HYDROPHILIC AND ORGANOPHILIC PROPERTIES OF ZEOLITES AND SILICA MOLECULAR SIEVES

By

Stuart G. Fegan

Thesis presented for the degree of

Doctor of Philosophy

University of Edinburgh

1985

MISSING PAGES ARE UNAVAILABLE

To my mother and father

Acknowledgements

The research described in this thesis would not have been possible without facilities, funds and guidance. The provision of facilities by the University of Edinburgh and funds by the Science and Engineering Research Council are appreciatively acknowledged. Special thanks must go to Barrie Lowe. For his guidance and for the never-ending enthusiasm he showed this work, I am extremely grateful.

I am indebted to members of the zeolite research group, past and present, for their help and valuable discussions and for typing what must at times have seemed an endless manuscript I thank Annette Erskine. Nameless though they may be, the assistance many others have given me is very warmly appreciated.

Declaration

This thesis is of my own composition and is an accurate account of research carried out by myself at the University of Edinburgh between April 1981 and March 1984.

_____

Abstract

The research work described in this thesis encompasses a number of different aspects of zeolite science. Involvement with the aqueous solution chemistry of zeolitic materials is prevalent throughout and the greater proportion of the work relates to the silica molecular sieve silicalite-1. The ability of this material to adsorb organic molecules from aqueous solution is described and adsorption isotherms for the uptake of α,ω-alkanediols are presented.

Whilst the aforementioned sorption studies were in progress it became apparent that these microporous silica sieves were far more complex solids than originally thought. In particular, the mode of synthesis was found to have a critical bearing on the resultant chemical compositions of the crystals. More specifically, alkali metal ions from reaction mixtures become incorporated in products even though crystals are virtually aluminium free. To learn more about this phenomenon and, more generally, to aquire a greater understanding of these solids detailed synthesis studies were undertaken. Crystallisation in the Na_2O-TPABr-SiO_2-H_2O and in the Amine-TPABr-SiO_2-H_2O systems has been investigated. The experimental work is complemented by a theoretical analysis of silica molecular sieve crystallisation.

A collection of the physicochemical properties of silicalite are discussed and these are compared and contrasted to properties typical of aluminous zeolitic materials.

The latter part of this thesis discusses the subject of salt imbibition by zeolites, the uptake of salts from aqueous solution into the intracrystalline channels and cavities. In general, aluminous zeolites were found to favour adsorption of inorganic salts, the more silicious materials preferring salts with organic character. The post-synthesis sorption of salts is correlated to the incorporation of guest species in zeolitic materials during synthesis.

The aforementioned salt imbibition studies were carried out using a new experimental procedure based on isopiestic vapour pressure measurements. The results presented show the powerful nature of this technique and demonstrate some of its many applications.

Contents

Acknowledgements

Declaration

Abstract

Chapter 1 Zeolite Science: Some Basic Concepts

1.1 Introduction 1

1.2 Structure, composition, properties, synthesis 2

References 26

Chapter 2 Analytical Methods

2.1 Introduction 29

2.2 Analytical Techniques: General Information 29

2.3 Analytical Methods: Experimental Details 33

2.4 Other Techniques 37

References 38

Chapter 3 Silicalite Synthesis in the Na_2O-TPABr-SiO_2-H_2O System

3.1 Introduction 39

3.2 Experimental 45

3.3 Results and Discussion 51

3.4 Conclusions 105

References 107

Chapter 4 Silicalite Synthesis in the Amine-TPABr-SiO_2-H_2O System

4.1 Introduction and Literature Review 110

4.2 Experimental 112

4.3 Results and Discussion 119

4.4 Conclusions 154

References 158

Chapter 5 A Theoretical Approach to Silica Molecular Sieve Synthesis

5.1 Introduction 160
5.2 Summary of the Equilibrium Model for Crystallisation of High Silica Zeolites 164
5.3 Crystallisation in Systems that Contain Strong Bases as Mineralisers 175
5.4 Crystallisation in Systems that Contain Amines as Mineralisers 219
5.5 Crystallisation in Systems that Contain Salts as Mineralisers 250
5.6 Concluding Remarks 254
References 258

Chapter 6 Properties of Silicalite-1

6.1 Introduction 260
6.2 Adsorption of Organic Molecules from Aqueous Solution 260
6.3 Chemical Composition of Silicalite-1: Some Related Properties 270
References 300

Chapter 7 Properties of Aluminous Zeolites 302
References 314

Chapter 8 The Use of Isopiestic Vapour Pressure Measurements to Study Adsorption by Zeolites

8.1 Introduction 316
8.2 Experimental 329
8.3 Results and Discussion: Adsorption of Electrolytes from Aqueous Solution by Zeolites 340
8.4 Application of the Isopiestic Technique to Study the Adsorption of Non-Electrolytes from Aqueous Solutions by Zeolites 385
8.5 Concluding Remarks 401
References 403

Appendices

I. Spectrophotometric Determination of Soluble Silica by the Molybdate Method.

II. Exploratory Crystallisations in Capillary Tubes.

III. Computer Programs Referred to in Chapter 5.

IV. List of Systems Investigated by the Isopiestic Technique.

V. Published Papers.

VI. Lecture Series and Courses.

CHAPTER 1

Zeolite Science: Some Basic Concepts

1.1 Introduction

The crystalline aluminosilicates known as zeolites possess remarkable properties. Their attributes predominantly stem from their structural uniqueness - zeolites are not dense solids, they have open 'honeycomb-like' topologies. Their structures and the properties they confer have intrigued scientists for many years and continue to do so to this day.

Since the early 1940's research activity in the zeolite field has steadily escalated and the scientific literature that now describes their synthesis, structures, properties and applications is vast. However, even though the cumulative efforts of industry and academia have amassed such a wealth of information, much still remains unknown, much has yet to be explored and as a subject for research zeolite science provides one of great diversity and unusual richness.

Historically, zeolites date from the discovery of stilbite by the Swede, Cronstedt, in the middle of the eighteenth century [1]. He observed that crystals of this mineral intumesced - they visibly lost water when heated. As a consequence 'zeolites', a mnemonic word derived from the classical greek 'zeein' (to boil) and 'lithos' (a stone), were named as a group of minerals. Although the first zeolites to be discovered all occurred in nature, many synthetic varieties are now known.

Almost 200 years elapsed between Cronstedt's discovery and germination of zeolite science - detailed systematic research did not begin until the 1940's. At this time, pioneering work was carried out by Barrer and co-workers in Britain and by Union Carbide Corporation in the United States. Research flourished after this initial impetus and industrial uses for zeolites were soon found. By the end of the 1950's, they were employed as sorbents to effect large scale separations, in the early 1960's they were taken up by the petroleum industry as cracking catalysts. Today zeolites are of immense technological importance.

The importance zeolites have assumed is ultimately attributable to their inherent microporosity. To the naked eye most zeolites are white flour-like powders which only rarely have any revealing macroscopic properties. Even the electron microscope seldom reveals more than morphological information, i.e. crystal size and shape. When 'viewed' at the submicroscopic molecular level though it soon becomes apparent why zeolites are such fascinating materials.

1.2 Structure, composition, properties, synthesis

Zeolites, felspars and felspathoids all belong to the group of crystalline silicates known as tectosilicates which are characterised by having three-dimensional framework structures. Unlike the felspars and felspathoids whose structures are relatively dense, zeolites have open frameworks and this is their distinguishing feature. Channels and cavities of molecular dimensions pervade crystals in orderly arrangements which are strictly imposed by periodicity.

The chemical composition of a zeolite can be represented empirically as:

$$M^{+n}_{x/n}[(AlO_2)_x(SiO_2)_y]^{-x}\ zH_2O$$

where M is a cation of valency n, y/x is greater than or equal to one and z is a function of the framework porosity and composition. The framework part of the structure (denoted in the square parentheses above) is composed of tetrahedra which consist of four oxygen atoms coordinated around so-called 'T-atoms' (T = tetrahedral). The tetrahedra join together, each one to four others, by sharing oxygen atoms so forming strong Si-O-Si and Si-O-Al bonds[a]. The resultant framework contains twice as many oxygen atoms as T-atoms, i.e. O/(Si + Al) = 2. The presence of trivalent aluminium atoms in tetrahedral sites gives the framework a negative charge and for electrical neutrality a stoichiometric number of cations reside in the intracrystalline channels and cavities. Zeolites can thus be considered as inorganic salts, albeit of a rather special type.

---

[a] Zeolites with framework Si/Al ratios less than unity have not been identified and cannot occur if Lowenstein's avoidance rule which disallows Al-O-Al linkages is observed.

The SiO_4 and AlO_4 tetrahedra that link to form the three-dimensional frameworks are sometimes called the primary building units (PBU's). Despite their apparently simple framework make-up, a multitude of different structures are known. This is principally because silica tetrahedra tend to form rings: 4, 5, 6, 8, 10 and 12 T-atom rings are all encountered in zeolite structures.

At present there are around 40 different known framework topologies [2], each one having a different system of channels and cavities. However, the structures of many novel synthetic phases have yet to be solved and the number of unique topologies is probably nearer 70. Various structure-classification schemes have been put forward most of which group together topologically related materials. Meier [3] proposed seven such groups named after representative members of each structure family: analcime, natrolite, chabazite, phillipsite, heulandite, mordenite and faujasite.

Besides viewing zeolite structures in terms of their primary building units, they can also be considered as polymers of larger sub-units, finite groups of tetrahedra. These larger sub-units were introduced by Meier [3] and called secondary building units (SBU's). They are depicted in Figure 1.1. All known structures can be assembled using just one of the SBU's shown. It is important to note that the construction of zeolites from SBU's is purely a crystallographic concept. Confusion could arise if the SBU's were thought to be the actual units from which zeolites were formed during crystallisation.

A further way of constructing frameworks uses the idea of tertiary building units (TBU's), assemblages of greater complexity than the SBU's such as cages, layers and chains. Sodalite (a felspathoid) and the industrially important zeolites, A, X and Y can all be built from 'β-cages', units which contain 24 tetrahedra made of single-4 and single-6 rings. The ways in which the β-cages link together giving the different structures are shown in Figure 1.2.

Many hypothetical zeolite structures have been predicted using these different building concepts. Such work can prophecy future discovery. One case history, that of zeolite omega, suffices to exemplify this. Prediction of the structure of this zeolite predated its discovery by several years.

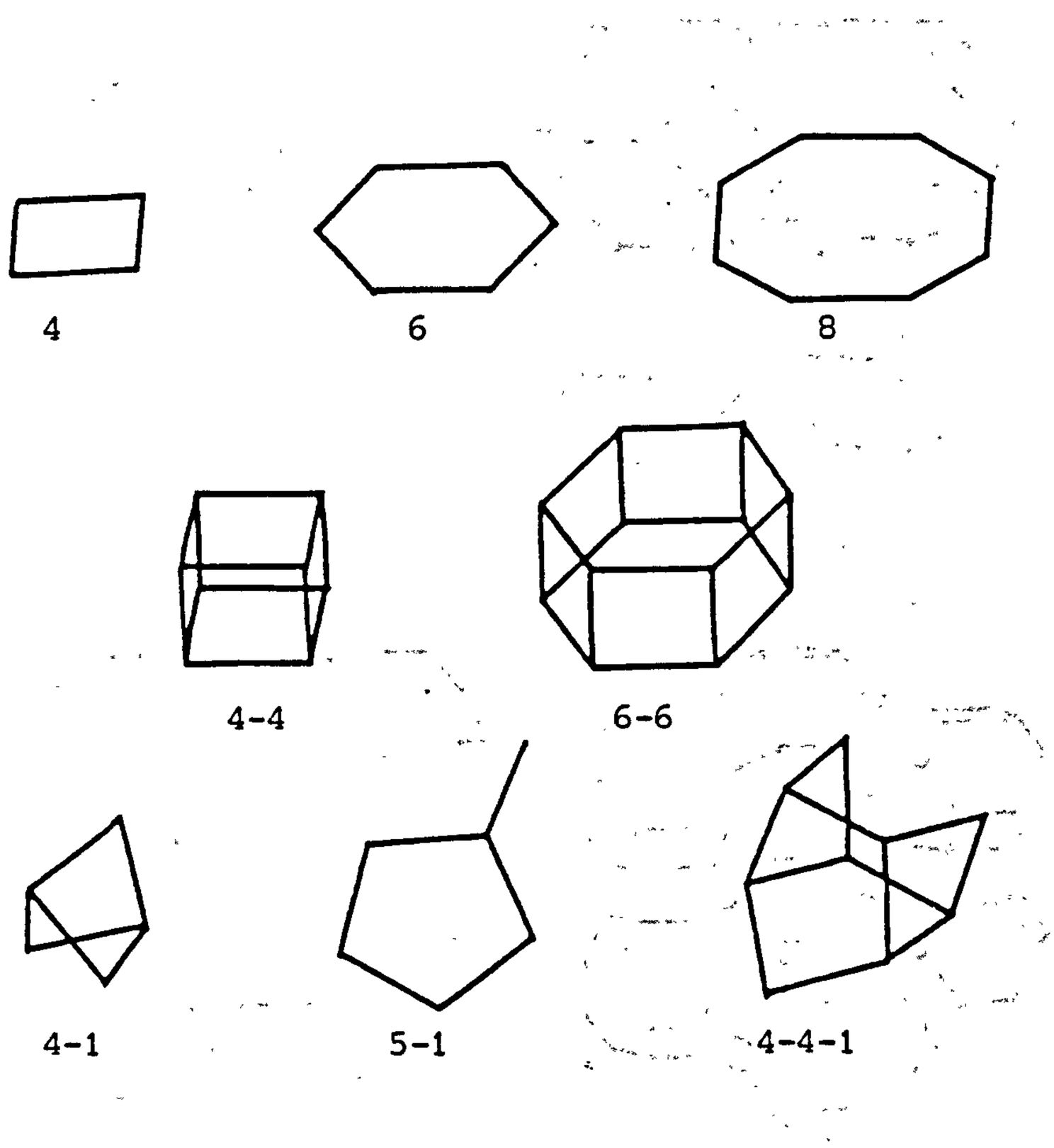

Figure 1.1 Secondary building units identified in zeolite structures [3]. Each straight line represents a T-O-T linkage.

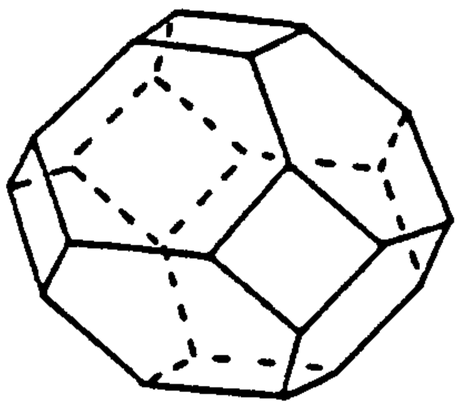

β-cage
(Sodalite cage)

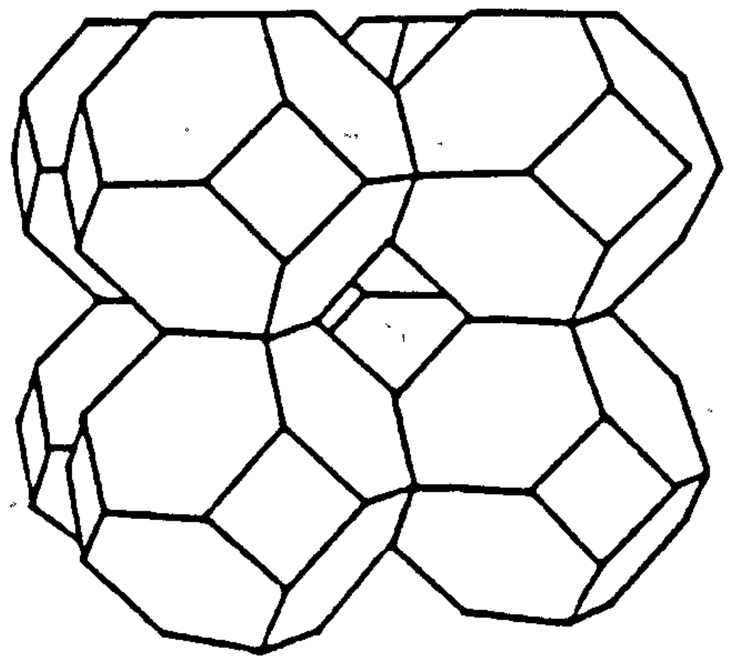

Sodalite

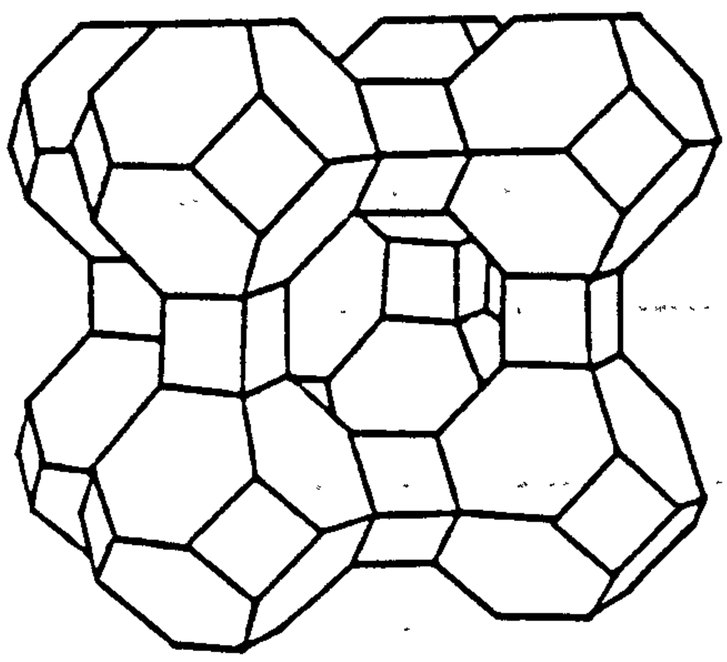

zeolite A

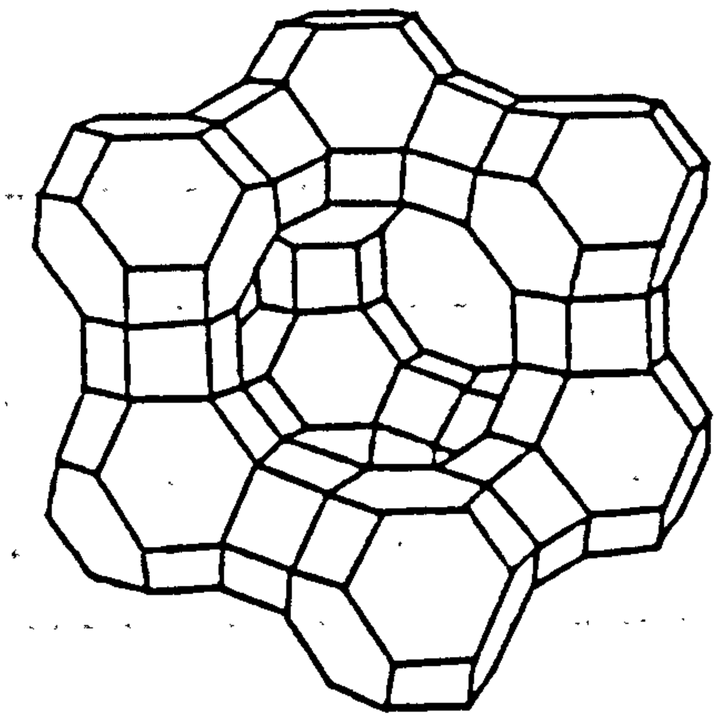

zeolites X and Y

Figure 1.2 Structures based on the sodalite cage

The porosity of zeolitic materials varies enormously, some have very tight structures whilst others have almost 50% of their volume void. Porosity is governed by the number and size of channels and cavities per unit crystal volume and is somewhat dependent on the dimensionality of the channel network. Zeolites with one-, two- and three-dimensional channel systems are known and, interestingly, all those in the latter two categories have interconnecting channel sets. Although hypothetically possible, zeolites with non-interconnected two- and three-dimensional channel networks have yet to be identified.

Their permeating channels give zeolites huge internal specific surface areas, sometimes the order of 1000 $m^2 g^{-1}$. These provide excellent adsorption surfaces for molecules that have free passage into the pore systems. Access to the intracrystalline pores is through channel apertures, sometimes called 'windows'. Both the number of T-atoms in the aperture ring and the presence of cations in the windows constrain access. The free dimensions of some T-atom rings are shown in Table 1.1.

Table 1.1 Free diameters of some T-atom rings [4]

Number of T-atoms in ring	4	5	6	8	10	12
Free diameter/Å	1.15	1.96	2.8	4.5	6.3	8.0

These dimensions give a rough estimate of the restriction imposed by aperture ring size on the 'molecular sieve' properties of the zeolite. Molecules above a critical size cannot be sorbed and thus, by prudent choice of zeolite, it is possible to separate compounds in admixture. This exclusion effect is the reason why zeolites are often synonomously termed 'molecular sieves'.

The most useful zeolites are those with 8, 10 and 12 T-atom windows because the dimensions of many molecules fall within the size of these openings. Ring distortion and puckering can additionally restrict access. Some windows are near circular in cross-section, others more elliptical. Window size and shape does not always reflect the cross-sectional characteristics of channels throughout their length though.

Table 1.2 Examples of zeolites with 1-D, 2-D and 3-D channel networks [2]

Dimensionality of channel network	Examples	No. of T-atoms in the windows	Approx. free dimensions of windows[a,b]
1-D	Ω	12	7.4 Å
2-D	Mordenite	12	6.7 x 7.0
		8	2.9 x 5.7
	Stilbite	10	4.1 x 6.2
		8	2.7 x 5.7
3-D	Faujasite[c] (zeolites X,Y)	12	7.4
	A	8	4.1
	Offretite	12	6.4
		8	3.6 x 5.2

[a] Both minimum and maximum values are given for non-circular apertures

[b] Free dimensions depend on the composition of the zeolite

[c] The mineral faujasite is isostructural with synthetic zeolites X and Y

Channels can be convoluted, broadening and narrowing at various points, and they may also be tortuous. Furthermore, different channel sets in the same zeolite often have different characteristics as can be seen from the examples given in Table 1.2.

In this introductory section it has only been possible to outline a few basic structural concepts. This brevity belies the significance of crystallographic studies which are of great importance to all in the zeolite field because many zeolitic properties are structure-dependent. Reference is made to the excellent works of Meier [3], Barrer [4] and Breck [5] for detailed appraisals of zeolite crystallography.

Zeolites can be classified into three groups on the basis of their framework Si/Al ratio (Table 1.3). Aluminous zeolites, those with a considerable amount of aluminium in their frameworks (Si/Al < 5), have substantial ionic character. They are 'solid electrolytes'.

Table 1.3 Categorisation of zeolites according to Si/Al ratio

	Si/Al	Examples[a]
Low	1 - 5	A, X, Y
Medium	5 - 10	Mordenite, Ω
High	>10	ZSM-5, ZSM-11, EU-1

[a] zeolites that can be crystallised over a significant compositional range sometimes fall into more than one category.

They contain a multitude of charge centres which generate considerable electrostatic fields within crystals. As vacant voids and channels are thermodynamically undesirable, zeolites readily sorb suitable molecules. Aluminous zeolites favour adsorption of polar and ionic species because of conducive adsorbate-adsorbent interactions. This

is why water is readily sorbed and tenaciously held by aluminium-rich zeolites. Pore-filling is often realised at extremely low water vapour pressures/concentrations enabling these zeolites to be employed as very effective dessicants. It is noteworthy that water occupies the cavities and channels of these aluminium-rich zeolites whilst they are actually crystallising. This has thermodynamic overtones which will be elaborated on shortly.

Adsorbed water can be removed by thermal treatment or evacuation and in most cases the process is reversible. In general, frameworks are strong and rigid and the zeolite structure is usually maintained upon dehydration with only minor shifts in the position of framework atoms. In contrast, there is often simultaneous movement of the counter-cations with loss of zeolitic water. Cations, unlike water molecules, must stay within the lattice to preserve electroneutrality but when they lose their water of hydration, the molecules with which they coordinate, they move to sites where they can favourably interact with the framework.

The property of ion exchange, inherent to zeolites, demonstrates cationic mobility in the more accepted sense. Many of the aluminium-rich zeolites, as-synthesised, contain alkali and alkaline earth metal cations. These cations can be replaced by others by post-synthesis ion exchange, a process which is routinely used to tailor zeolites for specific needs. The pockets of charge in a zeolite often act as adsorption sites and/or catalytically active centres and their nature is of critical importance. Exchange procedures usually involve contacting the zeolite, several times, with an aqueous salt solution containing the desired cation. The process is normally reversible. Although the openness of their frameworks readily allows cation exchange, ion sieve (exclusion) effects are observed if cations are large, analogous to molecular sieve action in adsorption. If large cations do enter the pore system, they can sometimes totally block channels. By judicious choice of the size of the exchange cation though, it is often possible to induce subtle changes to the 'mesh' of the sieve. If cations are sited at strategic points, such as at windows, exchange with cations of slightly different size can alter the effective channel aperture. Subsequent sorption behaviour is not necessarily only affected by alterations to the steric constraint. Sorption properties are also dictated by the field gradients within crystals and these depend on the specific nature of the cations.

Replacement of univalent ions by ones of higher valence (e.g. Na^+ by Ca^{2+}) introduces further factors. Replacements of this type necessarily reduce the cation density in the zeolite because multicharged cations have to counterbalance more than one framework negative charge. Such exchanges alter cationic positions, charge separation, charge distribution and field gradients within crystals. In addition, multivalent cations may hydrolyse. In summary, induced steric and/or electrostatic changes enable zeolites to be tailored by ion exchange for specific separative/catalytic work. The size, charge, location and number of cations in a zeolite are all important.

Although ion exchange is a versatile and routinely used modification tool for tuning zeolites prior to use, zeolites have inherent use as ion-exchangers. The ability of a zeolite to function efficiently as an exchanger depends on its exchange capacity and exchange selectivity. In practice, there is competition between the zeolite and the solution phase for cations. Often the zeolite prefers the least hydrated ions, the solution phase the highly hydrated ions. Some zeolites show remarkable preferences for certain ions and those with the greatest capacity, the most aluminous, are not always the most useful for exchange applications. A thorough review on ion exchange in zeolites was recently published by Sherman [6].

Ion exchange is widely used to prepare zeolite catalysts. As-made and as found in nature, most zeolites are catalytically inactive. Activation often involves converting the mother zeolite into a specific metallic form or into the acidic form. Most catalysis is carried out with the latter, namely with zeolites whose metal counter-ions (e.g. Na^+) have been replaced by protons H^+. Preparation of acid zeolites is usually a two-stage process involving firstly ammonium exchange and then calcination:

$$\text{Na-zeolite} + NH^+_{4(aq)} \rightleftharpoons NH_4\text{-zeolite} + Na^+_{(aq)}$$

$$NH_4\text{-zeolite} \xrightarrow{\Delta} \text{H-zeolite} + NH_3\uparrow$$

Aluminium-rich zeolites, if fully ammonium exchanged initially, often collapse on deammonation because the acid produced facilely attacks Al-O bonds. Partial ammonium forms can however be converted to semi-acid forms with retainment of structure.

Other ways of preparing H-form zeolites include exchange with polyvalent cations and direct exchange with mineral acids. In the former, acid sites are generated by an intracrystalline hydrolytic equilibrium of the type:

$$M(H_2O)_n\text{-zeolite} \rightleftharpoons M(H_2O)_{n-1}(OH)\text{-zeolite} + \text{H-zeolite}$$

M = polyvalent cation, e.g. La^{3+}

The reduced density of aluminium in the frameworks of silica-rich zeolites enables these materials to be converted to the H-form by direct exchange in acid solution. If conditions are not carefully chosen though, extensive dealumination may occur considerably reducing the number of resultant active sites. Sometimes controlled dealumination[a] is carried out to eliminate surface sites and confine reactions to the intracrystalline voids. H-form zeolites promote many acid-catalysed hydrocarbon conversion reactions inter alia isomerisation, alkylation, hydration, cracking, hydrocracking and reforming.

The first step in zeolite catalysis involves adsorption. Reactant molecules must be able to pass into the pore system and access active sites. The spatial arrangement of intermediate transition states and the size and egress of product molecules is also controlled by the cavity network. Zeolites largely superceded amorphous aluminosilicates as catalysts in the petroleum industry because of these 'shape-selective' advantages coupled with their increased activities.

A detailed synopsis of zeolite catalysis is outwith the scope of this work but one final point should however be mentioned. Catalytically active sites in zeolites, although often protons associated with the polyanionic framework, can also be separate phases within the zeolite such as metals, oxides, complexes and other occluded species. Such phases are not an inherent part of the zeolite structure and merely use the zeolite as a support. The first stage in the preparation of zeolites containing such phases often involves salt imbibition, the sorption of salts from aqueous solutions into the pores of the zeolite. This is

---

[a] Controlled dealumination can also be used to substantially increase the Si/Al ratio of the framework and so alter a zeolite's properties.

sometimes called impregnation in the catalysis literature. The imbibed salts can then be modified by a variety of methods (e.g. reduction, calcination) to form the desired active phase within the zeolite. Zeolite frameworks can also be lightly impregnated with salts to alter sorption behaviour. These are just two of the reasons why salt imbibition is an important field of research.

So far, attention has been largely focused on relationships between a zeolite's structure and its properties. Channel geometry, window size and blocking effects of cations have been discussed. Apart from their cation content, little has been said about their chemical composition, specifically the chemical make-up of the frameworks. There are basically two ways of chemically modifying a particular zeolite:

(i) by changing the exchange cations (already discussed),

(ii) by changing the Si/Al framework ratio.

Altering (i) and/or (ii) alters zeolitic properties.

The aluminium content of a zeolite largely controls its polarity. The most aluminous zeolites (Si/Al < 5) possess charged, heterogeneous surfaces and their intracrystalline voids contain a multitude of charged cations. These zeolites favour adsorption of water and other polar substances over non-polar species. They are often termed 'hydrophilic' zeolites because of this. In contrast, the sorptive selectivities of very silicious zeolites are quite the reverse. These sieves, some of which have only impurity level aluminium contents, possess few charged centres and have surfaces consisting predominantly of Si-O-Si linkages. These homogeneous surfaces can interact more favourably with non-polar molecules than they can with water and polar substances. Such zeolites are often called 'hydrophobic'.

The following exemplifies the aforementioned sorption selectivity differences. Aluminium-rich zeolites can remove compounds such as H_2O, NH_3, SO_2 and CO_2 from non-polar vapours and liquids contaminated with them. Chemists outwith the field probably know zeolites best for their drying capabilities - in many laboratories aluminous zeolites are routinely used to dry organic solvents. In direct contrast to this, very silicious materials are able to remove trace amounts of organic solutes from aqueous solutions. Although these zeolites are often

termed 'hydrophobic', it is clear that 'organophilic' is more apposite. Zeolites with intermediate Si/Al ratios display transitionary sorption properties. Work by Chen [7] on a series of dealuminated mordenites showed that sorption properties change from hydrophilic to hydrophobic as the Si/Al ratio increases. He attributed this to the increase in the number of homopolar Si-O-Si linkages and concommitant decrease in the number of aluminium atoms and associated charged cations in the zeolite.

In summary, zeolitic sorption behaviour is controlled by structure and composition. Compounds in admixture can be separated by:

(i) a molecular sieve effect: exclusion of some molecules on the basis of their size, and/or

(ii) a selectivity effect: exclusion of some molecules on the basis of their chemical nature.

The other two important properties of zeolites, ion exchange and catalysis, are also jointly governed by structure and composition.

Post-synthesis modification procedures such as ion-exchange and dealumination allow a zeolite's chemical composition to be varied independently of structure and thus enable a particular zeolite's properties to be tuned for specific uses. The composition of a zeolite, ready for use, may differ greatly from the original composition of the mother as-crystallised zeolite. Post-synthesis preparation procedures are time-consuming and often costly, especially if tonnage quantities are required by industry, but these drawbacks are largely unavoidable because only rarely is it possible to crystallise a zeolite with chemistry (Si/Al ratio, cation content) suitable for direct use. Although composition can be varied independently of structure after crystallisation, during crystallisation structure and composition are extremely interdependent. To successfully crystallise a particular zeolite structure, strict reaction conditions must prevail. These conditions will largely govern its composition and only rarely is it possible to directly crystallise a specific zeolite with broad compositional variation. The exceptions are certain high silica zeolites. Much of the underlying science governing 'synthesis' structure-composition relationships is still not well understood.

This has somewhat hindered progress in zeolite crystallisation and is probably the reason why so much work in this field has been done on an empirical basis, more or less by trial and error.

Early attempts to make zeolites in the laboratory were largely carried out by mineralogists endeavouring to replicate conditions under which natural zeolites formed. They had only limited success and were hindered by lack of product characterisation techniques. By the 1940's though, zeolites had aroused considerable interest and commercial possibilities were beginning to dawn. Systematic investigations into the synthesis and properties of zeolites thus began.

A general introduction to zeolite crystallisation now follows. An excellent book by Barrer reviews the topic in great depth [8].

Zeolites made in the laboratory fall into three categories:

(a) Those that are indistinguishable from natural species.

(b) Those which are structurally similar to natural zeolites but which have different composition (e.g. Si/Al ratio) and hence different properties.

(c) Those that have no natural counterparts.

Much of the synthesis quest has been geared to crystallisation of novel phases - new zeolites with novel properties are commercially of great value. Far less research has been carried out to specifically investigate kinetic/thermodynamic aspects of the crystallisation mechanisms.

Zeolites are crystallised under hydrothermal conditions. To make a zeolite at least four components must be admixed: a base, sources of silica and alumina[a], and water. The stoichiometry of a reaction mixture is usually represented as a list of the molar quantities of these components in oxide form[b], e.g. $xNa_2O\ ySiO_2\ zAl_2O_3\ wH_2O$ where x, y, z and w are numbers. If salts are additionally present in mixtures they are listed as such. Admixing components usually produces gels, thick solid-liquid slurries. The mixtures are alkaline and the amorphous

---

[a] A large number of different silica and alumina source materials can be used to formulate reaction mixtures.

[b] By definition $2NaOH \equiv Na_2O + H_2O$

solid partly dissolves producing soluble silicate/aluminosilicate species in various states of polymerisation. At a very general level, the most widely accepted mechanism for crystal growth involves a type of polymerisation between the crystallites and soluble silicate/aluminosilicate species in solution. The removal of ions from the solution phase, as a result of crystallisation, is accompanied by further dissolution of the gel. Reaction is complete when the disordered amorphous solid has all been converted to an ordered crystalline solid. Kinetics rather than thermodynamics often govern the products obtained. Many zeolites are only metastable and if left for long enough in their reaction solutions, their mother liquors, they will transform to more thermodynamically stable solids. This is known as Ostwald's rule of successive transformations.

The particular zeolite that crystallises is largely governed by the reaction mixture stoichiometry, especially the SiO_2/Al_2O_3 ratio and the nature of the cations present, and the crystallisation temperature. Factors such as the nature of the chemicals used, the method used to prepare the reaction mixture, aging gels at ambient temperatures prior to reaction and the degree of agitation during reaction are just some of the additional variables that can have effects. Perturbations caused by these variables can be kinetic and/or thermodynamic in origin.

Although systematic synthesis studies did not begin until the late 1940's, by 1960 many zeolite phases had been successfully crystallised. Well known examples include zeolites A, X, Y and L. Breck reviews crystallisation systems and structures obtained in his excellent book [9]. All the zeolites made during this formative development period had two inter-related features in common:

1. They were aluminium rich (Si/Al < 5).
2. They contained only inorganic cations.

Aluminous materials, although advantageous for some applications, also have inherent disadvantages. In general their stability under thermal, hydrothermal and acid conditions is relatively low because of the high density of aluminium atoms in their frameworks. It was imagined that more silicious zeolites would improve stability and therefore be beneficial for certain applications. This led to experimentation with organic cations in reaction mixtures.

In 1961 the first use of an organic cation, substituted ammonium ions , in zeolite synthesis was reported [10]. A large number of organic molecules, especially quaternary ammonium species, have since been employed in zeolite synthesis and proven highly successful [11]. Many novel zeolites have been discovered. Some of these, typified by Mobil's ZSM series are extremely silicious - some can be made with Si/Al ratios of 100 or more. It is interesting to note that the most silicious natural zeolites are clinoptilolite, mordenite and ferrierite with Si/Al ratios of about 5 .

The use of organic molecules in high silica zeolite synthesis heralded the concept of 'templating'. Usually organic molecules/cations become entrapped within crystals as they grow. They are sometimes considered to be structure-directing, namely the organic acts as a template around which tetrahedra organise so forming 'building blocks' for specific structures. However, all high silica zeolites are not organic-specific. For example, the zeolite EU-1 [12] only crystallises in the presence of hexamethonium ions but ZSM-5 [13] and ZSM-11 [14] can be made with several different organics. It is generally acknowledged that the best 'template' for making ZSM-5 is the tetrapropylammonium (TPA) cation but a multitude of other organics can act as guest species for this structure (see Table 1.4). Under certain reaction conditions, ZSM-5 can be crystallised from mixtures that contain no organics [15] and this casts uncertainty on the exact roles played by organic molecules when they are present in mixtures. Templating is currently a topic of much debate [11].

From a thermodynamic viewpoint, the organics can be considered as good stabilisers/pore-fillers. Open aluminosilicate frameworks, both aluminous and silicious, must be stabilised during growth by being filled with guest molecules. The former, being polar, are readily stabilised by water. Inorganic salts can also give additional stability to these materials. The hydrophilic character of aluminous zeolites thus manifests itself during synthesis. So too does the hydrophobic (organophilic) nature of silicious zeolites. For hydrophobic materials to crystallise in aqueous media, their porous crystals must be stabilised by organic molecules. Although these concepts are general, there are few exceptions. The stabilising effects are such that porous crystals will not form in the absence of 'suitable' guest species.

Table 1.4 Synthesis of zeolite and crystalline silica isotypes

Name of zeolite	Organics used for crystallisation[a]	Ref.	Name of pure silica analogue	Organics used for crystallisation[a]	Ref.
ZSM-5	TPA	13	Aluminium-free ZSM-5	TPA	16
			silicalite/silicalite-1	TPA	17
	Amines	18,19			
	Alcohols	20			
	Alkanolamines	21			
	Carboxylic acids	22			
	Transition metal complexes (organic)	23			
	'organic-free'	15			
ZSM-11	TBA	14,24	Aluminium-free ZSM-11	TBA	24
	Amines	18	Silicalite-2	TBA	25
ZSM-48	Amines	26,27,28	ZSM-48	Amines	26,27,28
	Bisquaternaries	29			
ZSM-12	TEA	30	TEA-Silicate	TEA	31
ZSM-39	Amines	32,34	ZSM-39	Amines	34
	Quaternaries	33			
KZ-1	Amines	35	KZ-1	Amines	35
KZ-2	Amines	35	KZ-2	Amines	35
EU-4	PTMA	36	EU-4	PTMA	36

[a] Organics are named according to chemical class except that quaternary ammonium compounds which promote crystallisation of a particular structure are specifically cited. Key: TEA = tetraethylammonium; TPA = tetrapropylammonium; TBA = tetrabutylammonium; PTMA = propyltrimethylammonium

Some correlation is observed between guest molecule type and crystallisation temperature. The most open water-stabilised aluminous zeolites are usually crystallised at low temperatures (T < 100°C). Higher temperatures tend to promote crystallisation of tight structured materials with lower water contents (especially if mixtures are inorganic) and also open organic-stabilised high silica zeolites.

In general, high silica zeolites can be made over much broader compositional ranges than can aluminous ones. Several have been successfully crystallised in aluminium-free form, from reaction mixtures that contain no specifically added aluminium source. At present there are eight of these silica molecular sieves known. These sieves, their zeolite isotypes and organics used in their synthesis are listed in Table 1.4. Of the materials listed, most is known about ZSM-5 type zeolites. ZSM-5 zeolites with vastly different Si/Al ratios have been made (minimum ~ 10, maximum >4000) and this has enabled its properties to be studied as a function of framework composition [37]. Some properties vary with composition, others do not (see Table 1.5).

Table 1.5 Properties of the zeolite ZSM-5 [37]

Properties of ZSM-5 independent of framework Si/Al ratio
Refractive index
X-ray pattern
Framework T-atom density
Channel size/micropore volume
Properties of ZSM-5 dependent on framework Si/Al ratio
Ion exchange capacity
(Ion exchange selectivity?)
Catalytic properties at H-ZSM-5
Hydrophobicity (water adsorption at constant P/P_o decreases as Si/Al increases)

The first patent covering an aluminium-free sieve was issued to Mobil in 1976 for their aluminium-free ZSM-5 [16]. A year later Union Carbide Corporation patented a porous crystalline silica, isostructural with ZSM-5, which they called 'silicalite' [17], sometimes referred to as 'silicalite-1'. These two patents appear to cover the same material.

Silicalite/aluminium-free ZSM-5 is most commonly crystallised in the Na_2O-TPABr-SiO_2-H_2O system (TPABr = tetrapropylammonium bromide). Although its aluminium bearing isotype, ZSM-5, can be made with a variety of different organics, silicalite requires TPA cations to crystallise. No aluminium is intentionally added to starting mixtures but nevertheless small amounts are usually unavoidably present. This arises from (i) impurities in reagents and/or (ii) impurities from the equipment used for the crystallisations. The products from the reactions therefore always do contain some aluminium - as synthesised products typically have Si/Al ratios between 1000 and 4000.

It is not apposite to call very silicious materials zeolites. A zeolite, by definition, is an aluminosilicate, i.e. it must contain aluminium. However, the properties of materials with Si/Al > 1000 are overwhelmingly dictated by their silicious natures, not their aluminium contents. Very silicious zeolites are probably better described as 'impure crystalline silicas'. Materials crystallised from 'aluminium-free' mixtures are generally referred to as molecular sieves, not as zeolites, even though their frameworks do contain trace amounts of aluminium.

A considerable part of the work presented in this thesis relates to silicalite[a] and a description of the structure of this material is therefore appropriate [38]. It should be remembered that silicalite and ZSM-5, although compositionally different, are structurally identical. It has already been mentioned that silicalite crystallises in the presence of tetrapropylammonium (TPA) ions. The as-synthesised product, the so-called silicalite precursor, has empirical composition

---

[a] The name 'silicalite' or 'silicalite-1' is used in preference to 'aluminium-free ZSM-5' henceforth to describe materials with ZSM-5 structure crystallised from reaction mixtures to which no aluminium source was specifically added.

4TPAOH 96SiO_2. Additionally, a little loosely bound water is also trapped within the crystals. The channel system is 3-dimensional and interconnected. Near circular zig-zag channels (free cross-section 5.4 ± 0.2 Å) perpendicularly intersect straight elliptical-shaped channels (free cross-section 5.7-5.8 x 5.1-5.2 Å). The channel network is schematically shown in Figure 1.3. The windows to both channel sets contain 10 silicon atoms enabling sorption of molecules of up to about 6 Å diameter. The pore volume is 0.19 $cm^3 g^{-1}$.

During crystallisation the void space is well filled by the quaternary molecules. They sit at the channel intersections - it is not possible for them to be elsewhere because of their size. After crystallisation the organic is removed by thermal treatment, usually by calcination in air at 500-600°C. This frees the pores and renders the material active for adsorption. Unlike aluminium-bearing ZSM-5, silicalite (ideally) has a neutral framework, no intra-crystalline cations and no ion-exchange capacity. The hydrophobic internal surface offers little attraction for water even at saturated vapour pressures. The small amount that is adsorbed is associated with:

1. Residual internal hydroxyl groups (often called silanol groups ≡Si-OH) that remain after the organic has been removed [38].
2. Silanol groups on the external surfaces of the crystals [37].

The outer surfaces of crystals are readily wetted by water because of the abundance of silanol groups on the crystal faces. Although silicalite's internal surfaces are hydrophobic, its external surfaces are hydrophilic - silicalite does not float on water. A material of similar structure called fluoride silicalite [39,40], which has unit cell composition 4TPAF 96SiO_2 has internal and external surfaces that are more hydrophobic than those of 'conventional' silicalite. Crystals of this material actually float on water [41], presumably due to the presence of surface Si-F groups.

Zeolitic materials with transitionary compositions span the range between the most hydrophobic molecular sieves and the most aluminous zeolites. Coupled with refinement procedures this gives rise to a plethora of structure-composition combinations. Additionally, germanium and gallium may replace silicon and aluminium and iron, boron and phosphorus can, under certain conditions, also be framework substituents.

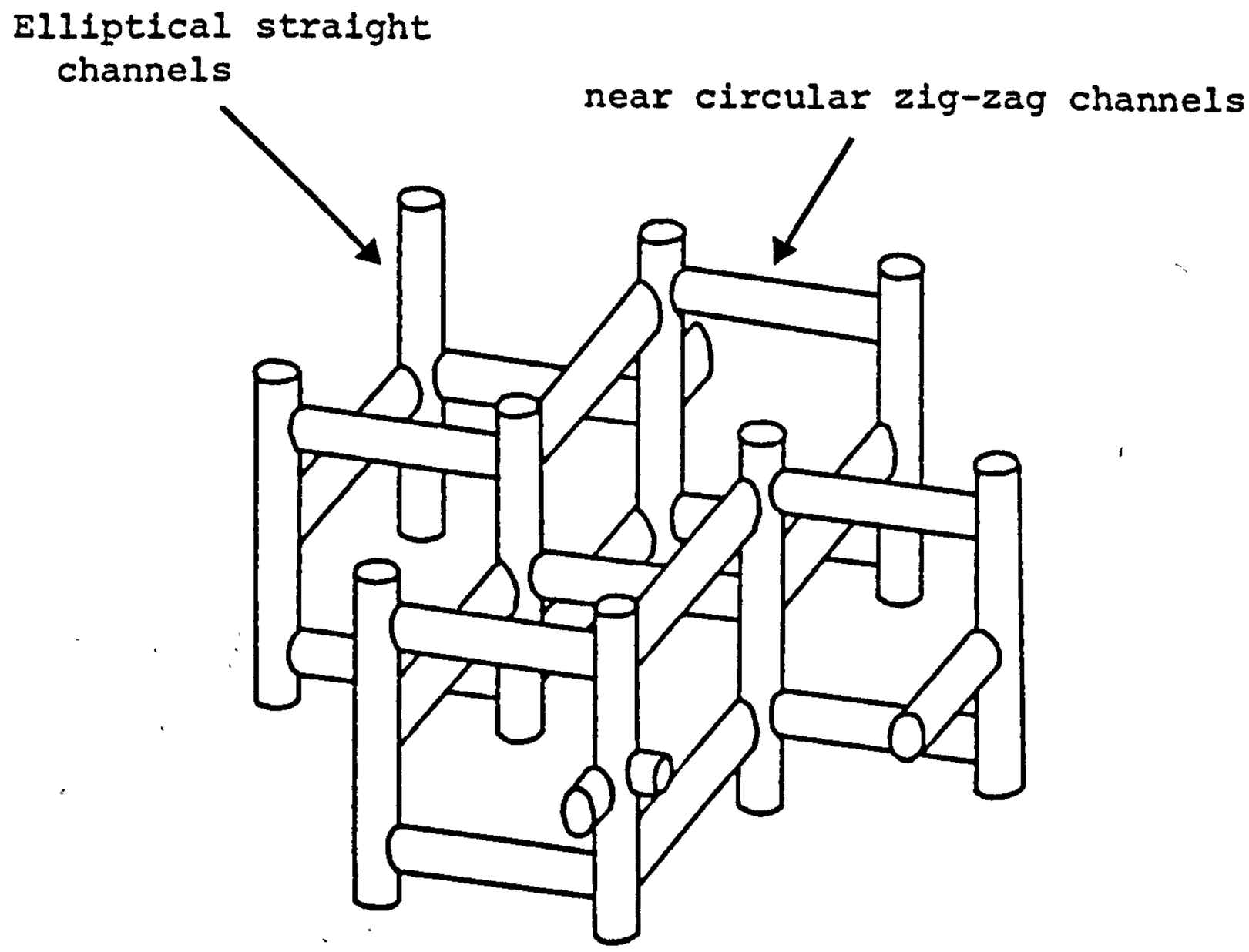

Figure 1.3 Channel structure of ZSM-5/silicalite

Table 1.6 Applications of molecular sieve zeolites [41]

ADSORPTION APPLICATIONS
A. Purifications
Drying
CO_2 removal
Sulphur compound removal
Pollution abatement
B. Bulk Separations
Normal/iso-paraffins
Xylene isomers
Olefin separation
O_2 from air
Sugar separation
CATALYTIC APPLICATIONS
Hydrocarbon conversions
Hydrogenation/dehydrogenation
Dehydration
Methanol to gasoline
Inorganic reactions
ION EXCHANGE APPLICATIONS
Removal of radioisotopes
Removal of NH_4^+ from waste-water
Detergent builder
Metals recovery
Fertilisers
Radioactive waste storage

To complete this review it is appropriate to mention some of the areas where zeolitic materials have found application. Both natural and synthetic zeolites have uses. The list given in Table 1.6 is by no means exhaustive but it suffices to show their versatility.

The past and projected destinies of zeolites in the United States shown in Table 1.7 reflect global trends in zeolite usage.

Table 1.7 Past and projected destinies of zeolites in United States commerce [42]

	1975	1980	1985
Catalysis	69%	14%	11%
Adsorption	31%	10%	8%
Detergency (ion exchange)	-	76%	81%
Total weight consumption (million lb)	58	325	495

The market for zeolite catalysts and sorbents has grown only modestly in the last decade. In contrast, there has been explosive growth in their use in detergents, as ion-exchangers (see Table 1.7).

Phosphates have long been used in detergents as builders to sequester hard water cations that are detrimental to the washing process. The eutrophication of lakes and streams by phosphates, amongst other chemicals, has led to new environmental pollution standards in many parts of the United States. Manufacturers have been forced to reduce phosphate usage and, in some cases, totally exclude phosphates from

detergent formulations. This legislation led to the introduction of zeolites as detergent builders. Zeolites remove the hard water cations, not by sequesterant action, but by ion exchange. It is ironic that the ability of zeolites to soften water, recognised long ago, has needed legislative forces to enable this use to be commercially exploited. Phosphate detergents are likely to be banned in other parts of the world if pollution problems do not abate. Indeed, Switzerland is to forbid their use from 1986 [43]. The future of zeolites in the detergent area looks assured.

The purpose of this chapter has been to outline basic concepts in zeolite science and to introduce zeolites as materials of great diversity. Several books [4,5,6,8] provide excellent background literature on most of the topics mentioned. In this thesis, detailed literature reviews on specific subjects are given in appropriate chapters.

At its outset a research programme should ideally have clear objectives. At the same time though, a certain degree of flexibility is desirable. When exploring unknown areas of science, problems cannot be foreseen and unexpected findings often warrant investigation.

The work presented in this thesis was carried out over a three-year period. Initially, the two main objectives were to investigate:

1. The uptake of organic molecules from aqueous solutions by silicalite and high silica zeolites. (Organophilic properties).
2. The uptake of salts, particularly inorganic salts, from aqueous solutions by aluminous zeolites. (Hydrophilic properties).

From an early stage in this work, anomalies, specific details of which are given in later chapters, were encountered with preparations of silicalite used for sorption studies. As a prerequisite to the pursuance of the sorption work, avenues had to be explored to ascertain where the root problems lay - sorption phenonema cannot be understood if the adsorbents themselves are not. There were several hints, subtle rather than glaringly obvious, that suggested the problems originated during crystallisation. A detailed study of silicalite

synthesis was thus felt paramount. Extensive synthesis studies have been carried out and much information has been brought to light. Time did not allow in-depth investigations of silicalite's organophilic sorption behaviour as originally anticipated but preliminary experiments in this area are documented. As will be seen, the synthesis work, which is described in Chapters 3-5, although not planned at the start of this research project, does complement other work in this thesis. Synthesis-property relationships are continually mentioned in the text. In Chapter 6, physical and chemical properties of silicalite are described. This chapter includes results that demonstrate the organophilicity of this material. To contrast this, Chapter 7 discusses the hydrophilic properties of aluminium-rich zeolites.

Chapter 8 describes an investigation of the uptake of salts from aqueous solutions by zeolites, the phenomenon of salt imbibition. Once again, hydrophilic-organophilic properties are very evident. The method used to carry out these experiments was completely novel and utilised isopiestic vapour pressure measurements. A great deal of time during the first nine months of this research programme was spent modifying and testing equipment and perfecting the experimental technique. The final chapter in this thesis looks retrospectively at the work accomplished.

Most chemistry is ultimately dependent on sound analytical methods. In Chapter 2, techniques used in the course of this work are introduced.

Chapter 1 - References

[1] A.F. Cronstedt
Akad.Handl.Stockholm, 1756, 17, 120.

[2] W.M. Meier and D.H. Olson
"Atlas of Zeolite Structure Types", published by the Structure Commission of the International Zeolite Association (1978).

[3] W.M. Meier
in "Molecular Sieves", Soc.Chem.Ind., London, 1968, p. 10.

[4] R.M. Barrer
"Zeolites and Clay Minerals as Sorbents and Molecular Sieves", Academic Press, London, 1978, Chapter 2.

[5] D.W. Breck
"Zeolite Molecular Sieves", Wiley, New York, 1974, Chapter 2.

[6] J.D. Sherman
in "Zeolites: Science and Technology" (NATO ASI Series), (Ed. F.R. Ribeiro, A.E. Rodrigues, L.D. Rollmann, C. Naccache), Martinus Nijhoff, The Hague, 1984, p. 583.

[7] N.Y. Chen
J.Phys.Chem., 1976, 80, 60.

[8] R.M. Barrer
"Hydrothermal Chemistry of Zeolites", Academic Press, London, 1982.

[9] Reference [5], Chapter 4.

[10] R.M. Barrer and P.J. Denny
J.Chem.Soc., 1961, 971.
Also: G.T. Kerr and G. Kokotailo,
J.Amer.Chem.Soc., 1961, 83, 4675.

[11] B.M. Lok, T.R. Cannan and C.A. Messina
Zeolites, 1983, 3, 282.

[12] J.L. Casci, B.M. Lowe and T.V. Whittam
European Patent application 42,226 (1981).

[13] R.J. Argauer and G.R. Landolt
U.S. Patent 3,702,886 (1972).

[14] P. Chu
U.S. Patent 3,709,979 (1973).

[15] R.W. Grose and E.M. Flanigen
G.B. Patent 1,574,840 (1980).

[16] F.G. Dwyer and E.E. Jenkins
U.S. Patent 3,941,871 (1976).

[17] R.W. Grose and E.M. Flanigen
U.S. Patent 4,061,724 (1977).

[18] L.D. Rollmann and E.W. Valyocsik
U.S. Patent 4,108,881 (1978).

[19] M.K. Rubin, E.J. Rosinski and C.J. Plank
U.S. Patent 4,151,189 (1979).

[20] J.L. Casci, B.M. Lowe and T.V. Whittam
European Patent Application 42,225 (1981).

[21] W.J. Ball, K.W. Palmer and D.G. Stewart
U.S. Patent 4,407,728, (1983).

[22] K. Iwayama, T. Kamano, K. Tada and T. Inoue
European Patent Application 57,016 (1982).

[23] L.A. Rankel and E.W. Valyocsik
U.S. Patent 4,388,285 (1983).

[24] M.K. Rubin, C.J. Plank, E.J. Rosinsky and F.G. Dwyer
European Patent Application 14,059 (1980).

[25] D.M. Bibby, N.B. Milestone and L.P. Aldridge
Nature, 1979, 280, 664.

[26] L.D. Rollmann and E.W. Valyocsik
European Patent Application 15,132 (1980).

[27] L. Marosi, M. Schwarzmann and J. Stabenow
European Patent Application 46,504 (1982).

[28] A. Araya and B.M. Lowe
J.Catal., 1984, 85, 135.

[29] J.L. Casci, B.M. Lowe and T.V. Whittam
British Patent Application 2,077,709 (1981).

[30] E.J. Rosinski and M.K. Rubin
U.S. Patent 3,832,449 (1974).

[31] R.W. Grose and E.M. Flanigen
U.S. Patent 4,104,294 (1978).

[32] B.P. Pelrine
U.S. Patent 4,259,306 (1981).

[33] J.L. Schlenker, F.G. Dwyer, E.E. Jenkins, W.J. Rohrbaugh, G.T. Kokotailo and W.M. Meier
Nature, 1981, 294, 340.

[34] D.M. Bibby and L.M. Parker
Zeolites, 1983, 3, 11.

[35] L.M. Parker and D.M. Bibby
Zeolites, 1983, 3, 8.

[36] J.L. Casci, B.M. Lowe and T.V. Whittam
European patent application 63,436 (1982).

[37] D.H. Olson, W.O. Haag and R.M. Lago
J.Catal., 1980, 61, 390.

[38] E.M. Flanigen, J.M. Bennett, R.W. Grose, J.P. Cohen, R.L. Patton, R.M. Kirchner and J.V. Smith
Nature, 1978, 271, 512.

[39] E.M. Flanigen and R.L. Patton
U.S. Patent 4,073,865 (1978).

[40] G.D. Price, J.J. Pluth, J.V. Smith, J.M. Bennett and R.L. Patton
J.Amer.Chem.Soc., 1982, 104, 5971.

[41] E.M. Flanigen
Proc. 5th Int.Conf. Zeolites, Naples (1980)
(Ed. L.V.C. Rees), Heyden, London, 1980, p.760.

[42] P.L. Layman
Chemical and Engineering News, 1982, 60(39), 10.

[43] Chemistry and Industry, 1984, Issue 11, p.387.

CHAPTER 2

Analytical Methods

2.1 Introduction

The principle aim of this chapter is to introduce the analytical techniques that have been extensively used during the course of this research and so avoid repetition in the chapters that follow. Sections in subsequent chapters give further experimental information.

The chapter is sub-divided into two sections. In the first, the analytical techniques used are introduced. The second section gives specific details about the analytical equipment (make and model) along with operating conditions and details of sample preparation prior to analysis.

2.2 Analytical Techniques: General Information

pH Measurements

The crystallisation of high silica zeolites and silica molecular sieves from amorphous gels is usually accompanied by a substantial increase in pH. This fact renders pH measurements useful as a means of monitoring the crystallisation process [1]. Foremost amongst the technique's advantages are its simplicity and speed. Samples from reaction mixtures (containing liquid and solid in admixture) only have to be cooled before measurements can be made. Other methods that have been used to monitor the crystallisation process, most commonly X-ray powder diffraction, require the solid to be separated from the liquid phase, washed free of adhering materials, dried and equilibrated with water vapour prior to analysis. These preparative steps take time - costly time if reaction over-run (transformation of products to more thermodynamically stable solids) is either in progress or imminent.

X-ray powder diffraction (XRD)

The most widespread applications of powder diffraction in zeolite science are (i) to monitor the progress of crystallisations and (ii) to characterise the final crystalline products - known diffraction patterns are used as 'fingerprints' to identify the product and determine its purity. Only a limited amount of structural information can be obtained by powder methods.

Sample preparation for XRD is critically important and this is especially so if the diffraction patterns of different samples are to be compared. Before samples are analysed they must be equilibrated with water vapour, ground to fine powder form (but not ground too severely otherwise crystal damage may occur) and extremely carefully packed into diffractometer slides. If any of these preparative steps are not strictly adhered to, results are difficult, and sometimes impossible, to interpret .

The crystallisation of zeolites involves the conversion of an amorphous solid into an ordered crystalline phase. As crystallisation proceeds, the solid phase becomes ever richer in crystalline material; the % crystallinity of the solid phase increases. Peak summation methods are widely used to determine the percentage of crystalline material present in samples taken during reaction.

Silicalite crystallisation has been extensively investigated in this work. In Figure 2.1, XRD patterns of samples taken during one particular synthesis run are shown. The % crystallinities of the samples were estimated from the area of the peak at ca. 23.1° 2θ relative to the area of the same peak in the most crystalline sample. Because this is the most intense diffraction line, it was felt unnecessary to use summation methods. In Chapters 3 and 4 crystallinity data, obtained by the aforedescribed method, is discussed in detail.

Microscopy

Product characterisation by microscopy is of the utmost importance. It is essential to have information about the size and shape of crystals. Also, small amounts of amorphous or crystalline impurity materials are often not detected by XRD but can be discerned by microscopic examination.

A Scanning Electron Microscope (SEM) is able to give 3-D images and allows crystals to be viewed under high magnification. Optical microscopy only gives 2-D vision (poor depth of field) and has inferior magnification capabilities to SEM. However, optical microscopy does have its advantages; sample preparation is easy and solids and liquids can be viewed in admixture.

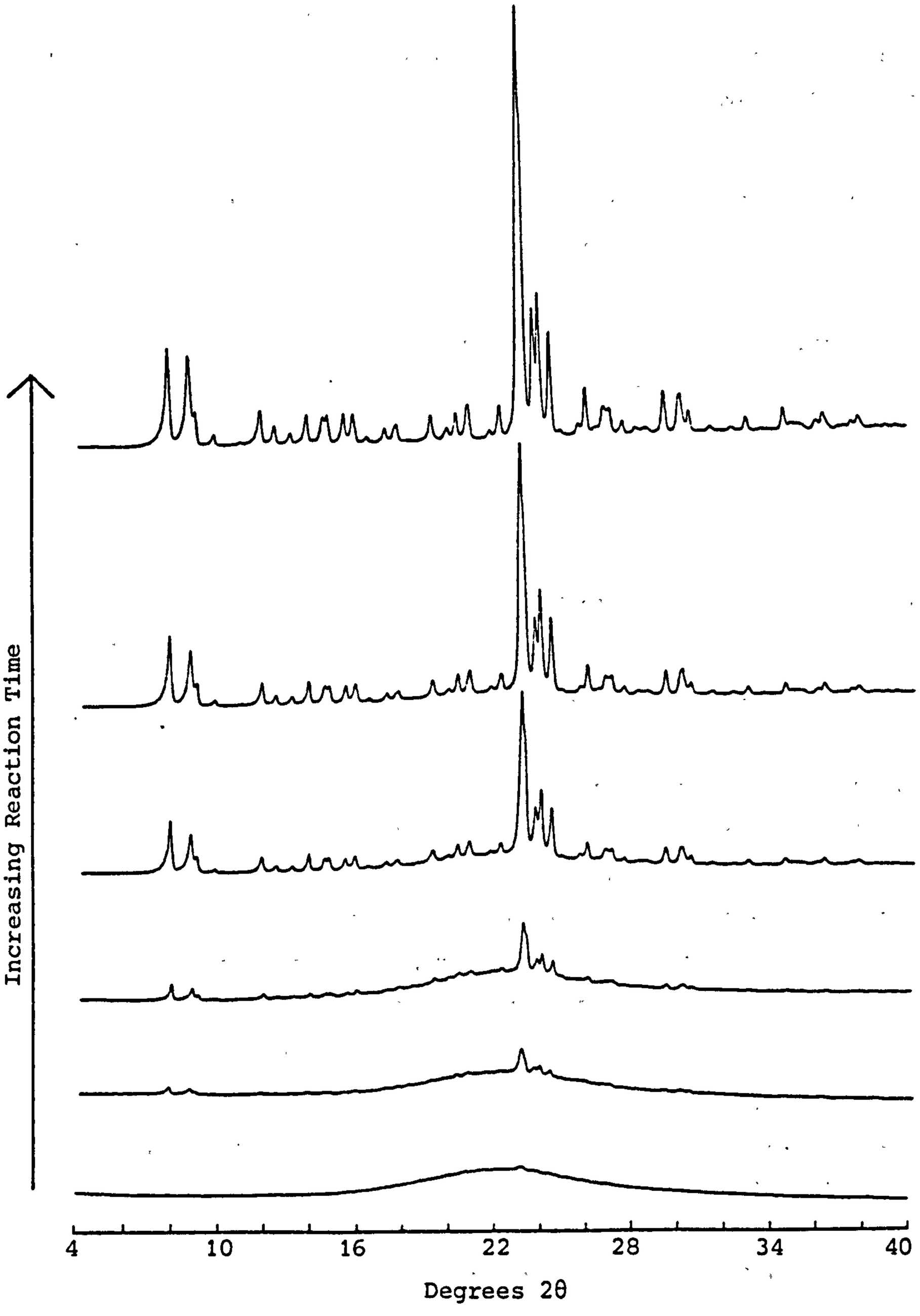

Figure 2.1 Crystallisation of silicalite from an amorphous gel as monitored by XRD analysis of samples taken during one particular synthesis run. The crystallinities of samples were determined from the relative areas under the peaks at ca. 23.1° 2θ. Crystallinity data obtained by this method is discussed in Chapters 3 and 4.

Chemical Analysis

X-ray fluorescence was used to determine the bulk compositions of crystalline materials. Multi-element analysis was obtained. Samples were fused into glass discs and analysed by the Department of Geology, University of Edinburgh[a].

Some samples were analysed by wet chemical methods (atomic absorption and emission) by ICI, Petrochemicals and Plastics Division, Wilton[b].

High silica materials that contained organic matter were analysed for carbon, hydrogen and nitrogen by the Department of Chemistry, University of Edinburgh.

Thermal Analysis

Thermal analysis techniques involve measurement of material properties as a function of temperature. Three such techniques have aided this research.

Thermal Gravimetric Analysis (TGA) measures weight changes in a sample as it is subjected to a temperature programme. In this work TGA has been used to determine the water and organic contents of zeolites. Differential Scanning Calorimetry (DSC) and Differential Thermal Analysis (DTA) measure the heat flow in and out of materials as a function of temperature. The differential heat flow between a sample and standard is measured by thermocouples. Exothermic and endothermic processes can be characterised. The two techniques are similar; DTA can be used at higher temperatures than DSC.

Prior to analysis by any of the above thermal analysis techniques, samples must be carefully prepared. Zeolitic materials must be well powdered and equilibrated with water vapour in a controlled atmosphere. Comparisons between results from the different techniques must be made with caution as the instrument configurations differ. During the course of this research it was found that some correlation was usually possible.

[a] The help of Dr. J.G. Fitton in obtaining the XRF analyses was greatly appreciated.

[b] The assistance of I.C.I. is acknowledged.

2.3 Analytical Methods: Experimental Details

Specific information that relates to the analytical techniques mentioned above is given below.

pH measurements

Equipment

Measurements were made with plastic bodied combination pH electrodes (EIL, type 1180/200/UKP) in conjunction with a Philips pH meter (type PW 9409). Latterly, some measurements were also made with a Pye Unicam 290 pH meter.

Conditions

The electrodes were standardised in pH = 9.20 reference buffer solution (BDH tablets) before sample measurements were made. The pH meters were set to record measurements at 20°C.

The pH of the reference solution was re-measured after a series of sample measurements had been made and only on a few occasions was there found to be any drift, i.e. the reference solution usually gave a pH reading of 9.20 ± 0.01. Where drift was observed, sample measurements were re-taken.

Sample Preparation

Samples from reaction mixtures were cooled to ambient temperatures in small pre-rinsed stoppered glass bottles. When cool, measurements were made. Stable pH measurements were obtained in 10-15 minutes. The electrode was carefully washed with distilled water between measurements. All samples from a particular reaction were re-measured after the reaction was complete so as to eliminate electrode errors and to allow time for samples to fully equilibrate at room temperature (which was usually close to 20°C). For the same reasons, the pH of samples from different reactions that were to be compared were measured at the same time.

X-ray powder diffraction

Equipment

Results were obtained using a Philips powder diffractometer. The configuration of the instrument was as follows. Samples were loaded by

an automatic sample changer (type PW 1170/02). The goniometer (PW 1050/80) was mounted on a highly stabilised x-ray generator (PW 1730/10) that provided $CuK_{\alpha_{1,2}}$ radiation (mean λ = 1.5418 Å). Scanning was controlled by a motor control unit (PW 1394). Detection was controlled by a channel control unit (PW 1390) and fed to either a pen recorder (PM 8203) or a teletype depending on whether the continuous or step scan mode was in operation. An AMR focusing monochromator (model AMR 3-202E) was fitted immediately before the detector (PW 1965/60).

Conditions

Normally a scan rate of 0.5° 2θ min^{-1} and a time constant of 4 were chosen for the analyses.

Sample Preparation

Powders were finely ground and left 'open' in the XRD laboratory to equilibrate with atmospheric water vapour for at least 12 hours before analysis. (A hygrometer adjacent to the instrument showed the relative humidity was usually in the 60-80% range). Finally, samples were carefully packed into slide holders and analysed. When comparisons were required, samples were analysed consecutively. The diffractometer was regularly calibrated with a piece of microcrystalline quartz stone.

Scanning Electron Microscopy

Equipment

A Cambridge Instruments type 604 Steroscan scanning electron microscope fitted with a Praktica L2 camera was used. Samples were coated with gold (SEM coating unit E5100, Polaron Equipment Ltd.) prior to analysis.

Sample Preparation

Fine powders were dispersed on aluminium pegs and coated with a film of gold (to make conducting and so prevent surface charge build-up during analysis).

Optical Microscopy

Equipment

The optical microscopy set-up consisted of a Vickers model M41 Photoplan Microscope fitted with a Pentax ME Super camera. A brass optical microscope (W. Watson & Sons, London) was also used on occasion.

Sample Preparation

Powders were dispersed in a solvent on a microscope slide. After solvent evaporation a layer of well dispersed solid remained. Samples were covered with glass slips and viewed. Solid and liquid mixtures (for example samples taken during crystallisation) were viewed without evaporation of the liquid phases.

Thermal Gravimetric Analysis

Equipment

Analyses were carried out on a Stanton Redcroft TG-770 Thermobalance.

Conditions

During runs, dry air flowed over the samples (4.5 $cm^3 min^{-1}$). The instrument was programmed to heat at 10°C min^{-1} and a typical sample weight of ca. 6 mg was used.

Sample Preparation

Small amounts of the solids were equilibrated with water vapour (in a closed system at 25°C over saturated NaCl solution, a_w = 0.753) for 3 or 4 days prior to analysis. Equilibrations were carried out in evacuated dessicators. Finely ground samples were placed in small stainless steel dishes which sat in recesses in a large stainless steel block. The block functioned as a thermal buffer and rested against the sides of the dessicator. Evacuation of the dessicators to the vapour pressure of water expedited equilibration. Dessicators were placed in thermostat baths held at 25.00 ± 0.04°C. Some samples were equilibrated in small glass bottles (instead of the steel dishes) in a different water bath at 25.0 ± 0.2°C.

The special dishes and blocks just described were designed for isopiestic vapour pressure measurements. Chapter 8 gives more comprehensive information about this equipment.

Differential Thermal Analysis

Equipment

A Stanton Redcroft DTA 674 instrument was used.

Conditions

Runs were carried out in a static air atmosphere at a heating rate of 10°C min^{-1}. The sample and the reference material (anhydrous Kaiser alumina) were placed in dimped platinum crucibles. Temperature differences were seen as peaks on the chart output. The actual weight of sample required for analysis depended on its powder density; ca. 70 mg was used on average.

Sample Preparation

Sample equilibration prior to analysis was as described for TGA above.

Differential Scanning Calorimetry

Equipment

The instrument used was a Du Pont DSC cell in conjunction with a Du Pont 990 Thermal Analyser.

Conditions

The sample (typical weight used, 3 mg) was placed in a small aluminium pan; an empty pan acted as the reference. The pans were positioned on raised platforms on a constantan disc which acted as the primary means of heat transfer to the sample and reference. The cell temperature was controlled by a silver heating block. The temperatures at the raised sample and reference platforms were monitored by Chromel-Constantan thermocouples. During runs, temperature differences were seen as peaks on the chart output. The areas under peaks were proportional to the energy involved in the transition and the mass of the sample. Dry air flowed over the samples during runs (50 $cm^3 min^{-1}$) and a heating rate of 10°C min^{-1} was always used. The maximum instrument temperature was 600°C.

Sample Preparation

Sample equilibration before analysis was as described above for TGA.

X-ray Fluorescence

Equipment

Analyses were carried out on a Philips spectrometer (model PW1450). Instrument calibration and sample analysis was carried out by the Department of Geology, University of Edinburgh.

Sample Preparation

Anhydrous samples were fused with a stoichiometric weight of flux (Johnson Matthey Spectroflux 105) and moulded into glass discs.

Elemental Analysis (C, H, N)

Equipment

Results were obtained on a Perkin Elmer 240 Elemental Analyser.

Sample Preparation

Sample equilibration prior to analysis was as described for TGA.

The operating conditions and sample preparations mentioned above were those most commonly employed. Unless otherwise stated in the text these conditions and preparative steps apply.

2.4 Other Techniques

Two other techniques should be mentioned at this stage:

Isopiestic Vapour Measurements

Isopiestic vapour pressure measurements have been used to study salt imbibition by zeolites. Full experimental details are given in Chapter 8.

Spectrophotometry

This technique was used to quantify the amount of silica in solution at the end of crystallisations (aluminium-free reactions) and by difference (knowing the total amount of silica in the reaction mixtures), the product yields were calculated.

The method relies on the fact that under certain conditions, orthosilicic acid reacts with a solution of molybdate in an acid medium to give an intense yellow coloration, due to α-molybdosilicic acid. The spectrophotometric method is based on this complex. As this technique was not used extensively during this research, it is inappropriate to outline the analytical procedure in this chapter; full details can be found in Appendix I.

Chapter 2 - Reference

[1] J.L. Casci and B.M. Lowe
Zeolites, 1983, 3, 186.

CHAPTER 3

Silicalite Synthesis in the Na_2O-TPABr-SiO_2-H_2O System

3.1 Introduction

Silicalite [1,2] is isostructural with the zeolite ZSM-5 [3,4] and is generally acknowledged to be the aluminium-free end member of the ZSM-5 compositional series [5]. This chapter describes a study of silicalite synthesis in the xNa_2O 2TPABr 20SiO_2 1000H_2O system. The aim of the study was to investigate the way in which the alkalinity and sodium content (x) of a reaction mixture affects the crystallisation of the silicalite precursor and the characteristics of the product. This introduction is split into two parts. First of all the relevant literature is reviewed and then the preliminary experimental work which prompted this investigation is described.

3.1.1 Literature Review

3.1.1.1 The Patent Literature

ZSM-5 was first synthesised by Argauer, Olson and Landolt in silicious systems that contained sodium and tetrapropylammonium (TPA) ions [3]. Numerous patents that cover alternative routes to this zeolite have appeared since. A detailed appraisal of this literature is outwith the scope of this review but the information and references given in Table 1.4 (Chapter 1) exemplify the diversity of reaction systems from which ZSM-5 type zeolites can be crystallised.

The first patent that covered an aluminium-free molecular sieve was published only eight years ago [6]; Dwyer and Jenkins (Mobil Oil Corporation, 1976) crystallised metal organosilicates, materials which as-synthesised contained both quaternary and metal species within their structures. Several of the examples given in the patent relate to crystallisation from reaction mixtures prepared with sodium hydroxide as the mineraliser and tetrapropylammonium bromide (TPABr) as the source of quaternary cations, i.e. similar mixture compositions to

those of the present investigation. Further examples show that the presence of chosen metal components in mixtures can effect incorporation of specific metal cations in the products. Metal ions incorporated included sodium, calcium, nickel and zinc. After thermal treatment to degrade the quaternary, it was stated that the metal ions could either be replaced by other cations, or, if desired, removed. The basic crystal lattices of these materials were unaffected by the metal species and x-ray diffraction showed the crystals were very similar in structure to the zeolite ZSM-5. These metal organosilicates are in fact 'aluminium-free' ZSM-5 and have been referred to as such [5]. In a recent specification aluminium-free ZSM-5 was synthesised by Kuehl [7] in systems that contained buffering agents to control the pH during crystallisation. The morphologies of the crystals produced were found to be dependent on the pH of the reaction medium.

A very close structural similarity to ZSM-5 was also shown by 'silicalite', a crystalline silica patented in 1977 by Union Carbide Corporation [1]. The silicalite precursor is crystallised hydrothermally in systems that contain alkylammonium cations (most commonly TPA), hydroxyl ions and a reactive form of silica. The precursor crystals contain organic material and have ideal unit cell composition 4TPAOH $96SiO_2$ [2]. However the crystals were found to contain metal species when metal ions were present in reaction mixtures. Calcination followed by treatments to remove the metal species produced silicalite, a porous crystalline silica polymorph. The silicalite precursor and the as-synthesised organosilicates of Dwyer and Jenkins are both crystallised under similar conditions, have similar structures and appear to be essentially the same material. This has already raised considerable argument about patent rights [8].

A silica polymorph with improved hydrophobicity called 'fluoride silicalite' was developed at Union Carbide's laboratories and patented in 1978 [9]. Reaction mixtures from which this material was crystallised were similar to those used to crystallise 'conventional' silicalite except that fluoride ions were present and the reaction pH was lower. Crystals produced were large and they gave an x-ray diffraction pattern very similar to that of ZSM-5. Infra-red spectroscopy showed that the improved hydrophobicity was due to the near absence of hydroxyl groups in the lattice.

A novel silica polymorph, crystallised in the presence of TPA ions and having a ZSM-5 type x-ray diffraction pattern, was claimed to be produced when either phosphate or sulphate ions were added to reaction mixtures [10]. Some phosphorus and sulphur were respectively found in the products. The morphology and thermal stability of the crystals were found to be slightly different from those of structurally similar materials.

3.1.2 The Open Literature

Outwith the patent literature silicalite synthesis has received little attention by researchers. Falth and Hakansson [11] studied silicalite crystallisation in the TPA_2O-SiO_2-H_2O system. Their main finding was that the amount of TPAOH used in mixtures, the reaction alkalinity, markedly affected the size of the crystals produced. The largest amounts gave very small crystals (ca. 1 μm) but when only small quantities were present large crystals (ca. 70 μm) formed. The aforementioned work [11] is the only paper in the literature devoted to silicalite crystallisation in its entirety.

A considerable number of studies relating to the synthesis of ZSM-5 have been published. This reflects the interest this material has aroused and more generally reflects the increasing attention that has been devoted over the last decade to the synthesis of zeolitic materials in systems that contain organic cations. Some of the papers on ZSM-5 synthesis are relevant to the present study because a number of workers have made comparisons between ZSM-5 and silicalite crystallisation and brought interesting information to light.

Lecluze and Sand [12] investigated crystallisation aspects of the ZSM-5/silicalite series. Increased rates of crystallisation were observed when the SiO_2/Al_2O_3 ratio of a reaction mixture was increased. They consider the ZSM-5/silicalite series as a continual isostructural series with silicalite being the aluminium-free end member.

Work by Chao et al [13] showed how reaction mixture stoichiometry and reaction conditions can affect the crystallisation of ZSM-5. Alkalinity was found to affect nucleation more than growth (at constant SiO_2/Al_2O_3) and they suggested that an optimum alkalinity for nucleation existed; at low and at high alkalinities induction periods

were prolonged. The chemical nature of the alkali used in reaction mixtures was found to be an important parameter; at constant alkalinity the rate of formation of aluminium-free ZSM-5 (silicalite) increased with increasing concentrations of tetrapropylammonium cations. Faster crystallisation kinetics were also observed when the SiO_2/Al_2O_3 ratio was increased at constant alkalinity. The nature of the silica source used in mixtures was shown to profoundly affect crystallisation. Rates of conversion increased in the order: silica gel < sodium silicate < colloidal silica.

Kulkarni et al [14] investigated ZSM-5 synthesis in systems that contained tetrapropylammonium (TPABr) and triethylpropylammonium (TEPBr) cations. The rates of nucleation and growth were lower when TEPBr was used. From their kinetic studies they inferred that an optimum alkalinity existed for nucleation and growth. Temperature was shown to markedly increase the kinetics of the crystallisation process.

Effects of crystallising ZSM-5 in systems that contained different alkali metal cations were investigated by Erdem and Sand [15] and Nastro and Sand [16]. The nature and amount of alkali metal present affected crystallisation kinetics and crystal morphology. Morphology changes were also studied by Mostowicz and Sand [17]. The use of salts and organic additives in reaction mixtures produced crystals of widely differing size and shape.

Nakamoto and Takahashi [18] crystallised ZSM-5 in alkali metal free systems. The only cations present in mixtures were TPA. Crystallisation rates increased as the alkalinity increased. Synthesis in alkali metal free systems has also been investigated by Bibby et al [19]; their systems contained ammonium (NH_4^+) and TPA ions. The principal benefit of carrying out crystallisation in these systems is that calcination of the products gives ZSM-5 in the H-form (i.e. catalytically active) without the need for preparative ion-exchange procedures.

Kinetic studies of ZSM-5 crystallisation have featured predominantly in the literature to date. Thermodynamic and mechanistic aspects of the crystallisations have received much less attention. Only Derouane and co-workers [20] have investigated the mechanism of ZSM-5 synthesis in any detail. Depending on the stoichiometry of

reaction mixtures and the nature of the reagents used to prepare them, they found that either of two crystallisation mechanisms can operate. Crystallisation occurred either by liquid phase ion transportation or by solid phase hydrogel transformation.

3.1.2 Preliminary Experimental Work

The structure and physical properties of silicalite have already been introduced in chapter 1. A study of the organophilic sorptive properties of this molecular sieve is described in chapter 6. Preliminary work in the aforementioned sorption study was carried out with material crystallised from reaction mixtures of composition $3.5Na_2O$ 2TPABr $20SiO_2$ $1000H_2O$. The mixtures were crystallised at 95°C and products were obtained in about 8 days. The products were used for sorption experiments after calcination to remove the entrapped tetrapropylammonium species from the silicalite precursors. These initial experiments successfully showed that organics were readily sorbed from dilute aqueous solutions. At the same time though the sorbents also displayed some anomalous behaviour. Stirring the silicalite crystals in water or dilute aqueous solutions produced substantial pH rises whereas identical experiments with crystals of the silicalite precursor did not. The increase in the hydroxide ion concentration was therefore due to species emanating from the pores of the sieve. Sodium ions were the only inorganic cations present in the synthesis mixtures and after calcination to remove the quaternary were the only ions that could be associated with the products. The observed pH increases were therefore caused by sodium hydroxide molecules being expelled into solution from the hydrophobic silicalite lattice. Steric restrictions do not allow sodium hydroxide molecules to escape until the pores have been freed of the large quaternary. After calcination, attempts to remove all the sodium from the lattice by repeatedly washing the material with water and by exchange in 1M ammonium chloride solution were unsuccessful. The amount of sodium that remained was far in excess of the trace levels of aluminium found. This residual sodium was undesirable as it introduced charged, hydrophilic centres into an otherwise hydrophobic lattice.

It seemed important that several questions were answered before furthering sorption studies. Is all the sodium in the sieve present as sodium hydroxide or are other sodium species present as well? Why are sodium species incorporated in silicalite? Why are they difficult to remove? Do they significantly affect the sorption properties of these materials? Although some of the information available in the literature was helpful, some was confusing. In their patent on silicalite [1] Grose and Flanigen state:

"When alkali metal hydroxide has been employed in reaction mixtures, alkali metal moieties appear as impurities in the crystalline product. Although the form in which these impurities exist in the crystalline mass has not yet been determined, they are not present as cations which undergo reversible exchange. ..... Neither silicalite nor its silicate precursor exhibits ion exchange properties".

In contrast Dwyer and Jenkins [6] inferred their metal silicates were exchangeable:

"The crystalline metal organosilicates as synthesised can have the original components thereof replaced by a wide variety of others according to techniques well known in the art. Typical replacing components would include hydrogen, ammonium, alkylammonium, aryl-ammonium and metals".

These patents therefore gave conflicting and unclear opinions of the nature of the metal species in these essentially identical materials. Just as the number and size of cations in aluminosilicate zeolites can markedly affect sorptive properties it seemed likely that any sodium species in silicalite, because of their size and hydrophilic nature, could profoundly alter sorption behaviour. Before pursuing sorption work it was felt desirable to have a greater understanding of the chemistry of these molecular sieves. As sodium moities were being incorporated during synthesis a detailed study of silicalite crystallisation was undertaken.

3.2 Experimental

3.2.1 Stoichiometry of the Reaction Mixtures

This study is concerned with synthesis of the silicalite precursor in the xNa_2O 2TPABr $20SiO_2$ $1000H_2O$ system and investigates the way in which the crystallisation and the characteristics of the resultant products are affected by the alkalinity and sodium content (x) of a reaction mixture when all other compositional parameters are kept constant. A total of nine reaction mixtures with x = 0.25, 0.50, 0.70, 0.85, 1.0, 2.0, 3.5, 5.0 and 6.5 (coded S1 to S9 respectively) were prepared and crystallised.

3.2.2 Equipment

The reactions were carried out in 1 litre screw-top polypropylene bottles equipped with stainless steel paddle stirrer units (Figure 3.1). Each bottle top was fitted with a bearing assembly which allowed the stirrer to rotate freely without any horizontal play. By means of two adjustable retaining rings screwed against the stirrer shaft the vertical position of the paddle was altered until its lower edge was ca. ½" above the base of the bottle. This provided efficient stirring of the mixture and prevented sedimentation of solid during reaction.

A small hole drilled in the top of the bottle allowed samples to be taken. This was sealed with a tight-fitting glass stopper at all times other than during sampling. The bottle and stirrer unit were clamped in position in a water bath and the drive from a motor, mounted vertically above the bottle, was transferred to the stirrer through a stainless steel shaft and connector bar. The set-up is shown in Figure 3.2. The water bath itself was made of copper sheet and a Fimonitor/relay system controlled four 1 kilowatt heaters which maintained the water temperature at 95 ± 1°C. To aid efficient thermostatting the water was continually stirred and its surface was insulated with polypropylene balls to reduce heat and water loss. A continuous flow of water into the bath from the mains coupled with an overflow kept the water level constant. Two identical water baths which could respectively accommodate 8 and 10 bottles at any one time were available for the experiments.

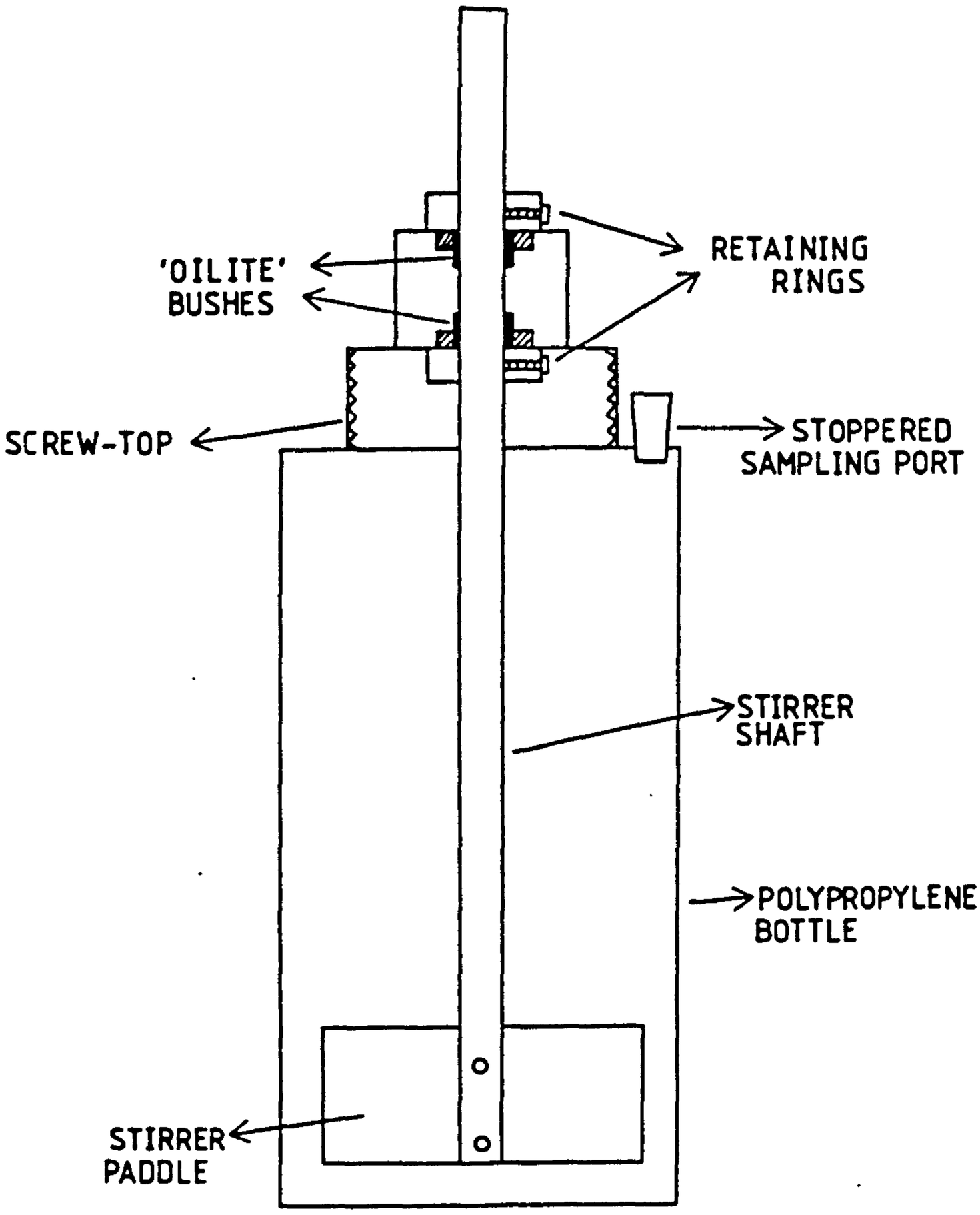

Figure 3.1 Polypropylene bottle and stirrer unit used for reactions at 95°C

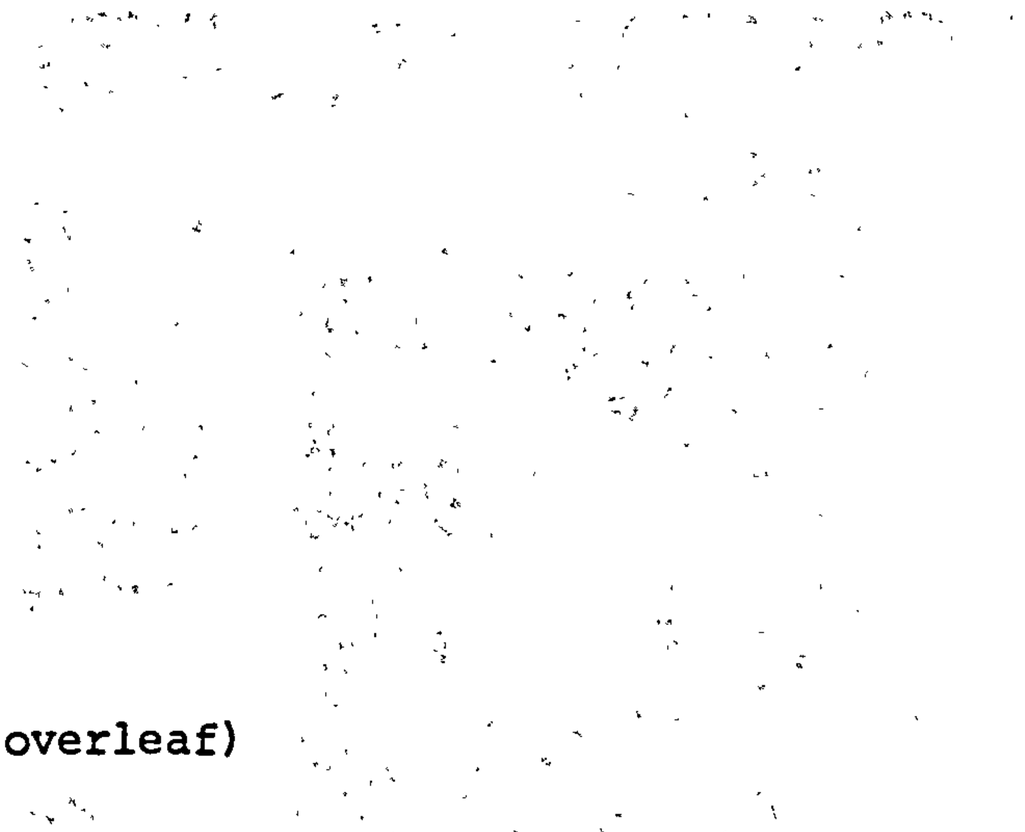

Figure 3.2 (see overleaf)

Polypropylene reactors in the 95°C water bath.

FIG. 3.2

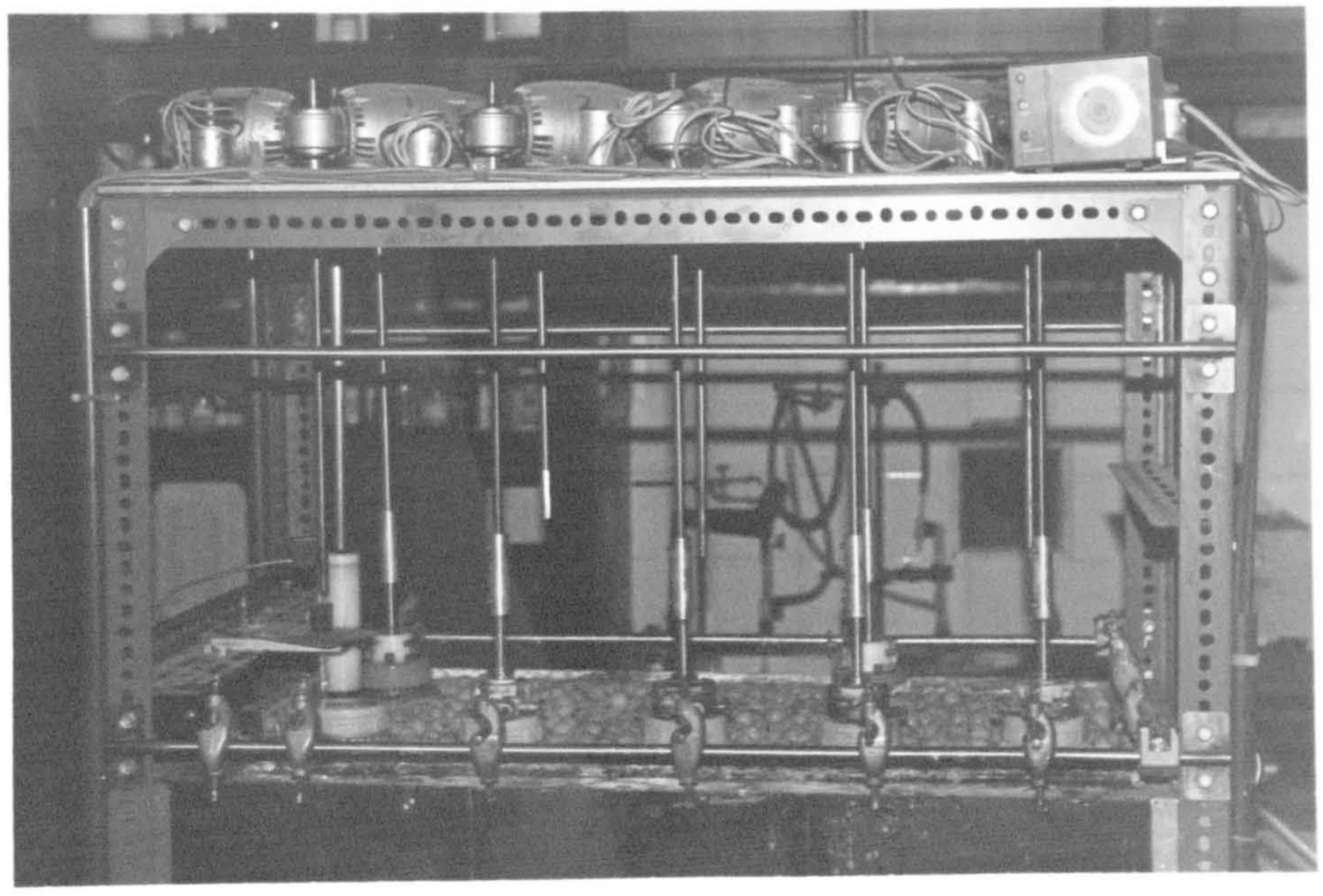

3.2.3 Materials

Details of the chemicals used to prepare the reaction mixtures are given in Table 3.1.

Table 3.1 Reagents used to prepare reaction mixtures

Chemical	Source/Grade
NaOH	Fisons plc, analar grade
TPABr	Fluka, purum grade
SiO_2	BDH Ltd., Cab-O-Sil M5
H_2O	Glass distilled

It is well known that the nature of the source silica used in synthesis can affect the crystallisation process. The amorphous silica employed in this study, Cab-O-Sil M5, was chosen because of its purity and large specific surface area. Cab-O-Sil is a fumed silica produced by hydrolysis of $SiCl_4$ in a hydrogen and oxygen flame at 1800°C. It has very low impurity levels as the reagents from which it is made are extremely pure. When used as the amorphous silica substrate in synthesis the large specific surface area of the Cab-O-Sil particles (ca. 200 m^2g^{-1}) gives an extensive liquid/solid interfacial contact area and this is often desirable. Although the Cab-O-Sil was received from the manufacturer as an apparently dry powder, some water is associated with the external surfaces of the particles; both siloxane bonds and hydrophilic silanol groups are present on the silica surfaces and, even at low water vapour pressures, water molecules are adsorbed. A sample of the Cab-O-Sil was analysed by thermal gravimetric analysis (TGA) with the result shown in Figure 3.3. At low temperatures the physically sorbed water is lost and the smaller high temperature weight loss is due to surface dehydroxylation, loss of chemical water. Duplicate analysis showed the Cab-O-Sil to have mean composition 97% SiO_2 3% H_2O by weight. This was taken into account when preparing reaction mixtures.

3.2.4 Preparation of the Reaction Mixtures

Care was taken to prepare all the reaction mixtures in exactly the same way. The silica and a portion of the water were stirred in a plastic measuring jug until a homogeneous slurry was obtained. The sodium hydroxide was dissolved in a small amount of distilled water in a pyrex beaker and stirred into the silica/water slurry. The beaker was washed several times with small aliquots of water to ensure all the sodium hydroxide was transferred to the mixture. Solid TPABr salt and the remaining water were added and stirring was continued until the mixture had a uniform consistency. Each reaction mixture was made up using 500 g of water and the amounts of the other reagents used were scaled in proportion. After preparation mixtures were immediately transferred to the polypropylene reactors and placed in the 95°C water bath. Reactions were timed from this moment. The mixtures were stirred at 150 rpm throughout. All but two of the reactions were carried out in the same water bath at the same time.

3.2.5 Sampling Procedure

The mixtures were sampled at regular time intervals throughout the reactions. Samples (ca. 8 cm^3) were normally taken after 2, 24, 48, 72, 96 ... hours although the longer reactions were sampled at 48 hour intervals. A tip-less 10 cm^3 pyrex pipette was used for sampling. It was immersed into the reaction mixture through the sampling port so enabling a representative sample containing both solid and liquid material to be withdrawn. Samples were placed in small plastic-stoppered glass bottles (ca. 12 cm^3 capacity) to cool; prior to use the glass bottles were rinsed with distilled water (to reduce the release of alkali from the new glass) and dried. Although it was necessary to stop the stirrer whilst sampling the procedure took barely half a minute and it was most unlikely this affected the reactions in any way.

3.2.6 Water Loss from Reaction Mixtures

The polypropylene bottles could not be completely sealed and water vapour was steadily lost during the reactions, principally through the bearing assembly. This loss was compensated by daily additions of small aliquots of distilled water, heated to 95°C, to the reaction mixtures. Prior to use several of the reaction bottles were filled with 500 g water, placed in the thermostat bath and their weight monitored over several days. From the results of these tests the addition of ca. 15 cm^3 of water per day to each bottle was deemed necessary if the water content in the mixtures was to be kept essentially constant. The level of the liquid in the mixtures was monitored visually throughout and the small unavoidable fluctuations in the water content that did occur are thought to have had little effect on the course of the reactions.

3.2.7 Criteria for Terminating Reactions

During reaction, amorphous silica is converted to crystalline material. The conversion is accompanied by considerable pH changes. The difference in appearance between the amorphous gel solid and crystalline solid in samples afforded a simple means of following the crystallisations. Reactions were terminated when samples appeared gel-free and when pH readings taken on consecutive days were near constant.

3.2.8 Product Preparation

The solid products were separated from their mother liquors either by filtration or centrifugation. In each case a portion of the mother liquor was passed through a 0.2 μm filter and retained for analysis. The solids were repeatedly washed with distilled water until the washings were near neutral (pH = 7 to 8) and bromide-free. Universal indicator paper was used for the pH test and the bromide test involved a standard silver nitrate procedure. The solids were then dried in an oven at 60°C.

3.2.9 Analytical Techniques used in this Study

After all the reactions were complete, the pH of each sample was re-measured. These measurements were made at the same time. The liquid and solid phases in the samples were then separated by the procedures outlined in section 3.2.8. After washing, the solids were dried at 60°C. Both the intermediate solid phases and the final bulk products were analysed by X-ray powder diffraction. The mother liquors were analysed for soluble silica by the molybdate method. The final crystalline solids were also analysed by thermal gravimetric analysis, optical microscopy and scanning electron microscopy. The chemical compositions of the solids were determined by X-ray fluorescence and C, H, N analysis.

3.3 Results and Discussion

Optical microscopy and scanning electron microscopy showed that only the reaction with lowest alkalinity (x = 0.25) did not fully crystallise. X-ray diffraction confirmed that all the crystalline products were silicalite and no crystalline impurities were detected.

Information about both the kinetics and thermodynamics of silicalite crystallisation has been obtained in this study. Crystallisation curves, plotted from XRD data, provided information about the reaction kinetics. The pH profiles gave a valuable insight into thermodynamic aspects of the crystallisations as well as a limited amount of kinetic information. The nature of the pH changes that occurred gave information about the crystallisation mechanism.

3.3.1 Crystallisation of the Reaction Mixture with x = 6.5 (Figure 3.4)

The large amount of base in this mixture initially dissolved all the amorphous silica. All crystallisation occurred from clear solution and a crystallisation curve could not therefore be plotted from XRD data. From the visual appearance of the samples taken it was apparent that some crystallisation occurred within the first 24 hours of the reaction. However subsequent crystal growth was slow and the final product yield was very low. The small increase in pH during reaction (see Figure 3.4) was caused by a reduction in the amount of silica in solution due to formation of the crystalline solid.

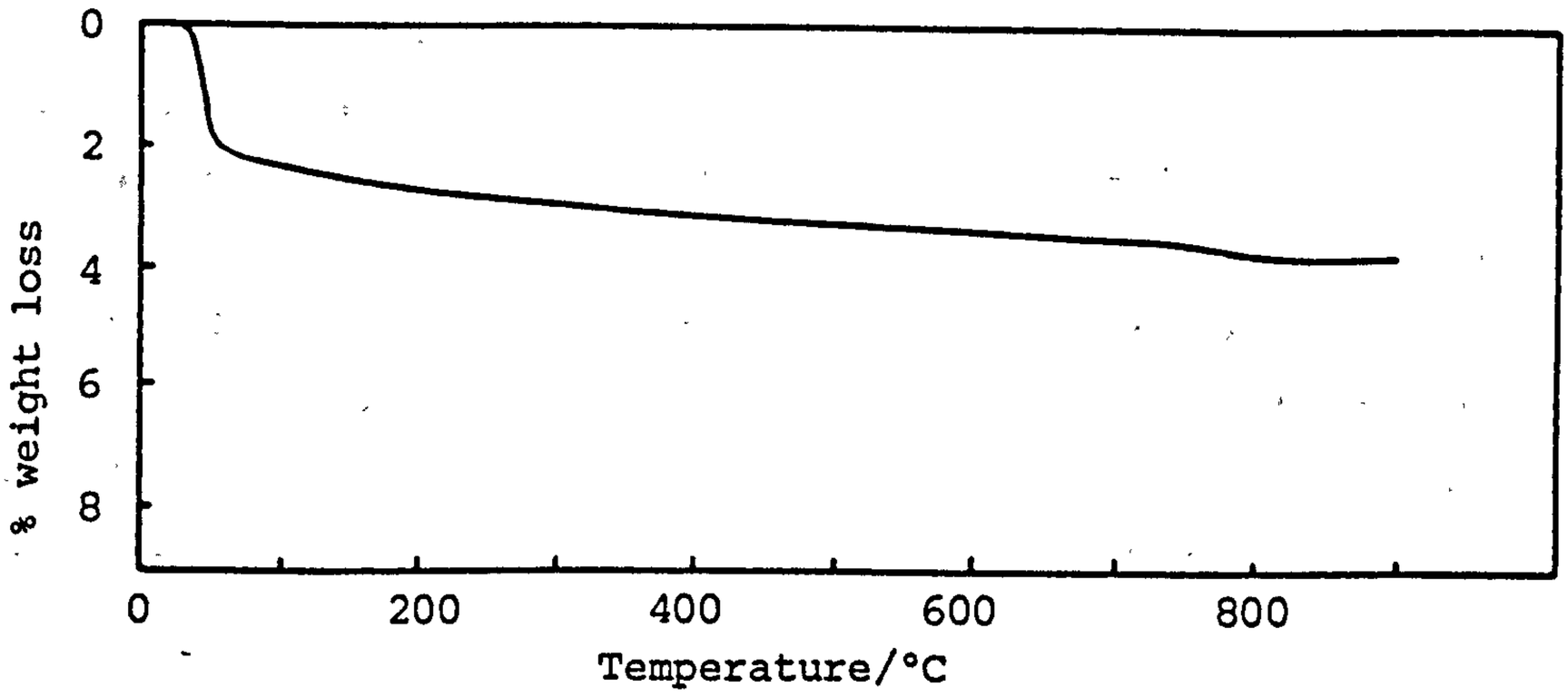

Figure 3.3 Analysis of Cab-O-Sil by TGA

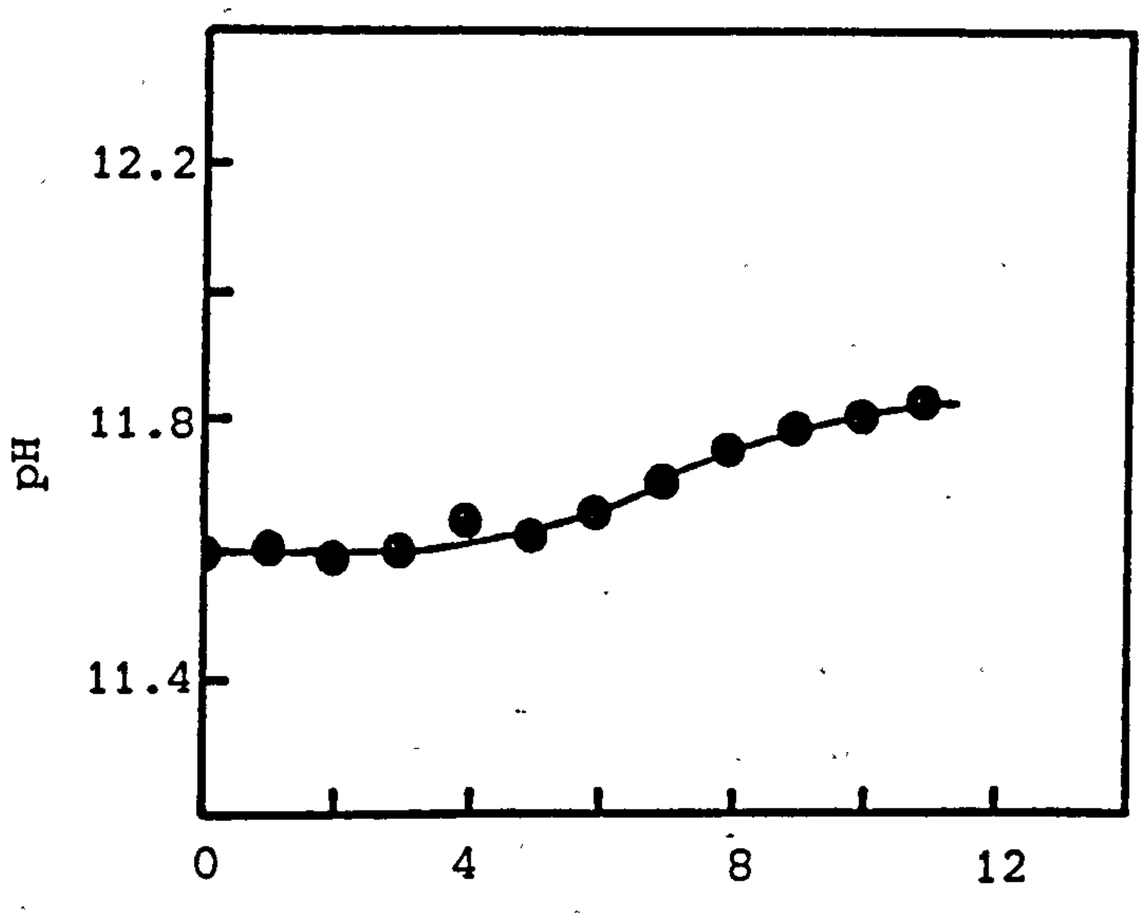

Figure 3.4 pH of samples taken during crystallisation of the reaction mixture with x = 6.5

3.3.2 Crystallisation of the Reaction Mixtures with x = 2.0, 3.5 and 5.0 (Figure 3.5)

In these reactions only a fraction of the solid amorphous silica initially dissolved. In all cases the pH remained almost constant throughout the induction period and the early stages of growth. Two solid silicas with different solubilities are present during the initial growth period but that with greater solubility (the gel solid) controls the species in solution. Growth occurs by a polymerisation reaction between soluble silicate species (the 'monomer') and the silicalite crystals (the 'polymer'). This reaction reduces the concentration of silicate species in solution and increases the hydroxide ion concentration. To re-establish concentrations of soluble species favoured by the amorphous solid the released hydroxide ions depolymerise some of the remaining gel. All three reaction mixtures contained substantial amounts of base and appreciable concentrations of silicate species were present in the solution phases. Consequently, they all have a buffer capacity that can cope with small changes in the hydroxide ion concentration. The results in Figure 3.5 show that little change in pH was observed during the initial stages of growth (crystallinity < ca. 40%). As the crystallinity increases the amount of amorphous silica present decreases and eventually the crystalline solid begins to control the nature of the soluble species through its solubility. Silicalite is less soluble than amorphous silica and the pH therefore starts to increase. In each case a very marked pH rise is observed when the crystallinity nears 100% and only small amounts of gel remain (see Figure 3.5). This rise indicates that the crystalline solid is in complete control of the species in solution. When all the gel has been depolymerised the final stages of growth occur from clear solution and the hydroxide ions released stay in solution and cause the pH to rise further. Crystallisation continues until an equilibrium is established between the crystalline solid and the solution phase. The small gradual rise in pH during the final stages of growth probably indicates the slow approach to this equilibrium. In part, this small rise could also be caused by conversion of the more soluble crystalline material to less soluble forms. At true thermodynamic equilibrium the pH should become constant.

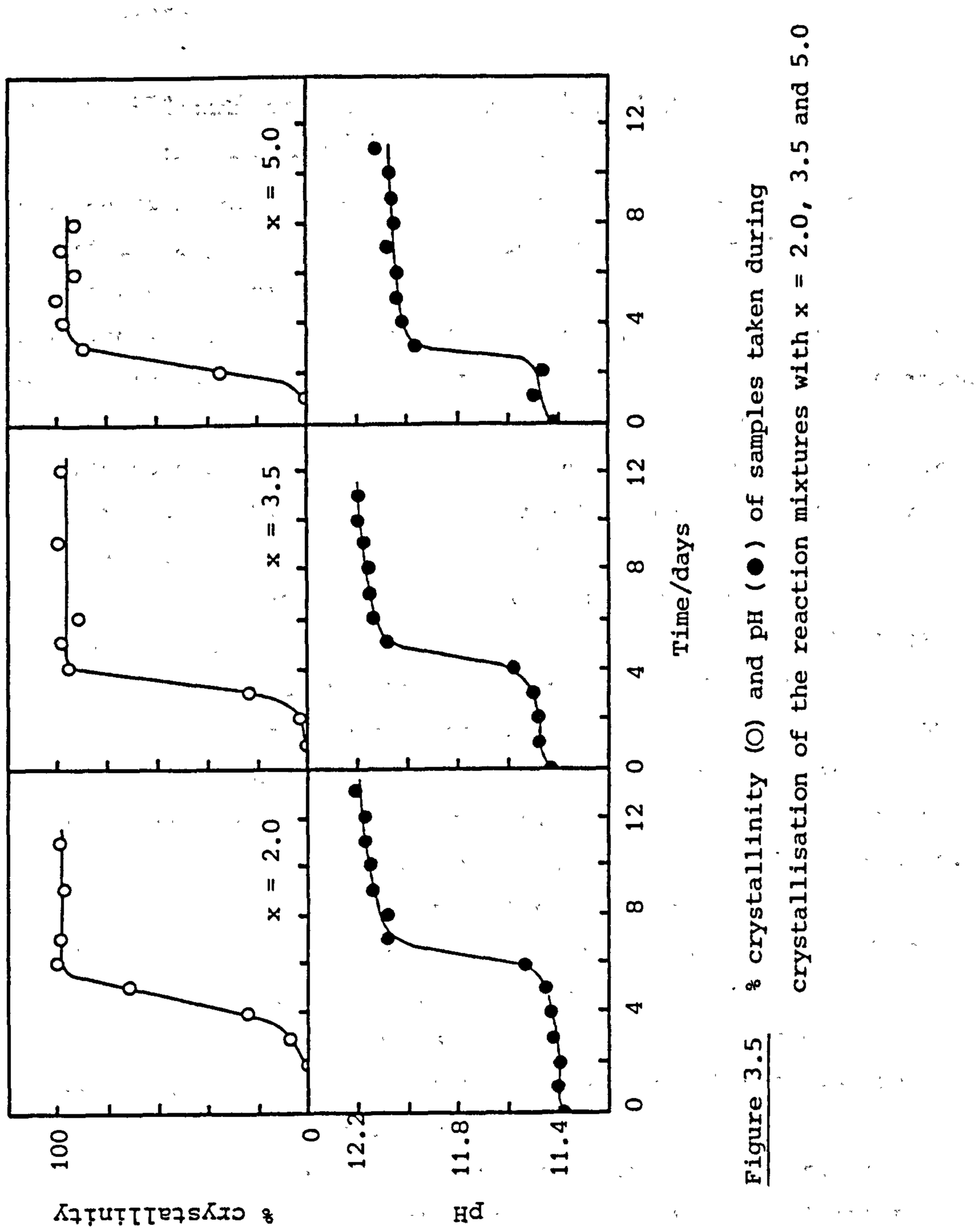

Figure 3.5 % crystallinity (○) and pH (●) of samples taken during crystallisation of the reaction mixtures with x = 2.0, 3.5 and 5.0

These mixtures contained base levels typical of those used to synthesise silicalite at low temperatures [1] and gave products in about a week at 95°C. The results in Figure 3.5 show clearly why pH measurements are of value. They provide information about the mechanism of crystallisation and unlike XRD they give a clear indication of when reaction is complete.

3.3.3 Crystallisation of the Reaction Mixtures with x = 0.70, 0.85 and 1.0 (Figure 3.6)

These reactions have considerably lower base contents. During the induction period the pH stayed constant but shortly after the onset of crystal growth the pH began to decrease. Silicalite has ideal unit cell composition 4TPAOH $96SiO_2$ and, as the quaternary is trapped within the framework, crystallisation is accompanied by a reduction in the amount of active base in the system. Low base reactions do not have the buffer capacity to cope with this loss and consequently pH decreases are observed. As crystallisation progresses the effective buffer capacity of these systems is continually reduced. The least buffered reaction (x = 0.70) showed the greatest pH fall. All the reactions showed marked pH rises when the crystallinity approached 100% similar to those observed for the higher base reactions (Figure 3.5) and due to the same effect; silicalite taking over control of the species in solution. However for these lower alkalinity reactions the pH increases are somewhat smaller and they occur at lower pH. Consequently, even after the pH has risen small amounts of amorphous silica are likely to remain. During the final stages of growth, after the major pH rise, the reactions with x = 0.70 and 0.85 showed another decrease in pH. This is due to removal of further base molecules from these systems caused by conversion of residual amorphous silica to crystalline material. Although these falls in pH are substantial, these low pH systems are exceptionally sensitive and unbuffered. This is especially so when the crystalline material controls the species in solution. The observed pH falls therefore represent only a small amount of further crystallisation and XRD did not in fact detect any significant crystallinity increases.

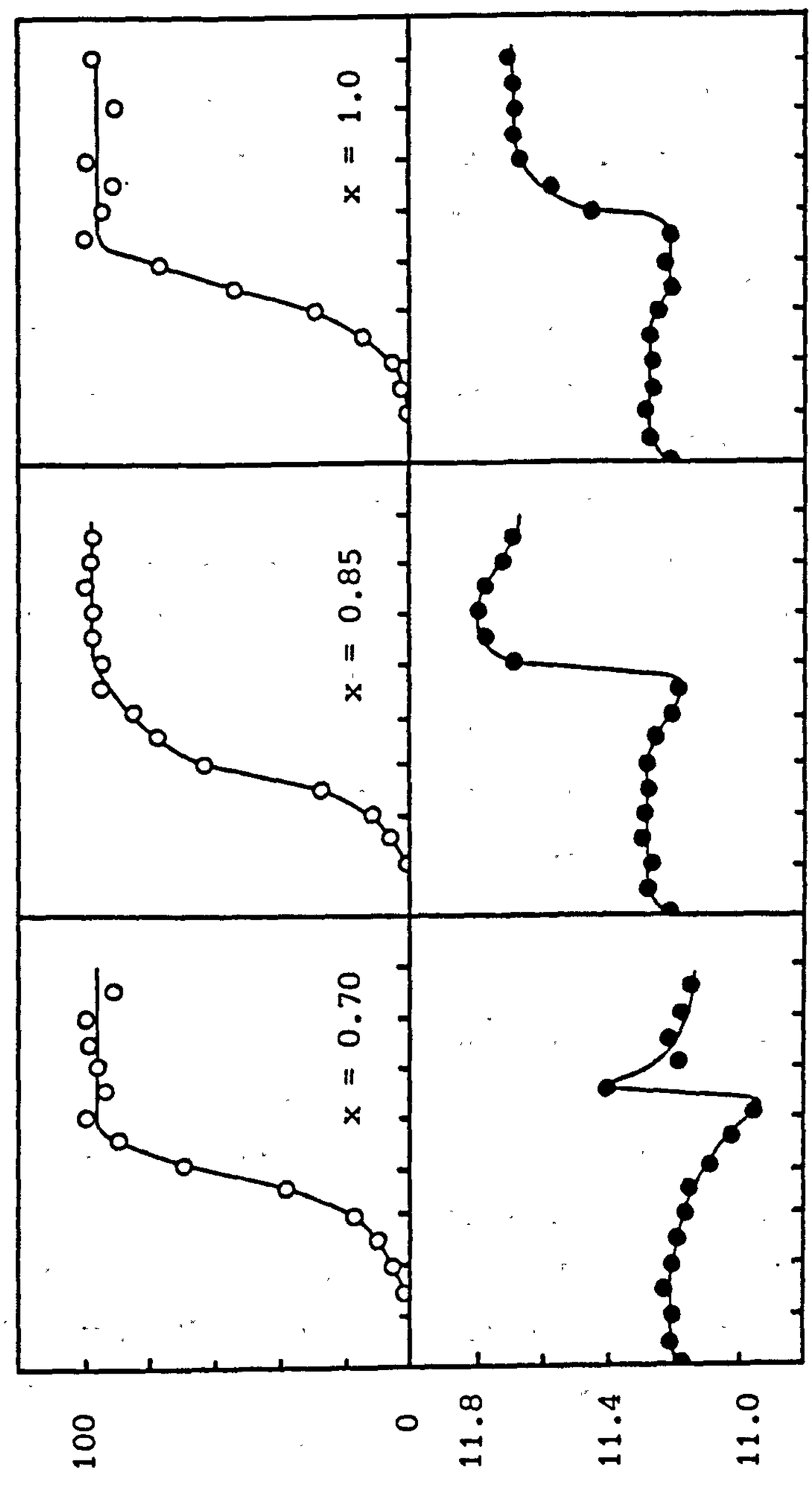

Figure 3.6 % Crystallinity (O) and pH (●) of samples taken during crystallisation of the reaction mixtures with x = 0.70, 0.85 and 1.0.

The pH profiles for the reactions with $0.7 \leqslant x \leqslant 5.0$ in Figures 3.5 and 3.6 all show a sudden increase in pH at near 100% crystallinity. In every case the solubility difference between the crystalline product and the amorphous silica causes this increase. For any given reaction the nature of the pH changes before and after the pH rise are similar; this is possibly an indication that they have the same origin. The higher alkalinity reactions (x = 2.0, 3.5, 5.0; Figure 3.5) show a gradual increase in pH both before and after the sudden pH rise indicative of the initial and final stages of solubility control transfer from the amorphous silica to the silicalite. The overall pH changes during these high alkalinity reactions are largely governed by solubility differences. The low alkalinity reactions (x = 0.70 and 0.85; Figure 3.6) show a pH fall before and after the marked pH rise. These decreases in pH are caused by the removal of base from unbuffered solutions during the crystallisation process. As the reaction alkalinity decreases the overall pH changes during reaction become increasingly dominated by base removal, not solubility transfer. The pH profile for the reaction with x = 1.0 shows regions of near constant pH before and after the major pH rise. This is probably a net result of the effects described for the higher and lower base systems. The results in Figure 3.5 and 3.6 have clearly illustrated that pH and XRD data provide complementary information about the course of these crystallisations.

3.3.4 Crystallisation of the Reaction Mixture with x = 0.50 (Figure 3.7)

The pH remained constant throughout the induc tion period and then steadily decreased until crystallisation was complete. Unlike all the higher alkalinity reactions no pH rise was seen at near 100% crystallinity. The removal of base has a dominant effect on the pH throughout crystallisation in this low alkalinity reaction and this effectively masks any pH rise due to solubility transfer. The final pH of this reaction is probably low due to absorption of some atmospheric CO_2.

3.3.5 Crystallisation of the Reaction Mixture with x = 0.25

This was the only reaction that did not fully crystallise. In order to convert 20 moles of amorphous silica to silicalite with ideal composition 4TPAOH $96SiO_2$ simple calculation shows that 0.42 moles of alkali metal oxide are required. This reaction did not therefore contain sufficient base to crystallise all the silica. The percentage crystallinity estimated from XRD measurements (63%) was close to the maximum (60%) attainable if all the silicalite crystallised with ideal unit cell composition.

The pH remained essentially constant for the first 11 days of the reaction and then started to decrease; a consequence of the removal of base molecules from the system by growing crystals. Throughout crystallisation the pH continued to decrease and after 47 days the reaction was terminated. The final reaction pH was 6.47. Absorption of atmospheric CO_2 affected the latter stages of this reaction. However CO_2 effects were not the cause of the pH decrease during the early stages of crystallisation. An 'organic-free' reaction of molar composition $0.25Na_2O$ $20SiO_2$ $1000H_2O$ carried out under identical conditions showed no significant pH change after 23 days (Figure 3.8). As no quaternary was present and no crystallisation occurred the pH remained constant.

The observed decrease in pH during the reaction with x = 0.25 coupled with the estimated crystallinity of the product show that even in low alkalinity reactions silicalite crystallises with unit cell composition close to 4TPAOH $96SiO_2$. If the incorporated TPA cations were associated with anions other than OH^- the pH would probably not have decreased and the crystallinity of the final product would have been much higher.

Most of the reactions carried out in this study were unaffected by atmospheric CO_2 and only the final stages of the two lowest base content reactions (x = 0.25 and 0.50) were probably perturbed. Reactions at low pH involving unbuffered solutions should ideally be carried out in closed systems.

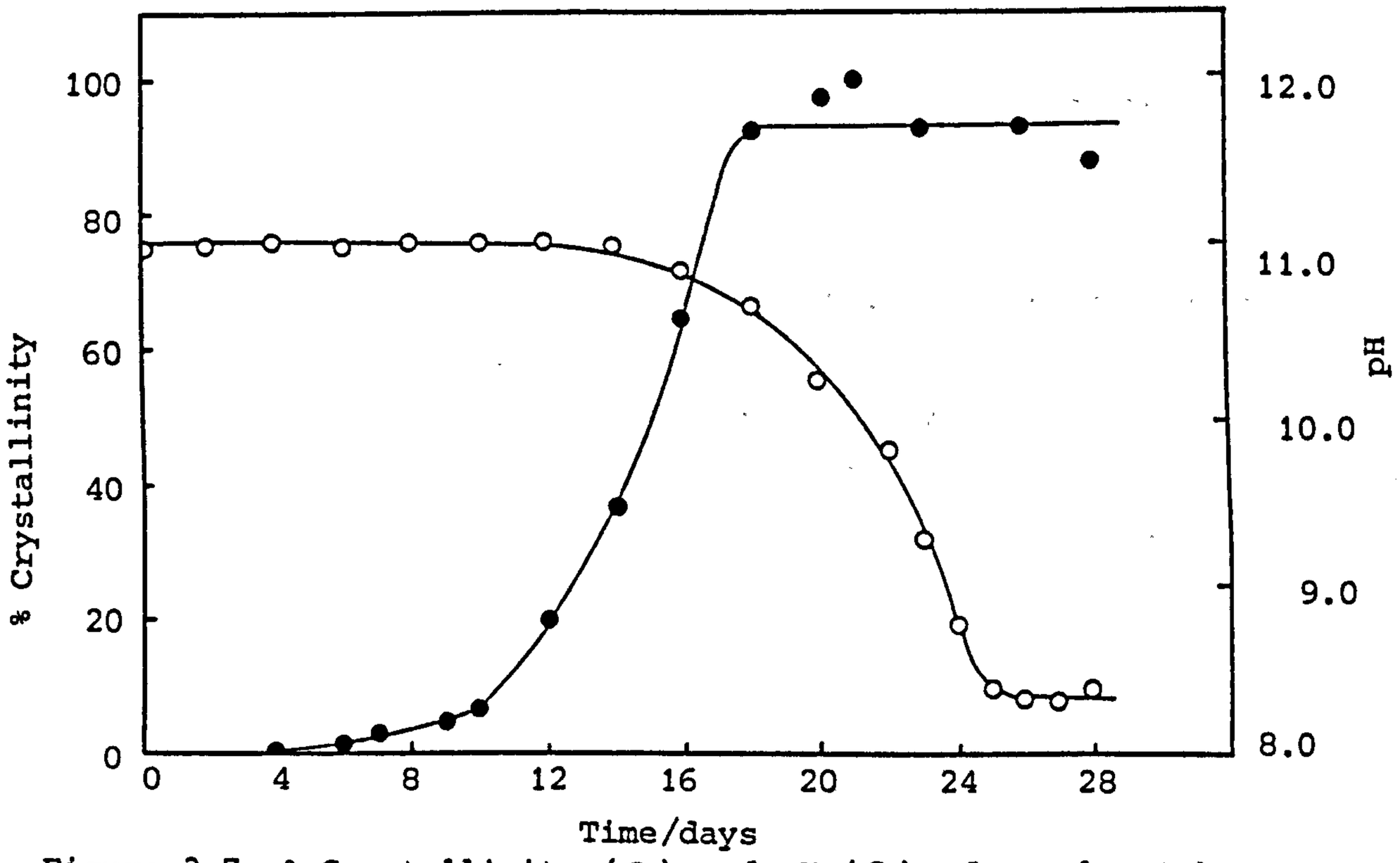

Figure 3.7 % Crystallinity (●) and pH (○) of samples taken during crystallisation of the reaction mixture with x = 0.50

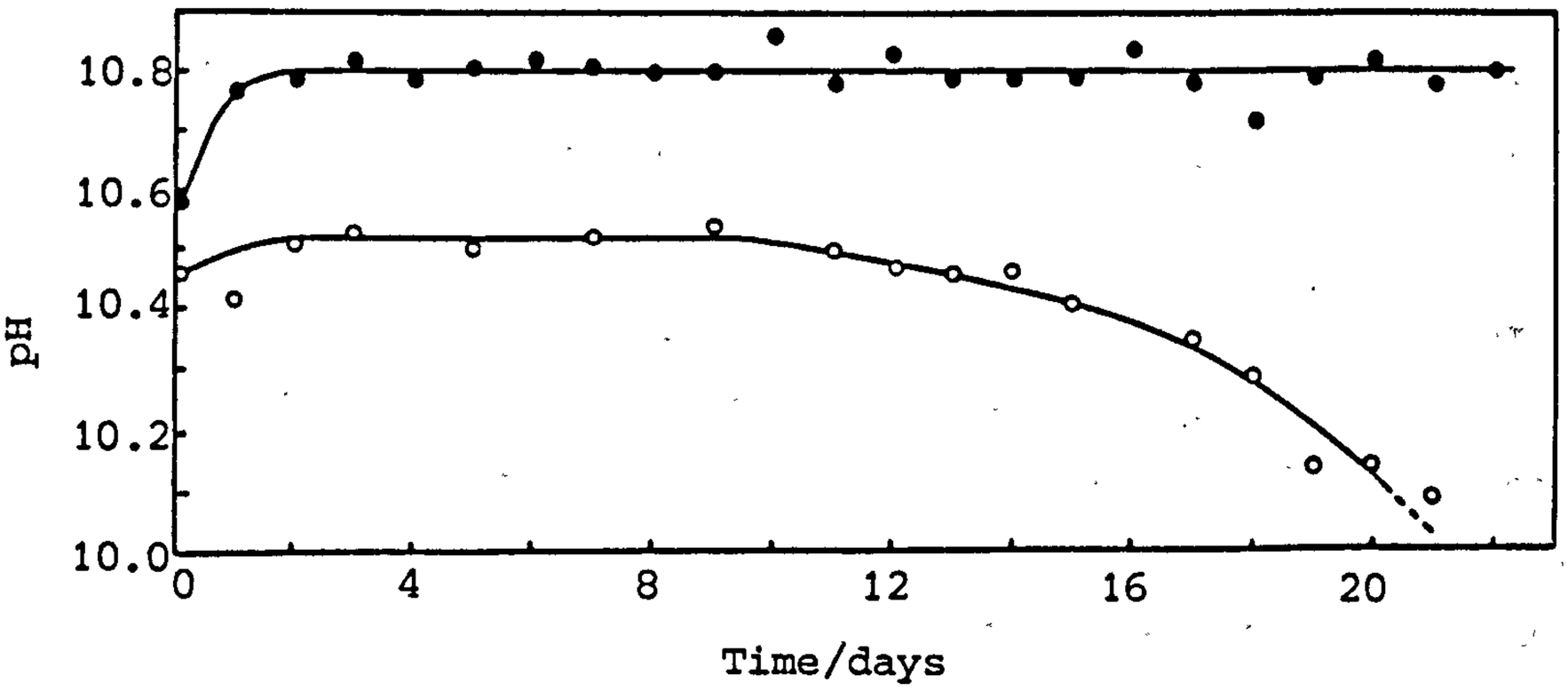

Figure 3.8 pH of samples taken during the early stages of crystallisation of the mixtures $0.25Na_2O$ 2TPABr $20SiO_2$ $1000H_2O$ (○) and $0.25Na_2O$ $20SiO_2$ $1000H_2O$ (●)

3.3.6 Observations from the Samples taken during Crystallisation

In addition to monitoring the reactions by pH, the changing appearance of the samples taken was informative and provided a simple means of following the crystallisations. Photographs of samples from six of the reactions are shown in Figure 3.9. The main points to note and features observed are summarised below:

(1) For the highest base content reaction (x = 6.5) all the amorphous silica initially dissolved. Only a small amount of solid subsequently crystallised. When the alkalinity was decreased less silica initially dissolved. This was particularly noticeable as the alkalinity decreased from 6.5 to 2.0. In converse, it can be assumed that as the alkalinity increased the concentration of silicate species in the solution phase during the induction period and early stages of growth increased. This is usually what is found.

(2) The samples taken after 2 hours were often of different appearance to those taken subsequently. This can clearly be seen for the reactions with x = 5.0 and 3.5. The samples appear to contain relatively little amorphous solid and the measured pH values were low (see also Figures 3.5 to 3.8). This indicates that the solid initially present is more soluble than the gel that subsequently forms - a ripening phenomenon.

(3) The volume of solid decreases as crystallisation occurs. This enabled the crystallisation kinetics to be qualitatively followed.

(4) When virtually all the amorphous solid has been converted to crystalline material, the solid settles leaving a completely clear solution phase. The silicalite controls the species in solution from this moment and this is often the time when a rise in pH occurs. The results and photograph shown in Figure 3.10 for the reaction with x = 0.85 illustrate this.

The points listed above show how simple observations can provide information about the crystallisation process.

x = 6.5	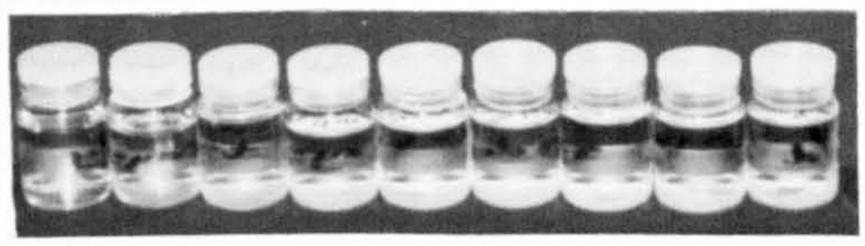 t = 2 h , 1 d , 2 d ....8 d
x = 5.0	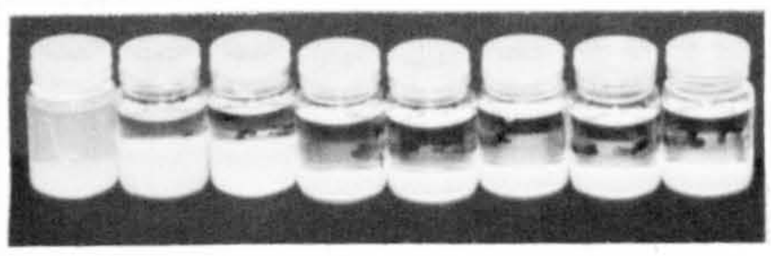 t = 2 h , 1d , 2 d ... ...7 d
x = 3.5	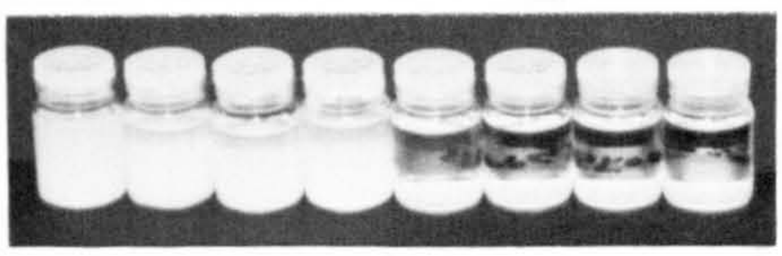 t = 2 h , 1d , 2 d... ...7 d
x = 2.0	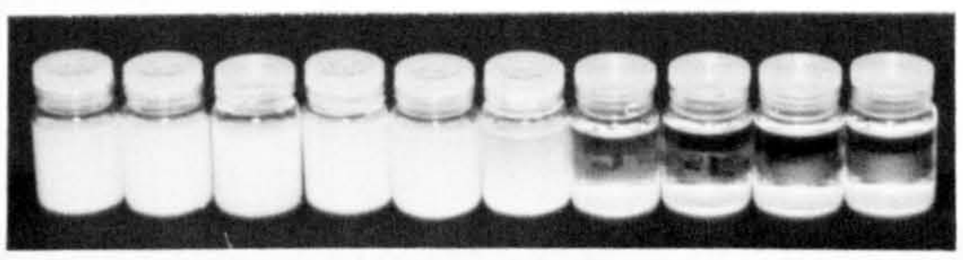 t = 2 h , 1d , 2 d ... ...9 d
x = 1.0	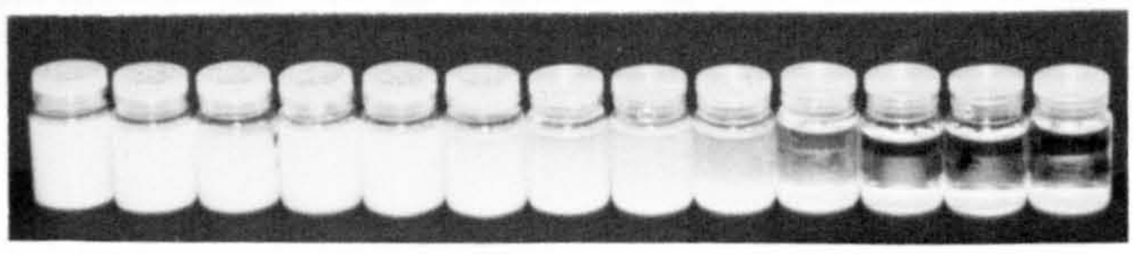 t = 2h , 1d , 2 d ... ...12 d
x = 0.5	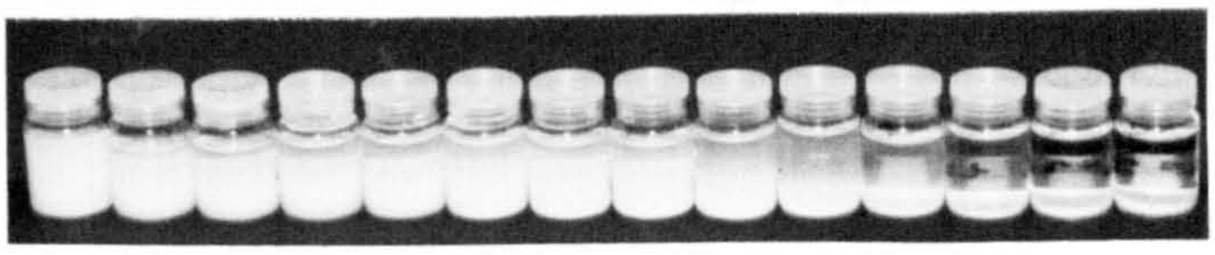 t = 2h , 2d , 4d... ...26 d

Figure 3.9 Crystallisation of silicalite from clear solution (x = 6.5) and from gels as monitored by the visual appearance of samples taken during the reactions

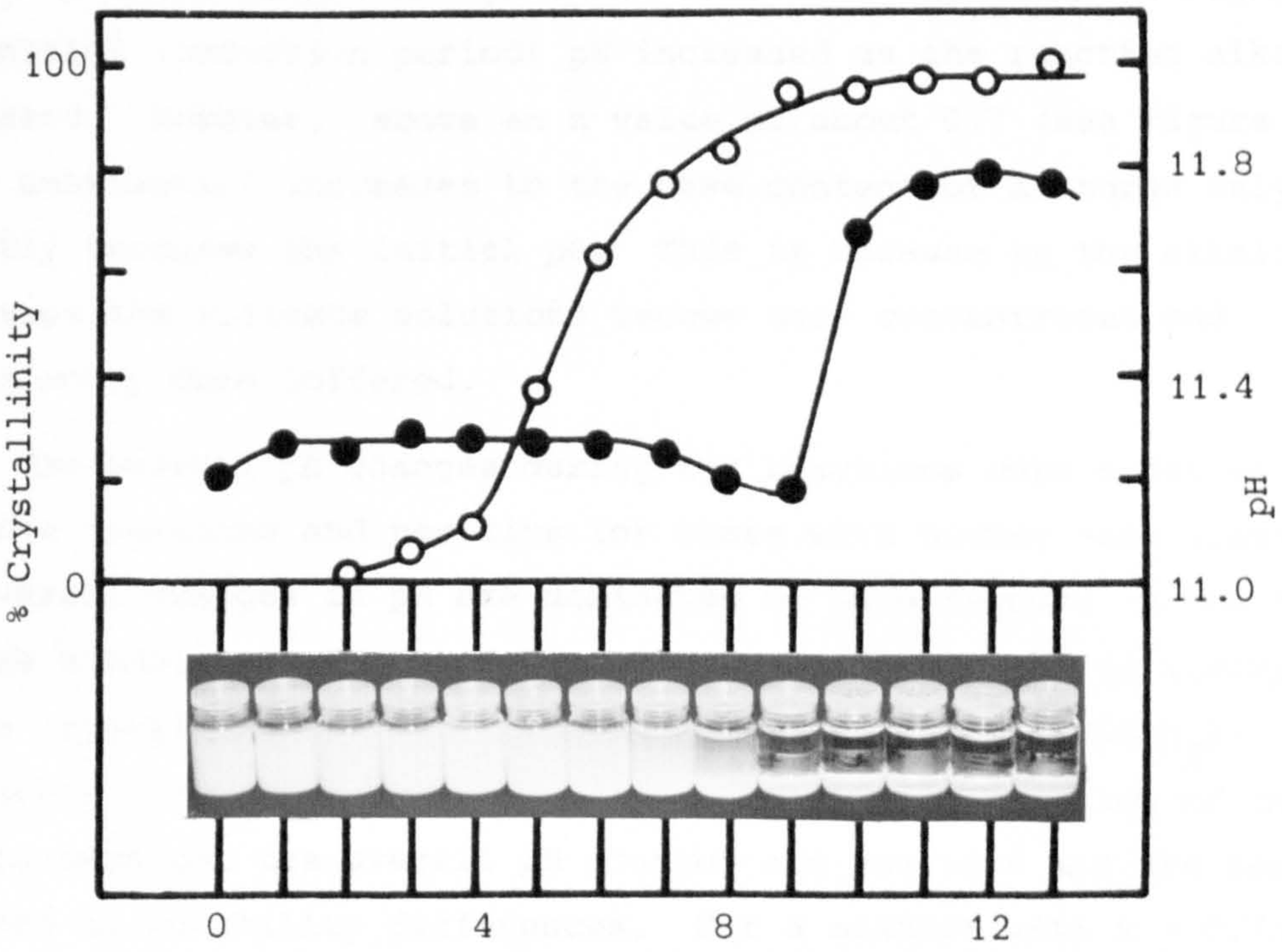

Figure 3.10 Comparison of pH (●) and crystallinity (○) measurements with the appearance of samples taken during crystallisation of the reaction mixture with x = 0.85.

3.3.7 Effects of Alkalinity on the Crystallisations

3.3.7.1 pH and Yields

During each reaction the pH remained essentially constant throughout the induction period and the initial stages of crystal growth. In all but one case (x = 0.25) the pH became near constant again when crystallisation was complete. The overall pH changes during the reactions, the concentration of soluble silica in the mother liquors and the product yields are given in Table 3.2 and shown in Figure 3.11. The initial (induction period) pH increased as the reaction alkalinity increased. However, above an x value of about 0.7 (see Figure 3.11) substantial increases to the base content of mixtures only slightly increase the initial pH. This is because as the alkalinity increases the silicate solutions become more concentrated and consequently more buffered.

The overall pH changes during the reactions were negative for low base reactions and positive for those with higher base contents. The overall changes in pH are dominated by base removal in the former because a substantial amount of the total base present is incorporated in the crystalline products (ideal composition 4TPAOH $96SiO_2$). For higher alkalinity reactions, a much smaller proportion of the total base is used up, the overall pH changes are positive and are largely governed by solubility differences. For a mixture with x = 0.75 the graph (Figure 3.11) predicts that there should be no overall pH change during reaction although the experimental results for the slightly lower alkalinity reaction (x = 0.70, Figure 3.6) show that substantial pH movements do occur during crystallisation even though there is little overall pH change (ΔpH = -0.04). Thus to obtain maximum information from pH measurements it is essential to take samples throughout a reaction.

The interpolated intersection at x = 6.7 represents the highest alkalinity from which crystallisation in the xNa_2O 2TPABr $20SiO_2$ $1000H_2O$ system under the conditions employed is possible. When x > ca. 6.7, conditions are too severe for nucleation and/or growth to occur.

Table 3.2 pH values and yields[a]

Reaction Code	x	pH_i	pH_f	ΔpH	c/mol kg^{-1}	% yield[b]
S1	0.25	10.52	6.47[c]	-3.52	0.002	63[d]
S2	0.50	11.03	8.26[c]	-2.77	0.002	99.8
S3	0.70	11.20	11.16	-0.04	0.015	98.6
S4	0.85	11.27	11.69	0.42	0.024	97.8
S5	1.00	11.27	11.69	0.42	0.036	96.8
S6	2.00	11.40	12.18	0.78	0.190	82.9
S7	3.50	11.48	12.20	0.72	0.364	67.3
S8	5.00	11.48	12.13	0.65	0.558	49.8
S9	6.50	11.60	11.82	0.22	1.022	8.0

[a] x = alkalinity of reaction mixture (mole Na_2O); pH_i and pH_f represent averaged values for the initial and final reaction pH; $\Delta pH = pH_f - pH_i$; c = concentration of soluble silica in mother liquor (molybdate method).

[b] Yields were calculated by subtraction of the silica in the mother liquor from the total silica in the mixture.

[c] Low because of absorption of carbon dioxide during reaction.

[d] From XRD measurements.

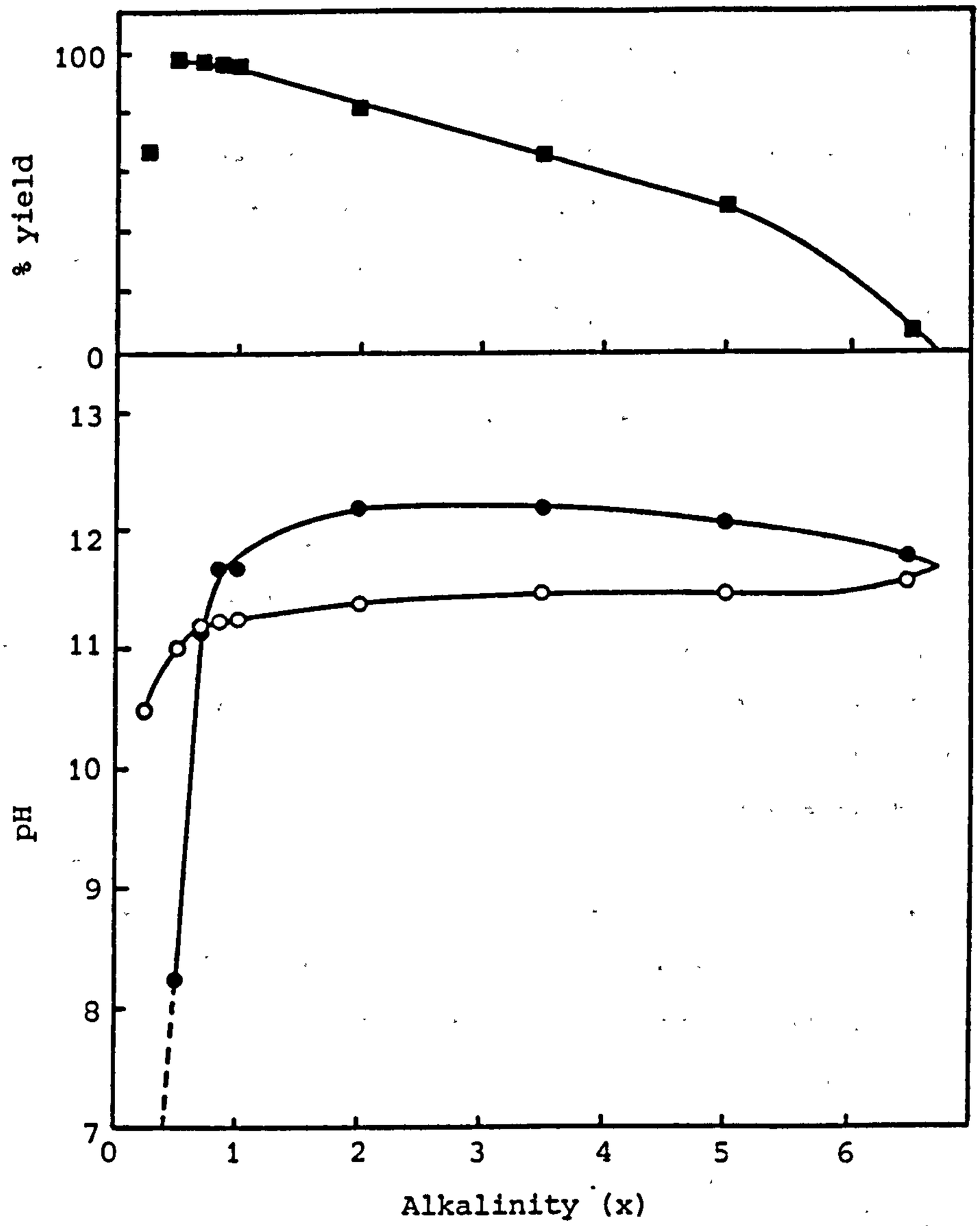

Figure 3.11 Initial pH (○), final pH (●) and product yields (■) as a function of reaction alkalinity

The pH is high and the sodium content of the mixture excessive. This is in good agreement with Grose and Flanigen [1] who found that not more than 6.5 moles of alkali metal oxide per mole of TPA_2O (by definition (see reference [1]) equivalent to 2TPABr) were desirable in synthesis mixtures.

The highest yields were obtained from the lowest base content reactions; the solubility of silicalite is much reduced at low pH. The low yield for the reaction with x = 0.25 was caused by the presence of insufficient base to crystallise all the silica. With increasing base contents and higher final reaction pH more of the silica stays in solution and lower yields were obtained (see Table 3.2). When x > ca. 6.7 no product is obtained. This is in good agreement with the limiting alkalinity estimated from the pH results.

3.3.7.2 Chemical Composition

Thermal gravimetric analysis (TGA) of each as-synthesised product showed a low temperature weight loss due to water desorption and a higher temperature weight loss (T > ca. 350°C) due to decomposition of the organic trapped in the channels. The estimated weight of organic per unit weight of anhydrous silicalite was almost identical in each case. The carbon and nitrogen contents of several of the products obtained from elemental analysis are compared to those estimated from TGA results in Table 3.3. The results are in good agreement and show that virtually all the channel intersections in the silicalite precursors are occupied by tetrapropylammonium species. The crystals therefore all contained close to four TPAOH molecules per unit cell of 96 SiO_2. This composition is empirical and does not represent the chemistry of the as-synthesised solids. Even at ambient temperatures many of the entrapped hydroxide ions are likely to attack the framework through the equilibrium shown below:

$$\underset{\text{TPAOH (solid)}}{\equiv Si-O-Si\equiv} \rightleftharpoons \underset{\text{TPA}^+ \text{ (solid)}}{\equiv Si-O^-} \quad HO-Si\equiv \qquad (3.1)$$

Table 3.3 Organic content of as-synthesised products

Reaction alkalinity (x)	Results from elemental analysis[a] %C	%H	%N	C/N atomic ratio	Results from TGA[a,b] %C	%H	%N	moles TPAOH pe unit cell[c]
0.5	8.98	1.95	0.82	12.8	8.7	1.9	0.9	4.0
1.0	9.00	1.93	0.89	11.8	9.0	2.0	0.9	4.2
2.0	8.57	2.11	0.91	11.0	8.7	2.1	0.9	4.1
3.5	8.14	2.07	0.78	12.2	8.4	2.0	0.8	4.0
5.0	8.31	2.06	0.79	12.3	8.5	2.1	0.8	4.0

[a] Samples were equilibrated with water vapour (a_w = 0.753, 25°C) before analysis

[b] Calculated assuming the weight loss below ∿350°C was due to H_2O, that above ∿350°C was due to TPAOH

[c] Assumes the anhydrous solid is 100% SiO_2

The silicalite precursor is therefore a salt of a strong base and a weak acid; an organosilicate. The framework bears a negative charge as a result of hydroxide ions breaking siloxane bonds. Thermal treatment probably pushes the equilibrium even further to the right and therefore calcination of the precursor leaves pairs of hydroxyl groups at many channel intersections:

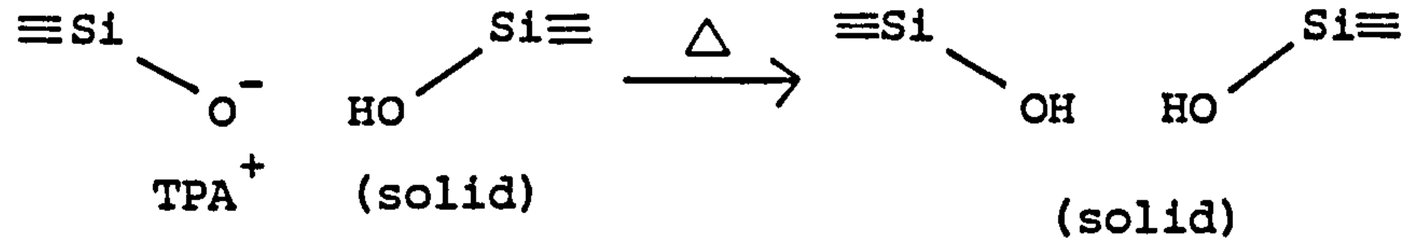

(3.2)

Such silanol groups are effectively lattice defects.

The chemical compositions of the reaction products, obtained by XRF analysis, are shown in Table 3.4. The trace aluminium levels found in the products from reactions with $0.25 \leqslant x \leqslant 2.0$ could not be accurately quantified by the analytical technique and the Si/Al ratios are given purely as an indication of the silicious nature of the frameworks. Significant aluminium levels were found in the products from the high alkalinity reactions ($3.5 \leqslant x \leqslant 6.5$). The low product yields and high impurity levels found indicate that aluminium incorporation is favourable in these high alkalinity reactions. It is likely that some of the aluminium impurities originated from the sodium hydroxide reagent and this in part explains why products from the high alkalinity reactions contained most aluminium. However the amounts found were considerably greater than the levels expected from the specified aluminium content of the sodium hydroxide reagent. Small but significant amounts of iron were also found in three of the products ($x = 0.25, 0.85, 3.5$) probably originating from the stainless steel paddles used to stir the reactions.

Only the product from the lowest alkalinity reaction ($x = 0.25$) did not show a sodium content in considerable excess of that required to balance the negative charge associated with tetrahedral impurity atoms (see Table 3.4). Empirically the incorporated sodium can be designated as the hydroxide (incorporation of sodium as a salt is less likely) and evidence for this is given in the discussion that follows.

Table 3.4 Chemical compositions of the reaction products

Reaction Code	x[a]	Wt %			Mole Ratios	
		Na_2O	Al_2O_3	SiO_2	10^{-3} Si/Al	Na/(Al + Fe)
S1	0.25	0.01	0.04	98.09	2.2	0.1
S2	0.50	0.32	0.04	97.73	2.2	9.9
S3	0.70	0.55	0.03	97.77	3.0	20.4
S4	0.85	0.50	0.03	97.77	3.1	11.9
S5	1.00	0.47	0.02	97.32	4.1	17.5
S6	2.00	1.31	0.03	97.76	2.8	46.3
S7	3.50	1.75	0.08	99.20	1.1	12.6
S8	5.00	1.57	0.07	97.40	1.1	28.5
S9	6.50	1.73	0.26	97.37	0.3	9.8

[a] Reaction alkalinity

The relationship between the sodium content of the reaction mixtures (the alkalinity) and that in the products is shown in Figure 3.12. In all cases only a fraction of the total sodium present is incorporated but the amount taken up increases with alkalinity. Increasing the alkalinity simultaneously increases both the sodium content of the mixture and the mean reaction pH and sodium incorporation may be dependent on both these variables (see later for elaboration). The amount of organic in the precursor crystals was independent of the sodium content (see Table 3.3). In contrast the claimed compositions of the metal organosilicates of Dwyer and Jenkins [6] indicate that metal species displace quaternary species from lattice sites.

The number of sodium atoms per unit cell was found to be linearly dependent on the mole fraction of sodium ions $2x/(2x + 2)$ in the reaction mixture (Figure 3.13). The minimum cation fraction for incorporation of sodium into the molecular sieve (0.24 ± 0.08) was within experimental error of the cation fraction (0.294) required to provide sufficient base to crystallise all the silica as $4TPAOH\ 96SiO_2$. Extrapolation of the straight line to a cation fraction of unity gives the maximum number of sodium ions that could be incorporated per unit cell from these reaction mixtures. The value (4.1 ± 0.5) suggests that the limiting unit cell composition of (Na, TPA)-silicalite in this system is $4NaOH\ 4TPAOH\ 96SiO_2$. Examples of syntheses in the patent literature that were comparable to the crystallisations carried out in this study all gave products containing less than 4 sodium ions per unit cell. The number "4" may have crystallographic implications.

The results obtained are insufficiently detailed for a mechanism for sodium incorporation to be proposed. Under synthesis conditions cations coordinate to the external surfaces of the crystals and as growth occurs could become entrapped in the frameworks. The pK_a of surface silanol groups and the ion-exchange equilibria involving the coordinated cations are likely to be important parameters in the incorporation mechanism.

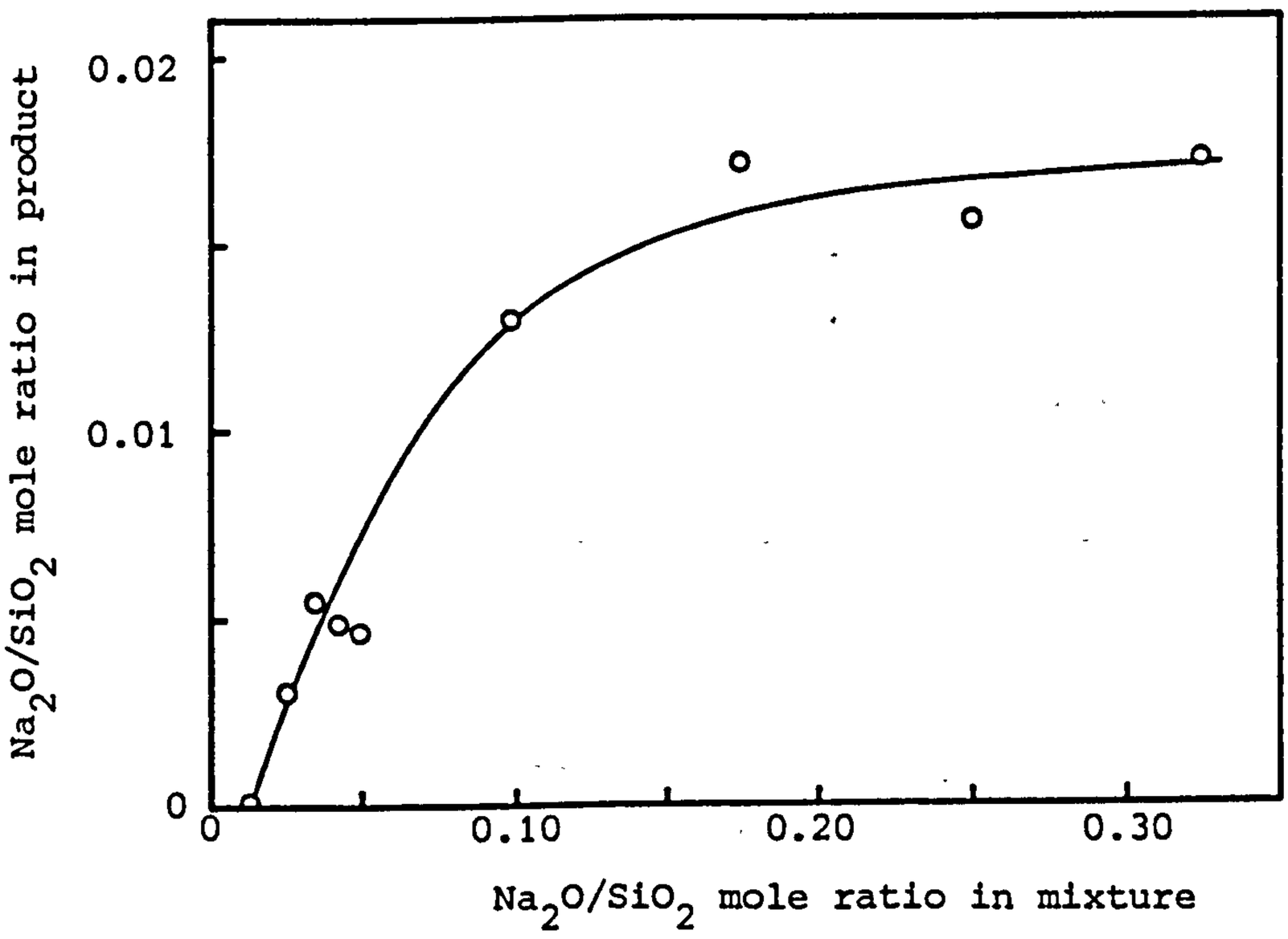

Figure 3.12 Relationship between the sodium content of the reaction mixtures and the sodium content of the crystalline products

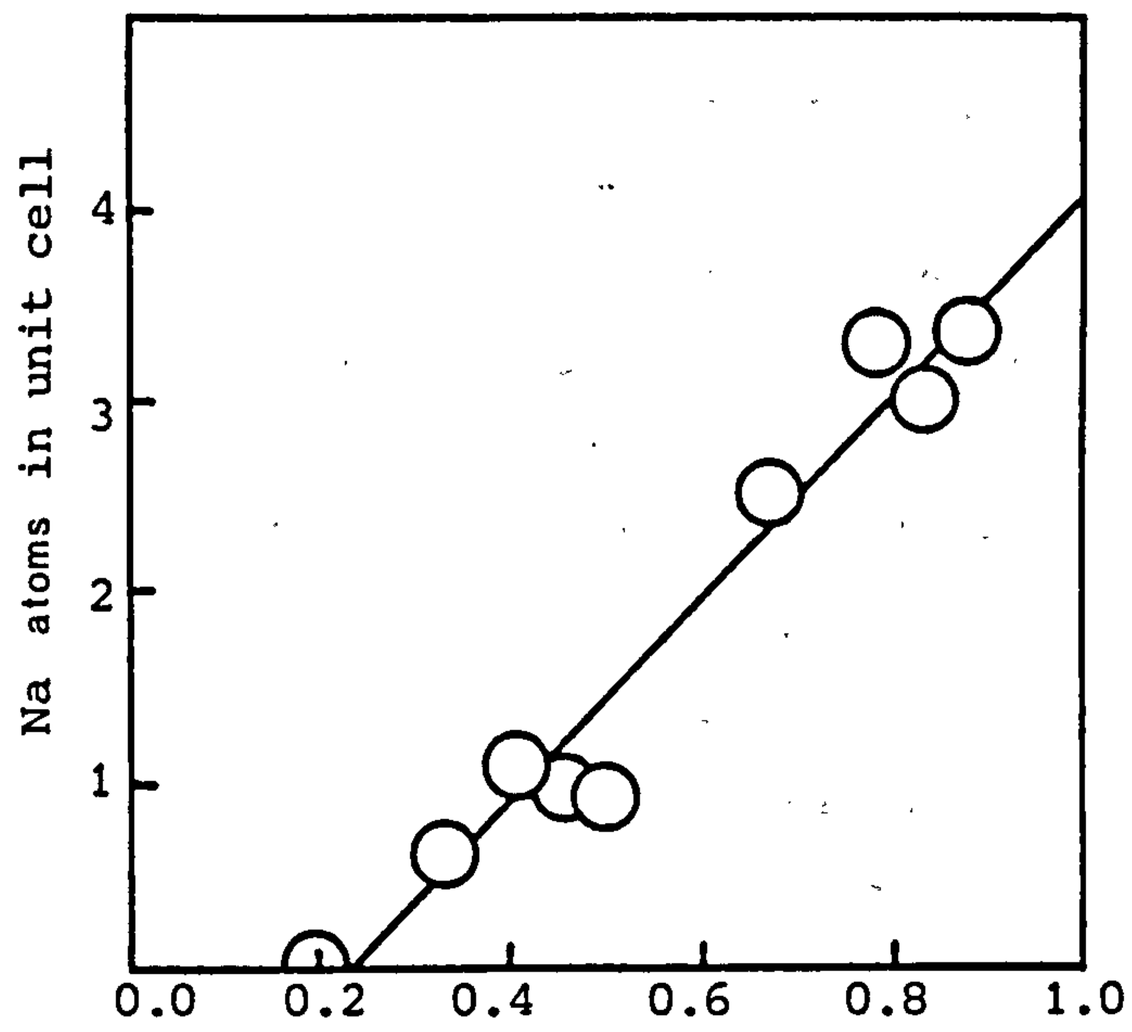

Figure 3.13 Number of atoms of sodium per unit cell as a function of the mole fraction $2x/(2x+2)$ of sodium ions in the reaction mixture.

Empirically the incorporated sodium is present as sodium hydroxide. Any sodium hydroxide molecules inside the molecular sieve are likely to coordinate to the framework through an equilibrium similar to that already described for TPAOH (equation (3.1)):

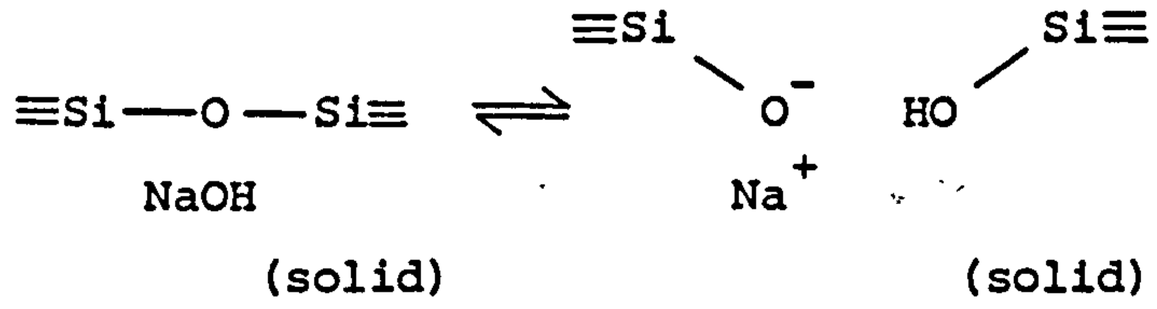

(3.3)

The anionic charge on the framework of the silicalite precursors is increased by sodium incorporation. During calcination to remove the organic most of the free base is likely to attack the framework.

Sodium ions coordinated to the lattice should be exchangeable, just as are cations in aluminium-free layer silicates, e.g. makatite [21]. After calcination it has been shown [1] that treatments with either aqueous HCl or NaCl solutions effectively remove the incorporated sodium. The acid treatment removes sodium by cation exchange as shown in Scheme I overleaf. As most of the incorporated sodium is believed to be attached to the framework (A), the acid treatment leaves the lattice defective with intracrystalline silanol groups (B). Clearly the positions of the equilibria that exist between (A) and (C) and between (B) and (D) are important in this respect. The successful removal of sodium by acid treatment shows that these materials are exchangers as was inferred by Dwyer and Jenkins [6]. The resultant silanol groups are only weakly acidic and after acid treatment re-exchange by simple means is impossible. By comparisch acid exchange in zeolites is usually readily reversible.

The salt treatment used to remove incorporated sodium probably operates by an anion exchange mechanism as outlined in Scheme II. The removal mechanism only involves the free base and no silanol groups are produced at the sites originally occupied by the sodium. Salt treatments would be unlikely to effect removal of sodium if the incorporated sodium itself was present as a salt, further evidence that the sodium is present as the hydroxide. As electrolyte occlusion in a hydrophobic lattice is thermodynamically unfavourable, salt molecules formed in the pores as a result of the anion exchange

Removal of sodium (alkali metal) from silicalite

Scheme I (Acid Treatment)

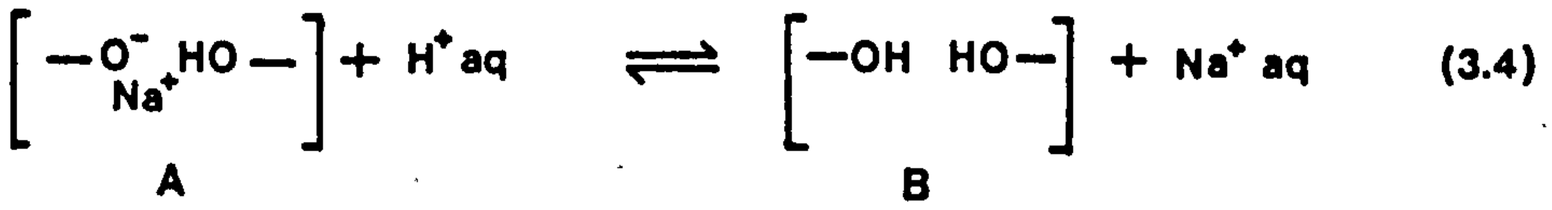

(3.4)

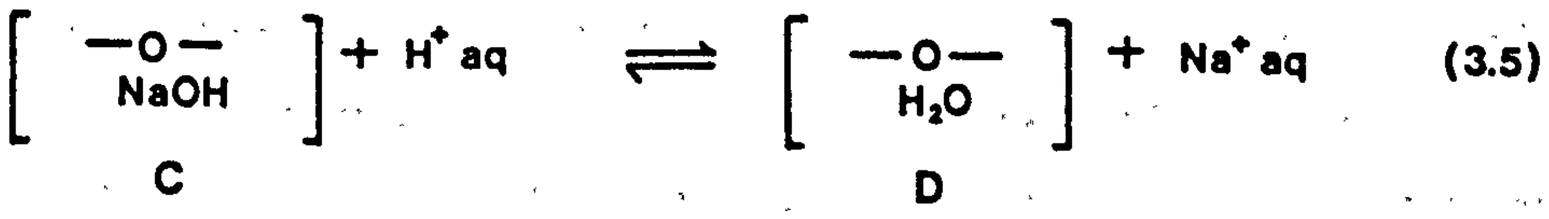

(3.5)

Scheme II (Salt Treatment e.g. NaCl)

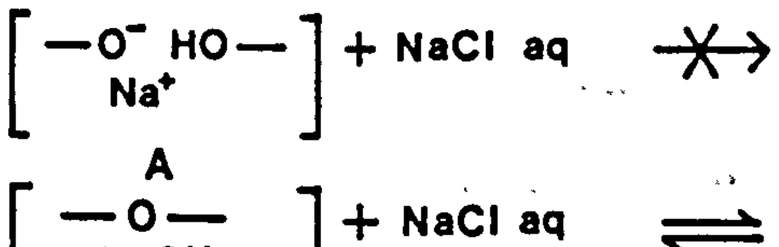

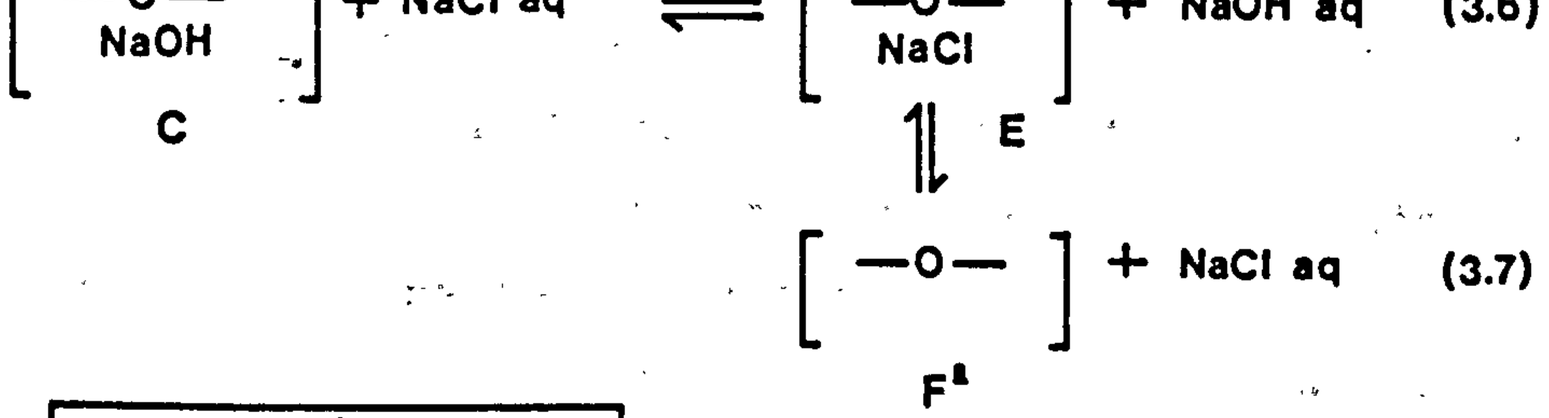

(3.6)

(3.7)

Scheme III (Hydrolysis)

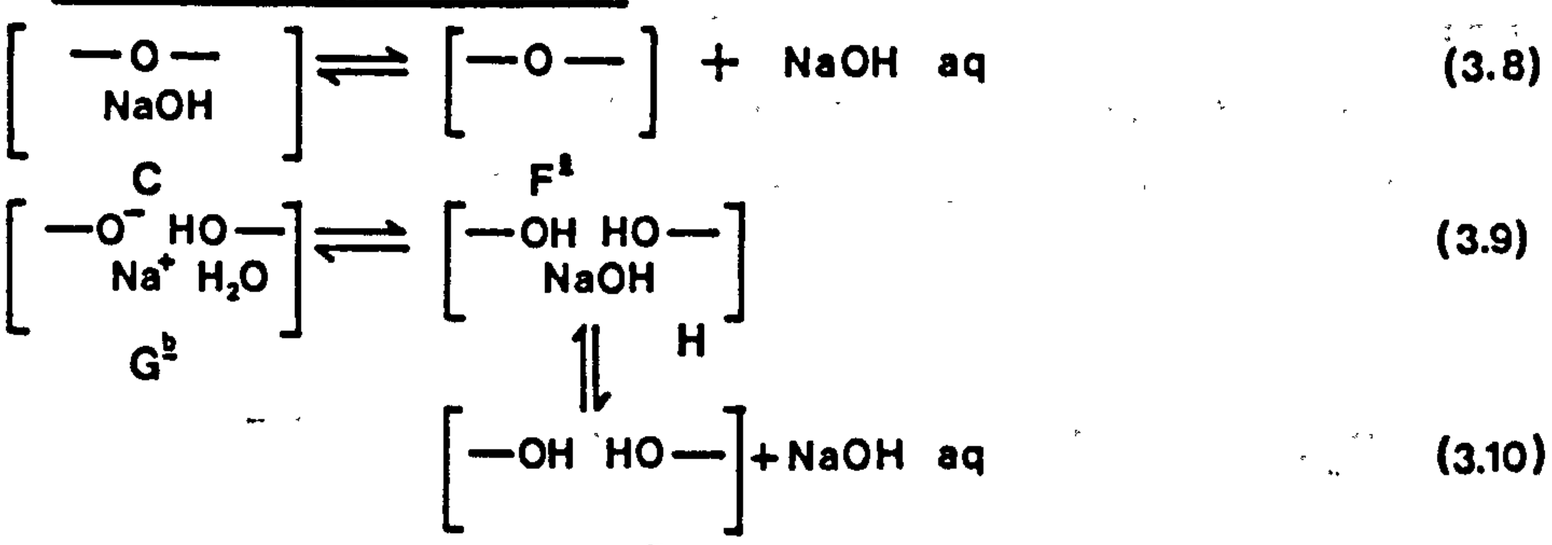

(3.8)

(3.9)

(3.10)

---

[a] Effectively the same as D.

[b] Effectively the same as A.

escape into the solution phase. For similar reasons free sodium hydroxide or sodium hydroxide molecules formed by hydrolysis can be expelled from the lattice as outlined in Scheme III. This causes the pH to rise when calcined products are stirred in water. However only a fraction of the incorporated sodium is readily removed by this hydrolysis mechanism. This may be because the sodium ions are strongly coordinated to the framework or because the sodium occupies different sites in the lattice. It is possible that some sites are in voids outwith the main channel system rendering both hydrolysis and escape of NaOH difficult.

Silicalite is a hydrophobic sorbent and before use it is desirable to remove any sodium from the lattice. The aforementioned equilibria show the importance of the preparative method used to remove the metal component. The silanol groups produced when sodium is removed by cation exchange and hydrolysis are effectively lattice defects similar to defects produced when tetrapropylammonium species are removed during calcination. When salt treatments are used to remove sodium the lattice remains far more intact. However a limited amount of cation hydrolysis is still likely to occur and give a lattice with extra silanol groups. These additional silanol groups give the materials enhanced hydrophilic character and this could significantly affect their adsorption properties. Although thermal treatment may partly anneal the lattice, it is unlikely that silicalite can be rendered free of all internal silanol groups.

The analytical data from this work has been compared with data from several patents. These patents all describe the synthesis of ZSM-5 type materials from aluminium-free, alkali metal containing reaction mixtures.

U.S. Patent 3,941,871 (Dwyer and Jenkins, Mobil Oil Corporation, 1976)
Reference [6]

U.S. Patent 4,061,724 (Grose and Flanigen, Union Carbide Corporation, 1977)
Reference [1]

Data from these patents is shown in Table 3.5 and plotted in Figure 3.14. Reaction mixtures were prepared using sodium hydroxide as the mineraliser and tetrapropylammonium bromide as the source of

quaternary cations. These mixtures differed in composition and the crystallisations were carried out at varied temperatures. Even so, agreement with the results obtained in this work is good. The enhanced sodium content of the product from one of the reactions given in Table 3.5 is probably due to the presence of additional sodium salts in the reaction mixture. All the products contained less than 4 moles of sodium per unit cell, i.e. $Na_2O/SiO_2 < 0.021$.

European Patent Application 93,519 (Kuehl, Mobil Oil Corporation, 1983)
Reference [7]

Data taken from this patent is shown in Figure 3.15. Buffering agents were used to control the pH during these reactions and many mixtures contained high concentrations of sodium species. Even so, the data shows that all products from low pH reactions contained little sodium. At higher pH more sodium was found in the products. From the analytical data in the patent it was calculated that ~1.4 wt% Na was the equivalent of four sodium ions per unit cell. Extrapolation of the curve in Figure 3.15 to this value suggests that crystallisation would have to be effected at high pH for a product to contain this amount of sodium. Three examples from the patent clearly show how pH can affect alkali metal incorporation. The relevant data is given in Table 3.6. The amount of tartaric acid added to mixtures was the only compositional variable and all reaction conditions were identical. The mole fraction of sodium in each mixture was the same. The results show that as the reaction pH decreased there was a reduction in the amount of sodium found in the product.

U.S. Patent 4,073,865 (Flanigen and Patton, Union Carbide Corporation, 1978)
Reference [9]

U.K. Patent Application 2,084,552 (Saleh, Norton Company, 1982)
Reference [10]

Fluoride silicalite (Flanigen and Patton) and another modified silicalite-like material (Saleh) were often crystallised at low pH in alkali metal rich systems. When synthesised under these conditions only small amounts of metal were incorporated in the products.

Table 3.5 Literature data relating to crystallisation of aluminium-free ZSM-5/silicalite

	Na_2O/SiO_2 in mixture[a,b]	Na_2O/SiO_2 in product[a]	Reaction temperature/°C
U.S. Patent 3,941,871 (1976)			
Example 2	0.13	0.011	150
Example 4	0.25[c]	0.018	100
Example 6	0.085[c]	0.020	100
U.S. Patent 4,061,724 (1977)			
Example 1	0.082	0.011	200
Example 2	0.081	0.011	200
Example 3	0.16[d]	0.018[d]	100
Example 6[e]	0.081	0.007	200

[a] Denotes molar ratios

[b] Refers to free alkali content

[c] Sodium salts were additionally present

[d] Refers to K_2O/SiO_2 ratios

[e] $(C_4H_9)_4PCl$ used as the source of quaternary cations. All other mixtures referred to in the table contained TPABr

Table 3.6 Data taken from the literature [7], showing the effect of reaction pH on the alkali metal content of 'aluminium free' ZSM-5

Data source: E.P.A. 93,519 (1983)

Molar reaction mixture composition	Example 6	Example 7	Example 8
NaOH	3.05	3.05	3.05
NH_4OH	4.2	4.2	4.2
$(CHOH.COOH)_2$	1.58	1.05	0.7
TPABr	1	1	1
SiO_2	19.8-19.9	19.8-19.9	19.8-19.9
H_2O	286	286	286
Initial pH	10.4	11.7	12.6
Final pH	10.13	10.67	11.06
ΔpH	-0.27	-1.03	-1.54
Product	ZSM-5	ZSM-5	ZSM-5 (+ quartz)
Product Composition			
wt % SiO_2	86.5	84.4	86.1
wt % Na	0.03	0.35	0.59
SiO_2/Al_2O_3 (mole ratio)	3420	3188	3114

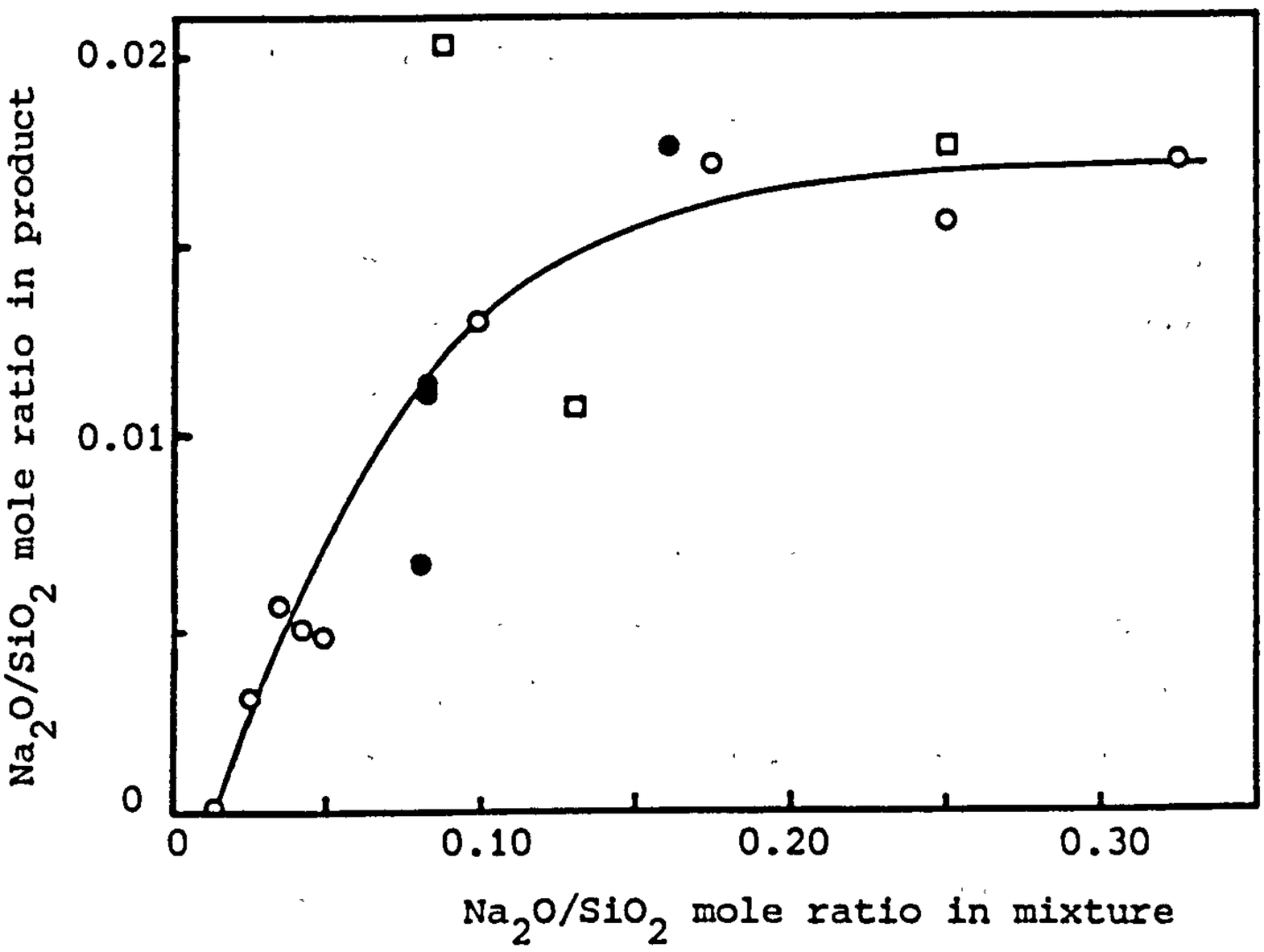

Figure 3.14 Relationship between the sodium content of reaction mixtures and the sodium content of crystalline products. Data taken from ref. [1], (●); ref. [6], (□); this work (○).

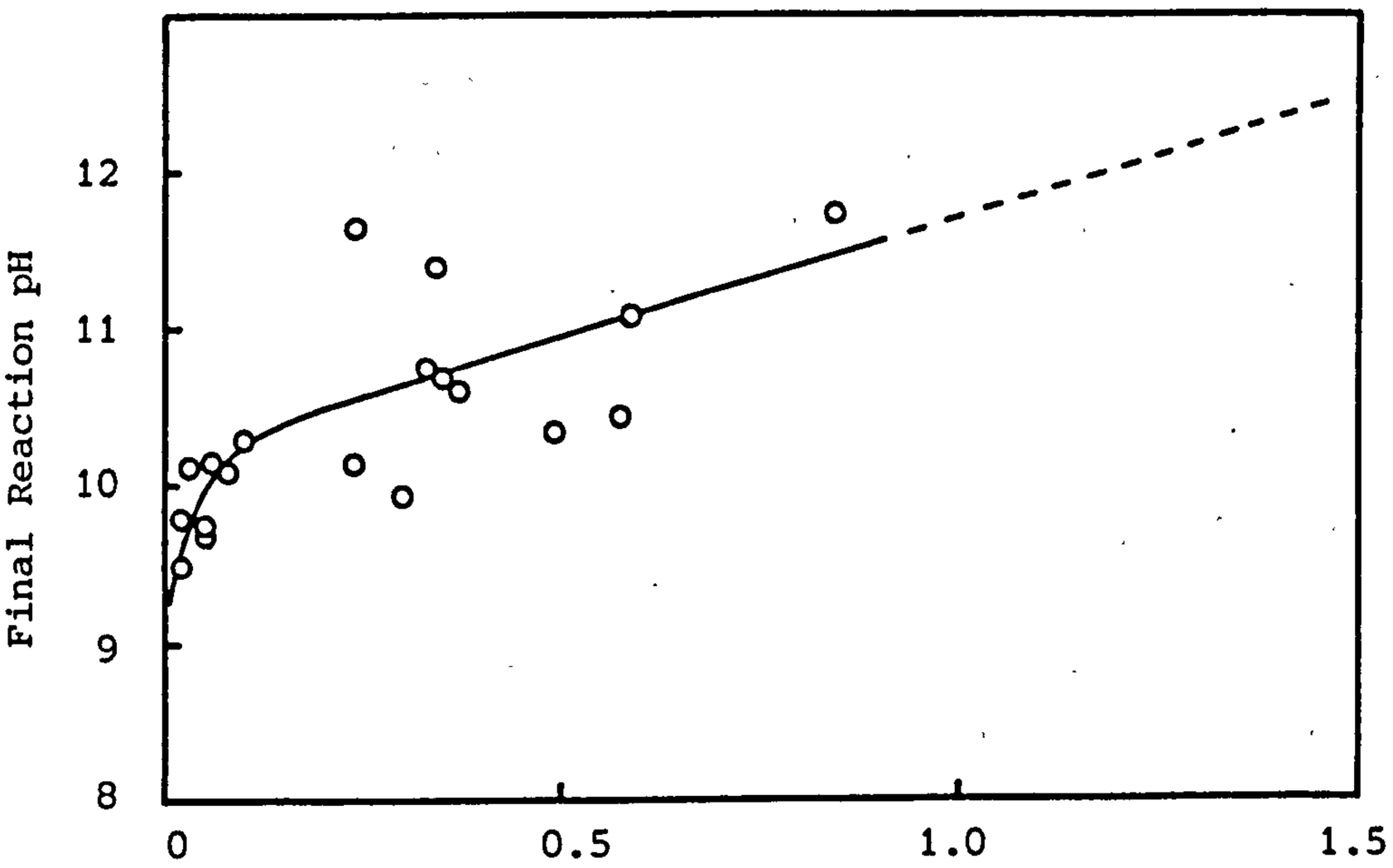

Figure 3.15 Relationship between the final reaction pH and the sodium content of 'aluminium-free' ZSM-5. Data taken from ref. [7].

These results from the literature confirm that pH is an important parameter controlling metal incorporation. Alkali metals are not taken up to any extent at low pH even in systems rich in alkali metal salts. This is good evidence that metals are not occluded as salts during synthesis. The fact that metal incorporation is pH dependent further suggests that the metal is present as the hydroxide. Both TPA and sodium species in the silicalite precursor can therefore be empirically designated as base molecules.

3.3.7.3 Solubility of Silicalite

Silicalite is less soluble than the amorphous silica from which it is crystallised and most of the pH results presented reflect this solubili difference by showing a marked pH rise at some stage during the crystallisation (Figures 3.5 and 3.6). After crystallisation is complete an equilibrium is established between the silicalite crystals and species in the solution phase. The final pH values in Figure 3.11 show an unexpected trend; the two highest alkalinity reactions (x = 5.0 and 6.5) give lower final pH values than those of immediately lower alkalinity (x = 2.0 and 3.5). Silicalite crystallised from high alkalinity reactions (e.g. x = 5.0 and 6.5) is believed to have increased solubility (see Table 3.2) due to the presence of large amounts of sodium in the lattice and high concentrations of sodium species in the solution phase. The outer surfaces of the crystals may be rich in sodium and have some amorphous character leading to increased solubility. This increased solubility causes the final pH values to be relatively low. At very high alkalinity silicalite is totally soluble and no crystallisation occurs.

During each reaction the mole fraction of sodium ions ($2x/2x + 2$) in the solution phase increased during crystallisation (Figure 3.16). This was because the TPA ions were concentrated in the products. For the higher alkalinity reactions ($2.0 < x \leq 5.0$) the increase in the solution phase sodium mole fraction coupled with the substantial pH increases that occurred during the crystallisations (Figure 3.5) is likely to have given crystals whose outer shells are enriched in sodium. Increases in pH and sodium mole fraction should both favour increased sodium incorporation and the distribution of the sodium in many of these products is therefore likely to be heterogeneous.

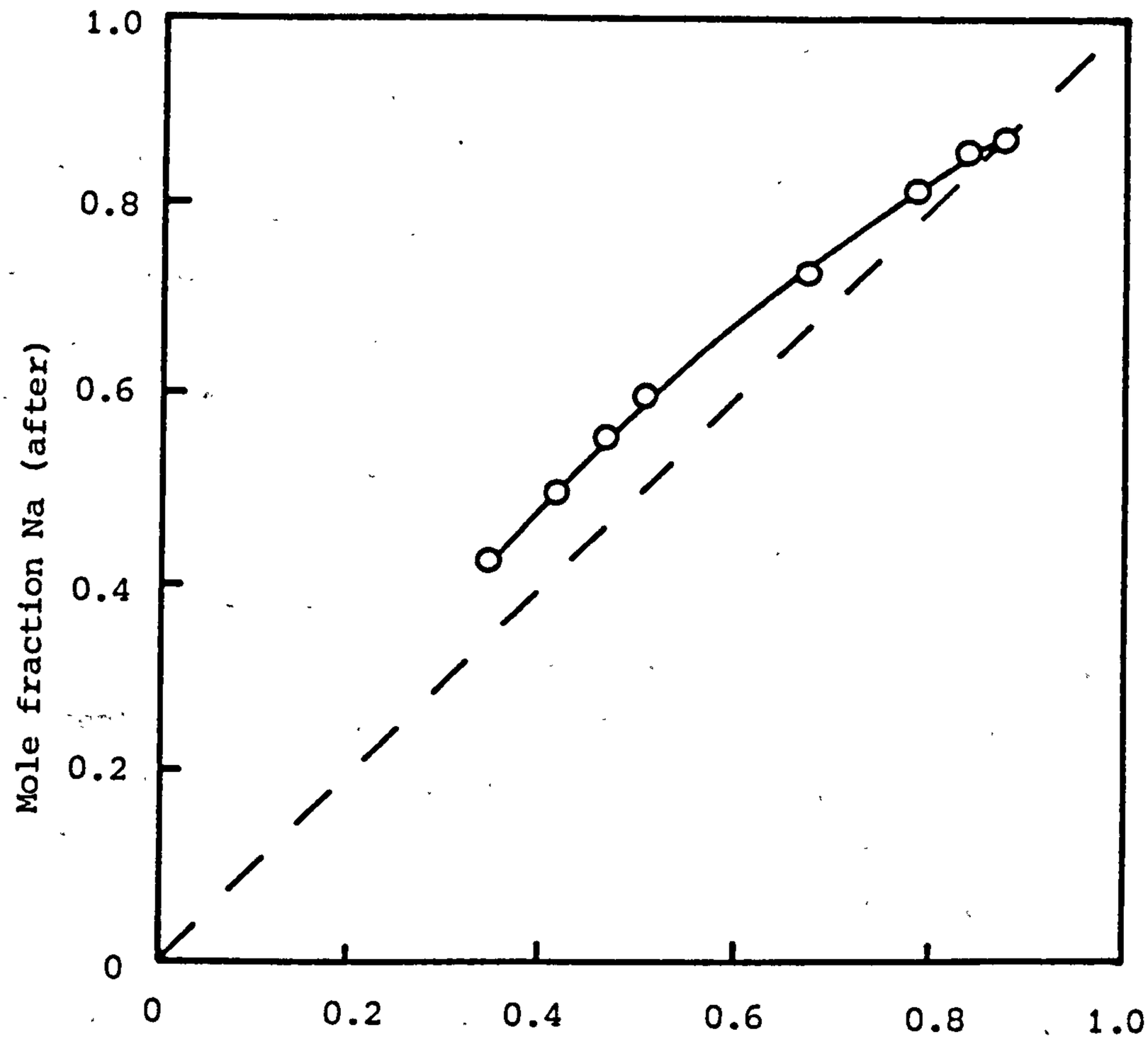

Figure 3.16 A comparison of the mole fraction of sodium ions in the solution phase before and after crystallisation. Mole fractions were calculated assuming no cations were coordinated to the silica surfaces. The mole fraction before crystallisation is given by $2x/(2x+2)$ where x is the reaction alkalinity. That after crystallisation was calculated by difference knowing the cation content of the products (Na^+ and TPA^+) and the product yields. All products were assumed to contain 4 moles TPA^+ per unit cell of $96SiO_2$.

3.3.7.4 Crystal Size and Morphology

The growth curves obtained from XRD (Figures 3.5-3.7) show that two distinct stages are involved in the crystallisations. Firstly, there is an induction period when nuclei are formed and then there is a period of growth during which the nuclei grow into crystals. The conditions prevailing during the induction period dictate the number of nuclei that form. As nuclei presumably 'assemble' from soluble silicate species, more nuclei form in solutions that contain high concentrations of silicate ions; the number of nuclei that form therefore increases as the alkalinity and initial pH of mixtures increases.

Growth occurred predominantly on primary nuclei and little secondary nucleation took place; this was indicated by the uniformly sized crystals that each reaction produced. Scanning electron micrographs of the crystals are shown in Figure 3.17. Twinning, though to different extents, was seen in all cases. The crystal size decreased as the alkalinity increased (Figure 3.18) because of the increasing numbers of nuclei that formed. Falth and Hakansson [11] found that alkalinity affected crystal size similarly. Crystals from the reaction with x = 6.5 were intergrown and additionally were unexpectedly large. When the alkalinity is excessive nucleation is inhibited and all (if any) growth occurs on what few nuclei there are (all crystallisation from the mixture with x = 6.5 occurred from clear solution and an alternative explanation for the large crystals could be that fewer nuclei form in the absence of a solid phase). The length/width ratio of the crystals increased as the alkalinity decreased (Figure 3.19); as the crystals get larger they also become more elongated. The graph suggests that when the reaction pH (alkalinity) is very low rod and needle shaped crystals should form. Kuehl [7] has shown this to be the case.

3.3.7.5 Reaction Kinetics

This synthesis study was primarily aimed at investigating thermodynamic aspects of silicalite crystallisation and the previous sections (3.3.7.1 to 3.3.7.4) have discussed alkalinity effects which are principally thermodynamic in origin. A limited amount of information about the crystallisation kinetics has been obtained from:

Figure 3.17 (see following three pages)

Scanning electron micrographs of the products from reactions S1 - S9.

S1

S2

S3

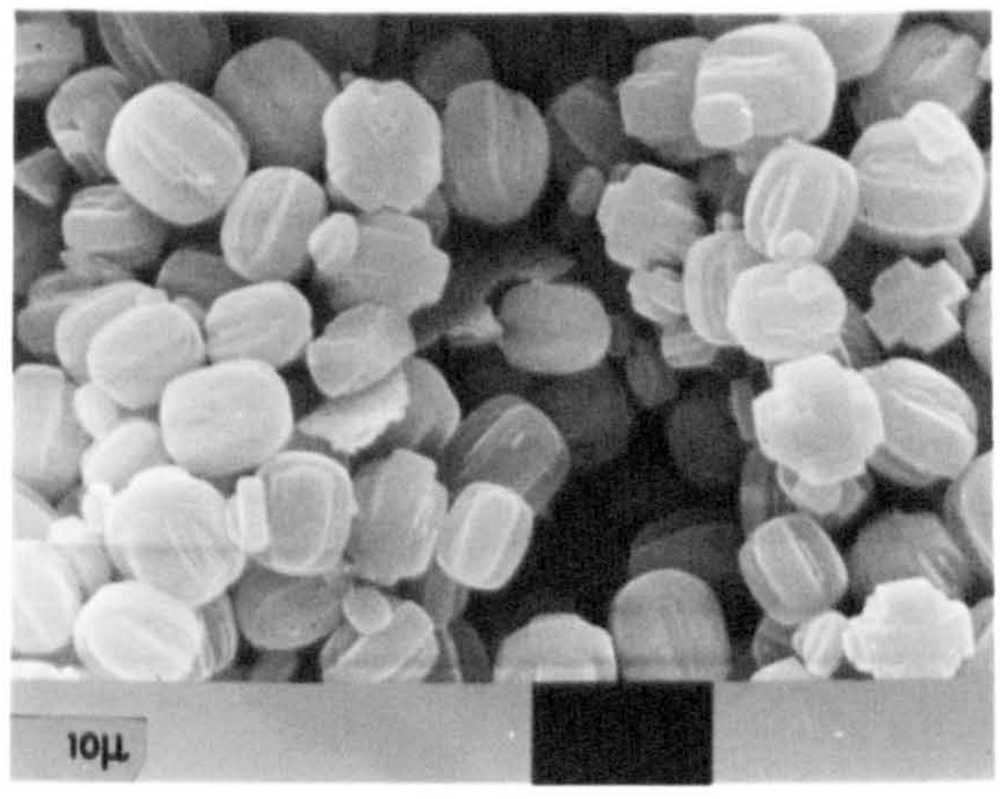

S4

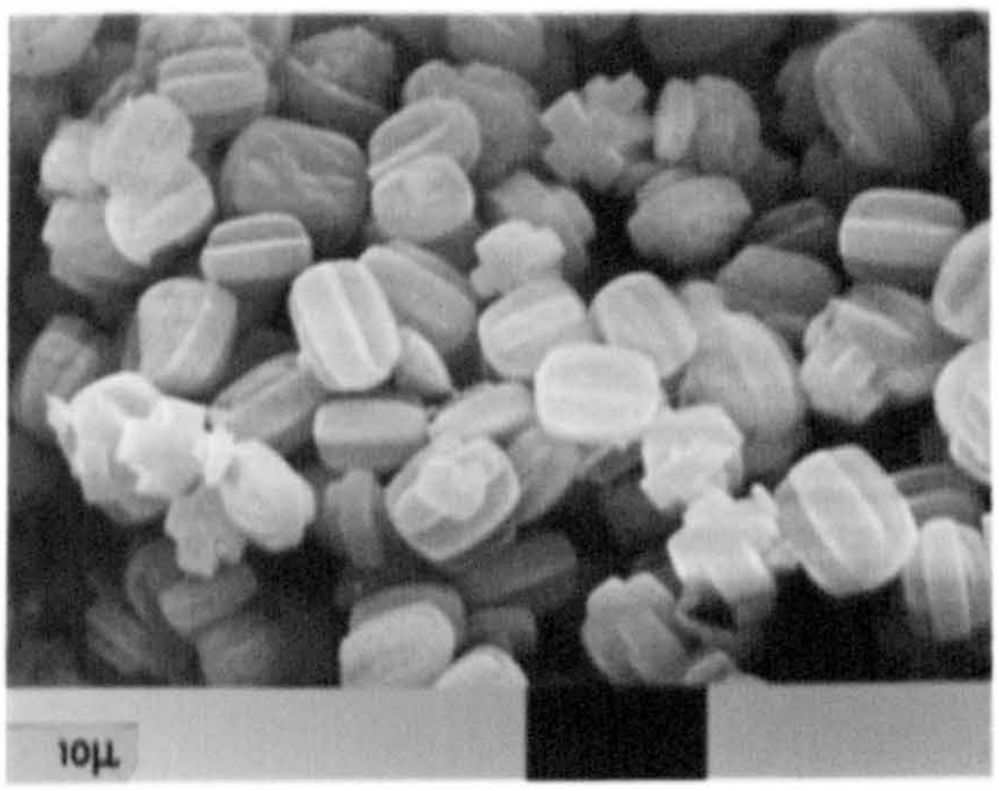

S5

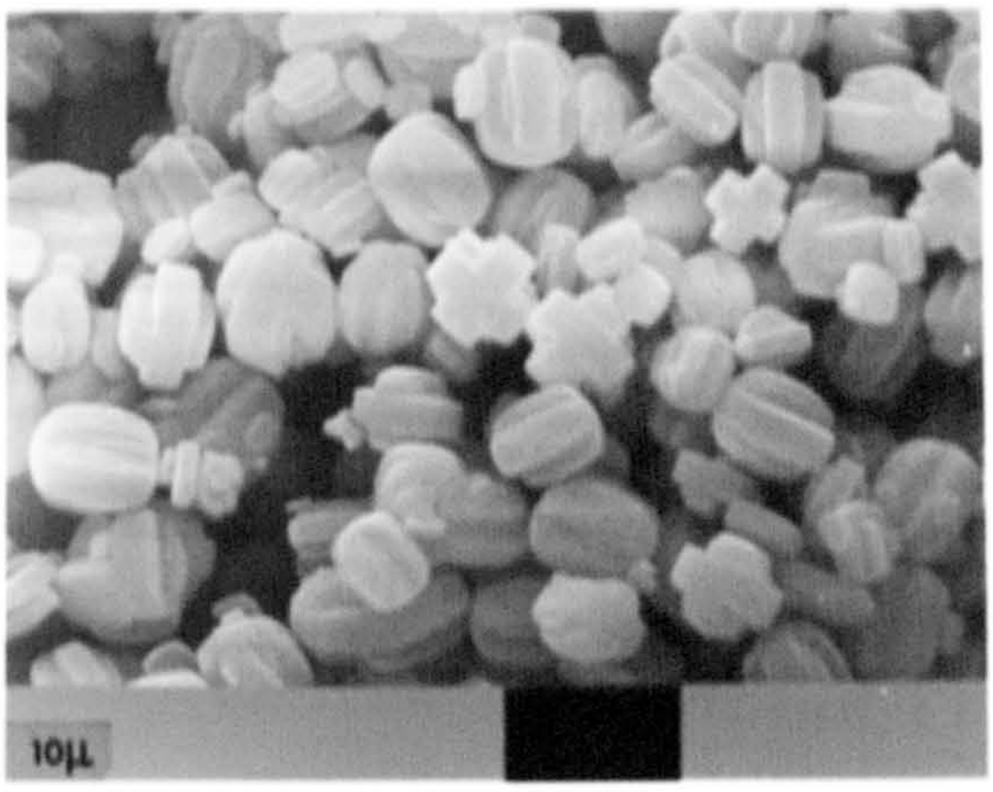

S6

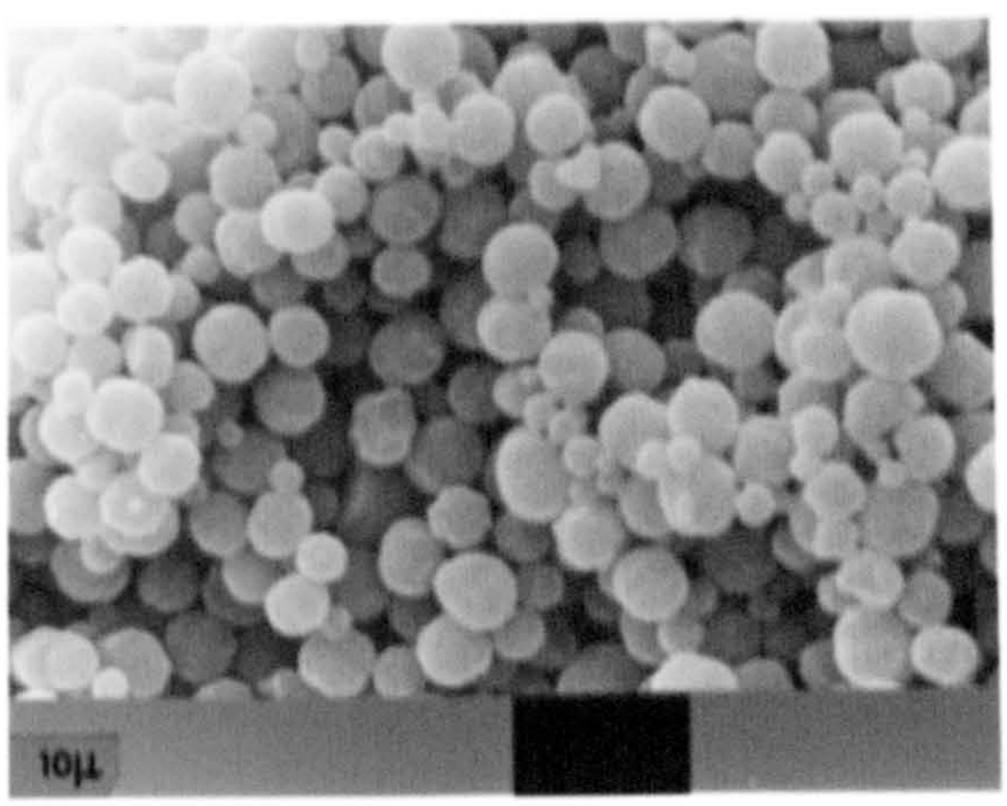

S7

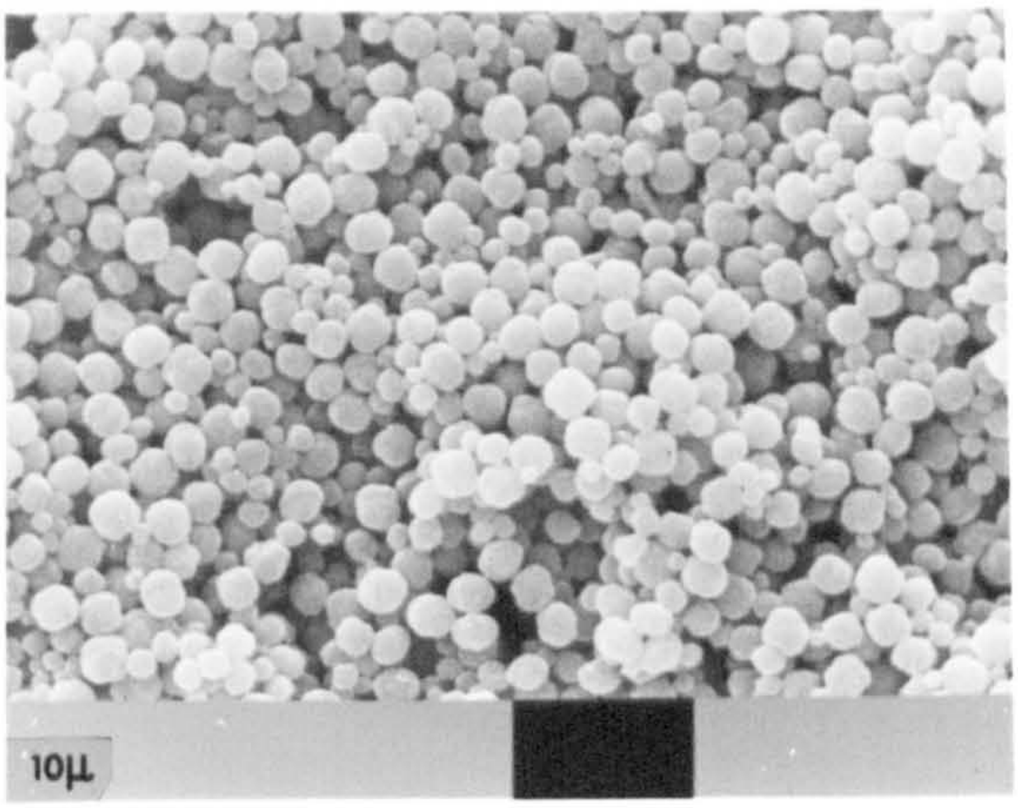

S8

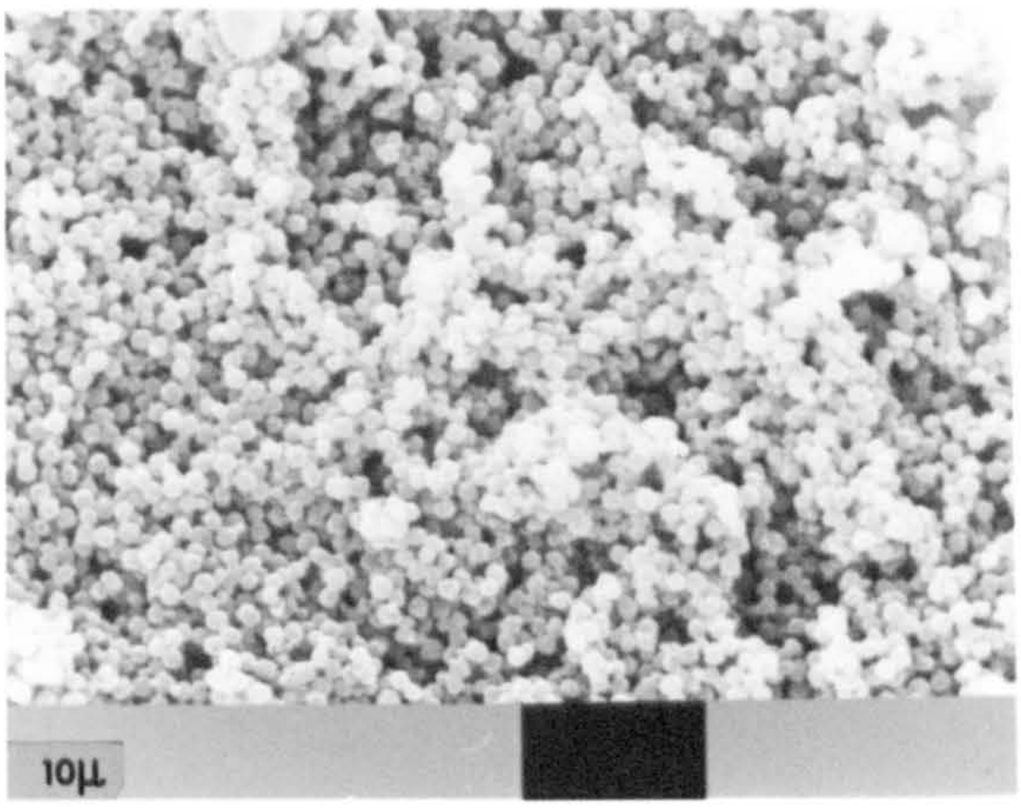

S9

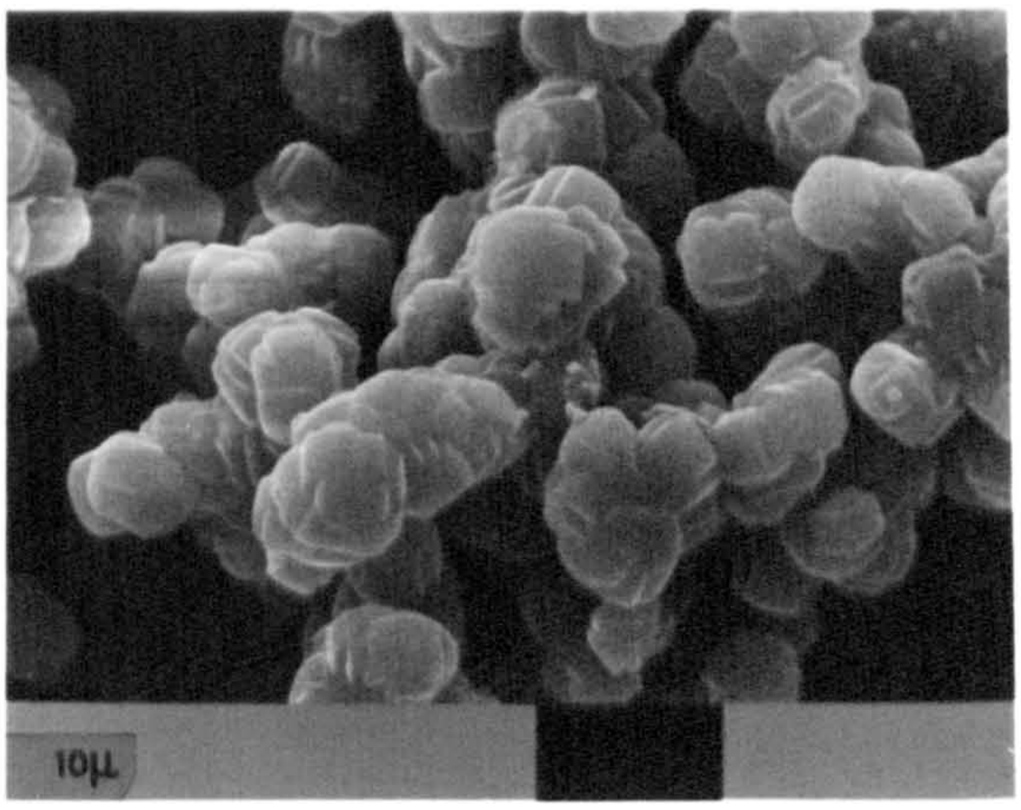

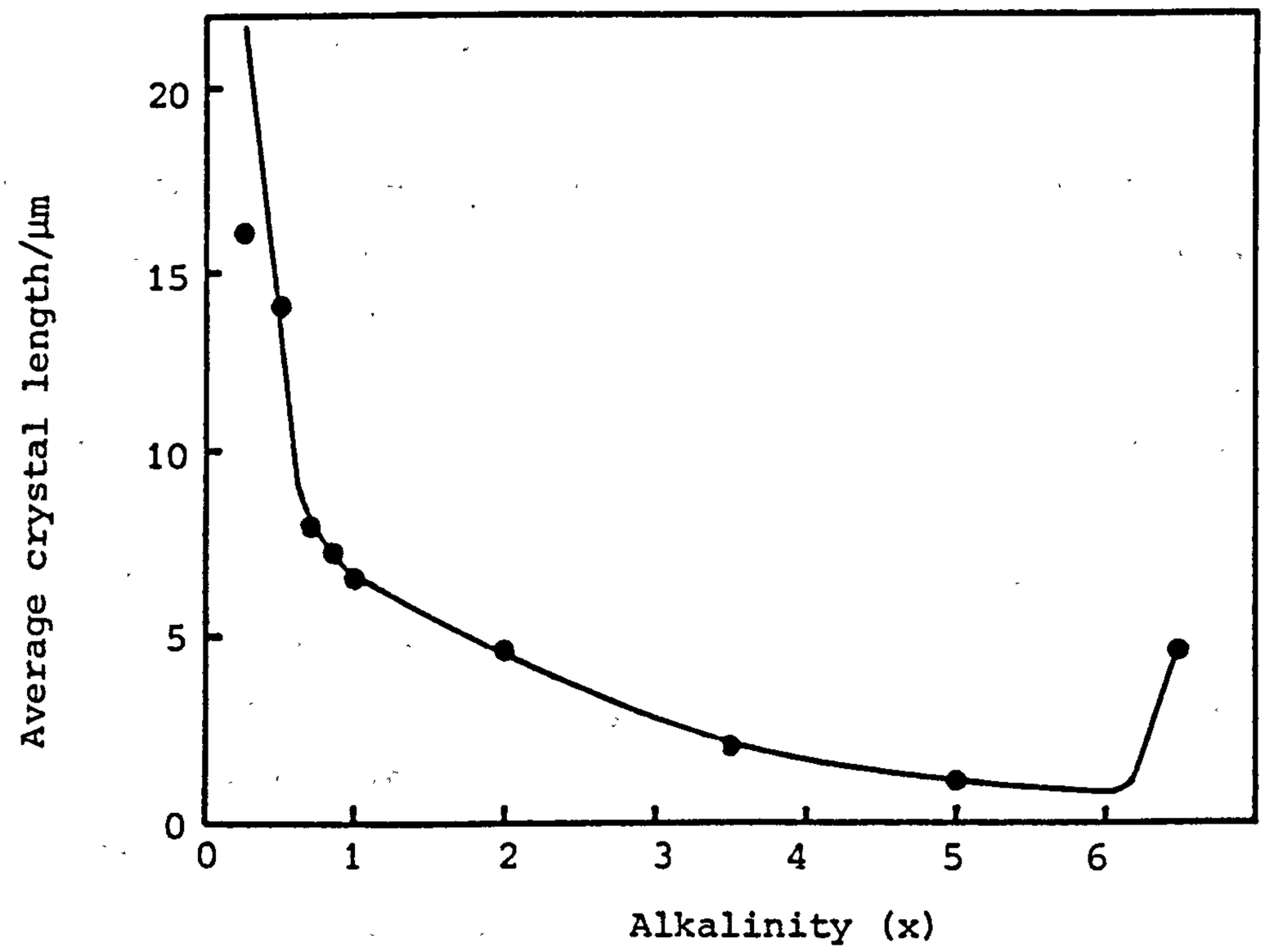

Figure 3.18 Average length of the silicalite crystals as a function of reaction mixture alkalinity. Each product consisted of crystals of fairly uniform size. Length measurements were made from microscopic examination (SEM) of between 5 and 10 crystals.

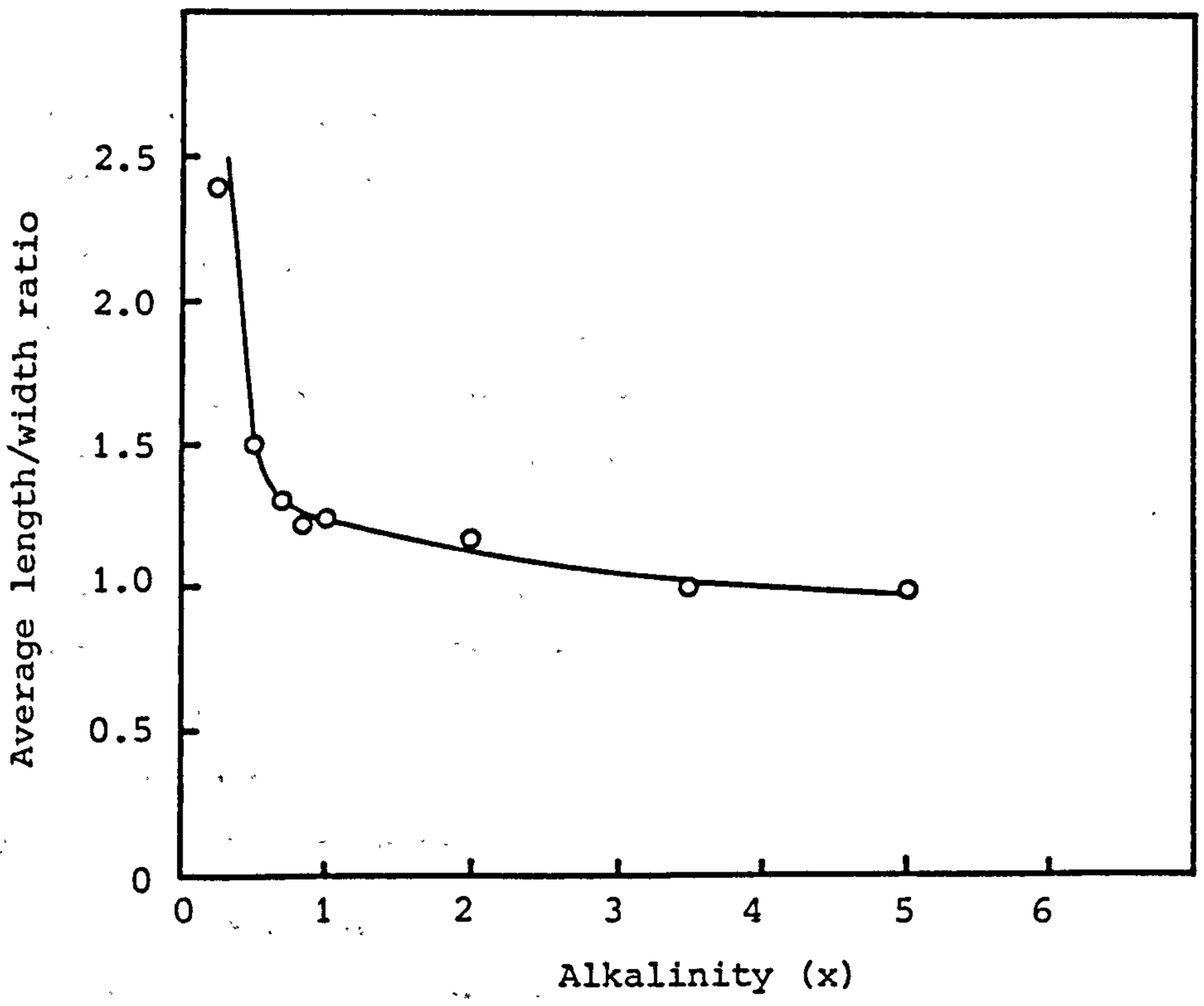

Figure 3.19 Average length/width ratio of silicalite crystals (from SEM measurements) as a function of reaction mixture alkalinity

(1) The appearance of the samples taken during the reactions.

(2) The pH profiles.

(3) The XRD crystallisation curves.

The most quantitative information was obtained from XRD although this technique is somewhat restrictive in the kinetic information it can give. The crystallisation curves, which are shown together in Figure 3.20, do not give quantitative information about the rate of nucleation or the rate of crystal growth. X-ray methods for determining the length of the induction period and for following the early stages of growth are unsatisfactory as very small crystals are X-ray amorphous [22] and crystals smaller than ~0.2 μm produce peak broadening. The results in Figure 3.20 show that crystalline material was first detected after ca. 1 day for the reaction with x = 5.0 and after ca. 4 days for the reaction with x = 0.50.

The percentage crystallinities were calculated from diffraction line intensities. These diffraction intensities are dependent on the amount of crystalline material present on a volume fraction basis. The crystallinities can be considered on a mass fraction basis by taking into account the different bulk powder densities of the amorphous silica and the silicalite although this presents difficulties because of the differing morphologies of crystals and differing states of aggregation of amorphous silica particles, both of which affect powder densities.

There are also difficulties preparing samples for XRD analysis. Powders can not always be packed in slides evenly, amorphous and crystalline powder fractions compress to different extents, crystals of different size and shape also compress differently and the crystals themselves can often fracture. XRD methods for determining crystallinity therefore have many drawbacks. For the discussion that follows it has been assumed that diffraction intensities directly give a measure of the amount of crystalline solid present on a mass fraction basis. Any errors introduced by this assumption may be small compared with others associated with the technique.

Each of the curves in Figure 3.20 show a linear region where the rate of crystallinity increase (R) is constant and at its maximum. This rate can be expressed on a mass fraction basis as:

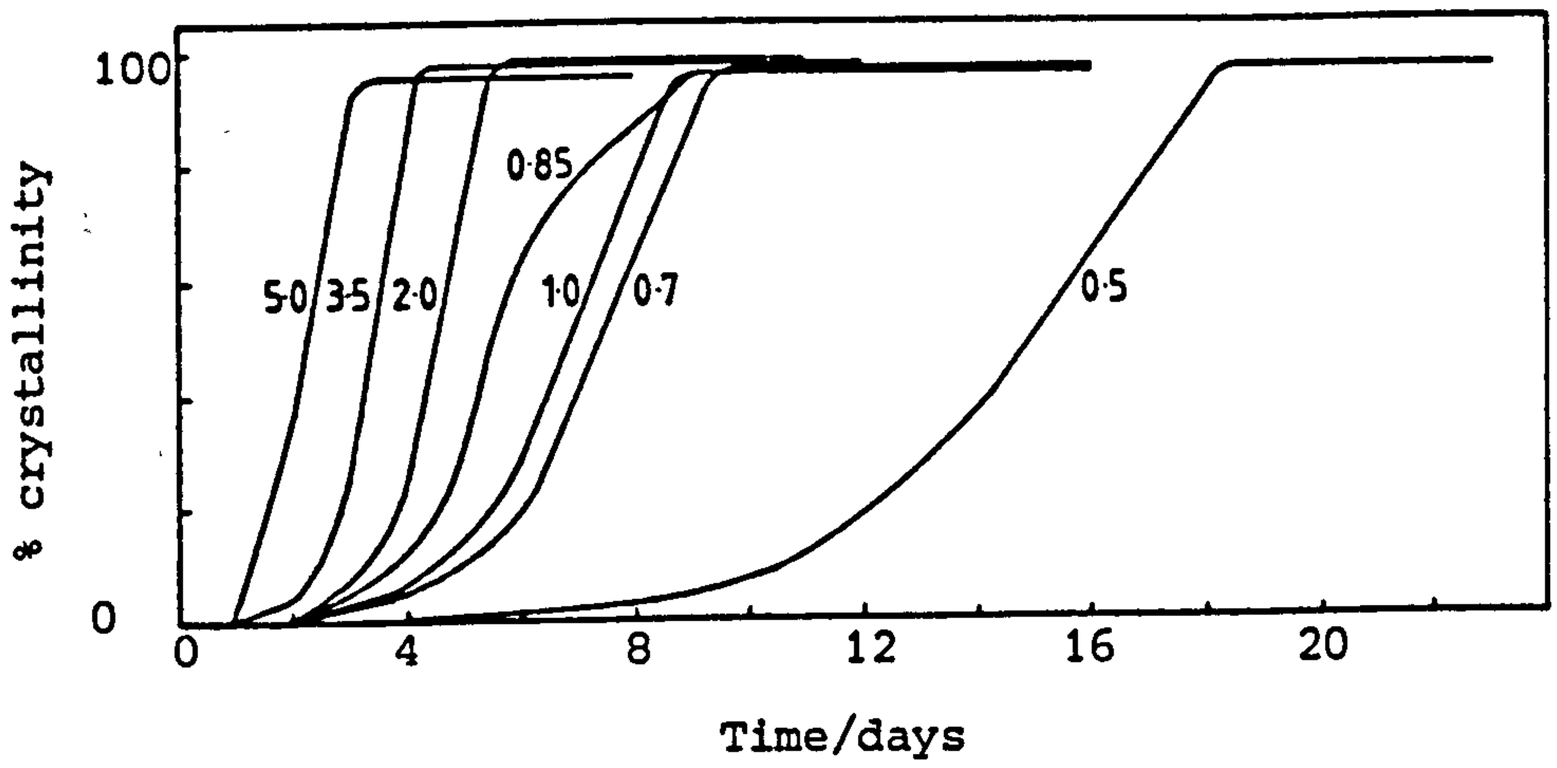

Figure 3.20 XRD crystallisation curves for silicalite crystallisation at 95°C from mixtures of composition xNa_2O 2TPABr $20SiO_2$ $1000H_2O$. The respective alkalinities (x values) are shown by the curves

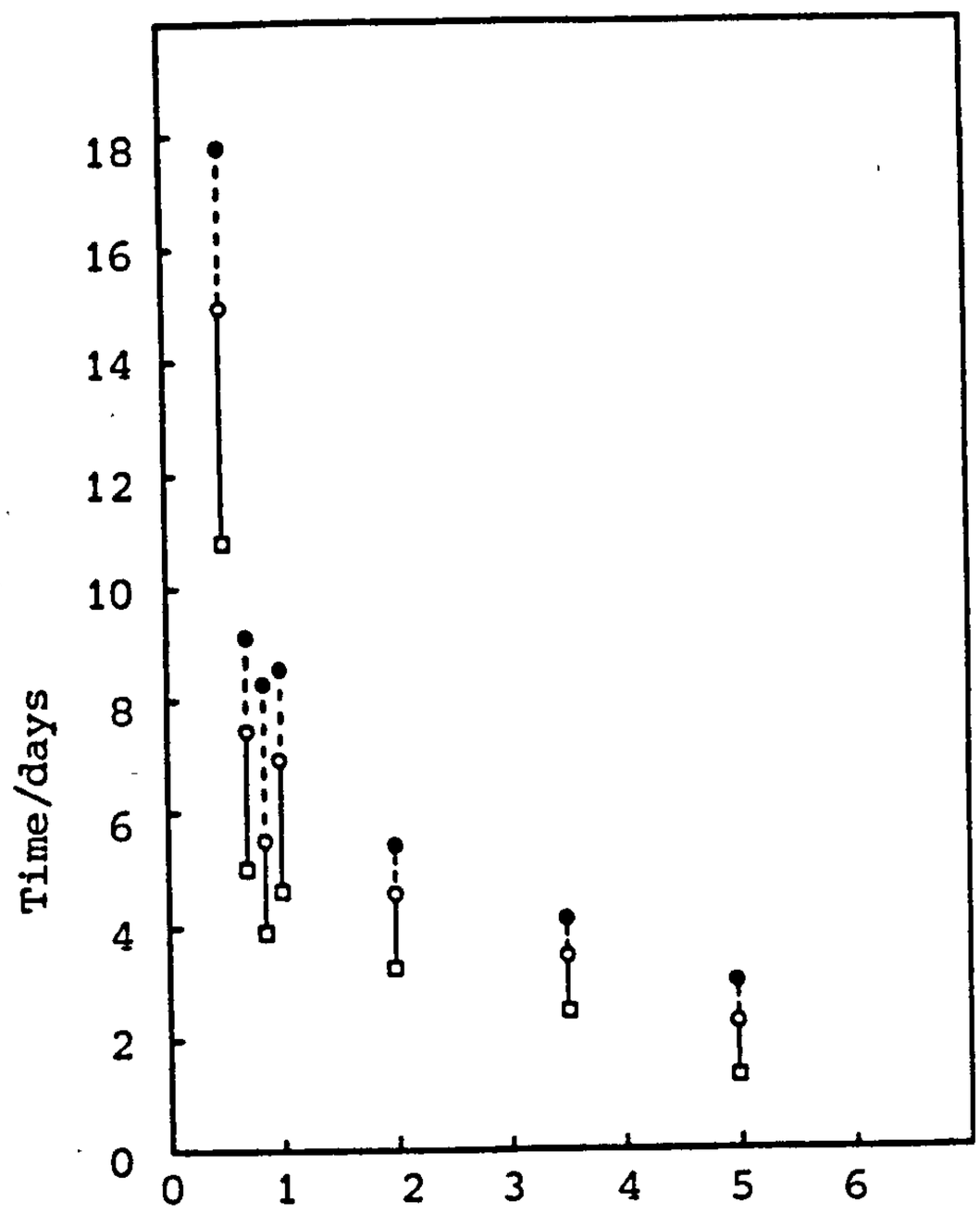

Figure 3.21 Effect of alkalinity on the time taken for the crystallinity of the solid phase in mixtures to reach 10% (□), 50% (○) and 90% (●).

$$R = \frac{MF_2 - MF_1}{t_2 - t_1} \qquad (3.12)$$

where MF_1 and MF_2 are the mass fractions of crystalline material in samples taken at times t_1 and t_2 respectively. The mass fractions can be expressed in terms of their component fractions:

$$MF_1 = \frac{C_1}{A_1 + C_1} \qquad (3.13)$$

$$MF_2 = \frac{C_2}{A_2 + C_2} \qquad (3.14)$$

where A and C represent the masses of amorphous and crystalline solid present at the denoted times. As crystals grow at the expense of the amorphous gel, i.e. the total mass of silica solid remains essentially constant during transformation of the gel, mass fractions at different times can be related:

$$MF_2 = \frac{C_1 + \Delta C}{(A_1 - \Delta C) + (C_1 + \Delta C)} = \frac{C_1 + \Delta C}{A_1 + C_1} \qquad (3.15)$$

where ΔC is the mass of amorphous silica converted to silicalite between times t_1 and t_2. The assumption that the total solid present remains constant during the period when gel is being transformed into silicalite is strictly valid only if the pH and solubility of the amorphous solid also remain constant during the transformation. Substituting equations (3.13) and (3.15) into (3.12) gives:

$$R = \frac{1}{(t_2 - t_1)} \left(\frac{\Delta C}{A_1 + C_1}\right) \qquad (3.16)$$

Equation (3.16) can be rewritten more generally:

$$R = \left(\frac{dC}{dt}\right) \frac{1}{(A + C)} \qquad (3.17)$$

where dC/dt represents the rate of crystallisation; the mass of crystalline material formed in unit time. It should be noted that the rate of crystallisation dC/dt and the rate of crystallinity increase (R) are distinctly different quantities. The latter is obtained from the slopes of the crystallisation curves and is dependent on both the rate of crystallisation dC/dt and on the amount of total solid present (A + C). Increasing the reaction alkalinity reduces the amount of total solid present during the gel-silicalite transformation stage and the near constant slopes of the linear portions of the crystallisation curves for the reactions with x = 2.0, 3.5, 5.0 (Figure 3.20) therefore indicate that the rate of crystallisation decreases as the alkalinity (x) increases from 2.0 to 5.0. In addition crystallisation from the reaction with x = 6.5 was observed to be very slow. Likewise, crystallisation was slow for the low alkalinity reactions (x = 0.25, 0.50). There is therefore an optimum alkalinity for the rate of crystallisation of silicalite in this system. At low alkalinity reduced concentrations of soluble silicate species are likely to lower the rate of crystallisation and it is possible that the controlling factor is the rate at which the amorphous gel is depolymerised. At high alkalinity increased hydroxide ion concentrations coupled with large concentrations of sodium ions lower the rate of crystallisation. It seems less likely that the kinetics of crystallisation in these high alkalinity reactions are controlled by the kinetics of gel dissolution. The optimum rate of crystallisation probably occurs when $1 \leqslant x \leqslant 2$.

Further kinetic information from the crystallisation curves is shown in Figure 3.21. In general the time taken for the crystallinity to increase from 10% to 50% increased as the alkalinity decreased. The time taken for the 50% to 90% transitions gave a relative measure of the slopes of the linear portions of the crystallisation curves. Anomalous behaviour was seen for one reaction (x = 0.85). The transition from 10% to 50% crystallinity was rapid, the 50% to 90% transition was relatively slow. The different form of the respective crystallisation curve was due to this (Figure 3.20). These anomalies were possibly caused by a 'seeding' effect accelerating the early stages of growth.

3.3.8 Related Reactions

In order to compare the results obtained in the xNa_2O 2TPABr $20SiO_2$ $1000H_2O$ system with other reaction systems, several further crystallisations were carried out. Details of these additional reactions are given in Table 3.7. Reaction conditions were unchanged: polypropylene bottles, 150 rpm, 95°C. The bottles used for reactions T2 to T7 had a modified bearing assembly which gave a better seal and so reduced water loss. Even so, small amounts of water were added to the reactions as required. An improved device, utilising a plastic syringe, was used to sample these reactions.

A comparison of the pH results from reactions T1, T2 and reaction S7 ($3.5Na_2O$ 2TPABr $20SiO_2$ $1000H_2O$) is shown in Figure 3.22. All three reactions contained the same amount of base. The addition of hexanediol slightly increased the initial and final pH (+0.06 and +0.02 respectively) and decreased the time required for the system to reach final equilibrium. It is possible that the observed effects arise simply from a reduction in the solubility of the amorphous silica and crystalline product, although other explanations are possible. For example the diol may sorb on the external surfaces of the solids, reducing the number of cations associated with the silica surfaces and increasing the base content of the solution phase.

Substantial increases in the initial and final pH values were found when all base was added as TPAOH (reaction T2, Figure 3.22) and also the time required for crystallisation was much reduced (relative to the isoalkaline sodium reaction S7). The reverse effects are seen in Figure 3.23. When extra sodium is added to a mixture the initial and final pH values are reduced and the crystallisation time is substantially increased. These results suggest that the solubilities of the amorphous and crystalline phases are increased by the incorporation of sodium ions, although ionic strength effects could also cause the pH trends observed. As for the kinetic effects, Chao et al [13] have also shown that at constant alkalinity crystallisation of ZSM-5 type materials is retarded by sodium ions. The results in Figures 3.22 and 3.23 show that silicalite crystallisation at constant alkalinity can differ substantially depending on mixture components.

Table 3.7 Related reactions: synthesis and product details

Reaction code	Mixture Composition[a]	pH_i	pH_f	ΔpH	Time/ days	Product
T1	$3.5Na_2O$ 2TPABr 2diol[d]	11.54	12.22	0.68	7	Silicalite-1
T2	$3.5TPA_2O$[e]	11.83	12.78	0.95	13	Silicalite-1
T3	$5.0Na_2O$ 2TPABr 5NaBr	11.32	11.91	0.59	27	Silicalite-1
T4	$3.5Li_2O$ 2TPABr	11.37	11.53[b]	0.16	8	Silicalite-1 + amorphous
T5	$6.5Li_2O$ 2TPABr	11.56	11.66	0.10	13	Silicalite-1 + amorphous
T6	$1Na_2O$ 2TBABr	11.32	11.36	0.04	30	Silicalite-2
T7	$1TBA_2O$[e]	11.64	11.78[c]	0.14	24	Silicalite-2

[a] All mixtures contained $20SiO_2$ $1000H_2O$

[b] Crystallisation was incomplete and the pH was decreasing when the reaction was terminated

[c] The pH was increasing when the reaction was terminated

[d] hexane-1,6-diol

[e] Quaternary ammonium hydroxides were obtained from Fluka

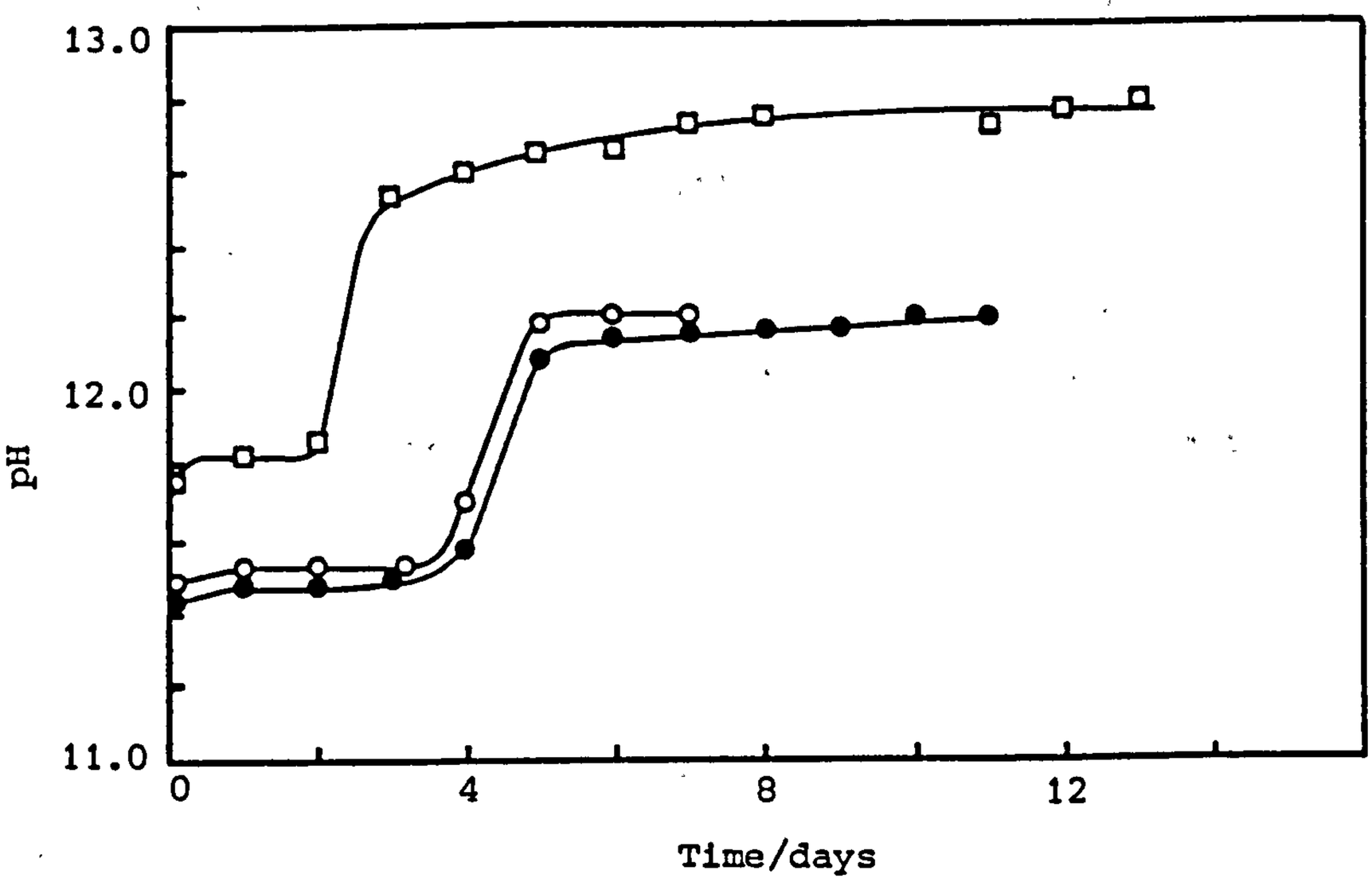

Figure 3.22 Comparison of pH profiles of reactions T1 (○), T2 (□) and S7 (●)

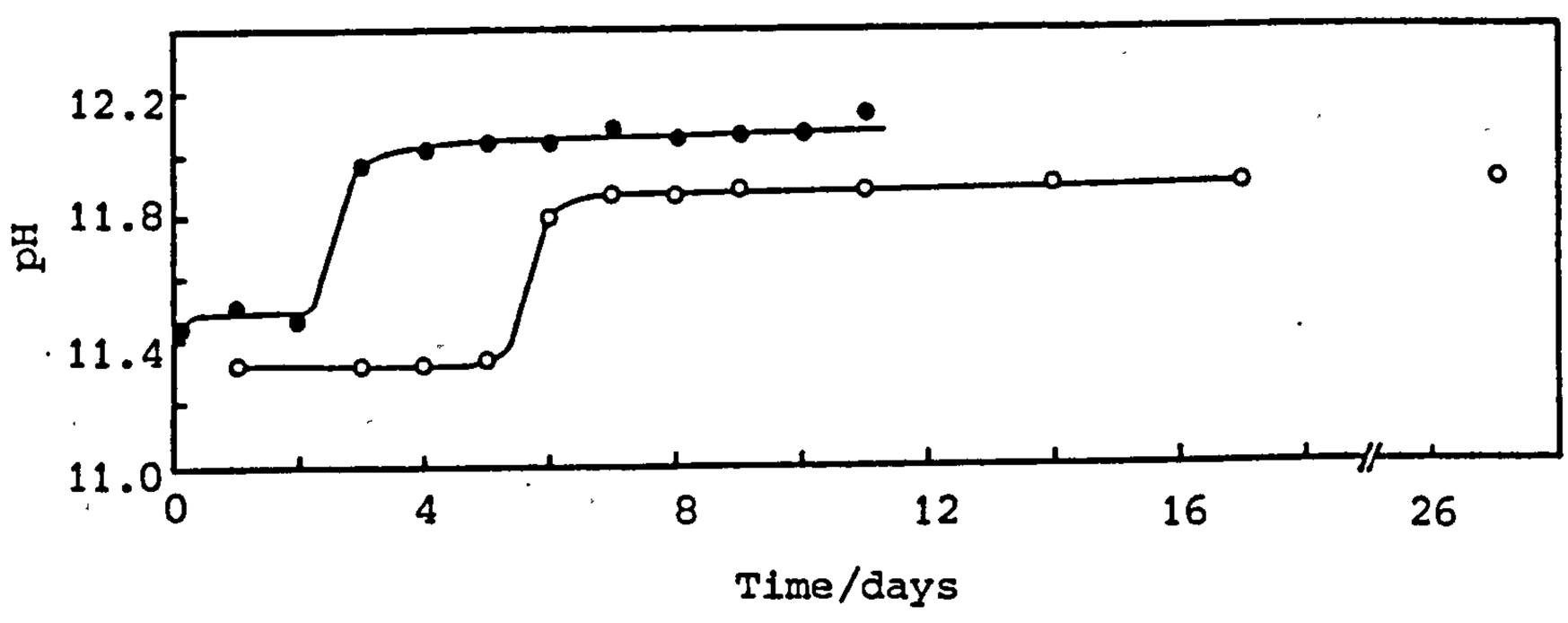

Figure 3.23 Comparison of pH profiles of reactions T3 (○) and S8 (●)

Two reactions, T4 and T5, were carried out using LiOH as base. The pH results are given in Figure 3.24. The initial pH values were lower (-0.11 and -0.04 respectively) than those of the reactions of corresponding alkalinity in the Na_2O system (S7 and S9). The pH curves also show several anomalous features:

(1) The mixtures contain substantial amounts of base and should have buffer capacities to cope with changes in the hydroxide ion concentration. However decreases in pH, due to the removal of base during crystallisation, were observed. Similar decreases were not observed for the reactions of some alkalinity in the xNa_2O series (S7 and S9).

(2) The pH rise during reaction T4 is small.

(3) Two small pH rises were seen during reaction T5.

Samples taken at the end of these reactions appeared to contain large aggregates of crystals. The solid sedimented rapidly leaving a clear solution. Both products appeared similar under the microscope. Examination of the product from reaction T5 by optical microscopy showed 'micelle' like clusters along with individual crystals. Scanning electron microscopy revealed the true nature of these clusters (Figure 3.25); crystals embedded in amorphous gel were seen. As much of the external surface of the clusters is covered with crystalline material, the silicalite is likely to control the solution phase species through its solubility. This in part explains why pH rises were seen even though all the gel had not been depolymerised. The local concentrations of soluble species inside the clusters may be high and in these lithium systems it appears that crystals grow predominantly from within the gel, not in the bulk solution phase. Mechanistically this seems similar to the gel-solid growth theory that some workers have favoured. X-ray diffraction showed the crystalline material was silicalite. However samples were only partly crystalline and gave weak diffraction intensities. It is unclear why crystallisation in the Li_2O system should be so different from that in the Na_2O system. In the latter crystals appear to grow in the bulk solution and optical microscopy showed they were never deeply embedded in gel. When samples were taken crystalline solid sedimented far more rapidly than amorphous material, evidence that the two solids were

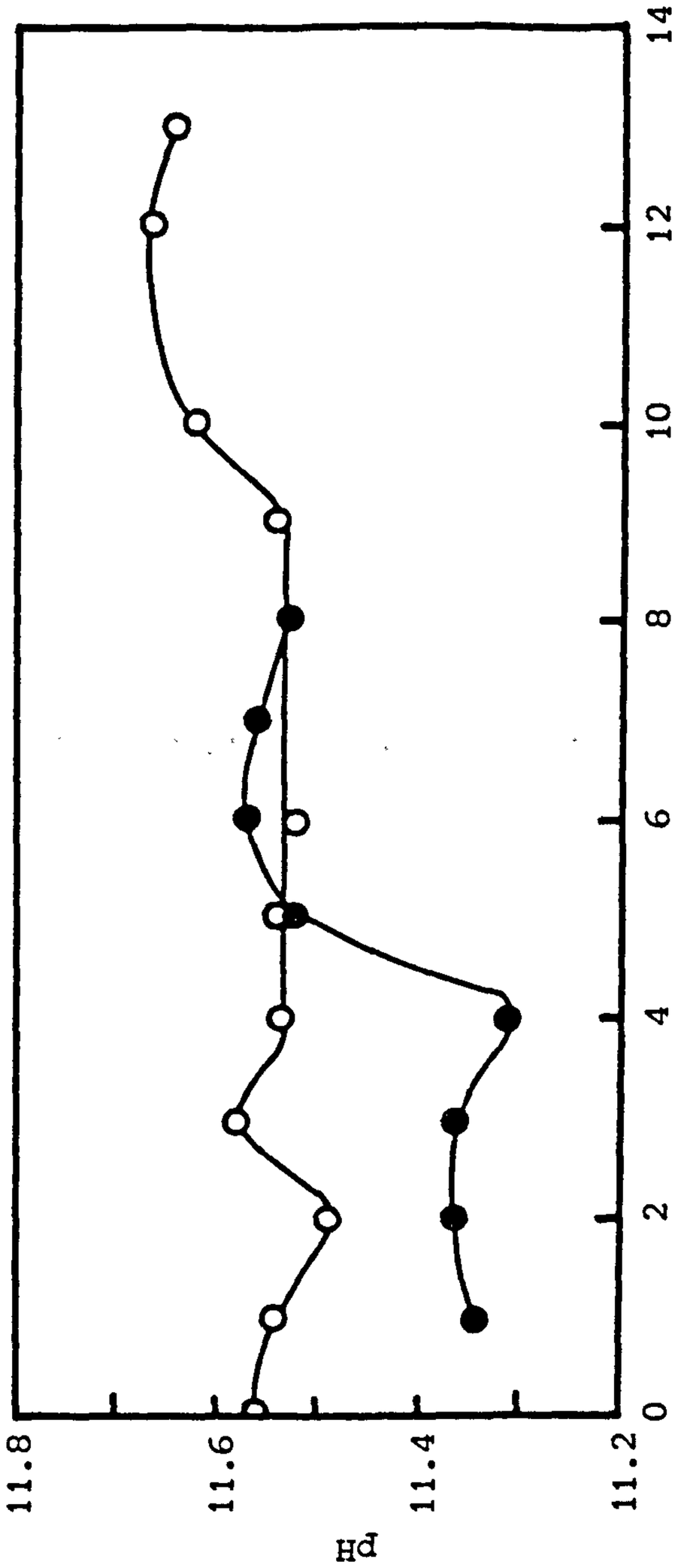

Figure 3.24 pH profiles of reactions T4 (●) and T5(○)

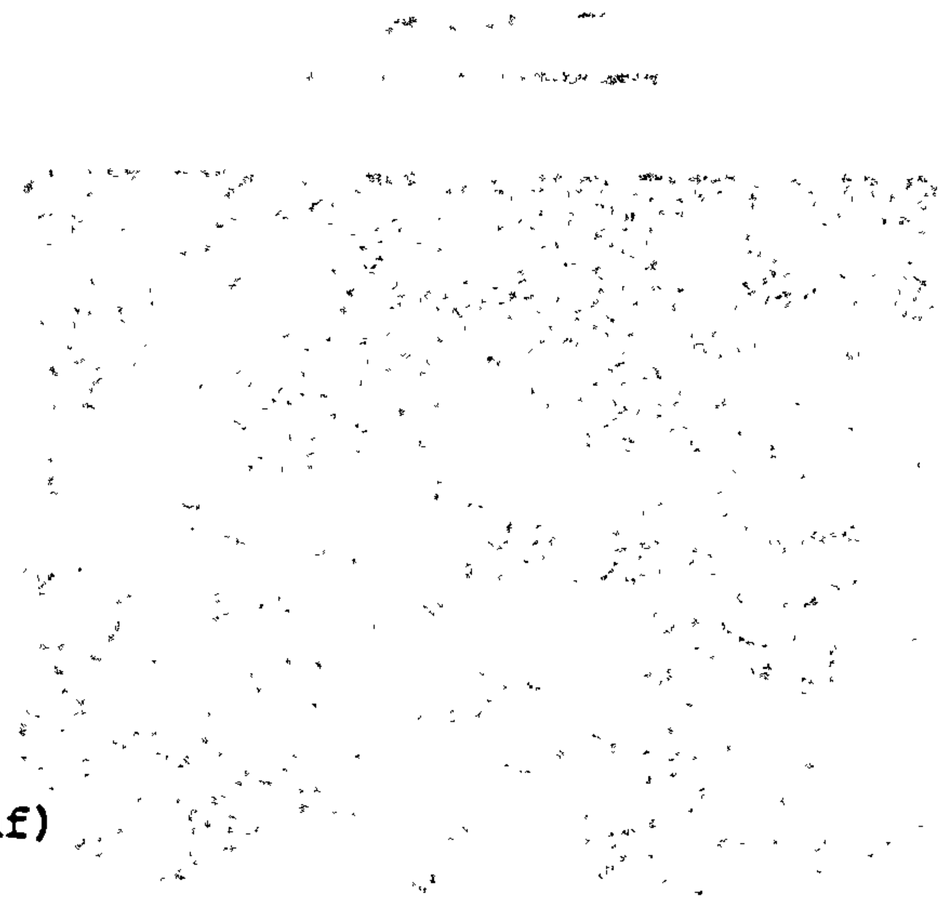

Figure 3.25 (overleaf)

Scanning electron micrographs of the product from reaction T5.

Product T 5

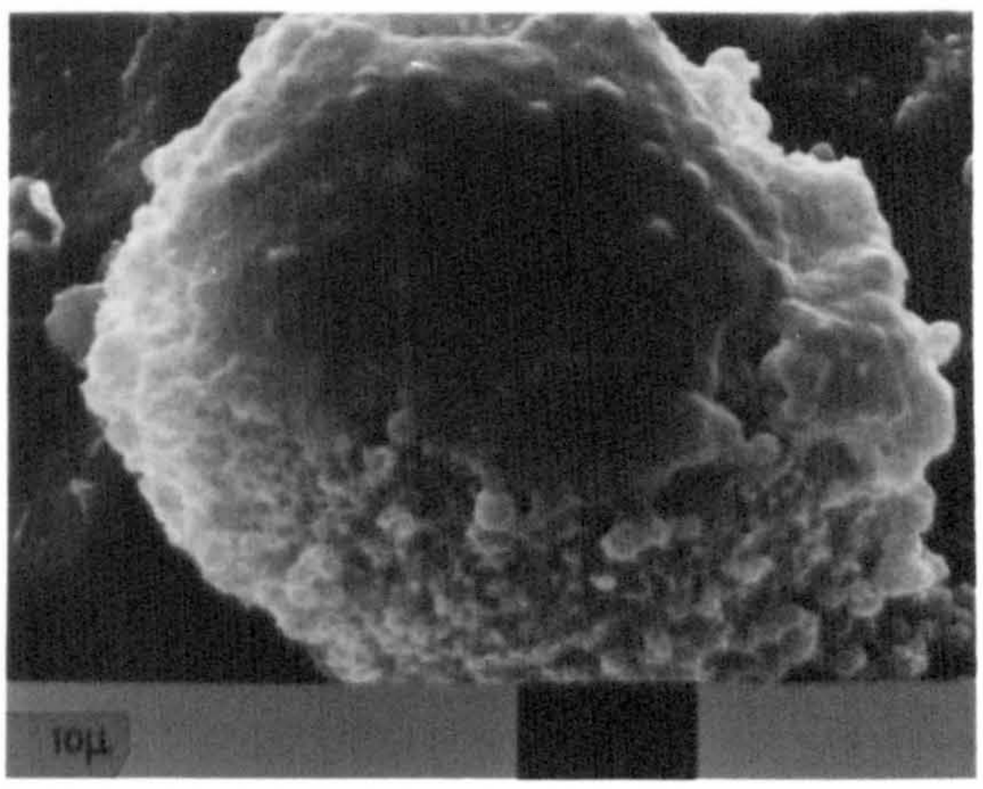

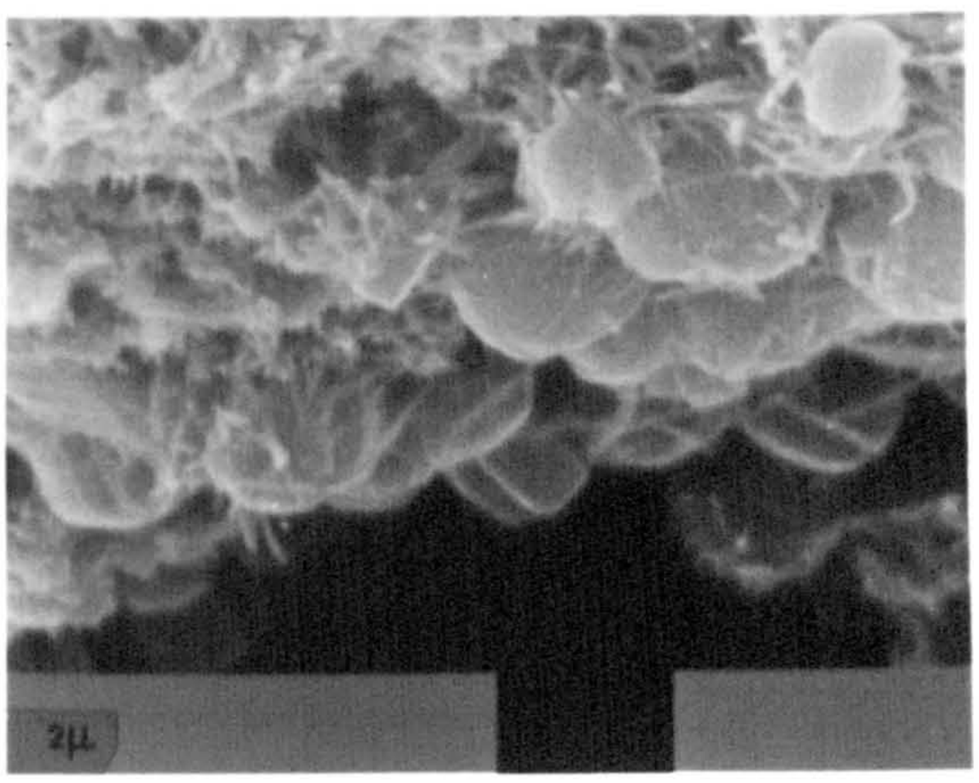

intimately attached. These observations strongly indicate that in the Na_2O system crystallisation occurs by a solution phase ion transportation mechanism. Time did not permit further investigation. These examples sufficed to show that the chemical nature of the alkali metals present in synthesis mixtures can markedly affect crystallisation.

The addition of TBABr (TBA = tetrabutylammonium) to reaction mixtures instead of TPABr produces systems from which silicalite-2 [23] readily crystallises. Silicalite-2 is isostructural with the zeolite ZSM-11 [24] and its precursor contains about 2.6 moles of TBA cations per unit cell of $96SiO_2$ [25]. Results from two silicalite-2 reactions, T6 and T7, are shown in Figure 3.26. For comparison the pH profile for the silicalite-1 reaction S5 (x = 1.0) is also drawn. All three reactions contained the same amount of base. The pH results for reactions T6 and T7 indicate that the solubilities of the amorphous silica and silicalite-2 were reduced in the alkali metal free system. Similar solubility effects were found for silicalite-1 synthesis (Figure 3.22). The observed pH falls indicate that the organic molecules entrapped in the silicalite-2 precursor during growth are TBAOH (empirically), analogous to the clathration of TPAOH molecules in the silicalite-1 precursor. The pH fall is greater for the alkali metal free reaction (T7). This is further evidence that the solubility of the amorphous silica has been reduced in this alkali metal free reaction; removal of base by the growing crystals has a larger effect on pH in this unbuffered system. The pH rise was very small for reaction T6 even though the product was fully crystalline. This may be because the product contains solubility increasing sodium species. Rubin et al [26] crystallised aluminium-free ZSM-11 (silicalite-2) and many products contained between 4 and 8 moles of sodium per unit cell. These levels are likely to have marked effects on the solubility of the crystals. It is interesting to note that these levels are greater than those that have been found in silicalite-1 samples (see section 3.3.7.2).

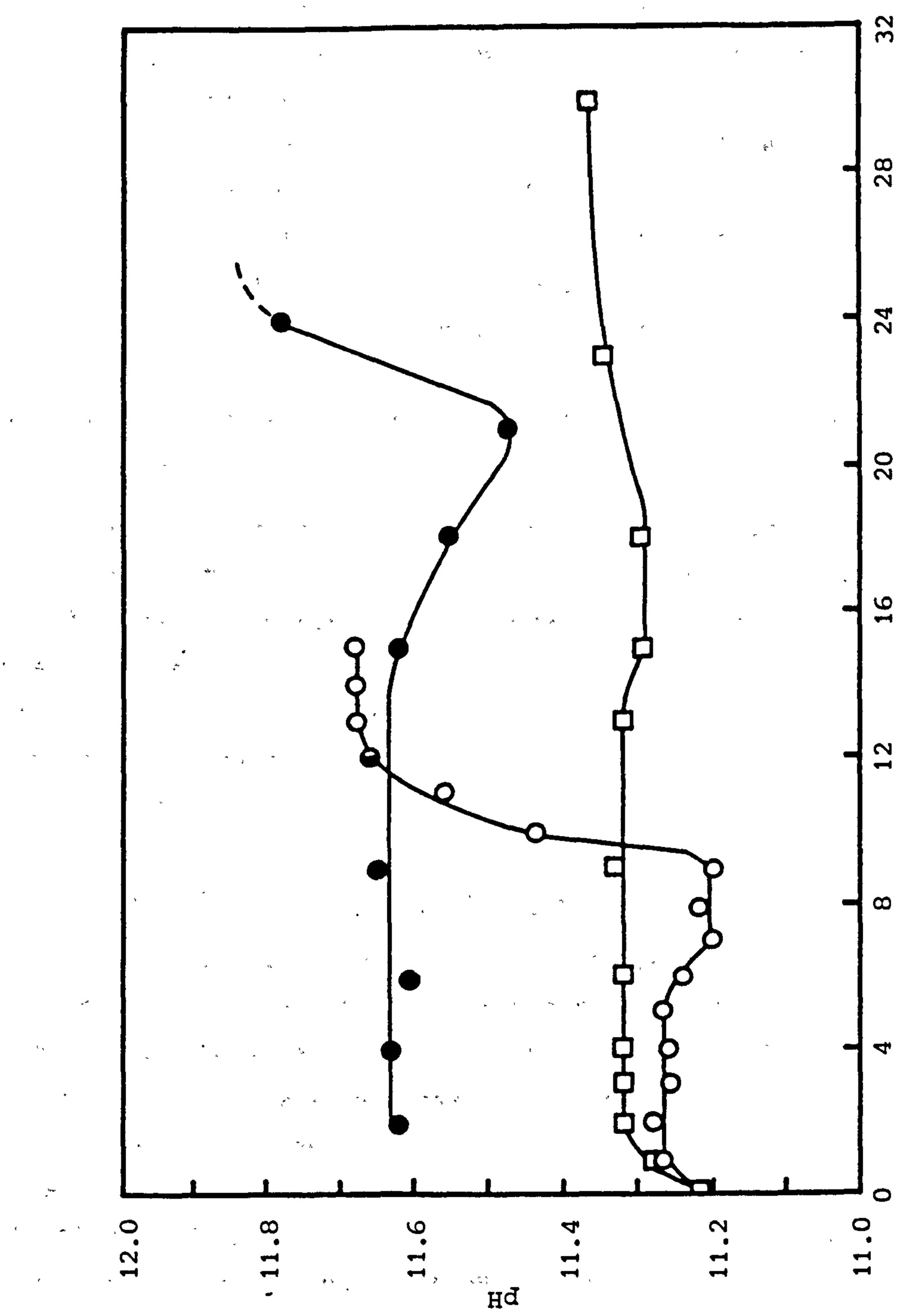

Comparison of pH profiles of reactions T6(□), T7 (●) and S5 (○)

Figure 3.26

The pH profiles of the silicalite-2 reaction T6 and the equivalent silicalite-1 reaction (S5) are compared in Figure 3.26. Features of the pH curves are summarised below:

(1) The induction period pH is higher for the TBABr reaction. This could be caused by solubility differences or steric effects involving surface-bound cations.

(2) Both pH profiles show a fall in pH indicating that base is being consumed.

(3) The pH rises occur when the crystalline silicas control the species in solution. The pH rise though is much reduced for the TBABr reaction. This may be because silicalite-2 is more soluble than silicalite-1.

(4) The silicalite-1 reaction crystallises significantly faster.

A detailed study of the effects of alkalinity on silicalite-2 crystallisation would no doubt be very revealing.

Results from these related reactions further exemplify the value of pH measurements. In the laboratory pH measurements give a simple and rapid means of monitoring the progress of a reaction. All the pH results presented in this work relate to synthesis of aluminium-free materials. The technique can also be used to monitor crystallisation of many high silica zeolites. Profiles obtained for the crystallisation of EU-1 [27] and ZSM-5 (Figure 3.27) illustrate this point.

3.3.9 Reproducibility of pH Measurements

In Figure 3.28 the pH results from reaction S7 (x = 3.5) are compared with those obtained for two repeat reactions, R1 and R2, of identical composition. Crystallisation was faster and the final pH higher for reaction R1 because water loss during reaction was purposefully not replenished. The results for the two other reactions show good agreement. Loss of water was made good in both these cases. The initial and final pH values differed by only 0.03 and 0.04 pH units. Duplicate reactions can therefore give concordant pH results. However fluctuations in measured pH values can occur if precautions are not taken. Factors that can minimise errors are listed below:

Figure 3.27 pH measurements made on samples taken during the crystallisation of high silica zeolites

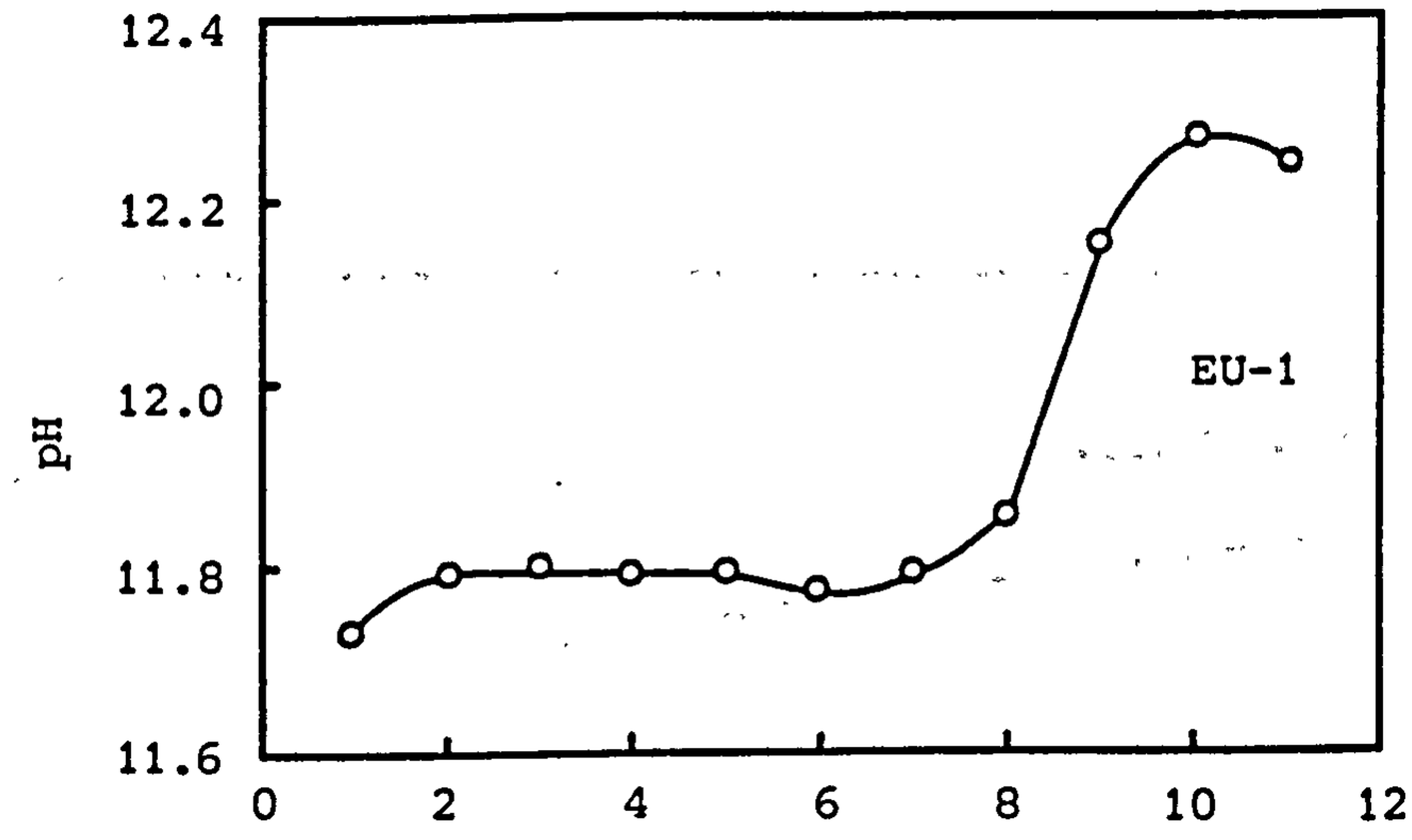

Mixture Composition: $10Na_2O$ 10Hex $60SiO_2$ Al_2O_3 $3000H_2O$
(Hex = hexamethonium bromide)

Reaction Conditions: Stirred 300 rpm, 200°C

Product: EU-1

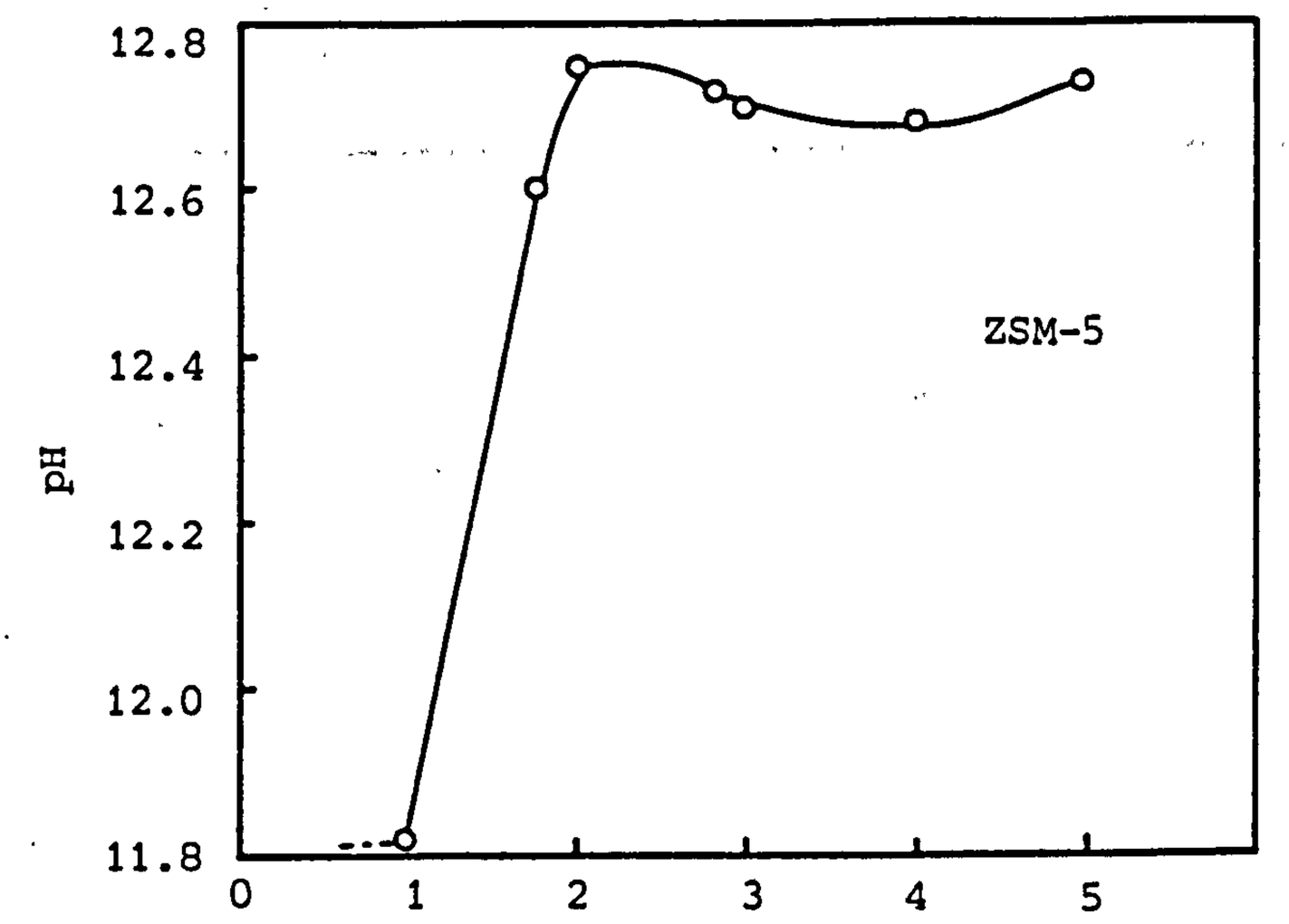

Mixture Composition: $10Na_2O$ 2TPABr $60SiO_2$ $2Al_2O_3$ $3000H_2O$

Reaction Conditions: Stirred 300 rpm, 150°C

Product: ZSM-5

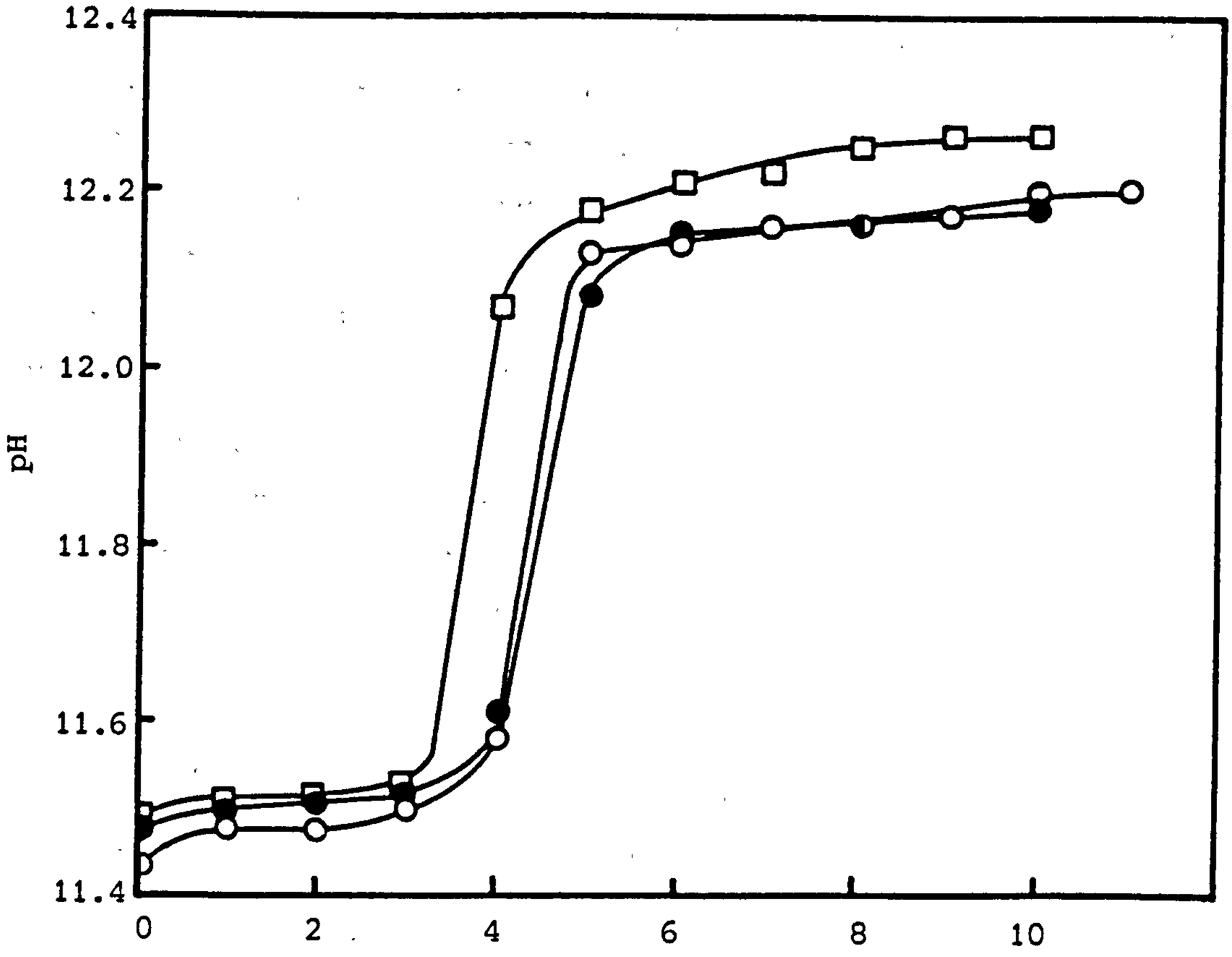

Figure 3.28 Comparison of the pH profiles of three identical reactions R1 (□), R2 (●) and S7 (○)

(1) Ensure the electrode response is rapid and no drifting occurs.
(2) Standardise the electrode with fresh buffer solution.
(3) Re-standardise the electrode regularly whilst taking measurements.
(4) Ensure the samples have been equilibrated at the same temperature prior to analysis.

Once samples have been taken and cooled the pH usually stabilises and if the aforementioned precautions are taken the pH of a given sample measured at different times will often differ by less than 0.05 pH units. Usually it is the relative differences in pH values that are important. When comparing pH values of samples taken from one reaction or from a series of reactions errors can be reduced by equilibrating all the samples under the same conditions and taking all the measurements at the same time.

All pH measurements taken at ambient temperatures merely reflect the pH of the reaction at elevated temperatures. After samples are taken, cooling often induces changes in the solutions. This can give rise to interesting phenomena and pH results. Such effects are discussed in the next section.

3.3.10 Effects of Temperature on Silicalite Solubility

The solubilities of most amorphous and crystalline silicas increase with temperature. If a solution is saturated or near saturated with respect to a solid silica at reaction temperature, cooling must either cause supersaturation of the solution phase, reorganisation of the species in solution or precipitation of silica. Many of the samples from the higher alkalinity reactions $x \geqslant 2.0$ showed some evidence of silica precipitation. This silica was sometimes seen as a gel-like phase that remained suspended after the bulk solid had settled. It appeared amorphous under the microscope. When reactions were terminated care was taken to separate precipitated silica from the bulk crystalline solid. In most cases the amount precipitated was very small. Associated pH changes, especially in buffered solutions, would also consequently be small.

Silica precipitation is most likely to occur when samples from high temperature reactions are cooled. For such reactions, the solubility differential is increased and there is more chance of silica coming out of solution and possibly contaminating crystalline material. Preliminary high temperature crystallisations showed interesting solubility effects and one reaction was repeated for detailed study.

A reaction mixture was prepared with x = 0.5 ($0.5Na_2O$ 2TPABr $20SiO_2$ $1000H_2O$) and crystallised at 150°C in an autoclave. The reaction was stirred at 300 rpm and samples were taken during the crystallisation. pH measurements were made about 30 minutes after taking samples. After the reaction was complete samples were stored in small glass bottles and over a year later pH measurements were re-taken. The two sets of pH measurements are shown in Figure 3.29. The first set of measurements showed a small pH rise after ca. 20 hours (a duplicate reaction showed this rise was reproducible). This rise was indicative of solubility control transfer from the amorphous silica to the silicalite. Samples taken after this time were gel-free. This result shows that in low pH systems the removal of base from the solution phase dominates the pH changes seen during reaction. This is in agreement with the results from reaction S2 (x = 0.50) carried out at 95°C (Figure 3.7). However, the final pH of the 95°C reaction was anomalously lower (by 1.94 pH units) than that of the 150°C reaction - the reverse situation was expected. This further indicated that CO_2 probably affected the latter stages of the 95°C reaction.

The pH measurements taken after ca. 1 year (Figure 3.29) were all substantially greater than those taken initially. The pH of one sample (t = 96 hours) was monitored kinetically and substantial pH rises were seen immediately after the sample was taken (Figure 3.30). Reorganisation of solution phase species or silica precipitation were the likely causes. It is unclear why changes continued over such a long period. The set of pH results obtained after a year (Figure 3.29) probably represented the stable pH values of the solutions after all changes had occurred. No precipitated silica was visible in any of the samples. It is significant that the observed differences in pH between the two sets of readings were smaller for the first two samples taken. These samples contained substantial amounts of amorphous silica and consequently

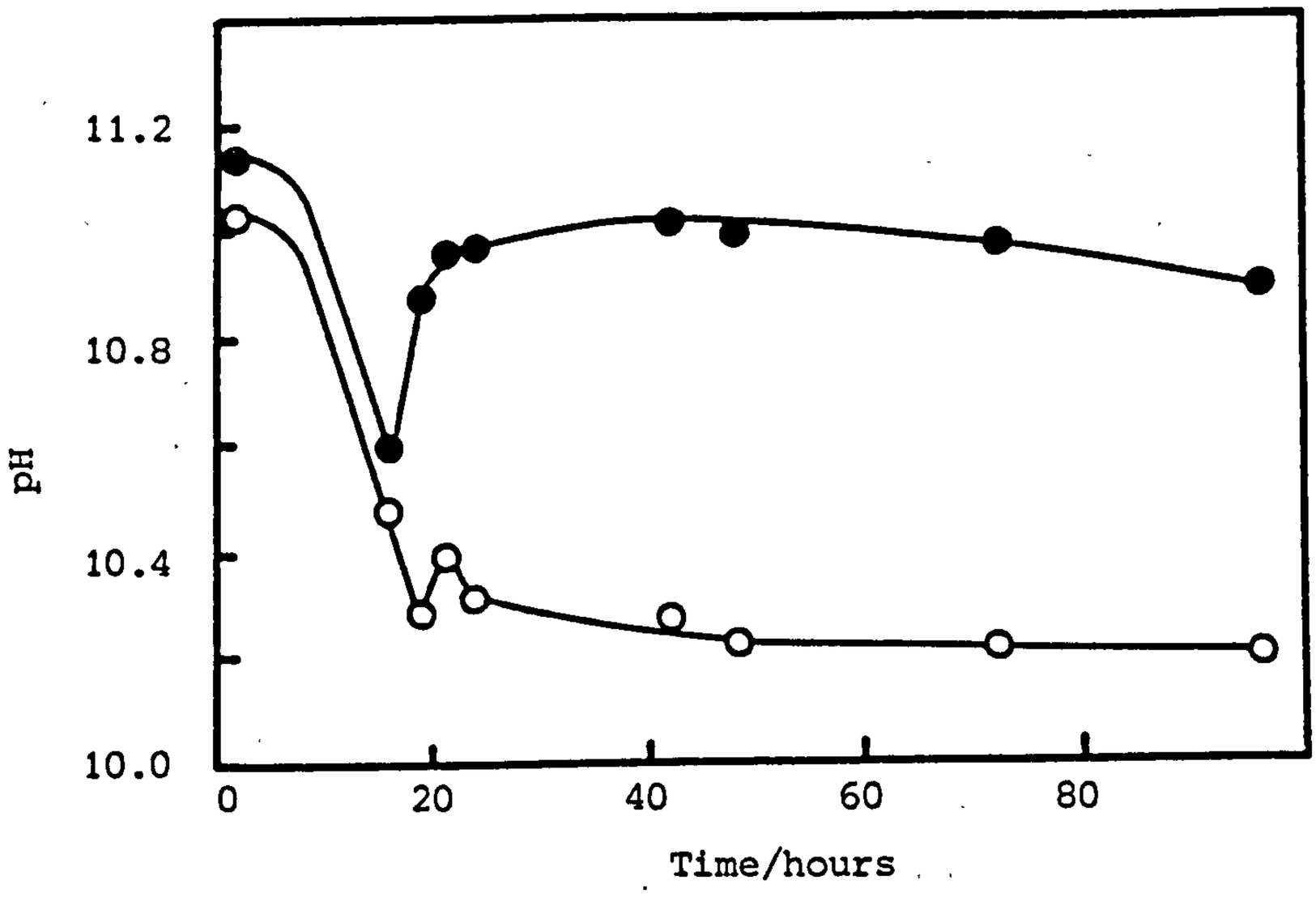

Figure 3.29 Comparison of pH measurements made on samples taken during crystallisation of a reaction mixture of composition $0.5Na_2O$ 2TPABr $20SiO_2$ $1000H_2O$ at 150°C. Measurements were made immediately samples had cooled (○) and over a year later (●).

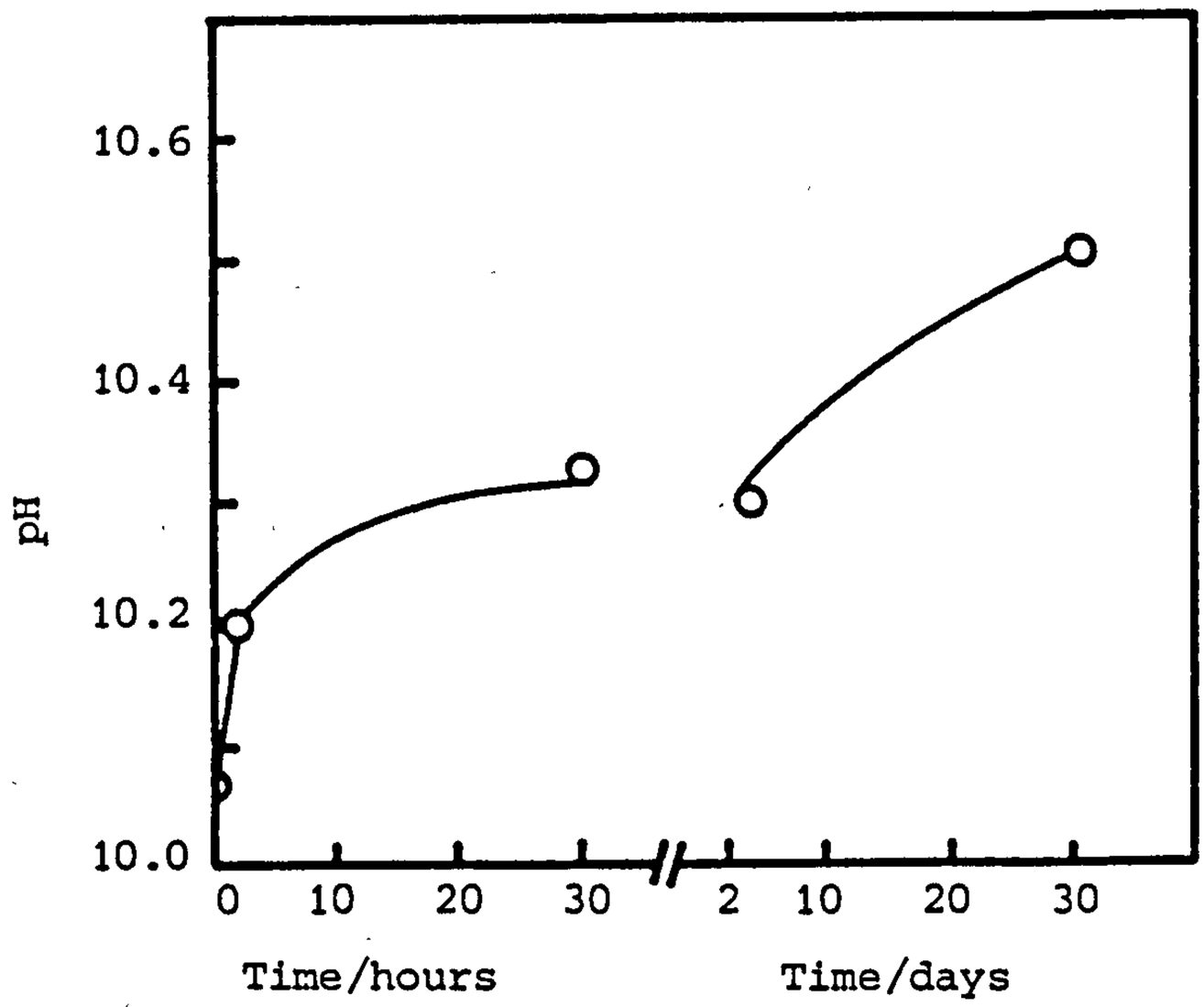

Figure 3.30 Time-dependent pH changes of a sample (t = 96 h) taken during crystallisation of the reaction mixture $0.5Na_2O$ 2TPABr $20SiO_2$ $1000H_2O$ at 150°C

they have a slightly greater buffer capacity to cope with pH changes. In addition, the temperature coefficients of solubility of the silicas are likely to differ. Similar time-dependent pH changes were not observed in samples from the reactions carried out at 95°C. These results show that to interprete pH results from high temperature reactions special care must be taken. Increases in sample pH consequent on cooling are most likely to be observed in unbuffered low pH systems.

3.4 Conclusions

A systematic study of silicalite crystallisation in the xNa_2O 2TPABr $20SiO_2$ $1000H_2O$ system has been undertaken. It has been shown that under the reaction conditions employed alkalinity (x) affects the following:

(1) Reaction pH
(2) Changes in pH during crystallisation
(3) Solubility of the amorphous and crystalline solids
(4) Product yields
(5) Chemical composition of the products
(6) Crystal size and morphology
(7) Reaction kinetics

Alkalinity probably affects the crystallisation of other silica molecular sieves and many high silica zeolites in similar ways and many of the points discussed are thought to have general applicability.

Alkali metal incorporation in the silicalite precursors seems to be predominantely controlled by the metal content of the mixture and the reaction pH. Certain aspects of the chemistry of these metal silicates have been discussed and further properties of these products are detailed in Chapter 6.

Other silica molecular sieves and high silica zeolites have been found to have metal cation contents above those required to balance framework aluminium (e.g. ZSM-5 [3, 28], ZSM-11 [26], ZSM-12 (TEA-silicate) [29], ZSM-39 [30], ZSM-48 [31] and KZ-2 [32]). Most of these 'excess' cations are likely to be chemically similar to metal ions in silicalite. Ion exchange work by Howden [33] showed that 'excess' cations in ZSM-5 could

be exchanged although no explanation for their presence was given. This further indicates that metal ions in aluminium-free molecular sieves should confer ion-exchange properties on these materials.

For some applications it is probably beneficial to have metal ions present. Their presence means there are lattice defects but as they are exchangeable they do provide a means of modifying sieving properties. In other instances removal of all metal ions is desirable. This is likely to be the case when silicalite is used to sorb organics from aqueous solutions as metal-free products having no charged centres should have greater organophilicity. Incorporated metal ions can be removed but treatments probably leave the lattice with increased numbers of broken siloxane bonds (≡Si-OH HO-Si≡) and this is undesirable. The lattice still has an enhanced number of defects and still has increased hydrophilicity. These problems can be avoided if silicalite is crystallised from alkali metal free mixtures. In chapter 4 silicalite synthesis in such systems is described.

Chapter 3 - References

[1] R.W. Grose and E.M. Flanigen
U.S. Patent 4,061,724 (1977).

[2] E.M. Flanigen, J.M. Bennett, R.W. Grose, J.P. Cohen, R.L. Patton, R.M. Kirchner and J.V. Smith
Nature, 1978, 271, 512.

[3] R.J. Argauer, D.H. Olson and G.R. Landolt
U.S. Patent 1,161,974 (1969)
Also, R.J. Argauer and G.R. Landolt
U.S. Patent 3,702,886 (1972).

[4] D.H. Olson, G.T. Kokotailo, S.L. Lawton and W.M. Meier
J.Phys.Chem., 1981, 85, 2238.

[5] D.H. Olson, W.O. Haag and R.M. Lago
J.Catal., 1980, 61, 390.

[6] F.G. Dwyer and E.E. Jenkins
U.S. Patent 3,941,871 (1976).

[7] G.H. Kuehl
European Patent Application 93,519 (1983).

[8] S. Budiansky
Nature, 1982, 300, 309.

[9] E.M. Flanigen and R.L. Patton
U.S. Patent 4,073,865 (1978).

[10] R.Y. Saleh
U.K. Patent Application GB2,084,552 (1982).

[11] L. Falth and U. Hakansson
Recent Progress Reports, 5th Int.Conf.Zeolites, (Ed. R. Sersale, C. Collela and R. Aiello), 1980, 37.

[12] V. Lecluze and L.B. Sand
Recent Progress Reports, 5th Int.Conf. Zeolites, (Ed. R. Sersale, C. Collela and R. Aiello), 1980, 41.

[13] K.-J. Chao, T.C. Tasi and M.-S. Chen
J.Chem.Soc., Faraday Trans. 1, 1981, 77, 547.

[14] S.B. Kulkarni, V.P. Shiralkar, A.N. Kostasthane, R.B. Borade and P. Ratnasamy
Zeolites, 1982, 2, 313.

[15] A. Erdem and L.B. Sand
J. Catal., 1979, 60, 241.

[16] A. Nastro and L.B. Sand
Zeolites, 1983, 3, 57.

[17] R. Mostowicz and L.B. Sand
Zeolites, 1983, 3, 219.

[18] H. Nakamoto and H. Takahashi
Chem.Lett., 1981, 1739.

[19] D.M. Bibby, N.B. Milestone and L.P. Aldridge
Nature, 1980, 285, 30.

[20] E.G. Derouane, S. Detremmerie, Z. Gabelica and N. Blom
Appl.Catal., 1981, 1, 201.

[21] H. Annehed and L. Falth
Recent Progress Reports, 5th Int.Conf. Zeolites
(Ed. R. Sersale, C. Collela and A. Aiello), 1980, 5.

[22] P.A. Jacobs
J.Chem.Soc., Chem.Comm., 1981, 591.

[23] D.M. Bibby, N.B. Milestone and L.P. Aldridge
Nature, 1979, 280, 664.

[24] P. Chu
U.S. Patent 3,709,979 (1973).

[25] J.B. Nagy, Z. Bagelica and E.G. Derouane
Zeolites, 1983, 3, 43.

[26] M.K. Rubin, C.J. Plank, E.J. Rosinsky and F.G. Dwyer
European Patent Application 14,059 (1980).

[27] J.L. Casci, B.M. Lowe and T.V. Whittam
European Patent Application 42,226 (1981).

[28] R.W. Grose and E.M. Flanigen
U.K. Patent 1,574,840 (1980).

[29] R.W. Grose and E.M. Flanigen
U.S. Patent 4,104,294 (1978).

[30] F.G. Dwyer and E.E. Jenkins
U.S. Patent 4,287,166 (1981).

[31] L.D. Rollman and E.W. Valyocsik
European Patent Application 15,132 (1980).

[32] L.M. Parker and D.M. Bibby
Zeolites, 1983, 3, 8.

[33] M.G. Howden
CSIR Report, CENG 413, 1982.

CHAPTER 4

Silicalite Synthesis in the Amine-TPABr-SiO_2-H_2O System

4.1 Introduction and Literature Review

When silicalite is crystallised from reaction mixtures that contain alkali metal cations, the as-synthesised crystals are always found to have a metal component; the products are metal organosilicates. The metal content can be considerable as has been shown by the results in Chapter 3 and elsewhere [1,2,3]. Charged metal cations are deleterious to the organophilicity of the lattice and so too are the silanol groups that may remain when the metal ions are removed. Preparation of silicalite in systems free of metal cations should give less defective and hence more organophilic products.

Two synthesis routes to alkali metal free silicalite are known. Several workers have crystallised silicalite in the TPA_2O-SiO_2-H_2O system [2,4,5,6]. The tetrapropylammonium hydroxide reagent ($2TPAOH \equiv TPA_2O + H_2O$) acts as both the source of quaternary cations and the source of hydroxide ions. As such, separate control of the base and TPA content of mixtures is not possible. In addition, commercially available TPAOH often contains alkali metal impurities [7] and is not easy to store (because of CO_2 absorption) or cheap (relative to TPABr mole per mole). Furthermore when large amounts of base are required to effect crystallisation, substantial amounts of the expensive quaternary often remain in solution at the end of the reaction and hence are wasted. There are therefore some drawbacks to the use of TPAOH in synthesis mixtures.

The second known route to silicalite from metal free mixtures is an adaption of the methodology used by Bibby et al [8] to crystallise metal free ZSM-5 and relates to the use of ammonium hydroxide in mixtures. Subsequent to the aforementioned work [8], von Ballmoos [9] and Ghamami and Sand [6] reported crystallisation of aluminium-free ZSM-5 (silicalite) in the $(NH_4)_2O$-TPA_2O-SiO_2-H_2O system. The latter also investigated synthesis in the $(NH_4)_2O$-TPABr-SiO_2-H_2O system.

When ammonium hydroxide ($2NH_4OH \equiv (NH_4)_2O + H_2O$) is used in reaction mixtures, ammonium ions can become incorporated in crystalline products [10] and although they, unlike metal cations, can be removed simply by calcination it is possible that residual associated defect sites (internal silanol groups) may remain in silicalite products.

This chapter details a study of silicalite crystallisation in the amine-TPABr-SiO_2-H_2O system, a route to alkali metal free silicalite that has not previously been reported. Mixtures are free of alkali metal cations, the use of TPAOH is avoided and separate control of the base and template concentration is afforded. The presence of amines in the mixtures has further advantages; their buffering ability enables the pH to be controlled during reaction and high product yields are obtained. It was envisaged that by judicious choice of amine, incorporation of the weak organic base in the silicalite crystals could be avoided. To that end the cyclic amine piperazine was used for the initial experiments. Before experimental details are given, mention is made of further literature salient to the present investigation.

Amines have been extensively used in zeolite synthesis [11]. In the main they have been employed as 'templates' and pore-fillers for high silica zeolites and, although weak bases themselves, in most cases they have been used in conjunction with strong inorganic bases such as sodium hydroxide. Presumably most of these reactions were carried out at relatively high pH as a consequence. Crystallisation of high silica zeolites (e.g. ZSM-5) at lower pH from systems which contained both weak and strong bases was investigated by Rollmann [12]. Neutralisation of all or part of the strong base added gave the low reaction pH conditions with most of the residual alkalinity derived from the weak base.

The studies described in this chapter detail silicalite crystallisation in the amine-TPABr-SiO_2-H_2O system. The reaction mixtures contain two organics, a relatively uncommon situation. Rollmann and Valyocsik [13] crystallised several high silica zeolites (e.g. ZSM-5, ZSM-35) from reaction mixtures that contained, in addition to the 'template' organic, a second organic component (quaternary ammonium compounds and amines) to modify the morphology of the crystals. The second organic was often bulky, virtually excluding any from being

trapped along with the template organic in the pores of the zeolite. The presence of two organics in synthesis mixtures (quaternaries and amines) was recently reported to have a synergistic effect on the crystallisation of ZSM-5 and ZSM-11 [14].

The reaction systems of the present investigation contain only weak bases as mineralisers and this too is a relatively uncommon situation in synthesis. There are only a few reports in the literature of such instances. Crystallisation of ZSM-48 [15] in the hexamethylene diamine-Al_2O_3-SiO_2-H_2O system (and also from Al-free mixtures) was investigated by Araya and Lowe [16]. Mixtures were free of alkali metal cations and the amine acted as the mineraliser and as the pore-filler for the crystals. It is of interest that the microporous crystalline aluminophosphates recently discovered and patented [17] are also made in systems which are free of alkali metal cations. Many crystallisations were performed in the amine-Al_2O_3-P_2O_5-H_2O system with an amine again functioning as both the base and the 'template'.

Crystallisation of silicalite-1 in the amine-TPABr-SiO_2-H_2O system is now discussed. Mixtures are free of alkali metal cations and at the planning stage of this work it was envisaged that the two organics would have separate roles; the amines would supply the alkalinity required for crystallisation whilst the TPABr would supply the structure-directing quaternary cations.

4.2 Experimental

4.2.1 Equipment

Syntheses were carried out in autoclaves and steel bombs. The stainless steel autoclaves (Figure 4.1) were designed and constructed by Baskerville and Lindsay Ltd. and had a capacity of 500 cm^3. Typically, they were charged to about 4/5 capacity; for safety reasons some void volume has to be left for gases and vapours and for liquid expansion at elevated temperatures. Each autoclave was equipped with a magnetically driven paddle stirrer, a dip-tube for sampling purposes, a sample valve, a pressure valve, gas inlet/outlet valves and a thermocouple pocket. The stirrer speed and temperature could be regulated and monitored. The gas valves were required for sampling

Figure 4.1 (overleaf)

A 500 cm^3 stainless steel autoclave with control unit

FIG. 4.1

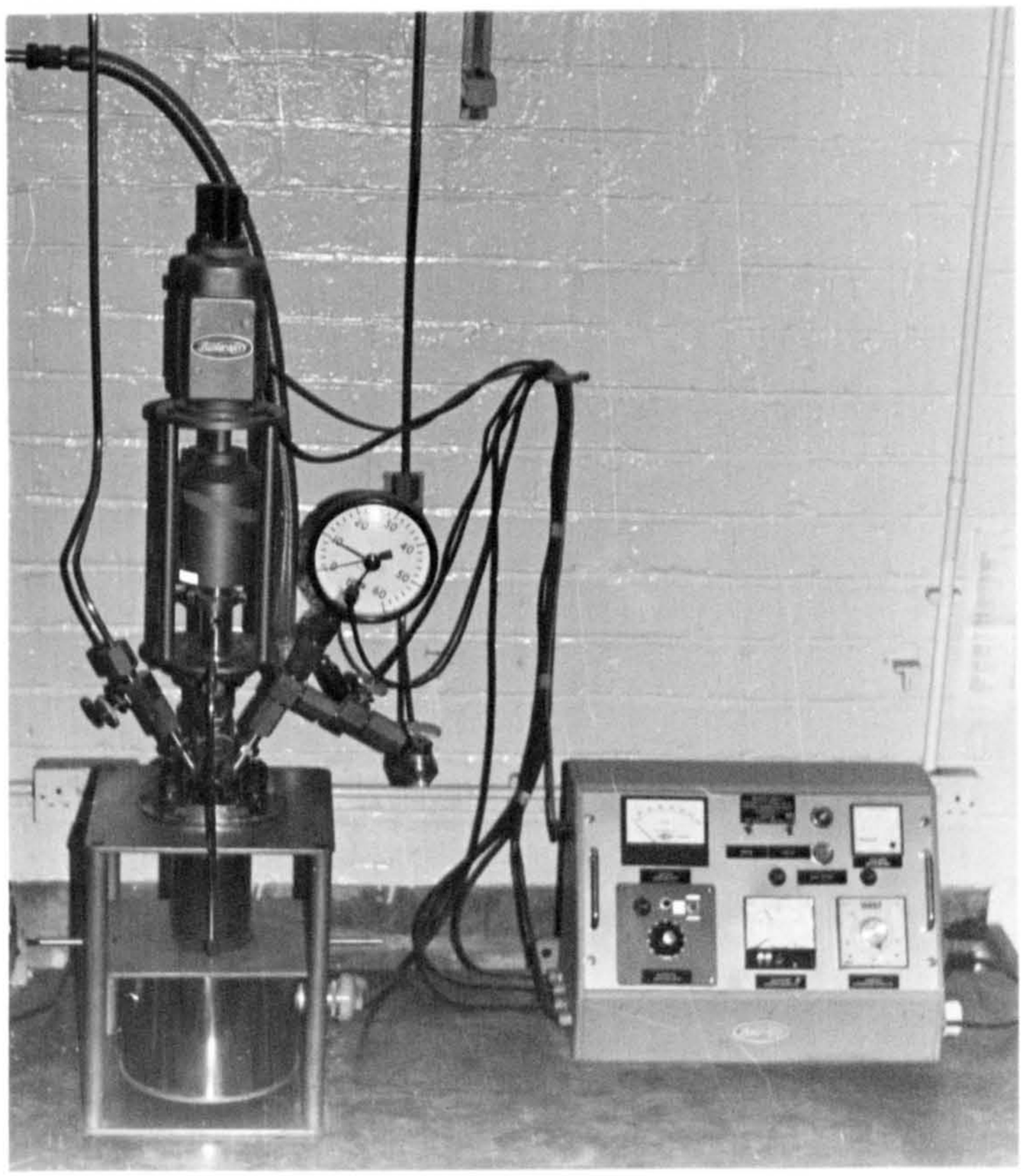

purposes on occasions when the autogenous reaction pressure was near atmospheric and therefore insufficient to force material through the dip-tube and out of the vessel. When this was the case, nitrogen was let into the autoclave before samples were taken and vented off immediately afterwards. An external heater controlled by a thermocouple pocketed inside the autoclave enabled the reactions to be thermostatted at any desired temperature. The thermostat controls were regularly calibrated with a Comark thermocouple. A meter enabled the pressure inside the autoclave to be monitored. Four identical autoclaves were available for the experiments and each was fitted with three safety devices in case of mishap; a pressure trip, a temperature over-ride and a bursting disk (45 atmospheres).

The screw-top stainless steel bombs (Figure 4.2) were fitted with teflon liners and were manufactured by engineers at the University of Edinburgh. They had a capacity of 30 cm^3. For safety reasons during runs a small space was again left void. The reactions were carried out in a thermostatted air oven under static conditions.

4.2.2 Materials

The amines used in the syntheses are shown in Table 4.1. The other reagents were silica (Cab-O-Sil M5, BDH Ltd.), tetrapropylammonium bromide (Fluka, purum grade) and glass-distilled water.

4.2.3 Synthesis procedure

The reaction mixtures were prepared in exactly the same way as those previously described (section 3.2.4) except that the amine was added (as received, not as an aqueious solution) in place of the sodium hydroxide solution. Typically mixtures for the autoclave reactions were made up using 400 g water, those for the bombs with 60 g water. Although the bombs could only accommodate about 25 cm^3, mixture preparatio was easier and weighing errors were smaller when a larger batch was prepared. After preparation mixtures were immediately charged to the reaction vessels and temperature control was initiated. Reactions were timed from this moment. All crystallisations were carried out in closed systems and were therefore not perturbed by absorption of atmospheric carbon dioxide.

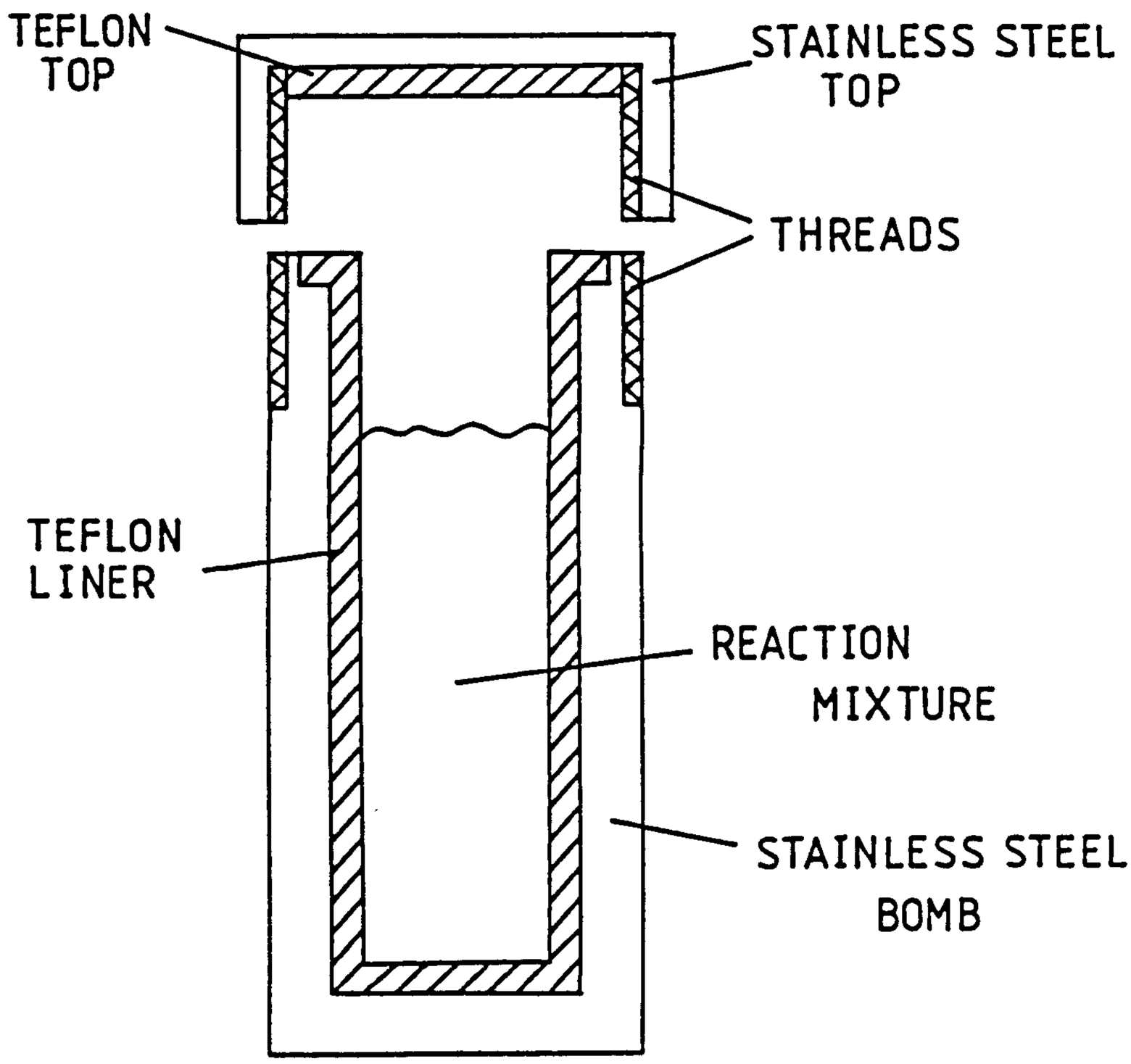

Figure 4.2 Schematic drawing of a stainless steel screw-top bomb

Table 4.1 Amines used in the reaction mixtures

NAME	FORMULA	SOURCE / GRADE
PIPERAZINE[a]	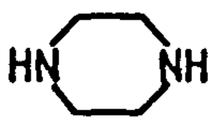	ALDRICH (98%)
1,4-DIAZABICYCLO(2,2,2)OCTANE	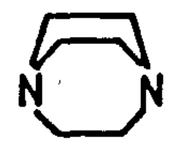	ALDRICH (97%)
l-METHYLBENZYLAMINE	$C_6H_5CH(CH_3)NH_2$	ALDRICH (98%)
TRIS(HYDROXYMETHYL)METHYLAMINE	$NH_2C(CH_2OH)_3$	BDH (>99%)

[a] as hexahydrate

During the autoclave reactions samples were taken. Once cool, pH measurements were made. Samples were stored in small glass bottles in a thermostatted room (20°C) and after reactions were complete pH measurements were re-taken. The bomb reactions were not sampled but periodically the bombs were removed from the thermostatted oven, quench cooled to room temperature under running water and opened so that pH measurements could be made. This did not require material to be removed from the bomb, the pH electrode itself was immersed into the mixture. The appearance of the solution phase was always noted and a minute amount of the solid was removed on a spatula for examination by optical microscopy. The bombs were open to the atmosphere for about 20 minutes on each occasion measurements/examinations were made. During this short time carbon dioxide absorption is not thought to have significantly affected the pH of any of the mixtures. After re-sealing the bombs were returned to the oven. These cooling/re-heating procedures probably perturbed the crystallisation kinetics but they are far less likely to have affected the overall course of the reactions, i.e. the positions of the initial and final solid-liquid equilibria. The bombs were opened about a day after the start of a reaction (to get a measure of the induction period pH) but only once or twice thereafter. The final reaction pH was always measured.

Most of the reactions were terminated on the basis of the following criteria: (i) a gel-free solid phase (optical microscopy), (ii) a clear mother liquor and (iii) concordant pH measurements on consecutive days (applicable to autoclave reactions only). The intermediate solids from the samples and all final products were separated from their respective solution phases and mother liquors and repeatedly washed with distilled water until the pH of the washings were near neutral and bromide free. The solids were dried in an oven at 60°C and then equilibrated with water vapour.

4.2.4 Analytical Techniques

The final products were characterised by XRD. The following techniques have also been used in this study:

pH measurements
Thermal gravimetric analysis
Differential thermal analysis
Elemental analysis (C, H, N)
Scanning electron microscopy
Optical microscopy

4.3 Results and Discussion

Details of the syntheses undertaken, the pH changes during the reactions and the products obtained are given in Tables 4.2 and 4.3. None of the mixtures contained sufficient base to initially depolymerise all the amorphous silica. Indeed the initial pH in all cases was relatively low. The crystallisations proceeded in three stages: (i) nucleation, (ii) growth of crystals at the expense of the amorphous gel and (iii) crystal growth from clear solution after depletion of all the gel. Crystals and gel usually fractionated when samples were taken and the growing crystals were often large enough to be seen under the optical microscope. In most cases there was evidence that growth occurred by a solution phase ion transportation mechanism. In the bombs the crystals and gel were sometimes seen in more intimate contact probably because of the static reaction conditions.

4.3.1 Reactions in the Piperazine-TPABr-SiO_2-H_2O System

The pH and X-ray diffraction results for reactions A1-A3 are shown in Figure 4.3. Each pH curve shows two regions of pH constancy, one during the induction period and the early stages of growth and the other during the latter stages of the reaction. The pH decreases during the reactions because base molecules are consumed as the crystals grow; silicalite has ideal unit cell composition 4TPAOH 96SiO_2. The incorporation of base into the crystals in effect generates acid in solution; it necessitates increases in the concentrations of protonated amine and hydronium ion in the solution phase to provide counter-charge for all the bromide ions that remain there. A more detailed discussion of these changes is given in Chapter 5.

Table 4.2 Autoclave reactions[a]: compositions investigated and products obtained

Reaction Code	Amine	Mixture Composition (moles)				Temp/ °C	Time/ days	Product[b]	Initial pH	Final pH	ΔpH
		Amine	TPABr	SiO_2	H_2O						
A1	Piperazine	5	2	20	1000	100	13	Silicalite-1	10.91	10.50	-0.41
A2	Piperazine	10	2	20	1000	100	14	Silicalite-1	11.04	10.75	-0.29
A3	Piperazine	15	2	20	1000	100	16	Silicalite-1	11.27	10.97	-0.30
A4	Piperazine	20	2	5	1000	100	19	Silicalite-1	11.14	11.07	-0.07
A5	Piperazine	1	2	20	1000	150	9	Silicalite-1 + Am	10.25	8.06	-2.19
A6	1-methylbenzylamine	2	2	10	1000	175	9	Silicalite-1	10.54	9.97	-0.57
A7	1-methylbenzylamine	2	-	10	1000	175	21	Cristobalite	10.41	10.78	+0.37
A8	Piperazine	5	2[c]	20	1000	100	98	Silicalite-2 + Am	10.90	10.47	-0.43
A9	TRIS[d]	5	1	10	1000	200	7	Silicalite-1 + Am	9.99	9.34	-0.65

[a] All reactions were stirred at 300 rpm

[b] Unless otherwise stated the products were fully crystalline as shown by X-ray powder diffraction, optical microscopy and in most cases SEM. (Am = amorphous material).

[c] TBABr used (tetrabutylammonium bromide; Fluka, puriss grade).

[d] Tris(hydroxymethyl)methylamine

Table 4.3 Bomb reactions[a]: compositions investigated and products obtained

Reaction Code	Amine	Mixture Composition (moles)				Temp/ °C	Time/ days	Product[b]	Initial pH	Final pH	ΔpH
		Amine	TPABr	SiO_2	H_2O						
B1	Piperazine	5	2	20	1000	150	7	Silicalite-1	10.70	10.53	-0.17
B2	Piperazine	10	2	20	1000	150	25	Silicalite-1	11.00	10.67	-0.33
B3	Piperazine	15	2	20	1000	150	25	Silicalite-1	10.94	10.71	-0.23
B4	Piperazine	1	2	20	1000	150	19	Silicalite-1 + Am	10.15	9.00	-0.85
B5	Piperazine	5	-	20	1000	150	25	Amorphous	-	10.67	-
B6	DABCO[c]	10	-	20	1000	150	25	Amorphous	-	10.40	-
B7	Piperazine	20	-	20	1000	150	12	ZSM-48 + Am	-	-	-

[a] All reactions were carried out under static conditions

[b] Unless otherwise stated the products were fully crystalline as shown by X-ray powder diffraction, optical microscopy and in most cases SEM. (Am = amorphous)

[c] 1,4-diazabicyclo[2,2,2]octane

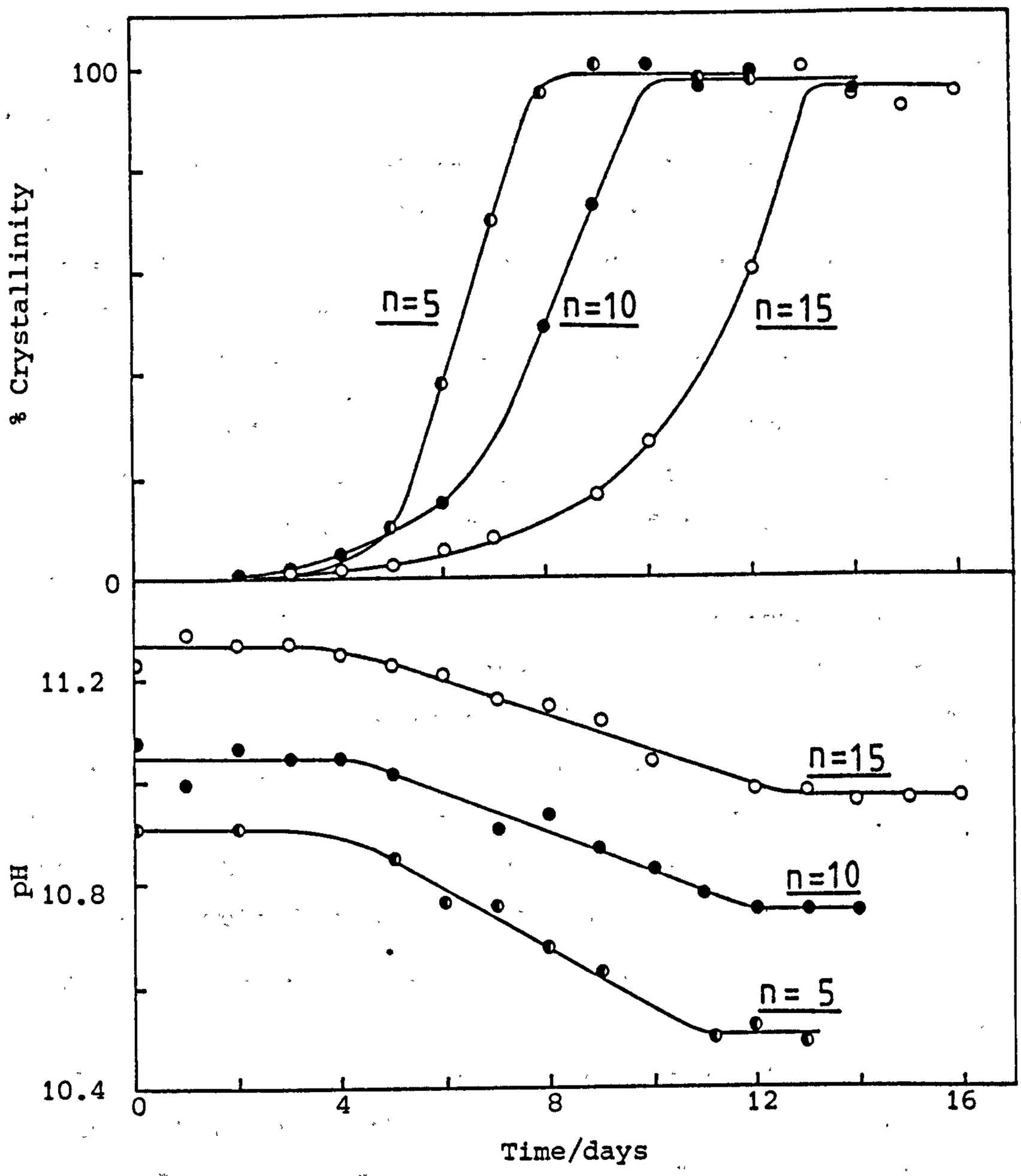

Figure 4.3 % crystallinity and pH of samples taken during reactions A1 (n = 5), A2 (n = 10) and A3 (n =15). Values of 'n' indicate the piperazine content of the mixtures, namely n-piperazine 2TPABr $20SiO_2$ $1000H_2O$

The 100°C autoclave reaction A1-A3 (Table 4.2) and the 150°C bomb reactions B1-B3 (Table 4.3) had identical compositions and the initial and final pH values of both sets of reactions exhibited the same trends with piperazine content (Figure 4.4) despite the fact the autoclave and bomb reactions were carried out under different conditions (stirred vs static, different reaction vessels). The greater solubility of the gel and crystalline phases at 150°C gives rise to slightly lower initial and final pH values. It is significant that even though all the pH measurements were made at ambient temperatures, the results in Figure 4.4 do correctly reflect the different solubilities of the amorphous and crystalline solid phases at different temperatures. It appears that equilibration at low temperature is slow and that high temperature equilibrium conditions are in effect frozen on cooling.

The samples taken during reactions A1-A3 enabled the crystallisations to be followed visually. Crystals and gel could be easily distinguished; after sampling the crystalline material sedimented rapidly and when gel was also present the solids fractionated into two distinct layers. For reaction A3 some quantitative measurements were made. The depths of the respective solid layers in the sample bottles, which were proportional to the volumes of the solids, were measured with a magnifier. The information obtained correlates well with the XRD and pH data (Figure 4.5). The results clearly show the transformation of the amorphous gel into a crystalline solid. The 'apparent' total volume of solid per sample decreased by ca. 80% during crystallisation.

The plots shown in Figure 4.3 contain a wealth of further information about reactions A1-A3. In each case, the point when maximum crystallinity is attained indicates when essentially all the gel has been polymerised although not the end of the reaction; the final stages of crystal growth occur from clear solution. This final crystallisation was accompanied by a considerable decrease in pH for reaction A1 (about 0.15 pH units), somewhat less for reaction A2 (0.08 pH units). For reaction A3 the pH and XRD results are in better agreement, i.e. pH constancy was observed immediately maximum crystallinity was attained. A possible explanation for the discrepancy between the pH and XRD results for reactions A1 and A2 is that crystallisation continues from clear solution (possibly a dilute sol) once all the amorphous gel has

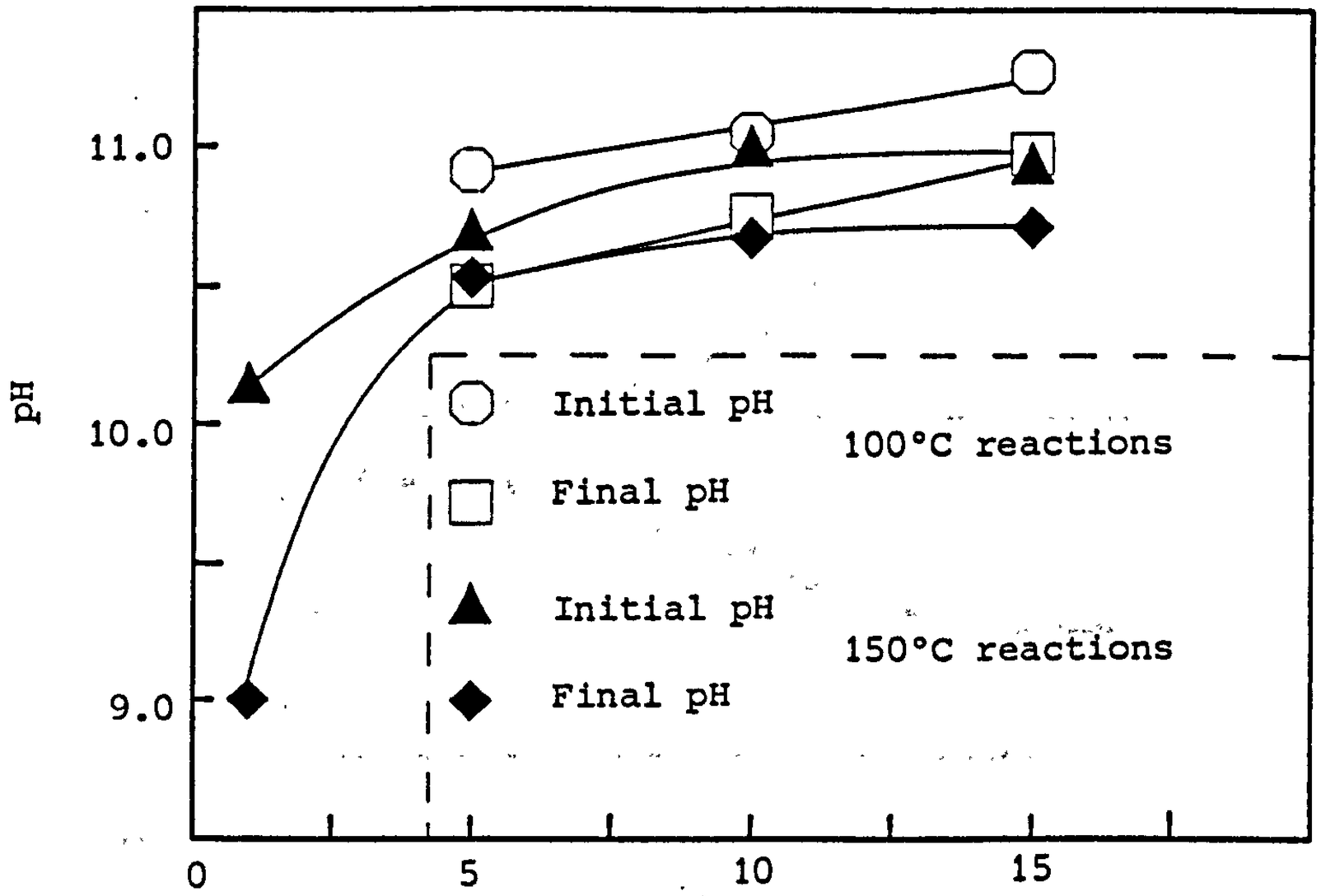

Figure 4.4 Overall pH changes that accompany silicalite crystallisation in the system n-piperazine 2TPABr $20SiO_2$ $1000H_2O$. Reactions at 100°C were carried out in autoclaves and stirred at 300 rpm, those at 150°C were carried out under static conditions in steel bombs.

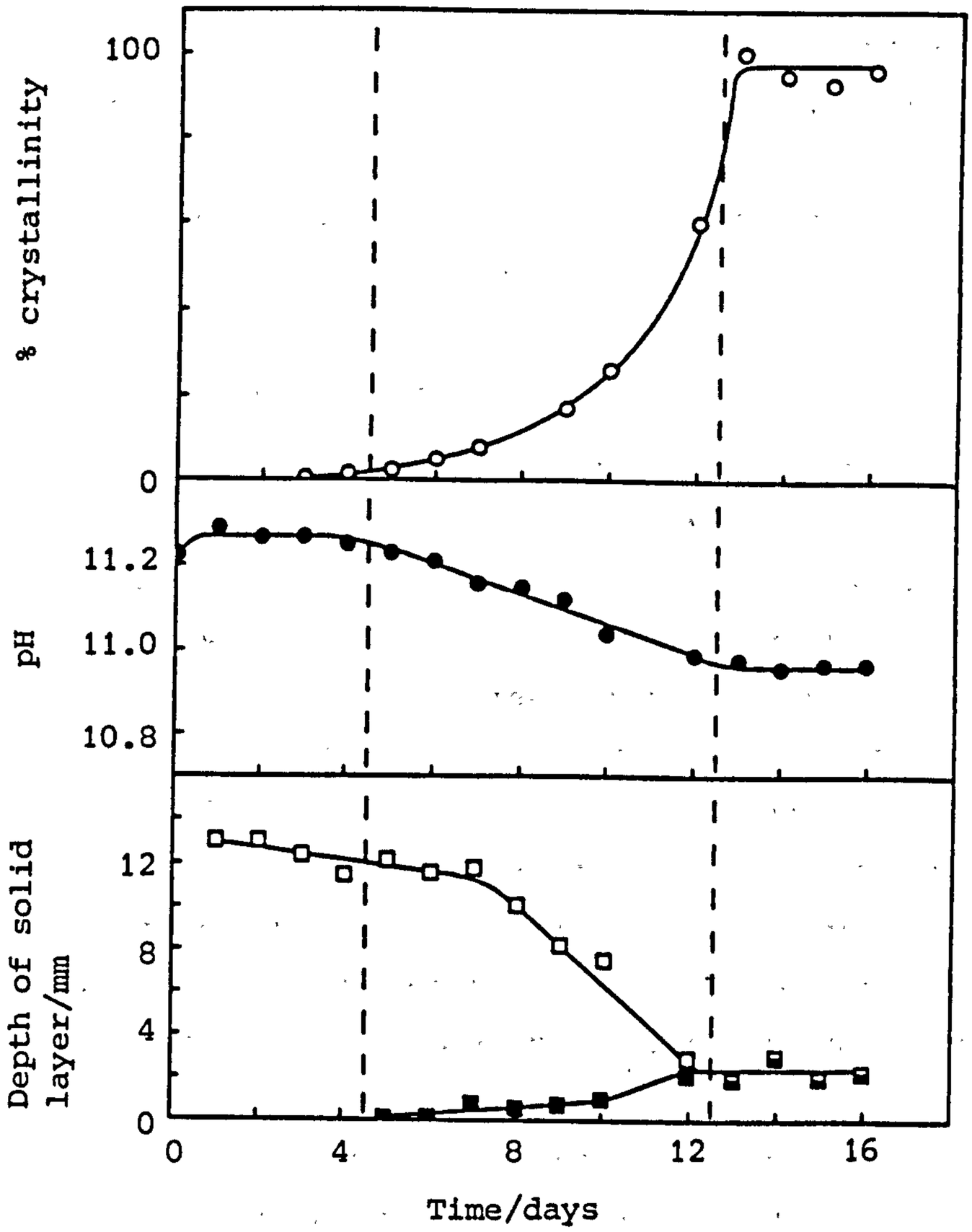

Figure 4.5 Correlation of the solid content of samples taken during reaction A3 with their crystallinity and pH: □, total depth solid; ■, depth of crystalline material

been consumed. It is probably significant that the effect is most marked in the least buffered system and it seems likely that the amount of extra crystallisation is relatively small. Recrystallisation of the more soluble crystals to less soluble forms could perhaps also contribute to the observed discrepancies. Buffering effects were probably the reason why no pH rises associated with solubility transfer were observed during any of the reactions at near 100% crystallinity. By comparison, when silicalite is crystallised in strong base systems mixtures are generally less buffered and pH rises are often observed; only in extremely unbuffered systems was the pH seen to fall throughout reaction (see Section 3.3). Theoretical aspects of the buffering action by amines are described in Chapter 5.

The crystallinity curves in Figure 4.3 gave information about the reaction kinetics. As a precautionary measure all three reactions were carried out in the same autoclave to eliminate possible effects of using different vessels. It can be seen from Figure 4.3 that the amount of amine in mixtures had little effect on the length of the induction period (as gauged from the onset of X-ray crystallinity) but it markedly affected the rate of crystal growth. As a consequence of the low and similar reaction pH values, the total mass of solid present during the gel-silicalite transformation period was probably large and similar in all three cases and the gradients of the crystallinity curves can therefore be compared to give a relative measure of the respective rates of crystallisation (see section 3.3.7.5 for explanation). From Figure 4.3 it can be seen that an increase in the piperazine content of the reaction mixture increased the reaction pH (as expected) but decreased the rate of crystallisation. This is an unusual situation. Normally crystallisation kinetics are retarded at high pH (see section 3.3.7.5) and often it is the increased concentration of hydroxide ions that is predominantly the cause. The pH of these amine reactions was relatively low and the growth kinetics here were not retarded by excessive alkalinity (hydroxide ion concentration). The pH(t) curves for reactions A1-A3 in Figure 4.3 also provide some evidence that crystallisation is retarded by an increase in mixture amine content; the time taken for the pH to fall from its initial value to its final one increased with the amount of piperazine in the reaction mixture

(A1, 7 d; A2, 7.8 d; A3, 8.5 d). The results indicate that optimum kinetics in this amine system would be seen at abnormally low pH. Rollmann [12] has also observed that the use of excess amine in reaction mixtures can severely retard the crystallisation process.

Results obtained from elemental analysis and thermal analysis indicated a possible cause of this anomalous kinetic behaviour. The carbon, hydrogen and nitrogen contents of the as-made crystals are shown in Table 4.4. If only TPA species were entrapped in the pores the expected C/N ratio would be near 12. The results clearly indicate that as the amount of piperazine in a mixture increases, so too does the amount of piperazine (C/N = 2) incorporated in the crystals (decomposition of either organic is unlikely under the comparatively mild reaction conditions). Moreover, there is insufficient space for any piperazine if TPA species occupy all channel intersections and the amine molecules must therefore be included in the crystals at the expense of the quaternary.

The fraction of piperazine molecules (f_p) in the as-made crystals is obtained from the formula:

$$y = \frac{12(1 - f_p) + 4f_p}{(1 - f_p) + 2f_p} \qquad (4.1)$$

where y is the C/N atomic ratio from analysis and $(1 - f_p)$ is the mole fraction TPA. Rearrangement gives:

$$f_p = \frac{12 - y}{8 + y} \qquad (4.2)$$

Calculated values of f_p are given in Table 4.4 and depicted in Figure 4.6. Over a tenth of the organic molecules in the product from reaction A3 are piperazine molecules.

Thermal analysis also gave evidence of piperazine incorporation in the crystals. Results from Differential Thermal Analysis are shown in Figure 4.7. The exotherm due to oxidative degradation of the TPA ions (330-510°C) is seen in all cases, the higher temperature exotherm (510-660°C) is due to decomposition of piperazine and is essentially absent when silicalite is crystallised in the presence of only small

Table 4.4 Carbon, hydrogen and nitrogen contents of reaction products (elemental analysis)[a]

Reaction Code	n[b]	%C	%H	%N	C/N atomic ratio	f_p[c]
A1	5	9.03	1.98	0.94	11.2	0.042
A2	10	9.04	2.03	0.97	10.9	0.060
A3	15	9.15	2.06	1.07	10.0 (±0.1)	0.113

[a] Results are given as wt %

[b] Piperazine content of reaction mixture (moles)

[c] Fraction of piperazine molecules in the as-synthesised crystals (calculated from equation (4.2)).

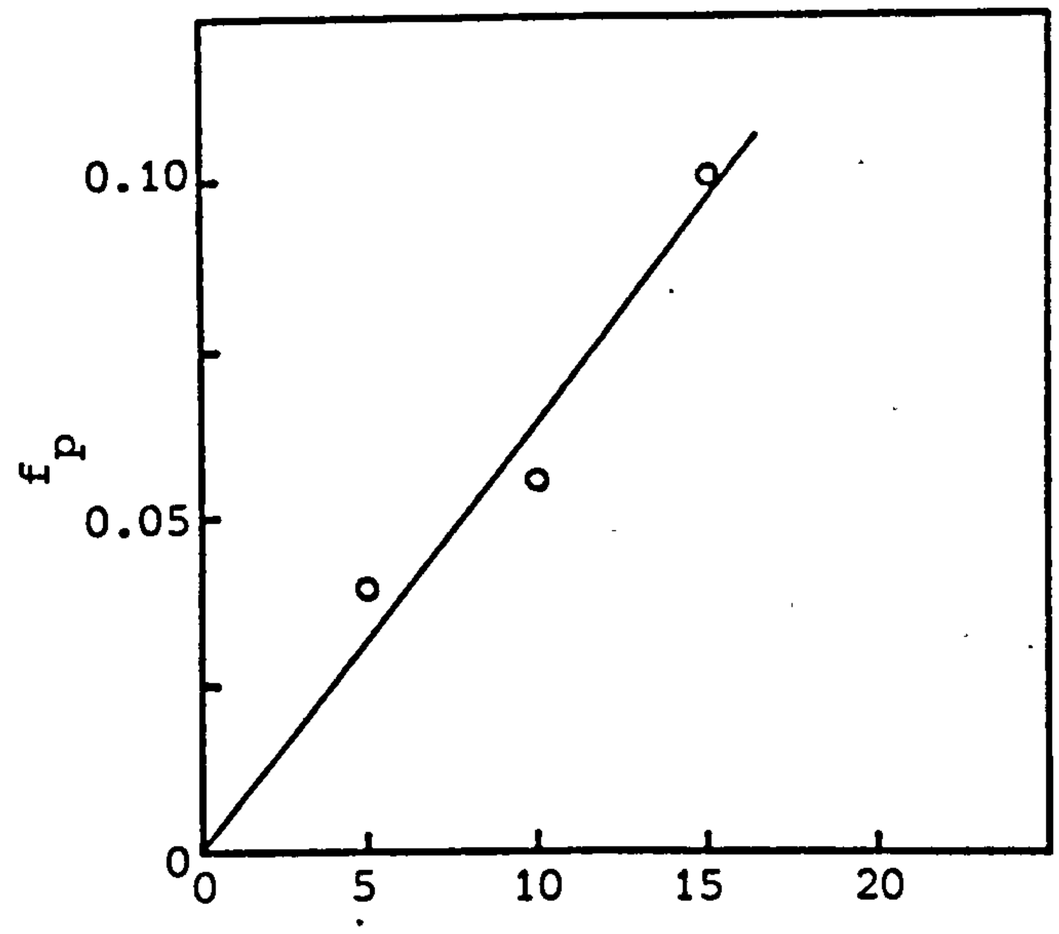

Figure 4.6 Relationship between the fraction of piperazine molecules in the silicalite precursor (f_p) and the number of moles of piperazine (n) in the mixture composition n-piperazine 2TPABr $20SiO_2$ $1000H_2O$

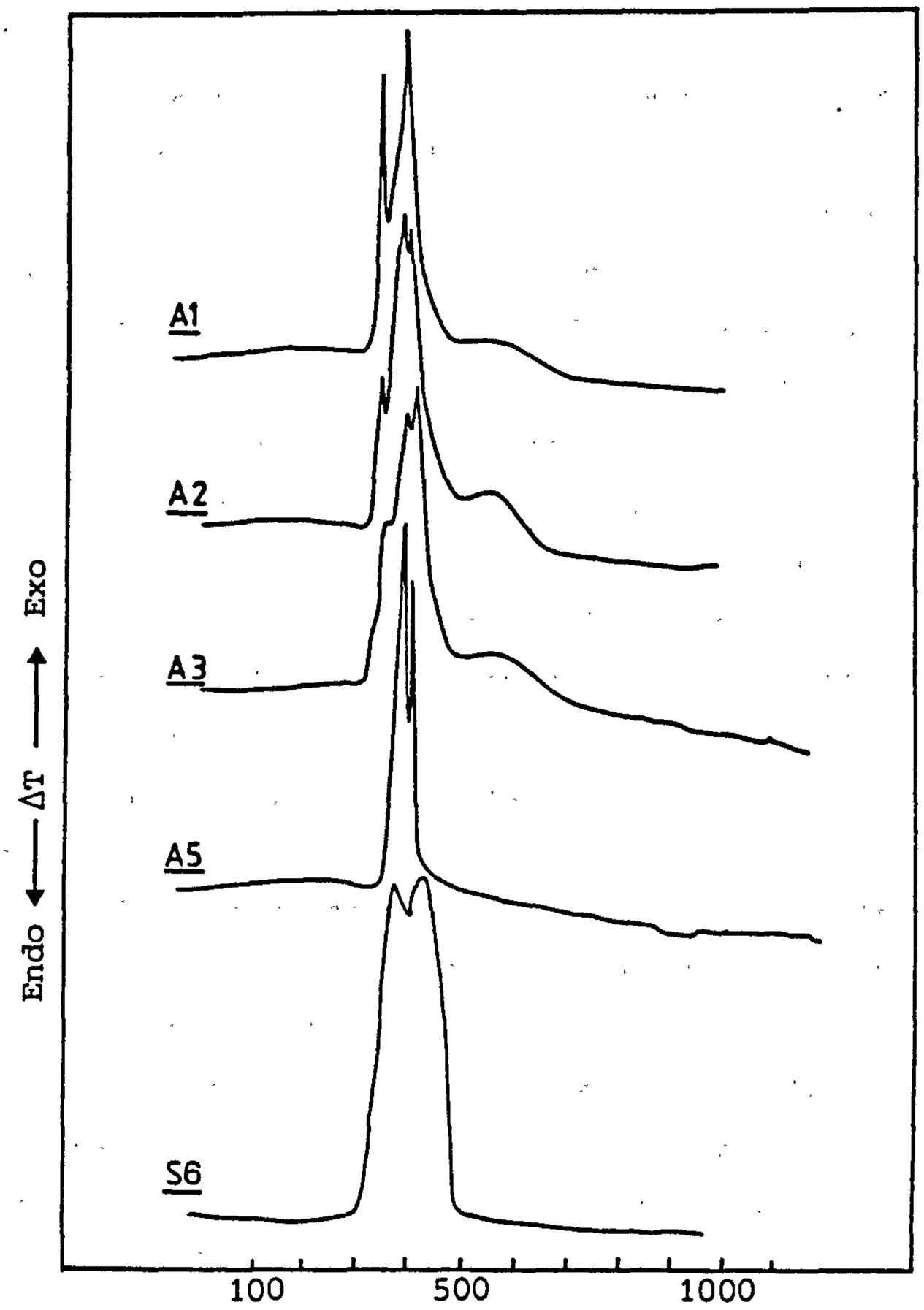

Figure 4.7 DTA curves of as-synthesised products. Product S6 was crystallised from a mixture of composition $2.0Na_2O$ 2TPABr $20SiO_2$ $1000H_2O$ at 95°C (see Chapter 3)

amounts of piperazine (reaction A5) and when crystallisation is effected in conventional strong base systems (reaction S6, see Figure 4.7).

Results from thermal gravimetric analysis are shown in Figure 4.8. Loss of water, decomposition of organic material and high temperature dehydroxylation (loss of chemical water) were observed in each case. The scheme outlined in Figure 4.9 was used to calculate the quantitative data given in Table 4.5. Losses B and C together (B+C = D) give a good estimate of the weight of $Org^{+}OH^{-}$ equivalent in the products and from the table it can be seen that the amount found per unit weight of anhydrous silicalite was near constant and slightly larger but similar to that expected if the crystals had ideal unit cell composition 4TPAOH $96SiO_2$ (wt TPAOH/wt SiO_2 = 0.141). However, as already mentioned, results from elemental analysis indicated some piperazine molecules were trapped in the crystals and from molecular weight considerations this necessitates that, in each case, an average of about two piperazine molecules (total weight of two molecules = 2 x 104.15 = 208.30 if each is assumed monoprotonated) displace each equivalent of TPAOH (M.Wt. = 203.37). Clearly entrapped piperazine molecules could also be unprotonated or diprotonated. Framework attack, although possible, is likely to be less extensive (mole per mole) than attack by TPAOH because piperazine is a weak base. However, amine incorporation, if substantial, could have adverse effects on the organophilicity of the crystals (increased lattice defects after calcination).

The similarity between the length of a piperazine molecule and the length of a propyl group on the quaternary is qualitatively shown in Figure 4.10(a) and as already mentioned it seems likely that at least two piperazine molecules are incorporated for each molecule of quaternary displaced (Figure 4.10(b)). Results obtained from thermal analysis do not allow calculation of either the exact number of inter-sections occupied by amine molecules or the exact number of amine molecules that displace each TPAOH molecule because of overlapping organic/water weight losses and the relatively small number of amine molecules present. Some intersections may contain two molecules, others one and some perhaps the likely maximum of four. Variation such as this would be expected if piperazine incorporation was a random process although not if it was thermodynamically controlled. Also, the very

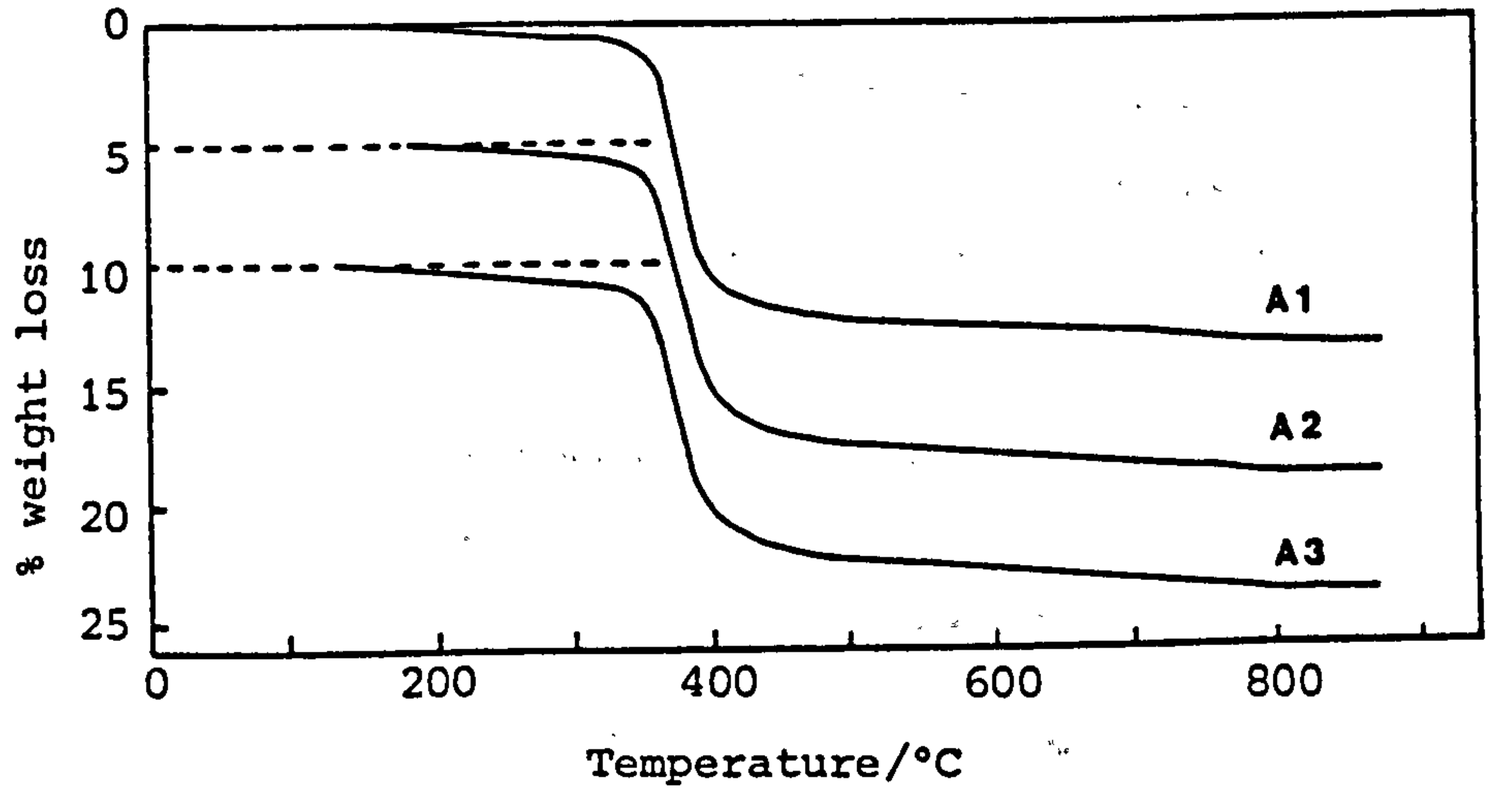

Figure 4.8 TGA curves of the as-synthesised products from reactions A1, A2 and A3. The curves are displaced by 5 units on the ordinate axis.

Figure 4.9 Scheme proposed for interpretation of TGA curves

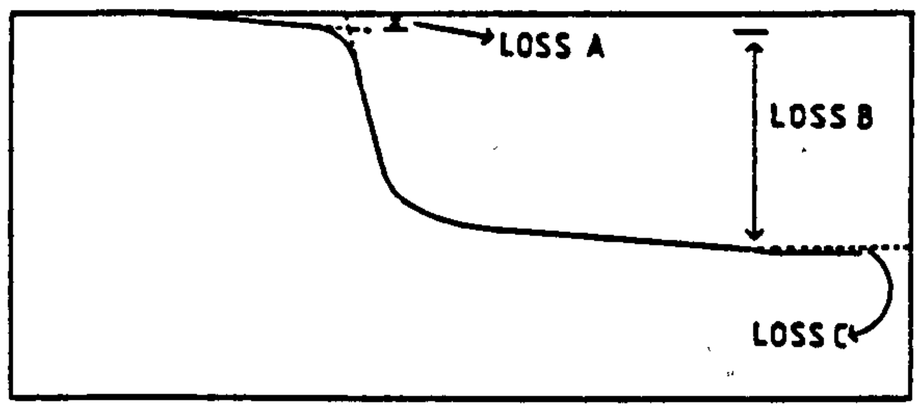

LOSS A (T<~350°C) : Dehydration ($-H_2O$)

LOSS B (T~350-750°C) : Decomposition of organic

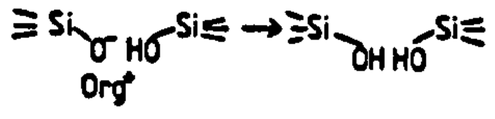

LOSS C (T~750-800°C) : Loss of chemical water

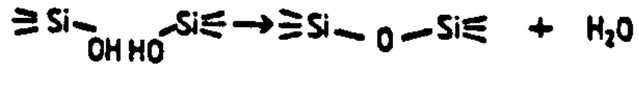

Notes:

(1) There is some overlap between losses A & B and losses B & C

(2) Both TPA and piperazinium cations (designated together as 'Org^+' in the scheme above) are present in as-made crystals. Some uncharged amine will also be present.

(3) Most of the organic cations will be co-ordinated to the lattice, little 'free' base will be present.

(4) All adjacent silanol groups probably do not dehydrate (loss C).

(5) Loss of physical and chemical water from the external surfaces of crystals will contribute to losses A and C respectively. However the external surface area is a small fraction of the total (internal + external) and therefore loss A can be assumed to give the intracrystalline water content and losses B and C together (D = B + C) give an estimate of the amount of organic base (Org^+OH^-) in the crystals.

Table 4.5 Results obtained from the TGA curves shown in Figure 4.8 using the scheme proposed in Figure 4.9

Reaction Code	Loss A wt %	Loss B wt %	Loss C wt %	Loss D[a] wt %	R[b]
A1	1.0	12.0	0.6	12.6	0.146
A2	1.0	12.5	0.4	12.9	0.150
A3	1.1	12.4	0.5	12.9	0.150
	(±0.1)	(±0.1)	(±0.1)	(±0.1)	(±0.002)

[a] D = B + C, the total weight loss due to the organic base

[b] R = D/(100 - A - D), the organic base to dry silicalite weight ratio

Figure 4.10 Schematic drawing of organic species in the channels of the silicalite precursor

(a)

TPA

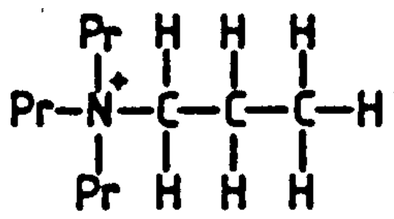

Piperazine

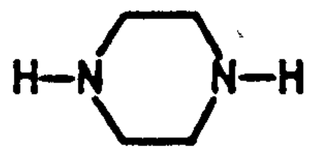

(b)

(TPA)-silicalite

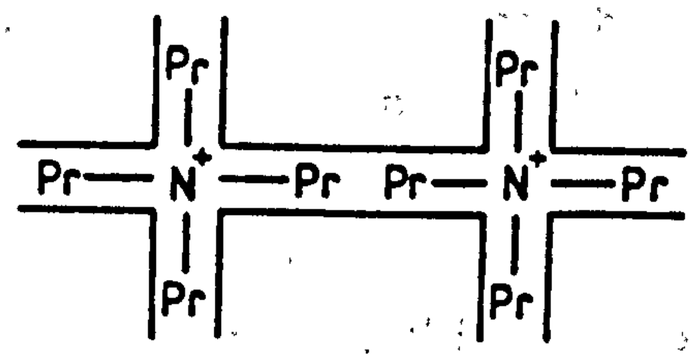

(TPA, piperazine)-silicalite

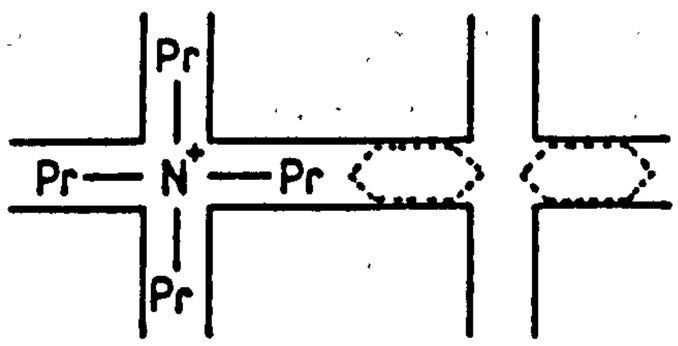

tight fit of piperazine molecules in the channels may cause selective channel occupation. By analogy, post-calcination sorption experiments show that very little cyclohexane, of similar cross-section, is sorbed into materials with silicalite-1 type structure [1,3,18]. The dual pore system of the crystals consists of circular and elliptical channels and piperazine molecules incorporated during synthesis may be preferentially sited; location in the elliptical channels seems likely. Regardless of the exact siting of the amine molecules, the vacant voidage in the precursor crystals is probably increased when piperazine is incorporated (TPA is the ideal fit for the channels). This would be expected to have an adverse effect on the thermodynamic stability of the crystals. This is probably a contributory reason for the anomalous kinetic results observed for reactions A1-A3 (Figure 4.3). At a mechanistic level, an increase in the amount of amine in a mixture is likely to cause increased competition between piperazine and TPA species for adsorption on or coordination to the surfaces of the gel and crystalline solids.

The results for reaction A4 show that the pH change during crystallisation can be controlled by careful choice of mixture stoichiometry (Figure 4.11). Reaction A4 contained more piperazine and less silica than reaction A3, a smaller percentage of the total base was consequently removed from the solution during crystallisation and the overall pH change therefore decreased (-0.30 and -0.07 respectively for reactions A3 and A4). Inspection of the samples taken during these reactions again showed the retarding effect of the amine. After 13 days the sample taken from reaction A3 appeared to be gel-free (confirmed by XRD, see Figure 4.3), whereas that from reaction A4 still contained amorphous material (after prolonged standing the 'solution' phase remained hazy because of small particles of amorphous material in suspension) even though this mixture contained only a quarter of the silica present in reaction A3. Anomalously the initial pH of reaction A4 was lower than that of reaction A3. The C/N atomic ratios of the organic material in the final products were similar (9.97 and 10.01 respectively). The results in Figure 4.11 show that if substantial amounts of amine are used in mixtures it is possible to buffer these systems and maintain near constant pH throughout crystal growth. This is thought to be beneficial. Such pH control is not possible when strong bases are employed as mineralisers as pH changes inherently accompany crystallisation (see section 3.3).

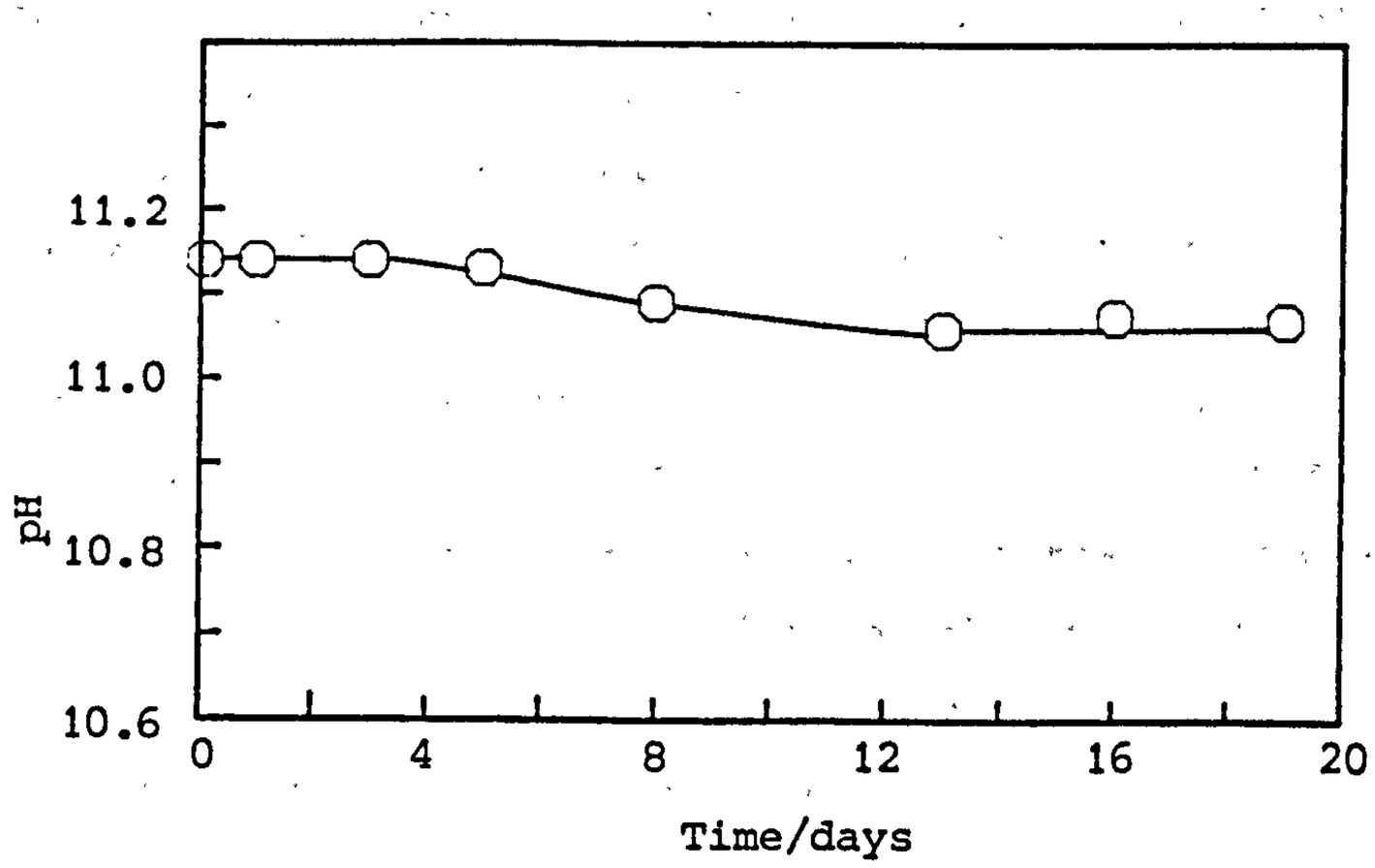

Figure 4.11 pH values of samples taken during reaction A4.

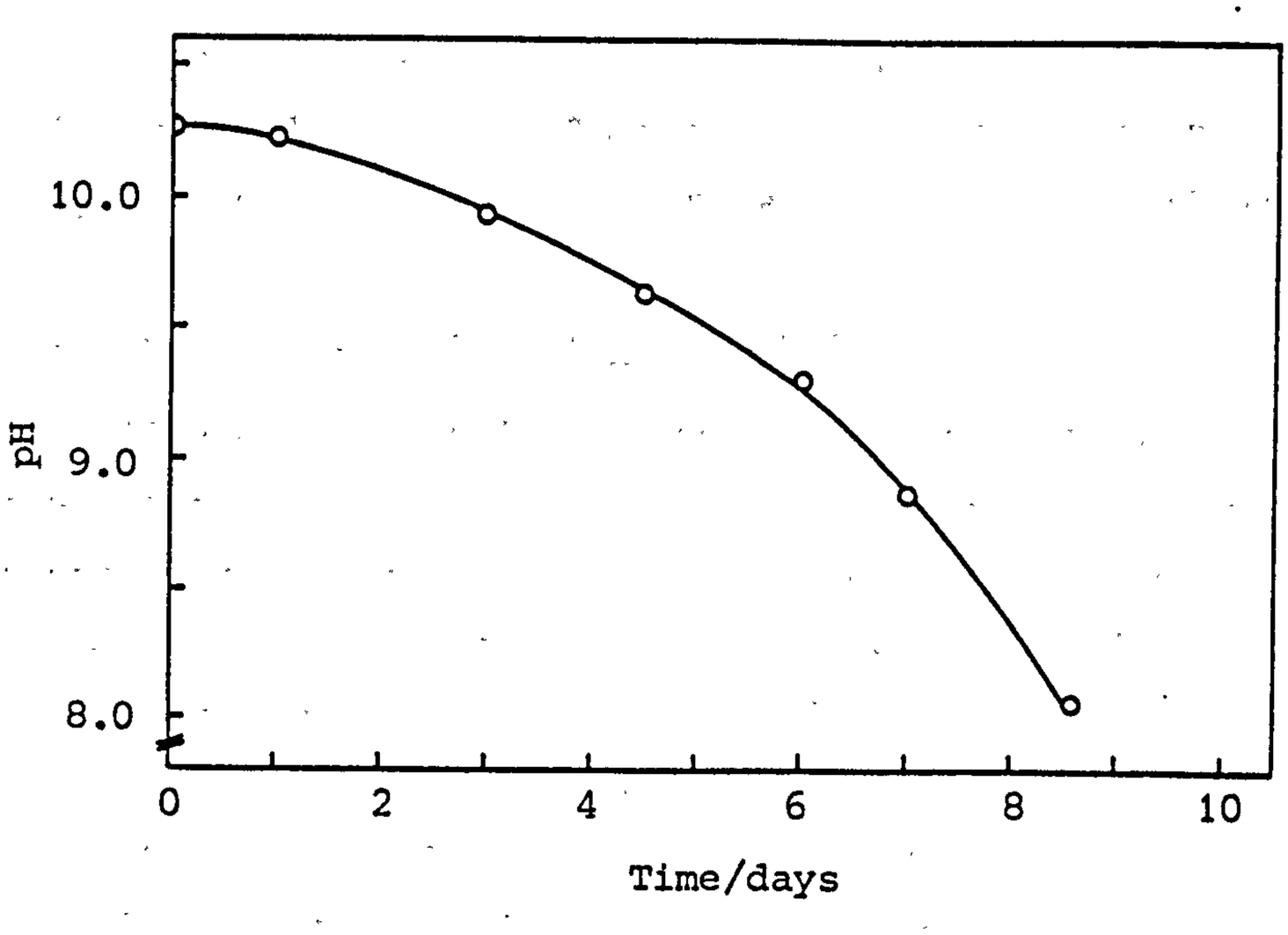

Figure 4.12 pH values of samples taken during reaction A5

If only small amounts of amine are used in mixtures (reactions A5 and B4), the pH is low, solutions are poorly buffered and large pH changes occur during crystallisation (see Tables 4.2 and 4.3). The pH results for reaction A5 are shown in Figure 4.12. This reaction was terminated at pH ∿8 because of the development of a yellow coloration in the solution phase (see later for explanation). Some amorphous material was found in the product. Repeat pH measurements were made, with a different electrode and pH meter, after samples had been stored for over 12 months. Considering the low pH of the solutions and their unbuffered nature the results agreed favourably with those in Figure 4.12. The second set of measurements were slightly lower and the difference increased as the pH decreased to a maximum of 0.2 pH units.

Evidence has been given for incorporation of piperazine in some of the products. In these instances the amine obviously actively participates in the crystallisation process. Under certain reaction conditions though the piperazine is probably less involved. For example, the organic material in the product from reaction B2 had C/N = 12.56 indicative of no piperazine incorporation. In such instances the piperazine can be considered merely as a supplier of the alkalinity (OH^-) required for crystallisation. To show the generality of this synthesis methodology, a number of other amines were used in this mineralising role.

4.3.2 Reactions with 1-methylbenzylamine

Silicalite was crystallised from a mixture that contained 1-methylbenzylamine as the mineraliser (reaction A6). In the absence of the TPABr, cristobalite formed (reaction A7). Reactions A6 and A7 both contained the same amount of total base and both products were highly crystalline. However the pH changes during the reactions were distinctly different (Figure 4.13). The pH decreased during reaction A6 because base is entrapped in the silicalite crystals as they grow. The amount of base in solution decreases throughout the crystallisation. Cristobalite, the product from reaction A7, is a non-porous crystalline silica. Base is not occluded in the crystals (compare TGA results in Figure 4.14) and the base content of the solution phase is not depleted during reaction. The pH rise observed simply reflects the solubility difference between the starting amorphous gel and the crystalline product. No cristobalite was detected in the product from reaction A6, showing the strong structure-directing effect of the TPA cations.

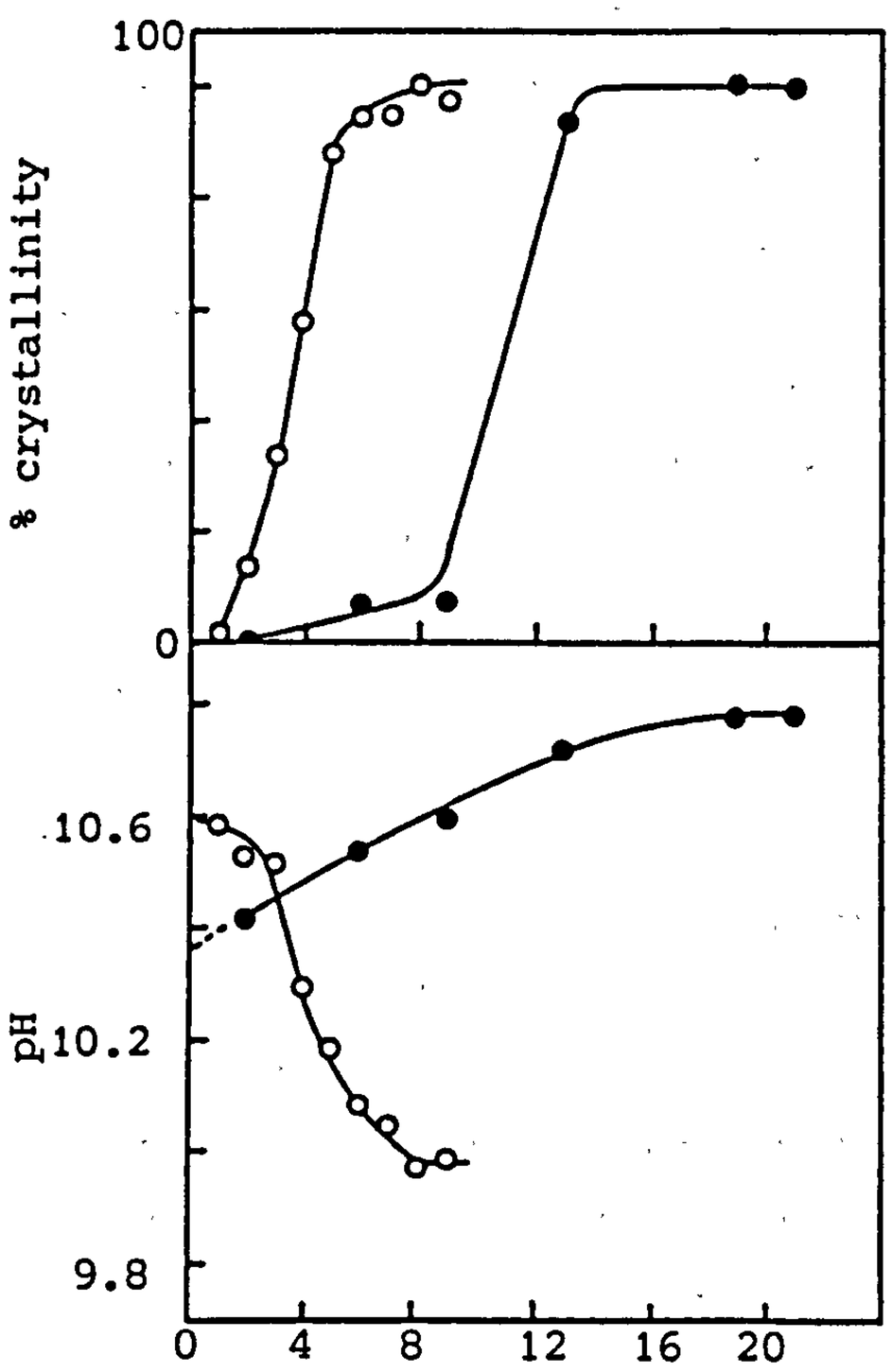

Figure 4.13 % crystallinity and pH of samples taken during reactions A6 (O) and A7 (●)

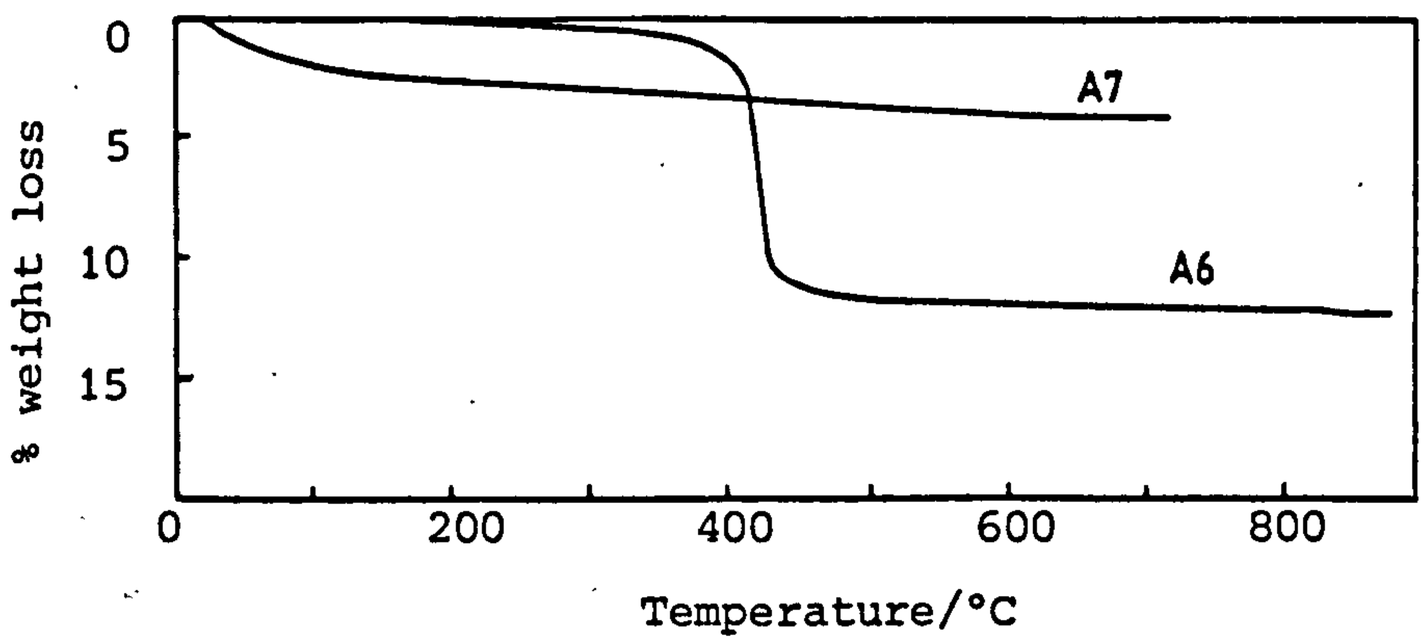

Figure 4.14 TGA curves of the as-synthesised products from reactions A6 (silicalite-1) and A7 (cristobalite).

4.3.3 Reactions in the Amine-SiO_2-H_2O System

Three further reaction mixtures were prepared without any quaternary salt. Microscopic examination of the products from the bomb reactions B5 and B6 showed no evidence of crystalline material. The amines used were piperazine and DABCO (diazabicyclo[2-2-2]octane) and the reaction time was 25 days in both cases. The bombs were re-heated to reaction temperature after adding some TPABr (equivalent to 2 moles in the molar composition). The stoichiometry of the mixture in bomb B5 was now identical to that of the starting composition of reaction B1. After reaction B5 (with TPA) had been heated for 10 days a fully crystalline product was obtained. The pH fell from 10.67 to 10.44 in good agreement with the pH change observed during reaction B1 (see Table 4.3). The crystalline material was identified as silicalite. After heating reaction B6 (with TPA) for 14 days the pH had fallen from 10.40 to 9.91. The solid product was silicalite along with a little unreacted amorphous material. These two reactions again show the strong directing effect of TPA cations. It is of interest that although no product crystallised from reaction B5 (prior to the TPA addition), ZSM-48 crystallised when larger amounts of amine were used (reaction B7). Thermal analysis showed piperazine was trapped in the crystals. Under Certain conditions therefore, reactions in the amine-SiO_2-H_2O system can produce microporous materials. Several workers [16,19] have reported crystallisation of ZSM-48 in this system. Clearly when a TPABr/ Amine combination is chosen to effect silicalite crystallisation, the amine and the reaction conditions employed must be carefully selected to avoid crystallisation of contaminant species. It is believed that in many instances the kinetics of silicalite crystallisation and its thermodynamic stability would be favourable and so enable pure products to be synthesised. Phase transformations caused by over-run would also be unlikely.

4.3.4 Reaction with TBABr

It has already been shown that different amines can be used in conjunction with TPABr to give silicalite-1. Amines can also advantageously be employed as mineralisers in reaction mixtures that contain other quaternary salts as structure-directors. The piperazine/tetrabutyl-ammonium bromide (TBABr) combination (reaction A8) produced silicalite-2 [20].

The pH results for this reaction are shown in Figure 4.15. The marked pH fall indicates when the bulk of the crystallisation occurs and indicates that base is consumed by the growing crystals. The reaction was slow by comparison with the analogous silicalite-1 reaction (reaction A1, Figure 4.3) although a better choice of mixture stoichiometry and reaction conditions would probably give silicalite-2 in a fraction of the time. Some amorphous material was seen amongst the silicalite-2 crystals from reaction A8. This was not unexpected as the reaction was terminated before pH constancy was attained (see Figure 4.15). The X-ray diffraction pattern of the as-synthesised product is shown along with that from the corresponding TPABr reaction (A1) in Figure 4.16. The silicalite-2 pattern has fewer lines because of its lower symmetry; as-synthesised crystals of silicalite-2 are tetragonal, those of silicalite-1 are orthorhombic.

The product from reaction A8 was analysed for C, H, N and the following amounts were found:

%C = 8.69 %H = 1.84 %N = 1.06

The calculated C/N atomic ratio was 9.56. This denotes very substantial incorporation of piperazine in the crystals (∿30% mole per mole since C/N ratios for piperazine and TBA are 2 and 16 respectively). Even if some of the quaternary had decomposed under the synthesis conditions (note that the low reaction pH and temperature reduce this possibility) and some tri-butylamine (C/N = 12) was occluded in the crystals the results still indicate piperazine incorporation. This incorporation may have considerable implications. Of the 4 channel intersections in a unit cell of silicalite-2 ($96SiO_2$) only about 2.6-3.0 can be occupied by TBA species[a] for steric reasons [21]. Entrapping small amines in the void channel space should increase the thermodynamic stability of the crystals, decrease their solubility and perhaps enhance reaction kinetics. Hydrophobic microporous silicas are more likely to crystallise in an aqueous environment if the void space, the volume not occupied by stabilising organic species, is minimised. Amine incorporation in silicalite-2 may therefore have a stabilising effect.

In contrast the incorporation of piperazine in silicalite-1 is not thought to benefit crystallisation kinetics and its presence in the crystals probably also has a de-stabilising effect. Tetrapropylammonium

---

[a]This gives a maximum weight ratio of organic to dry silicalite-2 of 0.135. The product from reaction A8 was found to have a weight ratio of 0.142.

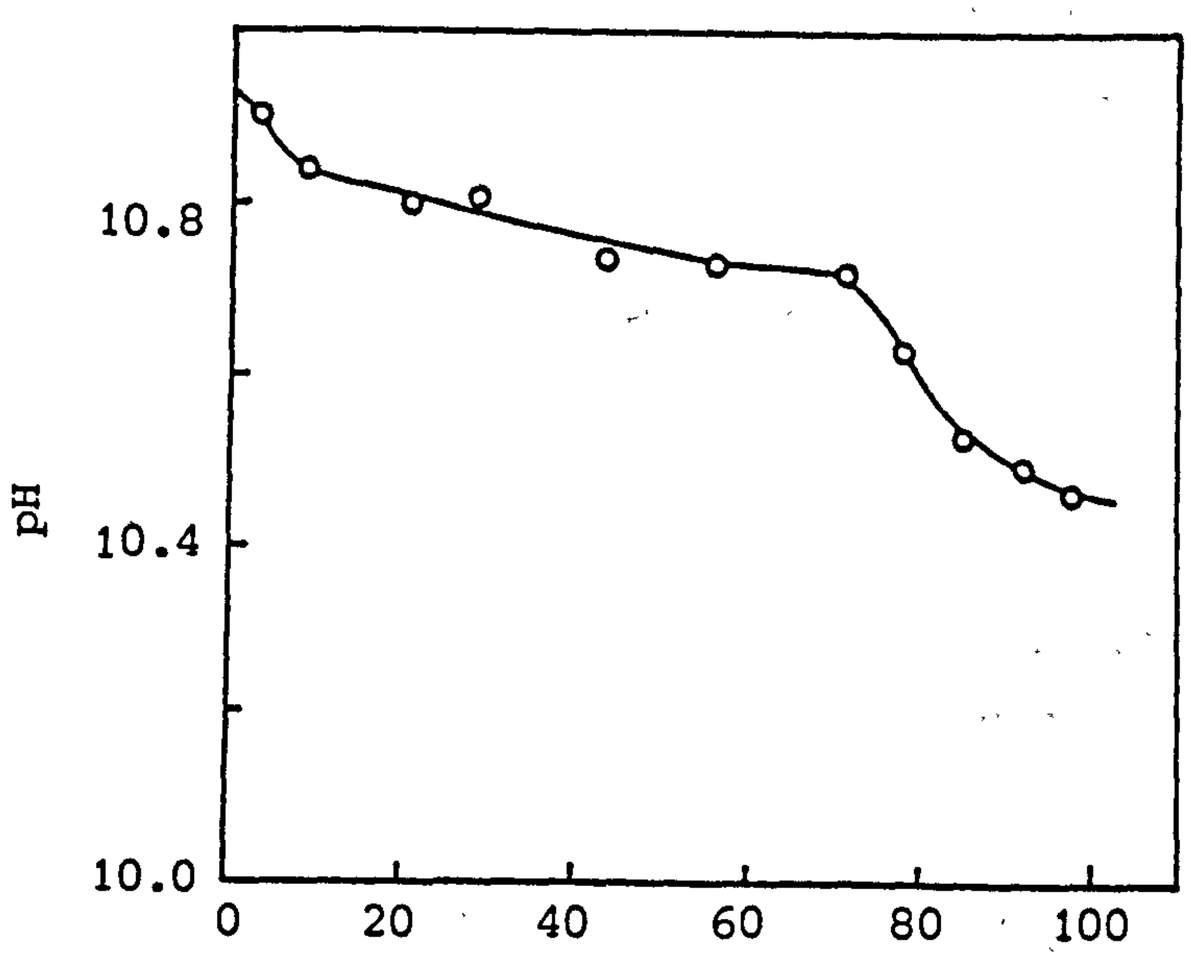

Figure 4.15 pH values of samples taken during reaction A8.

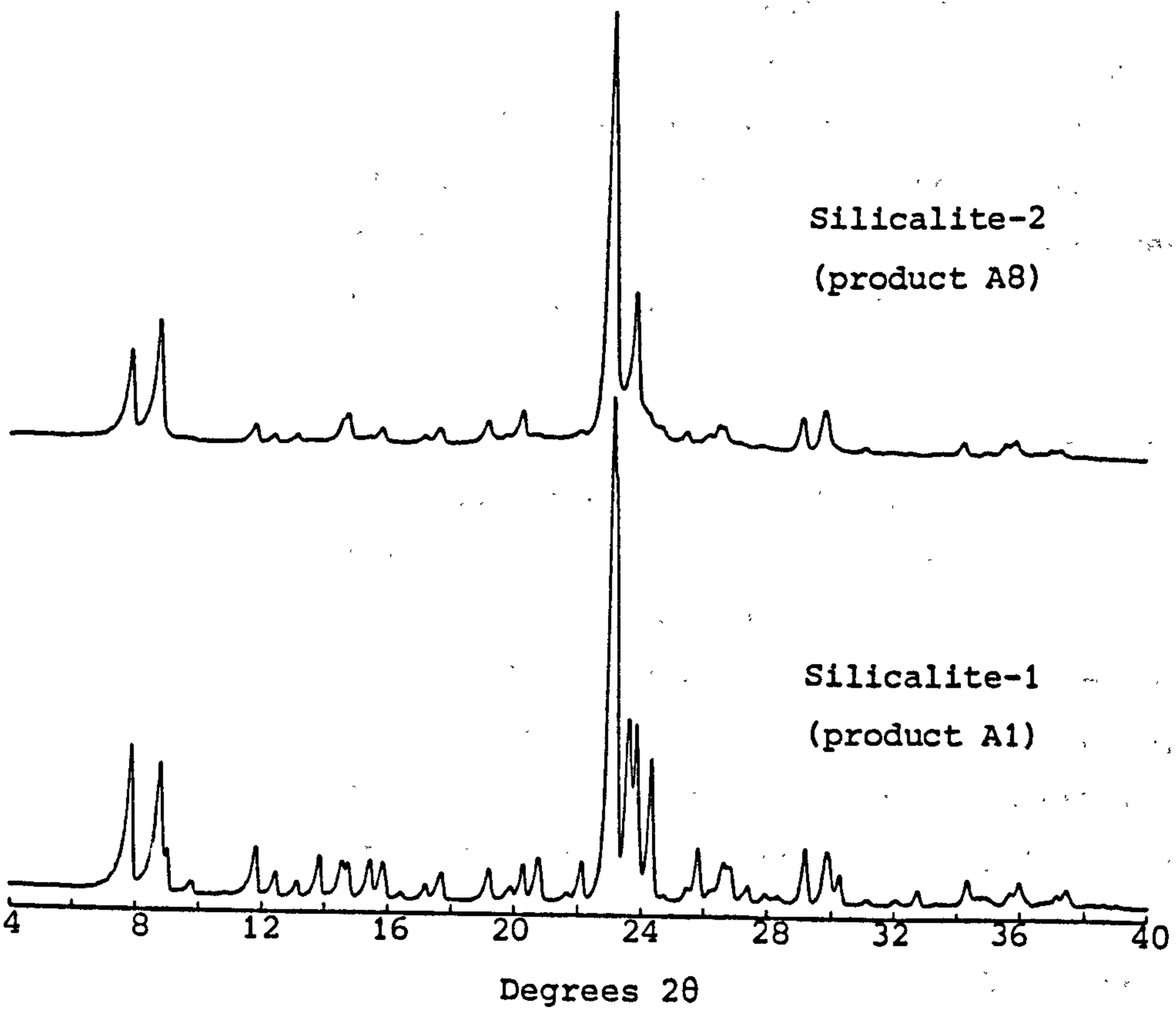

Figure 4.16 X-ray powder diffraction patterns of as-synthesised silicalite-1 and silicalite-2

species are the ideal 'fit' for the channel system and usually one molecule is located at virtually every channel intersection [21,22,23] (see also Chapter 3). Displacement by piperazine is likely to increase the void volume in the precursor crystals and result in increased solubility. The incorporation of amines other than piperazine would no doubt have similar detrimental effects unless the amine molecules (because of interactions with the framework through their size, geometry, chemical nature etc.) conferred stability on the silicalite crystals. The inclusion of amines in crystals can be avoided if they themselves are too large to be incorporated, i.e. by a steric exclusion effect.

Results presented so far have shown that under certain reaction conditions amines compete with quaternaries and act as pore-fillers. In most of the reactions investigated though the quaternary was preferentially incorporated. This exemplifies an important point; zeolitic materials, besides demonstrating marked selectivities in their post-synthesis sorption and ion-exchange behaviour, often do show a strong preference for incorporation of particular ions/molecules during their synthesis. Noteworthy, and pertinent to the present study, is the selectivity effect that was observed in the synthesis of Losod [24]. This aluminous zeolite (typically found to have Si/Al = 1) was crystallised from mixtures that contained large organic bases (e.g. bispyrrolidinium hydroxide) as the source of hydroxide ions and sodium salts (only on occasion NaOH) as the source of sodium ions. Although small enough to fit in the channels (i.e. not sterically excluded), no organic cations were ever found in the products. The highly charged (organophobic) lattice preferentially incorporated sodium ions to balance all the aluminium in the framework. The use of large organic bases in Losod synthesis made it possible to control the hydroxide concentration independently of the concentration of the cations (Na^+) built into the zeolite. The use of buffered amine systems in silicalite synthesis affords a similar effect. The amount of quaternary can be controlled independently of the alkalinity (not true if TPAOH used) and by careful choice of QBr/SiO_2 ratio (Q denotes a quaternary cation) use of expensive quaternaries can be optimised. Economic considerations are clearly of importance when commercial scale quantities of these materials are prepared.

4.3.5 Crystal Morphology

All the aforementioned crystallisations using amine/quaternary combinations were accompanied by a decrease in pH. The reverse is normally true when strong bases are used in mixtures (see section 3.3). The low final pH enables high yields to be obtained (at pH <11 yields are thought to be >98% based on silica. See section 3.3.7.1). In most cases the induction period pH was relatively low and consequently the amount of silica in solution was small. These conditions allow only limited nucleation and therefore enabled large crystals to be grown.

Under the electron microscope the products from reactions A1-A4 looked similar. Mixtures of twinned and single crystals of various sizes were seen. The largest crystals were about 8 μm in length. Micrographs of the products from reactions A1 and A3 are shown in Figure 4.17. Also shown are crystals from the lower pH, higher temperature reaction (A5) which were larger and more elongated. The observed crystal fragmentation was largely attributed to the stirred reaction conditions. The crystals of silicalite made with 1-methylbenzylamine (reaction A6) at high temperature were also large and rod-like.

Crystals of the silicalite products from the bomb reactions were all large and elongated as the micrographs in Figures 4.18 and 4.19 show. Some amorphous material can be seen amongst the crystals from reaction B4. It is of interest that although reactions B1 and B3 had identical mixture stoichiometries to reactions A1 and A3, the morphologies of the corresponding crystals differed (see Figures 4.17 and 4.18). This indicates that nucleation and growth are markedly affected by temperature and/or agitation. Both factors probably have effects. The low pH reaction B6 (see Figure 4.19) produced some crystals as long as 100 μm, indicative of reduced nucleation under these conditions. These results show that at low pH, and especially at high temperature, conditions are suitable for the growth of large crystals. When grown at low pH, the large silicalite crystals do tend to be rod- and needle-like as was suggested by the trend in the morphology of crystals grown in the xNa_2O 2TPABr $20SiO_2$ $1000H_2O$ system at 95°C shown in Figure 3.19 . Products obtained by Kuehl [3] from low pH mixtures were also often rod-like.

Figures 4.17 - 4.19 (see following three pages)

Scanning electron micrographs of reaction products

	A1
Figure 4.17	A3
	A5
	B1
Figure 4.18	B1 (optical micrograph)
	B3
	B4
Figure 4.19	B5 (after TPA addition)
	B6 (after TPA addition)

A1

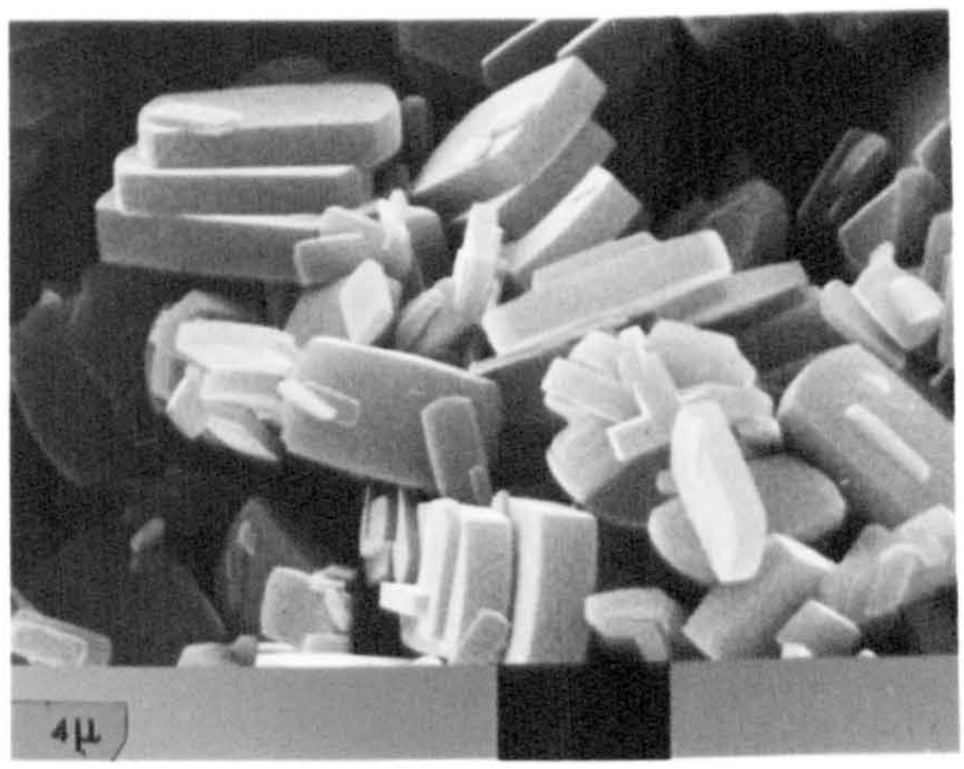

A3

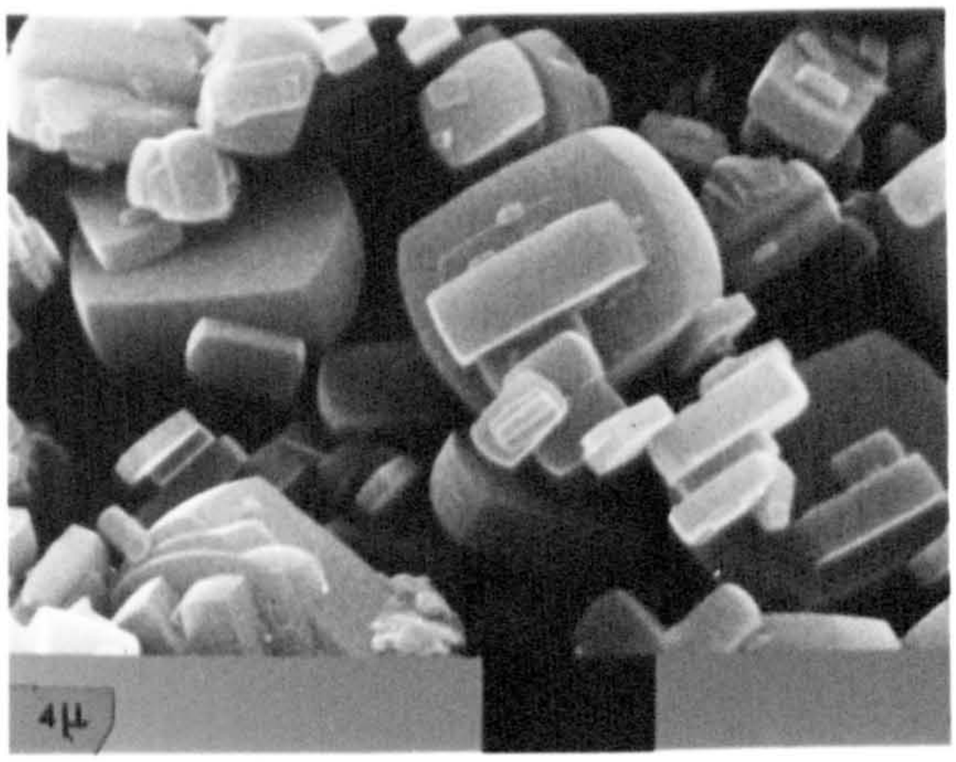

A5

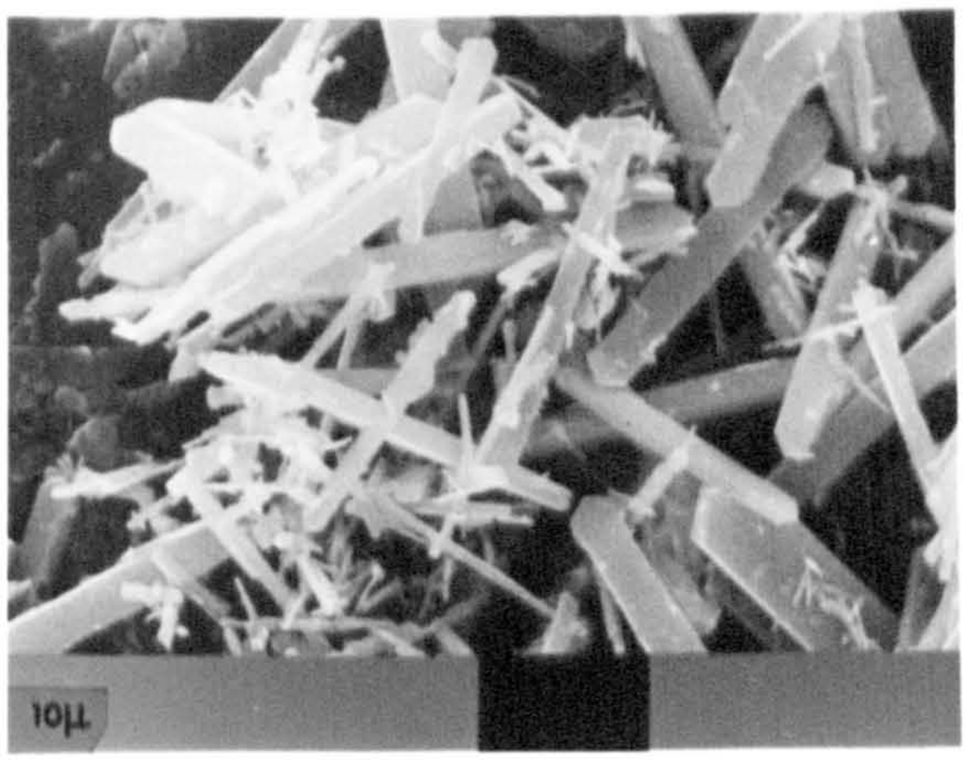

B1

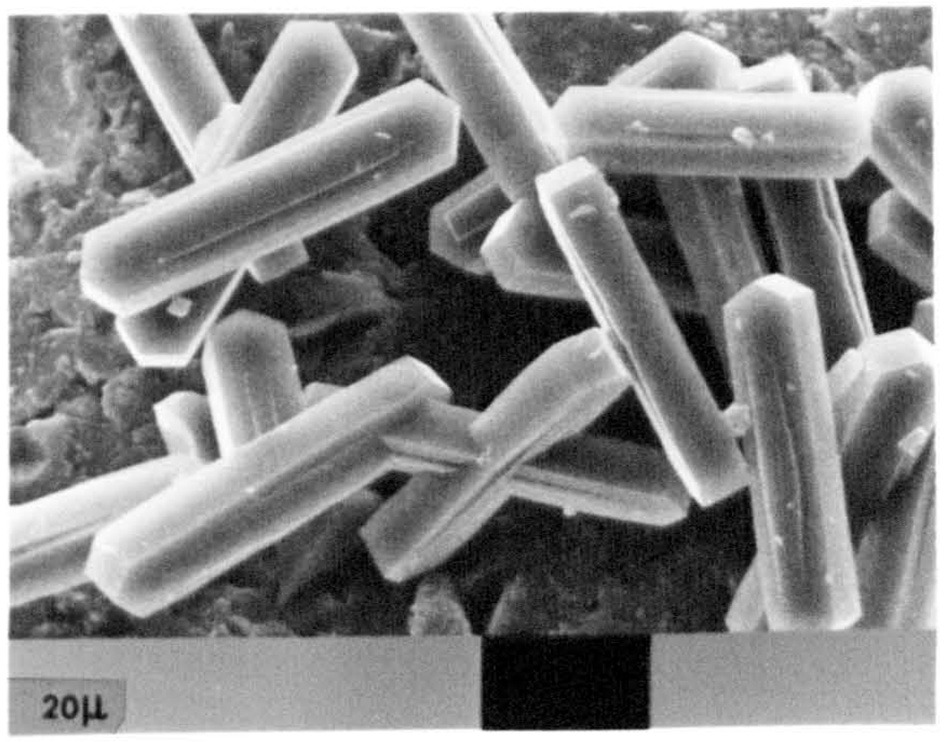

B1

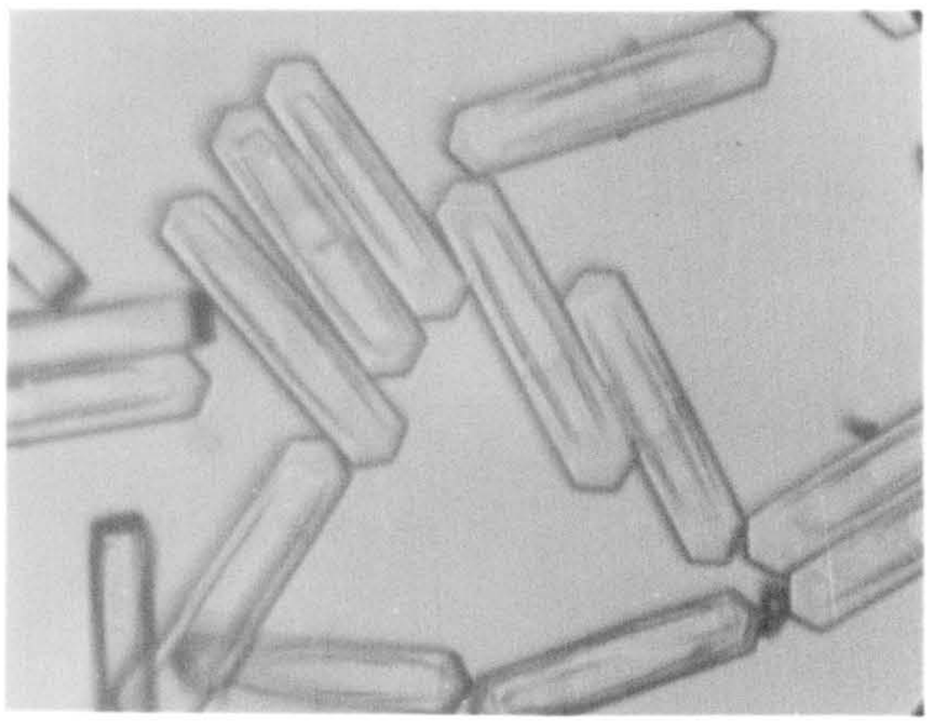

B3

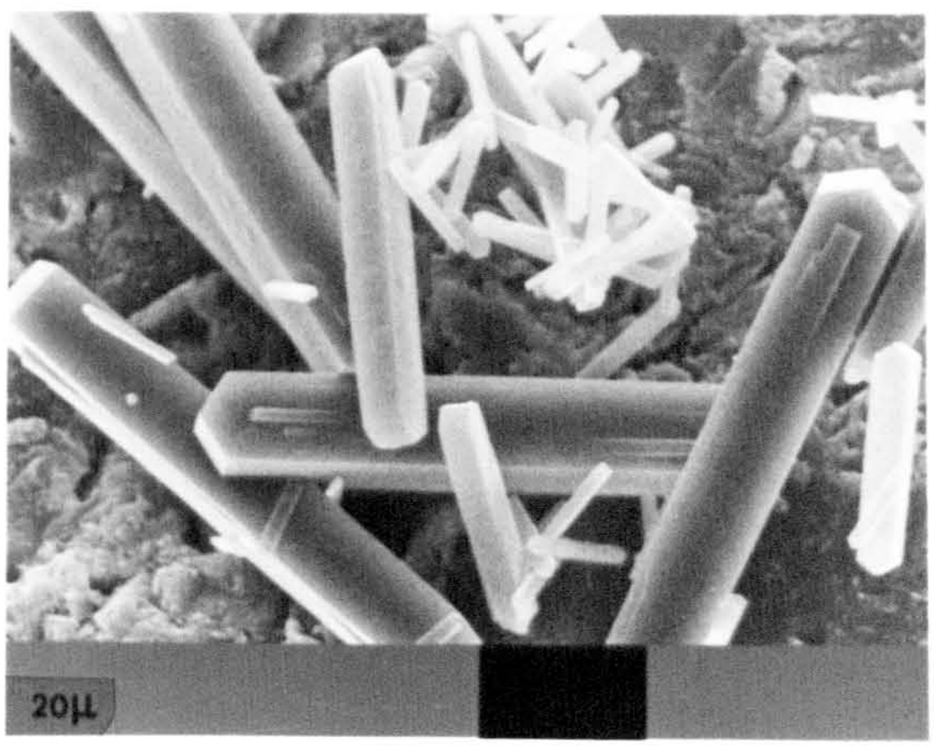

B4

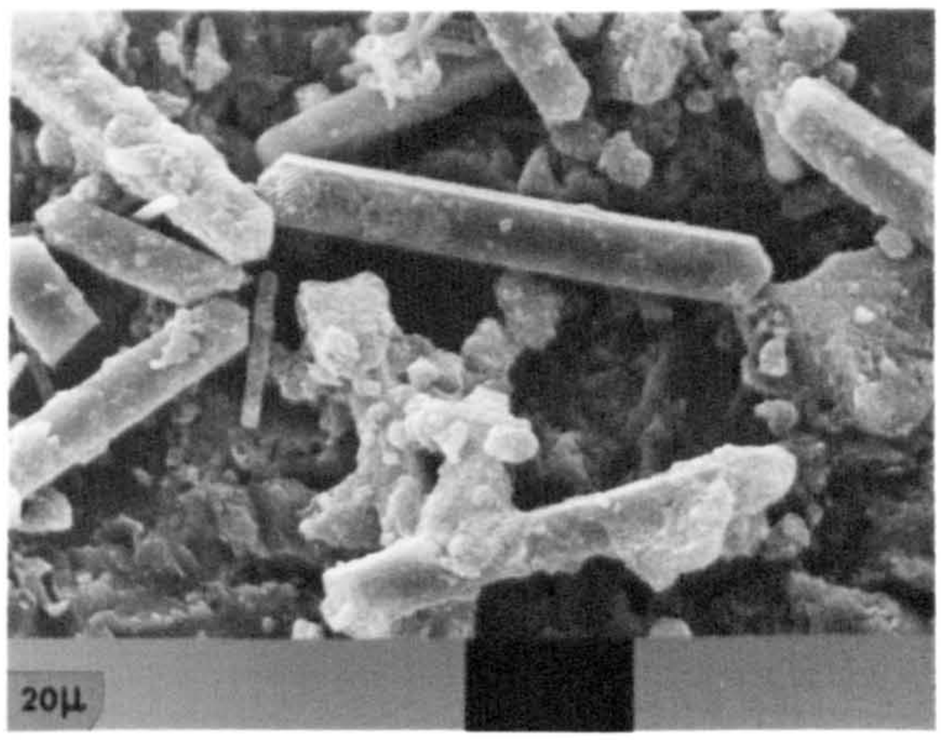

B5

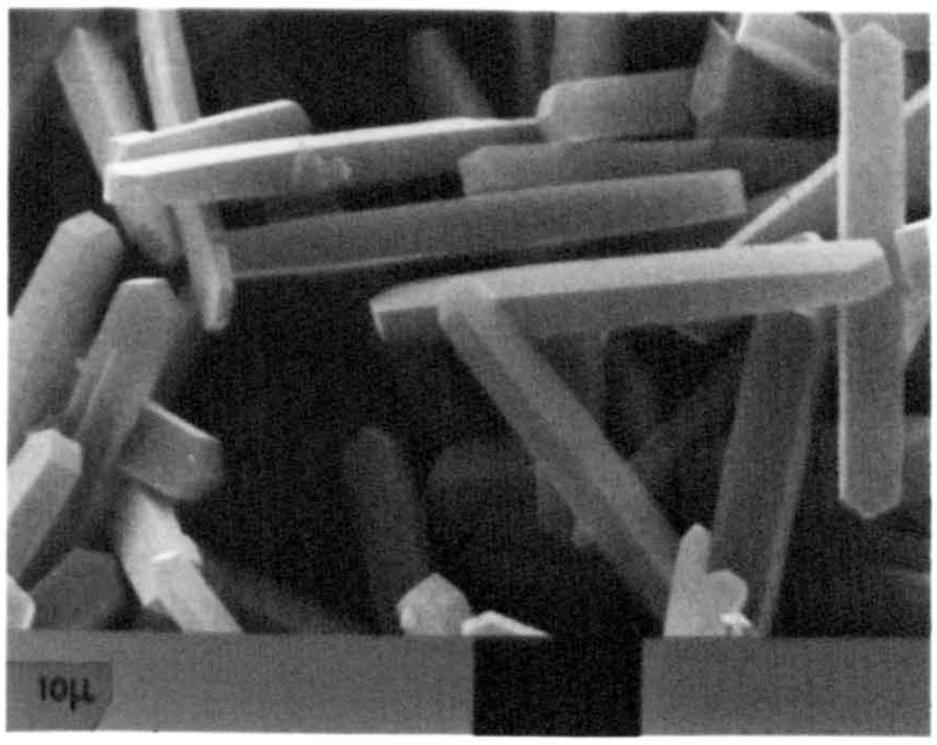

B6

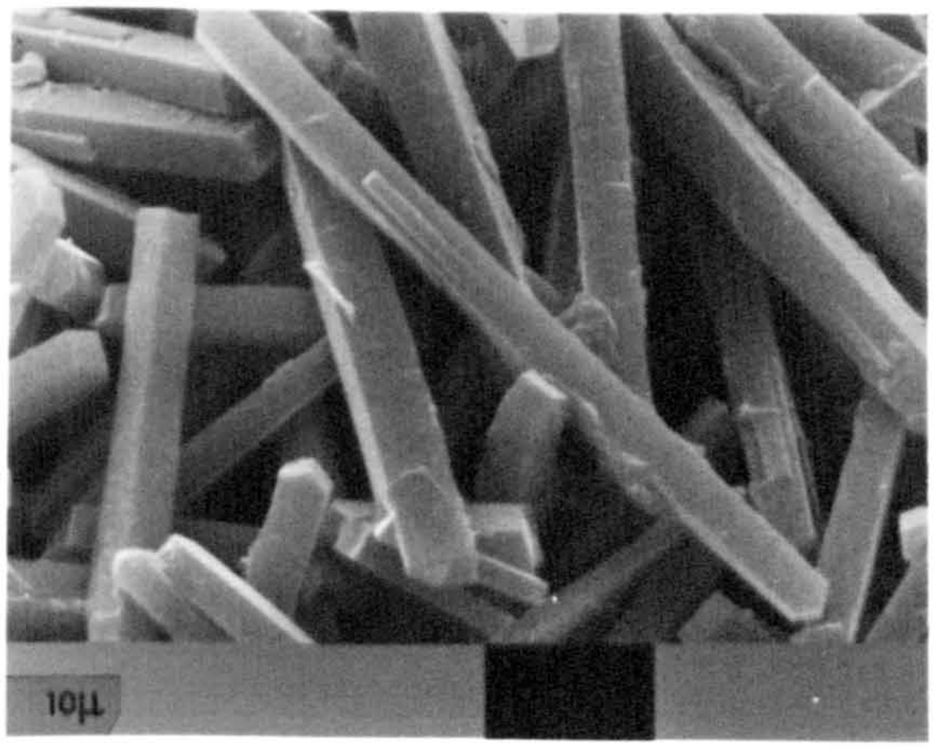

Crystals of silicalite-2 are shown in Figure 4.20. Synthesis at low pH in the presence of piperazine leads to elongation similar to that observed for crystals of silicalite-1. Interestingly the crystals of silicalite-2 though elongated retain their typical ovate shape. Crystals of silicalite-2 that were grown in a conventional strong base system are shown in Figure 4.20 for comparison.

4.3.6 Reaction with TRIS Buffer

In an effort to grow extremely large silicalite crystals one reaction was carried out at very low pH (reaction A9). TRIS buffer (tris(hydroxymethyl)methylamine) was used as the mineraliser. As the behaviour of this organic under hydrothermal conditions was unknown precautions were taken during the synthesis run. The reaction pH, temperature and pressure were monitored throughout. The results are shown in Figure 4.21. During the warm-up period the pH and pressure increased. After about 24 hours the pH began to decrease, perhaps indicative of crystallisation. A pressure increase was observed after about 75 hours and samples taken thereafter were discoloured. At first the solution phases were pale lemon in colour, samples taken later were intense orange. Oxidation of bromide to bromine was suspected and this was confirmed by the pungent smell of the samples. The pressure increase may not have been totally due to bromine vapour; some decomposition of organic, to smaller volatile fragments, may also have occurred. XRD analysis of the product gave only weak reflections but the crystalline material present was silicalite.

Bromine formation can be accounted for by the reactions shown below.

$$Br^- \rightarrow \frac{1}{2}Br_2 + e \qquad E^o = -1.087\ V$$

$$\underline{H^+ + \frac{1}{4}O_2 + e \rightarrow \frac{1}{2}H_2O} \qquad \underline{E^o = +1.229\ V}$$

$$H^+ + \frac{1}{4}O_2 + Br^- \rightarrow \frac{1}{2}Br_2 + \frac{1}{2}H_2O \qquad E^o = 0.142\ V$$

The overall reaction potential is +0.142 volts. The equilibrium constant K is written,

Figure 4.20 (overleaf)

Scanning electron micrographs of crystals of silicalite-2, the products from reactions A8 (top) and T6 (bottom). Details of reaction T6 were given in Chapter 3, section 3.3.8.

A8

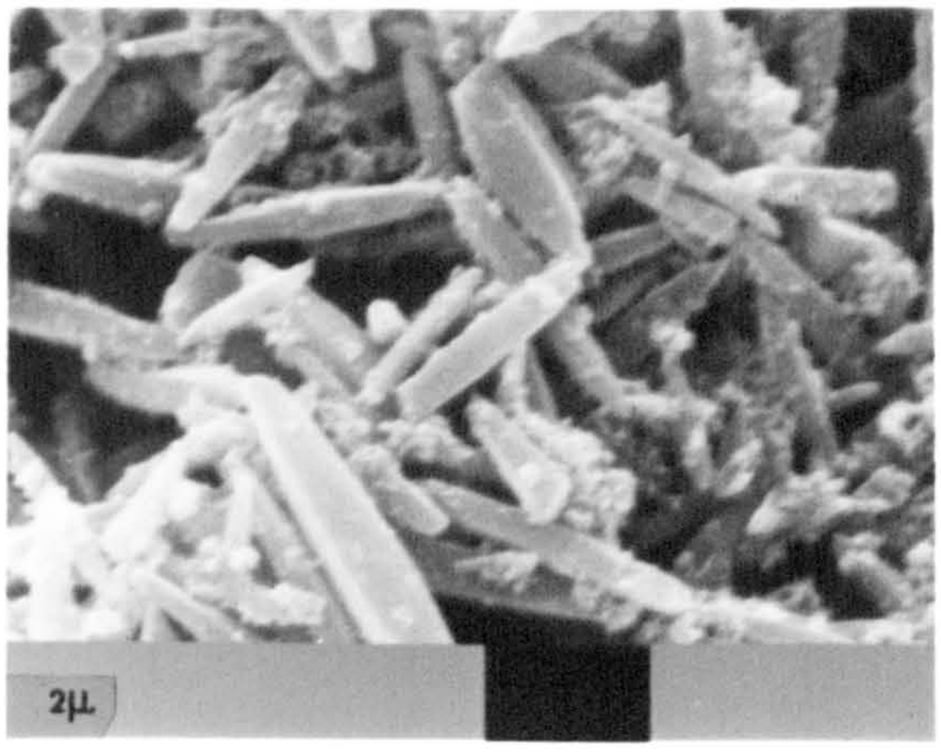

T6

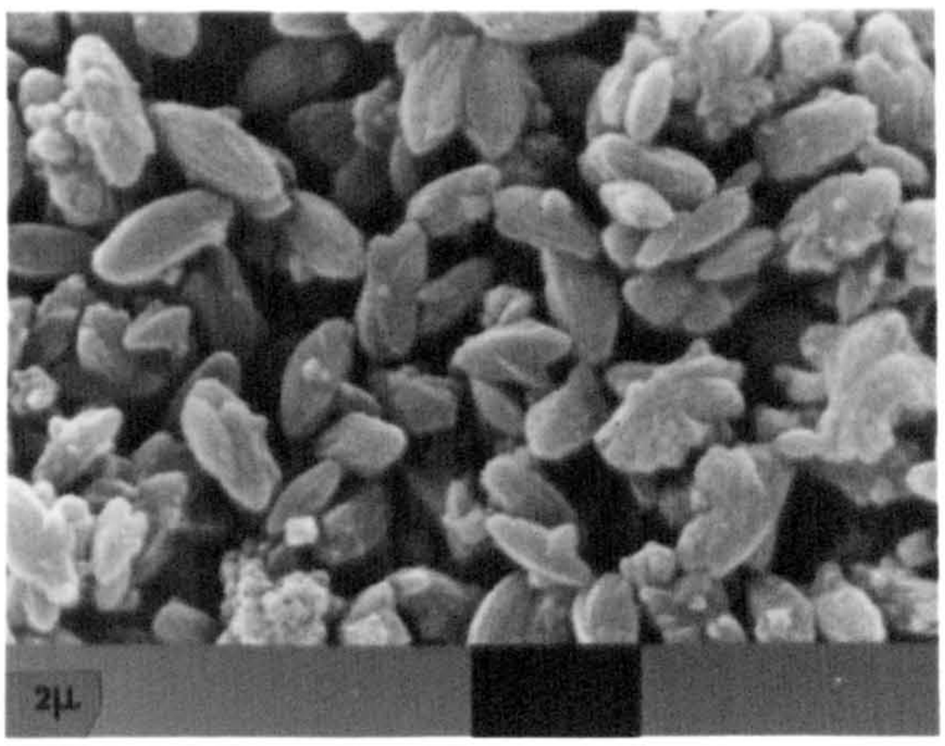

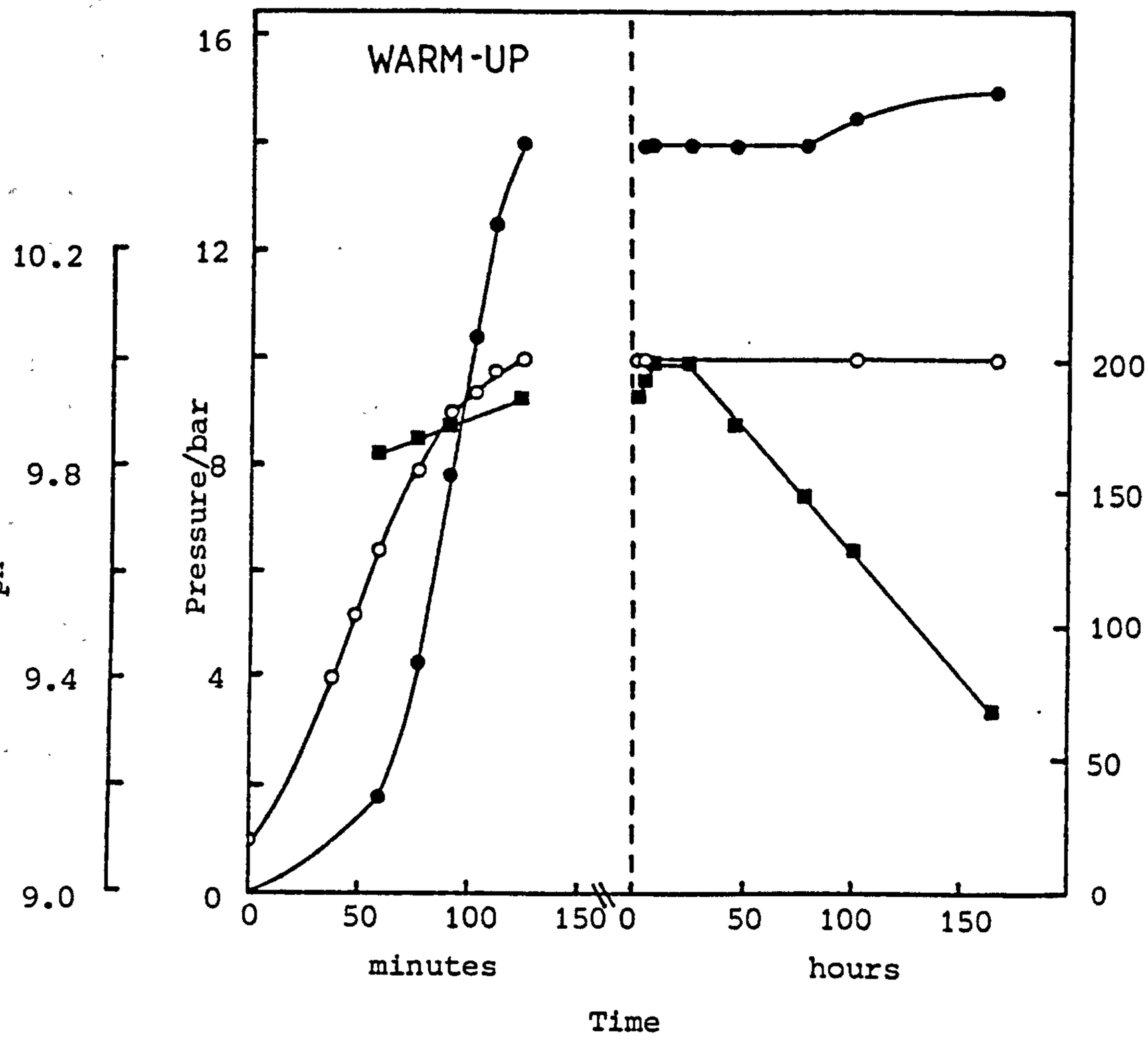

Figure 4.21 Parameters monitored during reaction A9: temperature (○), pressure (●) and sample pH (■)

$$K = \frac{[Br_2]^{\frac{1}{2}}[H_2O]^{\frac{1}{2}}}{[H^+][O_2]^{\frac{1}{4}}[Br^-]}$$

and was calculated to be 251.9 at 25°C. Bromine formation can be reduced by:

(1) lowering the amount of oxygen in the system,
(2) keeping $[H^+]$ small (i.e. higher pH reaction),
(3) keeping $[Br^-]$ small.

Three of the other low pH reactions investigated (A5, B4 and B6) also showed evidence of bromine formation. The solutions at the end of the reactions were pale yellow. To carry out low pH reactions alternative quaternary salts, e.g. TPACl could be used. The comparative reaction potential for chloride oxidation is -0.13 volts ($K = 6.34 \times 10^{-3}$); in aqueous solution oxygen oxidises bromide to bromine but not chloride to chlorine.

4.4 Conclusions

Silicalite-1 has been successfully crystallised in the amine-TPABr-SiO_2-H_2O system. When TBABr was employed as the structure-directing quaternary silicalite-2 crystallised. It is envisaged that ZSM-12 in aluminium-free form (the crystalline silicate made by Grose and Flanigen [25] is essentially this) could be made with tetraethylammonium (TEA) salts in combination with amines. As TEA compounds often decompose (via Hoffmann degradation) under high pH reaction conditions the possibility of crystallising ZSM-12 type materials at lower pH by this amine route is attractive.

Advantages and disadvantages of using these amine-quaternary systems to crystallise silicalite-type materials are summarised in Table 4.6. All products are free of alkali metal cations and only calcination is required before use. These benefits clearly also apply when syntheses are carried out in the Q_2O-SiO_2-H_2O system. Many of the drawbacks associated with the use of commercially available tetraalkylammonium hydroxides (see section 4.1) can be avoided by preparation of these reagents from the salts but procedures are time consuming and also when strong bases are used in mixtures considerable pH changes usually occur during reactions. Synthesis in the amine-QBr-SiO_2-H_2O system can be

Table 4.6 Advantages and disadvantages of the amine/quaternary salt route to silica molecular sieves

Advantages

(1) Amines and quaternary ammonium salts of high purity are commercially available.

(2) Reaction mixtures are free of alkali metal cations and hence so are crystalline products.

(3) The amounts of base (amine) and template (quaternary salt) in mixtures can be independently controlled (not true if quaternary ammonium hydroxides used).

(4) Wastage of expensive quaternary salt can be minimised.

(5) The presence of amines in mixtures gives enhanced pH control during crystallisation.

(6) Products only need to be calcined before use; treatments to remove alkali metal ions are not necessary.

(7) High product yields can be obtained because in general the final reaction pH is low; little of the silica remains in solution.

(8) The low pH reaction conditions enable large crystals to be grown.

Disadvantages

(1) Reaction kinetics can be adversely affected by low pH conditions. The presence of considerable amounts of amine in mixtures may also retard the crystallisation process.

(2) Incorporation of amine into crystals may increase the number of intracrystalline hydroxyl groups (defect sites) present in resultant products. It may also increase the solubility of the crystals. Such incorporation can be avoided by careful choice of amine - by an exclusion effect.

effected with a far greater measure of pH control. By careful selection of the amine (i.e. its pK_a) and the quantity used in mixtures it should be possible to crystallise silicalite (and other microporous silicas) over a narrow and chosen pH range. As long as systems are reasonably buffered, pH changes should be small and products should be fully crystalline. It is believed that organic buffers could be designed to give this pH control using chosen combinations of a variety of compounds: amines, amino-acids, carboxylic acids, organic salts of weak acids and bases. It should be possible to crystallise silicalite in quantity at pH as low as 7-8 in systems that contain organic buffers. This is not possible in unbuffered systems that contain only strong bases because the amount of product (of ideal composition 4TPAOH $96SiO_2$) that can be obtained is strictly limited by the amount of strong base present.

Kuehl [3] found that crystals of aluminium-free ZSM-5 (silicalite) with varied morphology could be obtained by control of the reaction pH. In the main, salts of organic acids were used to give this pH control. The initial reaction pH was sometimes as low as 9.0 and crystals grown were often rod-like. However the presence of large concentrations of metal cations and associated anions in mixtures is not thought ideal and the use of amines to give pH control, if producing similar morphology changes (the indications are favourable), is likely to offer improvement.

It has been shown that in some instances amine molecules become incorporated in the products along with the structure-directing quaternary species. Although perhaps detrimental in some cases (if the amine competes with the quaternary) it may have benefits in others (if the amine 'complements' the quaternary). Crystals containing more than one organic species are not common and crystallographically they may be of interest. The incorporation of amine molecules can be avoided if amines too large to be occluded are used in mixtures, i.e. by a steric exclusion effect.

It is of interest that fluoride silicalite [18] is crystallised under low pH conditions. This material has ideal unit cell composition 4TPAF $96SiO_2$ [26,27] and as salt molecules, not molecules of base, are entrapped in the precursor, little base is required in reaction mixtures to effect complete crystallisation. In one of the examples cited [18] the initial reaction pH was as low as 7.4. Rod-shaped crystals as large as 200 μm were reported, presumably indicative of the low pH

conditions limiting nucleation. Crystallisation of silicalite-1 at low pH using organic buffers should also produce exceptionally large crystals. For some applications of these materials big crystals may be desirable.

The procedures described in this chapter provide a novel synthesis route to silicalite-type materials and offer much scope for further research. In buffered low pH systems crystallisation can be controlled and this may facilitate the elucidation of hitherto unknown aspects of the crystallisation process.

Footnote:

During the course of the afore-described research, a number of exploratory crystallisations were effected in small glass capillary tubes. Reactions were followed by optical microscopy. Appendix II gives details of the successful syntheses, i.e. those which resulted in the formation of crystalline materials. Because of the small amounts of product obtained no attempt was made to characterise any of the solids.

Chapter 4 - References

[1] F.G. Dwyer and E.E. Jenkins
U.S. Patent 3,941,871 (1976).

[2] R.W. Grose and E.M. Flanigen
U.S. Patent 4,061,724 (1977).

[3] G.H. Kuehl
European Patent Application 93,519 (1983).

[4] L. Falth and U. Hakansson
Recent Progress Reports, 5th Int.Conf. Zeolites, (Ed. R. Sersale, C. Collela and A. Aiello), 1980, p. 37.

[5] K.-J. Chao, T.C. Tasi and M.-S. Chen
J.Chem.Soc., Faraday Trans. I, 1981, 77, 547.

[6] M. Ghamami and L.B. Sand
Zeolites, 1983, 3, 155.

[7] R. von Ballmoos
"The ^{18}O-Exchange Method in Zeolite Chemistry", Salle (Frankfurt) and Sauerländer (Aarau), 1981, p. 74.

[8] D.M. Bibby, N.B. Milestone and L.P. Aldridge
Nature, 1980, 285, 30.

[9] Ref. [7], p. 89.

[10] Ref. [7], p. 87.

[11] B.M. Lok, T.R. Cannan and C.A. Messina
Zeolites, 1983, 3, 282.

[12] L.D. Rollmann
U.S. Patent 4,296,083 (1981).

[13] L.D. Rollmann and E.W. Valyocsik
U.S. Patent 4,205,053 (1980).

[14] R.B. Calvert and L.D. Rollmann
European Patent Application 101,183 (1984).

[15] L.D. Rollmann and E.W. Valyocsik
European Patent Application 15,132 (1980).

[16] A. Araya and B.M. Lowe
J.Catal., 1984, 85, 135.

[17] S.T. Wilson, B.M. Lok and E.M. Flanigen
U.S. Patent 4,310,440 (1982).

[18] E.M. Flanigen and R.L. Patton
U.S. Patent 4,073,865 (1978).

[19] L. Marosi, M. Schwarzmann and J. Stabenow
European Patent Application 46,504 (1982).

[20] D.M. Bibby, N.B. Milestone and L.P. Aldridge
Nature, 1979, 280, 664.

[21] Z. Gabelica, E.G. Derouane and N. Blom
Appl.Catal., 1983, 5, 109.

[22] J.B. Nagy, Z. Gabelica and E.G. Derouane
Zeolites, 1983, 3, 43.

[23] E.M. Flanigen, J.M. Bennett, R.W. Grose, J.P. Cohen, R.L. Patton, R.M. Kirchner and J.V. Smith
Nature, 1978, 271, 512.

[24] W. Sieber and W.M. Meier
Helv.Chim.Acta., 1974, 57, 1533.

[25] R.W. Grose and E.M. Flanigen
U.S. Patent 4,104,294 (1978).

[26] G.D. Price, J.J. Pluth, J.V. Smith, T. Araki and J.M. Bennett
Nature, 1981, 292, 818.

[27] G.D. Price, J.J. Pluth, J.V. Smith, J.M. Bennett and R.L. Patton
J.Amer.Chem.Soc., 1982, 104, 5971.

Chapter 5

A Theoretical Approach to Silica Molecular Sieve Synthesis

5.1 Introduction

At a fundamental scientific level, less is known about the crystallisation of zeolites than is about their structures and properties. As a result, much research in the synthesis field has been based on empiricism and fraught with uncertainty. Even though the literature on zeolite crystallisation is substantial and ever increasing, speculative research still abounds. Progress in the 'art' has not been aided, indeed it is more apposite to say it has been positively hindered, by the technological importance zeolites have assumed because commercial politics dictate that valuable knowledge stays 'in house' and unpublished.

Mobil's ZSM zeolites, discovered in the late 1960's and early 1970's, marked an important turning point in the evolution of zeolite science - the advent of high silica zeolites (Si/Al > 10). Considerable research has since been devoted to the synthesis of materials of this type. A theoretical approach to the crystallisation of high silica zeolites, recently outlined in a publication by Lowe [1], considered the formation of these materials on thermodynamic grounds. No other account of its kind is to be found in the literature. The equilibrium theory that Lowe proposed for crystallisation is conceptually simple, it has widespread applicability and it forms the basis of the work presented in this chapter. Extensions to his model that have been made are described in detail.

The theoretical results presented in sections that follow were calculated with two aims in mind:

(1) To compare and contrast the experimental data already obtained for silicalite-1 crystallisation (Chapters 3 and 4) with theoretical predictions.

(2) To establish how the stoichiometry of a reaction mixture and the chemical composition of crystals produced can affect reaction thermodynamics.

The greater proportion of the results relate to hypothetical reactions and comparison with experimental data is therefore not possible. Nevertheless, it is believed features these results show may have important implications.

The principles of equilibrium are the key to the understanding of many chemical reactions and they are the essence of Lowe's theory. A thermodynamic treatment of zeolite crystallisation in aqueous media has to consider solution phase equilibria of two fundamental types - dissociation and solubility. General introductions to these equilibria and other concepts of solution chemistry relevant to this work are given in many standard physical chemistry texts and as such no repetition is attempted here. A basic knowledge of the following has therefore been assumed: the general theory of acids and bases, the law of mass action (chemical equilibrium), activity/activity coefficients, ionisation/dissociation, hydrolysis of salts, common ion effect, solubility product, dissociation of water, simultaneous equilibria, Le Chatelier's Principle, pH scale, strengths of acids and bases, buffer solutions and titrimetry. As the concept of buffering crops up repeatedly in discussions that follow, it is pertinent to elaborate a little on this particular subject.

Solutions that possess 'reserve acidity' and 'reverse alkalinity', a resistance to changes in pH upon addition of small amounts of acid and base, are termed buffer solutions. Usually such solutions consist of a mixture of a weak acid (HA) and its conjugate base (A^-) or a weak base (B) and its conjugate acid (BH^+).

Consider the equilibrium between a weak acid and its conjugate base. The dissociation of the acid is given by:

$$HA \overset{K_a}{\rightleftharpoons} H^+ + A^- \qquad (5.1)$$

and the degree of dissociation is governed by the acidity constant K_a:

$$K_a = a_{H^+} . a_{A^-}/a_{HA} \qquad (5.2)$$

where a_{H^+}, a_{A^-} and a_{HA} are the activities of the respective species. This expression can be approximated by replacing activities with concentration terms:

$$K_a = [H^+][A^-]/[HA] \qquad (5.3)$$

Taking logarithms and rearranging gives:

$$pH = pK_a - \log([HA]/[A^-]) \qquad (5.4)$$

where $pH = -\log[H^+]$ and $pK_a = -\log K_a$. The pH is controlled by the acid/conjugate base molar ratio. If $[HA] = [A^-]$ then $pH = pK_a$. This is the criterion for maximum buffering; addition of acid or alkali is least likely to affect the pH when solutions contain equivalent amounts of the acid and its conjugate base.

The analogous expression for dissociation of a weak base (B) is:

$$pH = pK_a - \log([BH^+]/[B]) \qquad (5.5)$$

and in this case maximum buffering occurs when $[BH^+] = [B]$. Weak acid buffer solutions have their buffer maxima on the acid side, weak base systems have theirs on the alkaline side. In general, buffer capacity is maintained over the range $pH = pK_a \pm 1$. Two final points should be mentioned - (i) titration curves for neutralisation of weak acids and bases demonstrate the manner buffer capacity varies with pH [2]; (ii) solutions can be buffered at a specific pH by judicious mixing of reagents.

The chemistry of silica

> *"Silica is by far the major component of the earth's crust, yet much remains to be learned of its chemistry and, in particular, its solubility in water".*
> *Ralph Iler (1979).*

The chemistry of silicas and silicates is intricate. The above words, taken from Iler's excellent book on the chemistry of silica [3], perhaps iterate the overriding reason why knowledge of so many facets of zeolite crystallisation is still poor. Zeolites are, of course, aluminosilicates but most contain far more silica than they do alumina and silicas/silicates and zeolites have much chemistry in common. If anything, the fact that aluminium is additionally present in parent solutions and gels makes the task of understanding zeolite crystallisation even more fraught with difficulty.

Silica is constantly dissolving and precipitating over much of the earth's surface. The dissolution process involves a hydrolysis mechanism and is catalysed by OH^- ions:

$$(SiO_2)_x + 2H_2O \rightleftharpoons (SiO_2)_{x-1} + Si(OH)_{4(aq)} \qquad (5.6)$$

When synthetic amorphous or crystalline silicas are in aqueous environments, equilibria identical to that above are set up. The immediate product of dissolution is orthosilicic acid $Si(OH)_4$, a hydrated monomeric unit of the silica solid. The resulting solutions are, however, complex and unlike most conventional solutions. They usually contain a wide variety of polymeric species in addition to monomer and at high pH ionisation occurs extensively producing silicate solutions.

The solubilities of amorphous silicas in water at 25°C are known to range between 70 and 180 ppm SiO_2 [4]; this refers to the concentration of SiO_2 (as $Si(OH)_4$) in equilibrium with the solid. Crystalline silicas have much lower solubilities. For example, quartz has a solubility of about 11 ppm SiO_2 in water at 25°C [5]. Increased dissolution occurs at elevated temperatures and at high pH.

5.2 Summary of the Equilibrium Model [1] for Crystallisation of High Silica Zeolites

The synthesis of most zeolites involves conversion of an amorphous solid to a crystalline solid in an aqueous alkaline solution. Reaction mixtures used to make high silica zeolites are silica-rich, typically they have molar SiO_2/Al_2O_3 ratios greater than 20, and in the development of this crystallisation model the small alumina contents in such mixtures were neglected. Reactions were considered to involve the transformation of an amorphous silica into a crystalline silica. As such, the theory is particularly suited for modelling crystallisation of dense crystalline silicas (e.g. quartz, cristobalite), silica molecular sieves (e.g. silicalite-1, silicalite-2) and certain other insoluble silicates, for example layer silicates. In these cases experimental data should agree best with the theoretical predictions. Fewer 'complexities' - possible sources of discrepancy between the theoretical and experimental results - are likely to manifest themselves if mixtures are aluminium-free.

The Solubility of Silica

Solid silicas dissolve in water - but only to a limited extent. As already mentioned, an equilibrium is established between the solid and orthosilicic acid $Si(OH)_4$ in solution. The activity, or if the activity coefficient term is taken as unity, the concentration of orthosilicic acid in equilibrium with the solid is the solubility product K_s:

$$K_s = [Si(OH)_4] \qquad (5.7)$$

Crystalline silicas are less soluble than amorphous silicas (K_s (crystal) < K_s (amorphous)) and for any given silica, K_s is dependent on certain experimental conditions, especially temperature, but independent of others, most notably pH.

As orthosilicic acid is a weak acid, ionisation is only partial:

$$Si(OH)_4 \overset{K_1}{\rightleftharpoons} Si(OH)_3O^- + H^+ \qquad (5.8)$$

$$Si(OH)_3O^- \overset{K_2}{\rightleftharpoons} Si(OH)_2O_2^{2-} + H^+ \qquad (5.9)$$

$$Si(OH)_2O_2^{2-} \overset{K_3}{\rightleftharpoons} Si(OH)O_3^{3-} + H^+ \qquad (5.10)$$

$$Si(OH)O_3^{3-} \overset{K_4}{\rightleftharpoons} SiO_4^{4-} + H^+ \qquad (5.11)$$

K_1, K_2, K_3 and K_4 are the dissociation constants for the first, second, third and fourth ionisations and the respective mass action relationships (neglecting activity coefficients) can be written:

$$K_1 = [Si(OH)_3O^-][H^+]/[Si(OH)_4] \qquad (5.12)$$

$$K_2 = [Si(OH)_2O_2^{2-}][H^+]/[Si(OH)_3O^-] \qquad (5.13)$$

$$K_3 = [Si(OH)O_3^{3-}][H^+]/[Si(OH)_2O_2^{2-}] \qquad (5.14)$$

$$K_4 = [SiO_4^{4-}][H^+]/[Si(OH)O_3^{3-}] \qquad (5.15)$$

For the crystallisation model, the solution phases in equilibrium with the solid silicas were idealised and assumed to contain only two silicate ions, $Si(OH)_3O^-$ and $Si(OH)_2O_2^{2-}$. These ions are likely to be the most abundant in many systems. However, the complexity of 'real' silicate solutions should not be totally forgotten. Other silicate ions, in various states of oligomerisation and ionised to different extents, will almost certainly be present as well. Substitution of selected values for the constants ($K_1 = (2 \times 10^{-10})$, $K_2 = (2 \times 10^{-12})$ and $K_s = 2.5 \times 10^{-3}$ and 1.8×10^{-4}) into equations (5.7, 5.12 and 5.13) enabled the pH dependence of the concentrations of $Si(OH)_3O^-$ and $Si(OH)_2O_2^-$ in equilibrium with two silicas of differing solubility (K_s) to be determined (Table 5.1 and Figure 5.1(a)). The results show that in near neutral solutions little ionisation of the acid occurs and little silica dissolves. At higher pH the concentration of undissociated acid in equilibrium with the solid remains unchanged but

Table 5.1 The pH dependence of the concentrations of silicate ions in equilibrium with solid silicas of differing solubility (calculated from equations (5.7), (5.12) and (5.13) using $K_1 = 2 \times 10^{-10}$ and $K_2 = 2 \times 10^{-12}$)

	$K_S = 2.5 \times 10^{-3}$			$K_S = 1.8 \times 10^{-4}$		
pH	$[Si(OH)_3O^-]$	$[Si(OH)_2O_2^{2-}]$	$[S_T]^a$	$[Si(OH)_3O^-]$	$[Si(OH)_2O_2^{2-}]$	$[S_T]^a$
7	5×10^{-6}	1×10^{-10}	2.51×10^{-3}	3.6×10^{-7}	7.2×10^{-12}	1.80×10^{-4}
8	5×10^{-5}	1×10^{-8}	2.55×10^{-3}	3.6×10^{-6}	7.2×10^{-10}	1.84×10^{-4}
9	5×10^{-4}	1×10^{-6}	3.00×10^{-3}	3.6×10^{-5}	7.2×10^{-8}	2.16×10^{-4}
10	5×10^{-3}	1×10^{-4}	7.60×10^{-3}	3.5×10^{-4}	7.2×10^{-6}	5.47×10^{-4}
11	5×10^{-2}	1×10^{-2}	6.25×10^{-2}	3.6×10^{-3}	7.2×10^{-4}	4.50×10^{-3}
12	5×10^{-1}	1×10^{0}	1.50×10^{0}	3.6×10^{-2}	7.2×10^{-2}	1.08×10^{-1}

[a] the total concentration of soluble silica ; ions plus orthosilicic acid.

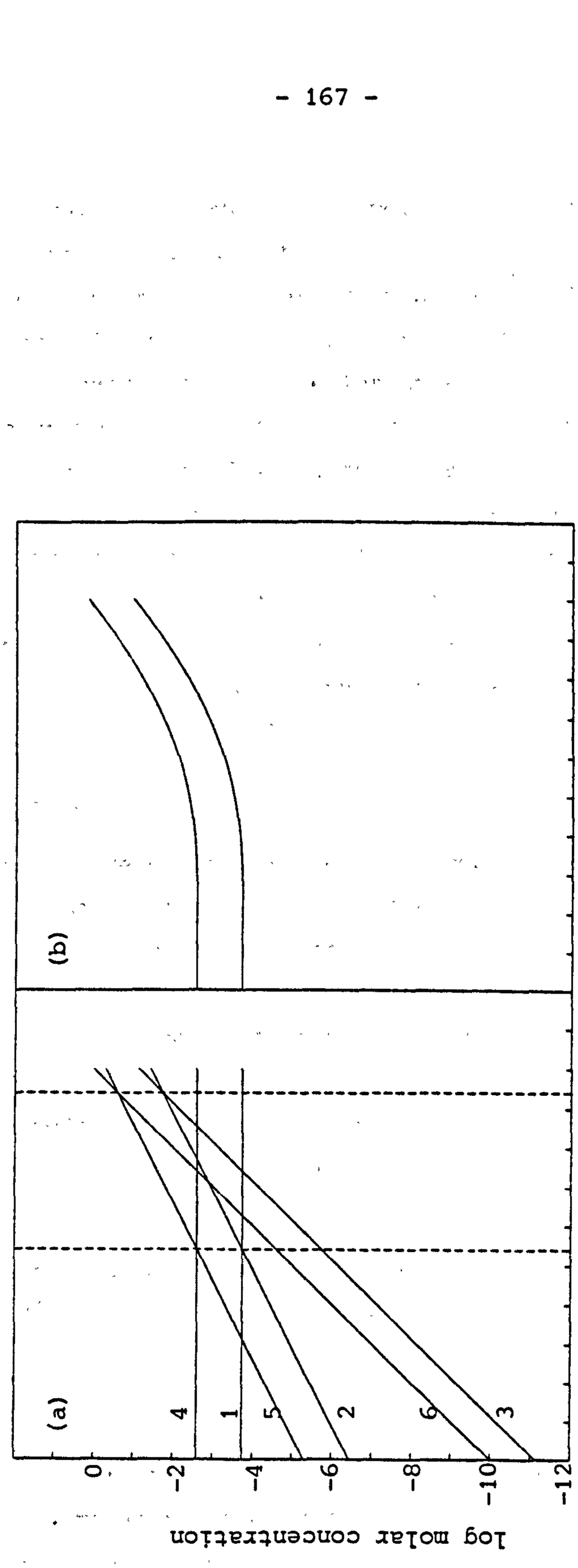

(a) pH dependence of the equilibrium concentrations of $Si(OH)_4$, $Si(OH)_3O^-$ and $Si(OH)_2O_2^{2-}$ in solutions that are in contact with solid silicas of differing solubility : 1, $Si(OH)_4$, $K_s = 1.8 \times 10^{-4}$; 2, $Si(OH)_3O^-$, $K_s = 1.8 \times 10^{-4}$; 3, $Si(OH)_2O_2^{2-}$, $K_s = 1.8 \times 10^{-4}$; 4, $Si(OH)_4$, $K_s = 2.5 \times 10^{-3}$; 5, $Si(OH)_3O^-$, $K_s = 2.5 \times 10^{-3}$; 6, $Si(OH)_2O_2^{2-}$, $K_s = 2.5 \times 10^{-3}$.

(b) pH dependence of the total silica in solution. Lower curve $K_s = 1.8 \times 10^{-4}$, upper curve $K_s = 2.5 \times 10^{-3}$

Figure 5.1

increased ionisation causes the amount of silica in solution to increase. Note that at high pH the doubly charged ion becomes increasingly important. These trends are not dependent on the specific solubility (K_s) of a silica (see Table 5.1) although the absolute concentrations of species in solution are. Figure 5.1(b) shows the solubility-pH continua drawn from the data in Table 5.1. The buffer capacities of solutions increase with pH as the concentrations of species in solution increase. Note that at any given pH, the greater the solubility (K_s) of the silica, the greater the amount of silica in solution and the greater the buffer capacity. Attention is also drawn to the fact that Figure 5.1(a) suggests that enhanced buffering may be observed at pH = 9.70 (when $[Si(OH)_4] = [Si(OH)_3O^-]$) and at pH = 11.70 (when $[Si(OH)_2O_2^{2-}] = [Si(OH)_3O^-]$).

Crystallisation

Consider reaction mixtures of composition $xM_2O\ ySiO_2\ wH_2O$ (M = alkali metal cation; x, y and w represent the molar quantities of reagents in the reaction composition). At the beginning of a reaction prior to nucleation, the solution phases contain $Si(OH)_4$, in equilibrium with the solid amorphous silica in the gel phase, along with silicate anions ($Si(OH)_3O^-$ and $Si(OH)_2O_2^{2-}$). The fraction of the total silica initially added to a mixture that dissolves depends on the amounts of all other components present although to the greatest extent on the base content.

The maximum molality (moles per kg water) of alkali metal cations $[M^+]$ in the solution phase is given by:

$$[M^+] = 2x/wM_w \qquad (5.16)$$

where x and w are the number of moles of alkali metal oxide and water in the molar reaction composition and M_w is the molar mass of water in kg. This assumes no base molecules are bound to the surface of the undissolved amorphous solid.

Crystallisation occurs only if the solubility of the crystalline solid is less than that of the amorphous solid, i.e. K_s(crystal) < K_s(amorphous). It is difficult to imagine how reaction could proceed if this was not true. After crystallisation is complete an equilibrium, similar to that established initially, is established between the crystalline solid and species in the liquid phase.

The solubility of the solid phase and the base cation concentration control the concentrations of silicate species in solution at the beginning and end of reaction. As electroneutrality must be preserved in solution, the concentrations of the ionic species are related by a charge equivalence equation:

$$[M^+] + [H^+] = [Si(OH)_3O^-] + 2[Si(OH)_2O_2^{2-}] + [OH^-] \qquad (5.17)$$

Points to note about equation (5.17):

(1) The doubly charged anion balances two negative charges.

(2) Relative to other terms, the term in H^+ is very small and can be neglected; the typical pH range for crystallisation is 10.5 to 12.5, i.e. $[H^+] = 10^{-10.5}$ to $10^{-12.5}$. Lowe also neglected the term in OH^- (because it too is relatively small) but in this work this term is included. Repeat calculations have in fact shown that omission of the OH^- term does not significantly alter results. Only at very high pH (>13), in pH regions generally unsuitable for crystallisation of silicas (and high silica zeolites), is the OH^- term actually likely to be important. Equation (5.17) thus simplifies to:

$$[M^+] = [Si(OH)_3O^-] + 2[Si(OH)_2O_2^{2-}] + [OH^-] \qquad (5.18)$$

The base cation concentration represents the alkalinity of a mixture and dictates (i) the total charge on anionic species in solution and, to a certain extent, also (ii) the total number of anions present. For any given base cation concentration though it is the solubility of the solid silica that controls the relative amounts of each

anion present. The lower the solubility of the silica, the lower the concentrations of silicate ions and the greater the concentration of hydroxide ions in solution.

The hydrogen ion concentration is largely controlled by the silicate ions through their dissociation equilibria and substitution of equations (5.7), (5.12) and (5.13) and the relationship for the ionic product of water K_w:

$$K_w = [H^+][OH^-] \qquad (5.19)$$

into equation (5.18) gives:

$$[M^+] = K_1K_s/[H^+] + 2K_1K_2K_s/[H^+]^2 + K_w/[H^+] \qquad (5.20)$$

This is the key expression in Lowe's theory. As K_1, K_2, K_s and K_w are constants, equation (5.20) allowed calculation of the equilibrium pH at the beginning and end of a reaction for any given base cation concentration ($[M^+]$). The initial reaction pH was determined by insertion of the initial cation concentration and the K_s value for amorphous silica into equation (5.20). The final pH was similarly evaluated using the final cation concentration and the K_s value for the crystalline silica.

The percentage of the total silica present as solid at the beginning of a reaction (G) and the product yield at the end of the reaction (Y) were calculated using the equation:

$$G \text{ or } Y = 100\left(\frac{\text{moles total } SiO_2 - \text{moles } SiO_2 \text{ in solution}}{\text{moles total } SiO_2}\right)$$

$$= 100(1 - (wM_w/20)(K_s + K_1K_s/[H^+] + K_1K_2K_s/[H^+]^2)) \qquad (5.21)$$

For his calculations Lowe assumed the cation concentration did not change during reaction. A range of values for the constants K_1, K_2 and K_s were used largely because there is some doubt about the accuracy of the reported values for the dissociation constants and K_s values

have only been reported for a few solids. Although not an ideal situation, the fact that these constants are not accurately known is not too serious a disadvantage. Far more important than the absolute values of the calculated parameters are the general trends and features the data shows. The selected values for the constants which were used throughout this work were typical of the values chosen by Lowe [1]:

$$K_1 = 2 \times 10^{-10}$$

$$K_2 = 2 \times 10^{-12}$$

$$K_s(\text{amorphous silica}) = 2.5 \times 10^{-3}$$

$$K_s(\text{crystalline silica}) = 1.8 \times 10^{-4}$$

$$K_w = 1 \times 10^{-14}$$

The K_s value used for the crystalline silica is the reported solubility of quartz at 25°C (11 ppm [5]). Values for the other constants are those applicable at ambient temperatures (see ref. [1] for discussion about choice of values for these constants). Experimental pH values, which were measured at ∿20°C, can therefore be favourably compared with theoretical results without temperature correction. It should be remembered though that the K_s values are likely to be considerably greater at reaction temperatures.

5.2.1 Extensions to the Equilibrium Model

Results in chapters 3 and 4 have shown that crystallisation of high silica zeolites, silica molecular sieves and dense crystalline silicas from amorphous gels typically proceed by the scheme illustrated in Figure 5.2. The crystallisation process can be split into stages:

(i) An induction period - establishment of an equilibrium between the amorphous silica (the gel) and soluble species in solution.

(ii) Growth of crystals at the expense of the amorphous solid.

(iii) Solubility control transfer and growth of crystals from clear solution.

(iv) Establishment of an equilibrium between the crystalline solid and soluble species in the mother liquor.

Figure 5.2 Schematic representation of the crystallisation process

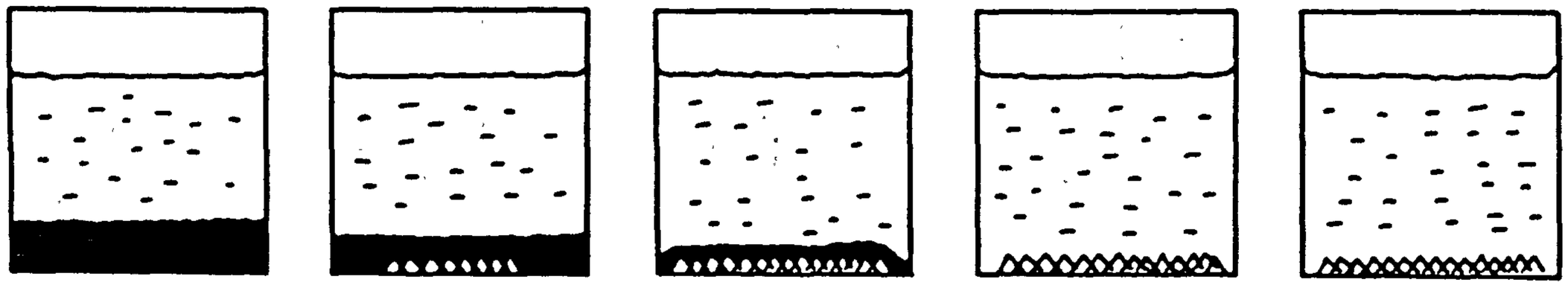

Reaction stage:	(i)	(ii)	(ii)	(iii)	(iv)
Solid phase:	A	A + C	A + C	C	C
Solid phase thermodynamically controlling species in solution:	A	A	A	-	C

Reaction stages: (i) induction period
(ii) crystal growth from the amorphous solid
(iii) crystal growth from clear solution and solubility control transfer
(iv) final equilibrium

The initial and final equilibrium positions (stages (i) and (iv)) can be determined using equation (5.20) as already described. The period when crystals grow at the expense of the amorphous solid can also be considered to be under thermodynamic control if it is assumed that during this period, removal of nutrients (principally silicate ions) by the growing crystals (crystallisation involves polymerisation between silicate ions and the crystal surfaces and,at least momentarily, causes the amount of silica in solution to decrease and the hydroxide ion concentration to increase) is slow compared with nutrient replenishment (effected by hydroxide attack on the gel solid) and re-establishment of the solid-liquid equilibrium. As crystals grow at the expense of the gel substrate, the crystallinity of the solid phase steadily increases but the amorphous solid that remains, the solid with the greater solubility, still controls the concentrations of species in solution. Modelling this period of growth is interesting because it is often accompanied by revealing pH changes. When the final traces of gel dissolve away the solid phase becomes entirely crystalline but, momentarily at least, the 'gel' will still control the species in solution through its solubility. The equilibrium at this point, referred to henceforth as the solubility transfer point, can be calculated (N.B. real systems would not be expected to behave so ideally - solubility transfer is likely to occur when a little amorphous solid is still present). Solubility transfer in tandem with crystallisation from clear solution then ensue. This period of the reaction is not under thermodynamic control and cannot be modelled. Eventually an equilibrium is established between the crystalline silica and soluble species in the mother liquor. It is thus possible to model the following stages of a reaction:

(1) The initial (induction period) equilibrium.
(2) The equilibrium at any stage during the period when crystals grow at the expense of the amorphous solid.
(3) The equilibrium at the solubility transfer point.
(4) The final reaction equilibrium.

Lowe calculated results only for the initial and final equilibrium positions. No attempt was made to model crystal growth at the expense of the gel solid or to calculate solubility transfer points. These represent extensions that have been made to his model. It should be mentioned that although only reaction mixtures that contain strong bases have been considered so far, the crystallisation theory can be well applied to weak base systems. Such systems are described in later sections.

5.2.2 Notation and Representation of Results

In tables and figures that follow reference is made to the three key equilibrium positions during a reaction, designated points A, B and C. All reactions proceed A → B → C where point A represents the equilibrium during the induction period, point B represents the equilibrium at the solubility transfer point and point C represents that at the end of a reaction.

The equilibrium theory gives no information about reaction kinetics or time dependent changes to any reaction parameters. For example, although pH changes that occur during reactions can be calculated, pH-time curves cannot be drawn to compare with experimental profiles. Instead, pH-yield curves (note that for any given reaction the product yield is a time dependent quantity) and line representations, that depict the pH changes that accompany crystallisation, are plotted. Changes in pH that occur during reactions are designated ΔpH_{B-A}, ΔpH_{C-B} and ΔpH_{C-A} to signify the change in pH between points B and A, points C and B and points C and A respectively. The latter represents the overall pH change during reaction.

As will be seen, the thermodynamic course of a reaction is dependent on the stoichiometry of the reaction mixture and the chemical composition of the crystals formed - it is not dependent on the absolute amounts of reagents in the mixture. For example, if a mixture was prepared and split into two parts, 90% and 10% by volume respectively, the thermodynamic courses of both reactions would be identical. For ease of data manipulation and interpretation it is convenient to calculate theoretical results from mixtures that contain 1000 g water. This is simply because mass action relationships involve concentration terms. All computer programs to facilitate calculations were thus written accordingly.

The following abbreviations have been used: $Si(OH)_4 = SH_4$, $Si(OH)_3O^- = SH_3^-$, $Si(OH)_2O_2^{2-} = SH_2^{2-}$.

5.3 Crystallisation in Systems that Contain Strong Bases as Mineralisers

5.3.1 Crystallisation in the $xNa_2O\ 20SiO_2\ 1000H_2O$ system.

Crystallisation from mixtures of composition $xNa_2O\ 20SiO_2\ 1000H_2O$ (x = 0.10 to 19.50) was modelled to illustrate how the theory can be applied to a specific reaction system. The results calculated show the effects of alkalinity on crystallisation. The products from these reactions were considered to be dense crystalline silicas such as quartz or cristobalite. It was assumed no base cations were entrapped in the crystals or coordinated to the external surfaces of the amorphous or crystalline solids, i.e. all base cations added to the mixtures remained in the solution phases throughout the reactions. No experimental data is available for comparison with this set of theoretical results.

Results were calculated using equation (5.16), (5.20) and (5.21). For any given alkalinity x, $[Na^+]$ was calculated (equation (5.16)) and the equilibrium pH values and yields determined (equations (5.20) and (5.21)). Note that because the base cation concentration was deemed to remain constant during reaction, this necessitates pH constancy until all the amorphous silica initially present as solid in the gel phase has been converted to the same mass of crystalline solid. Hence for these reactions, equilibrium conditions initially (point A) and at solubility transfer (point B) are identical and therefore no special computations were necessary to model crystal growth during the A-B transition or to calculate solubility transfer points. A computer program written in basic (file PHUP1 - see Appendix III for program details) facilitated calculations. The program was run on an Apple II microcomputer. The data is summarised in Table 5.2. The pH-yield plots in Figure 5.3 illustrate many of the features shown by the data:

(1) In each case, equilibrium conditions at points A and B are identical. This is simply because the base cation concentration remains constant during reaction. However, the solid phase is amorphous at point A, crystalline at point B.

Table 5.2 Simulated crystallisation in the $xNa_2O\ 20SiO_2\ 1000H_2O$ system
Chemical composition of the crystals: SiO_2

x	Initial (Point A) Solubility Transfer (Point B)			Final (Point C)			ΔpH_{C-A}
	$[Na^+]$	pH	G[a]	$[Na^+]$	pH	Y[b]	
0.10	0.011	10.30	98.8	0.011	11.21	99.3	0.91
0.25	0.028	10.66	97.5	0.028	11.49	98.4	0.83
0.50	0.056	10.92	95.5	0.056	11.68	96.9	0.76
0.70	0.078	11.03	93.9	0.078	11.77	95.8	0.74
0.85	0.094	11.09	92.8	0.094	11.82	95.0	0.73
1.00	0.111	11.15	91.7	0.111	11.86	94.1	0.71
2.00	0.222	11.36	84.7	0.222	12.04	88.7	0.68
3.50	0.389	11.52	75.0	0.389	12.17	80.7	0.65
5.00	0.555	11.62	65.6	0.555	12.26	72.9	0.64
6.50	0.722	11.69	56.5	0.722	12.32	65.0	0.63
8.00	0.888	11.74	47.6	0.888	12.37	57.3	0.63
10.00	1.110	11.80	35.9	1.110	12.42	46.9	0.62
12.00	1.332	11.84	24.4	1.332	12.46	36.6	0.62
14.00	1.554	11.88	12.9	1.554	12.50	26.3	0.62
16.00	1.776	11.92	1.6	1.776	12.53	16.1	0.61
16.50[c]	1.832	-	-	1.832	12.53	13.5	-
19.00[c]	2.109	-	-	2.109	12.56	0.7	-
19.50[c,d]	2.165	-	-	-	-	-	-

[a] % silica as amorphous solid initially and % yield at the point of solubility transfer

[b] % yield

[c] amorphous silica totally soluble

[d] crystals totally soluble

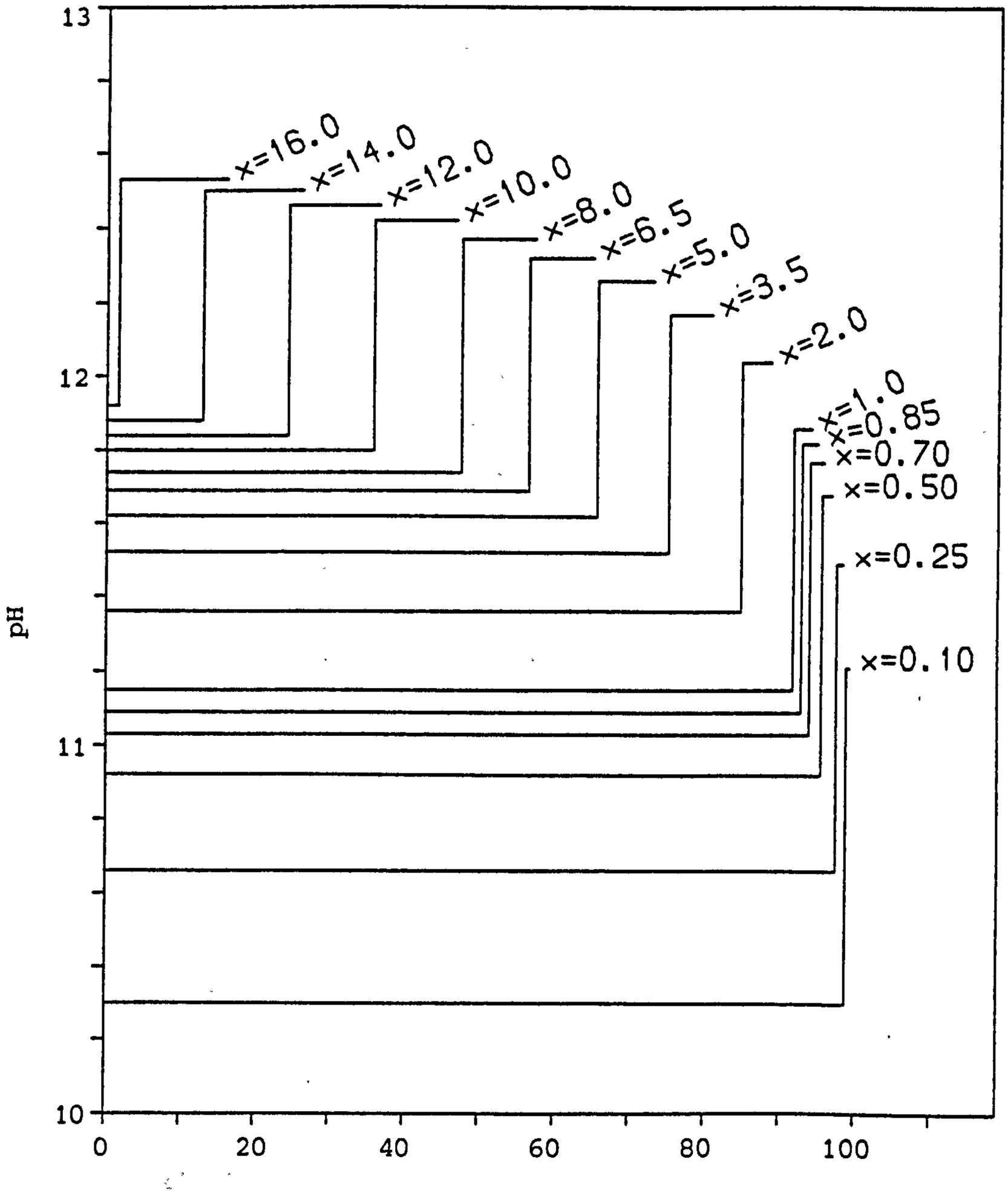

Figure 5.3 pH-yield curves for dense silica crystallisation in the $xNa_2O\ 20SiO_2\ 1000H_2O$ system. The initial horizontal portion of each S-shaped plot represents the A-B transition. The B-C transitions are depicted as separate vertical and horizontal sections for clarity only.

(2) The pH at points A, B and C increase with alkalinity (base cation concentration).

(3) In all instances where a product is obtained, pH_C is always greater than pH_B and the overall pH change (ΔpH_{C-A}) is always positive. The pH increase is caused by the decrease in the amount of silica in solution that results from transfer of solubility control from the amorphous silica to a silica with lower solubility. With increasing alkalinity (x) though, ΔpH_{C-A} decreases. This is a manifestation of the enhanced buffering at high pH in solutions rich with silicate ions.

(4) The amount of solid present always increases on crystallisation i.e. Y-G is always positive. This is because the crystalline solid is less soluble than the amorphous solid. However, both the amount of amorphous solid present initially (G) and the yield (Y) at the end of the reaction decrease as the alkalinity increases - at high pH increased ionisation causes the amount of silica in solution to increase (see Table 5.1 and Figures 5.1(a) and 5.1(b)). The amount of crystallisation that occurs from clear solution during the B-C transition (Y-G) increases as the alkalinity increases.

(5) At the start of reactions, the mixtures with x = 0.10 to 16.00 are heterogeneous, i.e. some amorphous solid is initially present. Those with x = 16.50 and x = 19.00 are initially homogeneous, i.e. the base content is very high and all the amorphous silica dissolves (the equilibrium theory cannot be used to determine the initial reaction conditions when this is the case). However some crystallisation does occur from the resulting clear solutions. For the reaction with x = 19.50, the alkalinity is too high for any crystallisation to occur. Thus there is an upper limiting alkalinity for crystallisation in this system.

(6) Crystallisation is possible at very low base levels ($x < 0.10$). Although crystallisation kinetics may be unfavourable at low alkalinity (low pH), the theory indicates that on the basis

of solubility (thermodynamic grounds) crystallisation can occur. It is interesting to note that many silicious minerals probably crystallise in nature under low pH conditions.

(7) The pH changes are not dependent on the amount of silica in mixtures - as long as some initially remains undissolved.

The effects of alkalinity on the product yields and the pH changes that occurred during the crystallisations are shown in Figures 5.4(a) and 5.4(b) respectively. The curves in Figure 5.4(b) depict how alkalinity affects the pH of solutions in equilibrium with the amorphous and crystalline silicas. Both curves show buffered regions; as x increases the gradients dpH/dx decrease (note that plots of pH vs base cation concentration are identical to the graphs shown). Crystallisation in the system under investigation corresponds to vertical movement from the lower curve to the upper curve at the respective x values. The figure infers that had some base become trapped in the crystals (diagonal movement between the curves) then pH rises would have been reduced.

The dependence of the pH on alkalinity (base cation concentration) for a wider range of K_s values was investigated by Lowe [1] (some of the results were re-calculated using equation (5.20) and are shown in Figure 5.5). For a given alkalinity the overall pH change increases as ΔK_s (K_s(amorphous) - K_s(crystal)) increased, i.e. enhanced solubility differences between substrate and crystals enhances the pH changes during reactions. It can also be inferred from Figure 5.5 that the transformation of a crystalline solid into a more stable crystalline material (Ostwald's rule) which causes a decrease in K_s must necessarily induce a further pH rise.

The results and discussion points relating to crystallisation in the $xNa_2O\ 20SiO_2\ 1000H_2O$ system are similar to those presented by Lowe. Crystallisation of dense silicas from some of these mixtures is thought possible. However the theory, as described, is not specific to one base; the theory takes the amount of base into account but not its chemical nature. For example, if other strong bases (e.g. KOH, quaternary ammonium hydroxides) were employed as mineralisers in these

Figure 5.4 (a) Percentage yield of dense crystalline silica from mixtures of composition $xNa_2O\ 20SiO_2\ 1000H_2O$ as a function of reaction alkalinity (x).

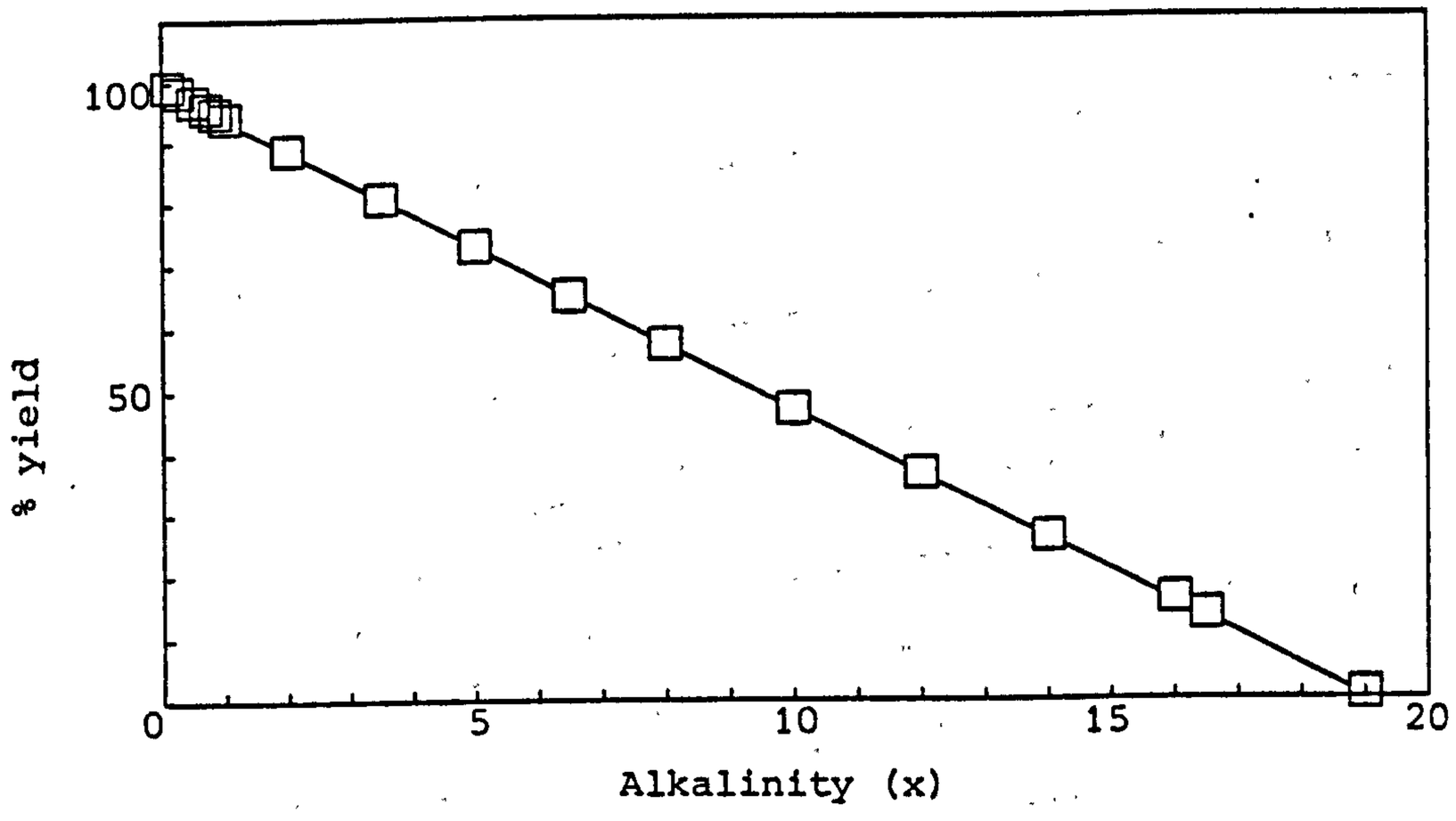

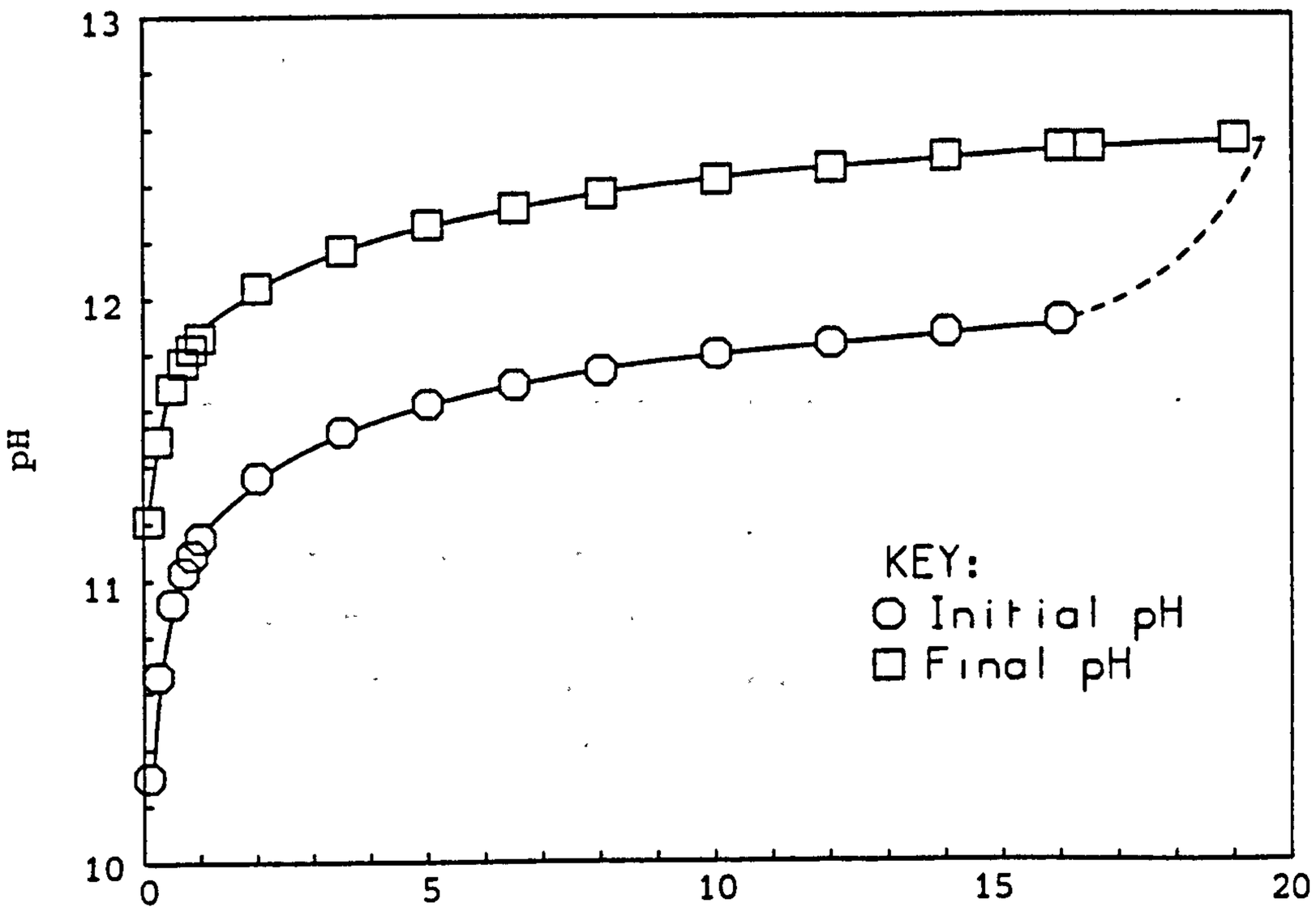

Figure 5.4 (b) pH changes during crystallisation of dense silicas in the $xNa_2O\ 20SiO_2\ 1000H_2O$ system as a function of reaction alkalinity (x). The upper limiting alkalinity is interpolated and correlates with the yield data in Figure 5.4(a).

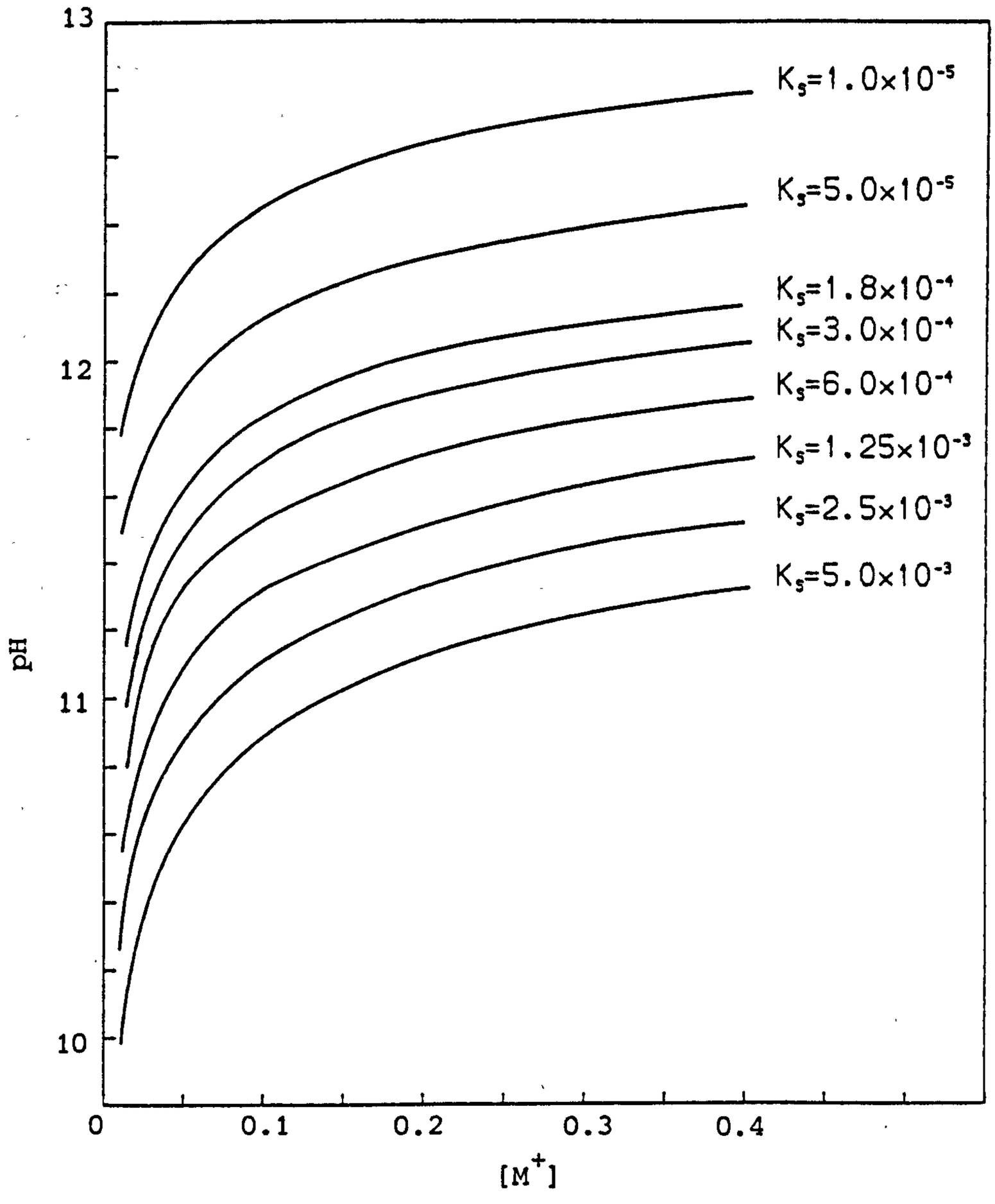

Figure 5.5 Dependence of pH on the concentration of base cations $[M^+]$ in solutions in contact with solid silicas of differing solubility (K_s) as calculated from equation (5.20).

mixtures instead of the sodium hydroxide, the calculated results would be identical to those already described (assuming the products were still dense silicas). The model can be made base specific by taking into account activity coefficient terms in mass action relationships. However there is little knowledge about the relevant coefficients and in any case for a general and simple thermodynamic treatment of crystallisation, it suffices to take all activity coefficients as unity and use concentration terms alone. Though likely to affect the absolute values of some reaction parameters at equilibrium, the fact that activity coefficients have been neglected is unlikely to alter the trends shown by the data.

The values of the proposed extensions to Lowe's theory outlined in section 5.2.1 have only been partly borne out by the results for dense silica crystallisation discussed above. This is because the base cation concentration remains constant throughout these reactions and, as a result, so does the pH throughout the period when crystals grow at the expense of the amorphous solid. If the base cation concentration changes as crystals grow, extremely informative pH changes are induced and it is such situations which are now considered.

Dense silicas, as the name indicates, have little void space within their structures. Crystals are compositionally almost 100% SiO_2. This is not true of microporous silicas whose open frameworks are usually stabilised during growth by being filled with guest molecules. The compositions of crystals can be substantially less than 100% SiO_2. The chemical nature of the guest species can markedly affect the pH changes that accompany crystallisation. Reasons for this are two-fold:

(a) The nature of the guest species is likely to affect the solubility of the solid (its K_s value).

(b) Guest species necessarily have to originate from the solution and their removal may perturb solution phase equilibria.

The effects of solubility (K_s) on the pH changes that occur during reactions have been covered by Lowe and briefly discussed above in relation to dense silica crystallisation. This point is considered no further. The results that are now presented were calculated assuming all product silicas had the same solubility ($K_s = 1.8 \times 10^{-4}$) irrespective of the chemical nature of the guest molecules. This has

enabled the effects of removing chemically different guest species from the solution phase during crystal growth to be evaluated independently of the solubility variable.

Possible guest molecule types are listed in Table 5.3 and their plausibility commented on. At present all known silica molecular sieves belong to categories (c) and (d), i.e. their pores are filled either with organic salts or organic bases during synthesis (reference is made to Table 1.4 in chapter 1). The best known silica sieve is silicalite-1 [9]. Silicalite-1 crystallises with ideal unit cell composition 4TPAOH $96SiO_2$ and thus during reaction the alkalinity of mixtures becomes partitioned between the solid and liquid phases. As will be seen, loss of base from solution has consequences.

Silicalite-1 crystallisation in the xNa_2O 2TPABr $20SiO_2$ $1000H_2O$ system is now discussed in detail. This particular system was chosen for study because experimental data was available (chapter 3) for comparison with the theoretical predictions.

5.3.2 Crystallisation of silicalite in the xNa_2O 2TPABr $20SiO_2$ $1000H_2O$ system

The base contents of these mixtures were equivalent to those used to model dense silica crystallisation in the previous section. Alkalinity was derived solely from the sodium hydroxide. The presence of the tetrapropylammonium bromide (TPABr) in the mixtures provided no additional alkalinity (it is the salt of a strong base and a strong acid) but it was deemed to direct silicalite-1 crystallisation.

In this system the charge balance equation relating the ionic species in solution is:

$$[Na^+] + [TPA^+] = [SH_3^-] + 2[SH_2^{2-}] + [OH^-] + [Br^-] \qquad (5.22)$$

Note that the $[H^+]$ term has been omitted from the left-hand side of the equation for the same reasons as before. The cations added to the mixture as base, the sodium ions, can be tentatively considered to balance the silicate and hydroxide ions in the solution. They can be

Table 5.3 Comments on the plausibility of guest molecule types for stabilisation of microporous silicas during crystallisation

Guest species	Comments
(a) Water	Hydrophobic surfaces are unlikely to be stabilised by water although some interactions probably occur. Hydrophilic microporous silicas have not yet been discovered but, like a silica gel, they would probably have a strong affinity for water and perhaps be water-stabilised during crystallisation.
(b) Void pores	Thermodynamically unlikely; microporous silicas need to be stabilised by guest molecules.
(c) Salts	Charged (hydrophilic) molecules act as guests only if they have appreciable organic character. One of the known microporous silicas, fluoride silicalite, is stabilised by TPAF [6,7].
(d) Bases	Organic bases act as stabilisers for the majority of the known microporous silicas (see Chapter 1, Table 1.4). Organic bases can be classified into weak and strong types.
(e) Acids	No acid-stabilised microporous silicas are known. Crystallisation of such materials may be possible from mixtures that contain weak organic acids under near neutral pH conditions. At elevated pH, organic acids are converted to salts.
(f) Other	Into this category fall uncharged molecules such as alcohols and a miscellany of other organics. Alcohols have found use in high silica zeolite synthesis but, as yet, not in silica molecular sieve synthesis. Other possible guests include (i) metal complexes with organic ligands and less likely (ii) dissolved gases (note that some clathrasils, tight-structured tectosilicates, are known to contain adsorbed gases as guest species [8]).

All the known silica molecular sieves are stabilised by compounds which are appreciably water soluble - yet hydrophobic silicas are best stabilised by hydrophobic molecules. There are many sparingly soluble/ insoluble organics which could perhaps function in a stabilising role if means of solubilising and dispersing them in aqueous media were found.

termed the 'effective cations' because they are base derived. The 'ineffective' cations are the tetrapropylammonium cations which can be thought of as providers of counter-charge for the bromide ions in solution. As the liquid phase is homogeneous specific cations cannot be differentiated into effective and ineffective types but this pseudo-categorisation does aid clarification of a salient point - the relative concentrations of effective and ineffective cations are necessarily equivalent to the relative amounts of base and salt added to mixtures (i.e. $2x/(2x + 2)$ in these reactions).

Prior to the onset of crystallisation, the concentration of effective cations $[C^+]$ is given by:

$$[C^+] = 2x/(1000M_w) \qquad (5.23)$$

where M_w is the molar mass of water in kg. Note that $[C^+] = [Na^+]$ at this stage. The charge balance equation that applies is therefore:

$$[C^+] = [SH_3^-] + 2[SH_2^{2-}] + [OH^-] \qquad (5.24)$$

This equation is identical to equation (5.22) except that the $[TPA^+]$ and $[Br^-]$ terms which are equivalent and cancel one another have been ommitted. Substitution of equations (5.7), (5.12), (5.13) and (5.19) into equation (5.24) gives an expression identical to equation (5.20):

$$[C^+] = K_1K_s/[H^+] + 2K_1K_2K_s/[H^+]^2 + K_w/[H^+] \qquad (5.25)$$

The initial equilibrium conditions were calculated using equation (5.25) substituting for $[C^+]$ and the K_s value for amorphous silica ($K_s = 2.5 \times 10^{-3}$). The amount of undissolved silica (S_u mol kg^{-1}) was calculated by subtracting the amount of silica in solution from the total amount in the system:

$$S_u = 20/wM_w - (K_s + K_1K_s/[H^+] + K_1K_2K_s/[H^+]^2) \qquad (5.26)$$

The percentage of the total silica that is undissolved (G) is given by:

$$G = 100S_u\ wM_w/20 \qquad (5.27)$$

If a given amount of this amorphous solid (S_c mol kg^{-1}) is converted to silicalite with composition 4TPAOH $96SiO_2$ the amount of base in solution decreases by an amount B_1 where:

$$B_1 = 4S_c/96 \qquad (5.28)$$

Because 1000 g water were assumed present in each reaction mixture the loss of base B_1 represents the decrease in the amount of base in solution on a concentration basis. The concentration of effective cations $[C^+]$ after removal of B_1 moles of TPAOH from the solution phase by the silicalite crystals is therefore:

$$[C^+] = [Na^+] - [B_1] \qquad (5.29)$$

where $[B_1]$ can be thought of as a virtual concentration representing the amount of base lost from solution. As crystallisation proceeds the effective cation concentration is continually reduced. After any given number of moles of the amorphous solid have been converted to silicalite, the effective cation concentration $[C^+]$ can be calculated using equation (5.29). Insertion of this value into equation (5.25) allows the pH to be calculated. At this pH the amount of silica in solution can be determined and hence the amount of gel remaining can be ascertained (by difference having allowed for the silica crystallised). Note that the gel still controls species in solution even though two different solid silicas are now present. Thus the period when crystals grow at the expense of the amorphous solid can be modelled thermodynamically. Crystallisation of silicalite in effect causes the following reaction to occur:

$$TPABr(aq) + NaOH(aq) \longrightarrow TPAOH(sil) + NaBr(aq) \qquad (5.30)$$

where TPAOH(sil) represents TPAOH within the silica lattice.

The removal of base from the solution during the growth period before solubility transfer is a titrimetric effect akin to adding acid to the system.

A computer program written in basic (file PHUP2) for an Apple II microcomputer was used to perform calculations. The computational methodology employed was as follows:

For each reaction alkalinity (x), the initial equilibrium was calculated (designated point A) using $K_s = 2.5 \times 10^{-3}$ for the amorphous solid. Fifty percent (by weight) of the undissolved amorphous solid was then considered to be crystallised. The new effective cation concentration was calculated and the new equilibrium parameters were determined. This process was repeated sequentially, each time 'crystallising' 50% of the remaining amorphous solid and re-calculating parameters. In effect, transformation of the gel into crystals was considered to be a stepwise process, equilibrium being re-established after crystallisation of portions of the amorphous solid. When the crystallinity of the solid phase (XL) on a mass basis:

$$XL = 100S_c/S_u \qquad (5.31)$$

was greater than 99.9% (i.e. when the solid was virtually entirely crystalline but the trace of amorphous solid was still solubility controlling), the calculated parameters were deemed to represent conditions at the solubility transfer point (point B) and the program terminated. The solubility transfer itself and the accompanying crystallisation from clear solution could not be modelled. The final equilibrium position (point C) was calculated by re-running the computer program using the K_s value ($K_s = 1.8 \times 10^{-4}$) for the crystalline silica. The program performed sequential crystallisation again (in effect on a less soluble substrate) until the crystallinity was greater than 99.9% (point C). The flow diagram in Figure 5.6 summarises the method used to calculate results, example output from the computer program is shown in Figure 5.7 and details of the program itself (file PHUP2) are given in Appendix III.

The results are collated in Table 5.4. The pH-yield plots in Figure 5.8 give a visual depiction of many of the features shown by the data. These features are now listed.

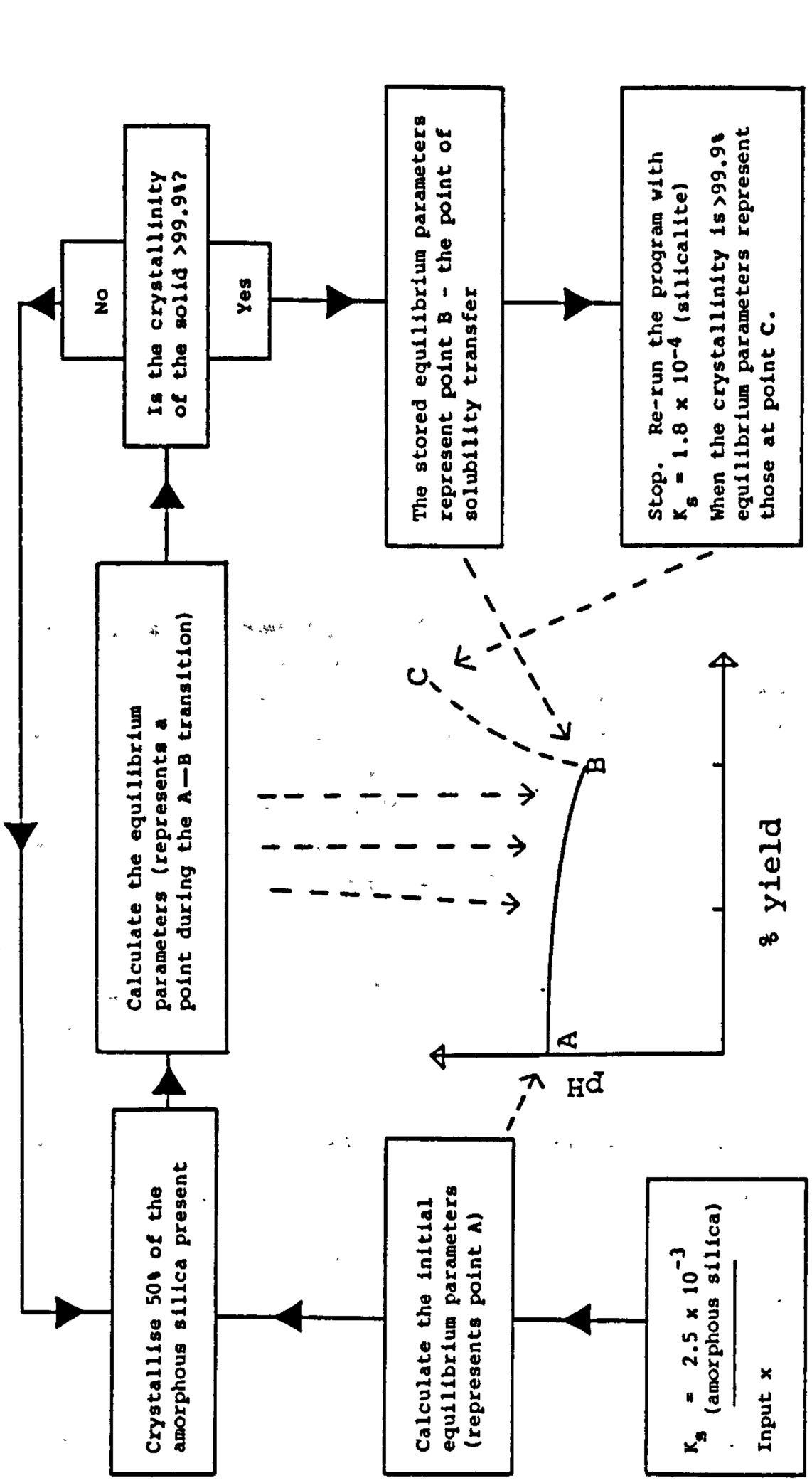

Figure 5.6 Flow diagram outlining the computational method used to model silicalite crystallisation in the xNa_2O 2TPABr $20SiO_2$ $1000H_2O$ system

Figure 5.7 Example output from the program (PHUP2) used to model silicalite crystallisation in the xNa_2O 2TPABr $20SiO_2$ $1000H_2O$ system

```
X=1
K1=2E-10
K2=2E-12
KS=2.5E-03

-------

(C+)=0.06727
PH=10.982
(S1)=0.04793
(S2)=9.1908E-03
Nos moles SiO2 in system=1.1102
Nos moles SiO2 in solution=0.05963
Nos moles solid SiO2 present (gel + xals)=1.0506
% Total SiO2 present as solid (gel + xals)=94.629
Nos moles gel present=7.0240E-04
Nos moles SiO2 xallised=1.0499
Nos moles base in xals=0.04374
% Total base tied up in xals=39.403
% Crystallinity=99.933
% Yield=94.566
NA/TPA ratio in solution=1.6502
NA/(NA+TPA)=0.6227
```

(N.B. These results related to the solubility transfer point (point B) for the reaction with x = 1.0. The program assumes 1000 grams of water are present in reaction mixtures)

Notation used in the Computer Output

(C+) = the effective base cation concentration

(S1) = the concentration of singly charged silicate anion

(S2) = the concentration of doubly charged silicate anion

(ST) = the total concentration of silica in solution

NA/TPA = the molar ratio of sodium to TPA ions in the solution

NA/(NA+TPA) = the mole fraction of sodium ions in the solution

Table 5.4 Simulated crystallisation in the xNa_2O 2TPABr $20SiO_2$ $1000H_2O$ system

Chemical composition of the crystals: 4TPAOH $96SiO_2$

	Initial (Point A)			Solubility Transfer (Point B)				Final (Point C)						
X	$[C^+]$	pH	G[a]	$[C^+]$	pH	Y[b]	L[c]	$[C^+]$	pH	Y[b]	L[c]	ΔpH_{B-A}	ΔpH_{C-B}	ΔpH_{C-A}
0.25[d]	0.028	10.66	97.5	-	-	-	-	-	-	-	-	-	-	-
0.50	0.056	10.92	95.5	0.010	10.25	98.9	82.4	0.010	11.16	99.4	82.8	-0.67	0.91	0.24
0.70	0.078	11.03	93.9	0.033	10.73	97.1	57.8	0.032	11.53	98.1	58.4	-0.30	0.80	0.50
0.85	0.094	11.09	92.8	0.050	10.88	95.9	47.0	0.049	11.65	97.2	47.6	-0.21	0.77	0.56
1.00	0.111	11.15	91.7	0.067	10.98	94.6	39.4	0.066	11.73	96.4	40.1	-0.17	0.75	0.58
2.00	0.222	11.36	84.7	0.182	11.30	87.2	18.2	0.180	11.99	90.7	18.9	-0.06	0.69	0.63
3.50	0.389	11.52	75.0	0.353	11.49	77.0	9.2	0.350	12.15	82.6	9.8	-0.03	0.66	0.63
5.00	0.555	11.62	65.6	0.524	11.60	67.4	5.6	0.521	12.24	74.5	6.2	-0.02	0.64	0.62
6.50	0.722	11.69	56.5	0.695	11.68	58.0	3.7	0.691	12.31	66.5	4.3	-0.01	0.63	0.62
8.00	0.888	11.74	47.6	0.866	11.73	48.8	2.5	0.861	12.36	58.5	3.0	-0.01	0.63	0.62
10.00	1.110	11.80	35.9	1.093	11.79	36.8	1.5	1.088	12.41	47.9	2.0	-0.01	0.62	0.61
12.00	1.332	11.84	24.4	1.321	11.84	25.0	0.9	1.315	12.46	37.4	1.3	0.00(2)	0.61(5)	0.61
14.00	1.554	11.88	12.9	1.548	11.88	13.2	0.4	1.542	12.49	26.9	0.8	0.00	0.61	0.61
16.00	1.776	11.92	1.6	1.776	11.92	1.6	<0.1	1.769	12.52	16.4	0.4	0.00	0.60	0.60
16.50[e]	1.832	-	-	-	-	-	-	1.825	12.53	13.8	0.3	-	-	-
19.00[e]	2.109	-	-	-	-	-	-	2.109	12.56	0.7	<0.1	-	-	-
19.50[e,f]	2.165	-	-	-	-	-	-	-	-	-	-	-	-	-

[a] % silica as amorphous solid; [b] % yield; [c] % total base removed by the crystals; [d] insufficient base to crystallise all the silica; [e] amorphous silica totally soluble; [f] crystals totally soluble

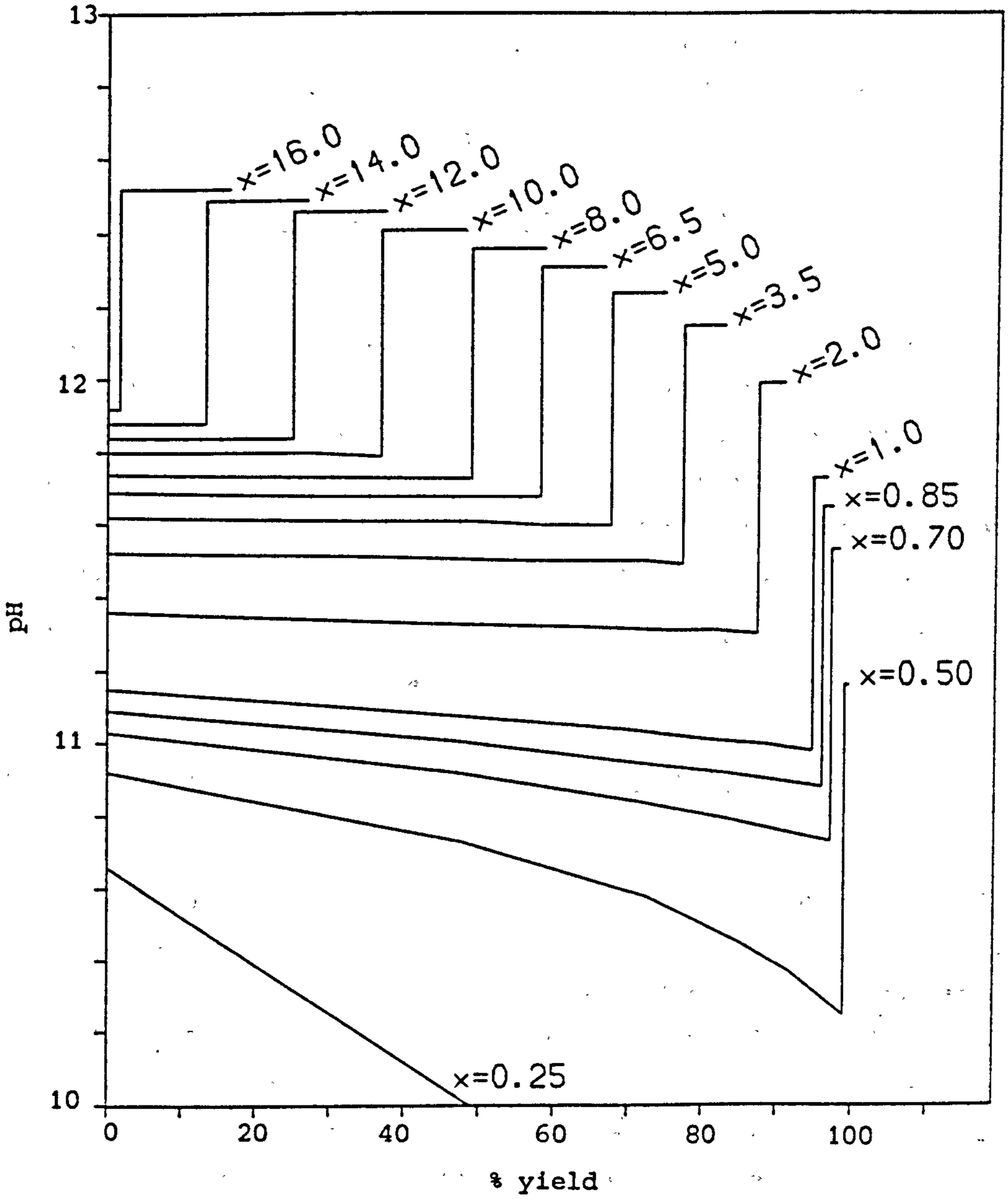

Figure 5.8 pH-yield curves for silicalite crystallisation in the xNa_2O 2TPABr $20SiO_2$ $1000H_2O$ system.
(N.B. the B-C transitions are depicted as separate vertical and horizontal sections for clarity only).

The initial equilibrium (point A)

As the reaction alkalinity increases:

(i) The induction period pH increases.

(ii) The amount of amorphous solid present decreases.

(iii) At very high alkalinity (x = 16.50 and 19.00) all the solid silica dissolves.

These features were expected as equilibrium conditions during the induction period (point A) are the same as those evaluated in the previous section (dense silica formation - section 5.3.1).

Crystal growth at the expense of the amorphous solid (the A-B transition)

(i) The pH fall (ΔpH_{B-A}), caused by the uptake of base molecules by the growing crystals, becomes more pronounced as the alkalinity decreases; low alkalinity reactions are unbuffered and a large percentage of their total base content is removed from solution during reaction. Over 80% of the base is consumed during this growth period for the reaction with x = 0.50.

(ii) The percentage of the total silica converted to crystals (Y) during this period decreases as the alkalinity increases.

Solubility transfer and crystal growth from clear solution (the B-C transition)

(i) In each case, the amount of silica in solution decreases and the pH and amount of crystalline solid present increase during this period. This is because silicalite is less soluble than amorphous silica. The amount of silicalite that crystallises from clear solution increases as the alkalinity increases. All crystallisation occurs from clear solution for the reactions with x = 16.50 and 19.00. When x = 19.50 conditions are too severe for any crystallisation to occur.

(ii) The largest pH rises during solubility transfer are seen for the low base, poorly buffered reactions.

These trends were also observed when dense silicas crystallise (section 5.3.1).

Summary

The effect of alkalinity on the yields and pH changes are summarised in Figures 5.9(a) and 5.9(b) respectively. When silicalite crystallises, unlike when dense silicas from (section 5.3.1), there is a minimum alkalinity (x = 0.42) below which reaction cannot go to completion. This is because the crystals consume base as they grow. At very low alkalinity (x < ∿0.45) the overall pH change during reaction is negative (i.e. $pH_C < pH_A$) because such a large proportion of the total base is removed by the crystals. Figure 5.10 shows that the overall pH change, a net result of the pH fall during the A-B transition and the pH rise during the B-C transition, reaches a small maximum between x = 2 and x = 3. At high alkalinity (x > ∿16.50) the overall pH change is reduced because all crystallisation occurs from clear solution. The interpolated intersection point denotes the upper limiting alkalinity.

5.3.2.1 Crystallisation of silicalite with composition pNaOH 4TPAOH $96SiO_2$

In the previous section it was assumed that silicalite crystallised with ideal unit cell composition 4TPAOH $96SiO_2$. Experimental results have shown that when silicalite is crystallised in the xNa_2O 2TPABr $20SiO_2$ $1000H_2O$ system the products have empirical composition pNaOH 4TPAOH $96SiO_2$ (p = 0 to 4 depending on the reaction conditions). A maximum of four NaOH molecules per unit cell is indicated by the experimental data (see chapter 3, Figure 3.13).

The theoretical results in Table 5.5, calculated using a modified version of program PHUP2, show how incorporation of NaOH affects reaction thermodynamics. For both a low and high base reaction (x = 1 and 10) silicalite was crystallised with variable chemical composition pNaOH 4TPAOH $96SiO_2$ (p = 0 to 4 for each x). The results show that:

(1) For the reactions with x = 1, the pH at points B and C decrease as the extent of NaOH incorporation increases. The yields correspondingly increase. Note that both the pH

Figure 5.9 (a) Percentage yield of silicalite from mixtures of composition xNa_2O 2TPABr $20SiO_2$ $1000H_2O$ as a function of reaction alkalinity (x).

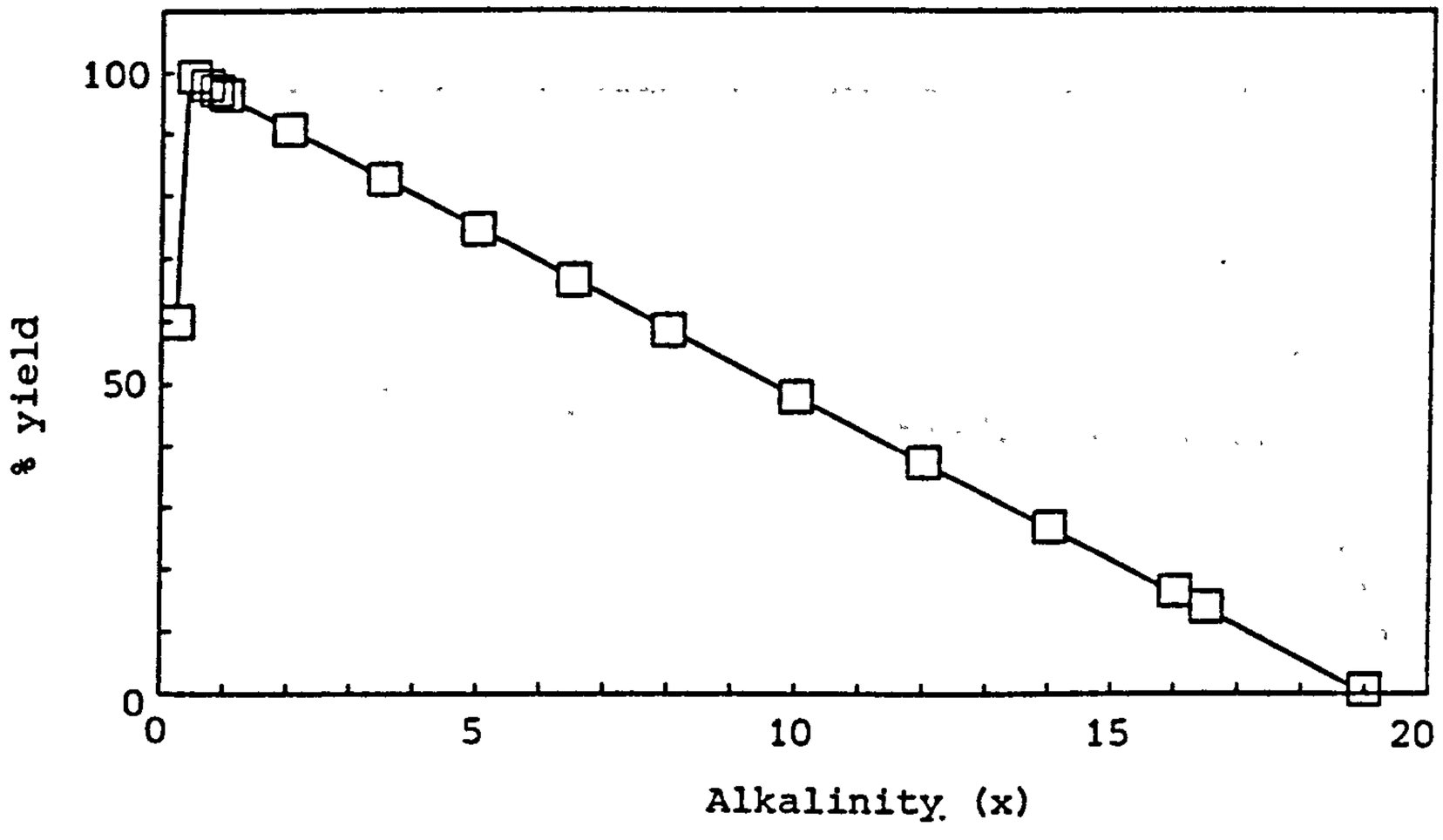

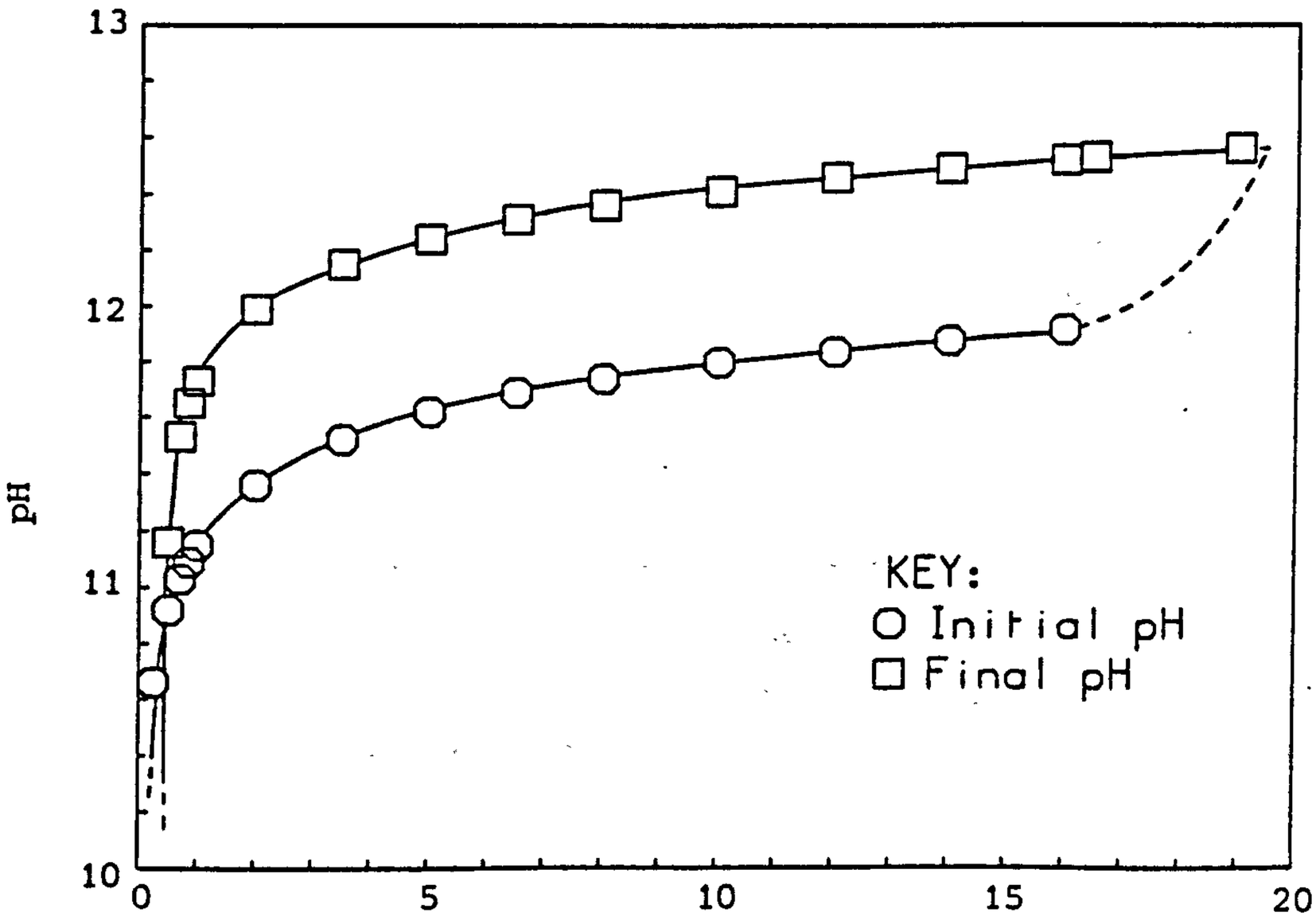

Figure 5.9 (b) pH changes during silicalite crystallisation in the xNa_2O 2TPABr $20SiO_2$ $1000H_2O$ system as a function of reaction alkalinity (x).

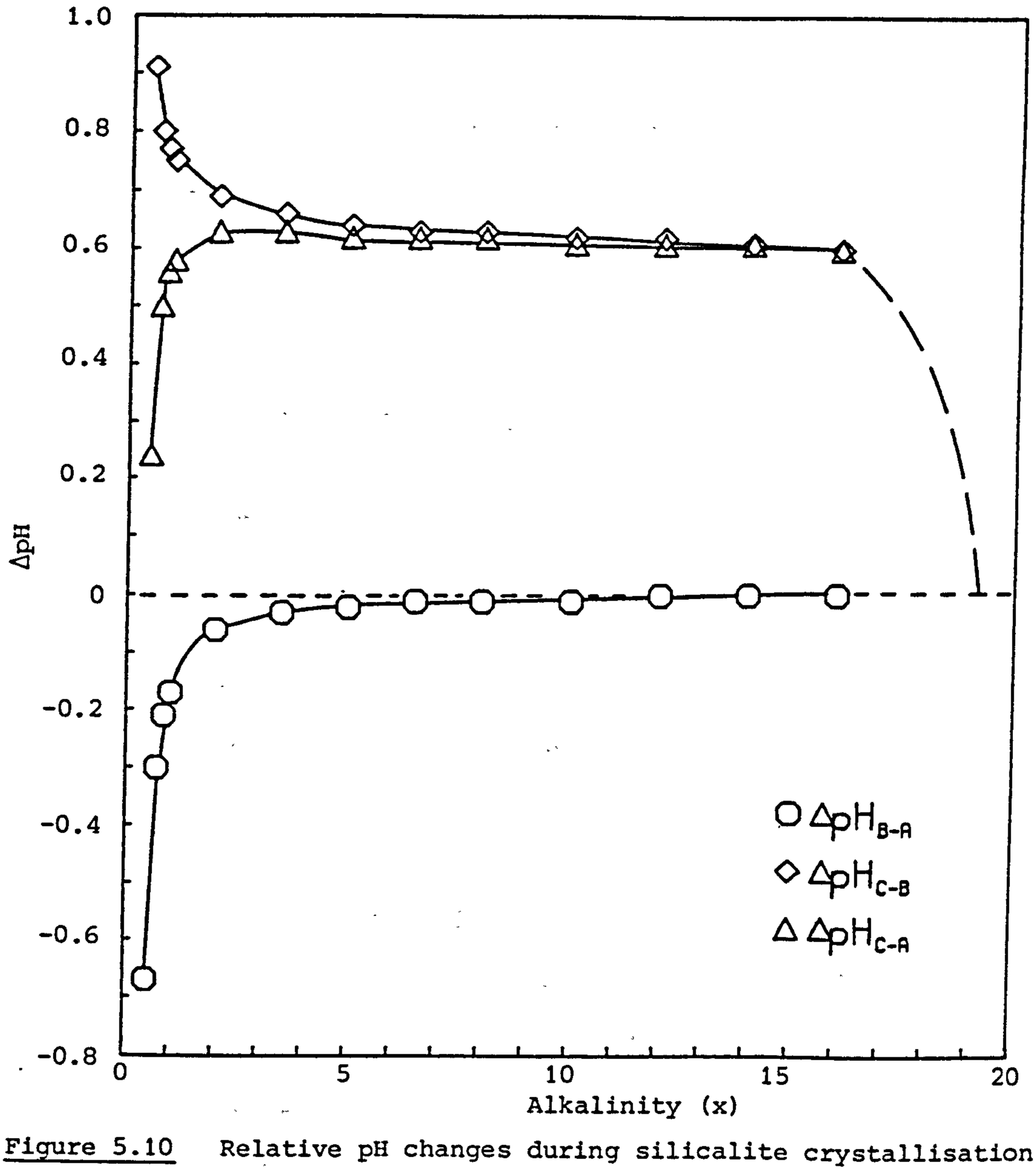

Figure 5.10 Relative pH changes during silicalite crystallisation in the xNa_2O 2TPABr $20SiO_2$ $1000H_2O$ system as a function of reaction alkalinity (x)

Table 5.5 Simulated crystallisation in the xNa_2O 2TPABr $20SiO_2$ $1000H_2O$ system

Chemical composition of the crystals: pNaOH 4TPAOH $96SiO_2$

x	p[d]	Initial (Point A)			Solubility Transfer (Point B)				Final (Point C)				
		$[C^+]$	pH	G[a]	$[C^+]$	pH	Y[b]	L[c]	$[C^+]$	pH	Y[b]	L[c]	ΔpH_{C-A}
1.0	0	0.111	11.15	91.7	0.067	10.98	94.6	39.4	0.066	11.73	96.4	40.1	0.58
1.0	1	0.111	11.15	91.7	0.056	10.92	95.4	49.7	0.055	11.68	96.9	50.5	0.53
1.0	2	0.111	11.15	91.7	0.044	10.84	96.3	60.1	0.043	11.61	97.5	60.9	0.46
1.0	3	0.111	11.15	91.7	0.032	10.72	97.2	70.8	0.032	11.53	98.2	71.5	0.38
1.0	4	0.111	11.15	91.7	0.020	10.55	98.1	81.7	0.020	11.39	98.8	82.3	0.24
10.0	0	1.110	11.80	35.9	1.093	11.79	36.8	1.5	1.088	12.41	47.9	2.0	0.61
10.0	1	1.110	11.80	35.9	1.089	11.79	37.0	1.9	1.082	12.41	48.2	2.5	0.61
10.0	2	1.110	11.80	35.9	1.084	11.79	37.3	2.3	1.077	12.41	48.5	3.0	0.61
10.0	3	1.110	11.80	35.9	1.080	11.79	37.5	2.7	1.071	12.41	48.7	3.6	0.61
10.0	4	1.110	11.80	35.9	1.075	11.79	37.7	3.1	1.065	12.41	49.0	4.1	0.61

[a] % silica as amorphous solid

[b] % yield

[c] % total base removed by the crystals

[d] moles NaOH per unit cell silicalite

fall (ΔpH_{B-A}) and the pH rise (ΔpH_{C-B}) become more pronounced as the amount of NaOH in the crystals increases (Figure 5.11(I)). These trends are a direct result of increased base loss from the solution phase during the A-B transition.

(2) For the reactions with x = 10, pH changes are unaffected by sodium incorporation (see Figure 5.11(I)). This is because the solutions are well buffered and only a small fraction of the total base (maximum 4.1% - for the product with composition 4NaOH 4TPAOH $96SiO_2$) is removed during reaction.

Analogous to the removal of base from solution during silicalite-1 (a tectosilicate) crystallisation is that during crystallisation of other classes of insoluble silicates such as layer silicates (e.g. makatite [10]). The latter contain an intrinsic negative charge on their silica frameworks which is usually counterbalanced by base cations. Although no results have been evaluated, it would be possible to model the crystallisation of silicates of this type using this theory.

Few of the base molecules inside silicalite crystals are likely to be present as discrete molecules. Attack on the silica framework will be rife (giving for example $\equiv Si\text{-}OH\ TP\overset{+}{A}\ \overset{-}{O}\text{-}Si\equiv$). As-synthesised silicalite is thus a salt - a silicate. Just as the internal surfaces are attacked by base, so are the external surfaces in contact with the solution and this externally bound base, like that inside, is 'lost' from the solution. The amount of base tied up in this way will be dependent on the nature of the base, the pH and the specific surface area of the crystals. In a similar manner, base will also be tied up on the amorphous solid at the beginning of the reaction. Its specific surface area is likely to exceed that of the crystals and so base lost to its surface will be greater. If not taken into account this surface base could be a cause of discrepancy between theoretical predictions and experimental results.

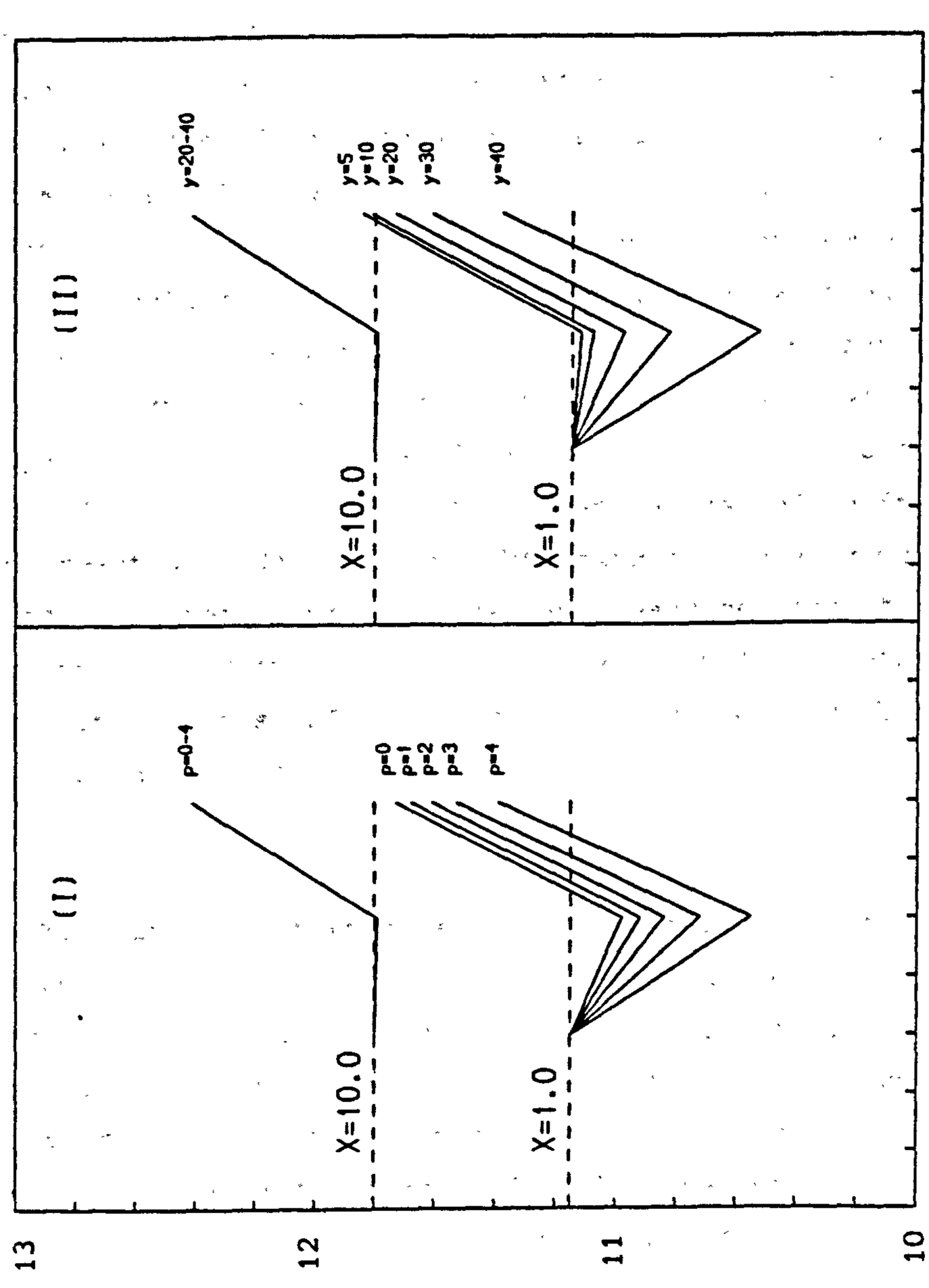

Figure 5.11 Line representations depicting pH changes that accompany silicalite crystallisation (the abscissae are scaled arbitrarily)

(I) System xNa_2O 2TPABr $20SiO_2$ $1000H_2O$; Crystal composition pNaOH 4TPAOH $96SiO_2$

(II) System xNa_2O 2TPABr $ySiO_2$ $1000H_2O$; Crystal composition 4TPAOH $96SiO_2$

With the aid of the manufacturer's data relating to the amorphous silica powder used as source silica in the experimental work (Cab-O-Sil M5; 200 ± 25 m^2g^{-1} in dry powder form), calculations indicate that only at very low base levels is the amount of base associated with the gel surface likely to be a significant percentage of the total (for the crystals it will be less significant). This loss in low base systems is partially offset by the fact that at low pH surface silanol groups are less likely to ionise and so base associated with the surface will be reduced. For reactions with an appreciable base content, and therefore a considerable buffer capacity, surface-bound base can be safely neglected in the theoretical calculations. If surface bound base is not taken into account for low base reactions, it is difficult to quantify the discrepancy between experiment and theory that could be caused. The problem is complicated by the fact that transformation of the gel into crystals is likely to be accompanied by a substantial decrease in the specific surface area of the solid phase and consequently a net release of surface base during reaction. In addition, obtaining accurate experimental pH measurements from unbuffered low base reactions has its problems; solutions are extremely sensitive to even small amounts of CO_2 absorption. Because of these problems surface bound base was neglected in all calculations.

Ways in which mixture alkalinity affects silicalite crystallisation have been discussed in some detail. As might be expected, altering the amounts of other mixture components can also affect the thermodynamic courses of reactions. The two sections that follow, respectively examine the perturbations that are induced when the amounts of silica and water in mixtures are changed. Calculations were performed using modified versions of the computer program already described (file PHUP2). As the modifications required were minor, and did not involve complicated re-programming, specific details are not given.

5.3.3 Crystallisation of silicalite in the xNa_2O 2TPABr $ySiO_2$ $1000H_2O$ system

The products from these reactions were considered to have ideal composition 4TPAOH $96SiO_2$. Crystallisation was simulated from mixtures of composition xNa_2O 2TPABr $ySiO_2$ $1000H_2O$ (x = 1 and 10; y = 5 to 40 for each x). Results are given in Table 5.6 and displayed in Figure 5.11(II). Features of note:

(1) For the low base mixtures (x = 1), pH changes are markedly affected by the silica content of the mixtures. Comparison with the results in Figure 5.11(I) shows that effects are similar to those already described for crystallisation of silicalite with variable composition (pNaOH 4TPAOH $96SiO_2$). This is not surprising because the amount of silica that crystallises dictates the amount of base lost from solution. For example, the pH changes that occur during the reactions $1Na_2O$ 2TPABr $40SiO_2$ $1000H_2O$ (product composition 4TPAOH $96SiO_2$) and $1Na_2O$ 2TPABr $20SiO_2$ $1000H_2O$ (product composition 4NaOH 4TPAOH $96SiO_2$) are identical. Note however that the kinetics of these reactions would probably differ appreciably because of the different amounts of silica in the mixtures and the different chemistries of the crystals.

(2) For the higher base reactions (x = 10), the silica content of a mixture has a critical bearing on whether any product is obtained. If crystallisation is to occur, the Na_2O/SiO_2 ratio in a mixture must be carefully selected. The pH changes during the reactions that did give products were little affected by the quantity of silica present (see Figure 5.11(II)). This is attributable to the high buffer capacity of these mixtures.

5.3.4 Crystallisation of silicalite in the xNa_2O 2TPABr $20SiO_2$ wH_2O system

The amount of water in a reaction mixture is a key reaction variable. Crystallisation of silicalite, with ideal composition, in the system xNa_2O 2TPABr $20SiO_2$ wH_2O (x = 1 and 10; w = 200 to 5000 for each x) has been simulated.

Table 5.6 Simulated crystallisation in the xNa_2O 2TPABr $ySiO_2$ $1000H_2O$ system
Chemical composition of the crystals: 4TPAOH $96SiO_2$

		Initial (Point A)			Solubility Transfer (Point B)				Final (Point C)				
x	y[d]	$[C^+]$	pH	G[a]	$[C^+]$	pH	Y[b]	L[c]	$[C^+]$	pH	Y[b]	L[c]	ΔpH_{C-A}
1.0	5	0.111	11.15	66.7	0.103	11.12	68.8	7.2	0.102	11.84	78.3	8.2	0.69
1.0	10	0.111	11.15	83.4	0.091	11.08	86.0	17.9	0.090	11.81	90.3	18.8	0.66
1.0	20	0.111	11.15	91.7	0.067	10.98	94.6	39.4	0.066	11.73	96.4	40.1	0.58
1.0	30	0.111	11.15	94.5	0.043	10.83	97.6	60.9	0.043	11.61	98.4	61.5	0.46
1.0	40	0.111	11.15	95.8	0.019	10.53	99.1	82.5	0.019	11.38	99.4	82.8	0.23
10.0	5[e]	1.110	-	-	-	-	-	-	-	-	-	-	-
10.0	10[e]	1.110	-	-	-	-	-	-	-	-	-	-	-
10.0	20	1.110	11.80	35.9	1.093	11.79	36.8	1.5	1.088	12.41	47.9	2.0	0.61
10.0	30	1.110	11.80	57.3	1.069	11.79	58.7	3.7	1.064	12.41	66.0	4.1	0.61
10.0	40	1.110	11.80	68.0	1.046	11.78	69.6	5.8	1.041	12.40	75.1	6.3	0.60

[a] %silica as amorphous solid

[b] % yield

[c] % total base removed by the crystals

[d] moles silica in mixture / composition

[e] amorphous silica and crystals totally soluble

Understanding of the discussion that now follows is aided if it is imagined that each mixture contained the same amount of water (1000 g). Increasing w therefore effectively decreases the absolute amounts of base, salt and silica present (N.B. not the relative amounts though). It is preferable to view the mixtures this way because the equilibria relating species in solution involve concentration terms. The results in Table 5.7 and Figure 5.12 show interesting features:

(1) In both sets of results (x = 1 and 10) the percentage of the total silica initially present as solid (G) and the induction period pH decrease as w increases. These trends were expected.

(2) The decreases in pH during the A-B transition are very small for the higher alkalinity reactions (x = 10) but considerable for the lower base reactions (x = 1). Regarding the latter, note that the pH decrease is almost independent of w (clearly seen in Figure 5.12). Reactions with small w contain most silica, a lot of base is lost during the A-B transition but the solution phases contain a lot of base to buffer this loss. Reactions with large w contain least silica, little base is lost during crystal growth but as the solution phases contain relatively little base in the first place (poorly buffered) substantial pH decreases are seen. The net result is that the observed pH decreases are fairly similar.

(3) Increases in pH during the B-C period for the mixtures with x = 10 are independent of w because of buffering effects. For the lower base mixtures (x = 1) the increases are greatest for reactions with large w (small concentration of base cations, lower pH, least buffered).

These results have shown that the water content of a mixture seriously perturbs reaction equilibria. It is in fact well known that choice of Na_2O/H_2O and SiO_2/H_2O molar ratios in mixtures is critically important.

Table 5.7 Simulated crystallisation in the xNa_2O 2TPABr $20SiO_2$ wH_2O system
Chemical composition of the crystals: 4TPAOH $96SiO_2$

		Initial (Point A)			Solubility Transfer (Point B)				Final (Point C)				
x	w[d]	$[C^+]$	pH	G[a]	$[C^+]$	pH	Y[b]	L[c]	$[C^+]$	pH	Y[b]	L[c]	ΔpH_{C-A}
1.0	200	0.555	11.62	93.1	0.334	11.48	95.6	39.8	0.332	12.14	96.7	40.3	0.52
1.0	500	0.222	11.36	92.4	0.134	11.21	95.1	39.6	0.133	11.91	96.5	40.2	0.55
1.0	1000	0.111	11.15	91.7	0.067	10.98	94.6	39.4	0.066	11.73	96.4	40.1	0.58
1.0	2000	0.056	10.92	90.9	0.034	10.74	94.1	39.2	0.033	11.54	96.2	40.0	0.62
1.0	5000	0.022	10.58	89.7	0.014	10.39	93.1	38.8	0.013	11.26	95.8	39.9	0.68
10.0	200	5.551	12.19	43.1	5.449	12.18	44.1	1.8	5.436	12.78	49.6	2.1	0.59
10.0	500	2.220	11.97	39.6	2.183	11.97	40.5	1.7	2.175	12.57	48.8	2.0	0.60
10.0	1000	1.110	11.80	35.9	1.093	11.79	36.8	1.5	1.088	12.41	47.9	2.0	0.61
10.0	2000	0.555	11.62	31.3	0.548	11.61	32.1	1.3	0.544	12.25	46.7	1.9	0.63
10.0	5000	0.222	11.36	23.6	0.220	11.36	24.3	1.0	0.218	12.03	44.5	1.9	0.67

[a] % silica as amorphous solid

[b] % yield

[c] % total base removed by the crystals

[d] moles water in mixture composition

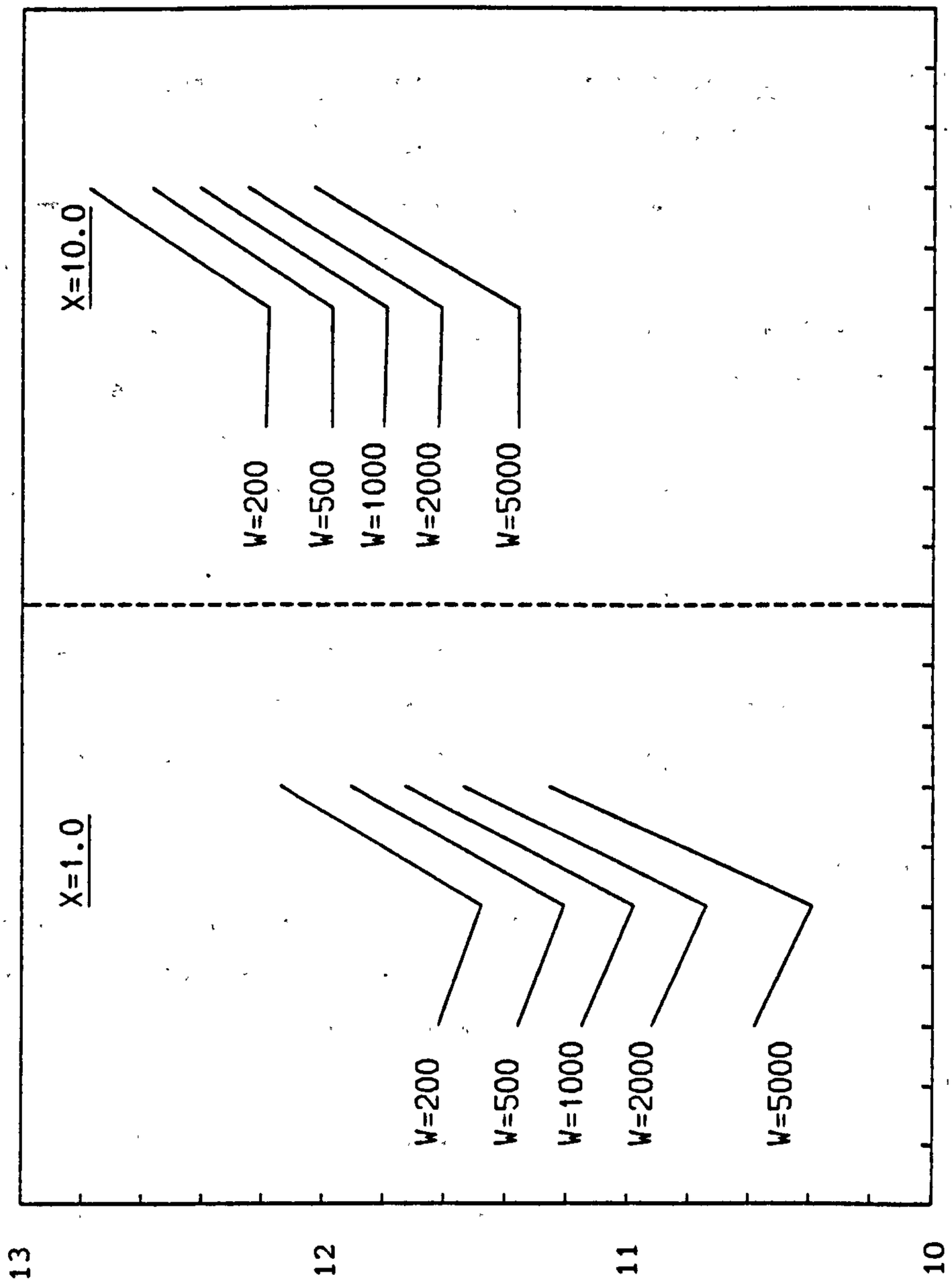

Line representations depicting pH changes that accompany silicalite crystallisation (the abscissae are scaled arbitrarily).

System xNa_2O 2TPABr $20SiO_2$ wH_2O; Crystal composition $4TPAOH\ 96SiO_2$

Figure 5.12

The manner in which alterations to mixture base, silica and water content affect the thermodynamics of silicalite crystallisation have been evaluated. As long as enough TPABr is present to enable reactions to go to completion (i.e. ca. 4 moles per 96 moles SiO_2), the theoretical equilibrium positions are not affected by excess. However experimental data disagrees with this; results suggest that the amount of quaternary salt in a mixture is a significant reaction variable. This point will be elaborated on shortly.

5.3.5 Crystallisation of microporous silicas in the xNa_2O 2TPABr $20SiO_2$ $1000H_2O$ system with other guest species

This section investigates ways in which the chemical compositions of crystals affect reaction equilibria.

Consider the reaction system xNa_2O 2TPABr $20SiO_2$ $1000H_2O$. Crystallisation of silicalite (composition 4TPAOH $96SiO_2$ and pNaOH 4TPAOH $96SiO_2$) in this system has already been simulated. Formation of dense silicas from these mixtures, although unlikely in practice, would be accompanied by pH changes identical to those obtained for dense silica crystallisation in the xNa_2O $20SiO_2$ $1000H_2O$ system (section 5.3.1). Crystallisation of microporous silicas with (a) void pores, (b) water filled pores (water lost from solution deemed negligible) and (c) salt filled pores (NaBr, TPABr - strong electrolytes) would also bring about pH changes identical to those calculated for dense silica formation. In each of these instances the alkalinity of mixtures (the base cation concentration) remains constant during reactions. The results that now follow show that complementary effects to those observed when strong base is removed (silicalite synthesis) are seen if crystal growth involves removal of strong acid molecules from solution.

The acid-containing crystals were deemed to have composition 4HBr $96SiO_2$ so that direct analogy was possible with the results calculated for silicalite crystallisation, i.e. effects of removing near equimolar amounts of acid and base from solutions have been compared. Results are listed in Table 5.8. Points to note:

Table 5.8 Simulated crystallisation in the xNa_2O 2TPABr $20SiO_2$ $1000H_2O$ system
Chemical composition of the crystals: 4HBr $96SiO_2$

	Initial (Point A)			Solubility Transfer (Point B)			Final (Point C)			
x	$[C^+]$	pH	G[a]	$[C^+]$	pH	Y[b]	$[C^+]$	pH	Y[b]	ΔpH_{C-A}
0.25	0.028	10.66	97.5	0.071	11.00	94.3	0.072	11.75	96.0	1.09
0.50	0.056	10.92	95.5	0.098	11.11	92.5	0.099	11.84	94.6	0.92
0.70	0.078	11.03	93.9	0.120	11.17	91.1	0.121	11.89	93.6	0.86
0.85	0.094	11.09	92.8	0.136	11.21	90.1	0.137	11.92	92.8	0.83
1.00	0.111	11.15	91.7	0.152	11.25	88.9	0.154	11.95	92.0	0.80
2.00	0.222	11.36	84.7	0.260	11.41	82.4	0.262	12.08	86.7	0.72
3.50	0.389	11.52	75.0	0.422	11.54	73.0	0.425	12.19	78.9	0.67
5.00	0.555	11.62	65.6	0.585	11.63	63.9	0.588	12.27	71.3	0.65
6.50	0.722	11.69	56.5	0.747	11.70	55.1	0.751	12.33	63.6	0.64
8.00	0.888	11.74	47.6	0.910	11.75	46.4	0.914	12.37	56.0	0.63
10.00	1.110	11.80	35.9	0.126	11.80	35.0	1.131	12.42	45.9	0.62
12.00	1.332	11.84	24.4	1.343	11.85	23.8	1.349	12.46	35.8	0.62
14.00	1.554	11.88	12.9	1.560	11.88	12.6	1.566	12.50	25.7	0.62
16.00	1.776	11.92	1.6	1.777	11.92	1.6	1.784	12.53	15.7	0.61
16.50[c]	1.832	-	-	-	-	-	1.838	12.53	13.2	-
19.00[c]	2.109	-	-	-	-	-	2.109	12.56	0.7	-
19.50[c,d]	2.165	-	-	-	-	-	-	-	-	-

[a] % Silica as amorphous solid ; [b] % yield; [c] Amorphous silica totally soluble;
[d] Crystals totally soluble

(1) Increases in pH are observed during the A-B period because of acid loss. The increase in pH decreases as mixture alkalinity (and buffer capacity) increases. These pH increases are in effect caused by the generation of base cations in solution:

$$TPABr(aq) + H_2O \longrightarrow HBr(sil) + TPAOH(aq) \qquad (5.32)$$

where HBr(sil) represents HBr within the silica lattice.

(2) The pH rise during the B-C transition decreases as the alkalinity increases. The net pH change during reaction ΔpH_{C-A} also decreases with increasing alkalinity. Note that these trends were also observed for silicalite crystallisation.

Although an acid-stabilised microporous silica is unlikely to crystallise in alkaline media, these results do complement and put in a clearer perspective those for the more practical situations (Figure 5.13). In well buffered systems (large x) pH changes are invariant of crystal composition and are principally governed by solubility differences. Crystallisation from low base mixtures (small x) is, however, accompanied by extremely diagnostic pH changes which reflect the chemistries of the crystalline phases. In low base mixtures removal of guest species from solution largely governs the overall pH changes that occur.

5.3.6 Comparison of theoretical and experimental results

Experimental results have been obtained for silicalite crystallisation in the xNa_2O 2TPABr $20SiO_2$ $1000H_2O$ system (Chapter 3). Before comparisons with theoretical results are made, ways in which the dynamics of real crystallisation processes upset the idealised reaction thermodynamics assumed in the theory have to be mentioned.

Experimental pH-time crystallisation curves normally show two regions of pH constancy - 'plateaux regions', one at the beginning of a reaction signifying that an equilibrium has been established between the amorphous gel and the solution phase species, the other at the end

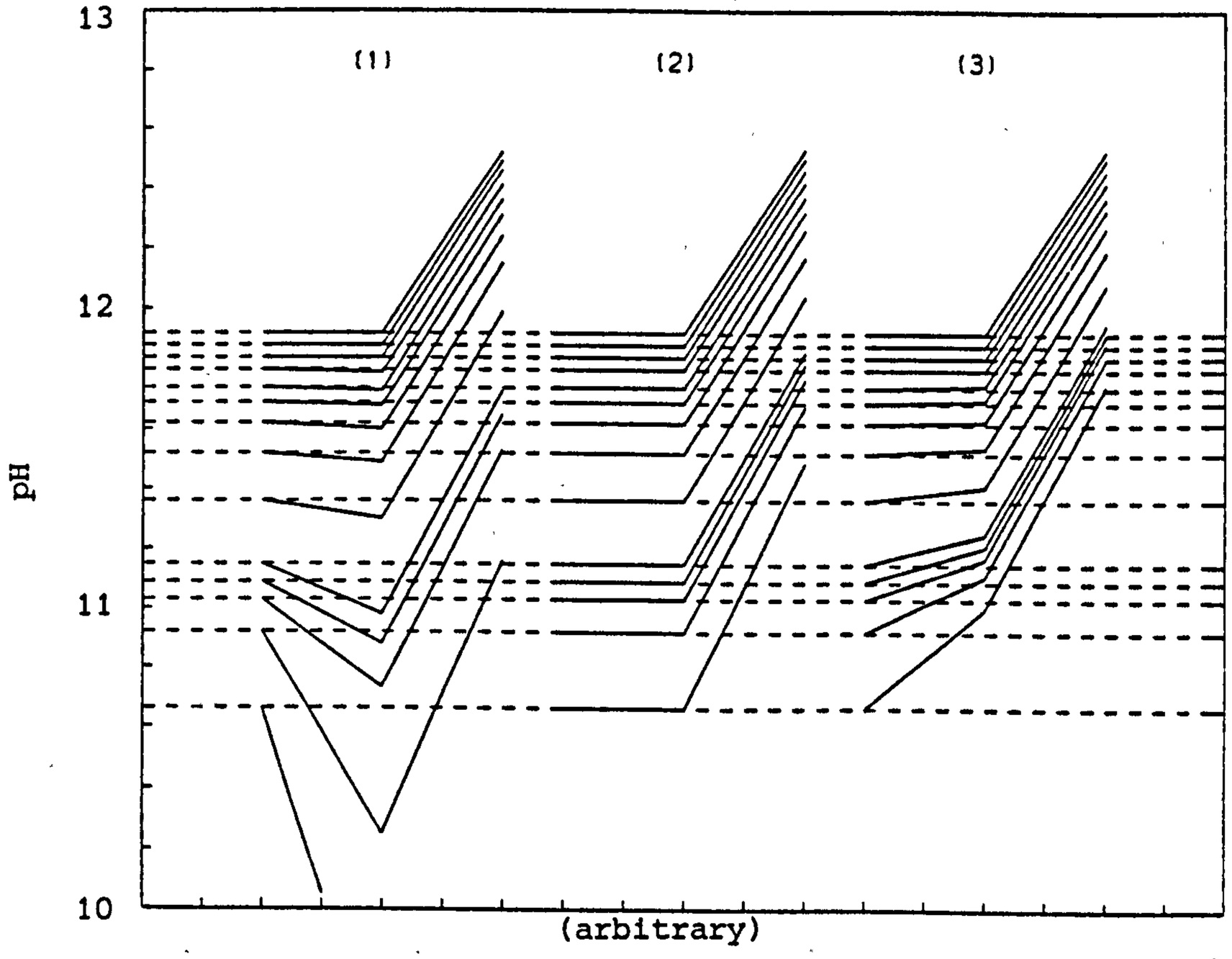

Figure 5.13 Line representations depicting the pH changes that accompany crystallisation of microporous silicas in the xNa_2O 2TPABr $20SiO_2$ $1000H_2O$ system. Reaction alkalinity (x) ranges from 0.25 (bottom plots) to 16.0 (top plots) - see Tables 5.2, 5.4 and 5.8 for details. Chemical compositions of the products:

(1) 4TPAOH $96SiO_2$

(2) (TPABr/H_2O/void) SiO_2

(3) 4HBr $96SiO_2$

The incomplete line denotes a reaction that cannot go to completion.

of the reaction denoting establishment of an equilibrium between the crystalline solid and the mother liquor. In practice, several samples of the reaction mixture are usually taken during these regions of pH constancy, values averaged and good estimates of the initial and final reaction pH obtained. Comparing these experimental values with theoretical values presents no problems - in real systems steady state situations are usually established at the beginning and end of reactions.

The points calculated for the A-B transitions and the solubility transfer points represent idealised positions which are likely to be seldom attained in practice. The crystallisation process is dynamic and only quasi-equilibria are very likely to be established whilst crystallisation is in progress. Experimental and theoretical solubility transfer points could therefore differ appreciably. Also, solubility transfer is likely to occur over a period of time, not necessarily suddenly, and will probably occur when most of the amorphous solid (but not all as assumed in the calculations) has been converted to silicalite. Some theoretical results were calculated to show the effect of 'early solubility transfer' on the form of reaction pH profiles.

Crystallisation of silicalite from reaction mixtures of composition xNa_2O 2TPABr $20SiO_2$ $1000H_2O$ (x = 0.5 and 10.0) was simulated with transference of solubility control prior to conversion of all the gel to crystals, i.e. when the crystallinity of the solid phase was in the 60% to 100% region. Results are shown in Figure 5.14. Ideal behaviour is denoted by the reaction pathway A-B-C. Pathways A-a-a'-C, A-b-b'-C etc. indicate routes caused by early solubility transfer (see footnote on Figure 5.14). The results for the low base reactions (x = 0.5) indicate that if solubility transfer occurs very early (crystallinity between 60% and 90%) then a pH fall, caused by removal of base as the residual gel crystallises, may be seen after the pH rise. If solubility transfer occurs when the crystallinity is greater than 90%, a pH fall is less likely to be observed. Even very early solubility transfer if unlikely to manifest itself on the pH profiles of high base reactions because of buffering effects at elevated pH (see results for x = 10.0, Figure 5.14).

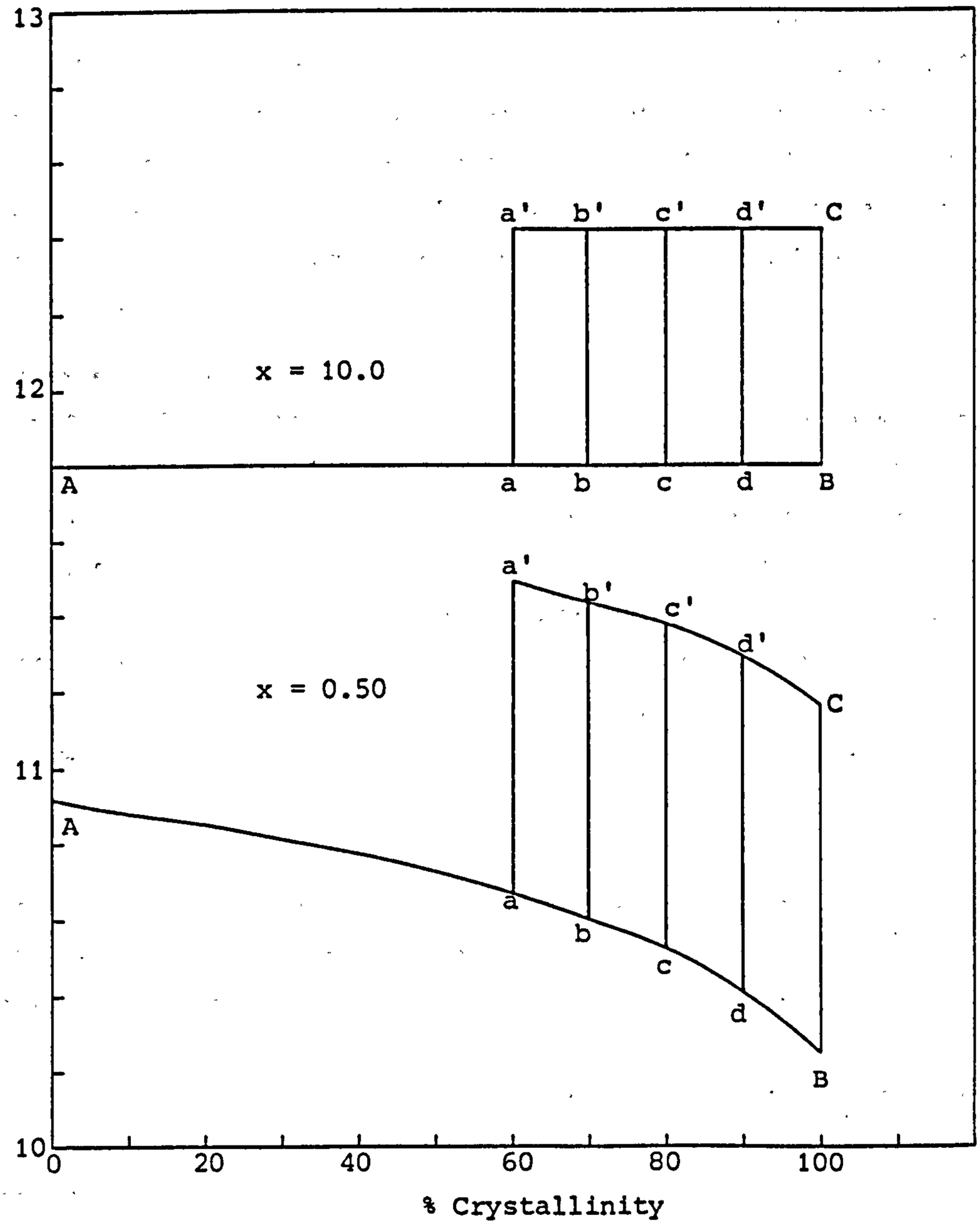

Figure 5.14 Changes to ideal reaction pathways (A-B-C) induced by early solubility transfer (pathways A-a-a'-C, A-b-b'-C etc.) during silicalite crystallisation in the xNa_2O 2TPABr $20SiO_2$ $1000H_2O$ system.

Footnote: Although the a-a',...., d-d' transitions are represented as vertical lines on the graphs, the crystallinities of the solid phases must necessarily increase during these periods of solubility transfer. The increases in crystallinity are only small for the reactions with x = 0.50, but considerable for those with x = 10.0

The experimentally obtained pH-time curves for silicalite crystallisation in the xNa_2O 2TPABr $20SiO_2$ $1000H_2O$ system are shown in Figure 5.15. The features shown by the experimental pH profiles are summarised in point form in Table 5.9 (see Chapter 3 for a more comprehensive discussion). The XRD crystallinity curves that complement these plots (chapter 3, Figures 3.5 - 3.7) show that the marked pH rises, due to solubility transfer, occur when the crystallinity is near 100%. Even though the experimental curves are 'rounded' by the dynamics of the crystallisation process, delineation of the A-B and B-C periods on the experimental plots in Figure 5.15 was possible and comparisons with the theoretical results have been made (N.B. points A, B and C being as defined previously).

The experimental pH values are compared to two sets of theoretical values in Table 5.10. The first set was evaluated assuming silicalite crystallised with ideal composition (4TPAOH $96SiO_2$), the second set was calculated assuming the crystal compositions were as experimentally found (i.e. pNaOH 4TPAOH $96SiO_2$ - see Table 5.10 for p values). The values chosen for the constants were those that have been used throughout this work (see end of section 5.2). The line representations in Figure 5.16 compare the experimental results with the theoretical set that assumed ideal crystal composition. Apart from the reactions with x = 0.5 and 6.5, the forms of the pH profiles theoretically predicted were also found in practice. A closer comparison between the absolute pH values is shown in Figure 5.17. In general the initial pH values correlate better than the final ones. The experimental final pH value for the reaction with x = 0.5 is markedly lower than predicted even after considering the NaOH in the crystals (see Table 5.10). The reason is probably attributable to CO_2 absorption by the unbuffered solution during reaction. Note also that no pH rise due to solubility transfer was observed during this reaction.

Constants were not varied to get a better data fit as agreement between experiment and theory was very reasonable. The results in Figure 5.5, although strictly applicable to dense silicas, in fact give a good indication of how the results for silicalite crystallisation (especially at high alkalinities) would be affected by altering K_s values.

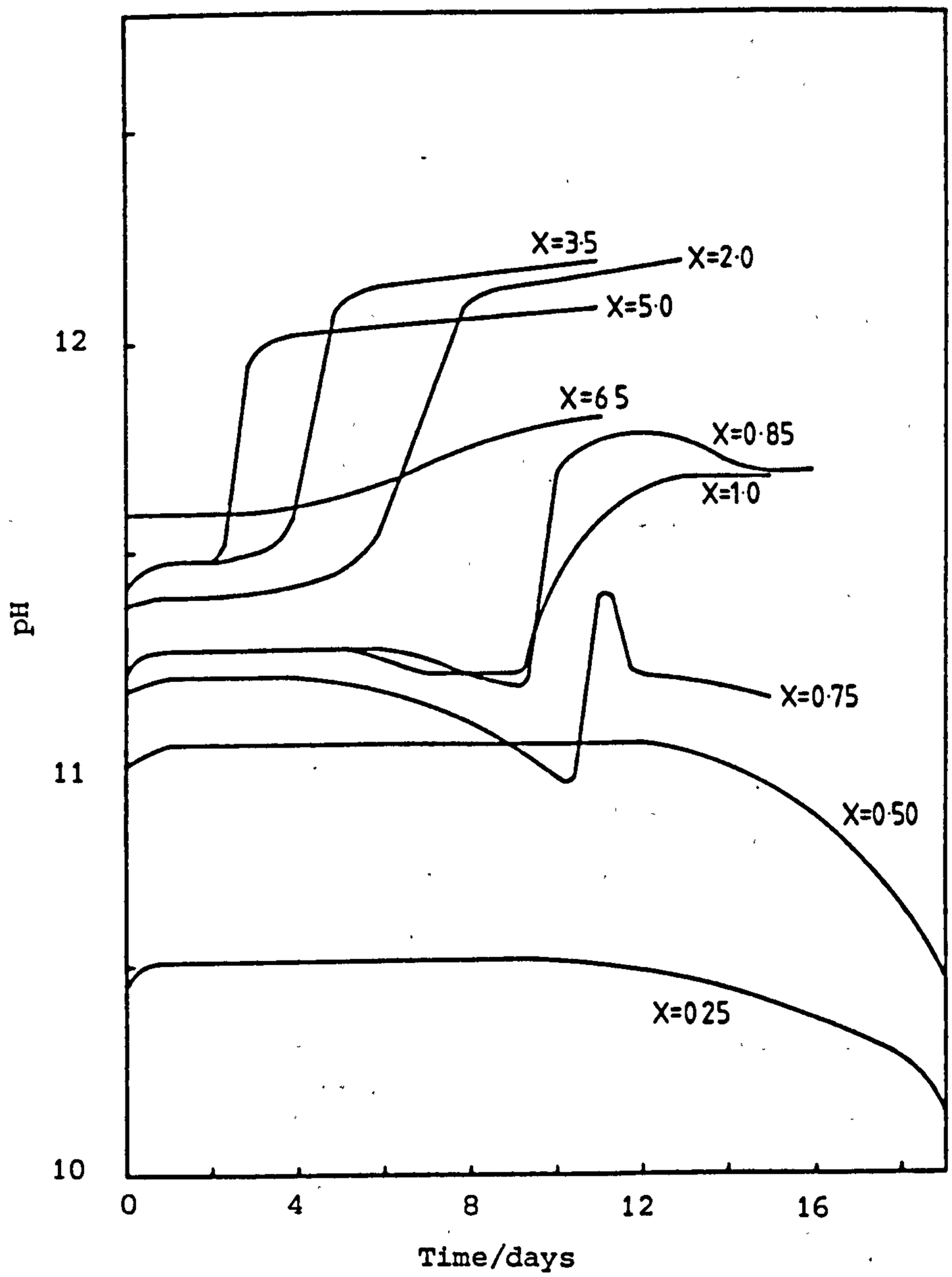

Figure 5.15 Experimental pH-time curves for silicalite crystallisation in the xNa_2O 2TPABr $20SiO_2$ $1000H_2O$ system at 95°C

Table 5.9 Comments on the experimental pH-time curves shown in Figure 5.15

Reaction Alkalinity (x)	Comments
0.25	There was a steady decrease in pH throughout this reaction (see section 3.3.5). Insufficient base was present to crystallise all the silica; to convert 20 moles of silica into silicalite with ideal composition requires 0.42 moles Na_2O in the reaction mixture. The crystallinity of the product (measured to be ~63%) was close to the maximum theoretically possible (60%) indicating that virtually all the base was consumed. The final reaction pH was 6.47.
0.50	The pH began to fall shortly after the onset of crystallisation and continued to fall until reaction was complete (see Figure 3.7). No pH rise due to solubility transfer was seen, probably because of CO_2 absorption.
0.70, 0.85, 1.0	During the A-B transition, decreases in pH caused by base loss were seen. The pH fall was especially marked for the lowest base reaction (x= 0.70). At these alkalinity levels crystallisation was relatively slow. This allowed the gel to control species in solution during the A-B period, i.e. the A-B period could be well modelled from a thermodynamic viewpoint.
	The profile for the reaction with x=1.0 shows a plateau region after the solubility transfer pH rise, the lower base reactions show decreases in pH (especially the least buffered reaction, x=0.70). These pH falls were probably caused by (i) early solubility transfer and/or (ii) CO_2 absorption.
2.0, 3.5, 5.0	Marked pH rises due to solubility transfer were seen. The small but gradual increases in pH that were seen prior to solubility transfer were probably due to a kinetic effect. Crystallisation was rapid in these systems (relatively) and the rate limiting step is thought to be the dissolution of the amorphous solid. Thus the A-B periods for these reactions are under poor thermodynamic control. The hydroxide ion concentration in solution is expected to be high.
	The gradual pH rises after solubility transfer show the slow approach to final equilibrium.
6.5	All the product crystallised from clear solution and the pH profile is distinctive because of this. No sharp pH rise due to solubility transfer was observed. The small gradual pH rise throughout reaction was caused by the steady decrease in the amount of silica in solution.

Table 5.10 Comparison of pH changes during silicalite crystallisation in the xNa_2O 2TPABr $20SiO_2$ $1000H_2O$ system

	Theoretical[b]			Theoretical[c]		Experimental			
x[a]	pH_A	pH_B	pH_C	pH_B	pH_C	Base in Unit Cell	pH_A	pH_B	pH_C
0.25	10.66	-	6.15[d]	-	6.15[d]	0.02NaOH 4TPAOH	10.52	-	6.47
0.50	10.92	10.25	11.16	9.69	10.66	0.60NaOH 4TPAOH	11.03	e	8.26
0.70	11.03	10.73	11.53	10.55	11.39	1.05NaOH 4TPAOH	11.20	10.95	11.16
0.85	11.09	10.88	11.65	10.79	11.58	0.95NaOH 4TPAOH	11.27	11.18	11.69
1.0	11.15	10.98	11.73	10.93	11.69	0.89NaOH 4TPAOH	11.27	11.20	11.69
2.0	11.36	11.30	11.99	11.25	11.95	2.50NaOH 4TPAOH	11.40	11.44	12.18
3.5	11.52	11.49	12.15	11.47	12.13	3.29NaOH 4TPAOH	11.48	11.50	12.20
5.0	11.62	11.60	12.24	11.59	12.23	3.00NaOH 4TPAOH	11.48	11.48	12.13
6.5	11.69	11.68	12.31	11.67	12.30	3.31NaOH 4TPAOH	11.60	-	11.82

[a] Reaction alkalinity

[b] Calculations assumed crystals had ideal unit cell composition 4TPAOH $96SiO_2$

[c] Calculations assumed crystals had compositions identical to those experimentally found (see adjacent column)

[d] Approximate pH, calculated assuming all base in reaction mixture consumed

[e] No solubility transfer point observed

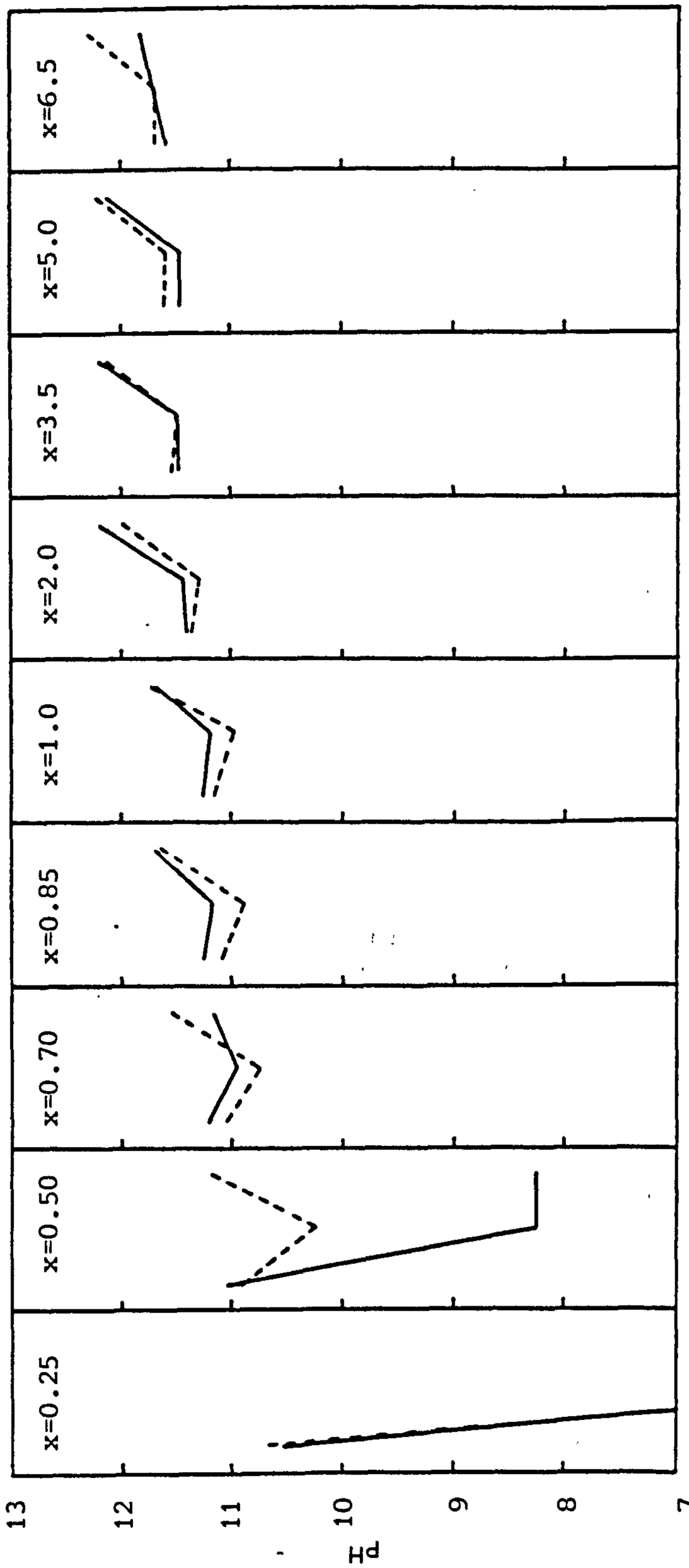

(arbitrary scales)

Line representations depicting the pH changes that accompany silicalite crystallisation in the xNa_2O 2TPABr $20SiO_2$ $1000H_2O$ system

———— Experimental results (95°C reactions)

---------- Theoretical results calculated using $k_1 = 2 \times 10^{-10}$, $K_2 = 2 \times 10^{-12}$, $K_s(gel) = 2.5 \times 10^{-3}$ and $K_s(silicalite) = 1.8 \times 10^{-4}$ (see section 5.3.2 for method of calculation). The products were assumed to have ideal unit cell composition 4TPAOH $96SiO_2$

Figure 5.16

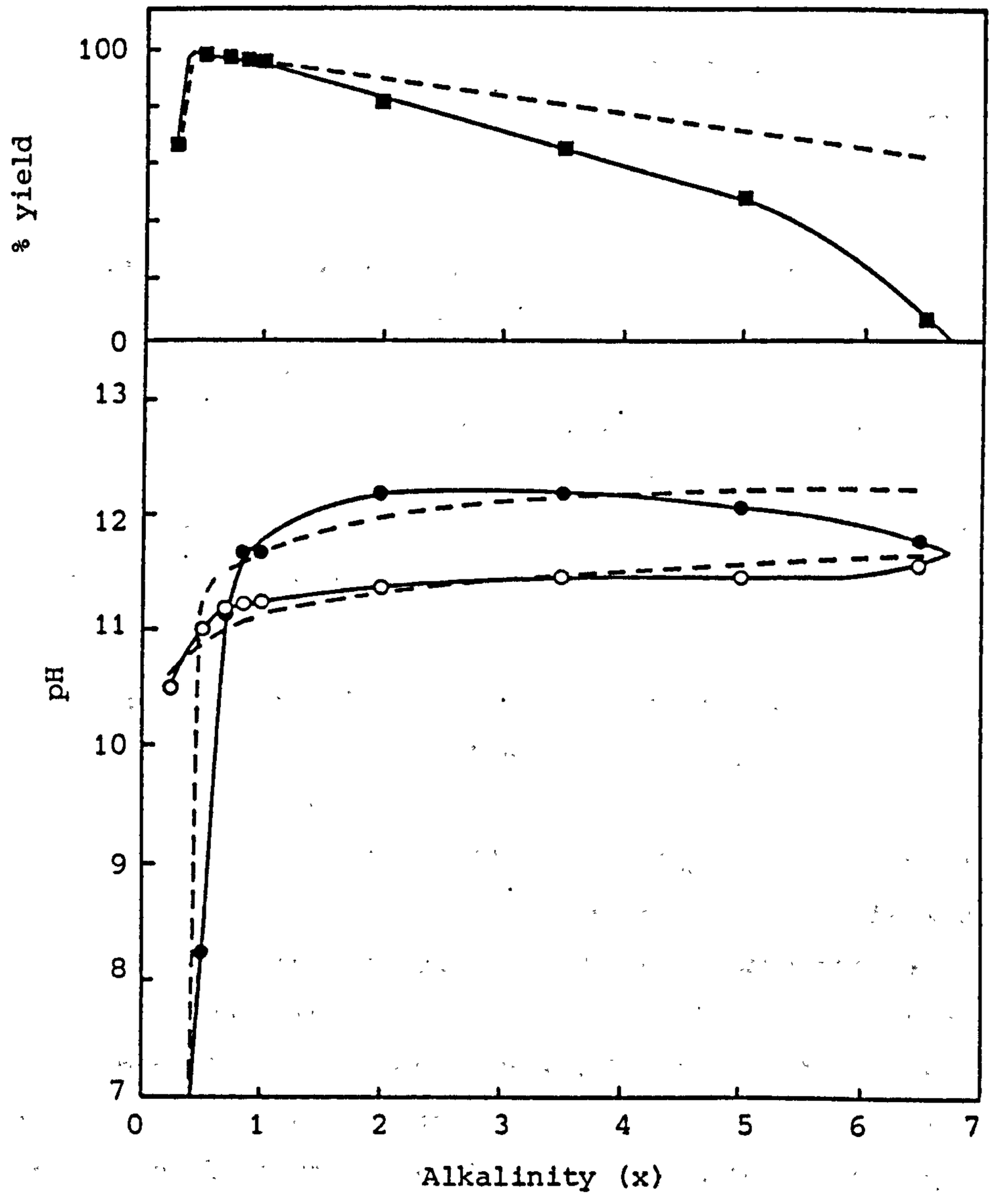

Figure 5.17 Comparison at the theoretically predicted (---) and experimentally determined (——) yields and pH changes for silicalite crystallisation in the xNa_2O 2TPABr $20SiO_2$ $1000H_2O$ system. The points denote the actual experimental values: O, initial pH; ●, Final pH; ■, Yield. Constants used for the calculations are shown in Figure 5.16. Products were assumed to have ideal composition.

Although the results in Figure 5.17 correlate well considering all the assumptions made in the theory, there are interesting discrepancies between the theoretical and experimental final pH values for the high alkalinity reactions (x = 5.0 and 6.5). The experimental results show a limiting alkalinity which is far lower than the theoretical limit (c.f. x ≅ 6.7 and x ≅ 19.25 respectively - the upper theoretical limit is shown in Figure 5.9(b)). Reasons for this are probably two-fold. Firstly, for high alkalinity reactions (high ionic strength) activity coefficients become significant. Had coefficients been considered in the theory, calculated hydrogen ion activities (which is what the experimental pH measurements represent) would be reduced. Also, the activities of the orthosilicic acid and the silicate ions would be reduced. As a consequence, concentrations of silicate species in solution would increase, less solid would be present and the upper limiting alkalinity, the point when crystals completely dissolve, would be moved to lower alkalinity and in better agreement with the experimental limit. There is however a second factor contributing to the discrepancies between results at high pH.

If theoretical results for silicalite crystallisation in the $xTPA_2O$ $20SiO_2$ $1000H_2O$ system (using TPAOH in mixtures, not the NaOH/TPABr combination) were evaluated, the results would be identical to those calculated in the xNa_2O 2TPABr $20SiO_2$ $1000H_2O$ system - because the theory is not base-specific. However if experimental synthesis were carried out in the sodium-free system, using TPAOH as both mineraliser and supplier of the quaternary cations, it is believed that some of the pH results, especially those for high alkalinity reactions, would differ substantially to those obtained in the sodium system. Trends might be similar but absolute values would probably differ appreciably. The key reason for this concerns the fact that sodium ions are present in mixtures (differences introduced by the higher ionic strengths of the sodium mixtures can be neglected for the purposes of this discussion). Sodium ions are present in solution and sodium hydroxide(empirically) is incorporated in the products, albeit sometimes only to a small extent. This inorganic base, both in solution and in the crystals is believed to have a destabilising effect on the silicalite, lowering its solubility

(K_s value). Experimental results have shown that the sodium content is linearly related to the mole fraction of sodium ions in the mixture (2x/(2x + 2)) and indicate that a maximum of four NaOH molecules per unit cell can be incorporated (see Table 5.10 and chapter 3, Figure 3.13). When the mixture alkalinity (x) is high, (i) a lot of sodium becomes entrapped in crystals and (ii) the solution phases are rich in sodium. Both these interrelated factors are believed to destabilise (increase K_s) the silicalite. These factors probably account for the downward tail-off in the experimental final pH values at high alkalinity. This tail-off is not predicted by the theory and the fact that the initial pH values do not fall away similarly is evidence that its origin lies with the crystalline products (Note that it is an upward tail-off that the theoretical results predict at high alkalinity (Figure 5.9 (b)). In effect the experimental results imply that if samples of the same silicalite batch were respectively put in equimolar sodium hydroxide and tetrapropylammonium hydroxide solutions, then crystals would dissolve to a greater extent in the former. This seems reasonable.

If silicalite is crystallised from sodium-containing mixtures, the presence of a considerable excess of the quaternary salt should be thermodynamically beneficial. If the mole fractions of sodium ions in the mixtures are reduced, products should contain less sodium, be less soluble, and hence enable better yields to be obtained. These same arguments are also likely to apply to crystallisation of other silica molecular sieves e.g. silicalite-2.

The solubility of silicalite has been discussed in relatively simple terms so far. As-synthesised silicalite has ideal anhydrous composition 4/96TPAOH SiO_2. The dissolution of this material is represented by the equation:

$$4/96TPAOH\ SiO_2 + 2H_2O \rightleftharpoons Si(OH)_4 + 4/96TPA^+ + 4/96OH^- \qquad (5.33)$$

and the solubility product (K_s) in concentration terms is given by:

$$K_s = [Si(OH)_4][TPA^+]^{4/96}[OH^-]^{4/96} \qquad (5.34)$$

If this relationship holds then the concentration of orthosilicic acid will be reduced in solutions of high TPA^+ and/or OH^- content (Note that it is really the activities of species that should be considered). However the small exponents of the respective terms in the solubility

product relationship (equation (5.34)) put relatively little dependence of $[Si(OH)_4]$ on the TPA^+ and OH^- concentrations over a wide range of reaction conditions. For example, if $[OH^-]$ is in the 10^{-5} to 10^{-2} range (pH = 9 to 12) then $[OH^-]^{4/96}$ lies between 0.62 and 0.83. If $[TPA^+]$ is in the 0.01 to 0.11 range (the latter is equivalent to 2 moles TPA^+ per 1000 moles H_2O in solution (c.f. reaction mixture compositions used in this work)) then $[TPA^+]^{4/96}$ lies between 0.83 and 0.91. The solubility product of silicalite can thus be approximated to the concentration of orthosilicic acid in solution and thought of no differently to the solubility products of solid silicas that are compositionally almost 100% SiO_2 e.g. amorphous silica, quartz. Equation 5.7 is therefore applicable to silicalite.

The main effect on an increase in pH is to cause increased ionisation of orthosilicic acid and through that increased solubilisation of silicalite. The concentration of orthosilicic acid in solution can be assumed to be independent of pH. The above arguments also hold for silica molecular sieves that contain other guest types. Errors introduced by these approximations are probably no greater than those associated with selection of values for some of the constants used in the theory. In addition, the generality of the model is lost if species other than orthosilicic acid are considered in solubility product relationships.

In chapter 4, a novel route to silicalite was reported which used amines as mineralisers. Products were free of alkali metal cations and changes in pH that accompanied crystallisation were vastly different to those observed when silicalite was crystallised from mixtures that contained strong bases. Crystallisation in amine systems is now discussed.

5.4 Crystallisation in Systems that Contain Amines as Mineralisers

Amines play a key role during the crystallisation of many high silica zeolites (see chapter 4 section 4.2 and reference [11]). Quite often their role is bifunctional; they act as mineralisers and they act as templates/pore-fillers. Although the alkalinities of mixtures are sometimes bolstered with strong base additions, it is reactions that contain amines alone as mineralisers that are considered here.

Crystallisation from mixtures that contain amines was approached theoretically by Lowe [1]. His equilibrium theory for crystallisation, already described for strong base systems, requires only minor modification for application to a weak base situation. The theory is again ideally suited for modelling crystallisation of aluminium-free materials.

5.4.1 Application of the Equilibrium Model [1] to crystallisation in systems that contain amines as mineralisers

Consider reaction mixtures of general composition $nRNH_2\ ySiO_2\ wH_2O$ where RNH_2 represents a monobasic amine and R is an alkyl or aryl group. In aqueous media, amines are partially protonated and solutions are alkaline:

$$RNH_2 + H_2O \overset{K_h}{\rightleftharpoons} RNH_3^+ + OH^- \qquad (5.35)$$

The hydrolysis constant K_h for this reaction is written:

$$K_h = [RNH_3^+][OH^-]/[RNH_2] \qquad (5.36)$$

and it inherently includes the essentially invariant water concentration term. The dissociation of the protonated amine is governed by the equilibrium:

$$RNH_3^+ \overset{K_a}{\rightleftharpoons} RNH_2 + H^+ \qquad (5.37)$$

and the acidity (dissociation) constant K_a is given by:

$$K_a = [RNH_2][H^+]/[RNH_3^+] \qquad (5.38)$$

It can readily be shown that:

$$K_a = K_w/K_h \qquad (5.39)$$

where K_w is the ionic product of water.

If it is assumed that no amine (charged or uncharged) is associated with the surface of the undissolved amorphous silica, then the total concentration of amine [A] in the reaction mixture is given by:

$$[A] = n/(wM_w) \qquad (5.40)$$

where n and w represent the molar quantities of amine and water in the mixture composition and M_w is the molar mass of water in kg. The total concentration of amine is related to the concentrations of protonated and unprotonated forms by the equation:

$$[A] = [RNH_2] + [RNH_3^+] \qquad (5.41)$$

Substituting equation (5.38) into (5.41) gives:

$$[A] = [RNH_3^+]\ ((K_a/[H^+]) + 1) \qquad (5.42)$$

and rearranging gives the expression:

$$[RNH_3^+] = [A][H^+]/(K_a + [H^+]) \qquad (5.43)$$

Electroneutrality must be maintained at all times in the solution and if, as before, $Si(OH)_3O^-$ (SH_3^-) and $Si(OH)_2O_2^{2-}$ (SH_2^{2-}) are the only silicate ions present, the following charge balance equation must hold:

$$[RNH_3^+] + [H^+] = [SH_3^-] + 2[SH_2^{2-}] + [OH^-] \qquad (5.44)$$

The $[H^+]$ and $[OH^-]$ terms were both neglected by Lowe but they are included here. Their omission makes only minor differences to computed results - except at pH extremes. In the analogous equation for strong base systems (equation (5.18)), the $[H^+]$ terms was neglected; when strong bases supply the aklalinity, pH values are (in general) considerably higher and therefore $[H^+]$ smaller.

Expressions for $[RNH_3^+]$,$[SH_3^-]$, $[SH_2^{2-}]$ and $[OH^-]$ (equations (5.43), (5.37), (5.12), (5.13) and (5.19)) can be substituted into equation (5.44) to give:

$$[A][H^+]/(K_a+[H^+])+[H^+] = K_1K_s/[H^+]+2K_1K_2K_s/[H^+]^2 + K_w/[H^+] \qquad (5.45)$$

This equation (solved for $[H^+]$)enabled the steady-state situations at the beginning and end of reactions to be evaluated ([A] was calculated from equation (5.40) and all other parameters bar $[H^+]$ are constants).

Results calculated by Lowe assumed no amine was incorporated in products i.e. all the base stayed in solution throughout reactions. It is possible to extend the basic theory, in an identical manner to the extensions described for strong base systems in section 5.2.1, to enable the period when crystals grow at the expense of the amorphous solid to be modelled and solubility transfer points to be determined. Incorporation of molecules within crystals has also been considered. Reference to points A,B and C (designation as before) is again made in tables and figures. A value of 10^{-10} was taken for the acidity constant (K_a) of the amine in all calculations. Values of the other constants were as previously cited (section 5.2).

5.4.2 Crystallisation in the $nRNH_2$ $20SiO_2$ $1000H_2O$ System

It was assumed that (i) the products from these reactions were dense silicas and (ii) all the amine, protonated and unprotonated, stayed in the solution phase throughout reaction. A computer program was written to solve equation (5.45) by iteration (manually at terminal). Results are presented in Table 5.11. The data shows the following features:

1. (point A): As the alkalinity (n) increases, the concentration of protonated amine and the pH increase and the percentage of the total silica present as solid and the RNH_3^+/RNH_2 ratio decrease.
2. (point B): All parameters at the solubility transfer point are identical to those initially - but the solid is totally crystalline.
3. (point C): As n increases, the parameters at final equilibrium show the same trends as they did at points A and B but their values have changed. In all cases the pH and yield increase during the B-C transition because the crystals are less soluble than the amorphous solid.

The most significant change induced by solubility transfer is the decrease in $[RNH_3^+]$ and consequent decrease in the pH-controlling RNH_3^+/RNH_2 ratio. These decreases, seen in all cases, can be explained by considering the hydrolysis equilibrium (equation 5.35). When the last of the gel dissolves, solubility transfer necessitates that hydroxide ions must be released into solution (i.e. the pH must rise). To preserve the equilibrium conditions, this increase in the hydroxide ion concentration is offset by conversion of some of the protonated amine to its unprotonated form (i.e. the base cation concentration decreases). The net effect is that the pH rise during solubility transfer is less than had the cations been strong base cations. The product yields obtained and the pH changes that occured are shown in Figure 5.18. The pH rise seen during reaction decreases as the alkalinity increases and the yields are high because the final pH in all cases is relatively low.

The effects of alkalinity on the crystallisation of dense silicas in this system are similar to those observed in the strong base system (section 5.3.1) apart from buffering effects due to the amine. This buffering reduces pH changes and enhances yields relative to equimolar

Table 5.11 Simulated crystallisation in the $nRNH_2$ $20SiO_2$ $1000H_2O$ system
Chemical composition of the crystals: SiO_2

	Initial (Point A) Solubility Transfer (Point B)				Final (Point C)				
n	$[RNH_3^+]$	$\frac{[RNH_3^+]}{[RNH_2]}$	pH	G[a]	$[RNH_3^+]$	$\frac{[RNH_3^+]}{[RNH_2]}$	pH	Y[b]	ΔpH_{C-A}
0.5	0.010	0.550	10.26	98.9	0.004	0.151	10.82	99.7	0.56
1	0.015	0.374	10.43	98.5	0.005	0.110	10.96	99.6	0.53
2	0.023	0.258	10.59	97.9	0.008	0.079	11.10	99.5	0.51
5	0.039	0.163	10.79	96.7	0.014	0.053	11.28	99.1	0.49
10	0.058	0.117	10.93	95.3	0.021	0.039	11.41	98.7	0.48
15	0.074	0.097	11.01	94.2	0.027	0.033	11.48	98.4	0.47
20	0.087	0.085	11.07	93.3	0.032	0.030	11.53	98.2	0.46

[a] % silica as amorphous solid initially and % yield at the point of solubility transfer

[b] % yield

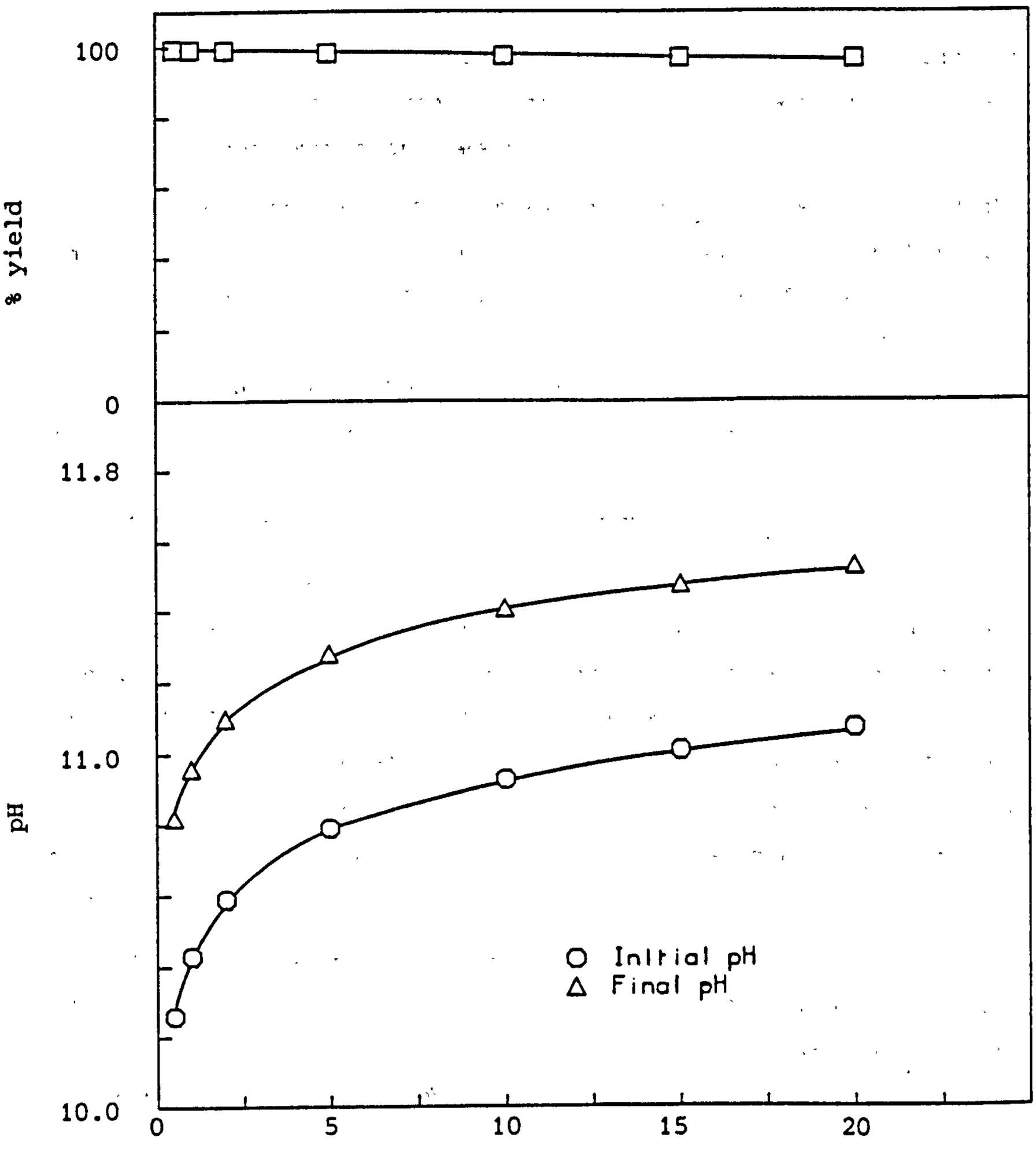

Figure 5.18 Effect of alkalinity (n) on the product yields and on the pH changes that accompany crystallisation of dense silicas in the $nRNH_2$ $20SiO_2$ $1000H_2O$ system

strong base reactions. Reasons for this are two-fold:

(i) Only a portion of the total amine is protonated (depends on K_a and the amount of amine present) and therefore 'active', i.e. associated with anions in solution. In strong base systems all base is active.

(ii) The amount of protonated amine decreases on solubility transfer whereas in strong base systems the base cation concentration does not.

The comparative curves drawn in Figure 5.19 show the pH changes that accompany crystallisation of dense silicas in equimolar strong and weak base systems. The graph suggests that if a stronger amine (e.g. $K_a = 10^{-12}$) was used in mixtures, pH changes would be intermediate between the weaker amine ($K_a = 10^{-10}$) and strong base systems. In fact results reported by Lowe did show this.

5.4.3 Crystallisation in the $nRNH_2$ $2TPABr$ $20SiO_2$ $1000H_2O$ system

If the product from these reactions was either (i) a dense crystalline silica or (ii) a microporous silica with void pores or pores filled with water or TPABr, then predicted pH changes at a given reaction alkalinity would be identical to those evaluated for dense silica formation in the $nRNH_2$ $20SiO_2$ $1000H_2O$ system (see last section). In all the aforementioned cases all the amine (the alkalinity) stays in solution throughout reaction.

The pH changes that accompany crystallisation of microporous silicas with other guest types (TPAOH, RNH_2, RNH_3Br and HBr) are shown in Figure 5.20. The sections that follow examine why such markedly different pH changes are observed. All products were considered to have the same solubility ($K_s = 1.8 \times 10^{-4}$).

Figure 5.19 A comparison of the relative changes in pH that accompany crystallisation of dense silicas in equimolar strong and weak base systems.
Upper curve: $xNa_2O\ 20SiO_2\ 1000H_2O$
Lower curve: $nRNH_2\ 20SiO_2\ 1000H_2O$ (using $K_a = 10^{-10}$)

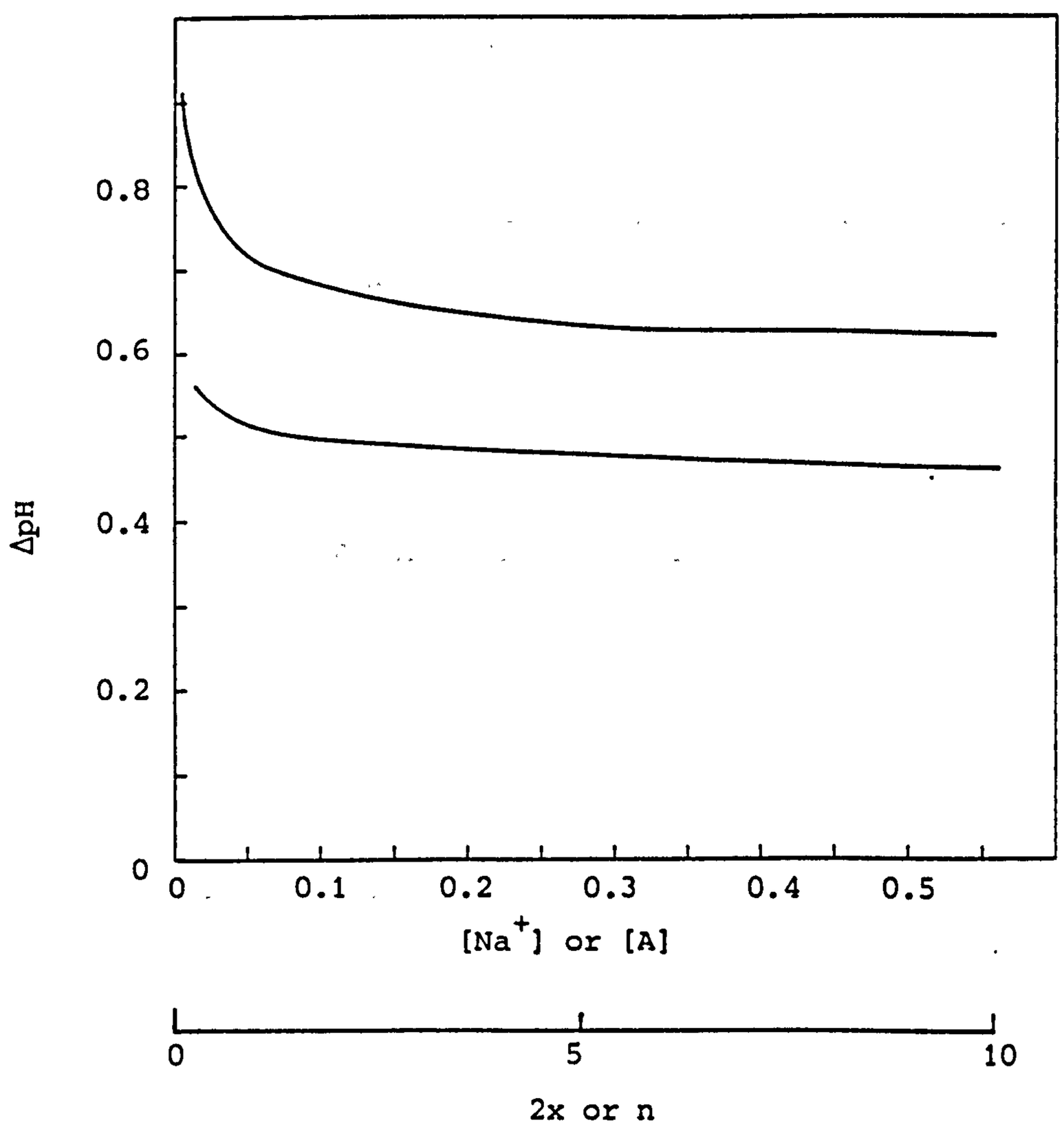

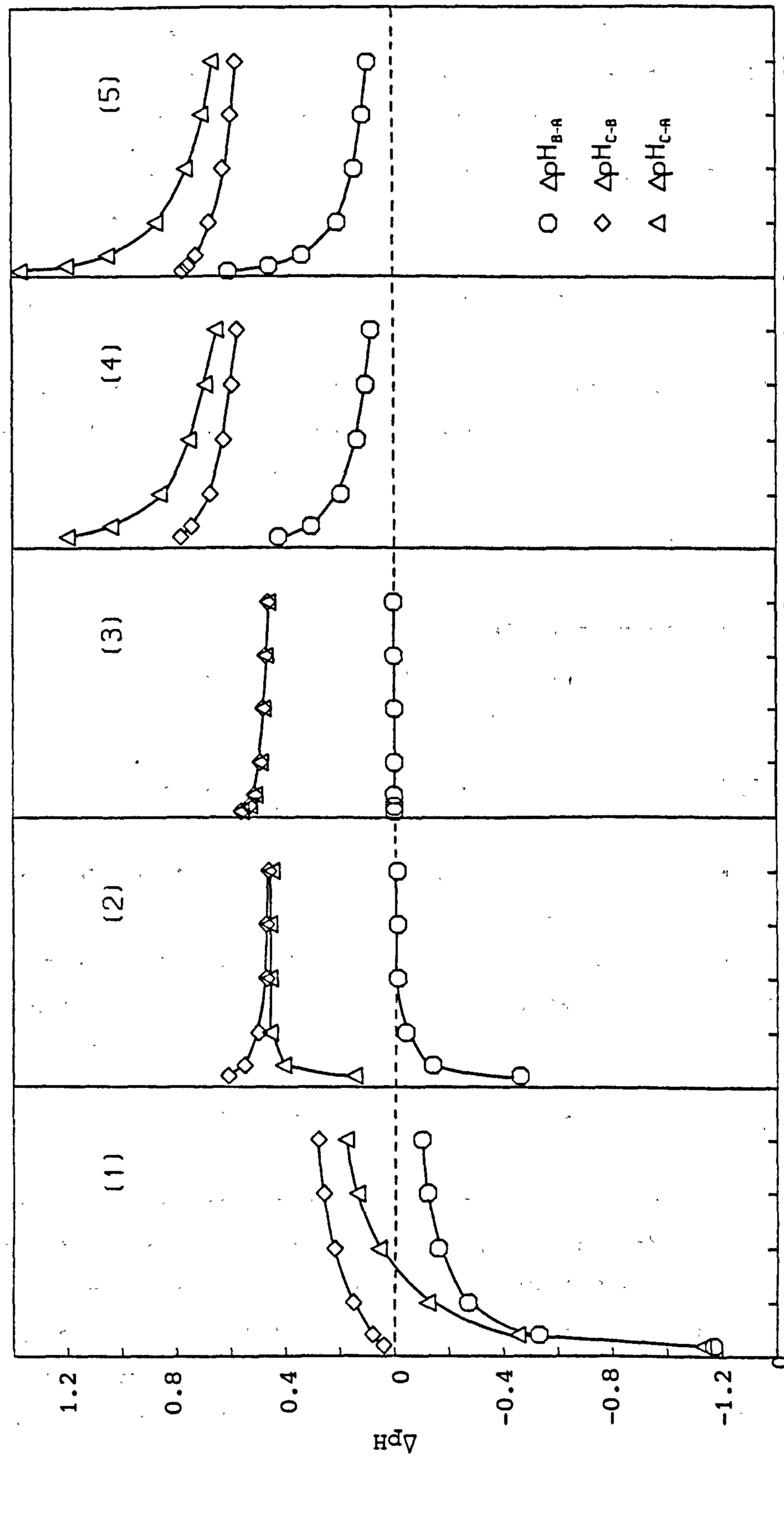

Figure 5.20 A comparison of the relative pH changes that accompany crystallisation of microporous silicas in the $nRNH_2$ $2TPABr$ $20SiO_2$ $1000H_2O$ system. Crystal compositions: (1) $4TPAOH$ $96SiO_2$; (2) $4RNH_2$ $96SiO_2$; (3) $(TPA)_2O$ $4HBr$ $96SiO_2$; (4) $4RNH_3Br$ $96SiO_2$; (5) $4HBr$ $96SiO_2$

5.4.3.1 Crystals containing TPAOH (silicalite)

The experimental results in Chapter 4 have shown that it is possible to crystallise silicalite in the RNH_2-TPABr-SiO_2-H_2O system. An understanding of the thermodynamics of silicalite crystallisation in this system is therefore of practical importance.

The full charge balance equation that relates the ionic species in the solution phase is:

$$[RNH_3^+] + [H^+] + [TPA^+] = [SH_3^-] + 2[SH_2^{2-}] + [OH^-] + [Br^-] \quad (5.46)$$

The concentrations of bromide and quaternary cations are initially equivalent (N.B. the quaternary cations are ineffective) and so equation (5.46) reduces to:

$$[RNH_3^+] + [H^+] = [SH_3^-] + 2[SH_2^{2-}] + [OH^-] \quad (5.47)$$

After nucleation, growth of crystals with composition 4TPAOH $96SiO_2$ (ideal chemistry assumed) removes strong base from the solution phase. In effect the following reaction occurs:

$$TPABr(aq) + RNH_2(aq) + H_2O \longrightarrow TPAOH(sil) + RNH_3Br(aq) \quad (5.48)$$

For each mole of TPAOH incorporated, one mole of cations (RNH_3^+ or, via dissociation of the protonated amine, H^+) become associated with bromide ions in the solution. Taking this into account, the charge balance equation that can be used to model silicalite crystallisation from these amine mixtures is:

$$[RNH_3^+] + [H^+] = [SH_3^-] + 2[SH_2^{2-}] + [OH^-] + [Br^-]^* \quad (5.49)$$

where $[Br^-]^*$ represents the concentration of bromide ions in solution equivalent, on an absolute molar basis, to the number of moles of TPAOH in the crystals. A computer program (file PHAMINE - see Appendix III) based on equation (5.49) (substitutions for the various terms as before) enabled the crystallisation process to be simulated. The computational methodology was similar to that used for silicalite crystallisation in

strong base systems (see section 5.3.2). Equilibrium conditions at points A, B and C and at points during the A-B transition were determined.

The pH changes that occur during crystallisation in these amine systems are governed by two factors:

(a) Buffering due to silicate ions. The greater the concentrations of silicate ions in solution (i.e. the higher the pH), the greater the resistance to pH change.

(b) Buffering due to the amine. For any given alkalinity (n) this is greatest when $[RNH_3^+]/[RNH_2] = 1$ (i.e. when pH = pK_a = 10). For reactions of different alkalinity, the buffer capacity depends on the individual concentrations of RNH_3^+ and RNH_2. Unless the absolute concentrations of these species are appreciable, buffering by the amine will not be significant. The situation is complicated by the fact that the amine buffer capacity is pH dependent and by the fact that some solutions are better acid buffers than base buffers and vice-versa. To understand the pH changes that occur during silicalite crystallisation all these factors need to be borne in mind.

The results, collated in Table 5.12, show interesting features. In each case, loss of TPAOH from the solutions during the A-B period causes the $[RNH_3^+]$ to increase. Consequently the RNH_3^+/RNH_2 ratio increases and the pH decreases. For the reaction with n = 1, the pH changes from 10.43 to 9.26 during this period, the RNH_3^+/RNH_2 ratio from 0.374 to 5.495. The point of maximum amine buffer capacity (pH = 10; RNH_3^+/RNH_2 = 1) is traversed and at point B the mixture is considerably less buffered, with respect to both the amine and silicate species, than it was initially.

The reactions with n = 2 to 20 also show pH falls during the A-B period but although, in each case, the silicate buffering decreases as the pH decreases, buffering due to the amine increases - the RNH_3^+/RNH_2 ratio approaches 1. The pH changes during this period, although reduced because of amine buffering, are still largely controlled by the induced changes to the silicate buffering. The overall result is that as the alkalinity (n) decreases, the magnitude of the pH fall during the A-B period increases. A similar although more pronounced trend was seen

Table 5.12 Simulated crystallisation in the $nRNH_2$ 2TPABr $20SiO_2$ $1000H_2O$ system
Chemical composition of the crystals: 4TPAOH $96SiO_2$

	Initial (Point A)				Solubility Transfer (Point B)				Final (Point C)				
n	$[RNH_3^+]^a$	$\frac{[RNH_3^+]}{[RNH_2]}$	pH	G[b]	$[RNH_3^+]^c$	$\frac{[RNH_3^+]}{[RNH_2]}$	pH	Y[d]	$[RNH_3^+]^c$	$\frac{[RNH_3^+]}{[RNH_2]}$	pH	Y[d]	ΔpH_{C-A}
0.5[e]	0.010	0.550	10.26	98.9	-	-	-	-	-	-	-	-	-
1	0.015	0.374	10.43	98.5	0.047	5.495	9.26	99.7	0.046	5.012	9.30	>99.9	-1.13
2	0.023	0.258	10.59	97.9	0.052	0.879	10.06	99.2	0.047	0.733	10.14	>99.9	-0.45
5	0.039	0.163	10.79	96.7	0.064	0.303	10.52	98.2	0.049	0.212	10.67	99.8	-0.12
10	0.058	0.117	10.93	95.3	0.081	0.172	10.77	96.8	0.052	0.103	10.99	99.6	+0.06
15	0.074	0.097	11.01	94.2	0.096	0.130	10.89	95.8	0.055	0.071	11.15	99.4	+0.14
20	0.087	0.085	11.07	93.3	0.108	0.108	10.97	94.8	0.059	0.056	11.25	99.2	+0.18

a Represents total protonated amine. Initially all protonated amine is associated with silicate and hydroxide ions

b % silica as amorphous solid

c Represents total protonated amine, some of which is associated with bromide ions

d % yield

e Insufficient amine present for reaction to go to completion

when silicalite was crystallised in strong base systems (section 5.3.2). It should be remembered that crystal growth during the A-B period is effectively accompanied by addition of strong acid to the solutions and the pH changes that occur are diagnostic of the ability of the mixtures to cope with acid additions.

During the B-C period, the product yield and pH increase. Solubility transfer, which in effect is <u>in situ</u> base generation, causes the pH to rise and thus to understand the pH changes that occur during this period base buffering by the mixtures has to be considered. The most important feature to be explained concerns why the pH rise during this period increases with alkalinity (n). The corresponding pH rise decreases with alkalinity when dense silicas crystallise from mixtures of the same base content (see Figure 5.20 and Figure 5.21) and the same is true when silicalite is crystallised in strong base systems (see Figure 5.13). The observed pH rises are governed by two factors:

(a) Buffering due to the amine and silicate species.
(b) The absolute amounts of base effectively added to these systems as solubility transfer and crystallisation from clear solution ensue.

At point B the reaction with n = 1 is poorly buffered by the amine but the effective base addition, caused by solubility transfer, is small because so little silica is in solution at low pH. This mixture can hence buffer the effects of solubility transfer and that is why only a small pH rise is seen ($\Delta pH_{C-B} = 0.04$).

As n changes from 2 to 20, the amine buffer ratio (at point B) decreases and buffering due to the silicate species increases. The effective base addition during the B-C transition increases with alkalinity - this is the dominant factor and it causes ΔpH_{C-B} to do likewise. The increase in $[OH^-]$ is of course partially offset by incorporation of TPAOH in crystals. Several low pH reactions were simulated as if the crystallisation from clear solution, accompanying solubility transfer, layed down an organic-free outer shell on the silicalite crystals i.e. no base was consumed during the B-C period. The results showed that loss of base during this latter growth is not a contributing factor to the observed pH changes. This is principally

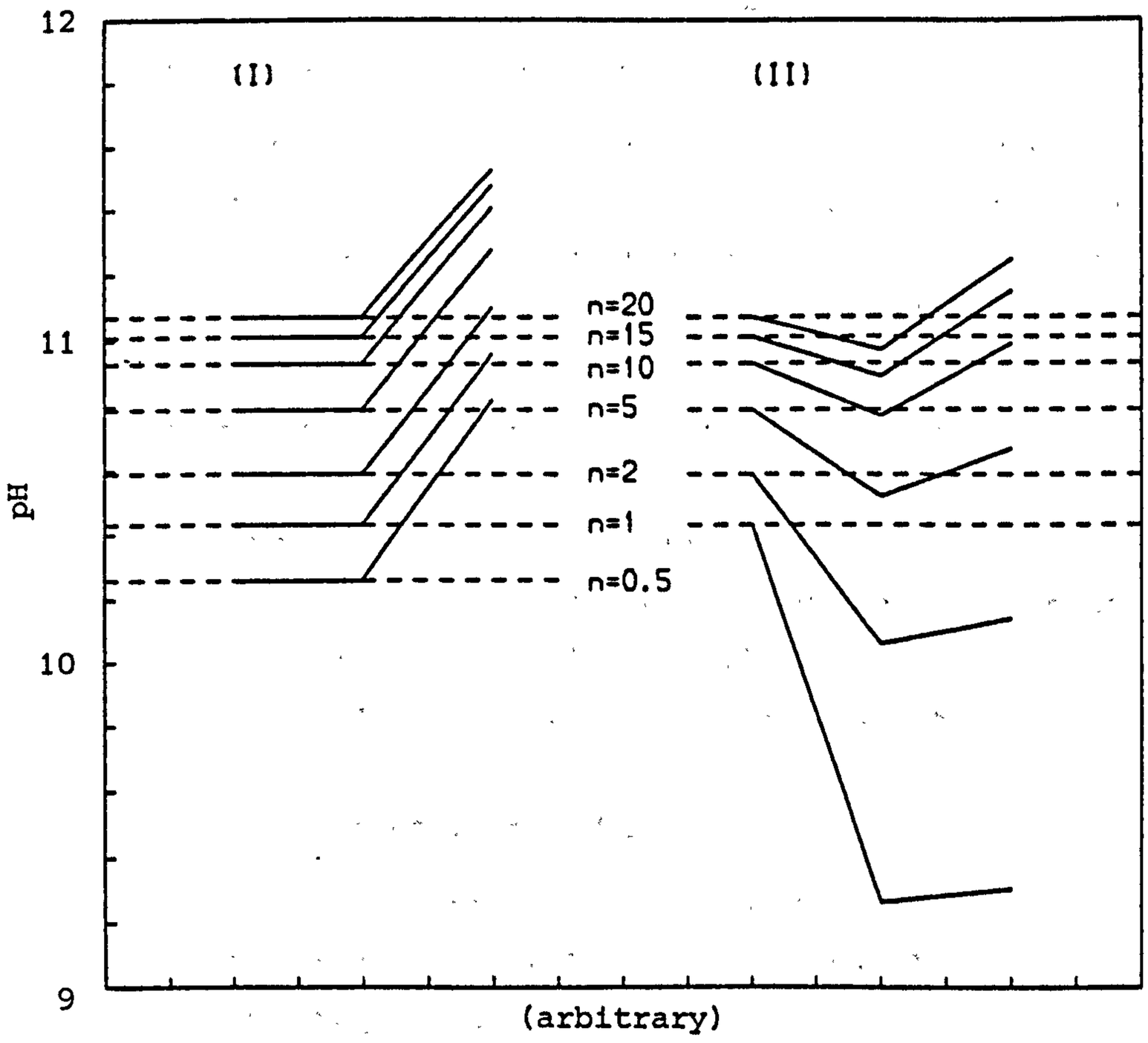

Figure 5.21 Line representation showing the changes in pH that occur during crystallisation in amine systems:

(I) $nRNH_2$ $20SiO_2$ $1000H_2O$;Product - dense silica (SiO_2)

(II) $nRNH_2$ $2TPABr$ $20SiO_2$ $1000H_2O$;Product - silicalite ($4TPAOH$ $96SiO_2$)

because so little growth occurs during solubility transfer if the pH is low. The pH changes during the B-C period are solely governed by the changes that are induced during the A-B transition. Figure 5.20 shows that the overall pH change is negative for the low alkalinity reactions and positive for those of higher base contents. For n ≈ 8 the overall pH change is zero, i.e. the pH changes during the A-B and B-C transitions cancel one another.

In summary, two types of buffering control the pH changes that occur during silicalite crystallisation in this amine system - acid buffering (during the A-B period) and base buffering (during the B-C period). Buffering is controlled by the amine and silicate components. It is important to note that factors which minimise the pH fall during the A-B transition (large n), maximise factors which induce a pH rise during the B-C period (see Figure 5.21). When silicalite is crystallised in strong base systems the reverse is true, i.e. factors which minimise or maximise the pH changes during the A-B transition do likewise to those after it (see Figure 5.13). These considerations are important if it is desired to design systems to quell pH changes.

5.4.3.2 Crystals containing RNH_2

The effective system under investigation is $nRNH_2$ $20SiO_2$ $1000H_2O$. The TPABr in the mixtures is superfluous. The crystals were assumed to have composition $4RNH_2$ $96SiO_2$ (c.f. silicalite).

The charge-balance equation which holds during crystallisation is:

$$([A]-[A]^*)\ [H^+]/(K_a + [H^+]) + [H^+] = [SH_3^-] + 2[SH_2^{2-}] + [OH^-] \qquad (5.50)$$

where [A]* reflects the amount of amine incorporated in the crystals. Results were computed from equation (5.50) and are given in Table 5.13 (N.B. the computer programs used to model crystallisation in this system and in systems that are discussed in sections that immediately follow were modified versions of file PHAMINE that was used to model silicalite crystallisation in amine sytems).

Table 5.13 Simulated crystallisation in the $nRNH_2$ 2TPABr $20SiO_2$ $1000H_2O$ system
Chemical composition of the crystals: $4RNH_2$ $96SiO_2$

	Initial (Point A)				Solubility Transfer (Point B)				Final (Point C)				
n	$[RNH_3^+]^a$	$\frac{[RNH_3^+]}{[RNH_2]}$	pH	G[b]	$[RNH_3^+]^a$	$\frac{[RNH_3^+]}{[RNH_2]}$	pH	Y[c]	$[RNH_3^+]^a$	$\frac{[RNH_3^+]}{[RNH_2]}$	pH	Y[c]	ΔpH_{C-A}
0.5[d]	0.010	0.550	10.26	98.9	-	-	-	-	-	-	-	-	-
1	0.015	0.374	10.43	98.5	0.005	1.072	9.97	99.3	0.002	0.263	10.58	99.9	0.15
2	0.023	0.258	10.59	97.9	0.017	0.340	10.45	98.4	0.006	0.101	11.00	99.6	0.41
5	0.039	0.163	10.79	96.7	0.035	0.177	10.75	97.0	0.012	0.057	11.25	99.2	0.46
10	0.058	0.117	10.93	95.3	0.055	0.122	10.92	95.5	0.020	0.041	11.39	98.8	0.46
15	0.074	0.097	11.01	94.2	0.071	0.100	11.00	94.3	0.026	0.034	11.47	98.5	0.46
20	0.087	0.085	11.07	93.3	0.085	0.087	11.06	93.4	0.031	0.030	11.52	98.2	0.45

[a] Represents total protonated amine. All protonated amine is associated with silicate ions and hydroxide ions

[b] % silica as amorphous solid

[c] % yield

[d] Insufficient amine present for reaction to go to completion

The data in Table 5.13 shows that the pH decreases during the A-B transition diminish as the alkalinity increases; the solutions get more buffered to loss of amine. The pH rise during the B-C transition decreases as the alkalinity (n) increases. This is the reverse of the trend observed if strong base (TPAOH) is trapped in crystals as they grow (silicalite crystallisation - see Figure 5.20). It should be noted that the uptake of RNH_3OH, either as discrete molecules or bound to the framework (analogous to strong base framework attack), is chemically identical to the uptake of RNH_2 ($RNH_3OH \equiv RNH_2 + H_2O$).

5.4.3.3 Crystals containing RNH_3Br

The compositions of the crystals were taken to be $4RNH_3Br$ $96SiO_2$. For the purposes of the theory the salt was considered a physical mixture of amine and acid ($RNH_3Br \equiv RNH_2 + HBr$). The charge balance equation that was used to model crystallisation was:

$$([A]-[A]^*)[H^+]/(K_a + [H^+]) + [TPA^+]^* + [H^+] = [SH_3^-] + 2[SH_2^{2-}] + [OH^-] \quad (5.51)$$

where $[A]^*$ represented the amount of amine (RNH_2) removed (as the salt) and $[TPA^+]^*$ represented the amount of base cations generated as a result of HBr incorporation (as the salt) in the crystals. The latter was considered to involve the following reaction:

$$TPABr(aq) + H_2O \longrightarrow HBr(sil) + TPAOH(aq) \quad (5.52)$$

Clearly for any given amount of crystallisation $[TPA^+]^* = [A]^*$.

Results are given in Table 5.14. Features of note are listed below:

(1) During the A-B transition pH rises are seen because of the incorporation of a salt of a weak base and strong acid. The effect is akin to adding base to the mixture. The low base, least buffered reactions, show the largest pH increases (see Figure 5.20).

(2) The largest pH rises during solubility transfer are also seen for the low base reactions.

(3) In all cases, the final pH attained is similar. Although starting off as weak base systems, crystallisation generates strong base in the solutions. At the end of these reactions

Table 5.14 Simulated crystallisation in the system $nRNH_2$ $2TPABr$ $20SiO_2$ $1000H_2O$
Chemical composition of the crystals: $4RNH_3Br$ $96SiO_2$

	Initial (Point A)				Solubility Transfer (Point B)				Final (Point C)				
n	$[RNH_3^+]^a$	$\frac{[RNH_3^+]}{[RNH_2]}$	pH	G[c]	$[RNH_3^+]^b$	$\frac{[RNH_3^+]}{[RNH_2]}$	pH	Y[d]	$[RNH_3^+]^b$	$\frac{[RNH_3^+]}{[RNH_2]}$	pH	Y[d]	ΔpH_{C-A}
0.5[e]	0.010	0.550	10.26	98.9	-	-	-	-	-	-	-	-	-
1	0.015	0.374	10.43	98.5	0.001	0.142	10.85	96.2	<0.001	0.024	11.63	97.4	1.20
2	0.023	0.258	10.59	97.9	0.008	0.129	10.89	95.7	0.001	0.023	11.63	97.4	1.04
5	0.039	0.163	10.79	96.7	0.022	0.106	10.98	94.7	0.005	0.022	11.65	97.2	0.86
10	0.058	0.117	10.93	95.3	0.041	0.087	11.06	93.5	0.010	0.021	11.68	96.9	0.75
15	0.074	0.097	11.01	94.2	0.057	0.077	11.11	92.4	0.015	0.020	11.70	96.7	0.69
20	0.087	0.085	11.07	93.3	0.070	0.070	11.15	91.6	0.020	0.019	11.72	96.5	0.65

[a] Represents the effective cation concentration

[b] Represents only a portion of the effective cations (TPA supply the rest)

[c] % silica as amorphous solid

[d] % yield

[e] Insufficient amine present for reaction to go to completion

each contains a considerable and similar amount of strong base and it is this base which largely governs the final equilibrium pH.

5.4.3.4 Crystals containing HBr

The charge balance equation that was used to model the crystallisation process was:

$$[A][H^+]/(K_a + [H^+]) + [H^+] + [TPA^+]^* = [SH_3^-] + 2[SH_2^{2-}] + [OH^-] \qquad (5.53)$$

where $[TPA^+]^*$ represented the amount of base cations generated in solution as a result of acid incorporation. Crystals were assumed to have composition 4HBr $96SiO_2$. The calculated results, shown in Table 5.15 and Figure 5.20, were very similar to those evaluated for RNH_3Br incorporation indicating that when a salt of a weak base and strong acid is removed from solution it is removal of the acid component which has the most serious effect.

The pH changes that accompany crystallisation of chemically different silicas from the same reaction mixtures ($nRNH_2$ 2TPABr $20SiO_2$ $1000H_2O$) have been evaluated and the results are now graphically summarised. The comparative line representations drawn in Figure 5.22 show how the pH changes during the A-B and B-C transitions are affected by the alkalinity and the guest molecule type. The overall pH changes that occurred during reactions are shown in Figure 5.23. For any given starting alkalinity, the overall pH change increases as the guest molecules change from base to acid character:

$$(TPAOH) \rightarrow (RNH_2) \rightarrow (TPABr,\ H_2O,\ void) \rightarrow (RNH_3Br) \rightarrow (HBr)$$

The most diagnostic pH changes occur when the amine content is low and solutions are sensitive to perturbation (see Figure 5.22). The pH profiles in Figure 5.24 for two iso-alkaline amine reactions (discussed in chapter 4) show that experimental pH changes that accompany crystallisation of chemically different silicas do exhibit the features that have just been theoretically predicted.

Table 5.15 Simulated crystallisation in the system $nRNH_2$ 2TPABr $20SiO_2$ $1000H_2O$
Chemical composition of the crystals: 4HBr $96SiO_2$

	Initial (Point A)				Solubility Transfer (Point B)				Final (Point C)				
n	$[RNH_3^+]^a$	$\frac{[RNH_3^+]}{[RNH_2]}$	pH	G[c]	$[RNH_3^+]^b$	$\frac{[RNH_3^+]}{[RNH_2]}$	pH	Y[d]	$[RNH_3^+]^b$	$\frac{[RNH_3^+]}{[RNH_2]}$	pH	Y[d]	ΔpH_{C-A}
0.5	0.010	0.550	10.26	98.9	0.003	0.137	10.86	95.9	<0.001	0.023	11.63	97.4	1.37
1	0.015	0.374	10.43	98.5	0.006	0.131	10.88	95.7	0.001	0.023	11.63	97.4	1.20
2	0.023	0.258	10.59	97.9	0.012	0.121	10.92	95.4	0.002	0.023	11.64	97.3	1.05
5	0.039	0.163	10.79	96.7	0.026	0.102	10.99	94.5	0.006	0.022	11.66	97.2	0.87
10	0.058	0.117	10.93	95.3	0.044	0.086	11.07	93.2	0.011	0.021	11.69	96.9	0.76
15	0.074	0.097	11.01	94.2	0.059	0.076	11.12	92.2	0.016	0.020	11.71	96.6	0.70
20	0.087	0.083	11.07	93.3	0.072	0.070	11.16	91.4	0.021	0.019	11.73	96.4	0.66

[a] Represents the effective cation concentration

[b] Represents only a portion of the effective cations (TPA supply the rest)

[c] % Silica as amorphous solid

[d] % yield

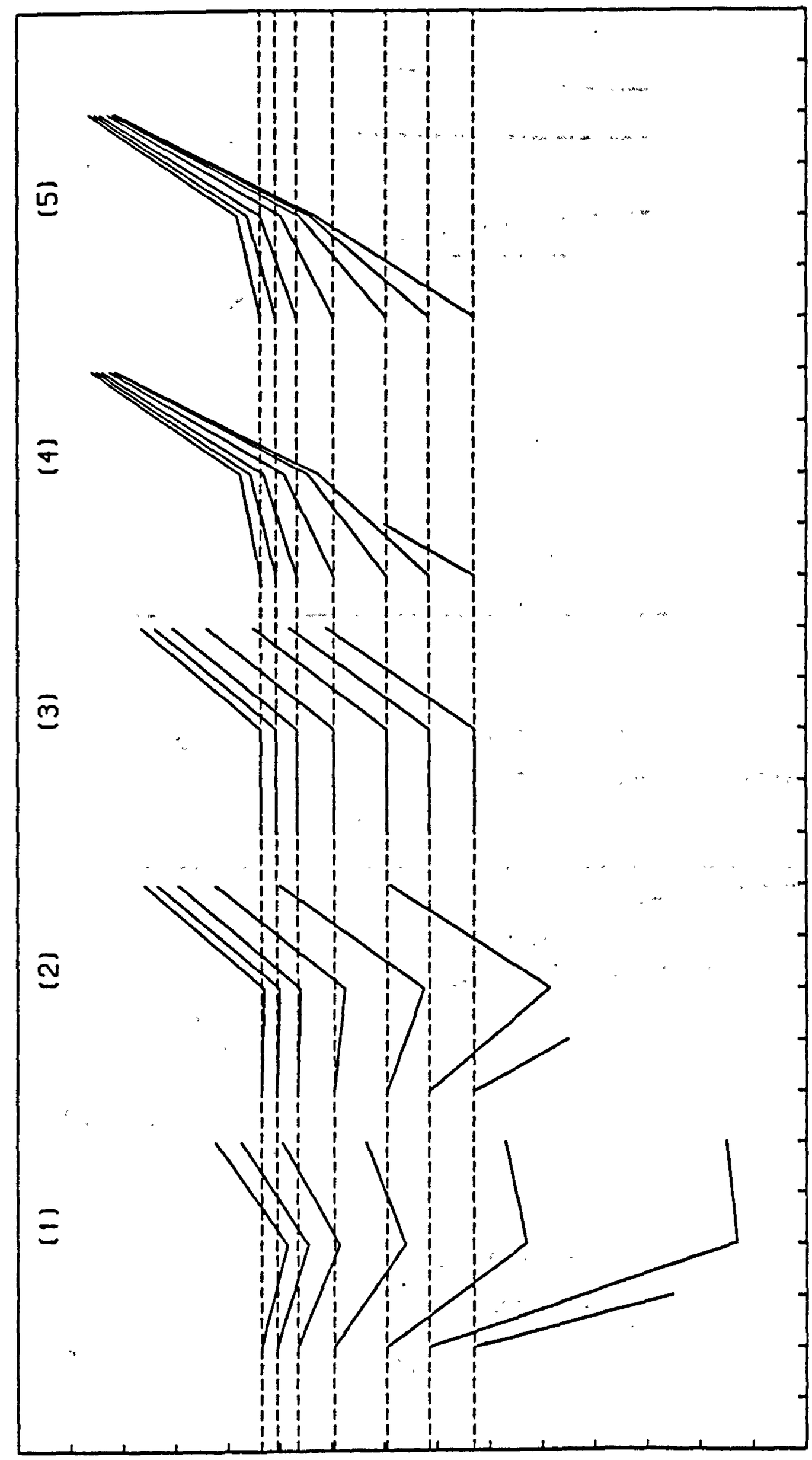

pH changes during crystallisation of microporous silicas in the $nRNH_2$ $2TPABr$ $20SiO_2$ $1000H_2O$ system for n = 0.5 (bottom plots), 1, 2, 5, 10, 15 and 20 (top plots).
Product compositions: (1) $4TPAOH$ $96SiO_2$; (2) $4RNH_2$ $96SiO_2$; (3) $(TPABr/H_2O/void)SiO_2$;
(4) $4RNH_3Br$ $96SiO_2$; (5) $4HBr$ $96SiO_2$ (N.B. Incomplete plots indicate reactions that cannot go to completion).

Figure 5.22

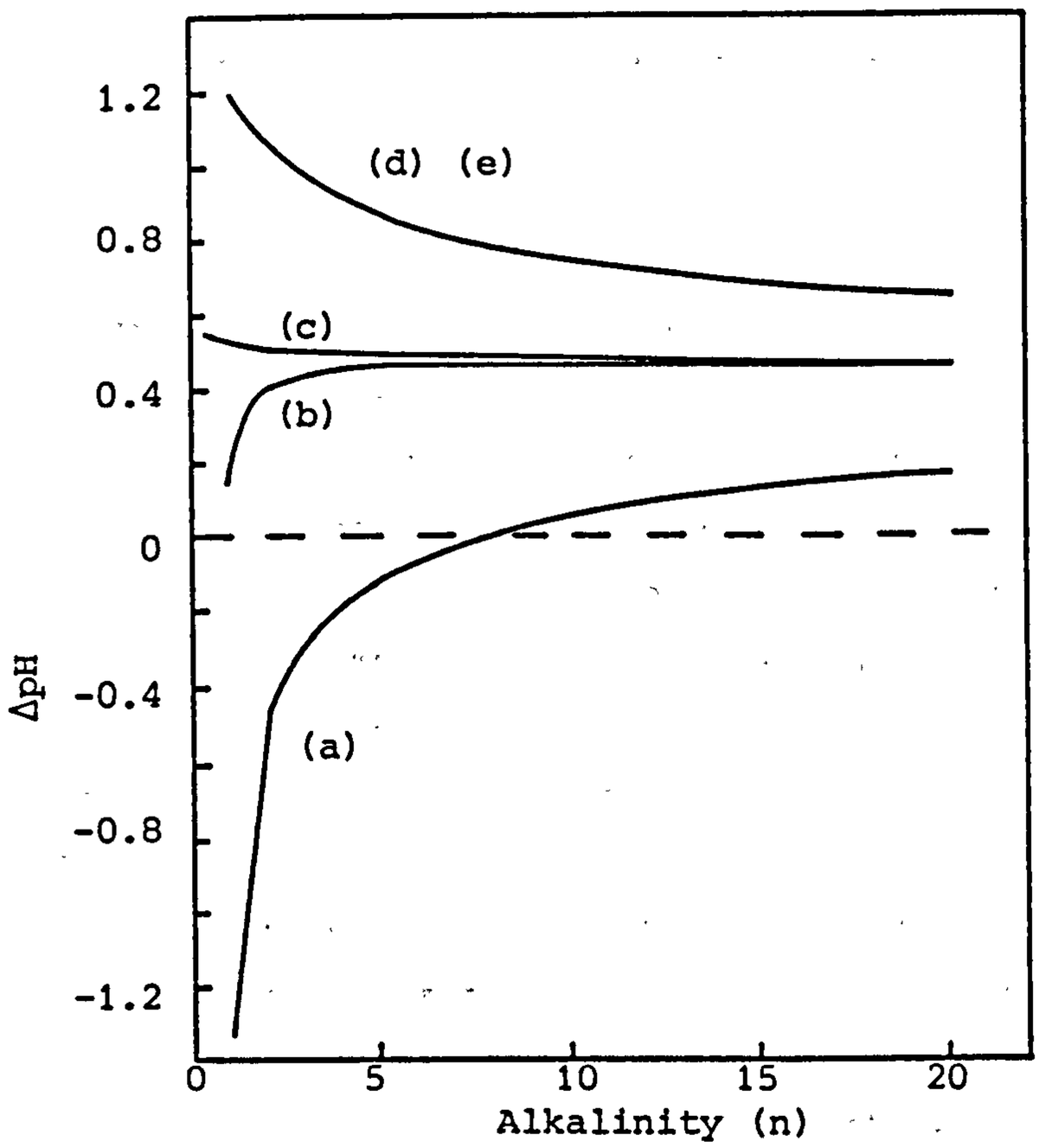

Product compositions:

(a) 4TPAOH $96SiO_2$

(b) $4RNH_2$ $96SiO_2$

(c) $(TPABr/H_2O/void)SiO_2$

(d) $4RNH_3Br$ $96SiO_2$

(e) 4HBr $96SiO_2$

Figure 5.23 Overall pH changes (theoretical) that accompany crystallisation of microporous silicas in the $nRNH_2$ 2TPABr $20SiO_2$ $1000H_2O$ system

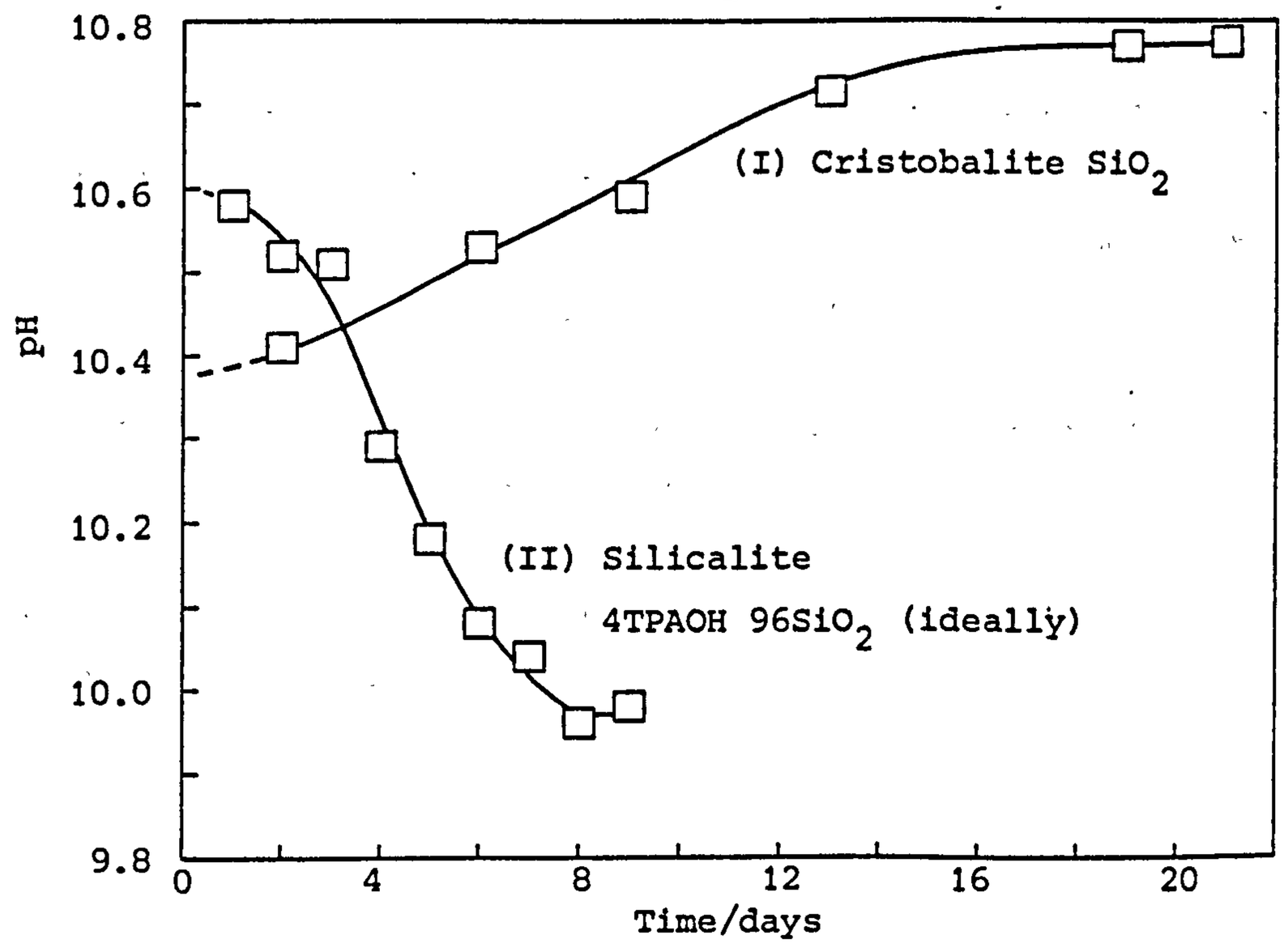

Figure 5.24 Experimental pH-time curves for crystallisations from reaction mixtures containing 1-methylbenzylamine (LMB)

(I) 2LMB $10SiO_2$ $1000H_2O$ 175°C Product: cristobalite

(II) 2LMB 2TPABr $10SiO_2$ $1000H_2O$ 175°C Product: silicalite

5.4.4 Comparison of theoretical and experimental results

Figure 5.25 shows theoretically and experimentally determined pH profiles (the data is shown in Table 5.16) for silicalite crystallisation from reaction mixtures that contain piperazine ($K_1 = 10^{-9.73}$, $K_2 = 10^{-5.55}$ at 25°C [12]). Calculations assumed piperazine was a monobasic amine; at these pH levels little of the diprotonated species will be present. No pH rises due to solubility transfer were observed experimentally. The predicted rises are in fact only small and in real systems such small rises could be masked by 'rounding' caused by the dynamics of the crystallisation process. Calculations assumed the crystals were of ideal composition although some piperazine was actually found in the products (discussed in chapter 4). It can be interpolated from the theoretical results in Figure 5.20 that this should have lessened the pH fall during the A-B transition and increased the pH rise during the B-C transition. Parameters were not altered to get a better fit between the theoretical and experimental data. The correlation obtained sufficed. It is of interest that both the experimental and theoretical pH decreases during the A-B period are almost linear with pH, i.e. they are straight lines on the plots. This is evidence that as the pH drops, the solutions still retain buffer capacity (due to the amine). In contrast, the experimental and theoretical pH profiles for silicalite crystallisation at similar pH levels in strong base systems (see Figures 5.15 and 5.8) are concave to the time (yield) axis during the A-B transition. This denotes a fall-off in buffer capacity (which is only supplied by silicate species in strong base mixtures).

Complex buffer action operates as silicalite crystallises in amine systems. Although pH changes are reduced by comparison with synthesis in strong base systems, improved pH control can be achieved by system design. Crystallisation in highly buffered systems is now investigated.

Table 5.16 Comparison of experimental and theoretical pH changes during silicalite crystallisation in the n-piperazine 2TPABr $20SiO_2$ $1000H_2O$ system

	Experimental[a]				Theoretical[c]			
n	pH_A	pH_B	pH_C	ΔpH_{C-A}	pH_A	pH_B	pH_C	ΔpH_{C-A}
5	10.91	b	10.50	-0.41	10.67	10.32	10.42	-0.25
10	11.04	b	10.75	-0.29	10.82	10.59	10.74	-0.08
15	11.27	b	10.97	-0.30	10.90	10.72	10.92	+0.02

[a] 100°C reactions (see Chapter 4 for further details)

[b] No solubility transfer point seen

[c] Calculations assumed piperazine was a monobasic amine with $K_a = 10^{-9.73}$

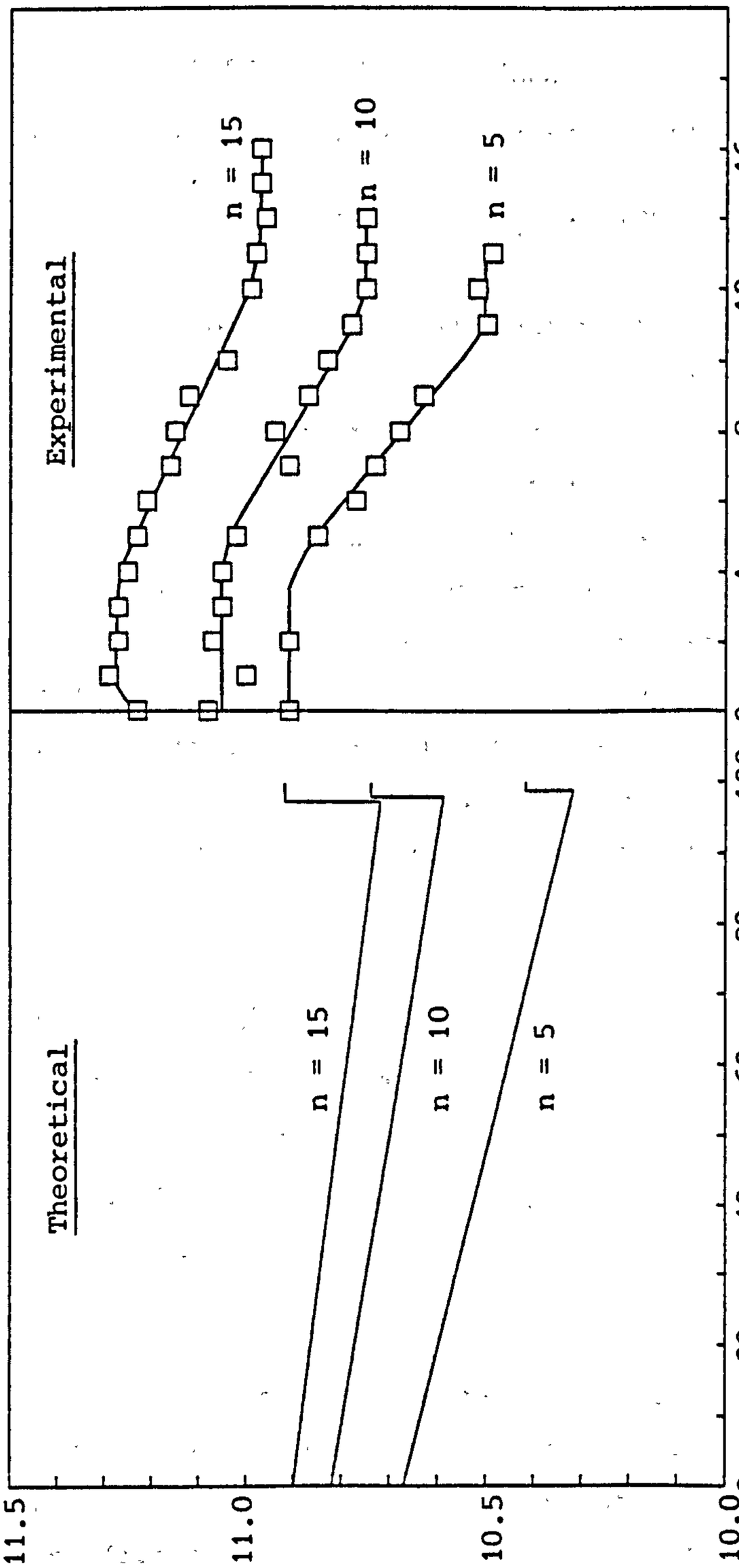

Figure 5.25 A comparison of the theoretically calculated and experimentally determined pH profiles for silicalite crystallisation in the n-piperazine 2TPABr $20SiO_2$ $1000H_2O$ system. Calculations used $K_1 = 2 \times 10^{-10}$, $K_2 = 2 \times 10^{-12}$, K_s(gel) = 2.5×10^{-3}, K_s(silicalite) = 1.8×10^{-4} and K_a(piperazine) = $10^{-9.73}$ (the piperazine was assumed to have ideal composition 4TPAOH $96SiO_2$. be monobasic). The products were assumed to have ideal composition 4TPAOH $96SiO_2$.

The experimental reactions were carried out at 100°C (see Chapter 4).

5.4.5 Crystallisation in highly buffered amine systems

Crystallisation in the $nRNH_2$ mHX $2TPABr$ $20SiO_2$ $1000H_2O$ system (n = 10, m = 0 to 9) is discussed in this section. The addition of strong acid (HX = HCl, HBr, HNO_3 etc.) to mixtures alters their alkalinity and buffering ability.

5.4.5.1 Crystal composition: SiO_2

Results were calculated using the charge balance equation:

$$[A][H^+]/(K_a + [H^+]) + [H^+] = [SH_3^-] + 2[SH_2^{2-}] + [OH^-] + [X^-] \qquad (5.54)$$

where $[X^-]$ represents the concentration of anions introduced by the acid addition. Note that this equation and hence calculated pH changes are independent of the nature of the strong acid. The results in Table 5.17 show that increased acid addition decreases the reaction pH (the RNH_3^+/RNH_2 ratio increases). For each reaction the amine buffer capacity is at a maximum at pH = 10. The pH rises during solubility transfer decrease as the reaction pH decreases (see Figure 5.26(I)). This is the opposite of the trend observed when crystallisation occurs from mixtures prepared without acid additions (see Figure 5.21(I)) and is due to the balance between buffering effects and the magnitude of the effective base additions during solubility transfer.

5.4.5.2 Crystal composition: $4TPAOH$ $96SiO_2$

The charge balance equation that was used to simulate the crystallisation process was:

$$[A][H^+]/(K_a+[H^+]) + [H^+] = [SH_3^-] + 2[SH_2^{2-}] + [OH^-] + [X^-] + [Br^-]^* \qquad (5.55)$$

where $[Br^-]^*$ represents the concentration of bromide ions in solution equivalent, on an absolute basis, to the number of moles of TPAOH in the crystals. Changes in pH during these reactions, calculated from the above equation, are shown in Table 5.18 and Figures 5.26(II) and 5.27. The results illustrate interesting features:

Table 5.17 Simulated crystallisation in the $nRNH_2$ mHX 2TPABr $20SiO_2$ $1000H_2O$ system
Chemical composition of the crystals: SiO_2

		Initial (Point A) Solubility Transfer (Point B)				Final (Point C)				
n	m	$[RNH_3^+]$ [a]	$\frac{[RNH_3^+]}{[RNH_2]}$	pH	G [b]	$[RNH_3^+]$ [a]	$\frac{[RNH_3^+]}{[RNH_2]}$	pH	Y [c]	ΔpH_{C-A}
10	0	0.058	0.117	10.93	95.3	0.021	0.039	11.41	98.7	0.48
10	1	0.088	0.189	10.72	97.1	0.060	0.122	10.91	99.7	0.19
10	2	0.130	0.305	10.52	98.2	0.113	0.256	10.59	99.8	0.07
10	4	0.230	0.706	10.15	99.1	0.223	0.670	10.17	99.9	0.02
10	5	0.283	1.037	9.98	99.3	0.278	1.003	10.00	>99.9	0.02
10	6	0.336	1.539	9.81	99.5	0.333	1.503	9.82	>99.9	0.01
10	8	0.445	4.058	9.39	99.7	0.444	4.005	9.40	>99.9	0.01
10	9	0.500	9.103	9.04	99.7	0.500	9.009	9.05	>99.9	0.01

[a] Represents total protonated amine

[b] % silica as amorphous solid

[c] % yield

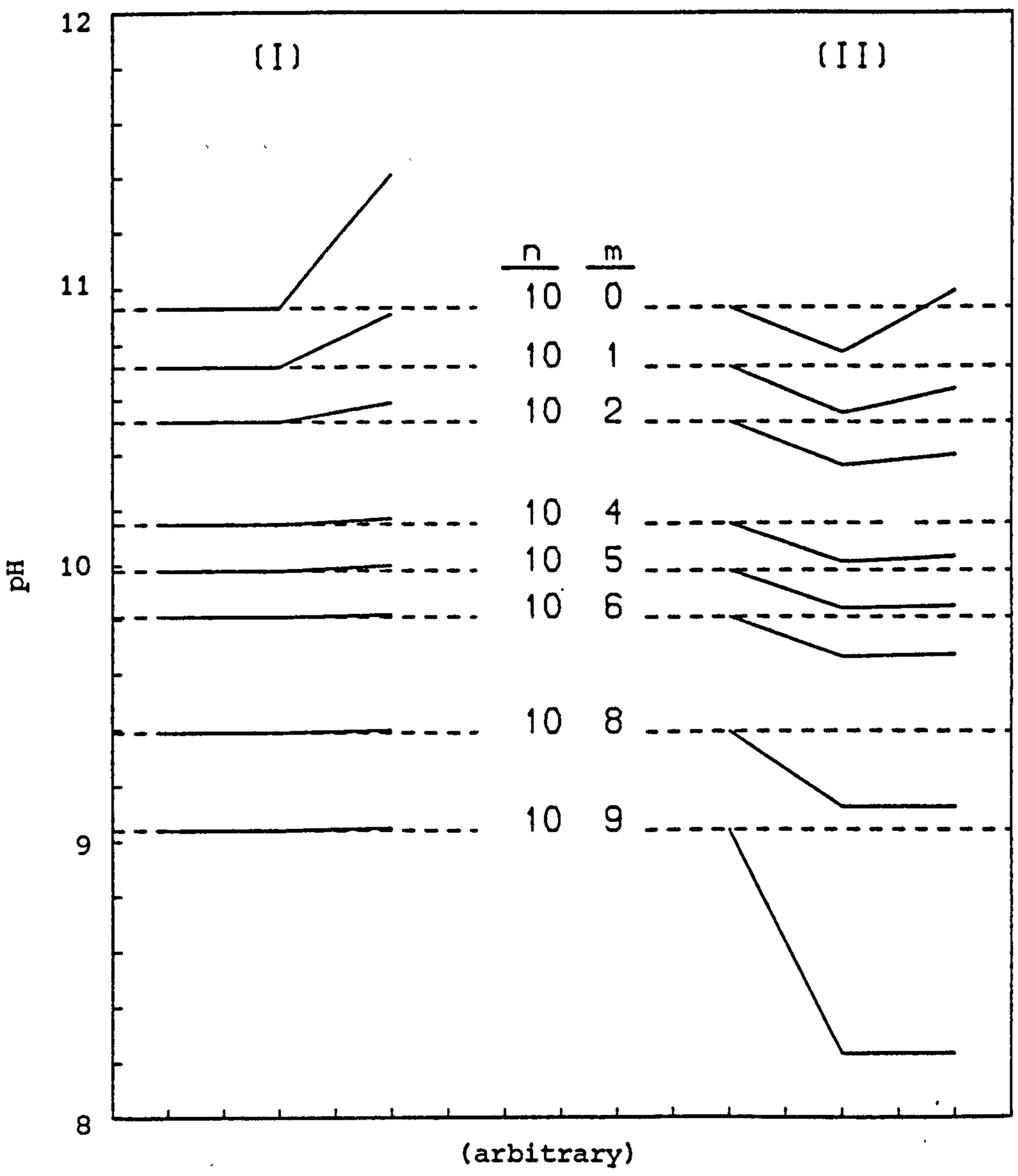

Figure 5.26 Crystallisation in the $nRNH_2$ mHX 2TPABr $20SiO_2$ $1000H_2O$ system. Product compositions: (I) SiO_2; (II) 4TPAOH $96SiO_2$

Table 5.18 Simulated crystallisation in the $nRNH_2$ mHX 2TPABr $20SiO_2$ $1000H_2O$ system
Chemical composition of the crystals: 4TPAOH $96SiO_2$

		Initial (Point A)				Solubility Transfer (Point B)				Final (Point C)				
n	m	$[RNH_3^+]^a$	$\frac{[RNH_3^+]}{[RNH_2]}$	pH	G^b	$[RNH_3^+]^a$	$\frac{[RNH_3^+]}{[RNH_2]}$	pH	Y^c	$[RNH_3^+]^a$	$\frac{[RNH_3^+]}{[RNH_2]}$	pH	Y^c	ΔpH_{C-A}
10	0	0.058	0.117	10.93	95.3	0.081	0.172	10.77	96.8	0.052	0.103	10.99	99.6	+0.06
10	1	0.088	0.189	10.72	97.1	0.122	0.280	10.55	98.1	0.104	0.230	10.64	99.8	-0.08
10	2	0.130	0.305	10.52	98.2	0.169	0.439	10.36	98.7	0.158	0.399	10.40	99.9	-0.12
10	4	0.230	0.706	10.15	99.1	0.273	0.971	10.01	99.3	0.269	0.939	10.03	>99.9	-0.12
10	5	0.283	1.04	9.98	99.3	0.327	1.44	9.84	99.5	0.324	1.40	9.85	>99.9	-0.13
10	6	0.336	1.54	9.81	99.5	0.381	2.20	9.66	99.6	0.380	2.16	9.67	>99.9	-0.14
10	8	0.445	4.06	9.39	99.7	0.491	7.64	9.12	99.7	0.490	7.58	9.12	>99.9	-0.27
10	9	0.500	9.10	9.04	99.7	0.546	58.9	8.23	99.8	0.546	58.9	8.23	>99.9	-0.81

[a] Represents total protonated amine

[b] % silica as amorphous solid

[c] % yield

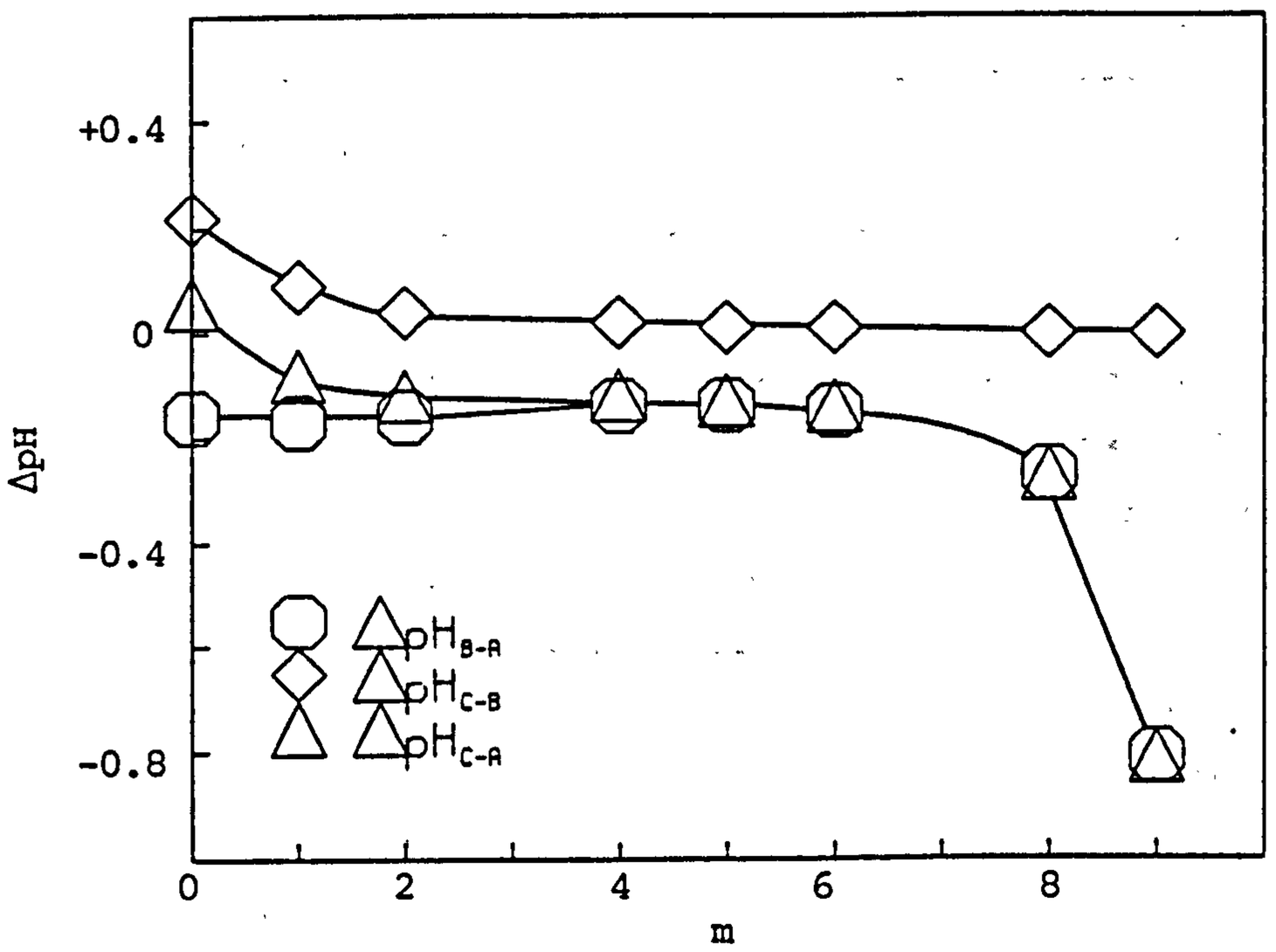

Figure 5.27 Relative pH changes during crystallisation of silicalite (4TPAOH 96SiO_2) in the 10RNH_2 mHX 2TPABr 20SiO_2 1000H_2O system as a function of the acid component (m) in reaction mixtures

(1) The pH decrease (caused by loss of TPAOH) during the A-B period passes through a minimum around the point of maximum buffering (pH = 10) and then decreases sharply (see Figure 5.27). The form of this curve is, not unexpectedly, similar to that of a titration curve for neutralisation of a weak base with a strong acid [2].

(2) The pH rise during solubility transfer decreases as the amount of acid added to a mixture (m) increases. At very low pH solubility transfer induces such small effects that, even though the amine buffers poorly, the reaction pH is little affected.

The results in Figure 5.26(II) and 5.27 show that in all cases a pH fall was observed during the A-B transition. Even though some of these solutions were well buffered, they were not well enough buffered to cope with the magnitude of the base loss. Figure 5.28 shows that this decrease can be reduced by buffer enhancement, i.e. increasing the amount of amine and its salt in mixtures.

It is important to mention that in all the amine systems discussed the acidity constant of the amine was taken to be 10^{-10}; the amine buffers at low pH in regions where the silicate species do not. If stronger amines were used in mixtures (smaller K_a) the amine and silicate buffer regions could well overlap. Effects of this are not easy to predict suffice to say results may differ somewhat from those presented in this work.

It was suggested earlier (in section 5.2 under 'The solubility of silica' and Figure 5.1(a)) that enhanced buffering in silicate solutions might be expected at pH = 9.70 (when $[Si(OH)_4] = [Si(OH)_3O^-]$) and at pH = 11.70 (when $[Si(OH)_2O_2^{2-}] = [Si(OH)_3O^-]$). The amount of silica in solution at low pH is so small that no buffering effects at pH ≈ 9.7 were borne out by any of the calculations. The buffer capacity of silicate solutions appears to increase continually with pH over the 7 to 12 range as the concentrations of silicate anions increase (see Figure 5.1(a) and (b)).

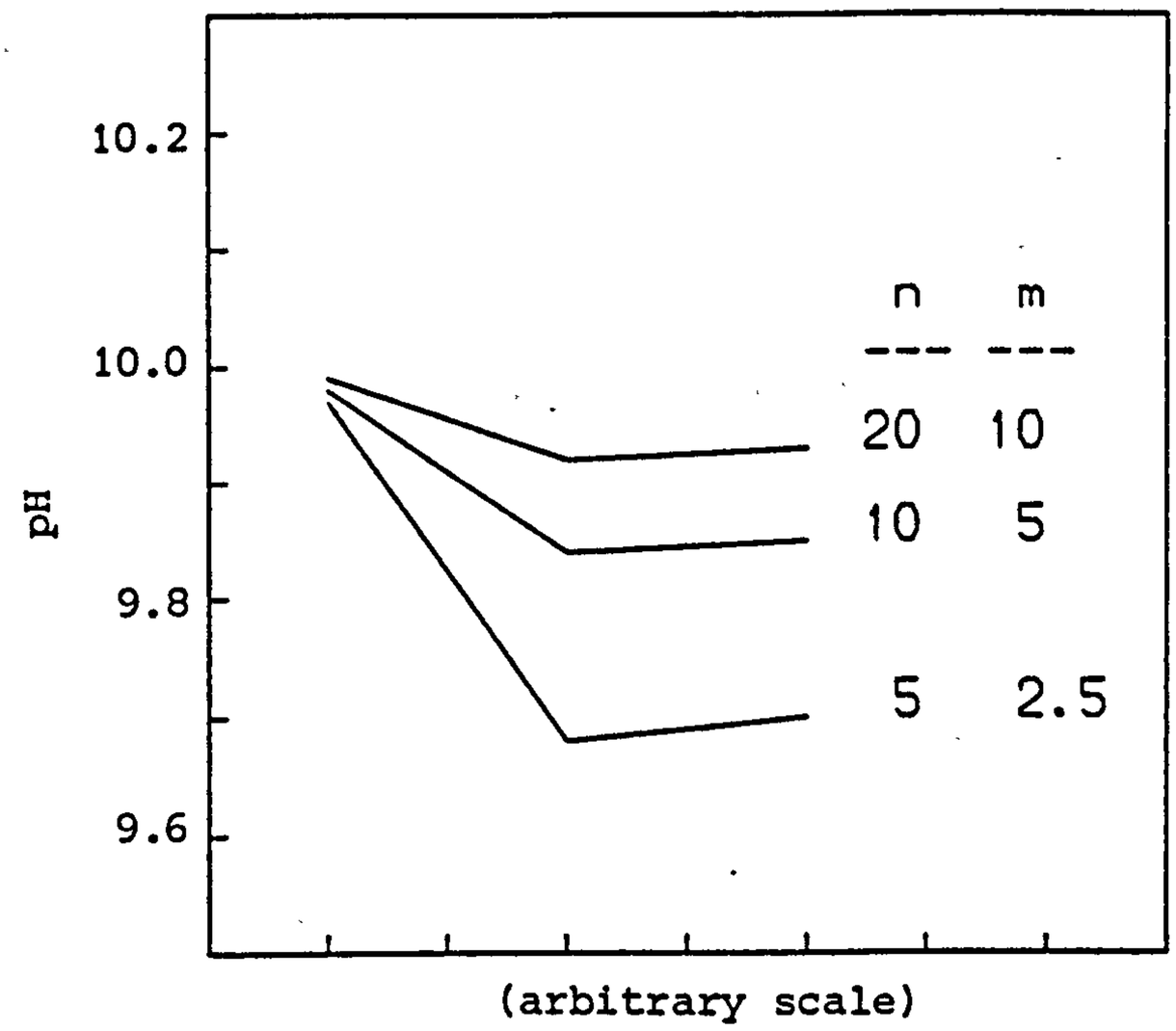

Figure 5.28 The effect of buffering on the pH changes during silicalite crystallisation in the $nRNH_2$ mHX $2TPABr$ $20SiO_2$ $1000H_2O$ system.

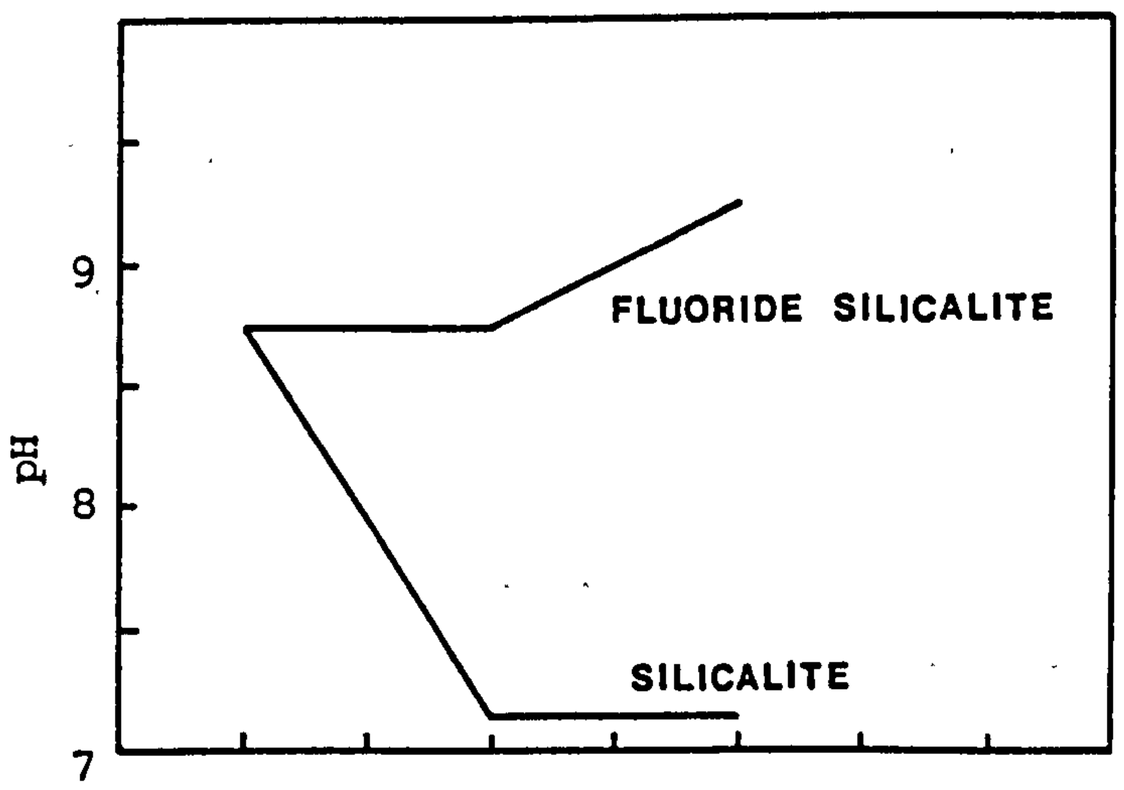

Figure 5.29 pH changes that accompany crystallisation of fluoride silicalite ($4TPAF$ $96SiO_2$) and silicalite ($4TPAOH$ $96SiO_2$) from reaction mixtures of composition $50TPAF$ $5SiO_2$ $1000H_2O$

5.5 Crystallisation in systems that contain salts as mineralisers

5.5.1 Theory

Aqueous solutions of salts of strong bases and weak acids, e.g. NaAc, NaF, are alkaline. This derived alkalinity can be used to effect crystallisation. Consider an aqueous solution of a sodium salt (NaA) of a weak acid (HA). The hydrolysis constant K_h governs the hydrolysis reaction:

$$NaA + H_2O \overset{K_h}{\rightleftharpoons} NaOH + HA \qquad (5.56)$$

The hydrogen ion concentration is controlled by the acidity of the acid:

$$HA \overset{K_a}{\rightleftharpoons} H^+ + A^- \qquad (5.57)$$

and the acidity constant K_a is written:

$$K_a = [H^+][A^-]/[HA] \qquad (5.58)$$

The total concentration of 'A' (as the ion A^- and the undissociated acid HA) is designated $[A_t]$:

$$[A_t] = [A^-] + [HA] \qquad (5.59)$$

Substituting equation (5.58) into (5.59) and rearranging gives:

$$[A^-] = (K_a + [H^+])/(K_a[A_t]) \qquad (5.60)$$

Crystallisation

Consider crystallisation in the NaA-TPABr-SiO_2-H_2O system. The ionic species in solution are related by the equation:

$$[Na^+] + [H^+] + [TPA^+] = [SH_3^-] + 2[SH_2^{2-}] + [A^-] + [OH^-] + [Br^-] \qquad (5.61)$$

Note that it is again assumed that only two types of silicate ion are present. With substitutions and necessary modifications to take into account the chemical make-up of crystals (similar to those used for amine and strong base systems), equation (5.61) enabled parameters at the steady-state reaction positions to be evaluated (method as before). Solubility transfer points have also been calculated.

5.5.2 Crystallisation in the sNaAc 2TPABr 20SiO_2 1000H_2O system. Crystal composition: SiO_2

The mineralising salt was chosen to be sodium acetate (K_a (acetic acid) = $10^{-4.76}$ at 25°C). Results were calculated using equation (5.61) (neglecting the $[TPA^+]$ and $[Br^-]$ terms) and are shown in Table 5.19A. Features to note:

(i) The initial pH is low even when large amounts of salt are present (very weak base).

(ii) Substantial pH rises occur during solubility transfer because systems are poorly buffered (pK_a = 4.76 for acetic acid). If crystallisations in systems of similar initial pH are compared, it is found that salt systems are poorly buffered relative to amine systems but more buffered than strong base systems.

(iii) Yields are very high.

Crystals containing TPAOH (silicalite)

The crystals were assumed to have ideal composition 4TPAOH 96SiO_2. The charge balance equation that was used to calculate results was:

$$[Na^+] + [H^+] = [SH_3^-] + 2[SH_2^{2-}] + [Ac^-] + [OH^-] + [Br^-]^* \qquad (5.62)$$

where $[Br^-]^*$ represents the concentration of bromide ions in solution equivalent, on an absolute molar basis, to the number of moles of TPAOH in the crystals.

Table 5.19 Crystallisation from reaction mixtures containing salts as mineralisers

A : sNaAc SiO_2 $1000H_2O$ Product composition SiO_2

B : sNaAc 2TPABr $ySiO_2$ $1000H_2O$ Product composition $4TPAOH\ 96SiO_2$

C : sNaAc 2TPABr $ySiO_2$ $1000H_2O$ Product composition $4TPAAc\ 96SiO_2$

			Initial (Point A)		Solubility Transfer (Point B)		Final (Point C)		
	s	y	pH	G[a]	pH	Y[b]	pH	Y[b]	ΔpH_{C-A}
A	5	5	8.25	99.1	8.25	99.1	8.77	>99.9	0.52
	5	50	8.25	99.9	8.25	99.9	8.77	>99.9	0.52
	50	5	8.75	99.0	8.75	99.0	9.27	99.9	0.52
	50	50	8.75	99.9	8.75	99.9	9.27	>99.9	0.52
B	5	5	8.25	99.1	-	-	-	-	-
	50	5	8.75	99.0	7.14	99.1	7.14	>99.9	-1.61
C	5	5	8.25	99.1	8.24	99.1	8.76	99.9	0.51
	5	50	8.25	99.9	8.13	99.9	8.66	>99.9	0.41
	50	5	8.75	99.0	8.75	99.0	9.27	99.9	0.52
	50	50	8.75	99.9	8.74	99.9	9.26	>99.9	0.51

[a] % silica as amorphous solid

[b] % yield

The results in Table 5.19B show that to effect complete crystallisation, mixtures must contain a lot of mineralising salt and relatively little silica. Removal of strong base during crystallisation is accompanied by a substantial pH fall (unbuffered solutions) but no pH rises are observed on solubility transfer - the mixtures are sufficiently buffered to cope with this.

Crystals containing TPAAc

The composition of the crystals was deemed to be 4TPAAc $96SiO_2$. Results were calculated from the equation:

$$[Na^+] - [S_1] + [H^+] = [SH_3^-] + 2[SH_2^{2-}] + [Ac^-] + [OH^-] \qquad (5.63)$$

where $[Ac^-]$ is given by:

$$[Ac^-] = (K_a + [H^+])/(K_a([Ac_t] - [S_1])) \qquad (5.64)$$

where $[S_1]$ represents the concentration of TPAAc lost from solution equivalent, on an absolute molar basis, to the number of moles TPAAC in the crystals. The results in Table 5.19C show that if salt is removed (the salt is that of a strong base and a weak acid) reactions readily go to completion (c.f. strong base removal). Only small pH changes occur during the A-B transition but substantial pH rises occur during solubility transfer.

5.5.2 Fluoride silicalite

Fluoride silicalite (4TPAF $96SiO_2$) is structurally similar to silicalite-1 (composition 4TPAOH $96SiO_2$) [6,7]. It is synthesised in systems that contain salts as mineralisers [13]. Mixtures generally require two salt components, one to provide the fluoride ions (e.g. NaF, KF) and the other to provide the quaternary cations (e.g. TPABr). TPAF is thus derived from the salt combinations. Consider formation of fluoride silicalite from reaction mixtures of composition sTPAF $20SiO_2$ $1000H_2O$. Calculated results were identical (to within 0.01 pH units) to those listed in Table 5.19C for formation of crystals of composition 4TPAAc $96SiO_2$ (from mixtures containing NaAc/TPABr) due to the fact that the acidity constants of the weak acids (HAc and HF) are almost identical (pK_a = 4.76 and 4.77 respectively).

Note however that silicofluoride ions will be present in mixtures and the model is therefore not strictly applicable to fluoride systems.

Figure 5.29 shows the markedly different theoretical pH changes that accompany formation of silicalite and fluoride silicalite from one particular reaction mixture (assuming silicofluoride ions are not present). Fluoride silicalite has to be crystallised at low pH because competition between TPAOH and TPAF for lattice sites increases at high pH. The presence of TPAF in pores renders the material more hydrophobic than silicalite probably because lattice attack by TPAF is impossible (unless hydrolysis to TPAOH and HF occurs). Consequently, after calcination to remove the organic, few internal silanol groups (hydrophilic centres) remain. The absence of hydroxyl groups in the fluoride silicalite structure has been shown by infra-red spectroscopy [13].

As-synthesised fluoride silicalite possesses a neutral framework and as such is a silica polymorph. Structural work indicates discrete TPAF molecules are present in the lattice [6,7]. It is believed there may be other salts that could stabilise microporous silicas. Just as fluoride silicalite requires low pH crystallisation conditions, it follows that there may be other molecules (for example salts and uncharged species) that could effectively function as stabilisers/guests for molecular sieves under low pH reaction conditions that could not under more severe alkaline conditions. Undoubtedly the presence of fluoride ions and/or other agents in mixtures to bring silica into solution at low pH would be beneficial.

5.6 Concluding Remarks

A theoretical approach to the formation of crystalline silicas has been made by application of the equilibrium model for high silica zeolite synthesis [1]. New theoretical concepts have been introduced:

(1) Removal of species from solution during crystal growth has been taken into account.

(2) The periods when crystals grow at the expense of the amorphous solid have been modelled.

(3) Solubility transfer points have been determined.

The theory has been applied to three different system types, namely those that contain strong bases, weak bases and salts as mineralisers. In each case the formation of chemically different crystals has been investigated. Clearly, the theory could also be applied to (i) crystallisation in systems that contain more than one base type (e.g $NaOH/RNH_2$ in combination) and (ii) instances where crystals remove more than one species type from solution during growth.

The results have highlighted both features that were expected and others that were not. All features though, even the 'predictable' ones, have been quantified and put in a perspective that has not been attempted before.

The crystallisation model is based on sound thermodynamic principles and results have been interpreted on equally sound thermodynamic grounds. Changes in pH that accompany crystallisation are governed by buffering effects in the solution phases and by the solubilities and chemistries of the solid phases. In strong base systems buffering is provided by silicate species alone and is appreciable only at high pH. In weak base systems additional buffering is conferred and this is especially significant at low pH. Enhanced pH control can be obtained if the compositions of reaction mixtures are judiciously chosen. The addition of strong acids to weak base systems [14] seems a particularly useful ploy and one which, guaging from the literature, has only been used on occasion.

A great deal has been discussed about pH changes and pH control. It is pertinent to consider why pH control is thought so important:

(1) Simply changing the alkalinity of a reaction mixture - the amount of base used, not its chemical nature - can result in the formation of completely different products. If considerable pH changes occur during crystallisation, either up or down, it is possible that in some instances this may cause movement between <u>crystallisation fields</u> and give rise to products that contain more than one crystalline phase. Of particular relevance here may be the fact that the number and type of silicate species in solution are highly pH

dependent (see Table 5.1 and Figure 5.1(a)). Note that silicate species are also known to be cation dependent. Control of pH may reduce the possibility of movement between fields. It should be mentioned that movement between fields can also occur at constant pH; as nutrients are consumed by the growing crystals, the chemistries of the solution phases and amorphous solid phases necessarily change.

(2) Control of pH may induce 'more uniform' nutrient uptake by growing crystals and may alleviate microheterogeneity. The ordering of silicon and aluminium atoms in high silica zeolites is a subject that has recently received considerable attention [15,16,17]. Could the aluminium distribution in zeolites be altered (and perhaps, as a result, their catalytic activity) by pH control during synthesis?

(3) Growth occurs at the external surfaces of crystals. Ion-exchange equilibria at the surfaces will probably be pH dependent. If pH changes occur, the nature of the growing surface must change - this is unlikely to be ideal.

(4) In general the rate of crystallisation increases with pH and pH fluctuations are undesirable from this kinetic point of view. It is thought beneficial to have a constant growth rate during crystallisation.

(5) In some cases secondary nucleation (of the same species) may be induced by pH changes. This is undesirable as it gives rise to products that contain crystals of different sizes.

(6) If systems can be designed to give a low final reaction pH then product yields should be high.

(7) Research studies - pH control may aid investigative work in the synthesis field.

Although the above list is not exhaustive, the points mentioned suffice to exemplify the importance of the pH parameter.

The crystallisation model does not take into account effects due to aluminium in mixtures. In general the solubilities of both amorphous and crystalline phases will be reduced if they contain aluminium. The theory has not yet been tested against experimental results from aluminium-containing systems.

Improvements to the theory could be made, perhaps most significantly by consideration of activity coefficients in mass action relationships. Nevertheless, as it stands, the theory does have its merits - in particular its simplicity and its generality. Better knowledge of the dissociation constants and solubility products would also be advantageous.

Two slightly different applications of the theory to situations of practical importance deserve mention. Firstly, the theory could be used to predict the changes that necessarily must occur when reaction mixtures are cooled from elevated temperatures to ambient, i.e. non-isothermal solubility changes that involve the same solid phase. Secondly, the theory could be used to model post-synthesis dissolution of high silica zeolites. This is an interesting area of zeolite science which has been little investigated. Dissolution is clearly an important consideration when applications of zeolites and silica molecular sieves involve contact with aqueous solutions. This point has been briefly discussed by Sherman [18] in relation to the use of aluminous zeolites as ion-exchangers. The prospective use of high silica zeolites and silica molecular sieves to sorb organic molecules from aqueous solutions (this topic is discussed in the next chapter) makes an understanding of dissolution of these materials of some significance.

The most important aspects of this work concern, not the specific results, but the general features that have emerged and the modelling approach that has been made. This work was carried out after experimental synthesis work was near completion. Amongst the ideas mentioned in this chapter are some which are thought worthy of practical investigation.

Chapter 5 - References

[1] B.M. Lowe
Zeolites, 1983, 3, 300.

[2] A.I. Vogel
"Textbook of Quantitative Inorganic Analysis", Longman, London, 1978 (4th Ed.), pp. 247-250.

[3] R.K. Iler
"The Chemistry of Silica", Wiley, New York, 1979.

[4] Ref. [3], pp. 30-62.

[5] Ref. [3], p. 31.

[6] G.D. Price, J.J. Pluth, J.V. Smith, T. Araki and J.M. Bennett
Nature, 1981, 292, 818.

[7] G.D. Price, J.J. Pluth, J.V. Smith, J.M. Bennett and R.L. Patton
J.Amer.Chem.Soc., 1982, 104, 5971.

[8] F. Liebau
Zeolites, 1983, 3, 191.

[9] E.M. Flanigen, J.M. Bennett, R.W. Grose, J.P. Cohen, R.L. Patton, R.M. Kirchner and J.V. Smith
Nature, 1978, 271, 512.

[10] H. Annehed and L. Falth
Recent Progress Reports, 5th Int.Conf. Zeolites, (Ed. R. Sersale, C. Collela and R. Aiello), 1980, 5.

[11] B.M. Lok, T.R. Cannan and C.A. Messina
Zeolites, 1983, 3, 282.

[12] H.B. Hetzer, R.A. Robinson and R.G. Bates
J.Phys.Chem., 1968, 72, 2081.

[13] E.M. Flanigen and R.L. Patton
U.S. Patent 4,073,865 (1978).

[14] L.D. Rollmann
U.S. Patent 4,296,083 (1981).

[15] R. von Ballmoos and W.M. Meier
Nature, 1981, 289, 782.

[16] E.G. Derouane, J.P. Grilson, Z. Gabelica, C. Mousty-Desbuquoit and J. Verbist
J.Catal., 1981, 71, 447.

[17] C.E. Lyman, P.W. Betteridge and E.F. Moran
in "Intrazeolite Chemistry", ACS Symp. Ser. 218, (Ed. G.D. Stucky and F.G. Dwyer), 1983, p. 199.

[18] J.D. Sherman
in "Zeolites: Science and Technology" (NATO ASI Series), (Ed. F.R. Ribeiro, A.E. Rodrigues, L.D. Rollmann, C. Naccache), Martinus Nijhoff, The Hague, 1984, p. 583.

Chapter 6

Properties of Silicalite-1

6.1 Introduction

By and large, the bulk of the synthesis work described in chapters 3-5 was undertaken in the latter period of these research studies. Work carried out at the beginning of the research programme showed silicalite was a complex solid with 'unexpected' properties. The present chapter details some of those properties. The value of the crystallisation studies in aiding the interpretation of results will become apparent.

Whereas the properties of a zeolite are dependent on its structure and composition, silica molecular sieves, whether they be materials that can be directly crystallised or materials produced by post-synthesis aluminium removal, should have similar properties. This is because ideally they should all be compositionally identical - 100% SiO_2.

As pointed out by Barrer [1],

> *"The silicalites and faujasite silica provide non-polar molecular sieves which are virtually devoid of cations and hydroxyl groups. Provided no detrital silica is present within the intrachannels, the sieve properties should be determined only by the framework geometries and so should be the same for all preparations. This aspect has not been investigated."*

In practice though, silica molecular sieves can be far from perfect and the abovementioned 'cations and hydroxyl groups' are important in this respect.

6.2 Adsorption of organic molecules from aqueous solution

6.2.1 Introduction

For chronological reasons it is appropriate to begin the results sections with this topic - the subject area investigated at the very start of the research programme.

It was recognised from an early stage that high silica zeolites that required organic void fillers for their crystallisation exhibit preferences for non-polar over polar sorbates in their post-synthesis adsorption properties. In the specific case of materials with ZSM-5 structure the relationship between aluminium (and associated cation) content and hydrophobicity is well established [2,3].

The ability of silicious zeolitic materials to adsorb organic solutes from aqueous solutions exemplifies their selectivity for non-polar sorbates. Moreover, this is an area with possible commercial applications. Organic molecules can be effectively 'concentrated' by adsorption onto molecular sieves and, if valuable, then efficiently stripped and processed. In other instances, it may be desired to dispose of the adsorbed molecules. Clearly such adsorption provides a potential means of removing toxic materials from wastewaters. It may be that certain industrial wastes that are required by legislation to be dumped at sea (at considerable expense) could be disposed of on land (relatively cheaply) if adsorption processes were able to sufficiently reduce the levels of toxic components. Whilst only speculative, this exemplifies one of the many possible ways in which the adsorption selectivities of silicious zeolitic materials could be utilised.

The experimental work carried out in this area relates to the uptake of α-ω alkanediols from aqueous solution by silicalite-1. At the time this work was undertaken there was only a sprinkling of data in the literature, mostly in patents, relating to the adsorption of organics from aqueous solution by silicious zeolitic materials. However it is apparent from the literature that has now been published that other workers were concurrently active in this field.

Milestone and Bibby reported the first detailed work on the subject [4]. Isotherms for the uptake of monohydric alcohols were obtained and it was found that the alcohol concentration at which adsorption saturation was realised decreased as the chain length (and organophilic nature) of the alcohol increased. It was pointed out that the reverse effects have been observed for alcohol adsorption on zeolites; water and the lower alcohols are adsorbed preferentially to those of greater chain length.

Much of the other relevant work published has also focused on alcohol adsorption from aqueous solution; by silicalite [5-9], by fluoride silicalite [10] and by ZSM-5 [11-13]. The potential value of an efficient means of isolating alcohols, particularly ethanol, from aqueous fermentation beers is the chief reason for this. Adsorption is more energy efficient than conventional separatory techniques such as distillation. In addition, the continuous removal of, for example, ethanol during its production by fermentation (by adsorption processes) would solve the problem of product inhibition which often occurs when the alcohol concentration in solution builds up; ethanol production is most rapid when its concentration in solution is low.

The studies by Milestone et al [11] on alcohol adsorption by ZSM-5 showed how zeolite aluminium and cation content affect alcohol uptake. Methanol and ethanol were adsorbed to a greater extent, at given solution concentration, as the aluminium content increased. The reverse trend was found for butanol. Propanol adsorption varied little with aluminium content. For a given ZSM-5, the amount of alcohol adsorbed was found to decrease as the size of the charge balancing cations increased. The effect was especially marked for Cs^+ forms of the zeolite.

6.2.2 Preliminary experiments

Silicalite-1 crystals, as-synthesised, contain TPA (tetrapropyl-ammonium) ions in their channels. Calcination of the silicalite precursor frees the pores of the organic material and gives an active organophilic sorbent. Upon cooling silicalite crystals to room temperature after calcination, some water and gases from the atmosphere are rapidly adsorbed. The TGA curve in Figure 6.1 shows this. However the bulk of the pore volume remains free because there is no attraction for substantial amounts of water to enter the channels. This is true even at saturated vapour pressures, $P/P_o = 1$ [14].

The adsorption of atmospheric gases at S.T.P., albeit limited and regardless of whether the specific molecules be N_2, O_2 or CO_2, reflects that there are sites within the lattice that can strongly interact with such molecules. As a result of this 'pre-adsorption', the addition of silicalite to aqueous solutions of organic solutes often gives rise to an

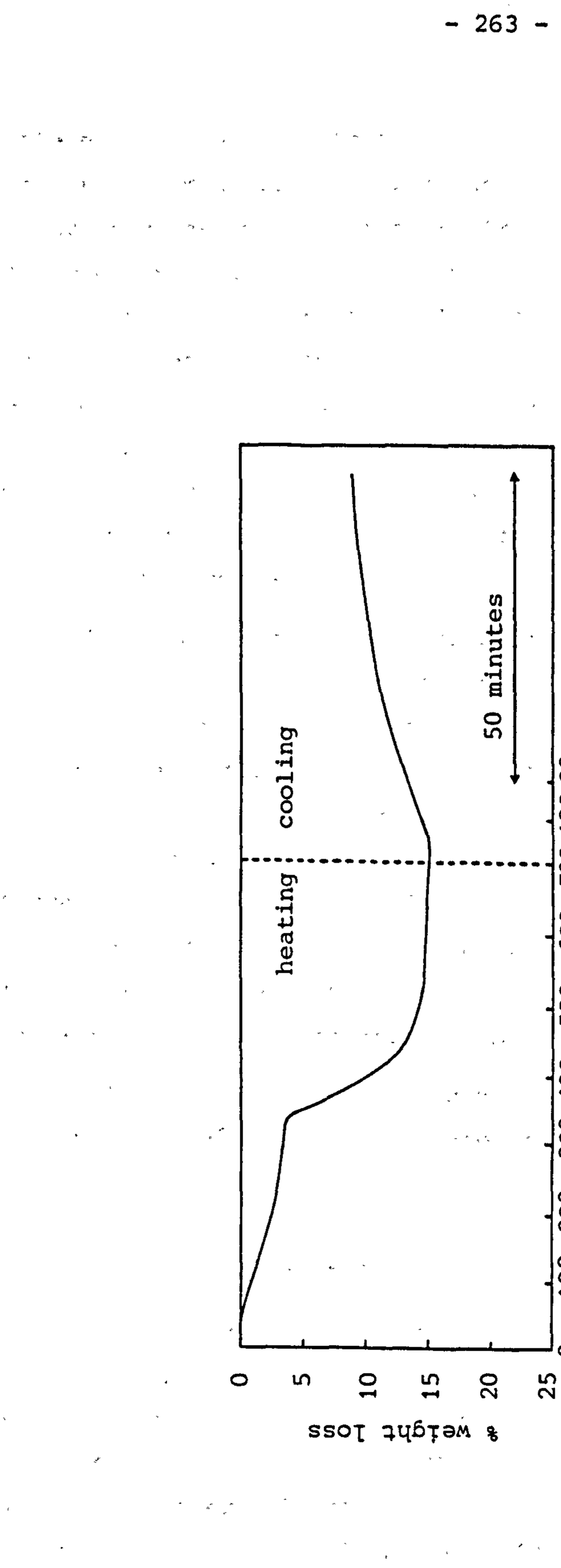

Figure 6.1 TGA curve for TPA-silicalite (sample S10) in flowing air. Weight losses due to water and organic can be seen. At 700°C, heating was stopped and the sample was left to cool down in the stream of 'dry' air. This cooling stage was not programmed. The sample rapidly scavenged water and gases from the flowing atmosphere as can be seen from the weight gain.

interesting visible effect; if extensive and rapid, adsorption of the organic molecules is accompanied by vigorous displacement of the adsorbed gases and a release of air bubbles, an effervescence, is observed. A number of qualitative tests were carried out using this phenomenon as an indicator of adsorption. The results are summarised in Table 6.1. The experiments showed, as expected, that the TPA ions in the channels of the silicalite precursor preclude adsorption and that large molecules can be excluded because of their size (e.g. 2,2-dimethyl-1,3-propanediol). Other experiments showed that where air release was observed, its rapidity could be used to give very qualitative information about adsorption kinetics.

Yet another experiment gave information about how strongly molecules are adsorbed. The addition of silicalite to ∿3 molal propanol solution was found to give 'explosive' release of air due to very rapid adsorption. Within a short time the release of air subsided totally. The solid phase was then isolated by filtration, although not washed in any way, and the filter-cake left in the open laboratory for ∿15 minutes. Subsequent re-immersion in fresh 3 molal propanol solution once again initiated vigorous 'bubbling' indicating not only the 'volatility' of the adsorbed propanol once samples are removed from solution but also the rapidity with which gases from the atmosphere are adsorbed.

All the abovementioned qualitative work preceded the quantitative adsorption experiments. The experimental procedure adopted for the latter is outlined below.

6.2.3 Experimental: Materials, Equipment, Procedure

The silicalite used for the work was crystallised from a reaction mixture of composition $3.5Na_2O$ 2TPABr $20SiO_2$ $1000H_2O$ at 95°C. The product was calcined at 450°C for 48 hours, washed with water, twice treated with 1M NH_4Cl solution at 80°C for 16 hours (10 cm^3 sol'n per gram solid) and then further calcined (450°C, 48 h; 550°C, 12 h). The final material, designated silicalite (S10), was then equilibrated with water vapour (a_w = 0.753, 25°C). Duplicate analysis of the equilibrated sample by TGA showed the solid to contain 2.85% (by weight) volatiles (mostly water).

Table 6.1 Results of qualitative tests showing the release (or not) of adsorbed gases when silicalite samples are added to aqueous solutions of organic solutes. Solution concentrations were ca. 1 molal.

		Adsorbate	Air release
Silicalite (calcined)	+	H_2O (no solute present)	No
	+	propanol	Yes
	+	hexanediol	Yes
	+	sucrose	No
	+	2,2-dimethyl-1,3-propanediol	No
Silicalite (as-synthesised)	+	hexanediol	No

The α-ω alkanediols used in the experiments were ethane-1,2-diol (Fisons, SLR reagent), butane-1,4-diol (Aldrich, 99+%), hexane-1,6-diol (Aldrich, 99%) and octane-1,8-diol (Aldrich, 96%). Glass distilled water was used throughout.

The experimental procedure adopted was as follows. Solutions of the diols of different concentrations were made up in glass conical flasks by adding known weights of solute to known volumes of water. Weighed samples of hydrated silicalite were added to each, the flasks were stoppered and then placed in a Townson and Mercer water bath thermostatted at 25.0 ± 0.1°C. The flasks were mechanically tumbled, using specially designed apparatus, during the equilibrations. Six flasks could be accommodated at any one time. In some cases, the need to use larger volumes of solution (>250 cm^3) required equilibrations to be carried out at the laboratory temperature with agitation being achieved through the use of magnetic stirrers.

Preliminary experiments showed that equilibration was usually complete within 12 hours. Upon attainment of a steady-state, the solid phases were isolated by filtration and carefully washed with small aliquots of cold distilled water - to remove adherent solution but not the sorbed organic. The silicalite samples were then dried, equilibrated with water vapour (a_w = 0.753, 25°C) and analysed by TGA to determine the amount of sorbed organic per unit weight of dry solid. For each experiment the equilibrium concentration of analyte in the solution was determined by difference after calculating the total amount of organic in the solid phase. Transfer of water between the solid and the solution was deemed negligible. The TGA curves showed that the low and high temperature weight losses, due to water and organic respectively, did not significantly overlap and the intracrystalline contents of the samples could be determined without difficulty. This was true even when the organic loading was low.

For some of the isotherm points, equilibrations were carried out using a 'desorption method'. Silicalite samples fully loaded with organic (by adsorption from relatively concentrated aqueous solution) were prepared and characterised by TGA to determine the organic contents. Known weights of loaded silicalite were added to known volumes of water and

equilibration carried out as before. The equilibrium contents of the solid phases and by inference the equilibrium solution phase concentrations were once again determined by TGA.

No systematic variation in the water content of the samples with organic loading was observed for any of the solutes under study. The results in Table 6.2 and Figure 6.2 show that clear relationships were however found between the solution phase concentration and the amount of organic adsorbed. Considering the isotherms collectively it can be seen that as the diol chain length increases the isotherm plateau moves to lower solute concentrations. A similar trend was found for the uptake of monohydric alcohols by silicalite [4].

The estimated maximum number of diol molecules per unit cell was 16.7 for ethane-1,2-diol and 8.1, 7.6 and 4.0 for the three higher diols respectively. The volumes occupied by the ethanediol and butanediol molecules were $\sim$0.16 and 0.12 cm^3g^{-1}. This compares with the crystallographic void volume of $\sim$0.19 cm^3g^{-1}.

Whilst the aforementioned adsorption experiments yielded interesting results, the work constituted 'preliminary' studies in a subject area that was originally planned to be a considerable part of the research programme as a whole. The work, as it turns out only a small fraction of the total work presented in this thesis, did however take a disproportionately long time to carry out. The cause was not experimental difficulties, it was simply that other findings and observations, many of which were 'unexpected' and brough to light whilst the sorption work was in progress, warranted more immediate investigation. The problems at hand related to the silicalite crystals - they were not as 'simple' solids as originally thought.

One final point is worth mentioning before some of the 'problems' encountered are discussed. Although silicalite does adsorb organic molecules from dilute aqueous solutions, practical applications in this area may be limited on account of 'poisoning' - selective adsorption of undesirable solutes. Similarly, adsorption results like those described above ideally require very pure solutes if the possibility of preferential adsorption of impurities is to be completely ruled out. The 'preliminary' nature of the experiments with the.

Table 6.2 Alkanediol adsorption from aqueous solution by silicalite[a,b]

n = 2		n = 4		n = 6		n = 8	
m	U_s	$10^2 m$	U_s	$10^4 m$	U_s	$10^6 m^c$	U_s
0.046	0.011	0.042	0.014	1.25	0.014	2.1	0.098
0.074	0.010	0.153	0.012	1.28	0.019	2.7	0.096
0.162	0.011	0.255	0.016	1.52	0.031	4.2	0.096
0.450	0.014	0.868	0.011	1.56	0.023		
1.049	0.067	1.44	0.025	1.58	0.063		
1.472	0.160	2.34	0.015	1.61	0.057		
1.494	0.086	2.40	0.013	1.64	0.047		
2.893	0.180	2.90	0.024	1.72	0.068		
		3.35	0.042	1.78	0.065		
		3.59	0.043	1.83	0.090		
		3.86	0.117	1.84	0.048		
		5.16	0.128	1.85	0.128		
		6.70	0.122	1.91	0.109		
		1.94	0.097				
		2.23	0.145				
		2.17	0.134				
		4.48	0.143				
		14.3	0.148				

[a] n = number of C atoms in α-ω diol, HO-$(CH_2)_n$-OH; m = equilibrium solution concentration (mol kg^{-1}); U_s = weight adsorbed diol/weight anhydrous silicalite.

[b] Data for the diols with n = 2, 4 and 8 refers to adsorption by silicalite sample S10. For n = 6, the first sorbate studied, silicalite (S2) was used. Samples S2 and S10 were crystallised from identical reaction mixtures under the same reaction conditions and were treated in the same way prior to carrying out the sorption work. Differences between the two solids (and hence differences in their sorption properties) were probably small.

[c] The calculated amounts of diol in solution at equilibrium were so small that they could not be accurately quantified. The concentration values probably hence have very considerable error.

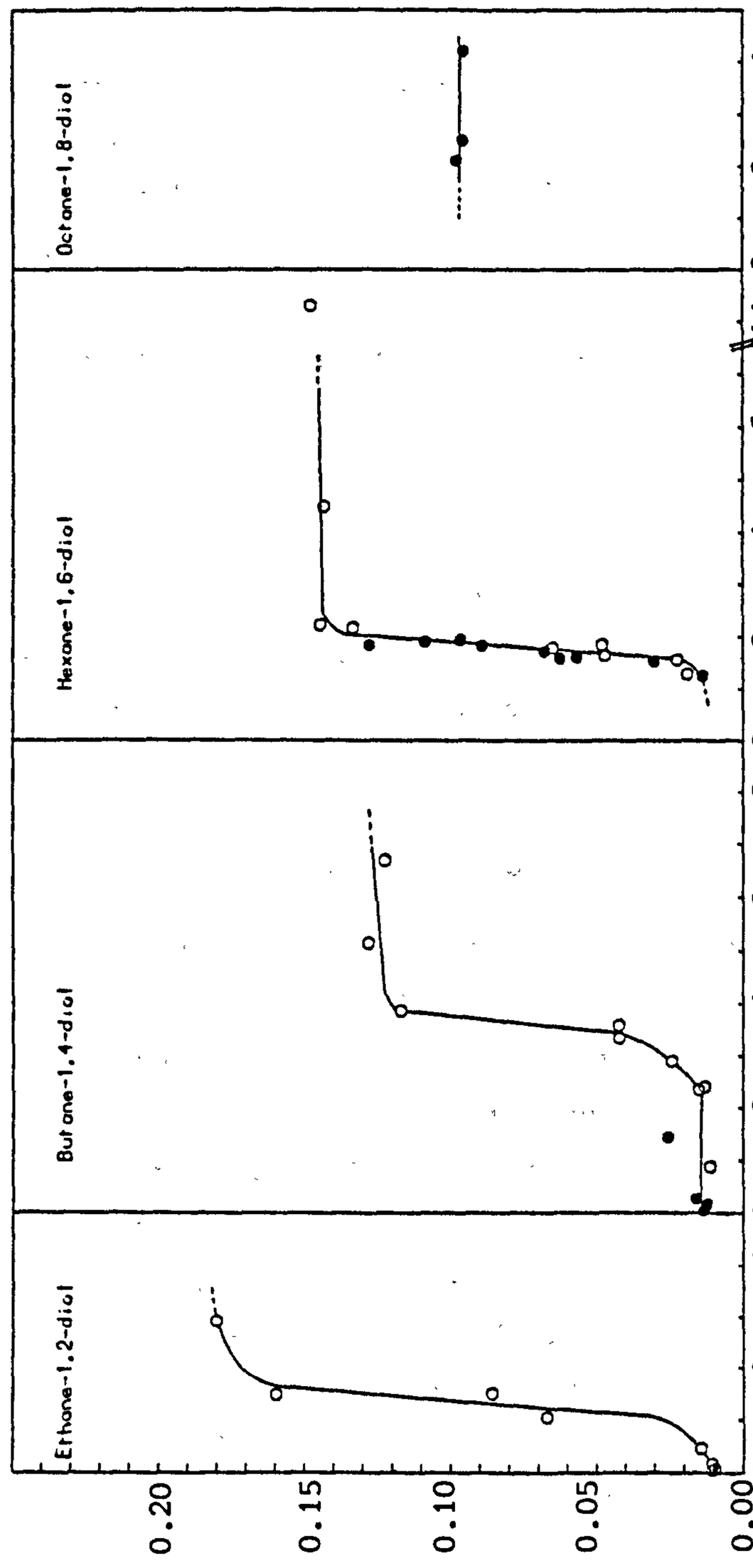

Figure 6.2 Adsorption isotherms for the uptake of α-ω alkanediols from aqueous solution by silicalite-1. The open and filled symbols represent data obtained by adsorption and desorption methods respectively. The data is shown in Table 6.2 (N.B. footnote b).

alkanediols did not warrant special solute purity and no evidence of impurity adsorption is believed to be indicated by the results. Problems with impurity adsorption are most likely to give spurious data when the equilibrium concentration of organic in solution is relatively large.

Although the purity of the organic solutes was not of too much concern, the same could not be said of the silicalite solids. Indeed it was about the 'impurity' of the silicalite sorbents that knowledge was sought.

6.3 Chemical composition of silicalite-1: Some related properties

Ideally, crystals of silicalite-1 should compositionally be 100% SiO_2. However, when the silicalite precursor is synthesised from reaction mixtures that contain alkali metal ions (quite often the reaction alkalinity is supplied by NaOH), metal ions are incorporated into products during the crystallisation process. This topic has been discussed at length in Chapter 3 and it is salient to point out that the work in that chapter was carried out with the specific aim of learning more about the chemistries of the silicalite products. It was seen as a pre-requisite to further study of silicalite's post-synthesis properties.

The alkali metal ion content of silicalite products is usually far greater than the levels of tetrahedral impurity atoms found (see Table 3.4, Chapter 3). It appears that alkali metal incorporation is dependent on (a) the amount of alkali metal present in reaction mixtures and (b) the reaction pH. Chapter 3 has discussed this point in detail. In the aforementioned chapter crystallisation of silicalite in the xNa_2O 2TPABr $20SiO_2$ $1000H_2O$ system at 95°C was investigated. Nine reaction mixtures were crystallised with x (the reaction alkalinity) ranging from 0.25 to 6.5. The products from these reactions (S1 to S9 respectively) provided interesting materials for further study because they differed considerably in composition.

Thermal gravimetric analysis of as-synthesised products S1 to S9 showed that all except product S1 (which was not fully crystalline) contained close to four TPAOH molecules per unit cell. In contrast, the amount of alkali metal in the materials differed considerably; product S1

contained least, product S9 most (see Table 3.4, Figures 3.12 and 3.13). Prior to calcination, the metal ions are confined by the TPA ions but like the organic they are empirically present in the silicalite precursor as base molecules (this was discussed in section 3.3.7.2). During calcination all this inorganic base is likely to be lattice bound ($\equiv Si\text{-}O^{-}Na^{+}$ HO-Si$\equiv$). Sites such as this render the materials 'defective' and also, to a certain extent, hydrophilic; some intracrystalline hydroxyl groups (hydrophilic centres) probably arise from removal of the organic (see equation (3.2)) but the presence of sites related to the inorganic base, if substantial in number, must inherently increase the hydrophilic nature of the solid. Also, it renders the materials silicates as opposed to silicas.

It became evident from early work that the presence of inorganic base in the silicalite lattice increased the amount of water subsequently sorbed (at controlled P/P_o). The water contents of products S1-S9 after calcination (Δ450°C, 24h; Δ550°C, 24 h) are shown in Figure 6.3. These values were determined from TGA curves and actually represent total volatile content; although some of this may be attributable to sorbed gases, most is believed to be water. Information available in the patent literature substantiated this general trend; the data in Figure 6.4 shows a clear relationship between product sodium content and equilibrium water uptake. These sorption results were obtained after outgassing the calcined materials at elevated temperatures and were hence not complicated by adsorption of gases.

Whilst the results in Figures 6.3 and 6.4 showed 'expected' trends (in that water was expected to be attracted to hydrophilic charged centres) it became apparent from a number of further experiments that interpretation of such water sorption data should be made with caution.

Consider a sample of a silicalite precursor that contains incorporated sodium and which has been equilibrated with water vapour. The sodium ions will be largely coordinated to the lattice through the equilibrium:

$$\equiv Si\text{-}O\text{-}Si\equiv \; + \; NaOH \rightleftharpoons \equiv Si\text{-}O^{-}Na^{+}\; HO\text{-}Si\equiv$$

Prior to calcination, all 'free' sodium hydroxide is sterically confined by the TPA template but this is not so after removal of the organic.

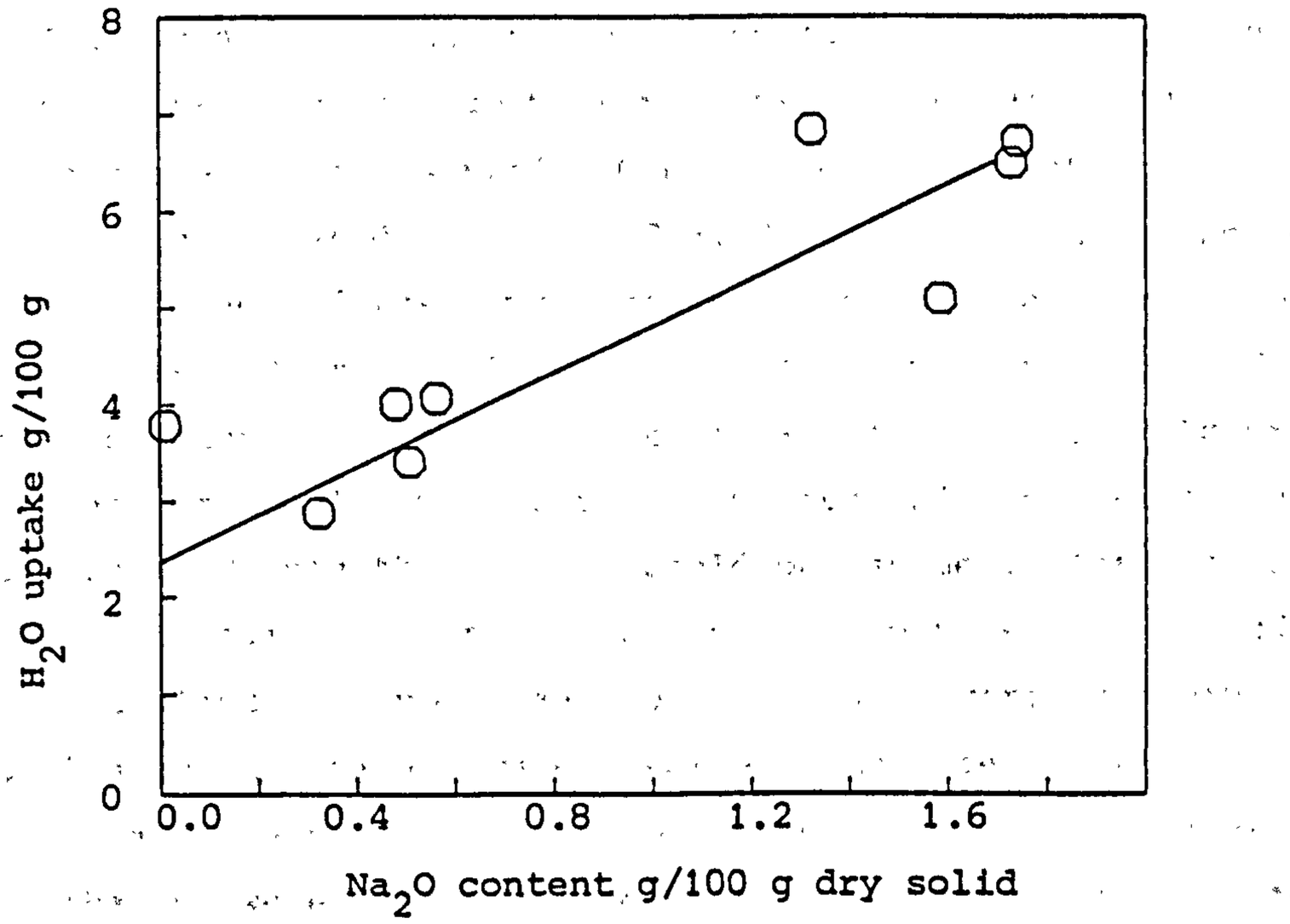

Figure 6.3 Water uptake by products S1-S9 as a function of their sodium content. The materials were calcined and equilibrated in an evacuated dessicator in a water bath at 25°C. Saturated sodium chloride was used to provide the vapour pressure control (P/P_o = 0.753). The special apparatus used for these experiments (the isopiestic apparatus) is described in Chapter 8. The water uptakes were determined by thermal gravimetric analysis.

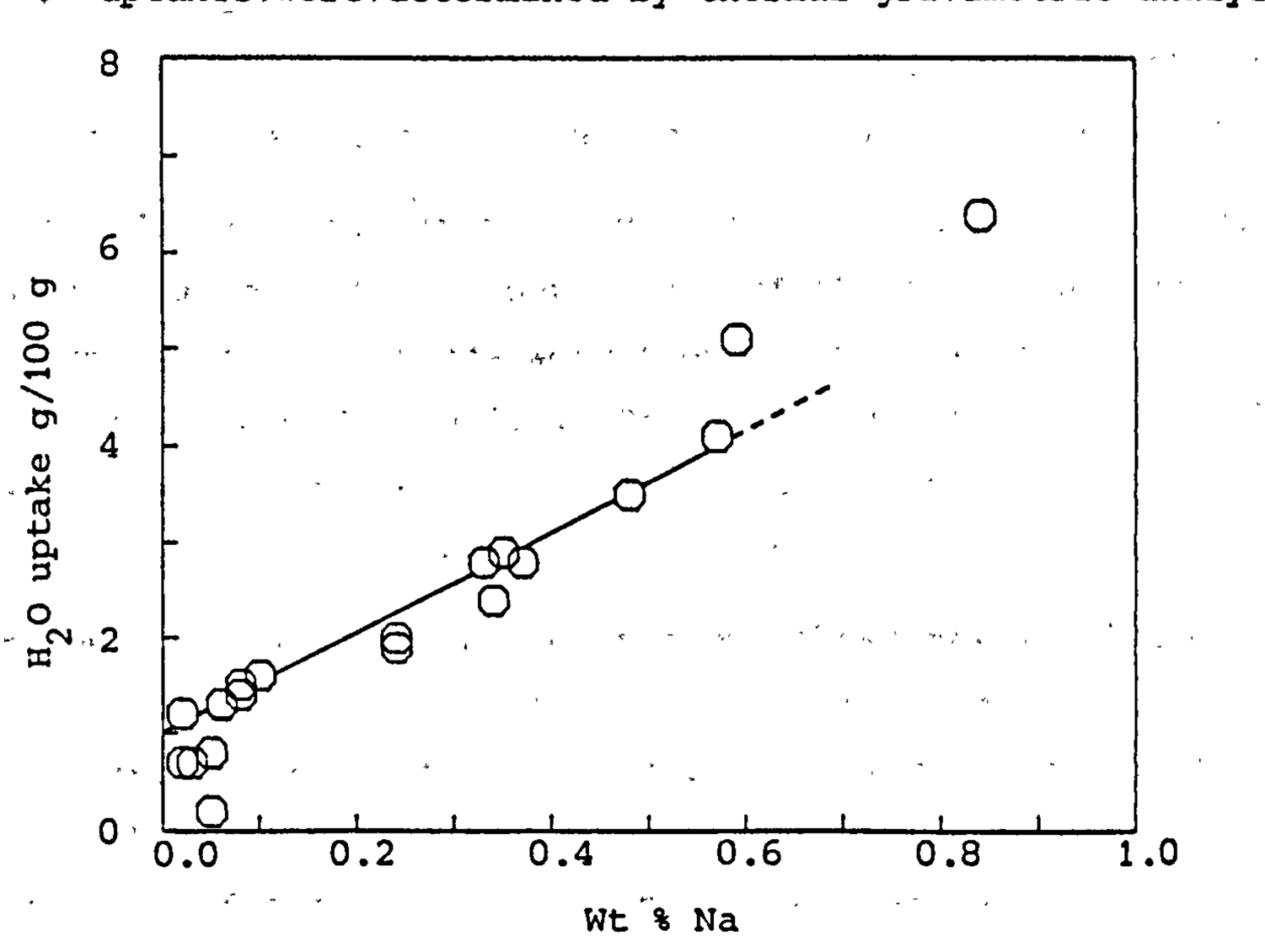

Figure 6.4 Water adsorption by silicalite at $P/P_o \approx 0.5$ as a function of crystal sodium content. The data is taken from the literature [15].

On adding small amounts of sodium containing silicalite (calcined, hydrated) to water, some sodium hydroxide readily enters solution; rapid pH rises are often observed. Controlled tests with products S1-S9 (calcined and equilibrated at a_w = 0.753, 25°C) gave interesting results. Small amounts of each of these products and each of their precursors were added to aliquots (∿8 cm^3 in glass bottles (∿12 cm^3 capacity)) of a dilute aqueous solution of thymol blue acid-base indicator. Adsorption of the indicator molecules was precluded because of their size and the solutions were so dilute that a_w = 1 could be assumed. After addition of the silicalite samples to the solutions the bottles were sealed with air-tight plastic stoppers and colour changes were monitored. Yellow to blue colour changes were observed immediately for the calcined samples that had an appreciable sodium content (S3-S9). The kinetics of the colour changes were reasonably consistent with the sodium contents of the materials. Product S1, the product with lowest sodium content, caused no colour change and for product S2 the change was only slight. The colour changes (thymol blue indicator range 8.0-9.6) were caused by emanation of sodium hydroxide molecules from the pores of the molecular sieves. The solutions containing the silicalite precursors all stayed yellow showing that in no instances were the observed effects due to entrained base - base accidently left on the crystals after synthesis.

The solids were left in the thymol blue solutions for 24 hours during which time no change in the colour of any of the solutions was detected. The pH of some of the solutions were then measured with the results shown in Table 6.3 and Figure 6.5. Based on rough calculations these pH values indicated that only a small fraction of the total sodium present in the products had entered solution.

Perhaps the most striking point about these tests was the rapidity of the colour changes when sodium rich silicalite samples were initially added to the indicator solutions; the changes were instantaneous. It was as if the base molecules were not just diffusing out of the pores, it was almost as if some of the base molecules were actually associated with the external surfaces of the crystals (which would account for the rapidity of the changes). Although only a hypothesis at the time, it was one which several earlier observations (which will be pointed out later) had tentatively suggested. To test this hypothesis several experiments were carried out and these are discussed below.

Table 6.3 Experiments with thymol blue indicator[a]

(Indicator pH range: 8.0-9.6)

Product[b]	Colour after adding sample[c]	Colour after 24 hours[d]	pH after 24 hours	Na^+/UC[e]
S1	Y	Y	8.06	0.02
S2	Y	Y/B	8.75	0.60
S3	B	B	9.54	1.05
S4	B	B	9.42	0.95
S5	B	B	9.62	0.89
S6	B	B	9.36	2.50
S7	B	B	9.61	3.29
S8	B	B	9.48	3.00
S9	B	B	9.42	3.31

[a] A concentrated stock solution of thymol blue was prepared by adding 0.0585 g solid indicator to 100 cm^3 water. A further solution was prepared by adding ∿20 drops of the stock to 100 cm^3 water. Aliquots of this solution were used for the experiments (∿8 cm^3).

[b] Samples were calcined (Δ450°C, 24 h; Δ550°C, 24 h) and hydrated (25°C, a_w = 0.753) before use.

[c] The initial solutions were all pale yellow (Y). A positive colour change (i.e. to blue (B)) indicates development of some blue colouration immediately after the crystals were added. In some cases (S5-S9) the colour changes were almost instantaneous.

[d] The bottles containing the solutions were stoppered during this time. No colour changes were seen after a further 6 days storage.

[e] Number of sodium ions per unit cell as determined by XRF analysis (see Table 3.4 for more details).

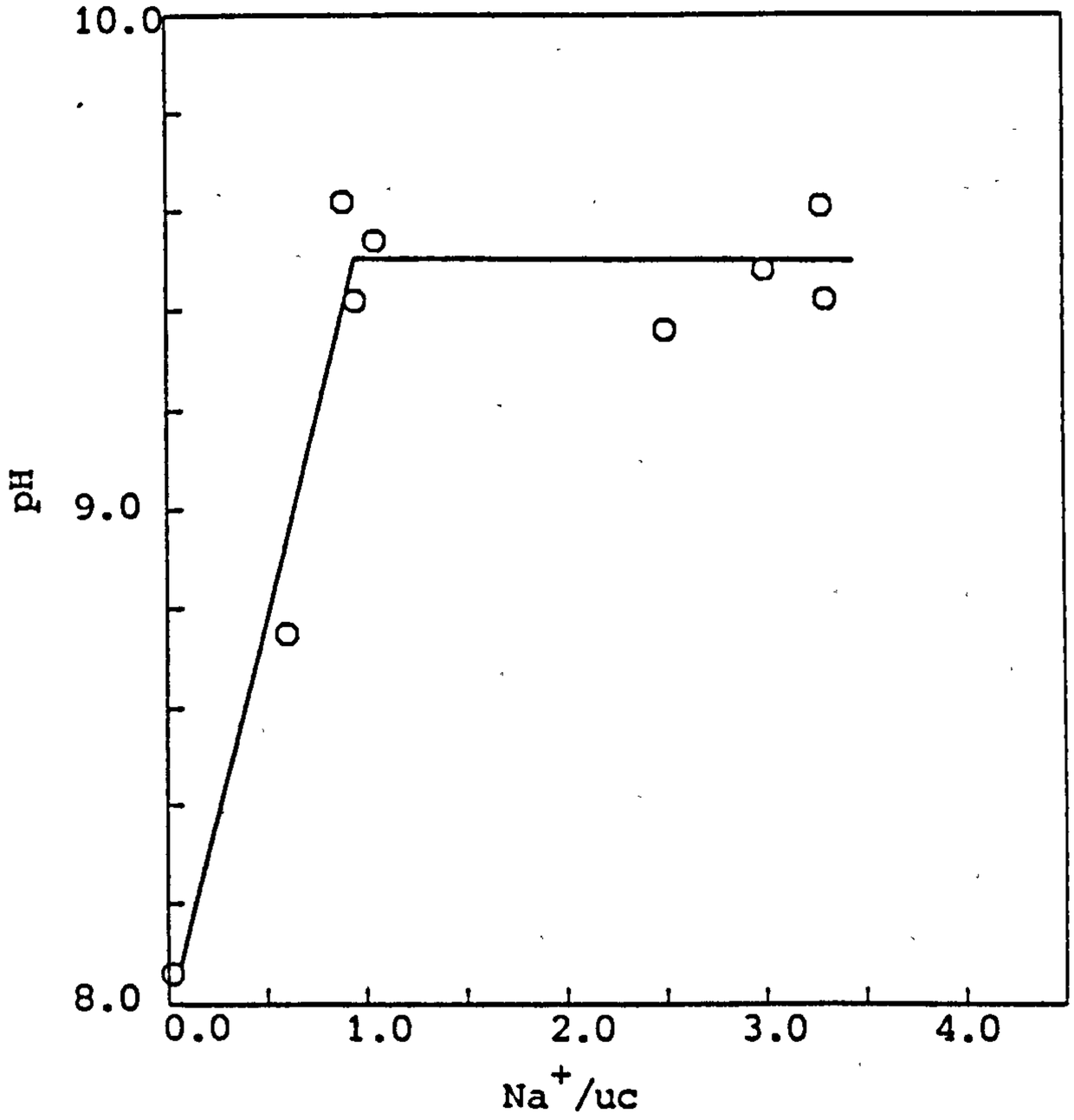

Figure 6.5 Relationship between the sodium content of silicalite products S1-S9 and the observed pH rise when small amounts of the calcined solids are put in water. These measurements were made in conjunction with the thymol blue indicator tests (see Table 6.3).

The first experiment involved thymol blue tests procedurally identical to those described above but using, instead of water, saturated sucrose solutions in which to disperse the indicator molecules. Sucrose solutions were used because sucrose is a non-electrolyte and is also too large to be sorbed. The addition of sodium rich silicalite (calcined and equilibrated at a_w = 0.753) to these initially faint yellow solutions produced slow but very observable colour changes; a blue haze developed around the crystals at the bottom of the small glass bottles. After some time the solutions had become quite blue - tests showed that vigorous shaking expedited these changes. The kinetics of the colour changes were probably adverse because of the extremely viscous nature of the sucrose solutions. The fact that colour changes were observed though has important thermodynamic implications; it shows that at the water activity of saturated sucrose solution and at the temperature of the experiment (the saturated solution was made up in a flask in a 25°C water bath, $a_w \approx 0.85$) sodium hydroxide molecules can emanate from the pores of sieve. It follows that if a sample of the silicalite is equilibrated with water vapour at $P/P_o \approx 0.85$ (the water activity of saturated sucrose solution) some sodium hydroxide must come to the external surfaces of the crystals. Thus simply exposing calcined silicalite samples to water vapour atmospheres can cause some relocation of their sodium contents from intracrystalline to extracrystalline. The samples used for the above thymol blue experiments were equilibrated at a_w = 0.753 beforehand and almost certainly this preparative step caused some relocation before the experiments were carried out (see below). Nevertheless, the implications of the experiments are not altered by this.

Although very simple in nature, the thymol blue tests were very revealing. Similar experiments with aqueous phenolphthalein solutions gave consistent results. With the latter, colour changes (clear to pink) are particularly easy to detect.

A number of 'solid phase' indicator tests were also carried out as a means of detecting 'surface base' associated with silicalite crystals. The silicalite samples used for these experiments were sodium rich products which had been calcined and equilibrated with

water vapour (a_w = 0.753, 25°C) and similarly equilibrated samples of their organic containing precursors. Grinding samples of the sieves with solid phenolphthalein crystals (white) caused immediate development of a pink colouration in the case of the calcined materials but no such change for the precursors. Further grinding of the former mixture intensified the colouration. These results are consistent with the presence of sodium hydroxide on the external surfaces of the calcined crystals. These molecules must have emanated from the pores during the preparative vapour phase equilibration; proof that at a_w = 0.753 (P/P_o) relocation of the sodium hydroxide is possible.

The indicator tests described above, both the solution and solid phase experiments, have been purposefully discussed without reference to specific silicalite samples. The various tests were carried out with a number of different samples so giving added weight to the conclusions drawn.

The relocation effects discussed above are complicated by a number of further factors. Sodium hydroxide molecules on the external surfaces of crystals may, like those that are intracrystalline, be co-ordinated to the silica surface or 'free'. An equilibrium is set up. The hygroscopic nature of sodium hydroxide will result in the rapid formation of a solution on the external crystal surfaces. The water activity and hence concentration of that solution will change until it is isopiestic (of equal vapour pressure) with the surrounding atmosphere. The amount of solution formed will depend on the number of base molecules that are free. The presence of a solution phase gives rise to spurious water adsorption data as it increases the total measured water uptake considerably. The validity of the water adsorption data given in some patents may be anomalous because of this effect. This is also true of the results in Figure 6.3.

Sodium rich silicalite samples often show orthorhombic symmetry after calcination as opposed to the monoclinic symmetry shown by their sodium free counterparts [16]. The work by Wu et al [16], along with experiments in this laboratory, has shown that simply leaving calcined samples of sodium rich silicalite open to the atmosphere can cause conversion to monoclinic symmetry. The explanation given [16] was

that "water had presumably caused relocation of the residual sodium species which enabled the framework structure to undergo a symmetry change". The nature of that relocation was not discussed and it may well be that the effect relates to the egress of at least a part of the lattice sodium (which constitutes the 'lattice loading') to the external surfaces of the crystals.

Also evident in the work of Wu et al [16] was a marked decrease in the diffraction line intensities after exposure of the sodium rich sample to the atmosphere (c.f. diffraction intensities immediately after sample calcination). Similar observations have been made in this laboratory on a number of occasions; treatments to remove the sodium from sodium rich samples invariably increase the diffraction line intensities. It is believed that the presence of external sodium in a solution on the untreated samples may be the cause of the observed intensity lowering.

Much has been said about relocation effects but there is still much to be learned. What proportion of the total sodium can egress from the pores and how is this affected by the total sodium content of the sample and conditions under which the material was crystallised? How important is the presence of water vapour in the relocation process? These are just some of the questions that remain unanswered.

Although organic molecules play an important role during the crystallisation of high silica zeolitic materials, inorganic entities such as bases and salts probably provide contributory stabilising effects in some cases. Post-calcination egress of such species (and/or similar species which become simply physically entrapped during synthesis) may be a far commoner occurrence than is realised. Indeed no reference to this possibility has been made till now. Zeolites that are crystallised in the absence of organics may also be stabilised by inorganic entities during synthesis but in many cases their removal is facile during product isolation/washing procedures and their 'effective' incorporation goes unnoticed. The situation is clearly different when inorganic species are physically entrapped by organic entities because not until after calcination is movement/removal possible.

A hypothetical example puts the concept in a rather different way. Suppose that a large amount of sodium chloride became entrapped (by organic species) in a silica molecular sieve during synthesis. After calcination much of the salt would want to egress from the hydrophobic pores - unless the material had a strong affinity for salt and this is unlikely for a silica sieve at ordinary temperatures (see Chapter 8). In practice, the salt molecules would probably move to the external surfaces of the crystals and, if the atmospheric vapour pressure was greater than that of saturated sodium chloride solution, the deposited salt would dissolve and form a solution isopiestic with the surrounding atmosphere. An equilibrium would be established between salt in the solution and salt in the pores. Whilst this example is only hypothetical it bears some analogy to the silicalite/NaOH case. Although sodium chloride under most conditions would not attack a silica framework, the opposite is true of NaOH and this fact makes the 'real' silicalite example more complex.

The vulnerability of the silicalite framework to attack by its own in situ base was investigated by a set of controlled experiments carried out as follows. Two silicalite samples, one with a low sodium content (sample S17) and the other with a high sodium content (sample S13) were crystallised, isolated from their mother liquors in the usual manner, calcined and hydrated. Both were then subjected to low temperature calcination/hydration cycles. The initial calcination frees the pores of organic material, the initial hydration causes egress of a portion of the incorporated sodium hydroxide molecules. The theory behind the subsequent calcination/hydration cycles was simple. It was envisaged that the calcination step would cause any free sodium hydroxide (in solution) to attack the framework whilst the subsequent hydration stage would set up once again a solution phase equilibrium:

$$\equiv Si\text{-}O\text{-}Si\equiv \; + \; NaOH(aq) \overset{\Delta}{\underset{+H_2O}{\rightleftharpoons}} \equiv Si\text{-}O^{-}Na^{+}\; HO\text{-}Si\equiv$$

However the situation is more complicated than this because co-ordinated cations can hydrolyse during the hydration step:

$$\equiv Si\text{-}O^{-}Na^{+}\; HO\text{-}Si\equiv \; + \; H_2O \rightleftharpoons \equiv Si\text{-}OH\; HO\text{-}Si\equiv \; + \; NaOH$$

Attack by base during the subsequent calcination stage at the same defect site would have no adverse effects. In contrast, attack at neighbouring sites would be detrimental; the low temperature calcination stage would probably not anneal the hydroxyl group 'defect' and materials with increased numbers of hydroxyl groups would result. The argument is equally relevant to internal attack by base. The chief aim of these experiments was thus to show that low temperature calcination/hydration cycles can cause considerable lattice damage and crystallinity loss.

Materials

The two silicalite samples used in the experiments were prepared as follows. The low sodium product, S17, was crystallised from a reaction mixture of composition $0.5Na_2O$ 2TPABr $20SiO_2$ $1000H_2O$ at 150°C. A mixture with molar stoichiometry $3.5Na_2O$ 2TPABr $20SiO_2$ $1000H_2O$ was used to make the high sodium product (S13). This reaction was carried out at 95°C. Both materials were carefully washed after synthesis and scanning electron microscopy showed both were free of amorphous material. X-ray fluorescence analysis showed sample S13 contained 1.75 Na atoms per unit cell. The amount of sodium in sample S17 was so low that it could not be quantified by the technique.

Procedure

The silicalite precursors were initially calcined in air at 550°C for 24 hours and thereafter were equilibrated with water vapour. Samples of both were then subjected to 21 calcination/hydration cycles. For the first nine cycles, the samples were first of all calcined at 450°C for 24 hours and then hydrated for 24 hours (25°C, a_w = 0.753, vapour pressure control by saturated sodium chloride solution). The latter 15 cycles were shorter. The calcination and hydration conditions were the same but timewise both were reduced to 1 hour duration. Intermittently, usually after every three cycles, samples were analysed by X-ray powder diffraction. The three most intense peaks in the silicalite diffraction pattern, those at ∿8.0°, 8.9° and 23.1° 2θ were monitored. As controls, samples of the same materials which had been hydrated but not subjected to the cycles were also analysed. The XRD work thus involved analysis of four samples.

For each, counts were accumulated for 10 seconds at 0.01° 2θ intervals around the three main diffraction line maxima. The crystallinities of the treated samples were calculated by count summation methods at the line maxima relative to the controls.

Results and Discussion

A selection of the diffraction results are shown in line diagram form in Figure 6.6. The principal features shown by the results are listed below:

(1) The crystallinity of the high sodium sample (S13) decreases considerably with the number of calcination/hydration cycles.

(2) The crystallinity of the low sodium sample (S17) is little affected by the treatments although substantial alterations in certain peak intensities were observed. In particular a decrease in intensity of the peak at ∿8.0° 2θ is accompanied by an increase in the intensity of the peak at ∿8.9° 2θ and vice-versa. These changes somewhat complicated the results analysis and are believed to be caused by crystal fracture and/or orientation effects - this point will be returned to later.

Changes in the crystallinities of the two samples were calculated relative to untreated samples by summing the counts at the three line maxima. The results are shown in Figure 6.7. The high sodium sample loses crystallinity as the number of calcination/hydration cycles increases. Visible evidence of this was seen in SEM micrographs (Figure 6.8). The treated sample of S13 differed considerably in appearance from its untreated counterpart; the crystals appeared to be 'welded' together. The exact role played by the extracrystalline base in this welding process is unclear. Such extensive crystal degradation and intercrystal silanol group condensation can only have occurred by the action of aqueous alkali, i.e. an external solution phase. The micrograph of the treated sample of the low sodium product (S17) shown in Figure 6.8 suggested, in agreement with the XRD results, little if any crystal degradation. Although the results leave no doubt that repeat calcination/hydration cycles can cause considerable damage to sodium rich silicalite samples, it is interesting to note that comparison of micrographs (a) and (b) in Figure 6.8 suggests that some damage occurs during the initial 'organic-removing' calcination of the silicalite precursor.

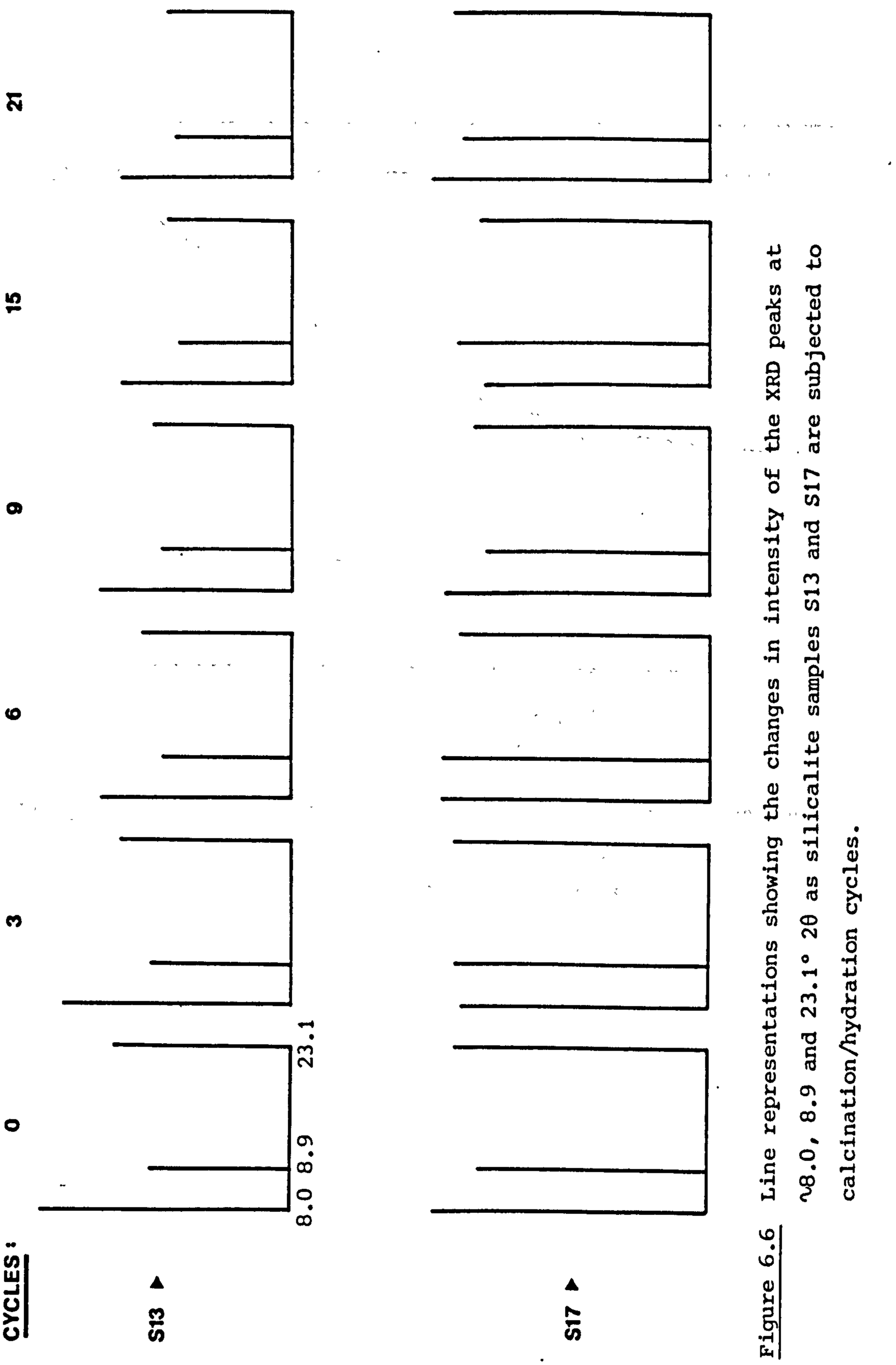

Figure 6.6 Line representations showing the changes in intensity of the XRD peaks at ~8.0, 8.9 and 23.1° 2θ as silicalite samples S13 and S17 are subjected to calcination/hydration cycles.

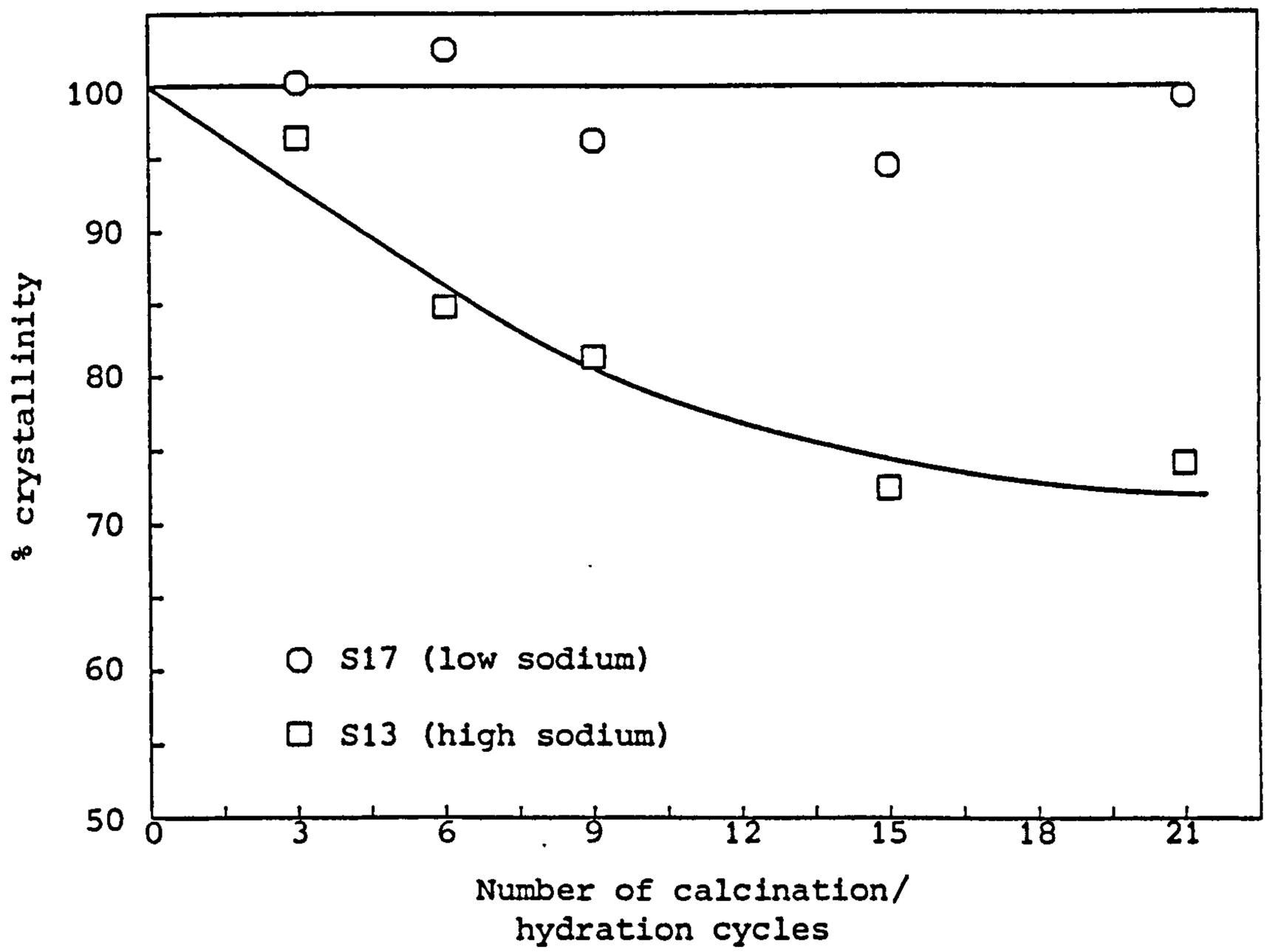

Figure 6.7 The effect of calcination/hydration cycles on the crystallinities of low and high sodium silicalite samples. See text for full details.

Figure 6.8 (overleaf)

Scanning electron micrographs of silicalite crystals:

(a) S13 (as-synthesised)

(b) S13 (after calcination to remove the TPA template)

(c) S13 (after 21 calcination/hydration cycles)

(d) S17 (after 21 calcination/hydration cycles)

FIG. 6.8

a

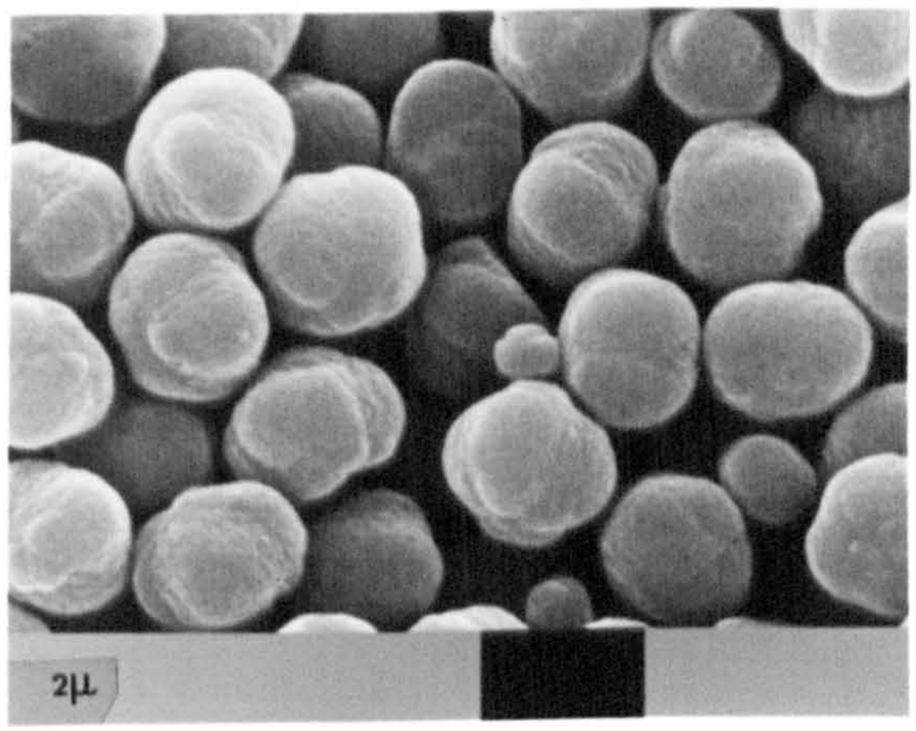

b

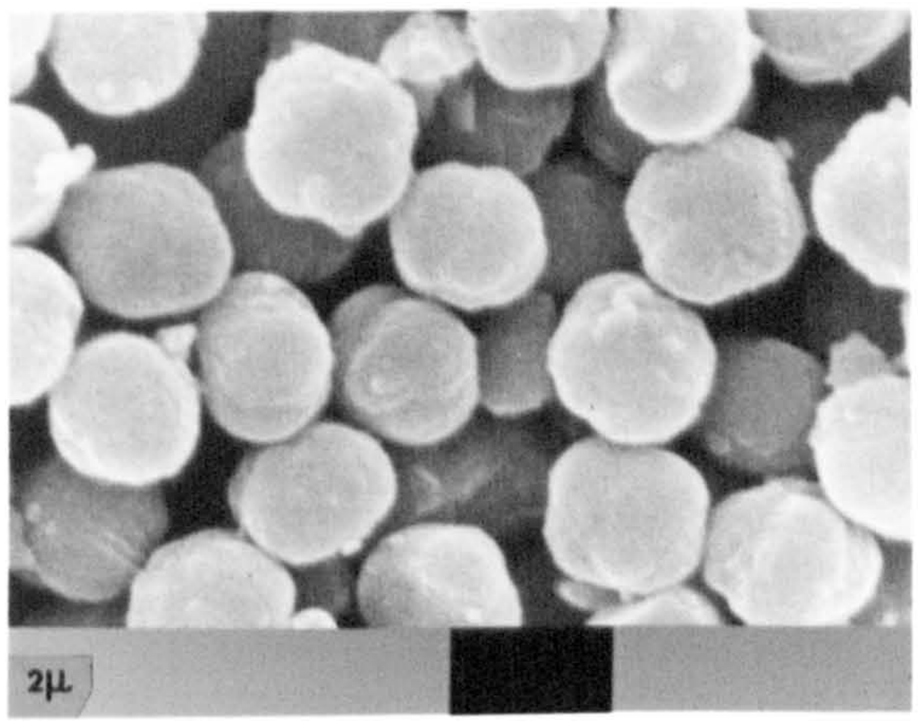

C

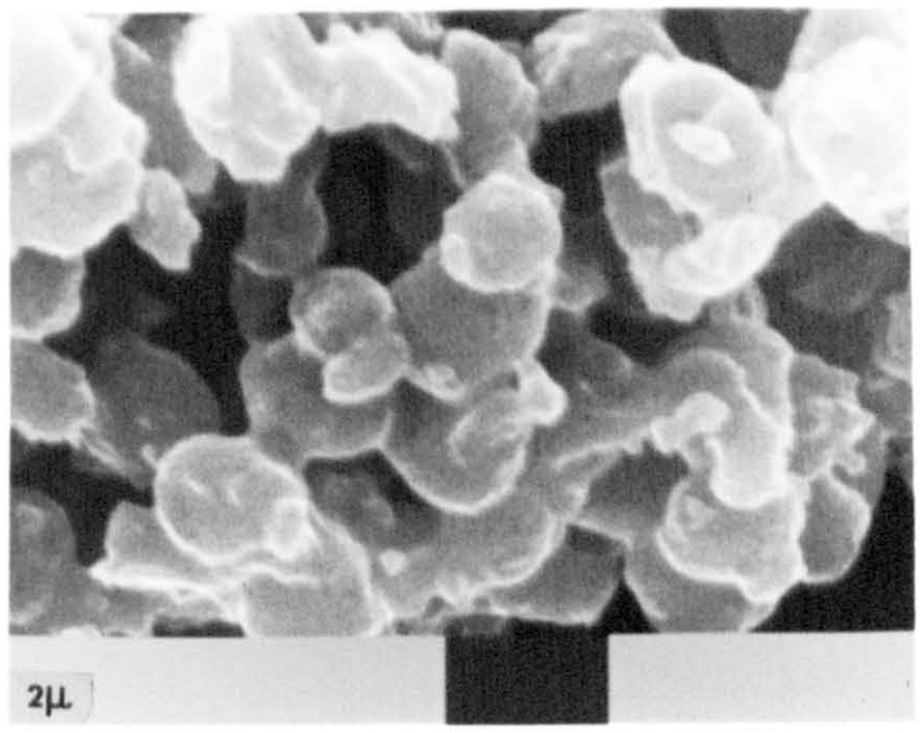

d

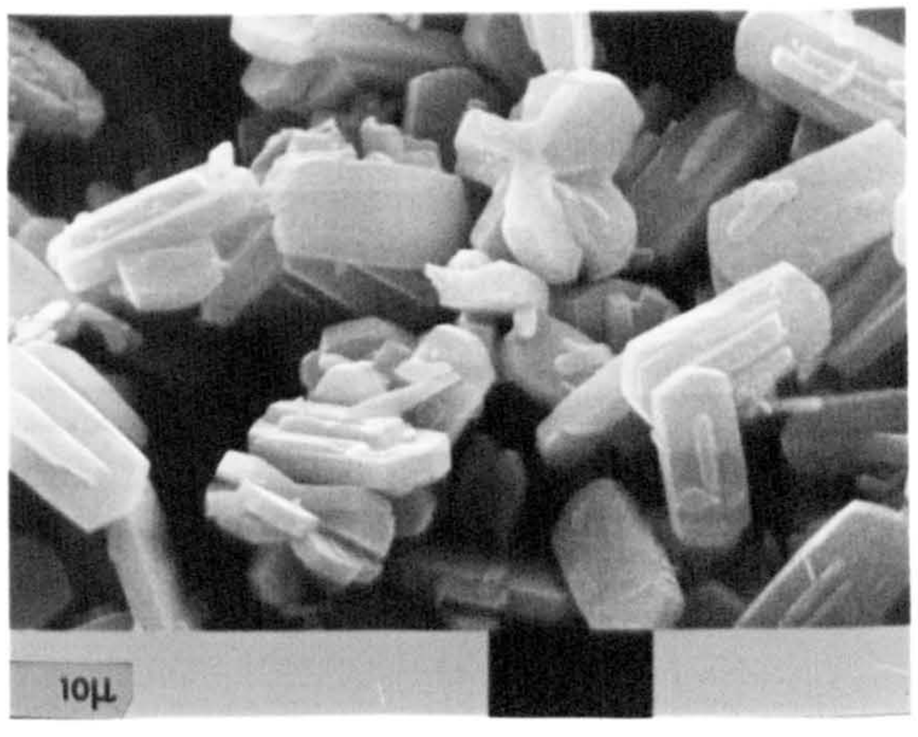

An important question to ask concerns the effect of incorporated sodium on the adsorption properties of silicalite products. Some of the preliminary sorption studies carried out in connection with the alkanediol work showed that silicalite samples with different chemistries did behave differently. In particular the work showed that TGA curves of samples containing sorbed organics differed in form depending on what treatments to remove incorporated metal ions had been employed. Milestone et al [4] have observed that silicalite's sorption properties vary from batch to batch and the data from the literature shown in Figure 6.9 also indicates that silicalite samples do behave differently.

In some instances the presence of alkali metal ions in silicalite may be desirable. Their presence suggests there should be exchange sites. In other cases, silicalite products free of metal ions are likely to be preferable. This can be achieved by direct crystallisation methods (as discussed in Chapter 4) or by post-synthesis treatment of the alkali metal containing materials.

Means of removing incorporated alkali metal ions by acid and salt treatments have been discussed earlier (see section 3.3.7.2). The removal treatments using NH_4Cl solutions (1M) that were employed in the preparation of the silicalite products for sorption studies were only partly successful. For example, the NH_4Cl treated product S10 used in the alkanediol work still contained 0.27 wt% Na_2O. Most of the inconsistencies encountered early on in that study are, in hindsight, believed to have been caused by the different chemistries of the silicalite products.

Whenever silicalite samples are treated with aqueous solutions the problem of crystal dissolution should be borne in mind. One experiment highlighted the problem; crystals of calcined silicalite (S13) were stirred in water ($\sim$10 ml g^{-1} silicalite) at 80°C for 48 hours. During that time emanation of base (NaOH) from the pores caused extensive framework attack. Examination of the crystals under a scanning electron microscope showed they had become considerably pitted (XRD confirmed loss of crystallinity) as a result of the contact with the alkaline solution (Figure 6.10). The parent material had no such etched appearance as can be seen from Figure 6.8(b).

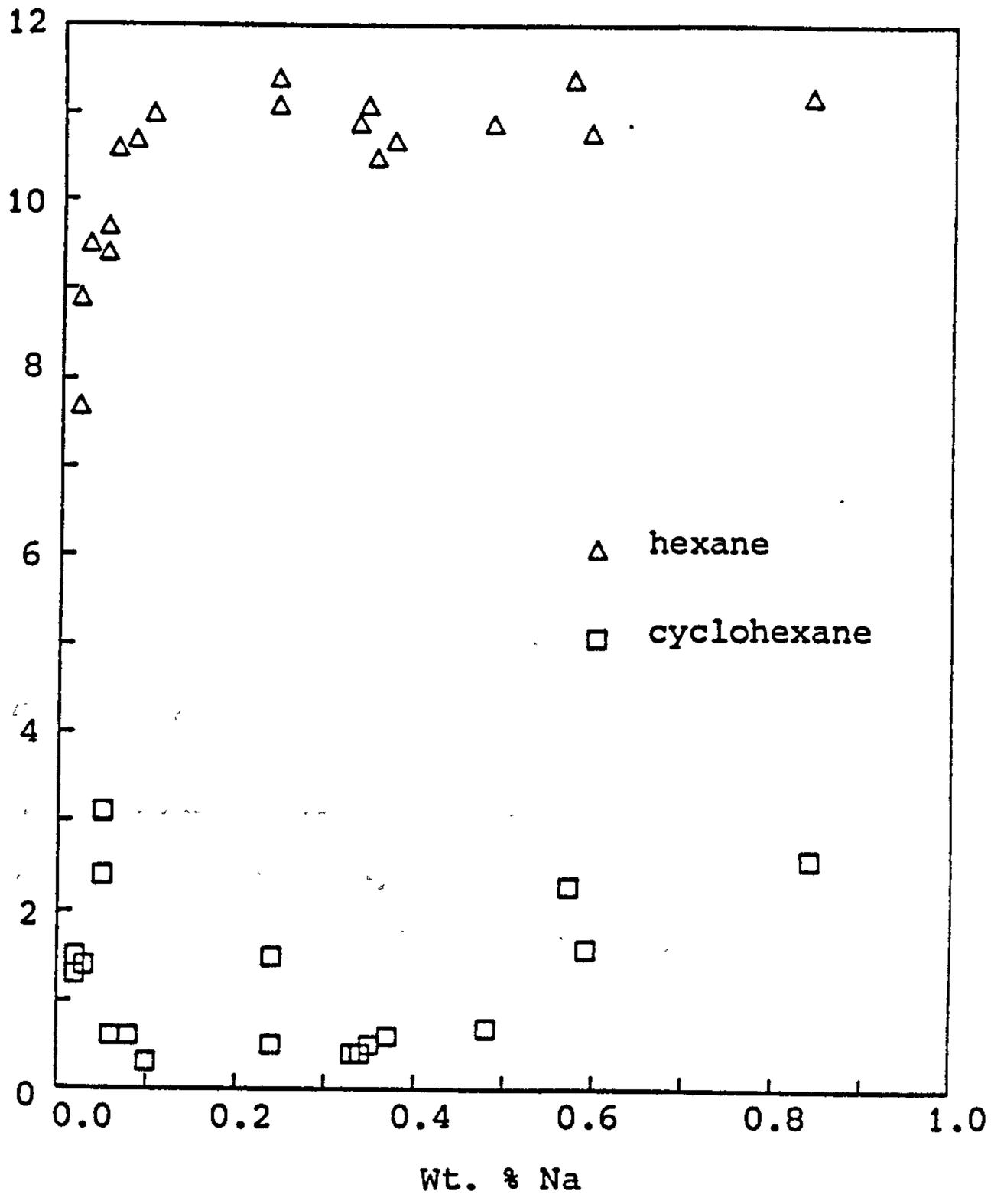

Figure 6.9 Literature data [15] exemplifying marked differences in the sorptive properties of silicalite products. Most of the products had Na/Al ratios considerably greater than unity. The effect of sodium incorporation on the hexane sorption results is very clear. The cyclohexane results show considerable scatter. (The adsorbate pressure was 2666 Pa for both organics).

Note: 0.80 wt % Na $\approx 2Na^{+}/UC$

Figure 6.10 (overleaf)

Scanning electron micrographs of silicalite (S13, calcined) after treatment with water (80°C, 48 h). The pitted surfaces are due to partial dissolution.

FIG. 6.10

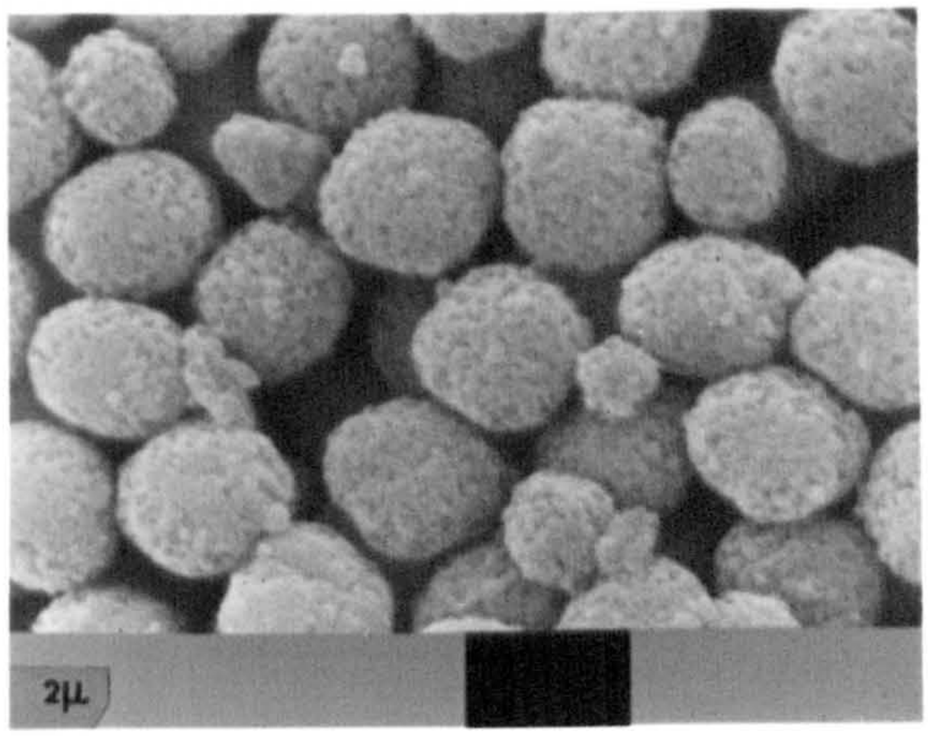

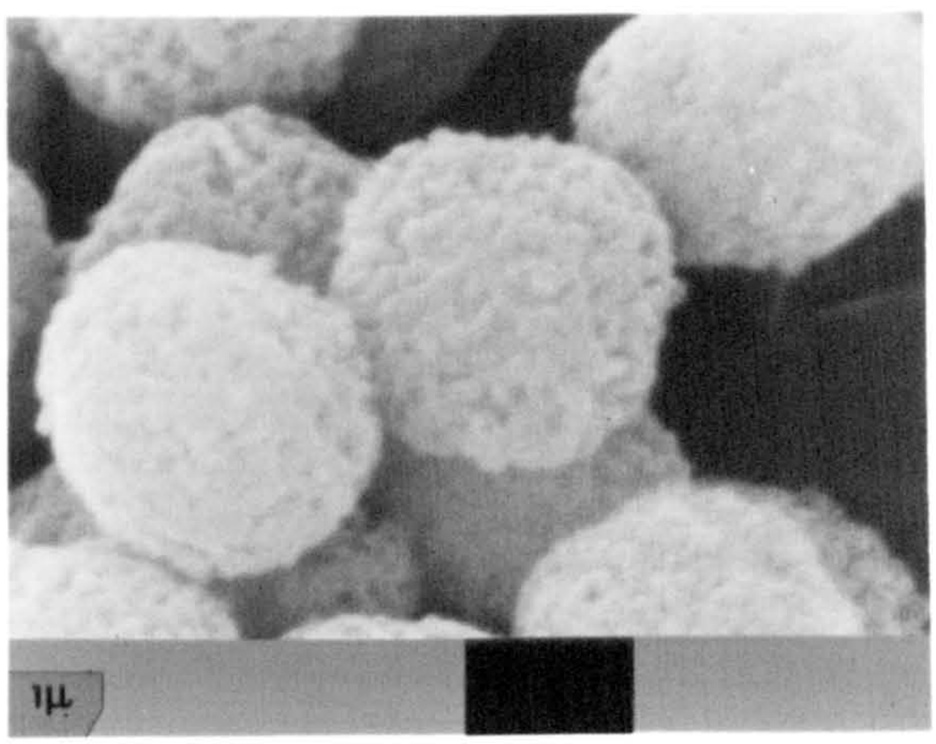

It is important to note that silicalite crystals are more prone to dissolve in alkaline media after (as opposed to before) calcination. Crystals containing the TPA template are stabilised against dissolution by the organic and this is an important facet of their crystallisation. A very simple experiment was undertaken to demonstrate the difference in solubility between silicalite and its organic containing precursor. A few crystals of each were put in capillary tubes that had been sealed at one end. Using a syringe, the tubes were then almost filled with 1M NaOH. Finally the open ends of the tubes were sealed under a flame. Both capillary tubes were then immediately placed in an oven thermostatted at 120°C. After ½ hour, the crystals were examined by optical microscopy (Figure 6.11). The results suggest that the organic template considerably stabilises the crystals against dissolution. The crystals of the precursor were in fact still intact after treatment at 120°C for 3 days. However the possibility of dissolution should be borne in mind every time molecular sieves are treated with aqueous solutions. This is of course especially true when calcined materials are involved and when the crystals contain inorganic base.

To avoid dissolution during post-calcination solution treatments it is best to either (i) carry out the procedures in buffered or acidic media and/or (ii) wash the crystals thoroughly with water immediately after calcination to remove as much 'labile' base as possible. Noteworthy is the fact that the sodium content of the crystals probably affects their inherent solubility. This point was discussed in Chapter 3. Also of note is that the thermal stability of the crystals is adversely affected by the presence of sodium. This was also observed by Saleh [17].

Much has been said about the 'defective' nature of silicalite solids and dissolution/degradation phenomena. On this general theme one final point should be mentioned. Removal of organic material from the pores of as-synthesised high silica zeolites and silica molecular sieves is often effected by air calcination. The high temperature oxidative reactions that result may, it is believed, cause damage to crystals. More specifically, the evolution of considerable amounts of water vapour (from oxidation of the organic) in conjunction with the localised 'hot spots' that must be associated with the oxidative reactions is unlikely to be ideal for frameworks. The adverse effects of calcination

Figure 6.11 (overleaf)

Optical micrographs of silicalite crystals (in capillary tubes) after treatment with 1M NaOH solution (0.5 h, 120°C): A - as-synthesised crystals; B - calcined crystals. Details of the synthesis of the silicalite (product B3, see Chapter 4) have been given elsewhere. The calcined sample was obtained from the precursor by thermal treatment in air (550°C, 24 h). The crystals are ∿75 μm in length.

FIG. 6.11

A

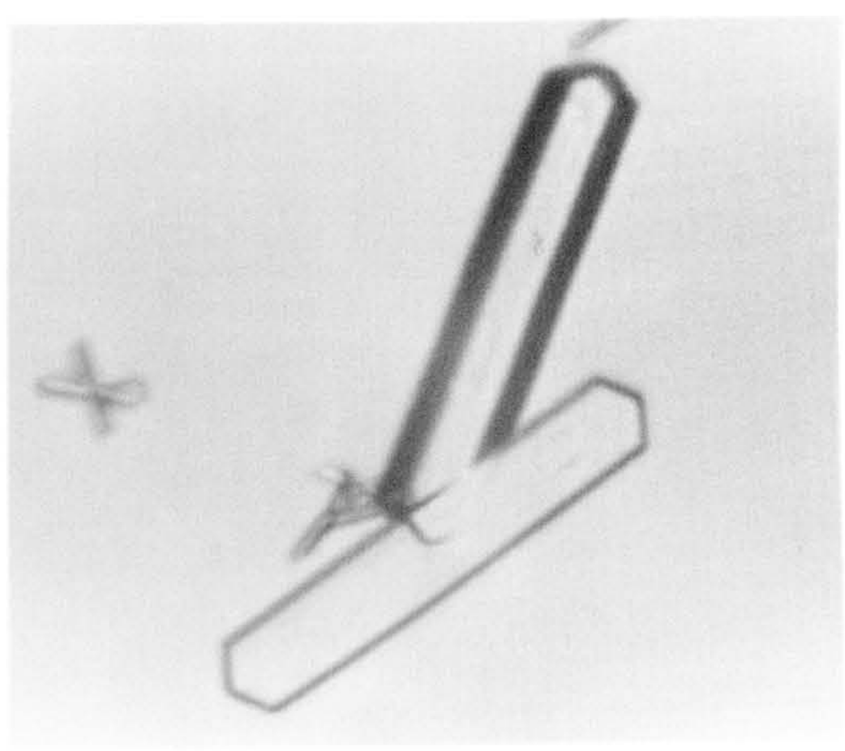

B

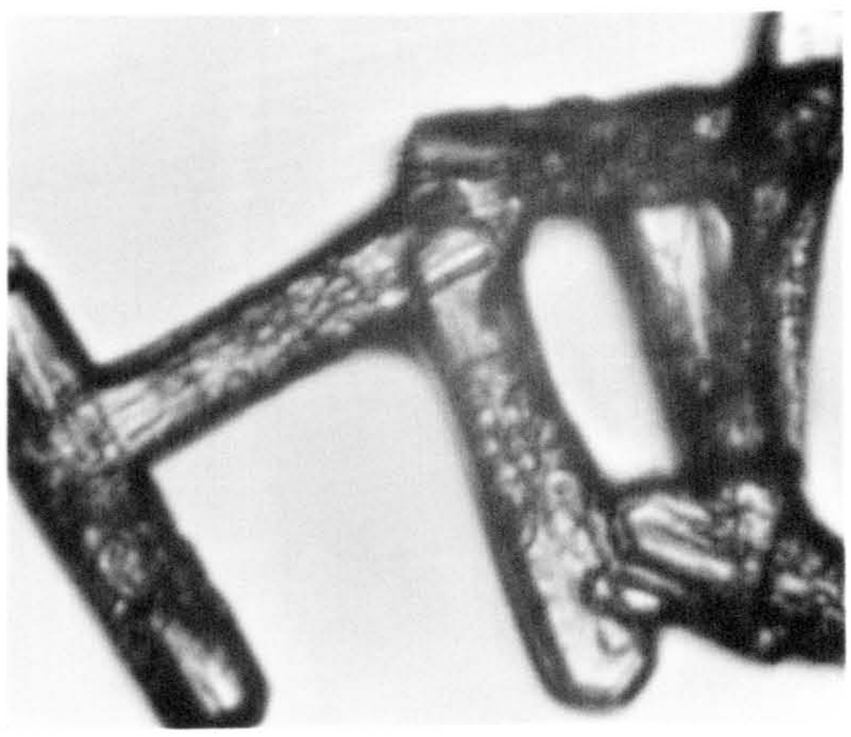

have also been pointed out by others [18,19]. Although only a speculative suggestion, it may be that two-stage calcinations, the first in a nitrogen atmosphere and the second (to remove possible coke deposits) in an air atmosphere, may have its advantages.

The first topic discussed in this chapter was the adsorption of organic molecules by silicalite. This subject also now forms the final topic; experimental results are presented which show that organic molecules can be sorbed by silicalite from the solid phase. Experimental evidence is given for the adsorption of hexanedioic acid by silicalite at room temperature (20 ± 2°C) in the apparent absence of a macroscopic fluid phase. These experiments were prompted by the discovery that solid 4-nitrophenol (whilst being used in trial solid phase indicator tests) was sorbed by silicalite.

The hexanedioic acid was dried at 60°C for 24 hours. The silicalite (coded S14) was crystallised froma reaction mixture of composition $0.5Na_2O$ 2TPABr $20SiO_2$ $1000H_2O$ at 150°C. The product was calcined in air (450°C, 48 h; 550°C, 48 h), acid treated (3 x 1 h, 80°C, 1M HCl, 10 cm^3 solution g^{-1} solid), washed, dried and equilibrated with the laboratory atmsophere for 12 hours. A mixture of the silicalite and the hexanedioic acid (9.2% w/w acid) was prepared by grinding the two solids in an agate mortar until uniformly mixed (ca. 3 minutes). For comparison a similar mixture (9.6 w/w acid) was prepared with the TPA filled silicalite precursor (for which intracrystalline sorption is not possible).

Both mixtures were examined immediately after preparation by thermal gravimetric analysis (TGA) and differential scanning calorimetry (DSC) with the results shown in Figures 6.12 and 6.13. In the case of the mixture with the silicalite precursor, the hexanedioic acid was lost by evaporation over the range 150 to 230°C and the TPA by oxidative degradation from 385 to ∿550°C. The DSC curve (Figure 6.13) shows an endotherm due to melting of the hexanedioic acid crystals and an exotherm due to loss of TPA from the silicalite lattice. In contrast the TGA curve for the mixture with silicalite (calcined) shows that the major loss of hexanedioic acid occurs at much higher temperature (225-425°C) and the DSC curve shows that this occurs endothermically up to 285°C and exothermically at higher temperatures. There is an

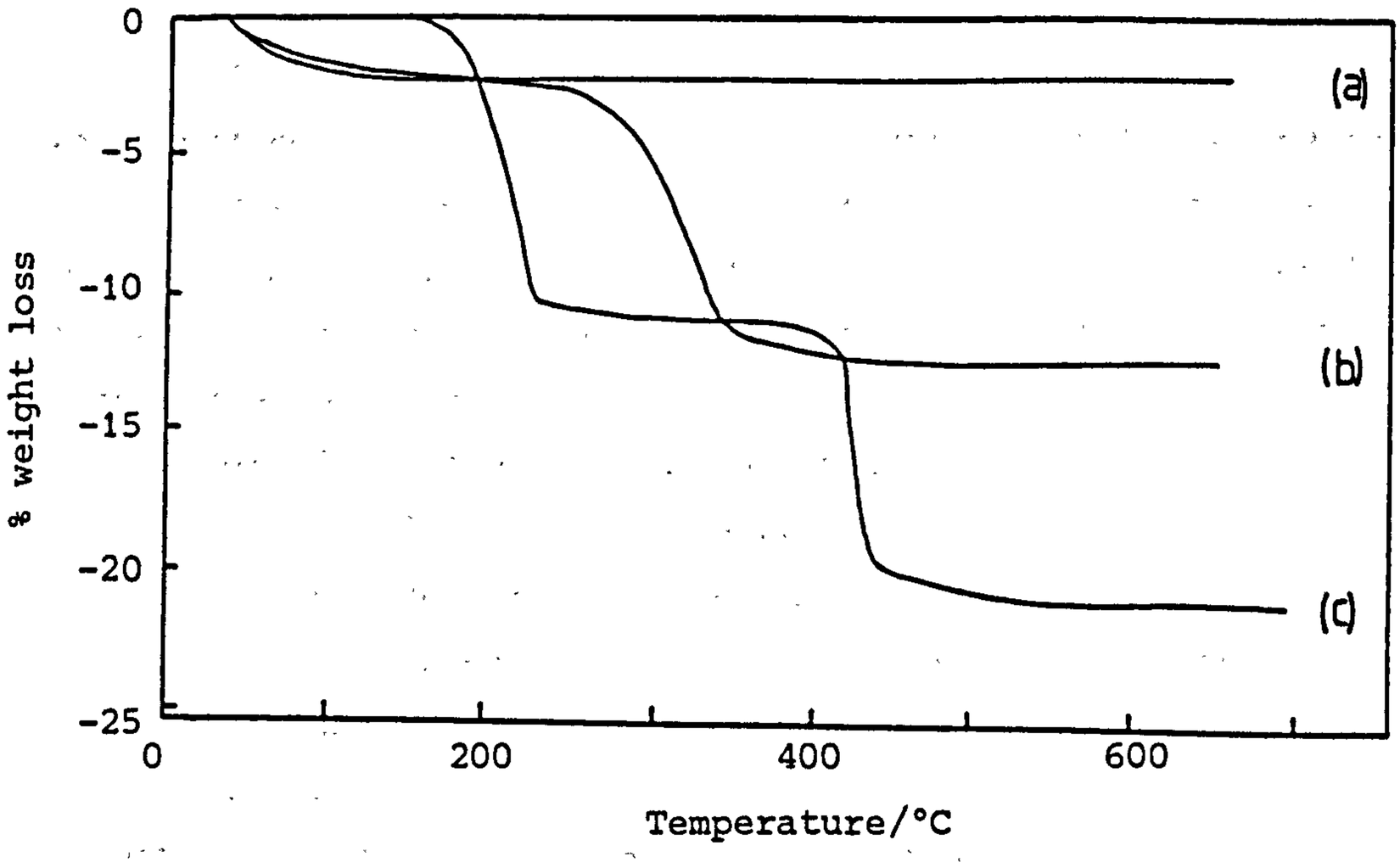

Figure 6.12 TGA curves for (a) silicalite, (b) silicalite + hexanedioic acid (after grinding) and (c) TPA-silicalite + hexanedioic acid (after grinding). Silicalite sample S14 was used for these experiments

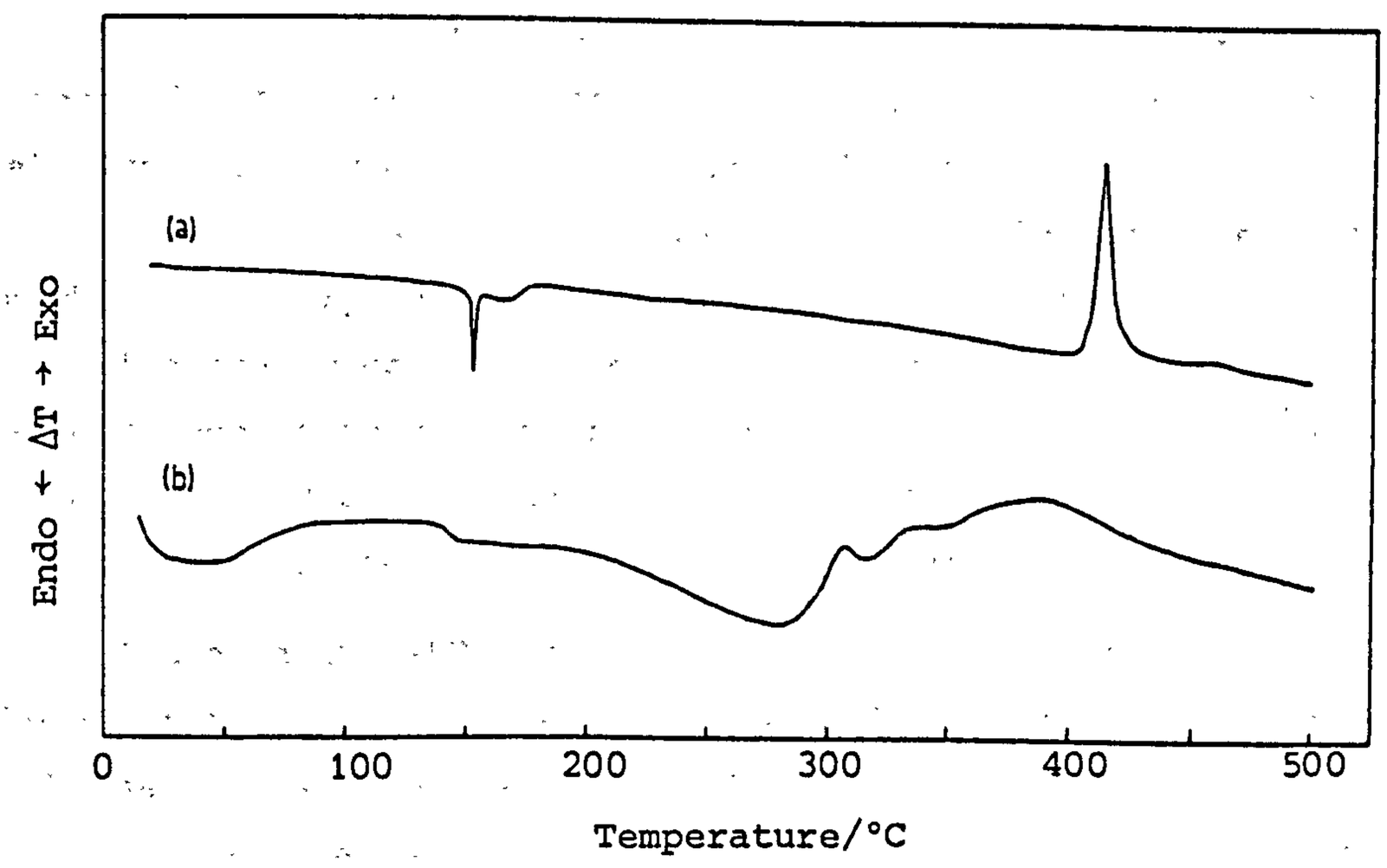

Figure 6.13 DSC curves for (a) TPA-silicalite + hexanedioic acid and (b) silicalite + hexanedioic acid. Both mixtures were analysed immediately after grinding.

endotherm from 20 to 90°C (loss of weakly sorbed water), but the melting point endotherm is completely absent. These observations are entirely consistent with the sorption of the acid into the silicalite channels.

A further mixture of acid and calcined silicalite (8.4% w/w acid) was prepared in a similar manner and examined by X-ray powder diffraction. Some acid was detected immediately after grinding but this decreased by ∿50% within 2 hours. The amount of acid decreased further during subsequent storage of the sample in an air-tight bottle. Throughout these experiments marked changes in the diffraction pattern of silicalite were observed. There were decreases in the intensities of the peaks at ∿8.0° and 8.9° 2θ; this is exactly the reverse of that observed when TPA is removed from the lattice by calcination and indicates the presence of organic within the channels. There was also a gradual decrease in the resolution of the doublet at 24.5° 2θ. This corresponds to a displacive transformation from monoclinic to orthorhombic symmetry [16] and is perhaps caused by the slow redistribution of the acid within the molecular sieve framework. These results and those obtained by TGA and DSC imply that most of the acid was sorbed by the sieve and that adsorption on the external surfaces of the twinned 20 μm crystals was slight.

The vapour pressure of hexanedioic acid at 20°C was estimated to be less than 10^{-4} mm Hg and hence sorption via the gaseous phase cannot account for the large amount sorbed in the short mixing time. The relative humidity of the laboratory (<75%) was too low for sorption via a transient aqueous solution phase. The only feasible mechanism is one in which intracrystalline sorption occurs by direct contact of the solid acid with the molecular sieve. As already mentioned, solid 4-nitrophenol has also been sorbed in this manner and, more generally, physical mixing probably provides a simple method by which silica molecular sieves and high silica zeolites can be loaded with a variety of organic compounds.

Although the XRD results described above gave good evidence for the adsorption of hexanedioic acid from the solid phase, other experiments with the same silicalite sample (S14) showed that grinding crystals alone can cause very marked intensity changes (Figure 6.14). This may be due

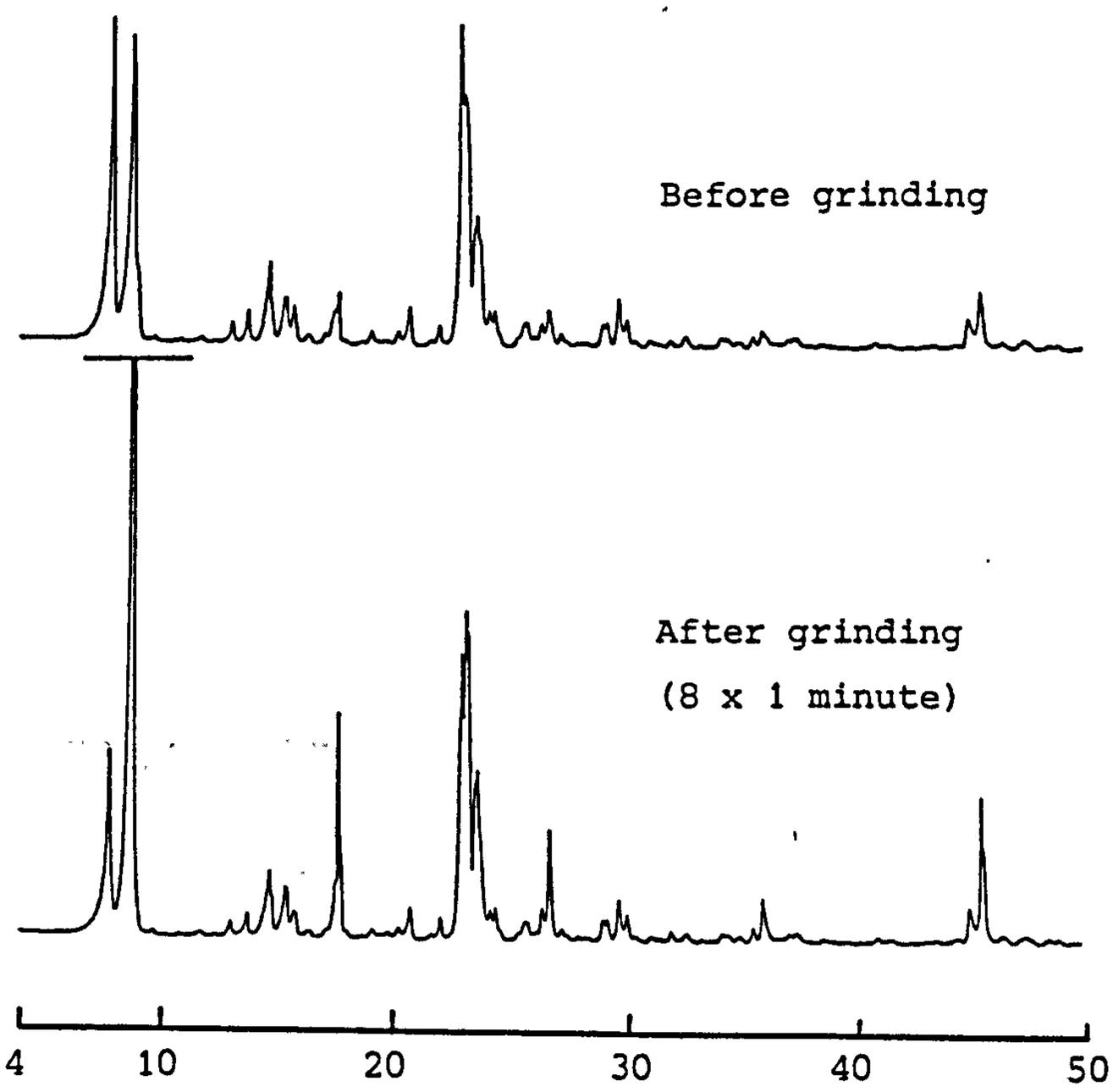

Figure 6.14 X-ray powder diffraction patterns of silicalite(S14) before and after grinding. In total, 8 x 1 minute grinding treatments were carried out. The changes in the line intensities were gradual. Major intensity increases were observed for the lines at ∿8.9, 17.9, 27.0, 36.2 and 45.6° 2θ. The line at ∿8.0° 2θ decreased in intensity considerably.

Figure 6.15 (overleaf)

Scanning electron micrographs of unground (U) and ground (G) crystals of silicalite (S14)

FIG. 6.15

Ⓤ

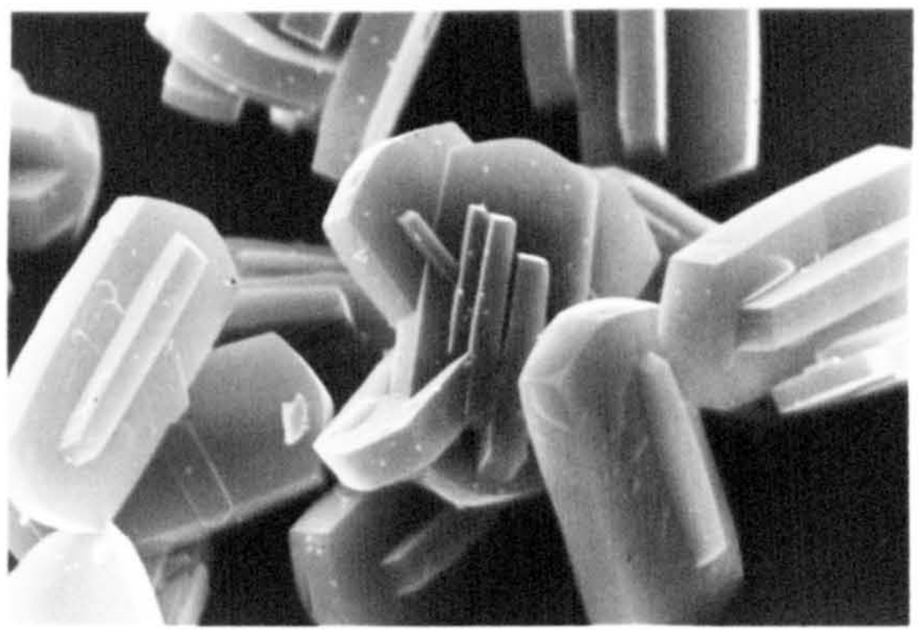

Ⓖ

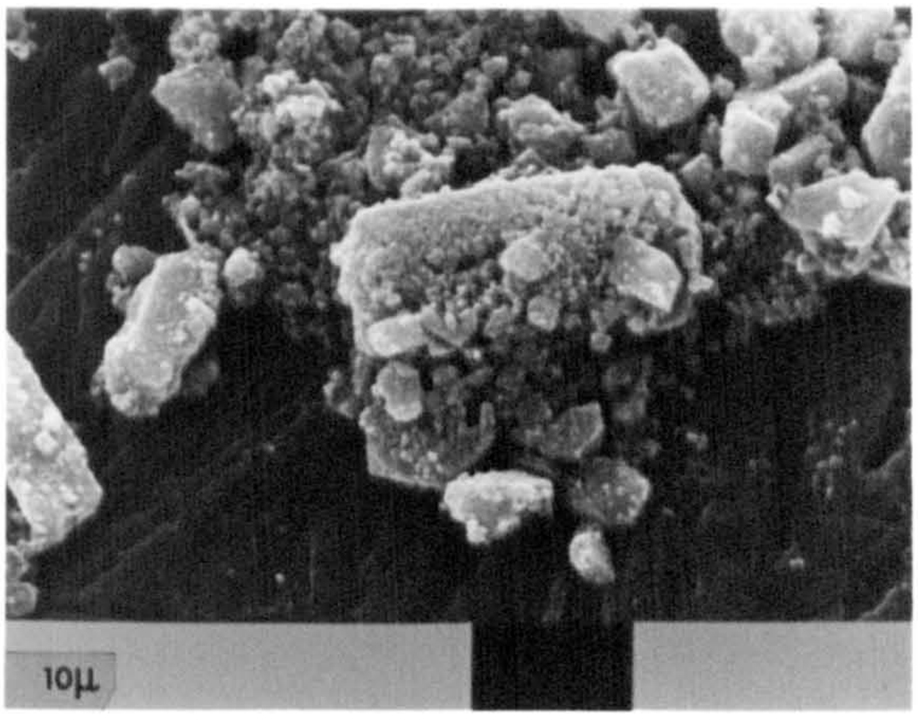

to preferred orientation of the sample presented to the X-ray beam or due to crystal fracture in certain planes. As Figure 6.15 shows, the grinding caused great damage to the crystals although the micrograph does not show the fragments to have specific form.

Concluding Remarks

Many of the points brought out by the results in this chapter are general in nature and probably have relevance to other silicious zeolitic materials besides silicalite-1. The work has shown that, although aluminium free and on that basis compositionally 'simpler' than zeolites, silica molecular sieves are complex solids. In the case of silicalite-1 there is still much to be ressearched.

Chapter 6 - References

[1] R.M. Barrer
"Hydrothermal Chemistry of Zeolites", Academic Press (London), 1982, p. 263.

[2] D.H. Olson, W.O. Haag and R.M. Lago
J.Catal., 1980, 61, 390.

[3] H. Nakamoto and H. Takahashi
Zeolites, 1982, 2, 67.

[4] N.B. Milestone and D.M. Bibby
J.Chem.Tech. Biotechnol., 1981, 31, 732.

[5] C.D. Chriswell, H.R. Burkholder and D.T. Gjerde
"Ethanol purification by Adsorption", Technical Quarterly Progress Report (1/4/81 - 30/6/81), Ames Laboratory, Iowa State University, 1981.

[6] S.M. Klein
M.S. Thesis, Ames Laboratory, Iowa State University, 1982.

[7] C.D. Chriswell, D.T. Gjerde, G. Shultz-Sibbel, J.S. Fritz and I. Ogawa
Report No. EPA-600/1-83-001, Ames Laboratory, Iowa State University, 1983.

[8] S.M. Klein and W.H. Abraham
AICHE Symp. Ser., 1983, 79 (280), 53.

[9] I.S. Maddox
Biotechnol. Lett., 1982, 4, 759.

[10] T.P.J. Izod and J.A. Duisman
U.S. Patent 4,375,568 (1983).

[11] N.B. Milestone and D.M. Bibby
J.Chem.Techn.Biotechnol., 1983, 34A, 73.

[12] A.J. Groszek
European Patent Application 101,254 (1984).

[13] R.M. Dessau and W.O. Haag
U.S. Patent 4,442,210 (1984).

[14] E.M. Flanigen, J.M. Bennett, R.W. Grose, J.P. Cohen, R.L. Patton, R.M. Kirchner and J.V. Smith
Nature, 1978, 271, 512.

[15] G.H. Kuehl
European Patent Application 93,519 (1983).

[16] E.L. Wu, S.L. Lawton, D.H. Olson, A.C. Rohrman Jr., and G.T. Kokotailo
J.Phys.Chem., 1979, 83, 2777.

[17] R.Y. Saleh
U.K. Patent Application GB2,084,552 (1982).

[18] G.T. Kokotailo and S. Sawruk
U.S. Patent 4,187,283 (1980).

[19] P. Chu, F.G. Dwyer and A. Huss
U.S. Patent 4,335,020 (1982).

Chapter 7

Properties of Aluminous Zeolites

The work described in the aforegoing chapters has focused almost exclusively on silicalite-1; its synthesis has been discussed in detail and a collection of its physicochemical properties have been described. There are generalities that can be drawn from those results that would probably also apply to other silica molecular sieves and whilst it is also believed that some of the arguments are relevant to certain high silica zeolites, some caution is warranted on this note. The presence of just small amounts of aluminium in synthesis mixtures can have a disproportionate influence on the crystallisation processes and even small quantities of aluminium in crystals can significantly alter their properties.

Attention is now turned to the properties of aluminous zeolites. The properties possessed by a zeolitic material are dependent on both its topological and chemical make-up and the principal aim of this short chapter is to put certain composition-structure-property relationships, some of which have already been mentioned, in perspective with the theme of this thesis. The first part of this chapter takes the form of a summary rather than a review and emphasis is placed on generalities rather than specifics. A few experimental results are given in appropriate places.

As already mentioned structural and compositional factors together determine the properties of zeolitic materials. The two elements of the compositional aspect are the framework make-up and the cation content. There are close links between these parameters, especially during synthesis. To crystallise a particular zeolite, stringent reaction conditions must be adhered to; a reaction mixture must be formulated correctly and heated under controlled conditions to obtain a desired product. Consequently, the chemical composition of a zeolite, as-synthesised, is usually limited to a fairly narrow range. Zeolites can, however, be flexibly tailored after synthesis by a number of means; for example, desired cationic forms can be obtained by ion exchange and framework compositions can be altered by selective removal of aluminium or silicon. Aluminium can be stripped from frameworks by acid extraction [1], silica can be preferentially removed by treatments with caustic solutions [2]. Other means of altering framework compositions are also known [3].

The aforementioned solution phase treatments that can be used to modify the T-atom compositions of zeolites can be closely correlated to conditions under which particular zeolites are crystallised. In general, aluminous zeolites are crystallised from high pH reaction mixtures (see Figure 7.1) and after synthesis are far more stable in alkaline solutions than they are in acid media. For example, experiments in this laboratory have shown that at pH = 4.0 (25°C) zeolite A (Si/Al = 1) dissolves extensively; the aluminium sites are attacked and framework collapse occurs. Although the presence of extensive amounts of aluminium in frameworks renders such materials unstable in acid media, it renders them, and the aluminium-rich amorphous gels from which they crystallise, relatively stable (insoluble) in alkaline solutions. Hence the need for high pH (>12) reaction conditions to crystallise aluminous materials. On the other hand, high silica zeolites and silica molecular sieves are crystallised at lower pH (typically 11 to 12.5) because silica is solubilised under more severe alkaline conditions. High silica materials are far more stable in acid solution than they are in alkaline media; although frameworks may be stripped of their aluminium in acid solution they remain structurally intact because their bulk is silica. In general zeolitic materials are stable in aqueous solutions under conditions only slightly less severe than those encountered during their synthesis although it should be mentioned that at extremes of pH both aluminous and silicious materials dissolve extensively, if not completely [4]. Various aspects of zeolite stability in aqueous media have been discussed by McDaniel and Maher [4a].

The fact that solubilisation of the silicon and aluminium components from frameworks is pH dependent is probably a contributory reason why certain zeolites have heterogeneous silicon-aluminium distributions [5,6,7]. This subject was mentioned in Chapter 5. The extent of aluminium incorporation into frameworks during synthesis is likely to be at least partly governed by pH and if substantial pH changes occur during crystallisations, as they commonly do during formation of high silica zeolites, there are likely to be consequential effects on the aluminium distribution in crystals; increases in pH during reactions should favour aluminium incorporation. It is of interest that although silicalite is crystallised from aluminium free reaction mixtures, results in Chapter 3 (section 3.3.7.2) showed that the greatest amounts were 'scavenged' from the higher pH preparations. This tallies with the aforedescribed argument.

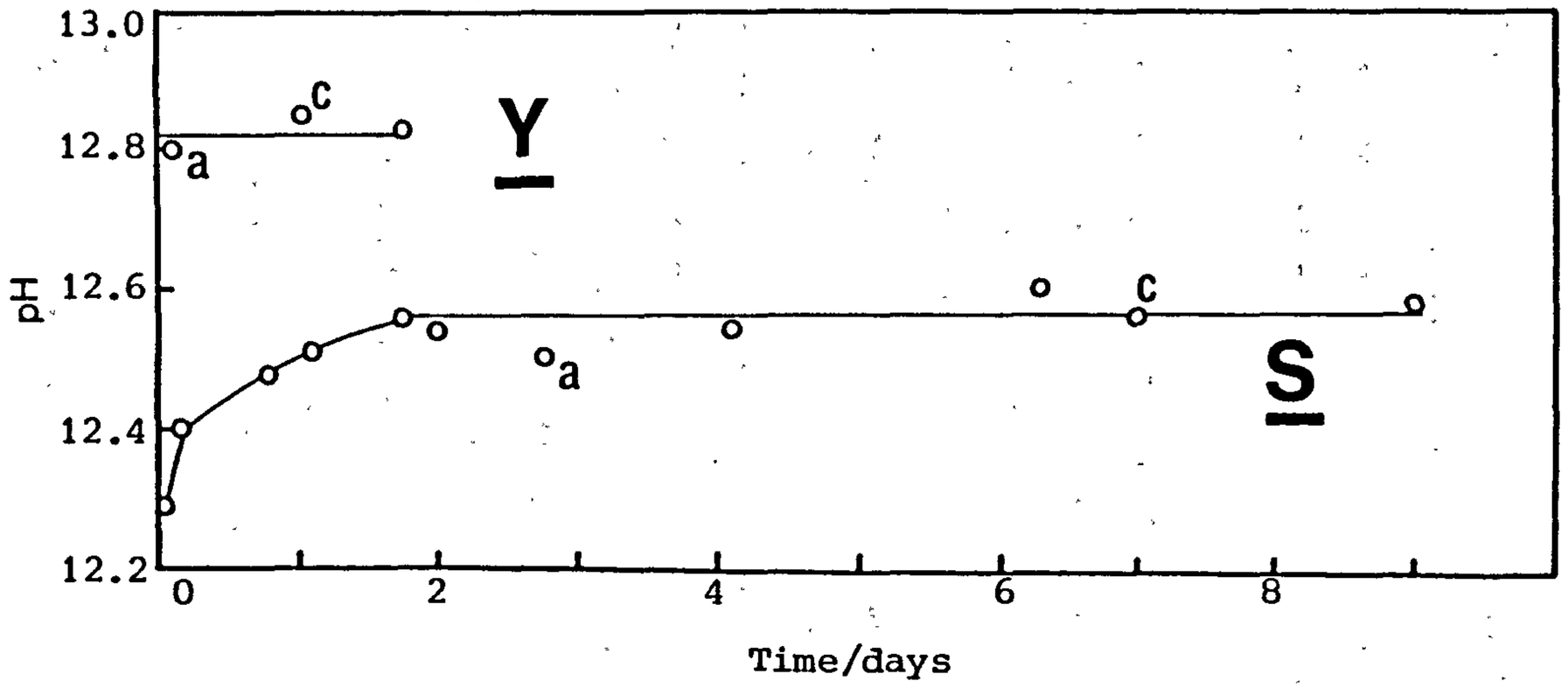

Figure 7.1 pH measurements made on samples taken during the crystallisation of zeolites Y and S from amorphous gels at 95°C. Some of the solid phases were later analysed by XRD as indicated in the diagram: a = amorphous, c = crystalline. The results show that crystallisation of these aluminous zeolites is not accompanied by significant pH changes. The reaction mixture compositions were:

zeolite Y $10.0Na_2O$ $20SiO_2$ $1.3Al_2O_3$ $400H_2O$ (mixture aged for 7 days at R.T. prior to reaction)

zeolite S $7.2Na_2O$ $20SiO_2$ $1.3Al_2O_3$ $675H_2O$ (mixture aged for 24 days at R.T. prior to reaction)

Substantial pH changes do not occur during crystallisation of aluminium-rich zeolites (the two profiles in Figure 7.1 show this) and Si/Al distributions that have been measured (see refs. [5]-[7]) appear to be near homogeneous throughout crystals. Clearly structural reasons and other causes besides crystallisation conditions may contribute to this.

The framework part of a zeolite is only one factor that confers solution phase stability on crystals. Stability is also likely to be affected by the nature of the exchangeable cations. In fact the actual crystallisation of many zeolites is highly dependent on the nature of the cations present in reaction mixtures [8]. The data in Table 7.1 shows what a dramatic effect the cation can have, totally changing the products obtained. Mechanistic reasons for these effects are unknown but important points are likely to be the ways in which cations interact with the frameworks and their effects on the silicate/aluminosilicate species in solution.

Two of the examples in Table 7.1 relate to synthesis mixtures that contain organic cations. The use of organic cations in synthesis was introduced after the realisation that zeolites with high Si/Al ratios and concomitant high thermal and hydrothermal stability were desirable for certain applications. High Si/Al framework levels were achieved by virtue of the fact that pores can only accommodate a certain volume of cations and there is a steric limitation on the number of bulky organic cations that can sit in channels. Initial syntheses with organic cations produced high silica forms of zeolites that had only previously been made with low Si/Al ratios but this fresh approach in zeolite crystallisation soon led to the discovery of novel phases.

Although clearly all aluminium sites require cationic balance, silicious materials made with organic cations are often found to contain a cationic excess and in many cases this is due to entrapped organic base. The role of this organic material is generally acknowledged as being one of pore-filling; silicious materials are stabilised during growth by being filled with organic molecules. Although specific 'templating' or 'structure-directing' effects by organic species are known, they are much rarer.

The incorporation of organic cations and organic molecules into silicious materials during crystallisation contrasts with the incorporation of inorganic cations, water and on occasion inorganic

Table 7.1 Literature data showing the relationship between the cation composition of some reaction mixtures and the crystalline products obtained [8]

	(Molar Ratios)		
zeolite	Na^+/SiO_2	TMA^+/SiO_2	K^+/SiO_2
Y	0.8	0.0	0.0
Omega	0.6	0.1	0.0
L	0.0	0.0	0.8
TMA-O	0.0	0.1	0.8

Reactions were static (100°C), with SiO_2/Al_2O_3 = 16-20, H_2O/SiO_2 = 14-25 and OH^-/SiO_2 = 0.7-0.9. The table shows that small changes in the cation content of mixtures gives rise to completely different zeolite products. It was asserted [8] that the cation was the cause of this.

molecules during the crystallisation of aluminous materials. Highly charged, polar, aluminous materials are stabilised by polar and polarisable entities. Although the organic species that stabilise high silica materials are often charged (e.g. quaternary ammonium species), it is their hydrocarbon 'character' that confer net stabilising effects.

The post-synthesis adsorption affinities of zeolites are not unlike their guest-type 'preferences' during synthesis. Consider the isotherms in Figure 7.2 which show the affinity of a number of different zeolites for water. The water content of the faujasite zeolites is dependent on their framework make-up and the nature of their exchangeable cations. The large caesium ions considerably reduce the intracrystalline space available for water. Nevertheless, water fills much of the void volume of all these faujasites because of their highly charged natures. Besides having strong affinities for water after synthesis, adsorbed water is able to stabilise these materials during their crystallisation.

Figure 7.2 shows that the high silica zeolite ZSM-5 adsorbs less water than the faujasites. This is partly due to its smaller pore volume but most significantly, in the context of this discussion, it is also partly because of its silicious nature. The figure shows that silicalite adsorbs even less water than the ZSM-5. In general, water is not able to stabilise high silica materials during their synthesis; they require organic entities to fill their voids during crystallisation.

Adsorption results that involve only one sorbate such as those shown in Figure 7.2 are widely used to characterise zeolitic materials. The relative affinity of a zeolite for different sorbates can be inferred and information about a zeolite's structure and its chemical make-up can be obtained from knowledge of its adsorption properties. However adsorption in single component systems does have its limitations and the affinity of a zeolite for one sorbate over another can only really be studied in a competitive environment i.e. by investigating adsorption from solutions, either liquid phase or gaseous/vapour phase. On the whole, adsorption by molecular sieve zeolites from solutions has received considerably less attention than adsorption in single component systems.

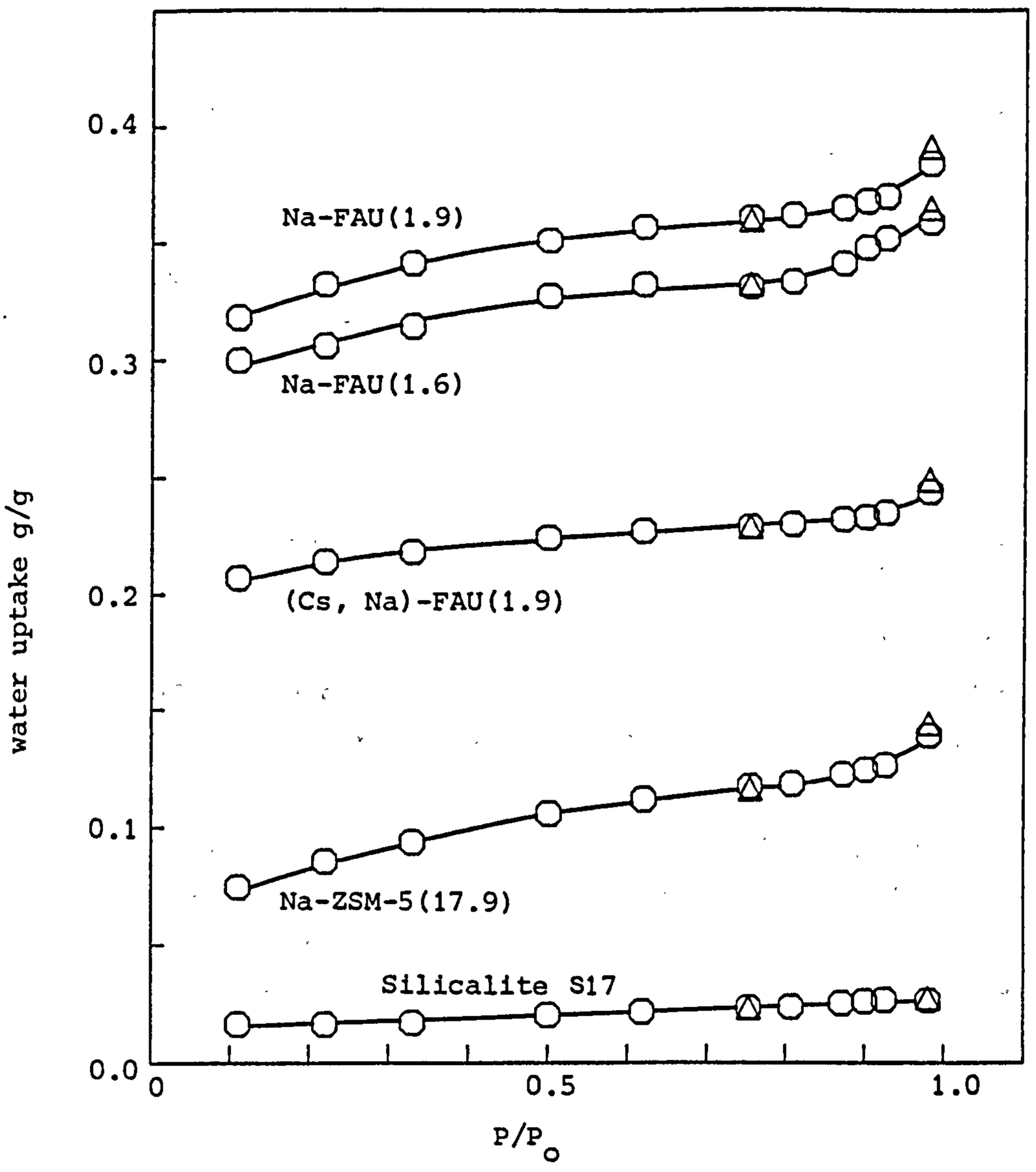

Figure 7.2 Water adsorption isotherms for some zeolitic materials with faujasite (FAU) and ZSM-5 structures. Silicon/aluminium ratios are shown in parentheses. More detailed compositional information, and also details of the synthesis of these materials, is given in Chapter 8. Explanatory notes are given overleaf.

Explanatory notes for Figure 7.2

The water adsorption results shown were obtained by equilibrating samples of the respective materials (in small stainless steel dishes) in a dessicator over saturated salt solutions with known vapour pressures. The amount of dry zeolite in each dish was known and by weighing the dishes the equilibrium water uptakes could be easily calculated. The equipment used, the 'isopiestic' apparatus, is fully described in Chapter 8.

The curves in the diagram show the 'plateaux' regions of the water adsorption isotherms. The upward inflexions of all but one of the plots at high P/P_o are probably due to capillarity effects. The silicalite crystals were relatively large and hence capillarity was not observed.

Repeat measurements were made at two vapour pressures (denoted by the triangles in the plots) after having (i) added small amounts of distilled water to the dishes containing the zeolite samples and then (ii) distilled the water off with a saturated solution of low water vapour pressure. This procedure 'compacted' the zeolite samples in the dishes and enhanced the capillarity effect upon subsequent equilibration at high P/P_o (0.98). The repeat results at lower P/P_o (0.75) were not affected by the procedure as capillarity is not a problem at this vapour pressure. These experiments were chiefly undertaken in connection with work which will be described in the next chapter.

The uptake of organic non-electrolytes from aqueous solution by silicalite-1 has been described in Chapter 6. Experimental results were given which showed the marked selectivities of this material for organic solutes. In contrast to this, aluminous hydrophilic zeolites prefer more polar solutes, in fact even ionic species. Aluminium-rich zeolites can adsorb inorganic salts from aqueous solutions and it is this phenomenon, often termed 'salt imbibition', that forms the bulk of the remaining work in this thesis.

Clearly adsorption from solutions, in this case from aqueous solutions, is a far more complex subject than adsorption in single component systems. That is true from both a theoretical standpoint and a practical one. The presence of more than one type of adsorbed species in the zeolite phase makes quantification of the contents of the zeolite difficult to say the least. This is certainly true in the area of salt imbibition from aqueous solutions where zeolites that contain intracrystalline salt and water are required to be analysed. These experimental difficulties are largely the reason why so little work has been done on the subject. Before the aforementioned difficulties are discussed in greater detail and before means of overcoming those difficulties are outlined, it is pertinent to review the relevant literature and explain, in the light of work already presented in this thesis, some of the reasons why salt imbibition is such an interesting topic for study.

As mentioned above, the imbibition of salts from aqueous solutions by zeolites is an important yet heretofore little investigated research area. The intracrystalline inclusion of salts is a particularly effective means by which the sorptive properties of zeolites can be modified [9]. Just as the entry to pores can often be constrained to different extents by exchanging the cations in a zeolite, it appears that the shape and size selectivity of a zeolite for sorbates can be controlled by quite small amounts of intracrystalline salt [9]. The imbibition of salts into zeolites is also a much used initial step in catalyst prepration and hence salt imbibition studies have implications for both sorptive and catalytic research. In addition, salt bearing zeolites are interesting compounds in their own right and speculative uses, including possibilities for chemical storage and chemical release, have been put forward [10]. As will be seen, the study of salt imbibition also has implications for zeolite synthesis.

Salt molecules can be introduced into zeolites from the molten state or, as already mentioned, by imbibition from aqueous solutions. To eliminate concurrent ion exchange, imbibition is usually studied with zeolites and salts that have a common cation. The imbibition of salts from melts has been studied by several workers [11-16] and although interesting results have been obtained, such work suffers the drawback that it does not allow the introduction of controlled amounts of salt into the zeolite channel system. Imbibition from aqueous solution does not suffer that disadvantage.

It is surprising that there are really only two authoritative works in the literature on salt imbibition from aqueous solutions [11,17], both of which were published over twenty years ago. Barrer and Meier [11] investigated the uptake of sodium chloride from aqueous solutions into zeolites Na-A and Na-X at 25°C and 100°C. Work by Barrer and Walker [17], the most detailed studies to date, involved the uptake of a variety of salts, mainly alkali metal halides, into faujasites and zeolite A. They found that salt uptake was little influenced by temperature or the salt anion but was considerably affected by the salt cation and the structure and the composition of the zeolite. Most of the imbibition results were interpreted as Donnan membrane processes as were the results of Barrer and Meier [11]. Some kinetic studies were also reported [17].

Structural studies on salt bearing zeolites have been reviewed by Barrer [18] and some of the researches that have investigated properties of salt-zeolite complexes are listed below:

Elution of imbibed salts [19]
Thermal properties of salt-bearing zeolites [14,15]
Spectroscopic studies of salt-zeolite complexes [13,16]
Migration of intracrystalline salts when subject to thermal treatments [20]

The thermal studies of Rabo et al [20] showed that high temperature heat treatments can drive imbibed salts from the α-cages of faujasites to the β-cages (salts imbibed at moderate temperatures cannot enter the β-cages). Compounds with interesting chemistries and potentially interesting catalytic properties resulted. The encapsulation of salt

(alkali metal nitrates, halides) into the β-cages stabilised both the zeolite and the salt against thermal degradation; the salt-containing zeolites and the trapped salts decomposed at higher temperatures than the parent materials. Similar effects were found by Barrer and Cole [21] when they entrapped salts directly during synthesis in the cages of sodalite and cancrinite. Unreported experiments [20] were also said to have shown that the zeolite-salt complexes had greater resistance to acid treatments than the parent zeolites themselves. The experimental results described in section 6.3 (Chapter 6) should be borne in mind here; there it was shown that the presence of the organic TPA template in silicalite-1 substantially reduced the solubility of these crystals (relative to the calcined material) in strong alkaline media. Indeed the stabilisation of high silica materials with organics is of prime importance for their formation and it is perhaps not surprising that certain aluminous zeolites, i.e. materials with substantial ionic character, are stabilised by inorganic salts during their crystallisation.

Aluminosilicate crystals in which inorganic salts are distributed throughout the anionic framework are well known in mineralogy [22]. Some zeolitic materials of this type, both synthetic and natural, are known [21-26]. The inclusion of salt guest species during synthesis is often found to be irreversible [21,23]; the salts can not be easily removed after crystallisation, showing that the encapsulation is an integral part of the crystallisation process itself. In some cases inorganic salts may even act as 'templates' and Barrer and Cole [21] reported interesting results on this subject. They made a variety of different sodalite and cancrinite compounds with salt guest species by applying different salts to the reaction mixtures. Small amounts of salt were sometimes found to direct the crystallisations. Salts were entrapped in the sodalite and cancrinite cages, often at the expense of water. Isotherms for salt and water uptakes into products as a function of the salt content of reaction mixtures were obtained and a theoretical treatment was given. It was generally observed that the presence of salts in the products improved their crystallinity and enhanced the yields obtained; the trapped salt stabilised the zeolite against dissolution in alkaline media.

The exact roles played by inorganic guests during crystallisation of aluminous materials probably differ from those played by organic guests during formation of silicious materials but there are clearly analogies that can be made. An extensive review by Barrer on the subject of salt imbibition, both during crystallisation and post-synthesis, is available [27]. A review article by Rabo [28] is also recommended.

For a number of reasons, therefore, post-synthesis salt imbibition studies are important:

(1) Salt imbibition provides a means of tailoring zeolites for specific catalytic and sorptive applications.
(2) Zeolite-salt complexes are interesting compounds with potential applications in their own right.
(3) A better knowledge of structure-stability relationships between salts and zeolites may have spin-off in zeolite synthesis and mineralogy.

The next chapter describes a new experimental approach to salt imbibition. The method was conceived and developed during this research program and involves the use of isopiestic vapour pressure measurements.

Chapter 7. - References

[1] N.Y. Chen
J.Phys.Chem., 1976, 80, 60.

[2] T. Onedera, T. Sakai, Y. Yamasaki and K. Sumitani
European Patent Application 87,720 (1983).

[3] R.M. Barrer
"Hydrothermal Chemistry of Zeolites", Academic Press, London, 1982, pp. 259-262.

[4] J.D. Sherman
in "Zeolites: Science and Technology" (Nato ASI Series), (Ed. F.R. Ribiero, A.E. Rodrigues, L.D. Rollmann and C. Naccache), Martinus Nijhoff, The Hague, 1984, pp. 593-598.

[4a] C.V. McDaniel and P.K. Maher
in "Zeolite Chemistry and Catalysis", (Ed. J.A. Rabo), ACS Monograph 171, 1976, p. 285.

[5] R. von Ballmoos and W.M. Meier
Nature, 1981, 289, 782.

[6] E.G. Derouane, J.P. Gilson, Z. Gabelica, C. Mousty-Desbuquoit and J. Verbist
J.Catal., 1981, 71, 447.

[7] C.E. Lyman, P.W. Betteridge and E.F. Moran
in "Intrazeolite Chemistry", (Ed. G.D. Stucky and F.G. Dwyer), ACS Symp. Ser. 218, 1983, p. 199.

[8] L.D. Rollmann
in "Zeolites: Science and Technology" (Nato ASI Series), (Ed. F.R. Ribiero, A.E. Rodrigues, L.D. Rollmann and C. Naccache) Martinus Nijhoff, The Hague, 1984, p. 111.

[9] R.M. Barrer, D.A. Harding and A. Sikand
J.Chem.Soc., Faraday I, 1980, 76, 180.

[10] Ref. [3], pp. 344-347.

[11] R.M. Barrer and W.M. Meier
J.Chem.Soc., 1958, 299.

[12] M.V. Susic, N.A. Petranovic and D.A. Mioc
J.Inorg.Nucl.Chem., 1971, 33, 2667.

[13] N. Petranovic, U. Mioc, M. Susic, R. Dimitrijevic and I. Krstanovic
J.Chem.Soc., Faraday I, 1981, 77, 379.

[14] N. Petranovic, S. Bojovic and M. Susic
in "Recent Progress Reports", 5th Int.Conf.Zeolites,
(Ed. R. Sersale, C. Collela and A. Aiello), 1980, p. 143.

[15] N. Petranovic and R. Dimitrijevic
in "Metal Microstructures in Zeolites", (Ed. P.A. Jacobs, N.I. Jaeger,
P. Jiru and G. Schultz-Ekloff), Elsevier, Amsterdam, 1982, p. 45.

[16] A.T. Petfield and R.P. Cooney
Aust. J.Chem., 1980, 33, 659.

[17] R.M. Barrer and A.J. Walker
Trans.Faraday Soc., 1964, 60, 171.

[18] Ref. [3], pp. 330-335.

[19] A. Araya and A. Dyer
Zeolites, 1981, 1, 39.

[20] J.A. Rabo and P.H. Kasai
in "Progress in Solid State Chemistry", (Ed. J.O. McCaldin
and G. Somorjai), Pergamon Press, Oxford, 1975, Vol. 9, p. 1.

[21] R.M. Barrer and J.F. Cole
J.Chem.Soc. (A), 1970, 1516.

[22] Ref. [3], p. 307.

[23] R.M. Barrier, J.F. Cole and H. Villiger
J.Chem.Soc. (A), 1970, 1523.

[24] R.M. Barrer, J.F. Cole and H. Sticher
J.Chem.Soc. (A), 1968, 2475.

[25] R.M. Barrer and J.F. Cole
U.S. Patent 3,674,709 (1972).

[26] R.M. Barrer and C. Marcilly
J.Chem.Soc. (A), 1970, 2735.

[27] Ref. [3], Chapter 7.

[28] J.A. Rabo
in "Zeolite Chemistry and Catalysis", (Ed. J.A. Rabo),
ACS Monograph 171, 1976, p. 332.

Chapter 8

The Use of Isopiestic Vapour Pressure Measurements to Study Adsorption by Zeolites

8.1 Introduction

The two sections that follow introduce the subject of isopiestic vapour pressure measurements. The first outlines the fundamental principles of the so-called 'isopiestic technique' and explains its use in solution chemistry, the second describes the application of the technique to study adsorption phenonema on zeolites.

8.1.1 Fundamentals of the isopiestic technique

The principle of the isopiestic technique is beautifully simple; if two or more solutions of non-volatile solutes in the same volatile solvent are placed in an enclosed space, then solvent will pass from one solution to another by distillation/condensation processes until the vapour pressures, and hence solvent activities, of all the solutions are equal. Solutions which have the same vapour pressure are said to be 'isopiestic'. At isopiestic equilibrium solutions of different solutes have different concentrations and, by careful determination of these equilibrium concentrations, sets of concentrations of solutions of different solutes which have the same solvent activity can be obtained. The technique is comparative and 'indirect' in that the precise value of the equilibrium solvent activity can be determined only if a reference solution, whose solvent activity as a function of concentration is either known from the literature or has been determined by a 'direct' method, is present during the equilibrations. Most researches with the isopiestic technique have involved aqueous solutions and sodium chloride has often been used as the reference electrolyte. Knowledge of the isopiestic molalities of different solutes gives valuable information about the chemistry of solutions. Osmotic and activity coefficients can be calculated and much learned of the behaviour of ions and molecules in solution.

Although solutions of several different solutes can be simultaneously investigated by the isopiestic technique, for the moment just two solutions, designated A and B, are considered. Suppose the vapour pressure of solution A is initially greater than that of B. Solvent will distil from the solution with higher vapour pressure to that with lower, i.e. from A to B. Eventually the vapour pressures of the solutions will equalise. However, since the distillation of solvent is accompanied by a temperature decrease and solvent condensation by a temperature increase, measures have to be taken to minimise differences in temperature between the solutions. If they are not, spurious non-isothermal steady-state situations may arise and the isopiestic solutions, although having equal vapour pressures, may have molalities significantly different from those expected. To avoid this occurrence, solutions are kept in good thermal contact so that heat can flow back and forth between them. Thermal contact is achieved by using materials of high thermal conductivity (a) to contain the solutions and (b) to provide an interconnecting medium between the solutions which in most cases has been a large metal block. The block functions as a thermal buffer.

Although the isopestic method is used to give information about steady-state situations between solutions, the kinetics of solvent transfer is an important practical consideration as it governs how quickly equilibrium is attained. Equilibration kinetics are greatly enhanced if the enclosed space in which the equilibrations are carried out is evacuated to the vapour pressure of water. This allows water molecules to pass more freely between solutions. The rate of equilibrium attainment also depends on a number of other factors; how much solvent needs to be transfered, the concentrations of the solutions (dilute solutions tend to take longer to equilibrate) and agitation (for example, gentle rocking of the solutions will expedite equilibration). Agitation also minimises thermal and concentration gradients within the solutions.

A typical isopiestic experiment might be carried out on the following lines; the procedure now described will give added clarity to what has already been said.

At the start, known weights of several solutes are placed in small tared dishes and the amounts added determined by careful weighing. Solvent is then added to each dish; the amounts added do not have to be accurately known but it is best if the solutions initially have similar concentrations and hence, to a first approximation, similar solvent activities. The

solutions are placed in good thermal contact in a container, quite often a dessicator of some sort. The dessicator is evacuated and put in a thermostatted environment, usually a well-regulated water bath.

The equilibration itself may take as little as a day (if the solutions are very concentrated) but it may take far longer, perhaps even a few weeks, if the solutions are very dilute. When equilibrium is deemed to have been attained the dishes are removed and weighed. These weighings, by difference with the initial weights, enable the amount of water in each dish to be determined and simple calculations then allow the molalities (moles solute per kilogram solvent) of the isopiestic solutions to be evaluated. All weights are usually corrected for air-buoyancy. Quite often, not just one but two or three solutions of each solute under investigation are equilibrated together in one experiment. The concordancy of the calculated equilibrium molalities of each different solute (at isopiestic equilibrium solutions of the same solute are isomolal) give a reliable indication that equilibrium has been satisfactorily attained and the mean solute molalities that can thus be calculated are more accurate than those that could be obtained from 'single dish' experiments.

Further equilibrations can be carried out by returning the dishes to the dessicator. If equilibration at a higher vapour pressure is required then a small amount of solvent can be placed in the base of the dessicator prior to evacuation. During the subsequent equilibration, this solvent, because of its higher vapour pressure, transfers to the solutions so diluting them. For a set of results at lower vapour pressure the dessicator can simply be evacuated for a prolonged period before an equilibration is commenced. Sets of isopiestic molalities of different solutes can be accumulated and the thermodynamics of solutions explored.

The isopiestic technique was introduced and named by Bousfield [1], improved by Sinclair [2] and developed into a sound experimental method by Robinson and Sinclair [3]. Results from systematic studies on aqueous electrolyte solutions obtained over a number of years by Robinson and colleagues have been collected in a single volume [4]. The technique has also been applied to water soluble non-volatile non-electrolytes [5,6].

An appreciation of the historical development of the technique has been given by Mallinson [7] and some of the most important experimental and procedural considerations have been reviewed by Luk'yanov [8] and others [7,9]. Since its inception, the isopiestic technique has made a substantial

contribution to the understanding of the physical chemistry of aqueous solutions and this elegant and inherently simple technique will no doubt continue to do so.

Two special applications of the technique, to determine solubilities [7,9] and to determine the dissociation pressures of crystal hydrates [10], deserve mention at this stage:

(a) Solubility measurements can be made very simply as follows. Initially a known weight of solute (usually a salt) is added to a tared dish and solvent added. A small amount of a saturated solution of the same salt plus excess solid is placed in another dish. The dishes are then equilibrated as described above. At equilibrium the former is exactly saturated and, after weighing to determine how much water is present in the dish, the solubility of the salt can be calculated.

(b) The second special application of the isopiestic technique, to determine the dissociation pressures of crystal hydrates, requires little explanation. In these experiments equilibrium weighings give information about the water content of a solid phase and in this respect this application, which involves only a solid-vapour equilibrium, is little different from widely practiced adsorption of gases and vapours onto solids. However a reference solution has to be present so that the equilibrium vapour pressures can be determined.

8.1.2 Application of the isopiestic technique to study adsorption by zeolites

It has already been pointed out that aqueous solutions have been extensively investigated by the isopiestic technique. For successful experiments with aqueous solutions, prospective solute molecules must satisfy two criteria: (i) they must be involatile in aqueous solution and (ii) they must be appreciably water soluble. The presence of vapour phase solute molecules renders experiments useless (the mass of solute in solution has to be conserved) and, regarding the second point, substances only sparingly soluble in water, whose solutions have vapour pressures that approach that of water, cannot be satisfactorily equilibrated. Such equilibrations take extended times and experimental difficulties are encountered when working at very high vapour pressures because of capillary condensation.

At 25°C most salts do not exhibit significant volatility, many are appreciably water soluble and the isopiestic method thus lends itself to investigation of their aqueous chemistry. For similar reasons, isopiestic vapour pressure experiments are ideal for investigating the adsorption of salts into zeolites from aqueous solutions. Salt imbibition, or salt occlusion, inclusion or impregnation as it has also been called, is a little-probed area of zeolite science and the application of the isopiestic method to its investigation solves most of the problems that have heretofore been the reason why so little research has been done in this field. As will be seen, the isopiestic method gives information that could not be obtained by other means.

To begin with, consider the uptake of a salt from aqueous solution into a zeolite; say NaCl into zeolite Na-X. To fully describe the steady-state situation that is eventually established between salt and water molecules in the solution phase and those in the solid zeolite phase, three parameters have to be accurately known:

(a) The concentration of salt in the solution phase.
(b) The amount of salt in the zeolite.
(c) The amount of water in the zeolite.

To understand the drawbacks of methods that have been used in the past to obtain this information and at the same time to outline some of the advantages of the isopiestic method reported herein, what might be considered a 'conventional' procedure is now described.

The method might be as follows. Known weights of dry zeolite, salt and water are put in a vial of some kind, the vial is closed and shaken or tumbled in a thermostatted environment until an equilibrium is established. For analysis the zeolite has to be separated from the solution and this presents an almost intractable practical problem. No matter how much care is taken, it is virtually impossible to wash the zeolite free of adhering salt without upsetting the salt inside its pores. Once separated though, a portion of the solution phase can be analysed for salt by conventional means (e.g. titrimetry, spectrometry) and its concentration determined. Knowledge of the initial solution concentration allows a value for the amount of salt imbibed to be calculated provided it is assumed that no transfer of water takes place between the zeolite and solution. If only a small amount of salt is taken out of solution though, large errors are inevitable. Alternatively, a portion

of the isolated zeolite phase can be directly analysed for its salt content although this too often poses problems. If the salt content is small, as it quite often is, quantification is again difficult.

The question as to how much water was present in the zeolite at equilibrium along with the salt is one which has invariably gone unanswered. It is possible to equilibrate a portion of the isolated zeolite-salt complex over a portion of the separated solution phase, i.e. the solution with which it was originally in equilibrium, and thereby determine the equilibrium water content. There are no questions to be raised about the validity of such a procedure, only its practical difficulty. What has to be queried is just how significant are the small changes to the vapour pressure of this solution that must inevitably occur during establishment of this 'vapour phase' equilibrium. Moreover, and regardless of the success of the latter step, it can be seen that a substantial amount of problematical analytical work is required to get any information about the uptake of salts into zeolites. For each point on an imbibition isotherm, the procedures have to be painstakingly repeated. Analytical problems become acute as the salt uptake diminishes.

The advantage of the isopiestic method to study salt imbibition will become apparent from the discussion that now follows. Consider once again the uptake of NaCl by zeolite Na-X. Imagine two small tared dishes, the first containing a known weight of NaCl and the second known weights of both NaCl and dry Na-X. If some water is added to each and the resultant solutions are equilibrated in good thermal contact in a thermostatted chamber then at equilibrium the solutions in the dishes will be isomolal. This is true irrespective of the amount of salt in the second dish adsorbed by the zeolite. At equilibrium the dish that contains solution only can be weighed and the concentration of the solution determined. This must necessarily also be the molality of the solution above the zeolite. The equilibrium situation is schematically shown below:

(I) 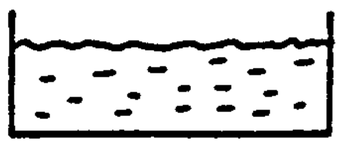 *solution only*

(II)  *solution + zeolite*

At equilibrium, the molality of the solution in dish (I) can be calculated. Because of the common solute, the molality of the solution in dish (II) can be inferred.

The beginnings of an analytical method to study salt imbibition should now be apparent. At equilibrium a simple weighing can give the concentration of the solution in contact with the zeolite.

The dish that contains solution and zeolite can also be weighed at equilibrium. This gives, by difference, the amount of total water in the dish some of which is adsorbed (intrazeolitic), the rest 'free' (in solution). The equilibrium situation can be described in terms of the masses of the components in the dish:

(a) The total amount of water in the dish (W_w), the experimentally determined parameter, is the sum of the water in the solution phase (w_w) and that in the zeolite ($\bar{w}_w$):

$$W_w = w_w + \bar{w}_w \qquad (8.1)$$

(b) The total amount of salt in the dish (W_s) is known and, as above, is the sum of the salt in the solution phase (w_s) and that in the zeolite ($\bar{w}_s$):

$$W_s = w_s + \bar{w}_s \qquad (8.2)$$

(c) The concentration of the solution phase, C, calculated from the solution only dish, is given by the equation:

$$C = w_s/w_w \qquad (8.3)$$

where w_s and w_w represent the amounts of salt and water in the solution that is in contact with the zeolite.

The parameters known are W_w, W_s and C but the above three equations (8.1-8.3) cannot be solved from this information because together they contain four unknowns (w_w, $\bar{w}_w$, w_s and $\bar{w}_s$). The problem, descriptively, is a very clear one; no information about how the water and salt are proportionated between the zeolite and solution phases has been obtained. It is worth mentioning at this stage that if assumptions were made, for example if the water content of the zeolite phase was deemed to have a certain value, then the problem reverts to a solvable one, i.e. 3 equations and 3 unknowns. However the water content of the zeolite is controlled jointly by the equilibrium water activity and the amount of salt imbibed and, as will be seen, assumptions such as the one made above have little justification.

Precise knowledge of both the water and salt contents of the zeolite phase is desired. To explain how this information is obtained imagine once again the NaCl/Na-X system with two dishes, one that contains solution only the other solution plus zeolite, being simultaneously equilibrated with a saturated solution of sodium chloride (in contact with excess solid salt). At equilibrium all three solutions are saturated and the amount of salt taken up by the zeolite would be the maximum possible from aqueous solution at the temperature of the experiment. The situation at equilibrium is visually depicted below.

(I)

solution only

(II)

solution + zeolite

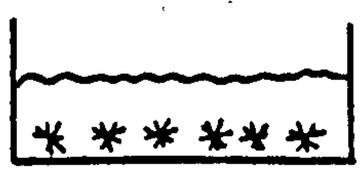

(III)

solution + solid salt

At equilibrium, the vapour pressures of the solutions in dishes (I) and (II) are dictated by the vapour pressure of the solution in dish (III). The solutions in dishes (I) and (II) are thus exactly saturated.

Consider the dish that contains the zeolite. The amount of solution present above the zeolite depends on what proportion of the salt initially added is free, i.e. not imbibed. If there is a large excess of salt, more specifically if the total weight of salt in the dish per unit weight of anhydrous zeolite is far greater than the equilibrium salt uptake per unit weight anhydrous zeolite, i.e. $W_s/W_z >> \bar{w}_s/W_z$, then a substantial amount of solution will be present with the zeolite at equilibrium. If the above experiment was repeated several times, each time with less and less salt in the zeolite dish, then the concentration of the solution above the zeolite would be the same each time (the equilibrium vapour pressure is controlled by a saturated solution) but the amount of solution present would be successively reduced; an increasing proportion of the total salt present is imbibed as the salt content in the dish is progressively lowered. On all occasions when $W_s/W_z > w_s/W_z$ a solution phase will be present at equilibrium but if $W_s/W_z \leqslant w_s/W_z$ there will be no solution phase and the dish that contains the zeolite will be 'dry'; all the salt is taken up by the zeolite and at equilibrium all the water that is present is intra-crystalline. This is the key principle of the application of the

isopiestic technique to zeolite adsorption studies. Zeolite and salt mixtures with salt/zeolite weight ratios that increment over a chosen range are each placed in a small dish. The dishes are not equilibrated individually as suggested above, they are all equilibrated together in the same chamber at the same time. At equilibrium some dishes will be 'dry', others will contain a solution phase. The weights of the dishes at equilibrium give the amount of water present in each and those that contain a solution phase have substantially greater water contents than those that do not. This fact allows graphical interpolation of accurate values for the amounts of salt and water present in the zeolite samples that are in equilibrium with a solution phase. The intracrystalline contents of each of the zeolite samples in equilibrium with a solution phase are the same per unit weight of dry zeolite.

The raw experimental results take the form of 'imbibition' graphs as schematically shown and described in Figure 8.1. The experimental procedure is akin to 'titrating' a zeolite with a salt at a chosen vapour pressure. Once all 'sites' for salt molecules within the zeolite at that vapour pressure are occupied (the 'end point'), additional salt manifests itself as a solution phase. In practice, 'V-shaped' graphs very similar in form to that shown schematically in Figure 8.1 were often obtained with the slopes of the two lines and the location of the intersection point dependent on the equilibrium conditions. It is noteworthy that results from many electrochemical titrations also take the form of 'V-shaped' graphs; in conductometric titrations for example, the conductance of a solution may diminish as a species is titrated and then increase again after the end point when excess titrant is present. In isopiestic experiments with zeolites it is the way the water contents of salt/zeolite mixtures vary as the 'end point' is first of all approached and then passed that give rise to graphs of this nature.

This introduction to isopiestic studies with zeolites, largely descriptive so far, now concludes with a detailed account of the theory involved.

In the isopiestic method, a group of small dishes of known weight, each of which contains roughly the same accurately known weight of dry zeolite, different known weights of a salt and some water are left in a closed chamber until isopiestic equilibrium is attained. At equilibrium

Figure 8.1 Schematic depiction of an 'imbibition' graph

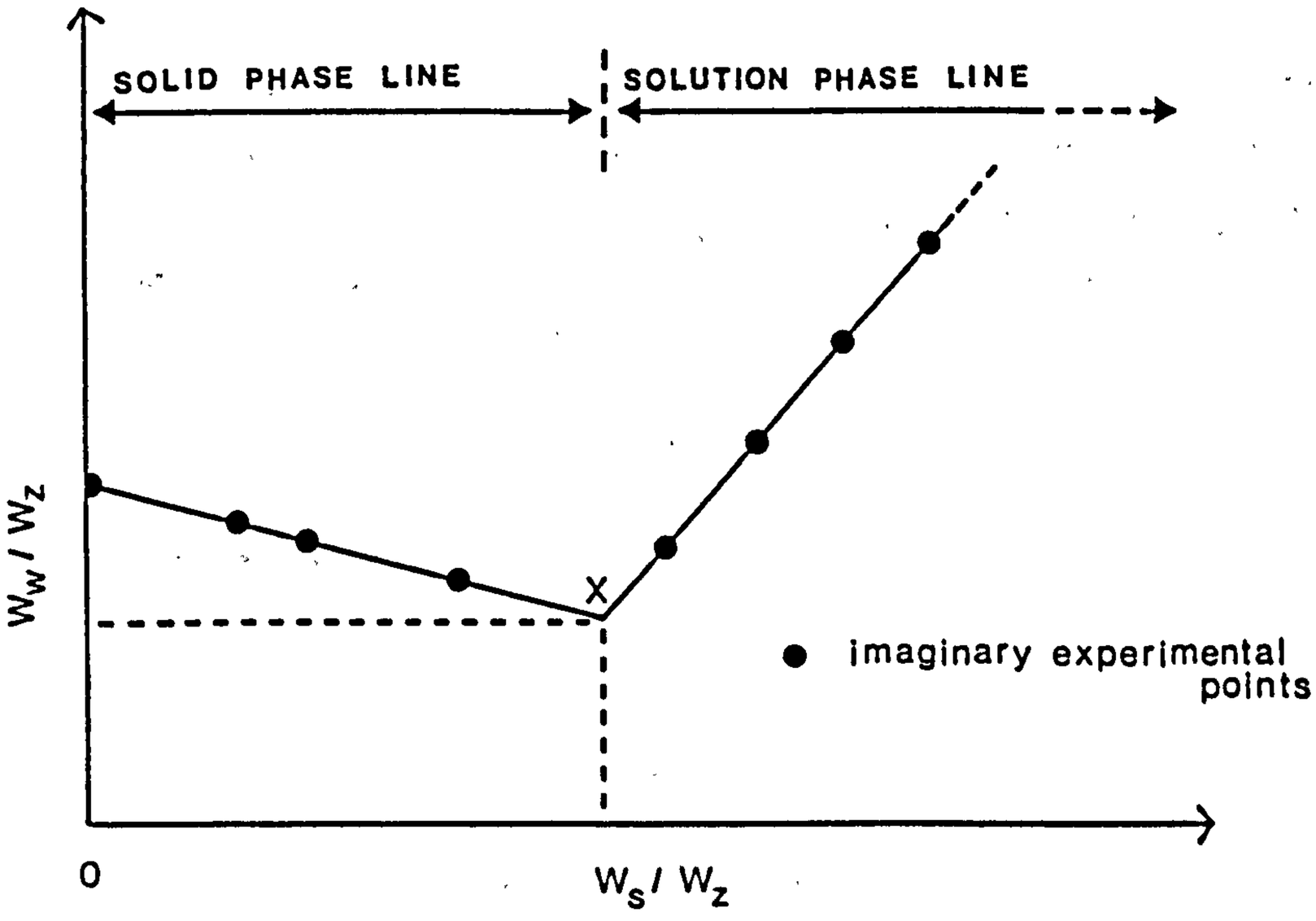

All salt and water is intracrystalline. Water is displaced from the pores by the salt.

Crystals are in contact with a solution phase. The water content of mixtures, W_w/W_z, increases with the salt content, W_s/W_z. The intracrystalline contents of the zeolite samples are the same per unit weight dry zeolite.

From the interpolated intersection point (X), the intracrystalline salt and water contents of the zeolite samples in contact with solution phases can be determined.

all solutions in the dishes have the same concentration irrespective of the amount of zeolite present and provided the zeolite samples are in contact with the solutions they will all contain the same amount of imbibed salt and water per unit weight of anhydrous zeolite.

Consider one of these dishes at equilibrium. The total amounts of water and salt (W_w and W_s) in the dish can be fractionated into the respective amounts in solution (w_w and w_s) and in the zeolite ($\bar{w}_w$ and $\bar{w}_s$) as shown by equations (8.1) and (8.2). Equation 8.1 can be rearranged as follows:

$$W_w = w_s(w_w/w_s) + \bar{w}_w \qquad (8.4)$$

Substitution of equation (8.2) into (8.4) gives:

$$W_w = (W_s - \bar{w}_s)(w_w/w_s) + \bar{w}_w \qquad (8.5)$$

and this can be rearranged in two steps as follows:

$$W_w = W_s(w_w/w_s) + \bar{w}_w - \bar{w}_s(w_w/w_s) \qquad (8.6)$$

$$W_w = W_s(w_w/w_s) + \bar{w}_s(\bar{w}_w/\bar{w}_s - w_w/w_s) \qquad (8.7)$$

Finally, equation (8.7) can be simplified by (1) designation of the weight ratios of water to salt in the solution (w_w/w_s) and in the zeolite ($\bar{w}_w/\bar{w}_s$) as R_{sol} and R_{zeo} respectively and by (2) replacement of absolute weights by weights per unit weight anhydrous zeolite. Equation (8.7) thus becomes:

$$W_w/W_z = R_{sol}(W_s/W_z) + U_s(R_{zeo} - R_{sol}) \qquad (8.8)$$

U_s is defined as the weight of salt imbibed per unit weight dry zeolite. Equation (8.8) is a key relationship; it represents the equilibrium situation in dishes that contain a solution phase and it represents what will be referred to hence as the 'solution phase' line. For a given water activity, i.e. a given solution concentration, R_{sol}, R_{zeo} and U_s are constant and hence W_w/W_z is linearly dependent on W_s/W_z. The slope of this line (R_{sol}) can be used to determine the concentration of the solution phases above the zeolite samples; the concentration is the reciprocal of R_{sol}. It is therefore not necessary to have 'solution only' dishes present during experiments.

The intercept of the line represented by equation (8.8) contains the terms for the salt and water contents of the zeolite samples in equilibrium with the solution phases, namely U_s and U_w (= $U_s R_{zeo}$) respectively. These terms cannot be separated without further experimental information. More specifically, information is required about the 'solid phase' line (refer to Figure 8.1).

If the ratio of salt to zeolite (W_s/W_z) in a dish is small, all of the salt is imbibed by the zeolite and at equilibrium there is no solution phase present. When this is the case, U_s is simply equal to the ratio of the weights of salt and zeolite in the dish and the amount of water sorbed by the zeolite is controlled by the amount of salt in the zeolite and by the water activity of the solution phases present in the dishes for which W_s/W_z is large. In many cases it is observed that for dishes in which there is no solution present:

$$W_w/W_z = k(W_s/W_z) + U_w^o \qquad (8.9)$$

where U_w^o is the amount of water adsorbed when there is no salt in the zeolite and k is an empirical constant. For a given water activity W_w/W_z is linearly dependent on W_s/W_z and this line usually has a negative gradient, i.e. salt displaces water from the pores of the zeolite. Equation (8.9) is the second key equation and represents the 'solid phase' line.

From the intersection of the lines represented by equations (8.8) and (8.9) (see Figure 8.1), the interpolated values of W_s/W_z and W_w/W_z represent the values of U_s and U_w, i.e. the salt and water contents of the zeolite samples that are in equilibrium with a solution phase. This is true irrespective of the form of equation (8.9), i.e. regardless of whether it is a straight line (as discussed here) or a curve (as sometimes observed). The accurate determination of the intersection point is critical to the success of the experiments and the amounts of salt and zeolite in each dish must be carefully chosen so that at equilibrium some dishes are 'dry' (and are on the solid phase line) and some contain solution (and are on the solution phase line).

Each set of experimental measurements corresponds to a particular water vapour pressure which is determined by the concentration of the solution phase above the zeolites. To make comparisons between results for different zeolites and salts it is best to arrange for each equilibration to be carried out under a pre-determined water vapour pressure. This is achieved by introducing a large quantity of a saturated salt solution (plus excess solid) into the equilibration chamber along with the dishes containing the zeolite samples. When equilibrations are carried out in this way the concentrations of the solution phases change until they have the same vapour pressure as the saturated solution. The equilibrium vapour pressure can be determined by a separate experiment or, if available, obtained from the literature.

As all results are obtained by gravimetric means, the method does not rely on specific properties of the solutes under study. Equilibrations can be repeated as often as desired until sufficient information has been obtained. At equilibrium, the concentration of the solution phase and the amounts of solute and water imbibed can all be determined.

To date the isopiestic method has been used in a variety of different physicochemical investigations. Most studies have involved solution phase work (for example, measurement of solute and solvent activities), only on occasion solid phase equilibrations (determination of the dissociation pressures of crystal hydrates). Thus the technique has been used to equilibrate either solids or solutions with vapours. The use of the isopestic method to study equilibria between solids and solutions has not been reported elsewhere. The experiments involve establishment of equilibria of three different types: (1) solution-vapour, (2) solution-solid and (3) vapour-solid. Generally speaking, it is more difficult to equilibrate solutions with vapours than it is solids with vapours, and that is why special equipment and precise experimental control are essential for these isopiestic experiments (see next section).

During the course of this work a substantial number of experiments were performed and it is only possible to present a portion of the results in this thesis. The work selected for presentation correlates with work in previous chapters and at the same time shows the capabilities and limitations of the isopiestic method. It is hoped that most of the results not reported here will eventually be published in the literature.

8.2 Experimental

8.2.1 Equipment

Most of the apparatus now described has been successfully employed in orthodox, 'solution only' isopiestic work [7,11]. Nevertheless, several modifications to equipment and many trial equilibrations, of a variety of different sorts, were carried out at the start of this work. In particular, the water bath arrangement (see later) had to be modified several times before satisfactory thermostat control was achieved, the optimum experimental procedures for the work in question had to be found and the procedures had to be thoroughly checked for reproducibility and accuracy.

Some of the equipment is shown in Figure 8.2. Small metal dishes with fitting lids were used for the experiments. Two types were available; gold-plated silver dishes fitted with teflon lids and stainless steel dishes fitted with stainless steel lids. Each dish had a volume of 9 cm^3 although in practice only a fraction of this was utilised. The dishes, which were originally made from 0.2 mm sheet and which were 1" diameter and 3/4" deep, sat snugly in circular recesses machined in a metal block. The gold-plated silver dishes sat in a gold-plated copper block, the stainless steel ones in a stainless steel block. Each block was 5" in diameter and 1" deep. The recesses were 3/8" deep and were machined symmetrically around the block. A small hole was drilled through the centre of each recess to facilitate removal of the dishes for weighing. These can be seen in Figure 8.2. A much larger hole drilled through the centre of the block ensured adequate vapour circulation during equilibrations.

The blocks sat in 6" 'Dry Seal' dessicators (Type 4, Jencon's Ltd.) which provided the closed systems in which the equilibrations were carried out. The set-up is shown in Figure 8.3. The dessicators were fitted with rubber "O"-ring seals and each dessicator top was modified to allow a lid carrier to be operated from outside the apparatus. The lid carrier was a perspex disc (with recesses to hold the lids in position) attached to a stainless steel rod which passed through a seal in the dessicator top. Figure 8.3 shows the lids raised as they should be during the course of an experiment.

Figure 8.2 (overleaf)

Equipment used in the isopiestic experiments:

A A metal block with dishes and lid carrier

B A modified dessicator containing a metal block

C The water bath arrangement

FIG. 8.2

(A)

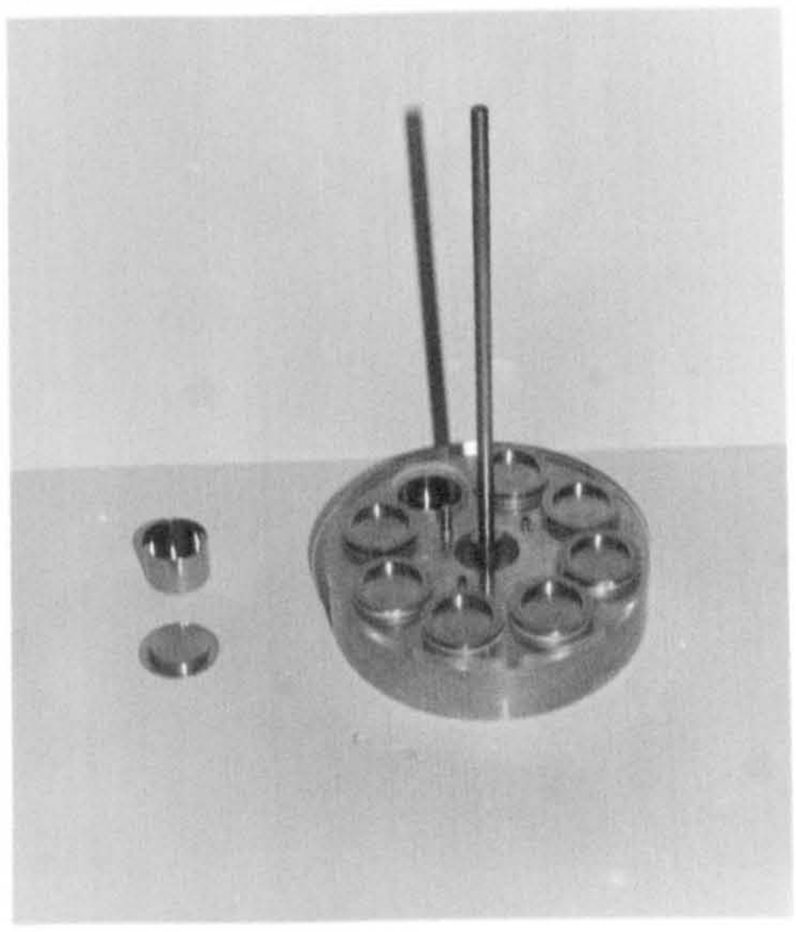

(B)

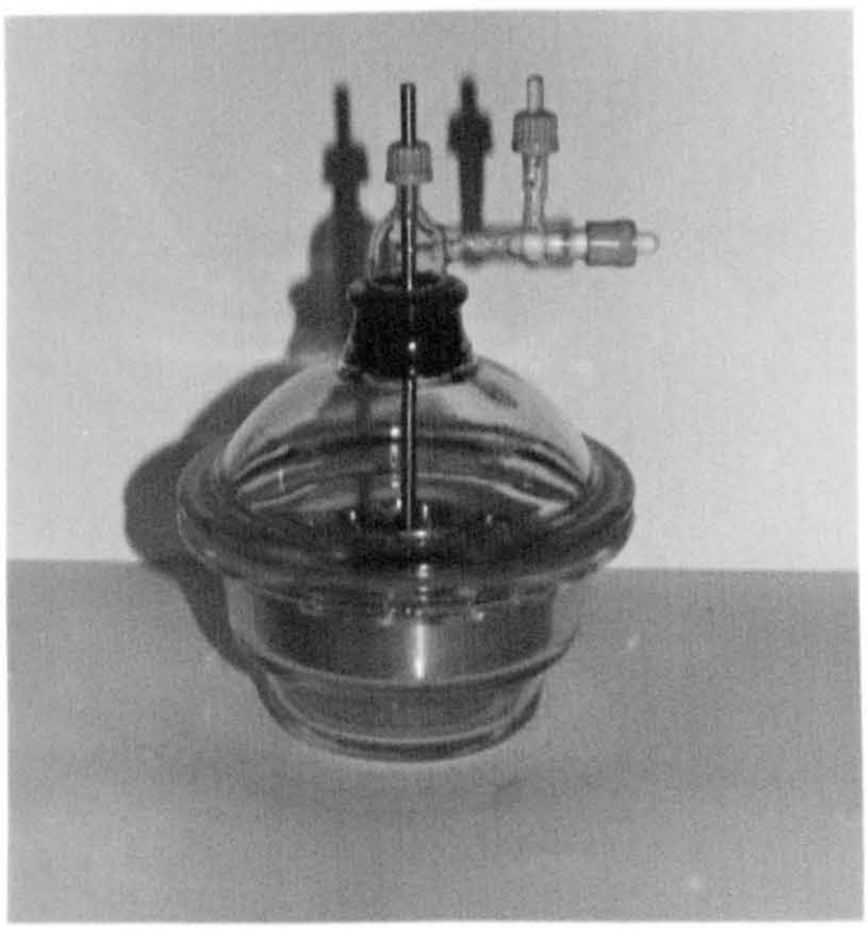

(C)

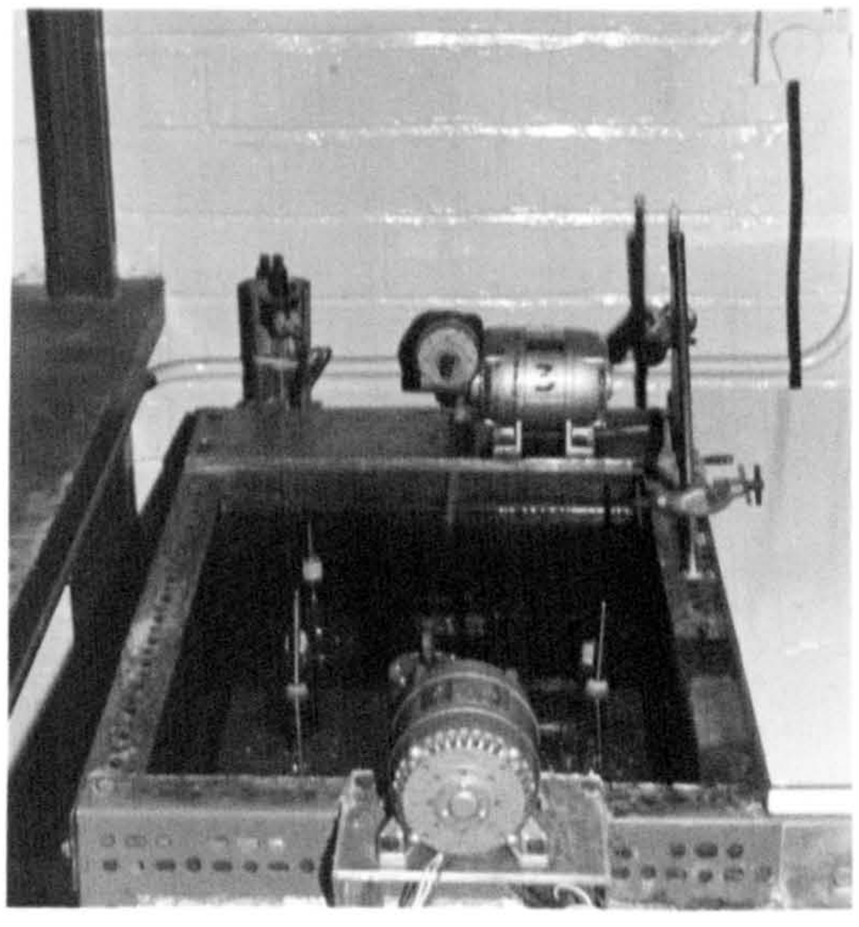

Figure 8.3 The dessicator arrangement

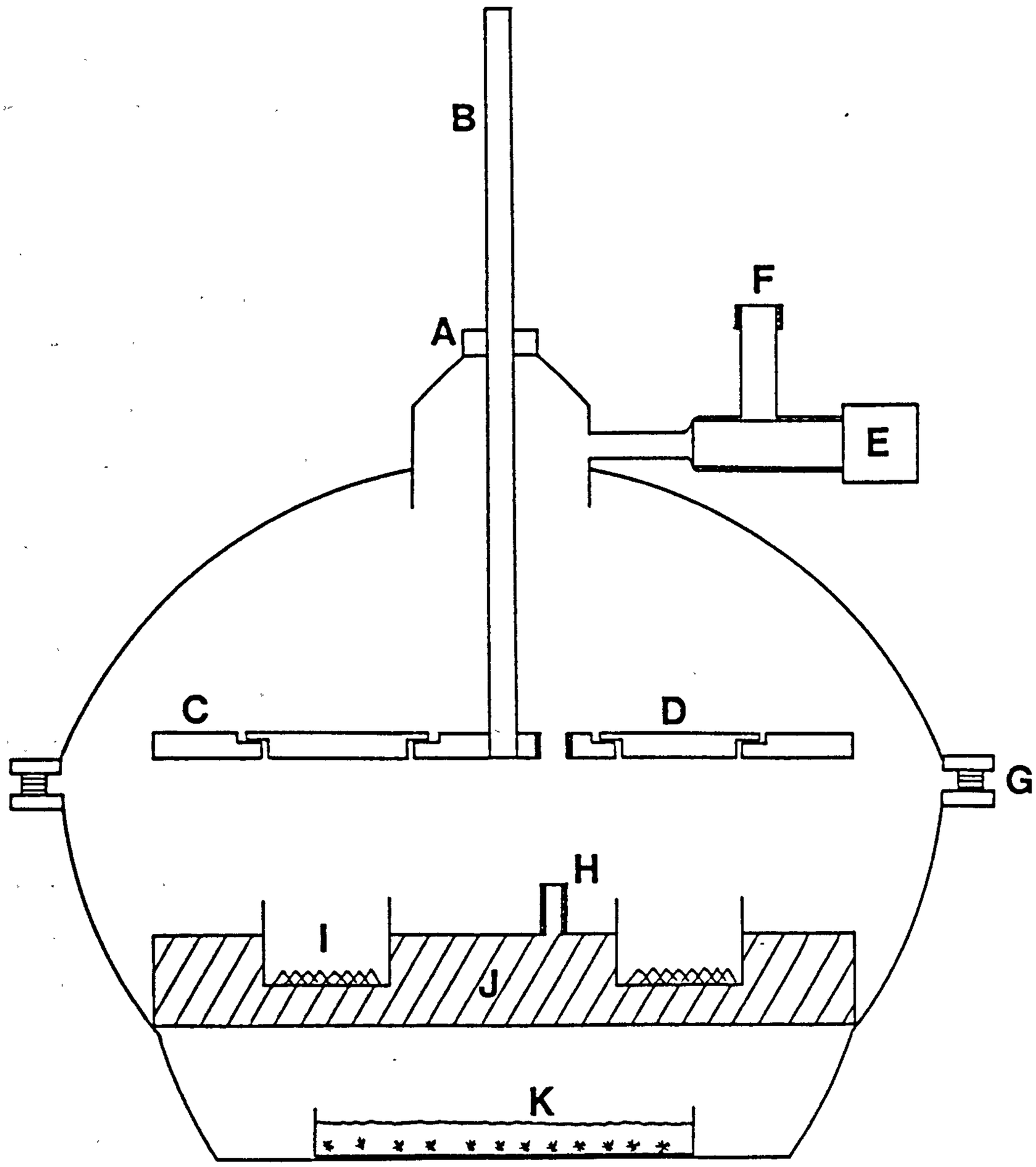

A _ seal
B _ steel rod for lid carrier
C _ perspex lid carrier
D _ lid for dish
E _ tap
F _ pump attachment
G _ 'o'-ring seal
H _ retaining thread
I _ dish + zeolite
J _ metal block
K _ saturated salt solution

The metal block was supported from the sides of the dessicator at its lower constriction and the saturated solution, that was often used to give pre-determined vapour pressure control during equilibrations, was contained in a petri-dish which sat in the base of the dessicator below the metal block. The dessicators were evacuated with a water-pump before equilibrations were commenced and a manometer in the pumping system enabled the air removal to be monitored. To avoid the solutions 'spluttering', as sometimes happens on evaucation, the rate of pumping was reduced to a satisfactory level by a piece of glass capillary tubing in the line between the apparatus and the pumping system.

At the end of an equilibration, the lids were lowered onto the dishes. The lid carrier was located on a screwthread, which protruded from the upper surface of the metal block, and secured with a nut. Air was then admitted to the dessicator, the block and dishes removed in one piece. The lipped lids formed a snug fit on the dishes and preserved the equilibrium conditions during this procedure. To weigh the dishes the block was placed on a specially constructed stand and dishes were successively removed by inserting a PTFE rod upwards through the small holes drilled in the centres of the block recesses. The dishes were handled at all times with a pair of specially designed tweezers with PTFE grips. At the start of this imbibition work weighings were made on a Unimatic balance (Stanton Instruments Ltd.). The aquisition of a Mettler electronic balance (Type AE163) considerably shortened the weighing procedures.

During the equilibrations the dessicators were positioned in recesses on a submerged board in a water bath. The water bath arrangement is shown in Figure 8.4. The bath was made of copper sheet and the water was thermostatted at 25 ± 0.04°C by a contact thermometer/ relay system which powered a small heater. A large booster heater was available for heating the water up to 25°C initially. The water temperature was regularly checked with a standard thermometer which had been calibrated against a Hewlett-Packard quartz crystal thermometer (model 2801A). With the latter instrument absolute temperatures can be calibrated to within ±0.02°C. The bath temperature range of 25 ± 0.04°C reflects this and in fact temperature fluctuations in the bath were only of the order of ±0.02°C at the outside. These temperature fluctuations are damped first of all by the glass dessicators and secondly

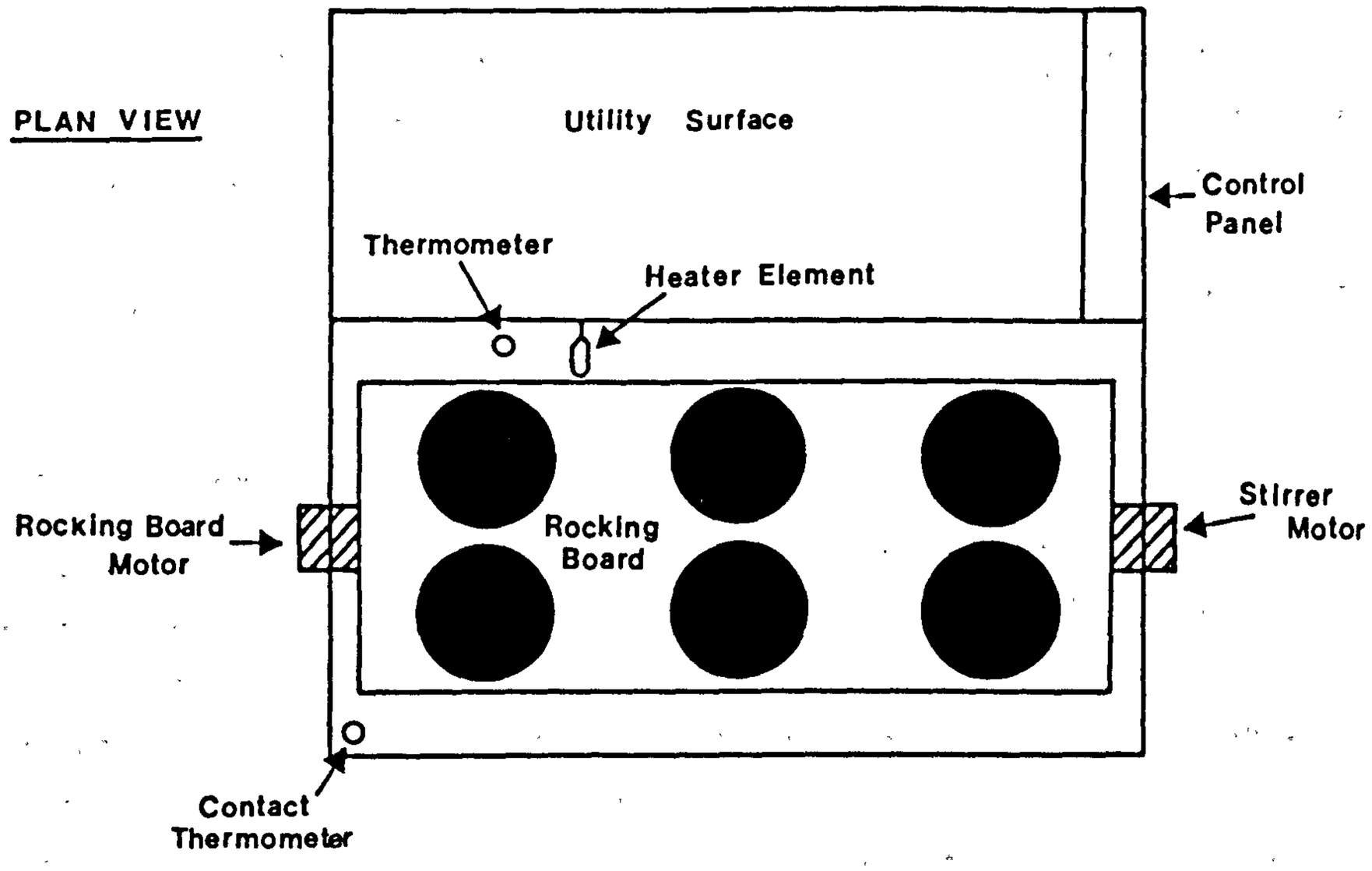

Figure 8.4 The water bath arrangement

by the metal blocks and dishes that contain the solutions and thus temperature differences between solutions were probably very small. Indeed they have to be for successful work.

The submerged board rocked gently to and fro at an angle of about 10° from the horizontal. A paddle stirrer, driven at 650 rpm by a Parvalux motor, provided additional agitation of the water that was necessary for satisfactory thermostat control. Six dessicators, each of which could hold eight dishes, could be accommodated in the bath at the same time.

8.2.2 Procedure

During all operations meticulous care was taken. First of all the dishes and lids were washed with distilled water, dried in an oven at 60°C and left for a few hours at room temperature to equilibrate with the atmosphere. Tests showed that weight constancy was rapidly attained. Each dish along with its lid was then weighed empty after which small amounts of zeolite were placed in each. The exact weights added were not required; the principle aim at this stage was to place between 0.35 and 0.5 g zeolite, on an anhydrous basis, in each dish. The dishes were put in a block in a dessicator and a petri-dish containing a saturated solution of sodium chloride (a_w = 0.753 at 25°C) was placed in the base of the dessicator. After evacuation the lids of the dishes were raised (using the lid-carrier) and the dessicator placed in the thermostat bath. The zeolite samples were allowed to equilibrate over the sodium chloride solution for at least 4 days. Kinetic tests showed that weight constancy was always attained after this time, although the equilibration times for different zeolites differed substantially. The dessicator was then removed from the water bath, the lids were lowered onto the dishes and air was admitted. The dishes were weighed as quickly as possible; with the electronic balance weighings were usually complete within two minutes. Weight loss/gain (to/from the atmosphere) during this procedure was never significant although a check was always made by weighing the first dish again at the end of a series of measurements. These weighings allowed calculation of the amount of equilibrated zeolite in each dish. A sample of the same zeolite equilibrated previously in the same manner and analysed (in duplicate) by thermal gravimetric analysis to obtain its water content enabled the weight of anhydrous zeolite in each dish to be calculated.

Quantities of a salt were then weighed into the dishes either as the solid or more usually, because of its greater accuracy, from a previously prepared stock solution of known molality. One dish that contained zeolite was usually left salt free. Solutions were handled either with pipettes or disposable plastic syringes. Freshly boiled distilled water (water almost free of dissolved gases tends not to splutter on evacuation) was added to each dish and the dishes returned to the dessicator. A saturated solution of the salt under study was usually used to control the system vapour pressure during the initial equilibration. The equilibration was carried out as before, usually for four days but sometimes for longer. At equilibrium the amount of water in each dish (sorbed + free) was obtained by careful weighing. At this stage the solution in each dish was saturated and the amount of salt imbibed was the maximum possible from aqueous solution at 25°C. Equilibrations with saturated solutions of higher vapour pressures reduced the salt uptake and enabled data to be accumulated and isotherms to be plotted. In some cases an independent measurement of the solute concentration at different vapour pressures was made by separately equilibrating the salt over each saturated solution.

8.2.3 Materials

Details of the synthesis and compositions of the zeolitic materials used in the experiments are given in Table 8.1. All the zeolites were used in the sodium form. The chemical compositions of the solids refer to the fully prepared, not the as-synthesised, materials. Details of the treatments used to prepare the materials prior to use are given below:

FAU(1.6)

This faujasite zeolite was obtained from BDH Ltd. Although in the sodium form, ion exchange procedures were carried out before use (1M NaCl, $\sim$10 cm^3 solution g^{-1} zeolite; 2 x 2 h at R.T., 1 x 12 h at 80°C).

FAU(1.9) and FAU(2.6)

Ion exchange procedures were carried out as for FAU(1.6).

Table 8.1 Synthesis and composition of zeolitic materials used in the isopiestic experiments

Reaction mixture (moles)								Product Composition (moles)[a,h]			Product code[g]
Na_2O	Al_2O_3	SiO_2	Organic	H_2O	Temp./°C	Time/h	Product[b]	Na_2O	Al_2O_3	SiO_2	
-	-	-	-	-	-	-	Y[c]	0.91	1	3.20	FAU(1.6)
10	2.33	20	-	400	95	5	Y	0.91	1	3.76	FAU(1.9)
10	1.30	20	-	400	95	42[d]	Y	0.91	1	5.11	FAU(2.6)
10	1	60	-	3000	150	72	ZSM-5	0.97	1	31.0	ZSM-5(15.5)
10	1	60	10[e]	3000	150	72	ZSM-5	0.90	1	35.8	ZSM-5(17.9)
0.5	-	20	2[f]	1000	150	48	silicalite-1	0.001	<0.001	96	S17

[a] after preparation procedures (see text)

[b] all products were free of crystalline and amorphous impurities as determined by XRD and SEM

[c] material obtained from BDH Ltd.

[d] mixture aged at R.T. for 7 days prior to reaction

[e] hexane-1,6-diol (BDH Ltd.)

[f] tetrapropylammonium bromide (Fluka)

[g] numbers in brackets denote approximate SiO_2/Al_2O_3 ratios

[h] the ZSM-5 samples were analysed by XRF, the compositions of the other four materials were determined by wet chemical methods (courtesy of ICI, Petrochemicals & Plastics Division).

ZSM-5(15.5)

This ZSM-5 was crystallised from an 'organic free' reaction mixture. The zeolite (which was in the sodium form) was not subjected to ion exchange treatments; it was desired to use the material in its as-synthesised state.

ZSM-5(17.9)

The entrapped hexanediol in the pores of the as-synthesised crystals was removed by air calcination (450°C, 72 h; 550°C, 24 h). Exchange procedures, as given for FAU(1.6), were then carried out.

S17

The TPA template was removed from the silicalite-precursor by calcination in air (450°C, 48 h; 550°C, 24 h). The crystals were then rendered free of incorporated sodium ions by acid treatment (1M HNO_3, ~10 cm^3 solution per gram solid, 2 x 1 h at R.T., 1 x 1 h at 80°C). A further calcination (550°C, 24 h; 650°C, 12 h) completed the preparation of the silicalite.

Na-A

One experiment was carried out with zeolite 4A (Na-A) obtained from BDH Ltd. The chemical composition of this material was not determined (the Si/Al ratio was assumed to be close to unity).

The salts used in the imbibition experiments are listed in Table 8.2. The halides were dried *in vacuo* at ~180°C and stored over P_2O_5 before use. The organic salts were used as received.

Glycerol (AnalaR) was obtained from BDH Ltd. and was dried and stored over zeolite 3A pellets prior to use. Glass distilled water was employed in all experiments.

The saturated salt solutions that were used to give pre-determined vapour pressure (water activity) control during the equilibrations were generally prepared from AnalaR grade salts. Table 8.3 lists the water activities of saturated salt solutions that were widely used during these studies. Where specific water activities are mentioned in the text, reference can be made to Table 8.3 for details of the specific saturated salt solutions used.

Table 8.2 Salts used in the imbibition studies

Salt	Source/Purity
Sodium chloride	Merck (Suprapure)
Sodium bromide	BDH (99%)
Sodium iodide	Merck (Suprapure)
Sodium acetate (received as the trihydrate)	Fisons (AnalaR)
Sodium benzenesulphonate	Fluka (purum grade)
Sodium pentanesulphonate (received as the monohydrate)	Fluka (purum grade)

Table 8.3 Water activities of saturated salt solutions at 25°C [11a]

Salt*	a_w	Salt*	a_w
KNO_3	0.9248	NH_4NO_3	0.6183
$BaCl_2.2H_2O$	0.9019	$NaBr.2H_2O$	0.5770
$ZnSO_4.7H_2O$	0.8710	$Ca(NO_3)_2.4H_2O$	0.4997
KCl	0.8426	$K_2CO_3.2H_2O$	0.4276
KBr	0.8071	$MgCl_2.6H_2O$	0.3300
NH_4Cl	0.7710	$K(C_2H_3O_2).1.5H_2O$	0.2245
NaCl	0.7528	$LiCl.H_2O$	0.1105

* The solid phase

8.2.4 Representation and calculation of results

The raw experimental results are presented as 'imbibition plots'. A schematic drawing of such a plot is depicted in Figure 8.1. In most cases, both the 'solid phase' and 'solution phase' portions of the plots were linear. The equations which represented these straight lines were evaluated by standard least mean squares methods and the intersection points were then calculated. A computer program was written in basic (for an Apple II microcomputer) to (i) undertake this numerical analysis and (ii) graphically plot the results.

Usually each imbibition plot was constructed from eight data points - the number of dishes, and hence salt/zeolite mixtures, in a dessicator was limited to eight. The W_s/W_z values of the mixtures were chosen to cover a considerable range in order to ensure that several points on both sides of the intersection points were obtained. Inevitably though, this was not always the case; in instances where very little salt was imbibed, most of the mixtures contained a solution phase and very few, sometimes only the salt-free solid, were dry. By interpolation though, imbibition data was still obtainable. This will become clear from the results presented. Of course it is possible to alter the W_s/W_z value of a mixture at any time during a series of isopiestic equilibrations in order to ensure there are points on both sides of the intersection value. This procedure was practiced on occasion.

8.3 Results and Discussion: Adsorption of electrolytes from aqueous solution by zeolites

8.3.1 NaCl + Na-Faujasite

Faujasite has one of the most open structures of all known zeolites. Entry to its pore network is through 12 T-atom windows and almost 50% of its crystal volume is void. As such, faujasites lend themselves to salt imbibition studies. Zeolites with faujasite structure can be crystallised under a variety of different conditions and as a result crystals with different chemical compositions can be made. This fact, coupled with the ability to modify the materials after synthesis if desired, means that a host of topologically identical but chemically different zeolites can be readily aquired. Ways in which their chemistries affect their properties, in the context of this work the extent to which they take up salts from aqueous solution, can be investigated.

Three faujasites have been used in this work. Two were crystallised in the laboratory, the other by a commercial manufacturer. As mentioned in section 8.2.3, each was crystallographically pure and each was converted to the sodium form by repeat exchange procedures. Their compositions, although already given in Table 8.1, are shown again in unit cell form below:

$67.2Na\ 6.6H\ [73.8AlO_2\ 118.2SiO_2]\ 237.4H_2O$ Si/Al = 1.60

$60.7Na\ 6.0H\ [66.7AlO_2\ 125.3SiO_2]\ 256.7H_2O$ Si/Al = 1.88

$49.1Na\ 4.9H\ [54.0AlO_2\ 138.0SiO_2]\ 242.8H_2O$ Si/Al = 2.56

The densities of the anhydrous materials were calculated to be 1.43, 1.41 and 1.39 g cm^{-3} respectively. For these calculations framework densities were taken to be 12.7 T-atoms/1000 $Å^3$ [12]. The water contents represent the amount adsorbed after equilibration at p/p_o = 0.753 (saturated sodium chloride solution) at 25°C. These water adsorption results show an interesting trend. As the silicious nature of the faujasite increases, the amount of water sorbed first of all increases; this is due to a reduction in the number of cations in the channels and concommittant increase in the void space available for water. However when the silicon content of the framework increases substantially, the 'hydrophobic' nature of the lattice dominates the effect of greater void space and less water is adsorbed.

The three faujasites mentioned above were designated FAU(1.6), FAU(1.9) and FAU(2.6) respectively, the numbers representing the approximate Si/Al ratios of the materials. The imbibition of sodium chloride by these three zeolites is now discussed. The NaCl/Faujasite system was chosen for initial study because imbibition data obtained by 'past' means on similar systems was available for comparison.

NaCl + FAU(1.9)

Figure 8.5 shows a selection of the experimental results as plots of W_s/W_z against W_w/W_z. Plots such as these will be referred to as 'imbibition plots' henceforth. Sodium chloride was readily imbibed by FAU(1.9) and straight lines corresponding to equations (8.8) and (8.9) were obtained. These lines have substantially different slopes and their intersection points were readily interpolated. Each plot refers to a different

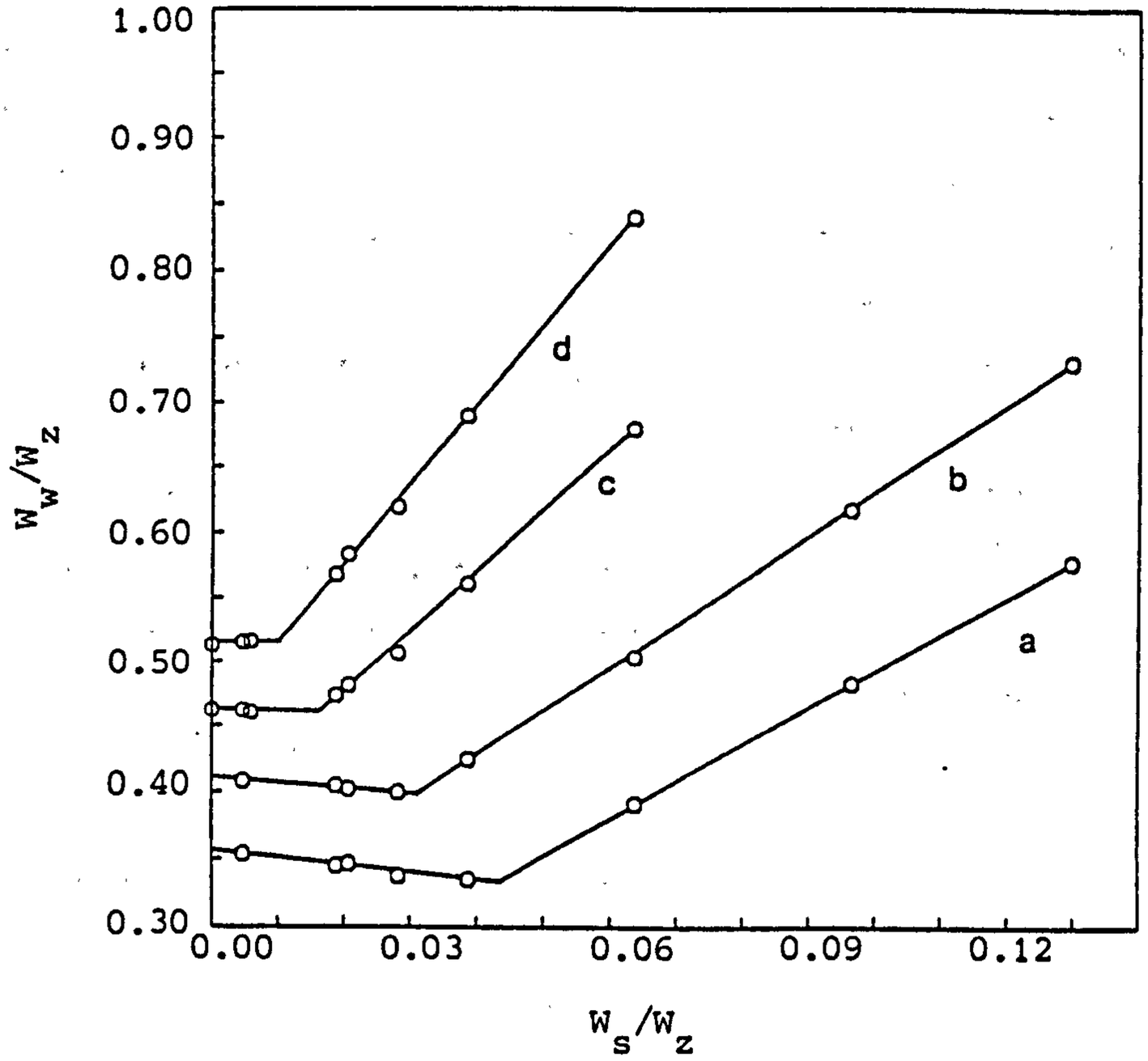

Figure 8.5 Imbibition plots for NaCl + FAU(1.9) at selected water activities: (a) 0.753; (b) 0.807; (c) 0.871; (d) 0.902. Plot (a) shows the maximum NaCl uptake possible from aqueous solution at 25°C; this equilibration was carried out over saturated sodium chloride solution. Plots (b), (c) and (d) have been respectively displaced by 0.05, 0.10 and 0.15 units on the ordinate axis for clarity.

water activity ($a_w = p/p_o$) and hence a different sodium chloride concentration. The lines with zero or negative gradients are given by equation (8.9) and represent the salt/zeolite mixtures that are 'dry'. The slope of these lines becomes more negative as the water activity decreases; this corresponds to an increase in the amount of water displaced from the zeolite by unit weight of imbibed salt. The lines with positive slopes in Figure 8.5 are given by equation (8.8) and represent salt/zeolite mixtures for which there is a solution phase at equilibrium. As the equilibrium solution concentration increases, the gradients of these lines decrease; the solution concentration is in fact given by the reciprocal of the gradient (see section 8.1.2). Note that some of the salt/zeolite mixtures that were 'solution phase' at low sodium chloride molalities become 'dry' as the equilibrium vapour pressure is lowered and more salt is imbibed. Parameters derived from the results in Figure 8.5 and from similar results at other water activities are shown in Table 8.4.

Figure 8.6 shows how the salt and water contents of the zeolite samples in equilibrium with solution change with the molality of the external solution phase. The water content of the zeolite samples in equilibrium with solution phases depends on the water activity of the solution phase and on the amount of salt imbibed. The effect of salt imbibition on the water content can be seen at high solution concentrations as the difference between U_w^o and U_w and it is clear that salt molecules displace some of the water. The known water and salt contents of the zeolite at each equilibrium position enabled an effective 'molality' of internal salt (m_i) to be calculated (see Table 8.4). Values are compared with the molalities of the external solution phases in Figure 8.7.

The maximum sodium chloride uptake from aqueous solution corresponds to that from saturated sodium chloride solution (Figure 8.5, plot (a)). The calculated value of the equilibrium solution phase concentration over saturated sodium chloride solution was 6.04 mol kg^{-1} and this corresponded to a salt uptake of 0.043 g/g and an internal salt molality of 2.21 mol kg^{-1} water.

Table 8.4 Imbibition results for NaCl + FAU(1.9)

a_w [a]	Solid phase line		Solution phase line		Intersection point		
	k [b]	U_w^o	R_{sol}	m [c]	$10^3 U_s$	U_w	m_i [e]
-	f	0.384	27.55	0.621	0.0	0.384	0.000
-	f	0.376	15.72	1.089	0.5	0.376	0.024
-	2.514	0.372	9.225	1.855	1.9	0.377	0.087
0.925	0.615	0.369	7.625	2.244	3.1	0.371	0.142
0.902	0.482	0.363	6.025	2.840	10.5	0.368	0.487
0.871	-0.249	0.362	4.619	3.705	16.2	0.358	0.776
0.843	0.129	0.358	4.023	4.254	25.2	0.362	1.194
0.807	-0.346	0.360	3.388	5.051	31.9	0.349	1.565
0.771	-0.537	0.357	2.871	5.961	37.0	0.337	1.879
0.753	-0.572	0.357	2.834	6.039	42.9	0.332	2.211
0.577	-0.524	0.352	d	-	49.1	0.327	2.572
0.428	-0.522	0.346	d	-	51.8	0.317	2.779
0.330	-0.559	0.337	d	-	59.9	0.306	3.378
0.111	-0.496	0.313	d	-	78.2	0.274	4.878

[a] controlled by saturated salt solutions (refer to Table 8.3)

[b] gradient of the solid phase line

[c] molality of the external solution phase, mol kg^{-1}

[d] no solution phase present

[e] molality of the salt 'solution' in the zeolite, mol kg^{-1} water

[f] gradient assumed to be zero, i.e. $U_w = U_w^o$

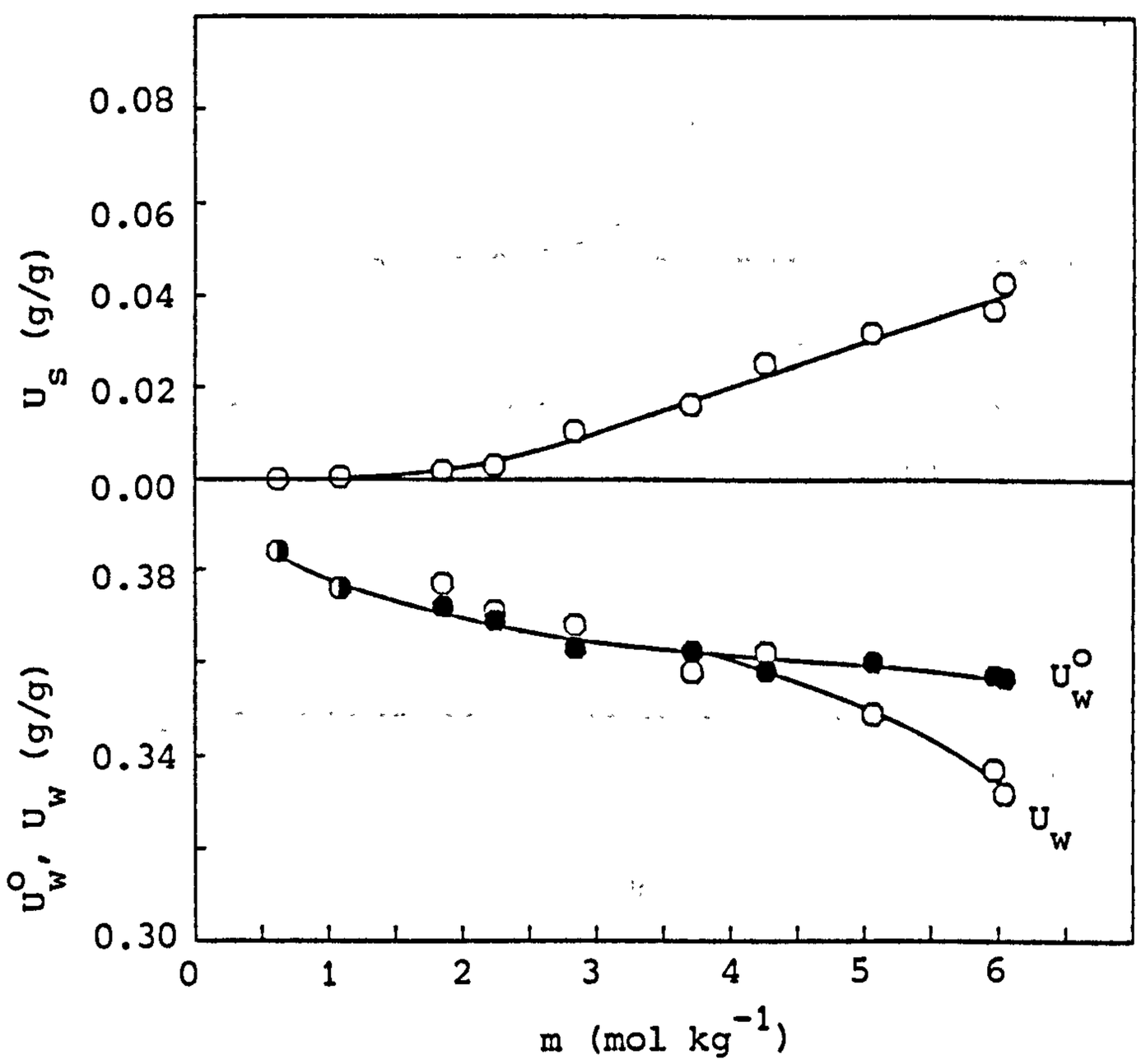

Figure 8.6 Uptake of NaCl and water by FAU(1.9) as a function of solution phase molality (m). U_w^o represents the water content of the salt free zeolite, U_w and U_s represent the water and salt contents of the zeolite samples in contact with a solution phase.

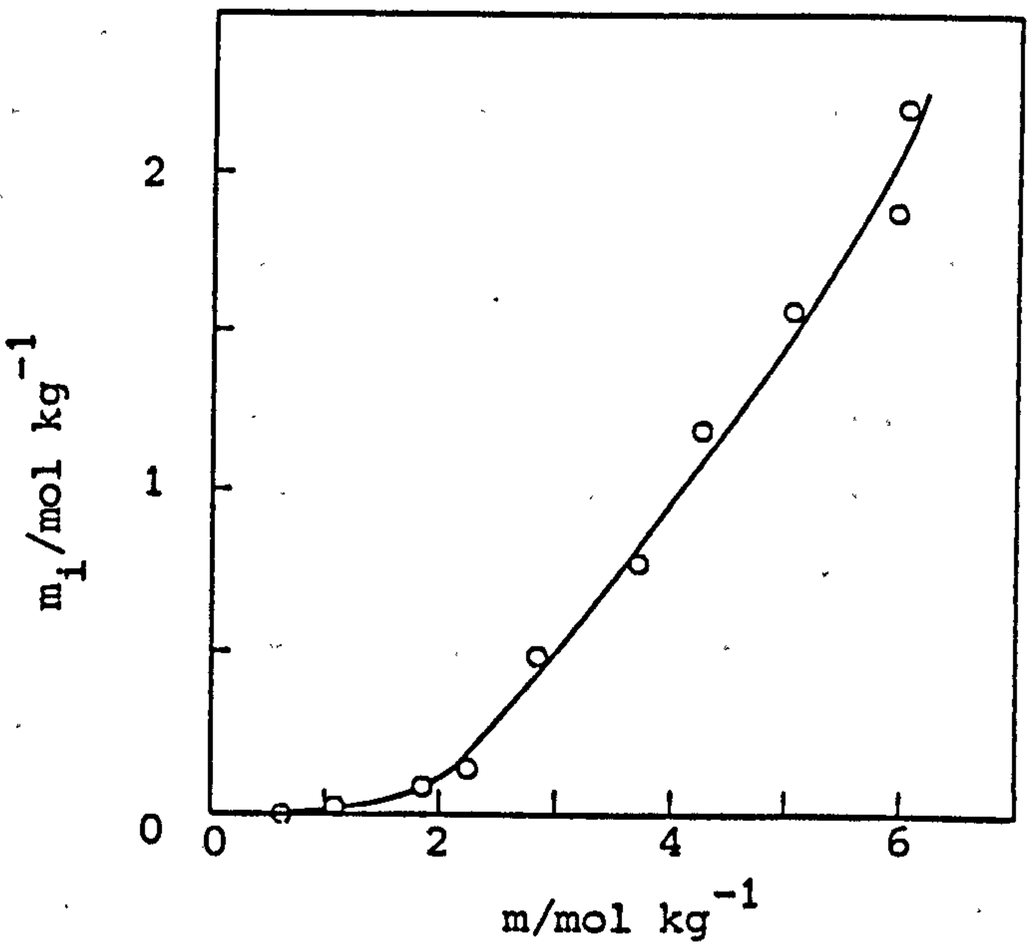

Figure 8.7 Internal molality (m_i) of NaCl in FAU(1.9) as a function of the solution phase molality (m).

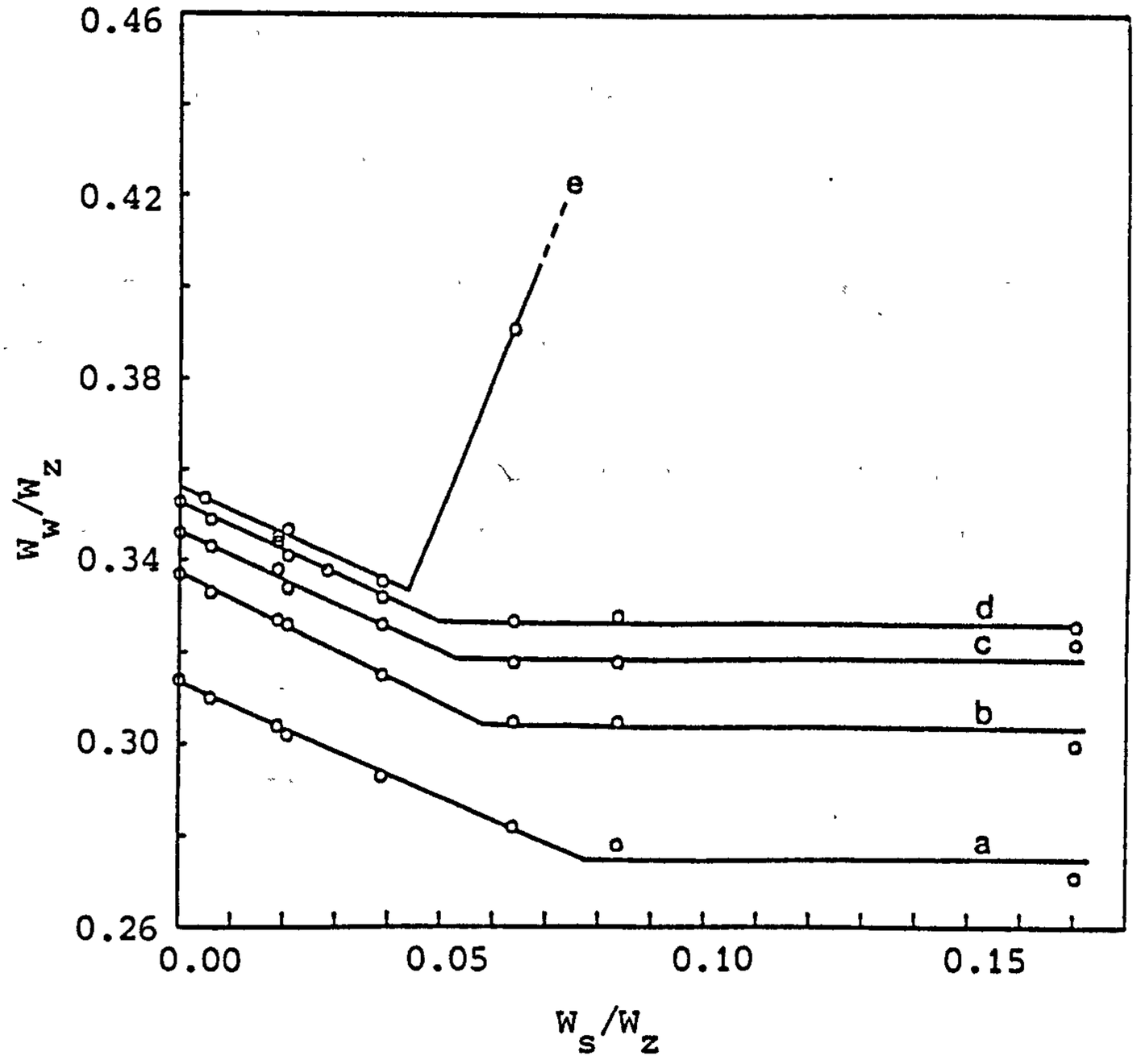

Figure 8.8 Imbibition results for NaCl + FAU(1.9) at water activities below that of saturated sodium chloride solution (a_w = 0.753). The equilibrium water activities were (a) 0.111; (b) 0.330; (c) 0.428; (d) 0.577 and (e) 0.753.

Greater salt uptakes were observed when the zeolite samples were equilibrated with sodium chloride at water vapour pressures below that of saturated sodium chloride solution. Experimental results obtained under these conditions are shown in Figure 8.8. The lines with negative slopes correspond, as before, to situations where all salt is imbibed whereas the horizontal lines are for zeolite samples that contain the maximum amount of imbibed salt, at the specified water vapour pressures, in equilibrium with solid salt. In these instances there is no solution phase and the excess salt is in contact with the external surfaces of the zeolite crystals. The intersections in Figure 8.8 correspond to the values of U_s and U_w for zeolites that contain the maximum amount of imbibed salt and these are given in Table 8.4.

Figure 8.9 shows the internal molality of NaCl in the zeolite as a function of water activity. The linear portion corresponds to equilibrations with NaCl solutions and the curved portion to equilibrations involving the zeolite and solid NaCl at water activities below that of saturated sodium chloride solution.

These results show that under the experimental conditions employed equilibria are readily established between the zeolite and a solution phase and at lower water activities between the zeolite and a solid surface salt phase. When water from a saturated salt solution in contact with a zeolite is isothermally distilled off (as it was during these experiments) further salt molecules are taken up into the pores of the zeolite. Very similar although less controlled procedures are often the first step in the preparation of zeolite catalysts. Catalytically active components, for example nickel, are often impregnated into zeolites as salts. Procedures involve adding a zeolite to a concentrated salt solution and then driving the water off with heat treatment. It is important to note that subsequent handling of zeolites salt-loaded by such methods requires care. Salt-loaded zeolites have to be stored in conditions of controlled humidity and temperature if the salt is to remain within the zeolite and the experiments described below demonstrate this clearly.

PAGE NUMBERING AS ORIGINAL

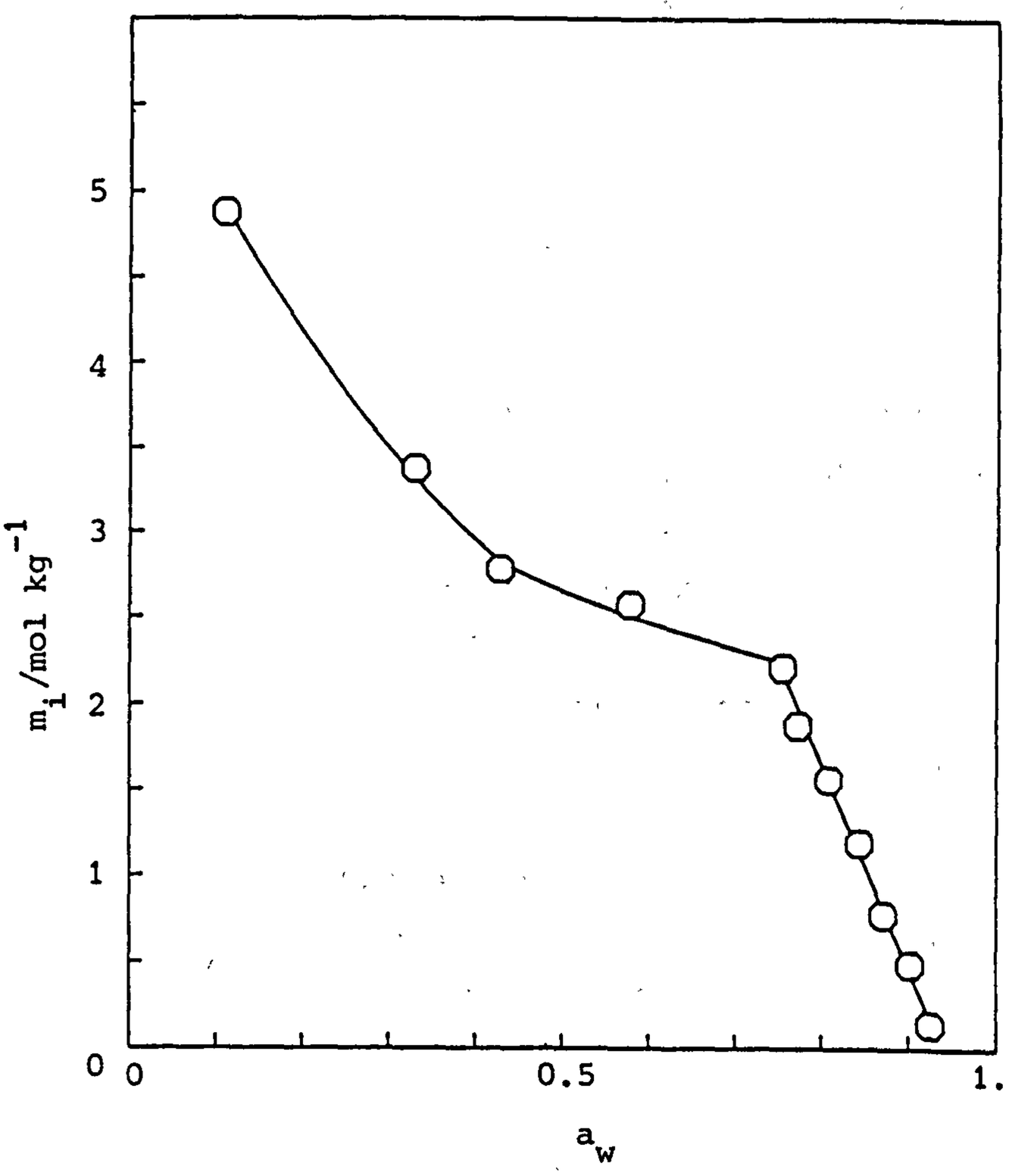

Figure 8.9 Internal molality (m_i) of NaCl in FAU(1.9) as a function of water activity

To show that salt molecules readily move between the zeolite and a surface salt phase, several experiments using X-ray powder diffraction were undertaken. Solid sodium chloride in contact with the external surfaces of zeolite crystals should, if crystalline, be readily observable by XRD; pure sodium chloride has an intense diffraction line at ∿31.8° 2θ. XRD experiments were carried out on the NaCl/FAU(1.9) mixtures used in the aforementioned salt imbibition studies. These experiments were performed once all the imbibition data for the NaCl/FAU(1.9) system had been accumulated as the samples could not be disturbed in any way during the series of isopiestic equilibrations. The procedure adopted was straight-forward. The equilibrations over saturated $MgCl_2$ and LiCl were repeated (Figure 8.8 shows the results originally obtained at these two vapour pressures - plots (b) and (a) respectively) and, after each, three selected salt/zeolite mixtures (with W_s/W_z = 0.0387, 0.0637 and 0.1703) were removed from the dessicator and immediately analysed by XRD for surface salt. Results are shown in Figure 8.10 along with drawings of the two original imbibition plots that have already been given in Figure 8.8. Crystalline NaCl was detected in the salt/zeolite mixture with W_s/W_z = 0.0637 after equilibration over $MgCl_2$. This mixture contains more salt than can be imbibed at this vapour pressure and the presence of surface salt was expected from the imbibition plot. The imbibition results for equilibration over saturated LiCl indicated that no surface salt should be seen in this same mixture and this was borne out by XRD analysis as Figure 8.10 shows. However after leaving the sample in the laboratory for a short time (at 71.5% R.H. and 18°C) a sodium chloride peak was detected. This peak increased in intensity over time as salt emanated from the zeolite's pores and the sample equilibrated with its surrounding atmsophere (Figure 8.11). Had the laboratory been more humid, the deposited sodium chloride would have eventually dissolved.

NaCl + FAU(1.6)

The faujasite used for this experiment was the most aluminous of the three available. Imbibition results for NaCl into FAU(1.6) are shown in Table 8.5. Figure 8.12 shows some of the imbibition plots that were obtained. The four uppermost plots (a-d) show the effects of altering the equilibrium solution phase concentration; as the molality of the

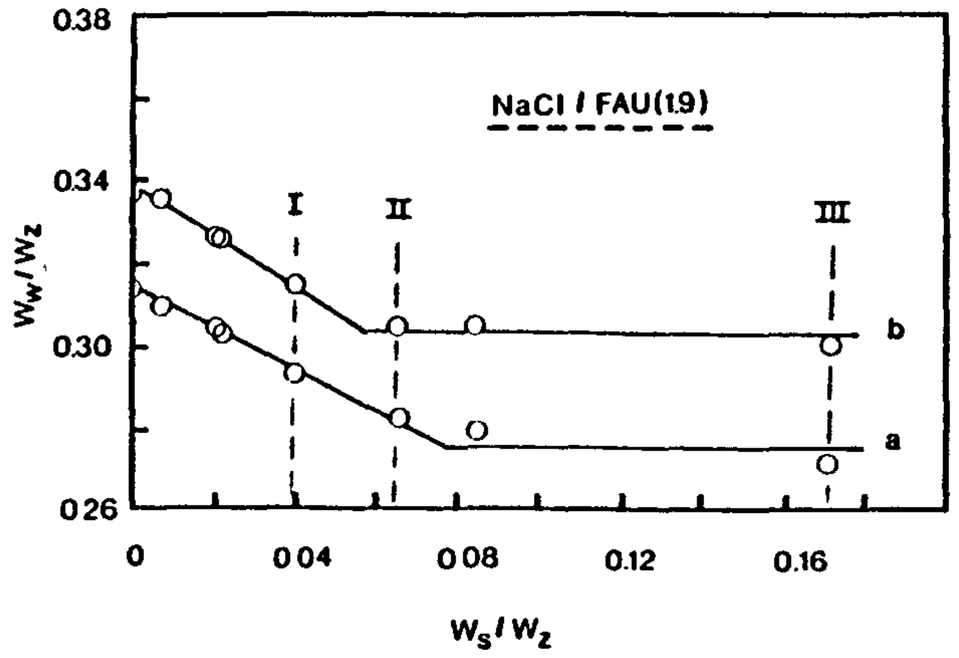

Plot a : $a_w = 0.11$

Plot b : $a_w = 0.33$

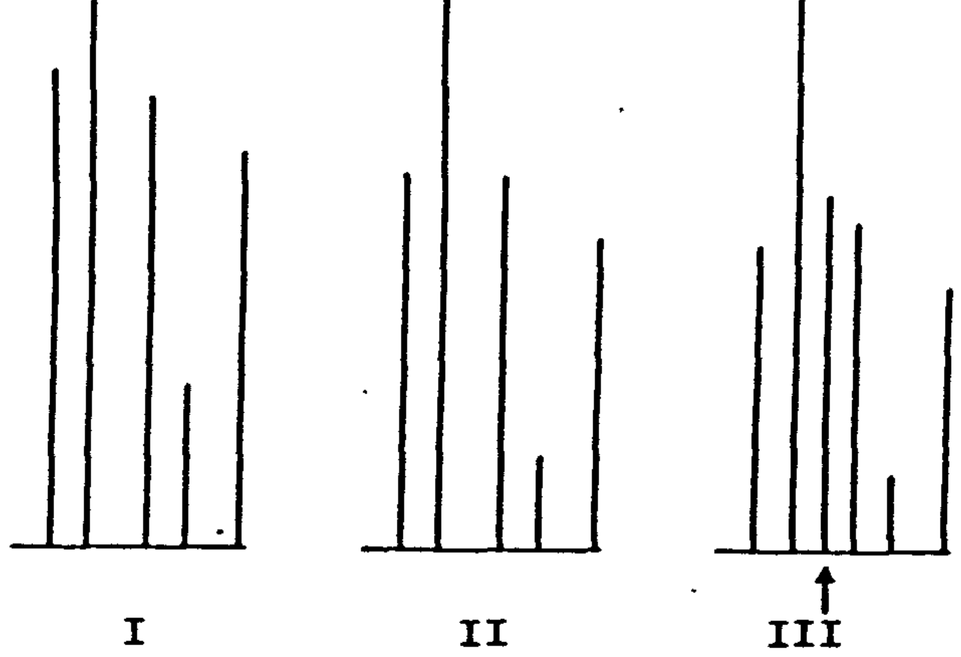

(after equilibration at $a_w = 0.11$)

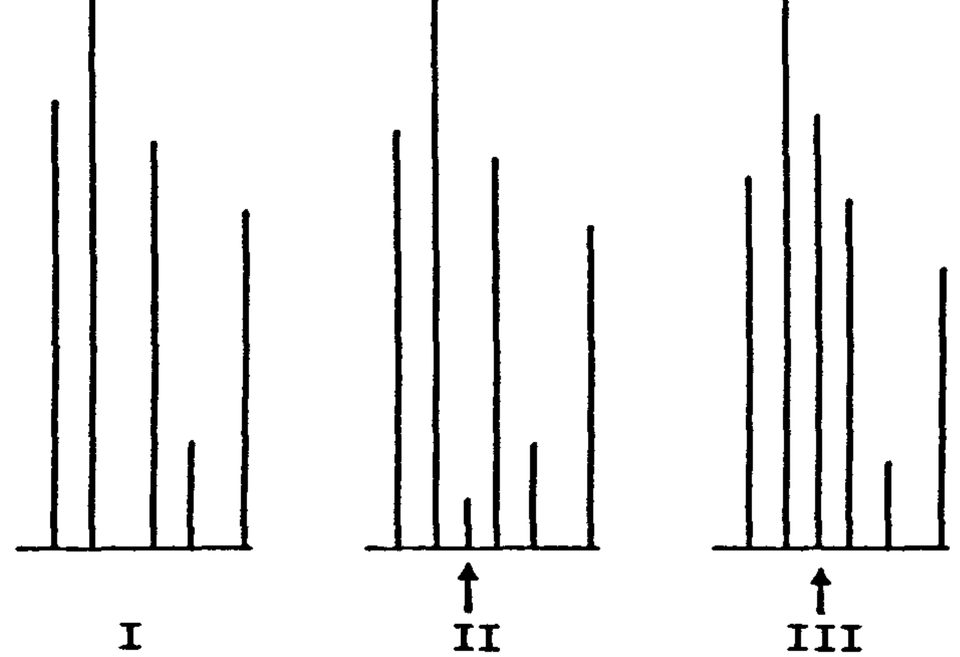

(after equilibration at $a_w = 0.33$)

Figure 8.10 Line representations of the X-ray powder diffraction patterns of three NaCl/FAU(1.9) mixtures (between 30-34° 2θ) after equilibration at $a_w = 0.11$ and $a_w = 0.33$. The W_s/W_z values of the mixtures were (I) 0.0387, (II) 0.0637 and (III) 0.1703. The arrows indicate the presence of a diffraction line due to crystalline NaCl, all other lines are due to the zeolite. The XRD results correlate with the imbibition plots shown.

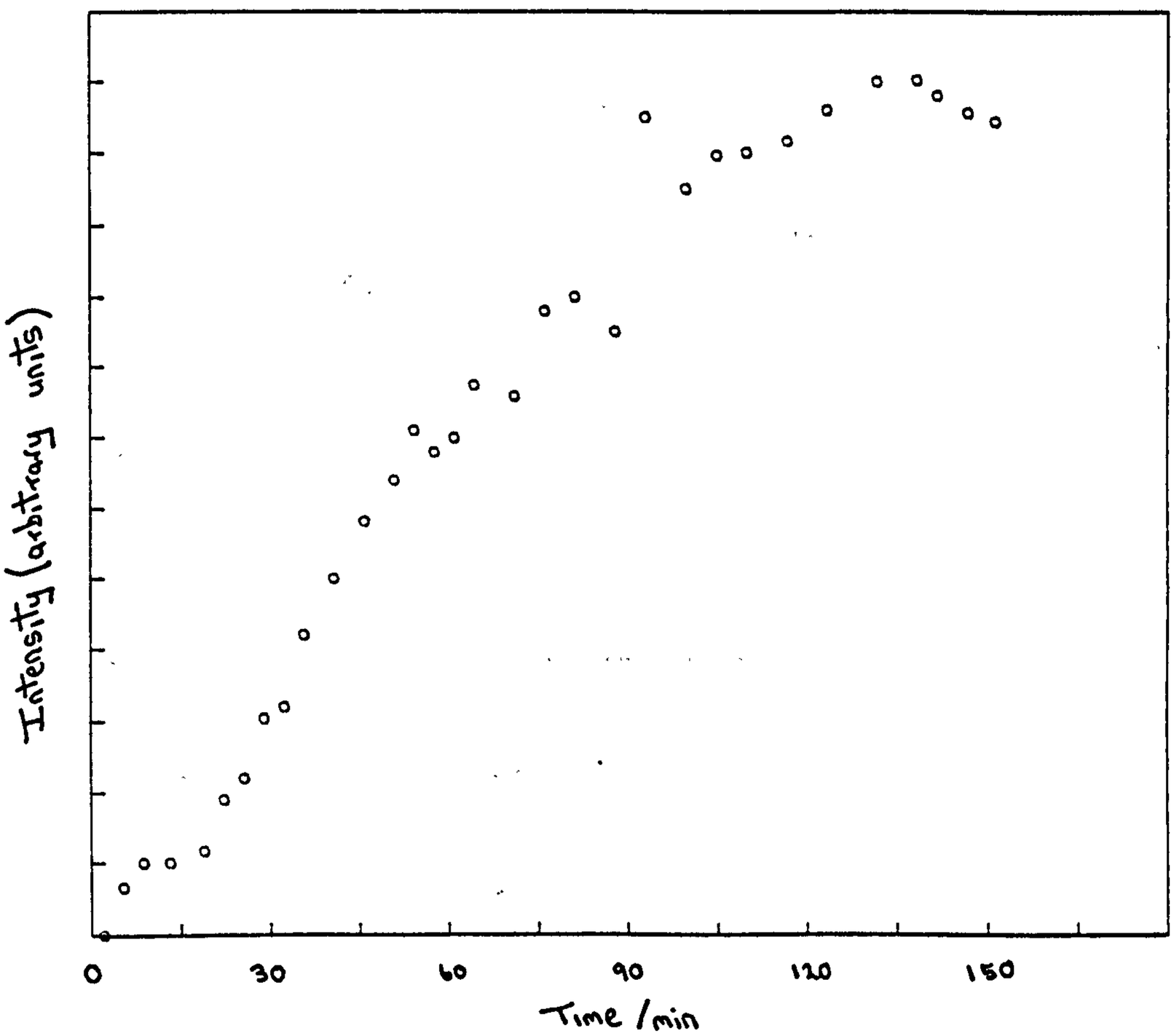

Figure 8.11 Intensity of the XRD peak at ∿31.8° 2θ (due to NaCl) as a function of time for the NaCl/FAU(1.9) mixture with W_s/W_z = 0.0637. The mixture was equilibrated at a_w = 0.11 prior to the experiment and then scanned continuously for several hours. During this procedure the sample was 'open' to the laboratory atmosphere (71.5% R.H., 18°C). This atmosphere caused salt to egress from the pores of the zeolite.

Table 8.5 Imbibition results for NaCl + FAU(1.6)

	Solid Phase Line		Solution Phase Line		Intersection Point		
a_w [a]	k [b]	U_w^o	R_{sol}	m [c]	$10^3 U_s$	U_w	m_i [e]
0.925	f	0.346	7.903	2.165	7.9	0.346	0.391
0.902	f	0.347	6.183	2.768	13.3	0.347	0.655
0.871	0.465	0.341	4.899	3.493	22.1	0.351	1.077
0.843	0.221	0.339	4.087	4.187	29.6	0.345	1.469
0.807	0.098	0.336	3.440	4.974	38.3	0.340	1.928
0.753	-0.091	0.334	2.790	6.133	51.0	0.329	2.649
0.618	-0.426	0.330	d	-	50.5	0.308	2.802
0.500	-0.491	0.327	d	-	57.0	0.299	3.264
0.428	-0.509	0.324	d	-	58.2	0.294	3.384
0.330	-0.523	0.315	d	-	61.8	0.282	3.743
0.225	-0.503	0.307	d	-	61.3	0.276	3.796
0.111	-0.481	0.294	d	-	63.9	0.263	4.163

* see Table 8.4 for footnotes

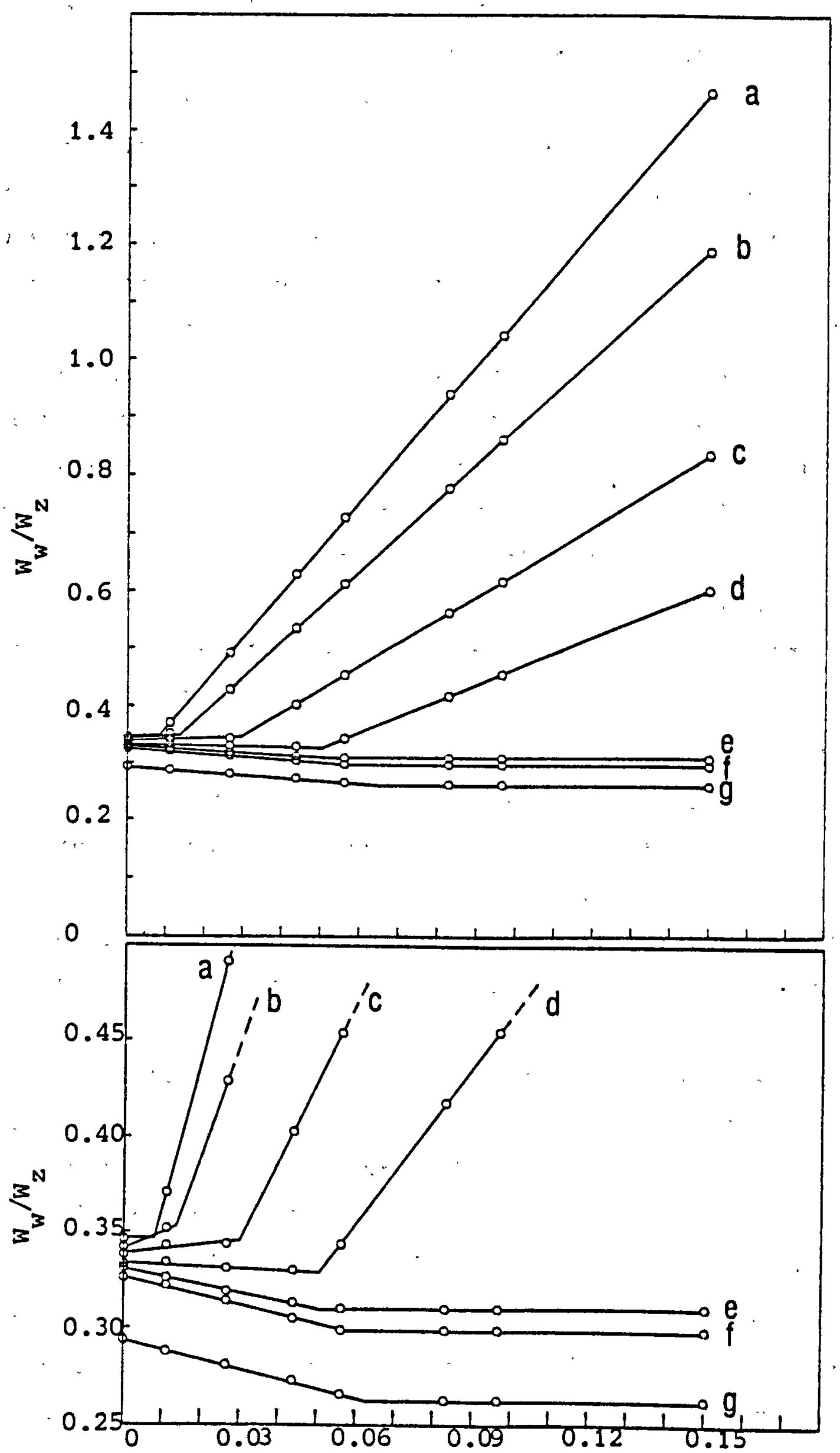

Figure 8.12 Imbibition plots for the NaCl/FAU(1.6) system at different water activities: (a) 0.925, (b) 0.902, (c) 0.843, (d) 0.753, (e) 0.618, (f) 0.500, (g) 0.111. The lower figure is simply a larger scale version of the upper and shows the intersection points with greater clarity.

solution increases, salt is taken up to a greater extent. The lowermost plots (e-g) in Figure 8.12 represent equilibria, between the zeolite samples and solid salt, at vapour pressures below that of saturated sodium chloride solution. As before, it was observed that salt is imbibed to a greater extent when equilibrations are carried out under these conditions. The lower diagram in Figure 8.12 is simply a larger scale version of the one above and it shows the intersection points with greater clarity. The horizontal sections of plots (e-g) are parallel and represent situations in which zeolite samples that contain the maximum amount of imbibed salt are in equilibrium with solid salt on the external surfaces of the crystals. It can be clearly seen that as the equilibrium water vapour pressure is decreased, the intersection point moves to higher W_s/W_z and lower W_w/W_z values. The portions of plots (e-g) with negative gradients represent salt/zeolite mixtures for which all the salt is imbibed. The gradients of these portions are similar. The results at low and high water activities are summarised in Figure 8.13.

Several points about the high water activity results deserve mention. Figure 8.12 shows that at high vapour pressures (for example, plots (b) and (c)) the 'solid phase lines' have positive gradients; the presence of small amounts of imbibed salt apparently increases the water content of the zeolite (relative to the salt-free material). However there could be alternative explanations for these results. They could for example be a simple artifact of the system arising from slightly inhomogeneous salt/zeolite mixtures; the high water contents could be due to the presence of a solution phase in part of the sample. Microcapillarity problems may also be contributory. The effect is not unique to either the zeolite, FAU(1.6), or to sodium chloride as similar effects have been observed with other zeolites and salts.

At very high vapour pressures (e.g. plot(a), Figure 8.12) all the experimental salt/zeolite mixtures contained a solution phase and only the dish that contained salt-free zeolite was 'dry'. However the plot indicates, as can be seen from the figure, that some salt is imbibed - the solution phase line does not extrapolate to the water content of the salt-free zeolite at that vapour pressure. If the zeolite samples in equilibrium with solution phases are deemed to have water contents equivalent to that of the salt free zeolite, i.e. if the 'imaginary' solid phase line is assumed horizontal, an intersection point can be

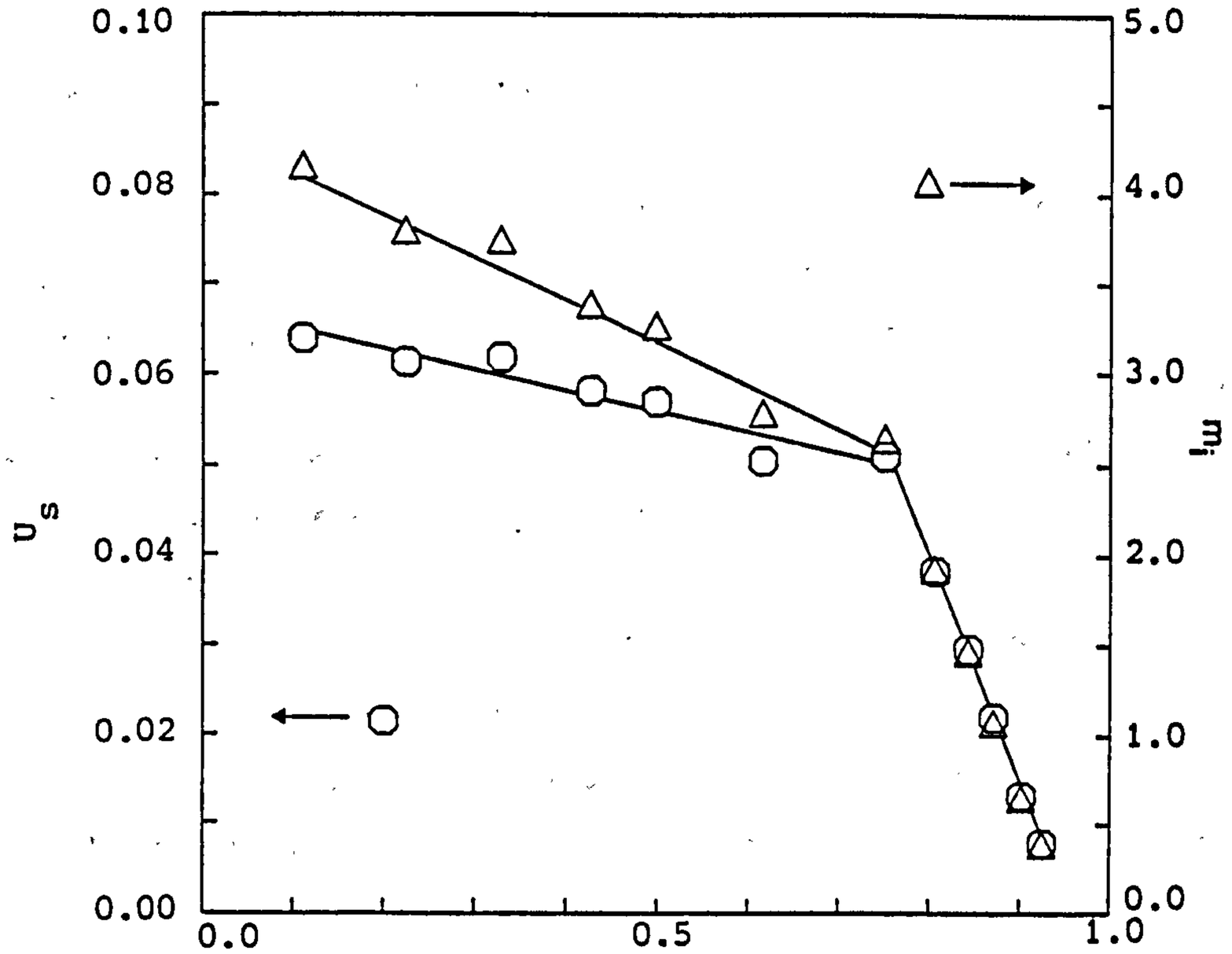

Figure 8.13 Imbibition of NaCl into FAU(1.6) as a function of water activity. Both the salt uptake (U_s) and the internal salt molality (m_i) are shown. Both plots show a distinct break at a_w = 0.75, the water activity of saturated NaCl solution.

calculated and the amount of imbibed salt determined. Clearly the solid phase line may actually have a positive gradient and would be expected to have if the trend of plots (b) and (c) continued at higher vapour pressures. However, as the gradient of the solution phase line is large and positive under these equilibration conditions, the amount of imbibed salt determined from the intersection point is similar regardless of whether the solid phase line is taken to be horizontal or of positive gradient. The respective values for the water contents of the zeolites differ somewhat more though. It was not felt necessary to set up a further experiment with salt/zeolite mixtures of low W_s/W_z values to investigate imbibition from dilute solutions further. The most interesting areas for investigation are the salt uptake from relatively concentrated aqueous solutions and from the solid phase at vapour pressures below that of saturated sodium chloride solution. Work has shown though that, if desired, isopiestic experiments can be set up with low ratio salt/zeolite mixtures and results successfully obtained.

These isopiestic experiments with zeolites involve equilibration of salt/zeolite mixtures of known but different stoichiometries at different vapour pressures and subsequent determination of their water contents. In the case of the NaCl/FAU(1.6) mixtures, data presented so far has been in the form of imbibition plots, plots of W_s/W_z against W_w/W_z. This same data can be graphically presented in a rather different way; for each salt/zeolite mixture a water adsorption isotherm can be plotted (Figure 8.14). These isotherms differ from orthodox isotherms in that, relative to the salt-free zeolite, the water contents of the salt/zeolite mixtures are either depressed (if salt is imbibed) or increased (if salt is present as a solution). The extent of depression/enhancement depends on the salt/zeolite weight ratio and on the equilibrium vapour pressure. At low water activities, the isotherms of certain salt/zeolite mixtures, those that contain the maximum amount of imbibed salt with excess solid salt on the zeolite crystal surfaces (curves F, G and H in Figure 8.14), are coincident. The isotherms for these mixtures (F-H) are characterised by discontinuitues at $a_w = 0.753$, the water activity of saturated sodium chloride solution, when the surface salt dissolves to form an external solution phase. Marked increases in the water content of the mixtures with low W_s/W_z ratios are observed at water activities above 0.753 because in these cases the salt/zeolite

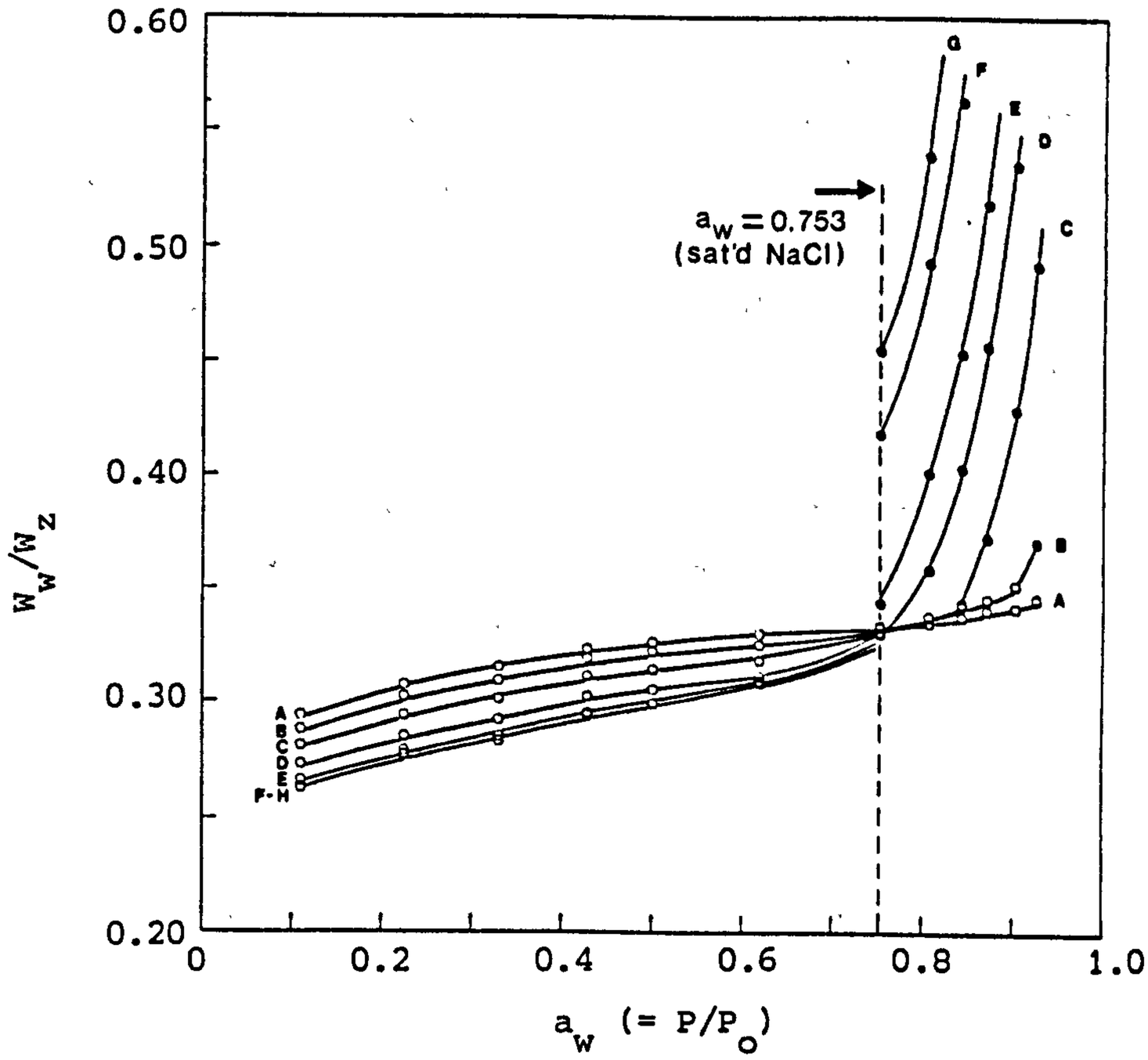

Figure 8.14 Water adsorption isotherms for NaCl/FAU(1.6) mixtures with different W_s/W_z ratios: (A) W_s/W_z = 0, (B) 0.0110, (C) 0.0265, (D) 0.0437, (E) 0.0561, (F) 0.0829, (G) 0.0966, (H) 0.1496. The filled circles denote situations where some of the water is present in an external solution phase.

stoichiometries are such that salt only begins to egress from the pores at high vapour pressures. Water adsorption isotherms of salt loaded zeolites thus show very characteristic features. Similar isotherms could arise if salts were ever accidently left in contact with zeolite samples. If zeolites are not washed free of adherent and/or adsorbed salts after synthesis or after, for example, post-synthesis ion exchange procedures then water adsorption results could be anomalous. Similar situations to this could arise in instances where inorganic salts are entrapped in high silica zeolites by organic pore-fillers. After calcination, movement of such salt molecules is no longer restricted and they may well egress from the channels and render water adsorption data spurious. Indeed high silica zeolites would not be expected to have a strong affinity for the retainment of 'synthesis entrained' inorganic salts within their pores.

The phenomenon of salt hydrolysis deserves mention with regard to the isotherms discussed above. If a small amount of FAU(1.6) is put into water a substantial pH rise is observed due to cation hydrolysis (hydronium ion exchange).

$$\text{Na-Z} + \text{H}_2\text{O} \rightleftharpoons \text{H-Z} + \text{NaOH(aq)}$$

Hydrolysis occurs because the zeolite is the salt of a weak acid and a strong base and is suppressed in solutions that contain the same cation as the zeolite.

By inference though, it follows that if the zeolite is equilibrated with water through the vapour phase a hydrolysis equilibrium must be set up and this must involve some free sodium hydroxide. The point raised here concerns the whereabouts of these sodium hydroxide molecules. The amount of sodium hydroxide produced by hydrolysis is small and this can be gauged from the pH values attained when samples are put in water (pH = 10-11). By analogy with the results for NaCl imbibition, it follows that the sodium hydroxide is likely to remain in the lattice at low and intermediate vapour pressures but will egress and form a solution phase on the external surfaces of zeolite crystals at high water vapour pressures. This same effect would be expected of many other aluminous zeolites. Zeolites that contain a substantial amount of aluminium and which are highly

charged would be expected to readily imbibe charged species and the effect of sodium hydroxide egress would probably only be seen at very high vapour pressures. Such egression though may be a contributory reason, along with capillarity, to the enhanced water uptakes on zeolites that are often observed at high vapour pressures (see Figure 7.2).

The presence of base molecules formed by cation hydrolysis, or base molecules entrained during synthesis, in the pores of high silica zeolites is probably a more serious problem. Electrolytes such as NaOH would not be expected to be readily imbibed by organophilic materials; such molecules would be far more likely to egress from the channels and from solutions, even at low vapour pressures. Spurious and enhanced water adsorption data would result. Discussions and results in Chapter 6 relating to silicalite-1 have already highlighted this problem.

NaCl + FAU(2.6)

FAU(2.6) was the most silicious of the three faujasites used in these studies. Even so, sodium chloride was readily imbibed by this zeolite (Table 8.6 and Figure 8.15). Figure 8.15 shows that at low water vapour pressures the salt/zeolite mixtures with weight ratios close to the equilibrium salt uptake (i.e. close to the intersection point) had anomalously high water contents. This suggested that these mixtures were not in true equilibrium; apparently too much solid salt was present on the crystal surfaces and too little present in the zeolite's pores. This was probably due to sample inhomogeneity and it is significant that this problem was only encountered at low vapour pressures when the zeolite samples were equilibrated with solid salt. Understandably equilibrium is more readily attained for mixtures that have salt/zeolite weight ratios either substantially less or greater than the equilibrium (intersection) salt uptake. Clear intersections (from which results were calculated) were interpolated from the salt/zeolite mixtures that were in 'true' equilibrium.

To test the reproducibility of the isopiestic method, a second experiment was carried out with NaCl/FAU(2.6) mixtures different from those previously used but covering the same weight ratio range. Results obtained at two different water activities are compared with those originally obtained in Figure 8.16. For the equilibrations over

Table 8.6 Imbibition results for NaCl + FAU(2.6)

	Solid phase line		Solution phase line		Intersection point		
a_w [a]	k [b]	U_w^o	R_{sol}	m [c]	$10^3 U_s$	U_w	m_i [e]
0.925	f	0.355	7.828	2.186	2.7	0.355	0.129
-	f	0.353	6.818	2.510	3.8	0.353	0.186
0.871	f	0.352	4.816	3.553	9.7	0.352	0.473
0.843	-0.118	0.351	4.054	4.222	17.0	0.349	0.834
0.807	-0.238	0.350	3.398	5.037	23.6	0.345	1.172
0.753	-0.333	0.349	2.751	6.220	34.8	0.337	1.769
0.618	-0.450	0.346	d	-	43.2	0.326	2.265
0.500	-0.485	0.341	d	-	44.7	0.320	2.391
0.428	-0.489	0.338	d	-	51.7	0.313	2.829
0.330	-0.524	0.339	d	-	58.4	0.300	3.329
0.225	-0.523	0.323	d	-	65.5	0.289	3.880
0.111	-0.493	0.306	d	-	68.8	0.272	4.320

* see Table 8.4 for footnotes

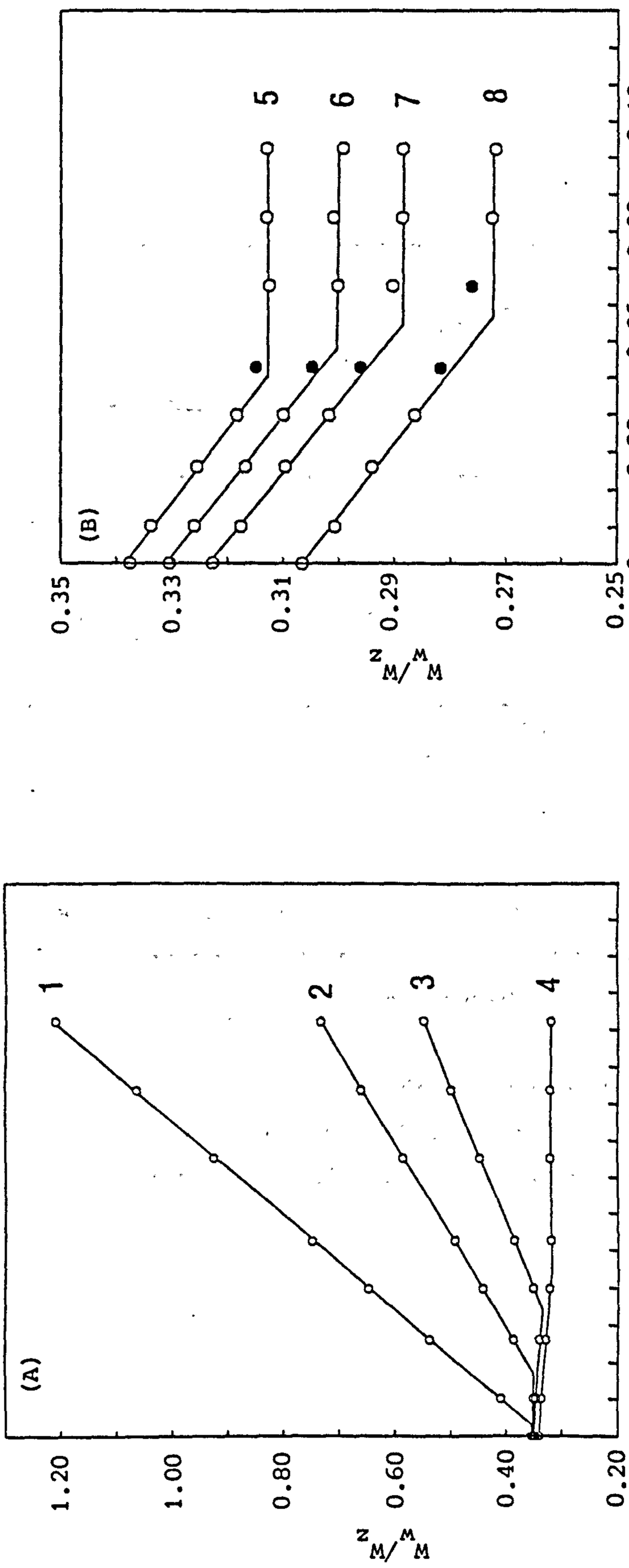

Figure 8.15 Imbibition plots at different water activities for the NaCl/FAU(2.6) system

(A) The plots correspond to the following water activities: 1, 0.925; 2, 0.843; 3, 0.753; 4, 0.500

(B) The plots correspond to the following water activities: 5, 0.428; 6, 0.330; 7, 0.225; 8, 0.111. The filled circles probably represent non-equilibrium situations.

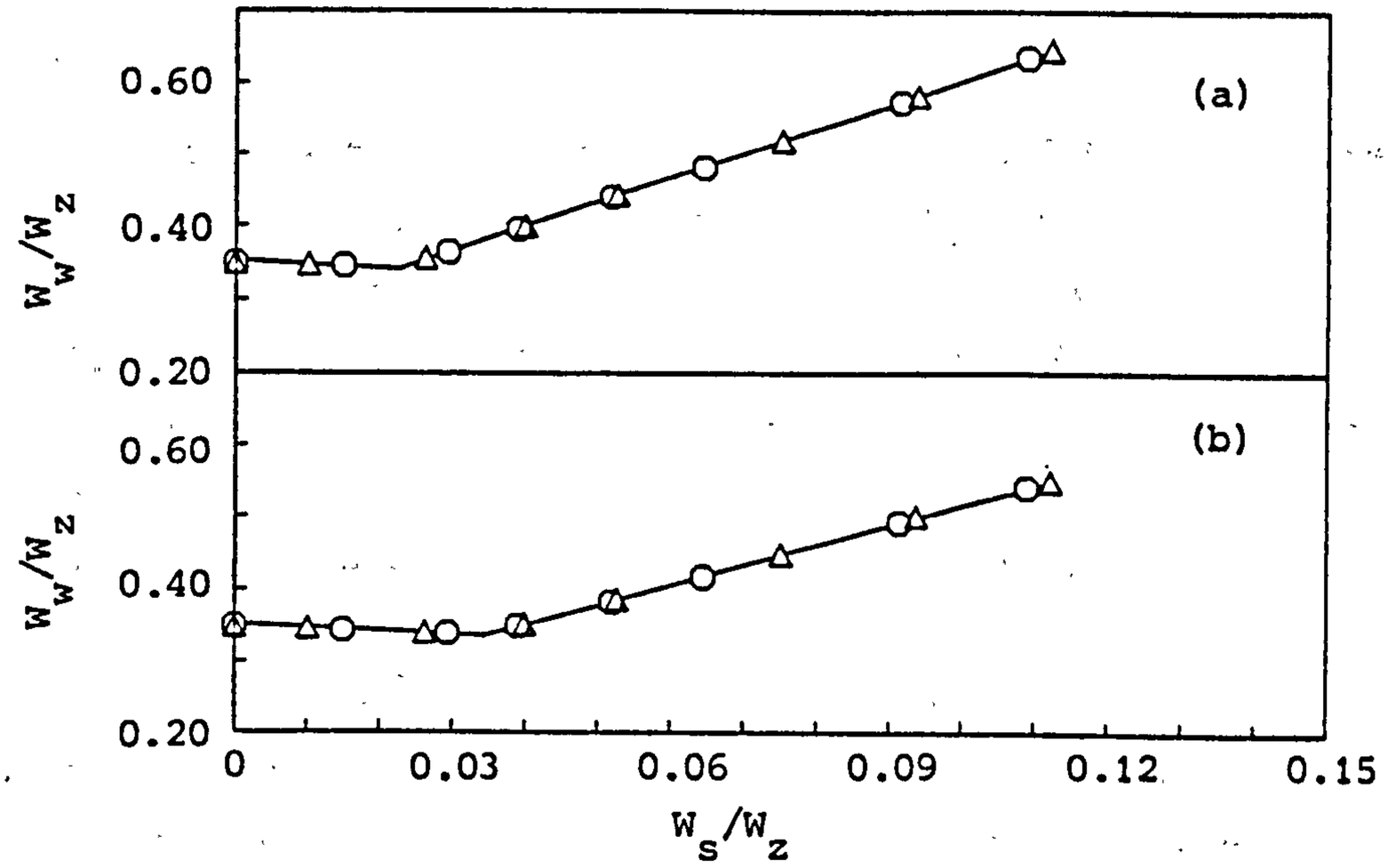

Figure 8.16 Imbibition plots for the NaCl/FAU(2.6) system at two different water activities: (a) a_w = 0.807 (saturated KBr); (b) a_w = 0.753 (saturated NaCl). The different symbols represent results obtained from independent experiments. The concordancy of the results shows the reproducibility of the isopiestic method.

saturated sodium chloride solution, the U_s values (0.0348 and 0.0351), the U_w values (0.3371 and 0.3366) and the external solution phase molalities (6.220 and 6.209) were in excellent agreement. Over saturated KBr solution the U_s values (0.0236 and 0.0239), the U_w values (0.3447 and 0.3436) and the solution concentrations (5.037 and 4.997) also agreed favourably. These results show that with care reproducible data can be obtained.

The initial set of results for the NaCl/FAU(2.6) system are summarised in Figure 8.17; the salt uptake (U_s) and the internal salt molality (m_i) are plotted against water activity. A distinct break at $a_w = 0.753$ (saturated NaCl solution) was again observed. No hysteresis was apparent as the order in which the equilibrations were carried out shows (see Figure 8.17). In practice, isopiestic equilibrations can be effected in any desired order.

Comparison of the imbibition results for NaCl + Faujasite

A comparison of the uptakes of NaCl into FAU(1.6), FAU(1.9) and FAU(2.6) as a function of water activity is shown in Figure 8.18. Each plot shows a distinct break at the water activity of saturated sodium chloride solution. For the equilibrations between the zeolites and sodium chloride solutions ($a_w \geqslant 0.753$), the amount of sodium chloride taken up depends on the chemical nature of the faujasite and on the solution phase concentration. At any given concentration though, the most aluminous faujasite, FAU(1.6), imbibed most salt. The reverse was true of the least aluminous material, FAU(2.6). The linear, high water activity ($a_w \geqslant 0.753$) portions of the plots in Figure 8.18 show this. The salt uptakes in this figure have been given as millimoles NaCl per litre crystal volume which allows the amount of imbibed salt in zeolites with different chemistries and hence different densities to be directly compared. These results generally suggest that small highly charged inorganic salts such as sodium chloride have greater affinity for zeolites of similar characteristic, i.e. the more aluminous types. Similar uptakes of sodium chloride into faujasites were found by Barrer [13].

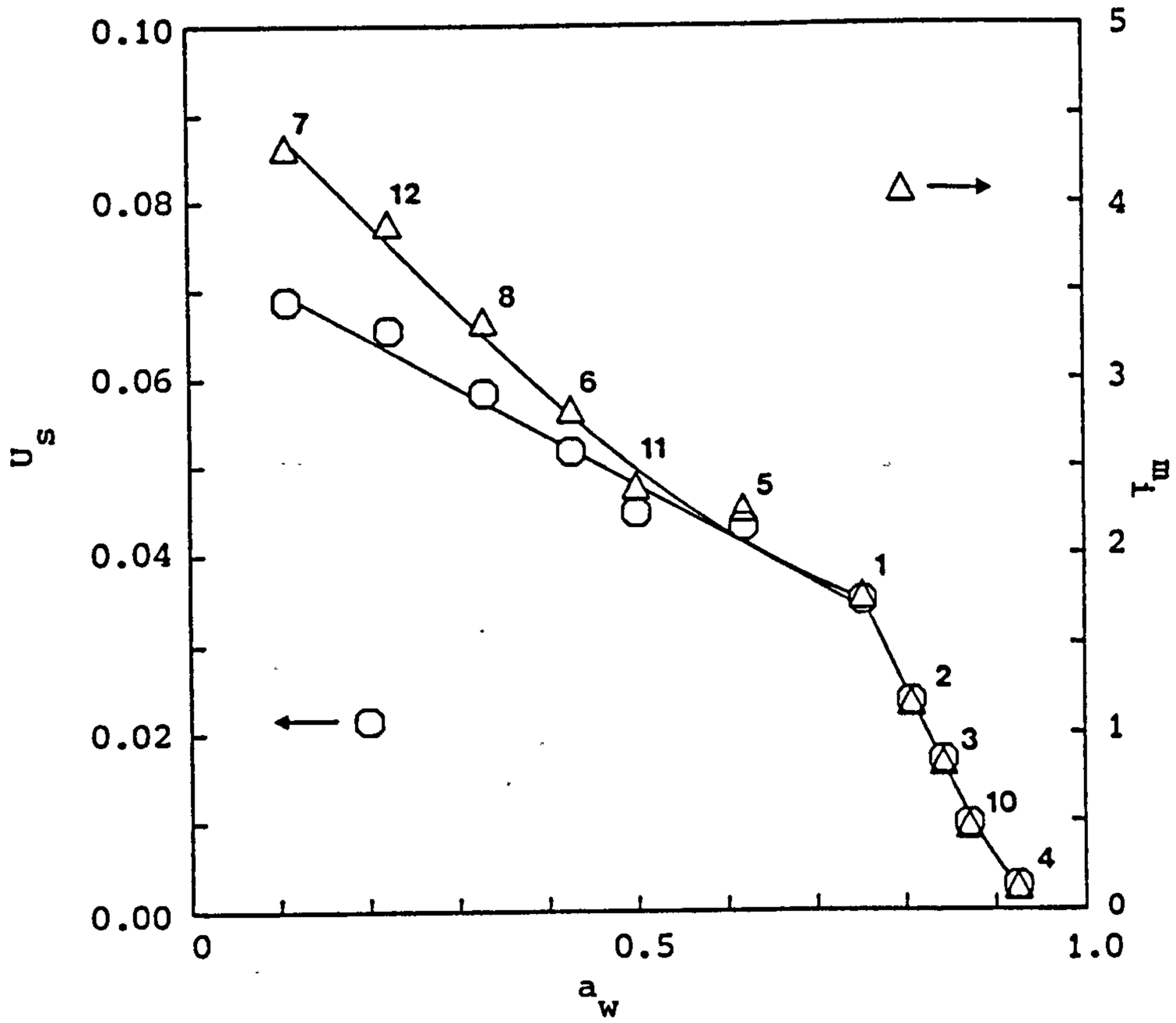

Figure 8.17 Imbibition results for NaCl + FAU(2.6) as a function of water activity. Both the internal molality of salt m_i and the salt uptake U_s are depicted. The numbers indicate the order in which the equilibrations were carried out and show that no hysteresis was observed.

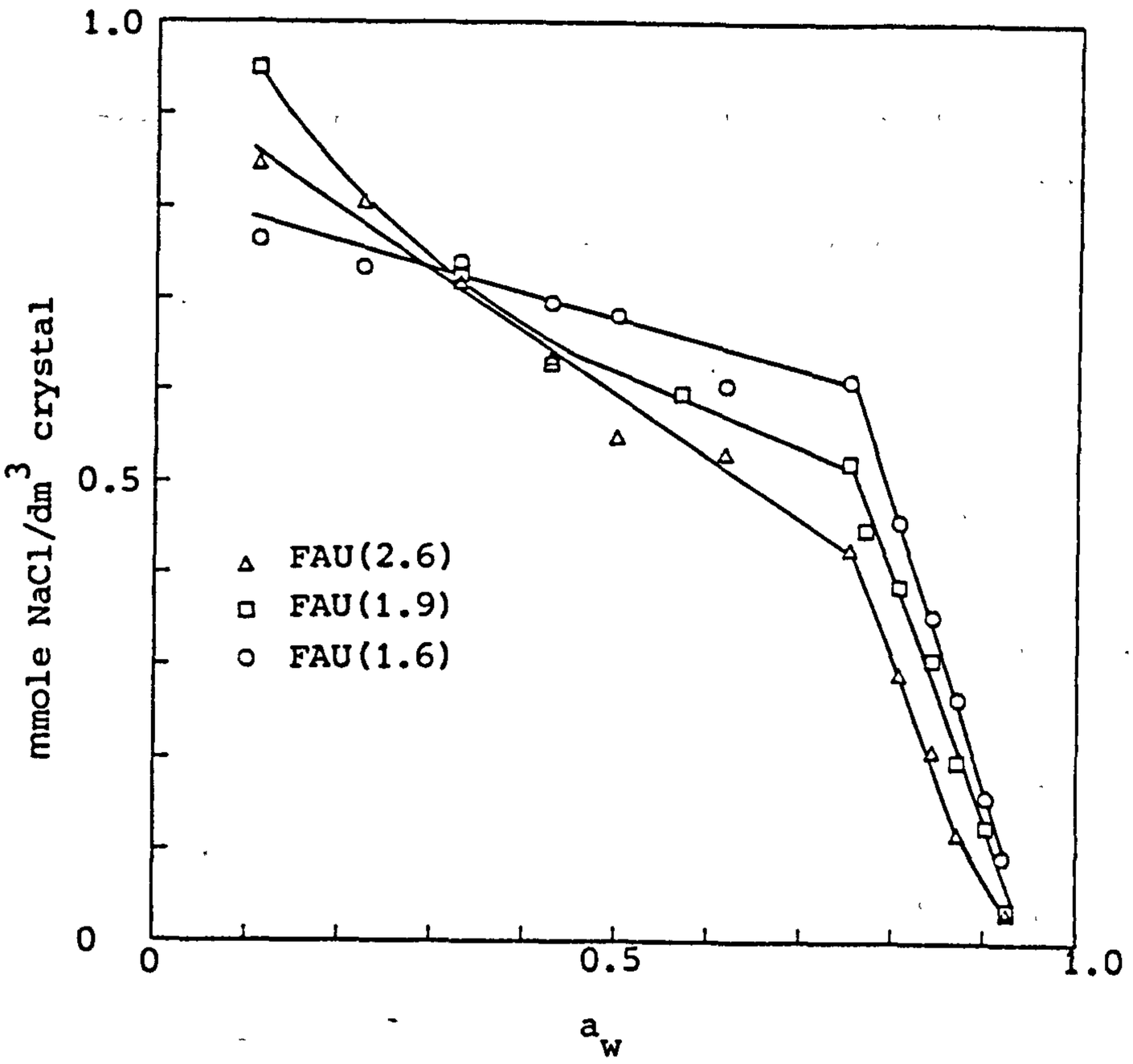

Figure 8.18 Imbibition of NaCl into Na-faujasite as a function of water activity.

At water activities below that of saturated sodium chloride solution, for equilibria between solid salt and the zeolites, the relative salt uptakes by the three faujasites show a more complex trend (Figure 8.18). Consider first of all the results for FAU(1.6) and FAU(2.6), the most aluminous and silicious materials respectively. At intermediate water activities FAU(1.6) imbibed more salt than FAU(2.6) but it can be seen from Figure 8.18 that as the water activity was lowered further the salt uptakes of these materials first of all approach one another and at very low water activities FAU(2.6) actually imbibes more salt than FAU(1.6). The faujasite of intermediate Si/Al ratio, FAU(1.9), shows a trend compatible to the aforementioned at intermediate water activities although an anomalously high salt uptake was observed at very low water activity. Reasons for this are unknown but two points should be borne in mind:

(1) True equilibration between two solids cannot be easy to attain under these experimental conditions. However, the results show systematic trends and it is believed that they represent if not true equilibria then something close to it.

(2) The interpolated salt uptakes at low water activities ($a_w < \sim 0.3$) for FAU(2.6) may be low. As Figure 8.15(B) shows, and as already explained, equilibrium at low water activities was difficult to attain and it may be significant that no such problems were encountered with the other two faujasites. More specifically, the plots shown in Figure 8.15(B) are drawn with linear 'solid phase' portions but if these portions were curved then interpolated intersection points, although difficult to estimate in practice, would be shifted to much higher W_s/W_z values. Hence for FAU(2.6) far more salt may actually be imbibed than thought. If this is the case, then the respective salt uptakes of the three faujasites at very low vapour pressures (Figure 8.18) would be completely the reverse of what they were at intermediate and high vapour pressures.

The salt and water uptakes of FAU(1.6) as a function of water activity are shown in Figure 8.19. Salt displaces water from the pores at all but the highest water activities (lowest salt loadings). The same trends were observed with the other two faujasites.

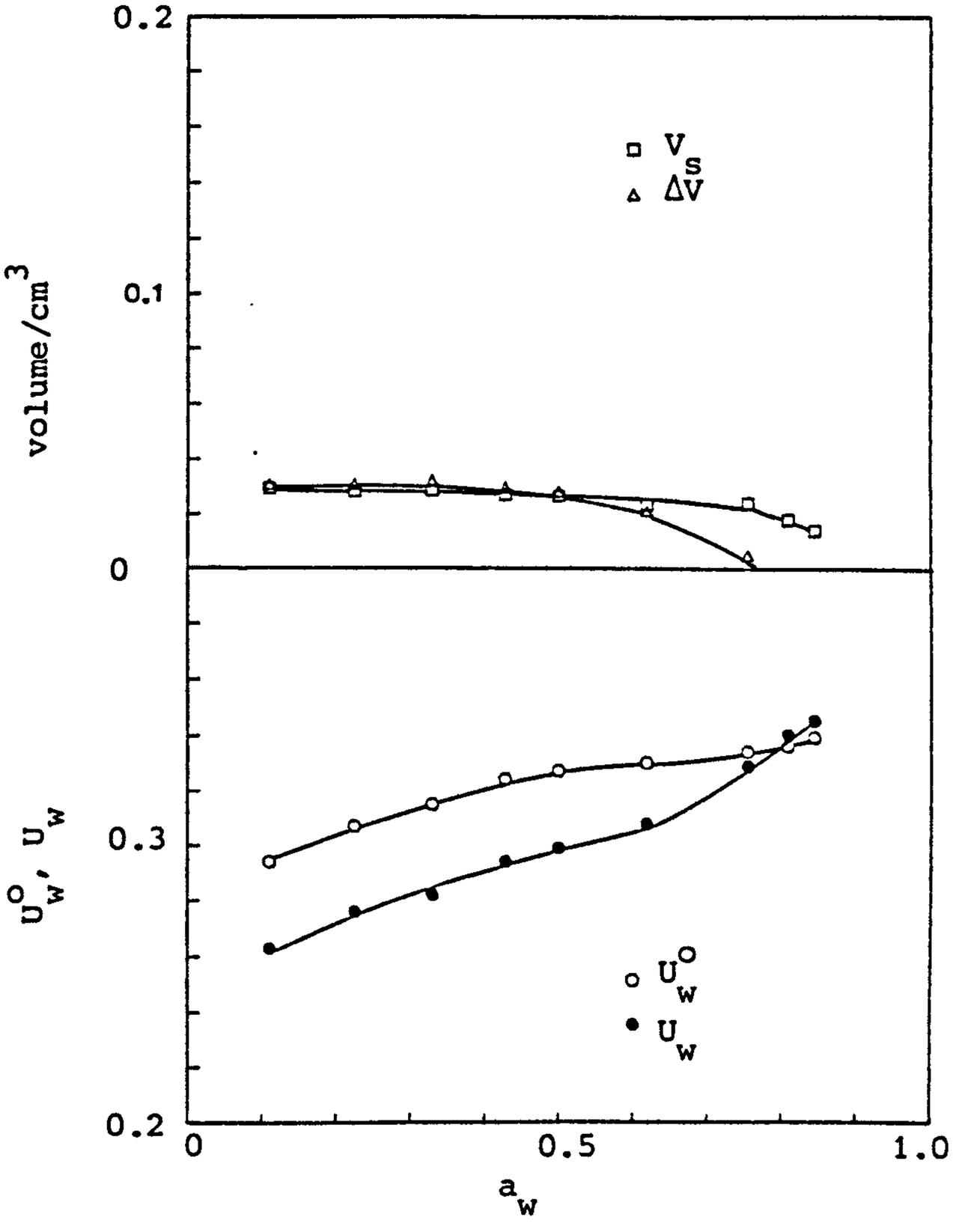

Figure 8.19 Salt and water uptake by FAU(1.6) as a function of water activity. Salt displaces water from the pores as can be seen by the difference between U_w^o and U_w at all but the highest water activities. The volume of salt imbibed (V_s) is compared to the volume of water displaced ΔV ($= U_w^o - U_w$) in the upper graph. The densities of the intracrystalline salt and water were taken to be 2.165 and 1 g cm^{-3} respectively.

8.3.2 NaI and NaBr + FAU(1.9)

FAU(1.9) was used to investigate the comparative uptakes of NaCl, NaBr and NaI from aqueous solutions. Full imbibition results for NaBr and NaI will be given elsewhere but imbibition plots obtained for the salt uptakes from their saturated solutions are given in Figure 8.20. Derived parameters are shown below in Table 8.7.

Table 8.7 Imbibition results for the uptake of NaCl, NaBr and NaI from their saturated solutions by FAU(1.9)

Salt	m^a	U_s	U_w
NaCl	6.039	0.043	0.332
NaBr	9.343	0.125	0.317
NaI	12.63	0.241	0.276

[a] molality of solution phase, mol Kg^{-1}

Reported values [7] for the solubilities of the halides at 25°C (determined by the isopiestic method) are 6.15, 9.18, 12.32 mol Kg^{-1} respectively and the solubility values shown in Table 8.7 differed from these by only 1.8%, 1.8% and 2.6% respectively. From the saturated solutions of the halides, 0.73, 1.21 and 1.61 millimoles of NaCl, NaBr and NaI per gram anhydrous zeolite were respectively imbibed.

As the isopiestic method is a gravimetric technique it is well-suited for investigating the imbibition of high molecular weight salts such as NaI. In the particular case of NaI, the weight of salt imbibed from its saturated solution was equivalent to about 25% of the crystal weight. Experiments at low vapour pressures, that involved equilibration of the zeolite with surface salt, showed that once again considerably more salt can be imbibed under these conditions.

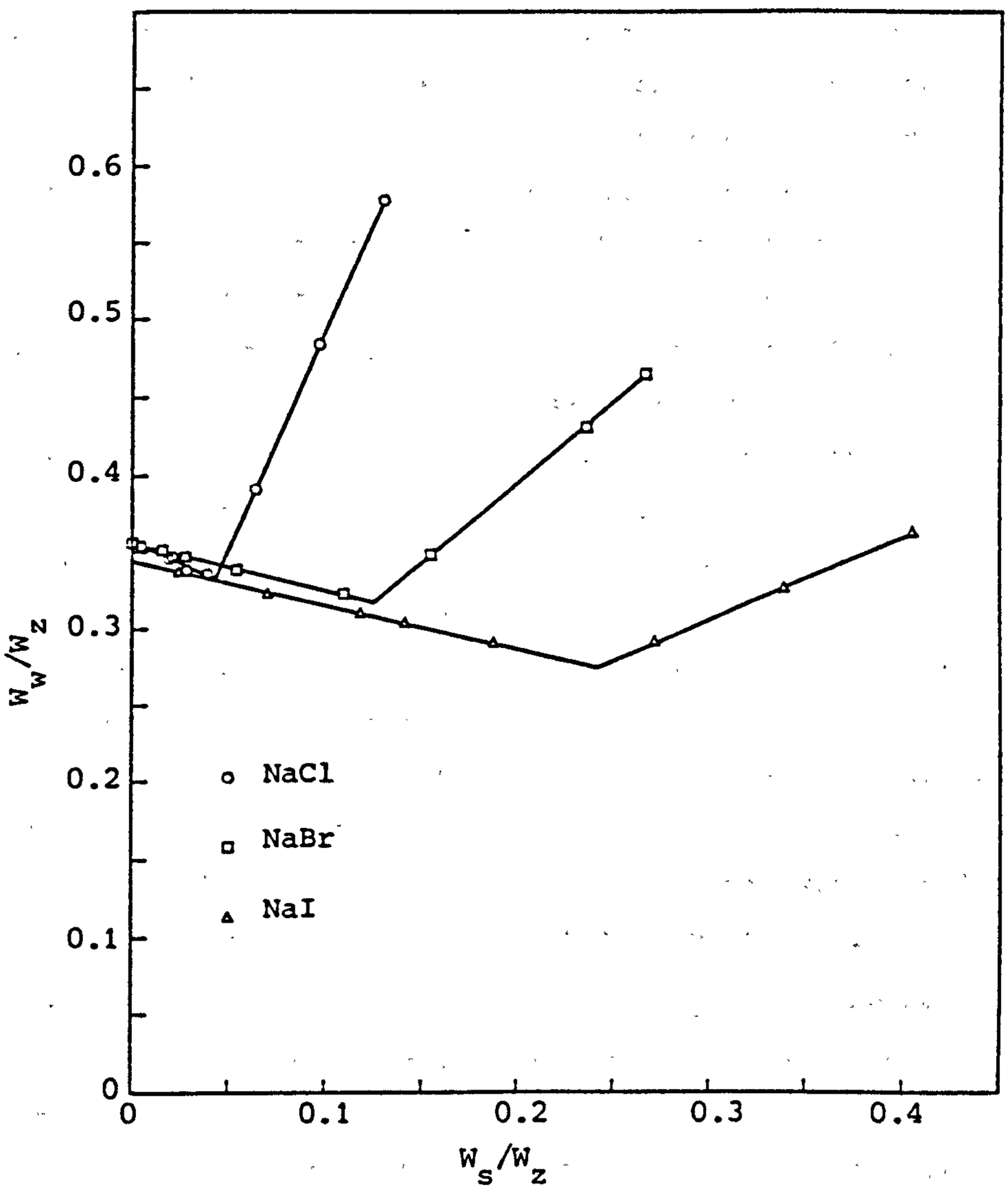

Figure 8.20 Imbibition plots showing the uptakes of NaCl, NaBr and NaI into FAU(1.9) from their saturated solutions.

8.3.3 NaCl + Na-A

Zeolite A has a similar void crystal volume to that of faujasite zeolites but windows of much smaller size. Entry to the pore system is controlled by 8 T-atom rings and is further constrained by the presence of cations in the windows. Results from isopiestic experiments on the NaCl/Na-A system are shown in Figure 8.21. The results show that no salt is imbibed even from saturated sodium chloride solution. No intersection points were obtained and the linear plots, which are represented by equation (8.8), extrapolate on the ordinate axis to values which represent the water contents of the salt-free zeolite Na-A at the various vapour pressures. Equilibration at lower vapour pressure (a_w = 0.33) indicated only a small amount of salt uptake (<0.01 g/g). Repeat experiments over a narrower W_s/W_z range were not done to accurately quantify this uptake. The fact that salt imbibition was not observed is surprising although in agreement with studies by Barrer [14]. The sizes of the sodium and chloride ions do not exclude them from entry. It may be that the salt uptake is very slow at 25°C, i.e. the results may reflect kinetics rather than thermodynamics, although another possible explanation is that the very high negative charge on the framework (zeolite A has Si/Al = 1) precludes the imbibition of salt molecules.

The experimental arrangement for investigation of the NaCl/Na-A system differed from the norm in that two of the eight dishes that could be accommodated in the dessicator contained no zeolite, only salt. These dishes, which hence contained only solution at equilibrium, were used to calculate the isopiestic molalities of sodium chloride at different vapour pressures. These values are compared to the molalities of the sodium chloride solutions determined from the slopes of the W_w/W_z against W_s/W_z plots in Table 8.8. The two solution only dishes gave concordant molalities on each equilibration, the difference between the two ranging between 0.06% and 0.09%. Molalities graphically evaluated from the water contents of the salt/zeolite mixtures differed from the mean molalities of the two solution only dishes by between 2.2% and 3.9%. These discrepancies are not believed to have serious implications and they may be partly due to slight zeolite dissolution/hydrolysis. Experiments were usually carried out with zeolite present in all dishes and the equilibrium solution phase concentrations were deduced graphically from the data obtained.

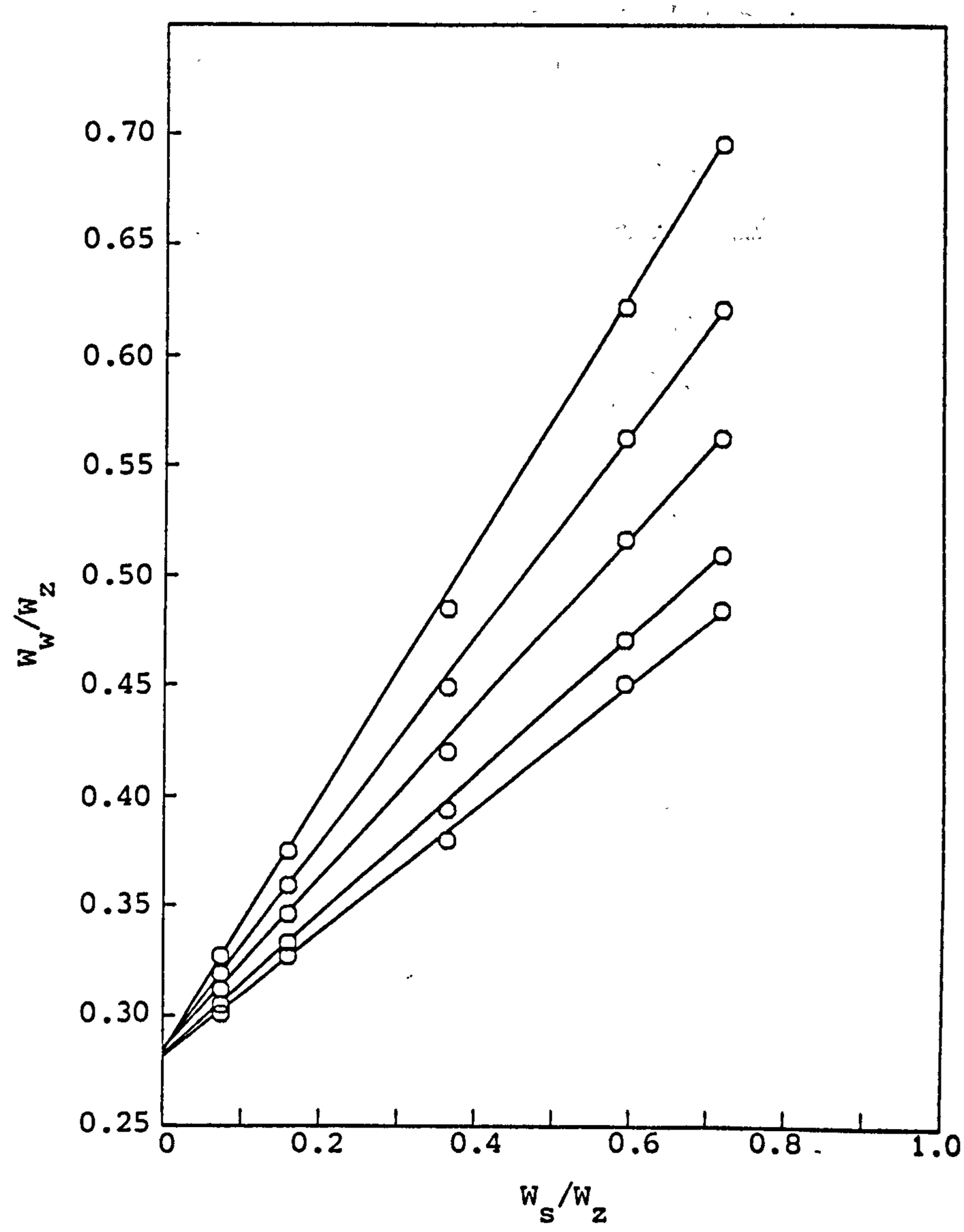

Figure 8.21 Imbibition results for the NaCl/Na-A system. The lines correspond to the following solution concentrations:
6.01 (lowest plot), 5.39, 4.39, 3.63 and 2.98 (uppermost plot) mol Kg^{-1}

Table 8.8 Comparison of solution molalities calculated from 'solution only' dishes with those calculated from imbibition plots for the NaCl/Na-A system. The solution only dishes and the dishes containing salt and zeolite were equilibrated in the same dessicator at the same time.

Molality (imbibition plot)	Molality (solution only)
6.007	6.1577
	6.1525
5.389	5.5084
	5.5032
4.392	4.5057
	4.5028
3.628	3.7596
	3.7565
2.978	3.0750
	3.0731

8.3.4 Other salt/zeolite systems

The chief aim of this section is to put this salt imbibition work in perspective with the theme of this thesis - organophilic and hydrophilic properties of zeolitic materials. This section includes further imbibition results, some of which will be only discussed in part and will be reported in full elsewhere.

Figure 8.18 has shown that the amount of sodium chloride taken up by faujasite zeolites at any given solution concentration gets less as the silicious nature of the zeolite increases. If this trend was to continue, higher and higher Si/Al faujasites would be expected to imbibe less and less salt. The same would be expected of other high silica zeolites and work has shown that no sodium chloride is imbibed from aqueous solution by ZSM-5(17.9) at 25°C (Figure 8.22). A very small amount was imbibed at low vapour pressures but it was difficult to discern and quantify because the water content of the zeolites were so little perturbed in relation to the salt-free material; to obtain an accurate intersection under these conditions it is necessary for the water content of the zeolite to be considerably depressed.

Although of completely different structure to faujasite, the results for the ZSM-5 were not unexpected; aluminous zeolites readily take up inorganic salts from aqueous solution, high silica materials do not. If a salt has organic character though, this should enhance the likelihood of its uptake from aqueous solution by the more silicious zeolite types. Experiments with three organic salts, sodium acetate, sodium benzenesulphonate and sodium pentanesulphonate, were carried out with this aim in mind. The main points brought to light by this work are discussed below.

Although sodium chloride was not taken up by ZSM-5(17.9) from aqueous solution, sodium acetate was readily imbibed (Figure 8.23). The figure compares the imbibition plots for sodium acetate uptake from its saturated solution by ZSM-5(17.9) and FAU(1.9). Although the amount adsorbed by the ZSM-5 was less than was taken up by the faujasite these results are significant and the imbibition of other fatty acid salts into these zeolites would be elucidating.

The uptake of sodium benzenesulphonate into FAU(1.9) was unusual in that no imbibition occurred from aqueous solutions of this salt and

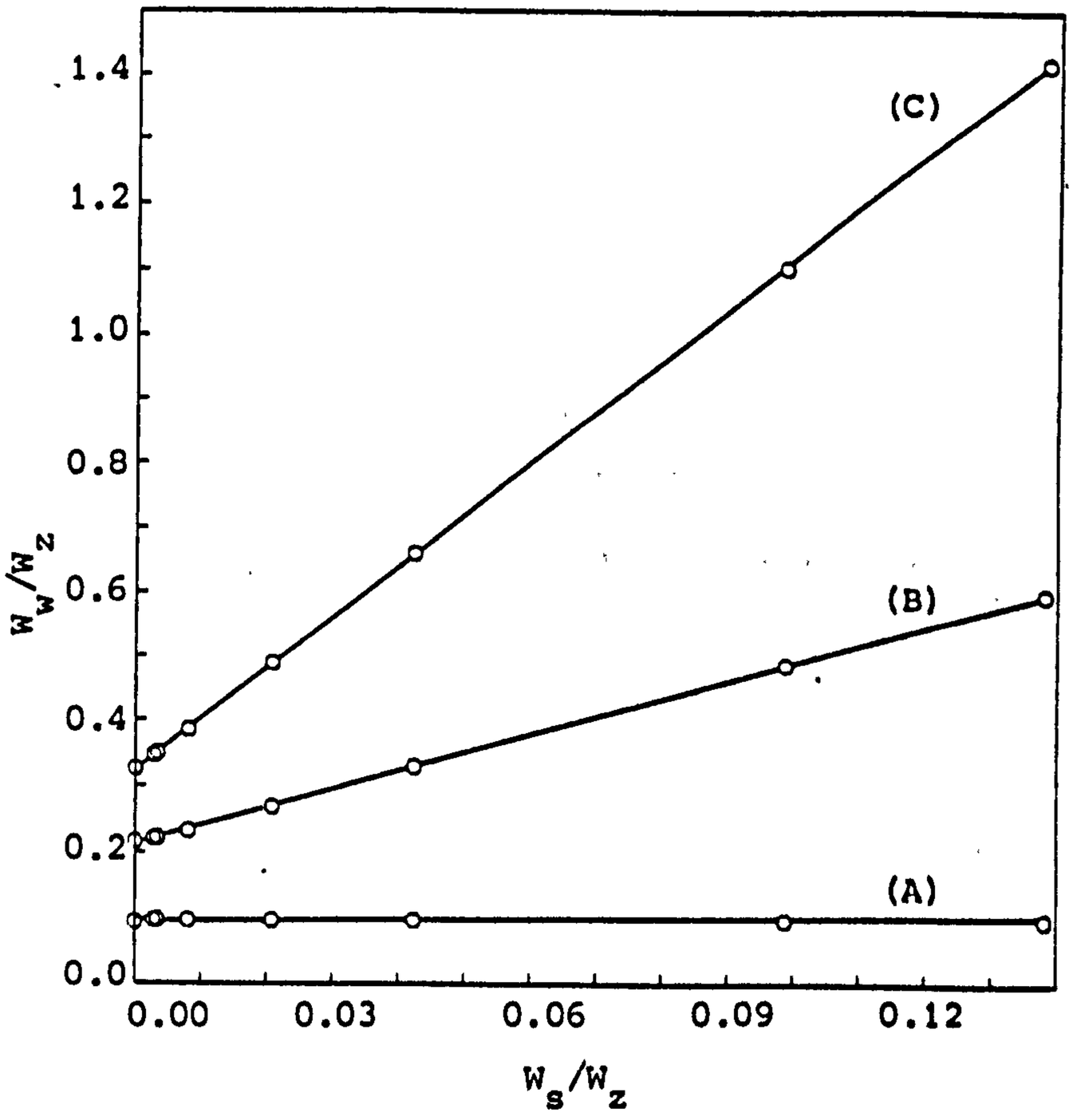

Figure 8.22 Imbibition plots for the NaCl/ZSM-5(17.9) system. The equilibrium water activities and solution concentrations (where applicable) were: (A) $a_w = 0.330$; (B) $a_w = 0.753$ (saturated sodium chloride solution), $m = 6.191$ mol Kg^{-1}; (C) $a_w = 0.925$, $m = 2.163$ mol Kg^{-1}. Plots (B) and (C) are displaced by 0.1 and 0.2 units respectively on the ordinate axis.

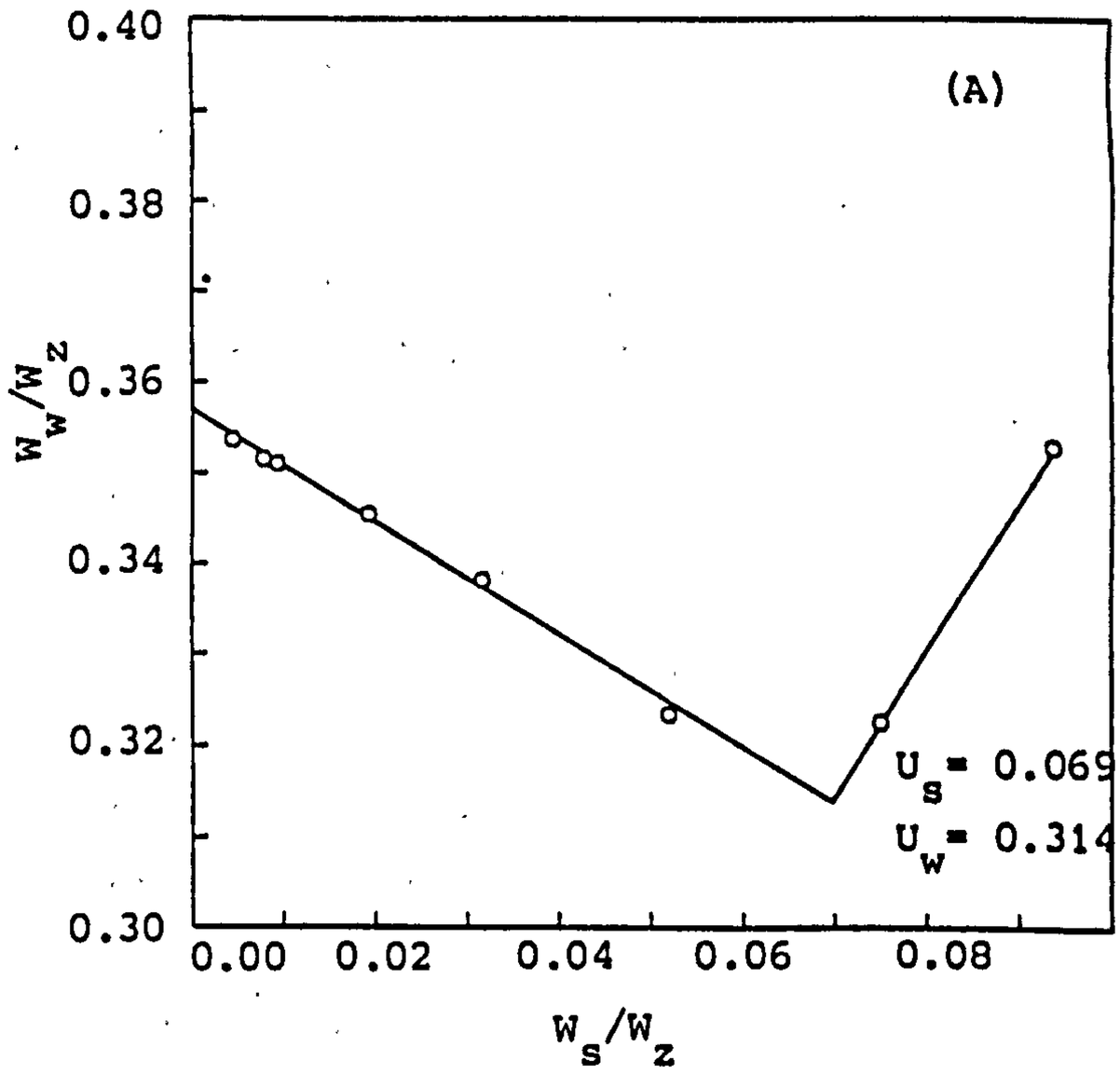

Figure 8.23 Imbibition plots showing the uptake of sodium acetate into (A) FAU(1.9) and (B) ZSM-5(17.9) from its saturated solution. From plot (B) the solution concentration was calculated to be 5.86 mol Kg^{-1}.

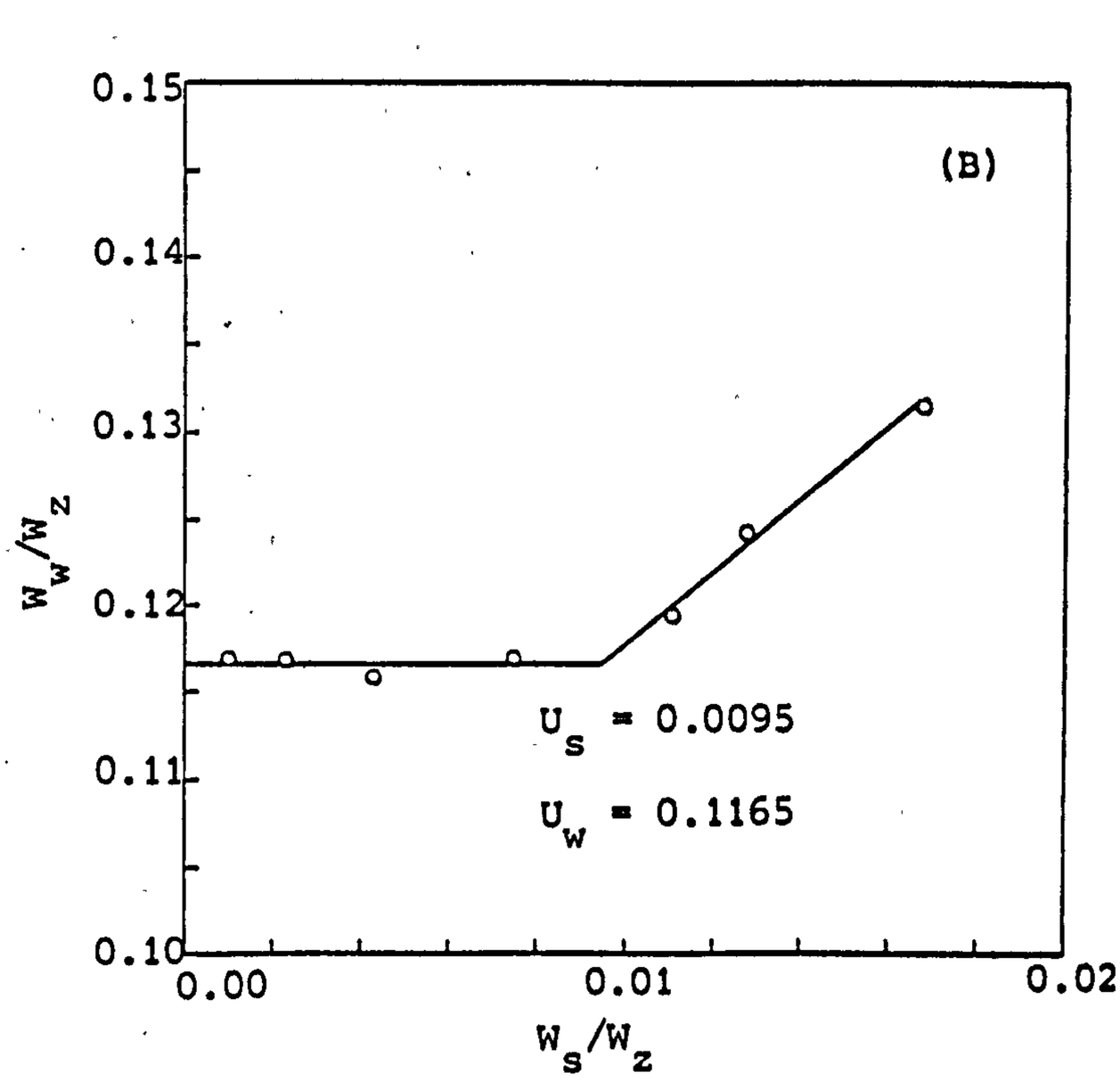

It was not until the water vapour pressure was lowered considerably that salt was taken up by the zeolite. The imbibition plots in Figure 8.24 and the isotherm in Figure 8.25 show this. The data is given in Table 8.9. The plots in Figure 8.24 show that sodium benzene-sulphonate crystallised on the zeolite crystals as a hydrate, i.e. the slopes of the portions of the imbibition plots which represent zeolite samples in equilibrium with solid salt on their external surfaces are of positive gradient. From the gradient of these plots the surface salt was deemed to be the monohydrate.

Little uptake of sodium benzenesulphonate by silicalite was detected as Figure 8.26 shows. This may be due to a steric effect. A scanning electron micrograph of surface salt in intimate contact with the silicalite crystals is shown in Figure 8.27. The salt was seen as discrete lumps as oppose to a fine salt layer completely covering the surfaces of crystals. If the same is true of other salt/zeolite solid mixtures it is not surprising that the solid-solid equilibria that exist at low vapour pressures are sometimes difficult to establish.

Sodium pentanesulphonate was taken up by silicalite(S17) to a greater extent than by FAU(1.6) as Figure 8.28 shows. The organic character of the salt is clearly influential here; high silica zeolites and silica molecular sieves readily imbibe salts that have appreciable organic character. This has implications for both catalyst preparation and synthesis the reasons for which should be clear.

Although the presence of large amounts of salts in pores may have detrimental effects on the sieving properties of zeolites it is well known that of the many ways by which the sorptive properties of zeolites can be modified the introduction of small amounts of salt can be particularly effective. The isopiestic method is ideal for the preparation of such materials. The salt-zeolite complexes so prepared can be used directly or, if desired, can be further treated. For example, imbibed organic salts could be thermally decomposed to give oxides, imbibed transition metal cations could be reduced to the metallic state and zeolites loaded with inorganic salts could be subjected to high temperature firing to perhaps drive salt molecules into smaller voids outwith the main channel system not ordinarily accessible to them. The isopiestic method, apart from its principal use to study imbibition phenomena from aqueous solutions, thus allows ready preparation of

Table 8.9 Imbibition results for sodium benzenesulphonate + FAU(1.9)

a_w [a]	m [c]	U_w^o	U_s	U_w	m_i [e]
0.925	2.342	0.356	-	-	-
0.807	[d]	0.363	-	-	-
0.618	[d]	0.357	0.025	0.342	0.400
0.500	[d]	0.352	0.058	0.318	1.013
0.330	[d]	0.342	0.095	0.287	1.837

*See Table 8.4 for footnotes

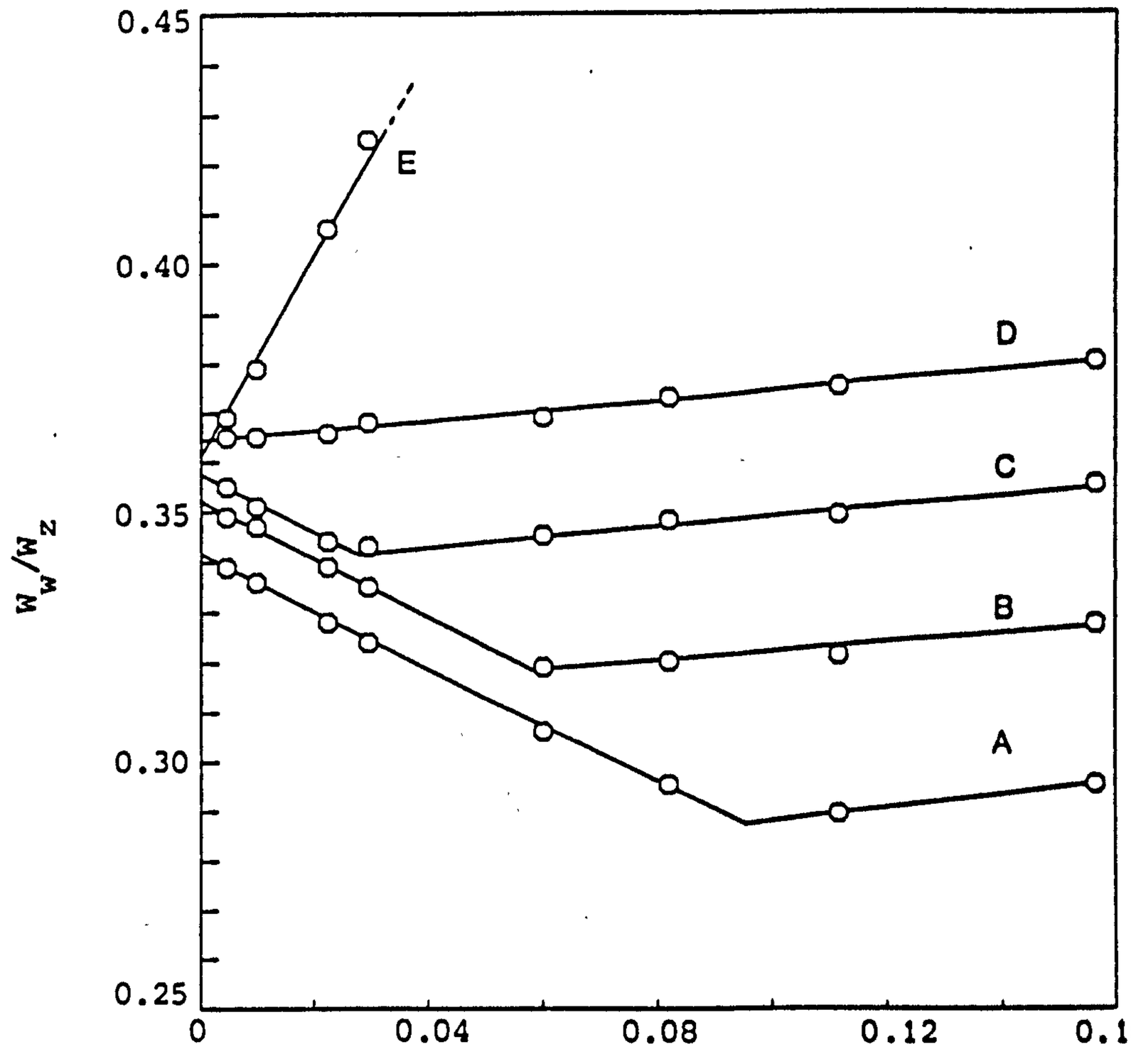

Figure 8.24 Imbibition plots for sodium benzenesulphonate + FAU(1.9) at different water activities: (A) 0.330, (B) 0.500, (C) 0.618, (D) 0.807, and (E) 0.925.
Plot (E) intercepts the ordinate axis at a lower value than plot (D); although undetectable, it may be that a small amount of salt is imbibed at these water activities so causing this apparently anomalous result.

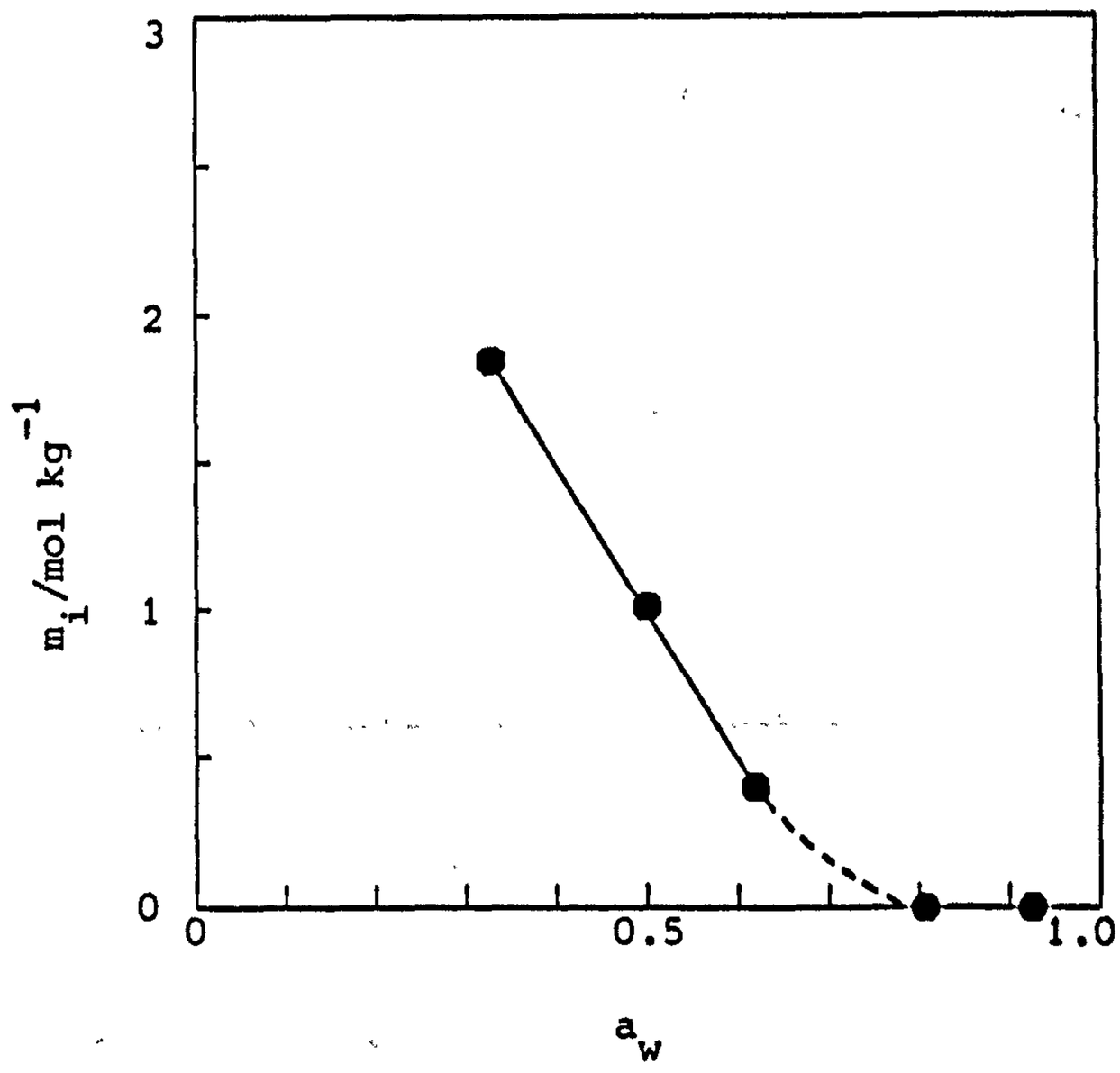

Figure 8.25 Internal molality (m_i) of sodium benzene-sulphonate in FAU(1.9) as a function of water activity.

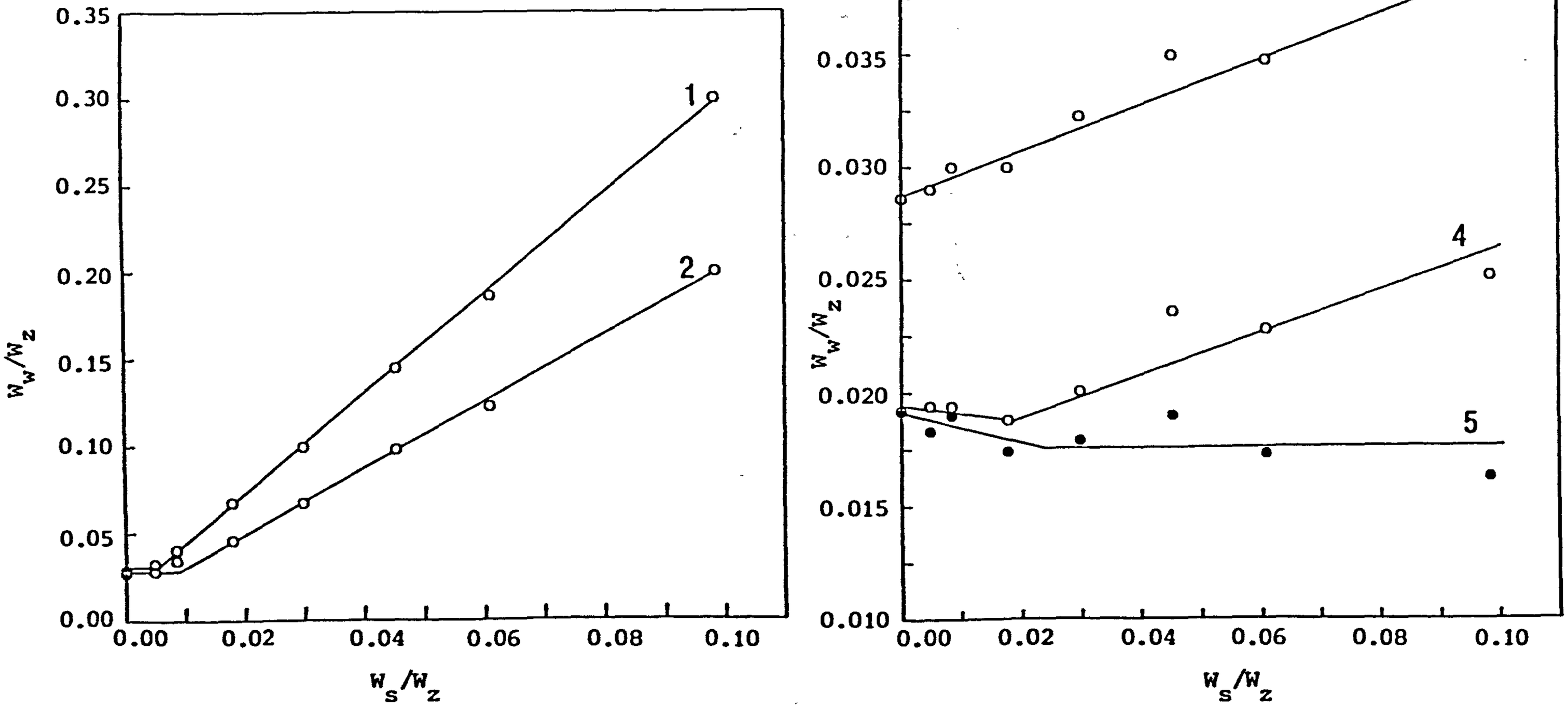

Figure 8.26 Imbibition plots for sodium benzenesulphonate + silicalite(S17) at different water activities: (1) 0.925, (2) saturated sodium benzenesulphonate (a_w unknown), (3) 0.871, (4) 0.330, (5) 0.225. The amount of salt taken up from its saturated solution (m = 2.91 mol kg^{-1}) was small (<0.01 g/g). The results at lower water activities (plots (3)-(5)) were difficult to interprete because of the very low total water contents. Plot (3) anomalously indicated no salt imbibition. It could be that the adsorption detected from the solution phase in plots (1) and (2) is indicative of adsorption on the external surfaces of crystals and that imbibition into the pores only occurs at much lower vapour pressures. The salt in contact with the external surfaces of the crystals loses its water of hydration at very low vapour pressures.

Figure 8.27 (overleaf)

Scanning electron micrographs of silicalite (S17):

(a) As-synthesised.

(b) After calcination and preparative acid treatments.

(c) crystals in contact with sodium benzenesulphonate (isopiestic experiment).

FIG. 8.27

a

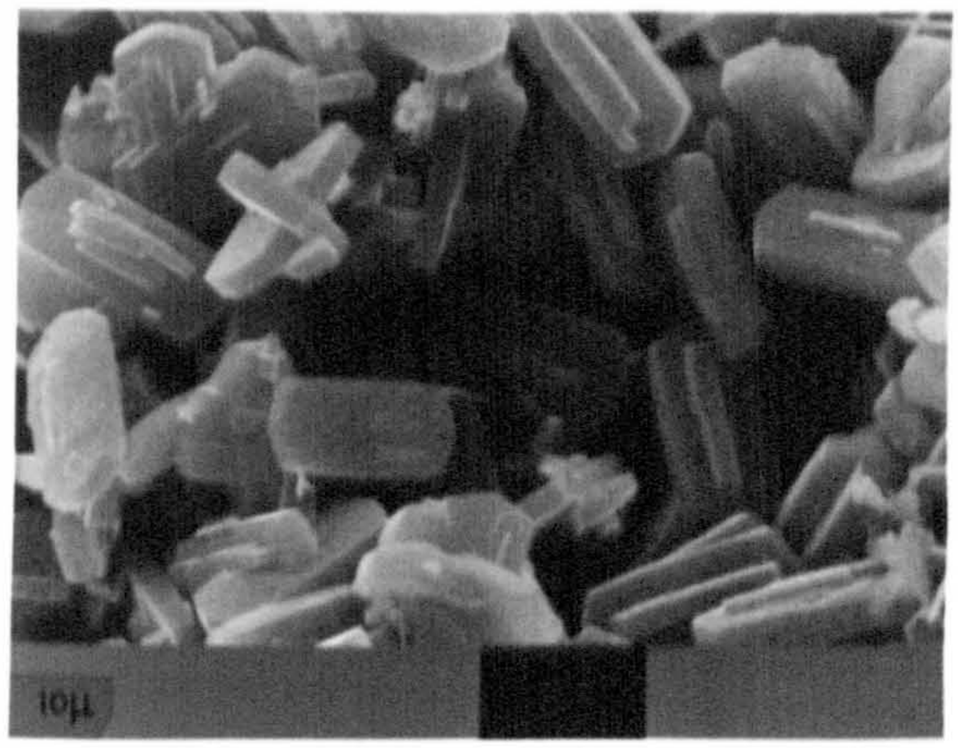

b

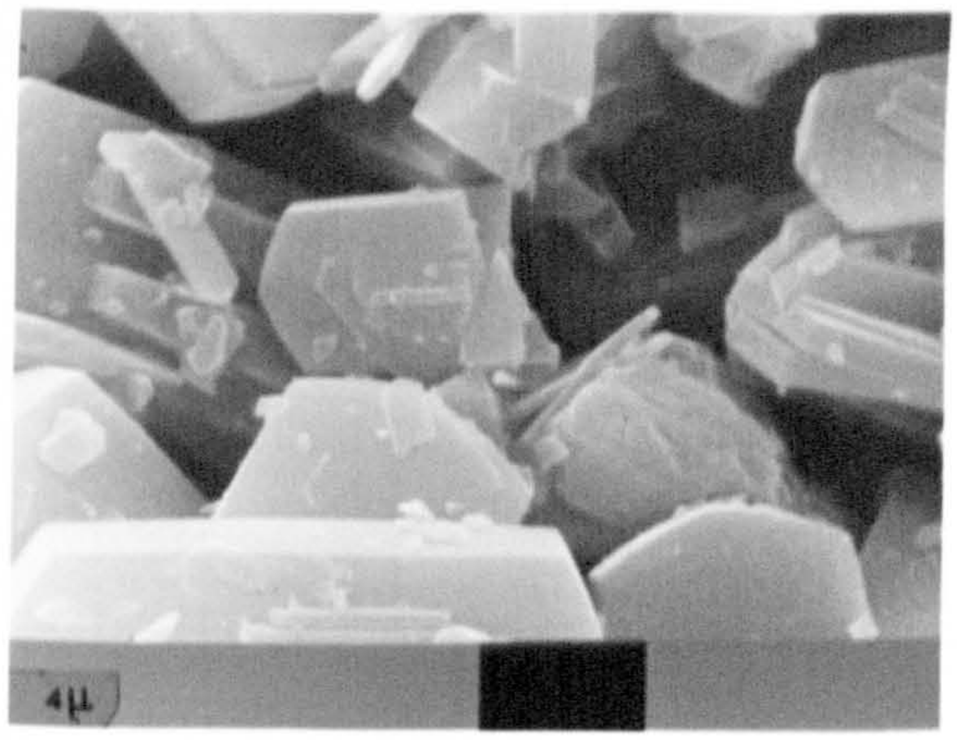

c

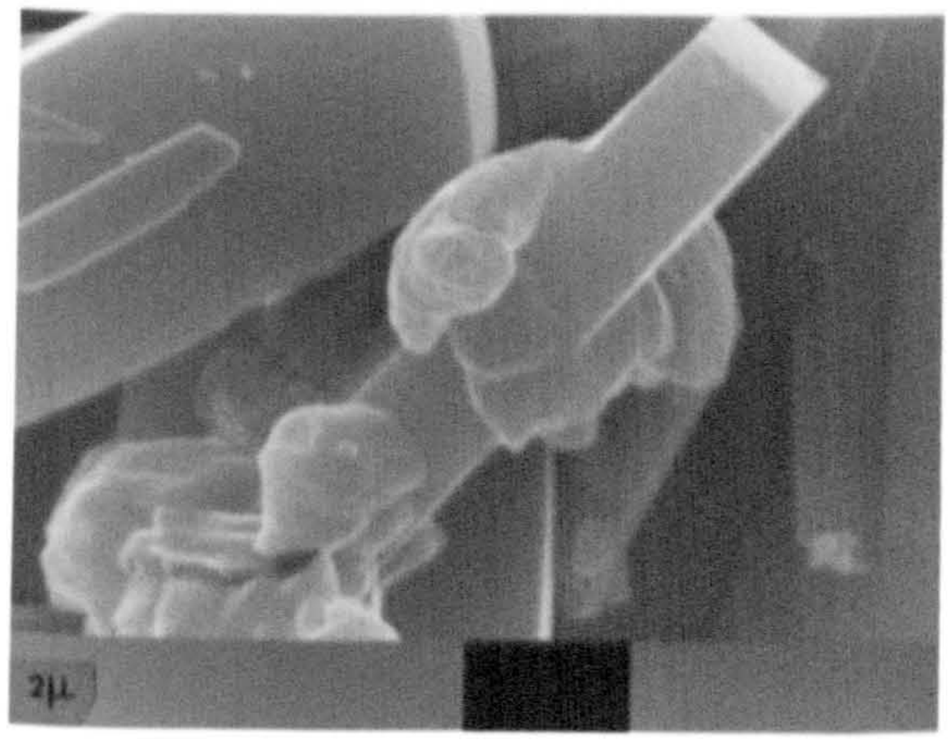

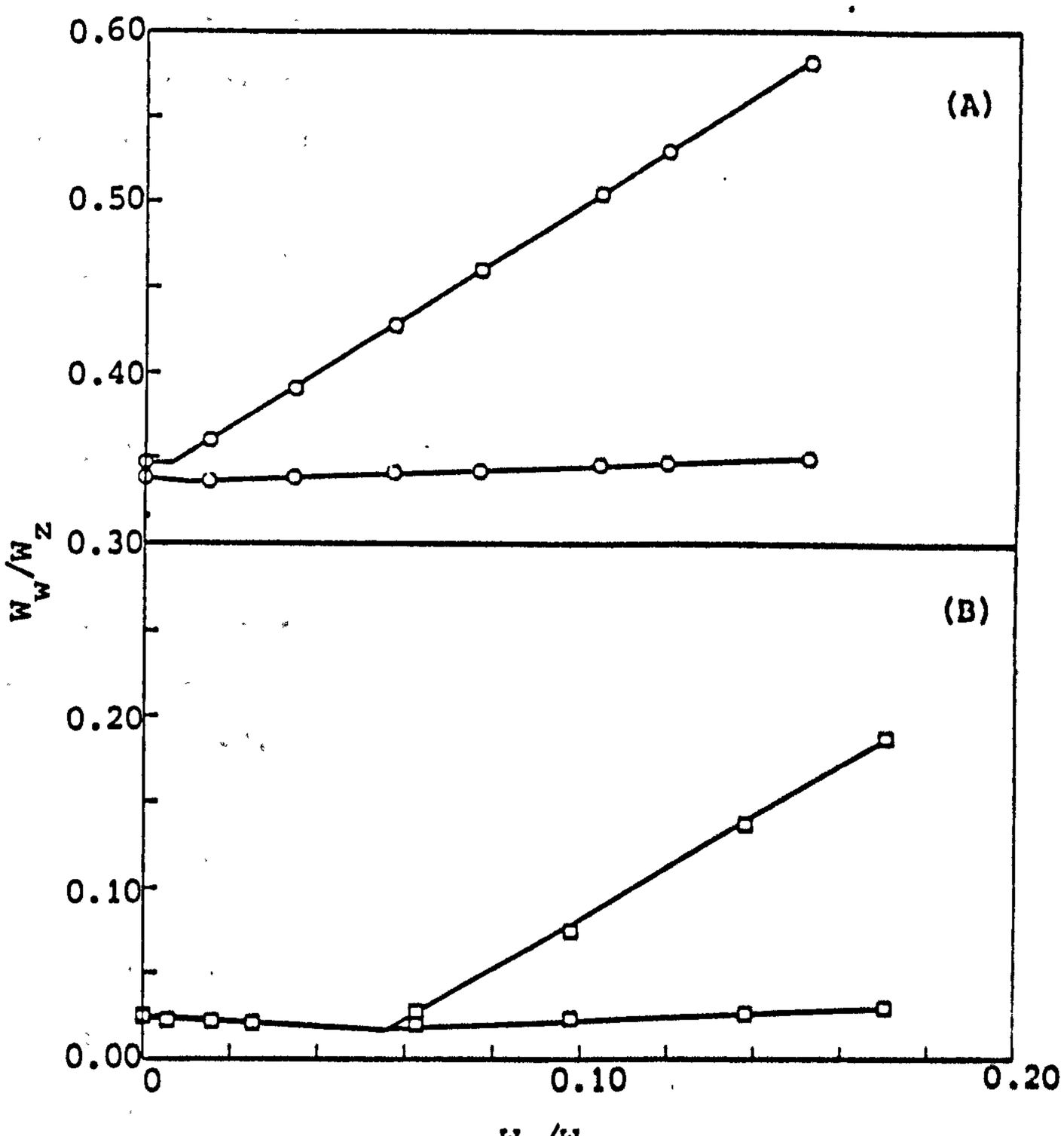

Figure 8.28

Imbibition plots for the uptake of sodium pentanesulphonate into (A) FAU(1.6) and (B) silicalite(S17) at two water activities: (i) $a_w = 0.925$ (saturated KNO_3); (ii) $a_w = 0.753$ (saturated NaCl). At $a_w = 0.925$, the mean molality of the external solution phases was 3.68 mol Kg^{-1}. Solid salt was in equilibrium with the zeolitic materials at $a_w = 0.753$. The surface salt was present as its monohydrate. These results show that silicalite imbibes sodium pentanesulphonate to a greater extent than FAU(1.6).

salt-loaded materials as the first step in the preparation of a variety of different guest-zeolite complexes. Zeolites can, of course, be salt-loaded from melts but not with the control and regulation that the isopiestic method confers.

8.4 Application of the isopiestic technique to study the adsorption of non-electrolytes from aqueous solutions by zeolites

The results described in foregoing sections demonstrate the elegant and powerful nature of the isopiestic technique for studying salt imbibition by zeolites. The technique is not limited to this area though; the uptake of involatile non-electrolytes by zeolites can also be investigated using the isopiestic method. The theory described in section 8.1.2 applies to all involatile solutes regardless of whether they be electrolytes or non-electrolytes. However the number of non-electrolytes that are both involatile in aqueous solution and appreciably water soluble, the two essential criteria for successful isopiestic experiments, is restricted. In the case of organic non-electrolytes, solubility and volatility are largely determined by molecular weight and functional group considerations.

The next section describes an investigation of glycerol adsorption by three different zeolitic materials. Aqueous solutions of glycerol have been previously studied in 'orthodox' isopiestic work [5].

8.4.1 Adsorption of glycerol from aqueous solutions

Imbibition plots at selected water activities for glycerol adsorption into zeolite FAU(1.6), ZSM-5(15.5) and silicalite(S17) are shown in Figures 8.29-8.31. Derived parameters from these plots and similar plots at other water activities are shown in Tables 8.10-8.12.

Glycerol was readily adsorbed by all three of the materials under study. Figures 8.29 and 8.30 show plots with linear 'solid phase' lines; displacement of water in the pores of FAU(1.6) and ZSM-5(15.5) by the glycerol is linear. At very low water activities, almost all the water in ZSM-5(15.5) is displaced by glycerol (Figure 8.30). Figure 8.32 shows, on a volume basis, the water, glycerol and total contents of the zeolite as a function of water activity. At all water activities,

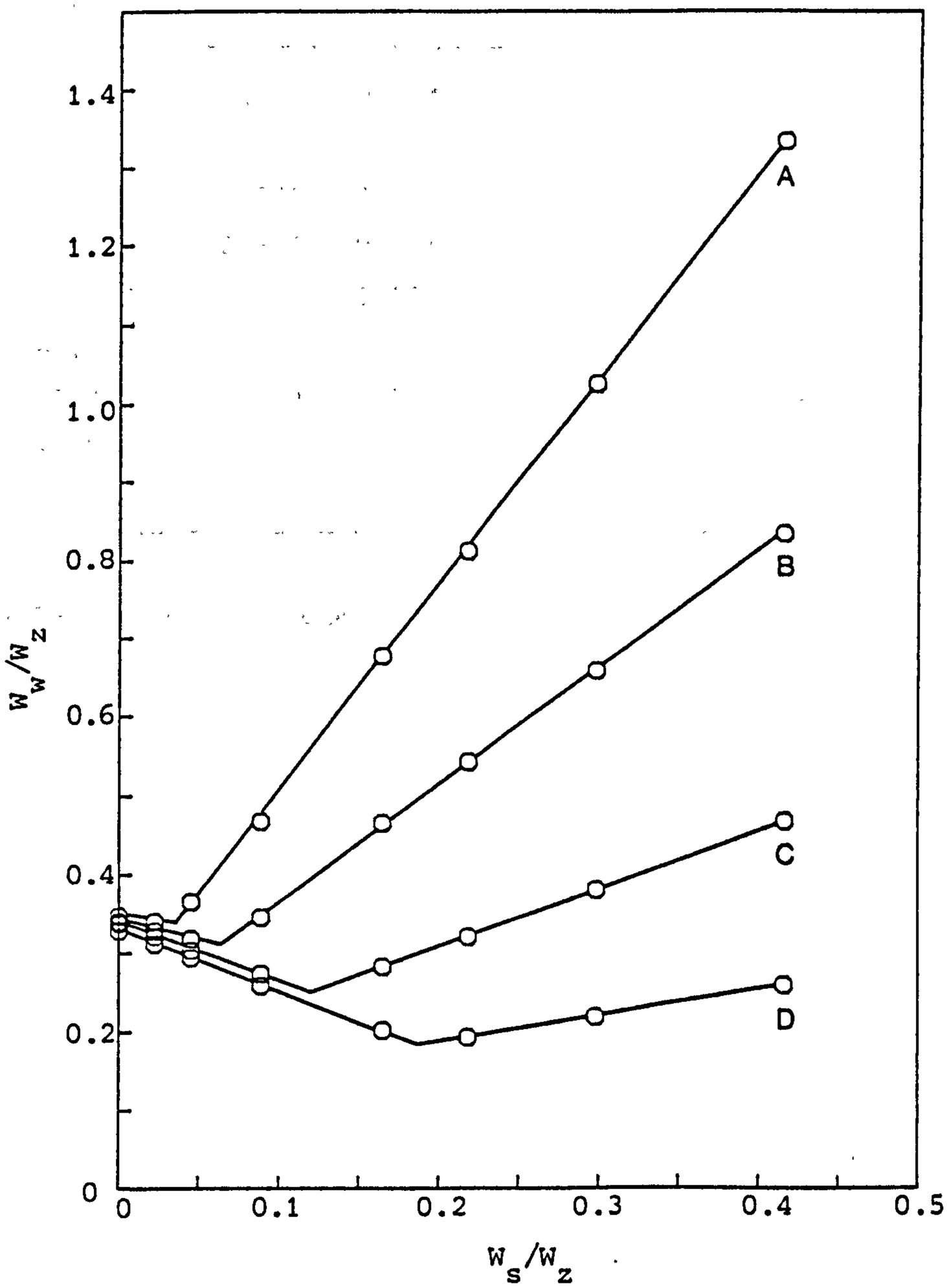

Figure 8.29 Imbibition plots for glycerol + FAU(1.6) at selected water activities: (A) 0.925; (B) 0.871; (C) 0.753; (D) 0.577

Table 8.10 Imbibition results for glycerol + FAU(1.6)

	Solid phase line		Solution phase line		Intersection point		
a_w [a]	k [b]	U_w^o	R_{sol}	m [c]	U_s	U_w	m_i [e]
0.925	-0.335	0.347	2.624	4.138	0.036	0.335	1.168
0.871	-0.501	0.340	1.478	7.350	0.062	0.309	2.190
0.807	-0.651	0.336	0.964	11.27	0.096	0.274	3.804
0.753	-0.729	0.337	0.731	14.86	0.121	0.249	5.287
0.708	-0.742	0.333	0.564	19.25	0.138	0.231	6.510
0.618	-0.735	0.326	0.381	28.52	0.166	0.191	9.455
0.577	-0.783	0.329	0.323	33.63	0.188	0.182	11.21
-	-0.796	0.325	0.244	44.50	0.210	0.158	14.41
0.428	-0.794	0.323	0.187	58.02	0.228	0.142	17.50

* See Table 8.4 for footnotes

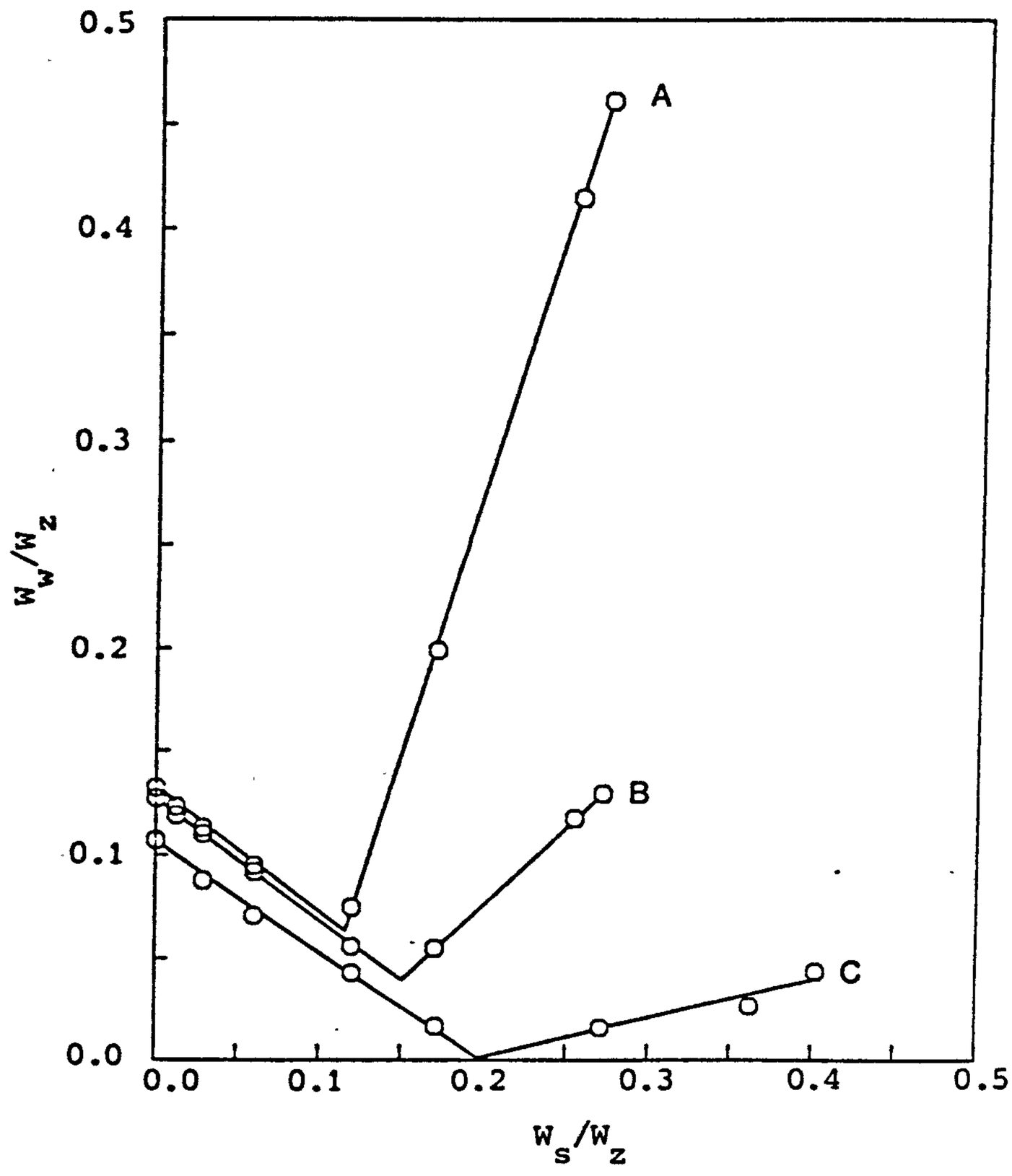

Figure 8.30 Imbibition plots for glycerol + ZSM-5(15.5) at different water activities: (A) 0.925; (B) 0.753; (C) 0.330

Figure 8.11 Imbibition results for glycerol + ZSM-5(15.5)

	Solid phase line		Solution phase line		Intersection point		
a_w[a]	k[b]	U_w^o	R_{sol}	m[c]	U_s	U_w	m_i[e]
-	-0.403	0.138	10.08	1.078	0.081	0.106	8.294
-	-0.483	0.135	8.336	1.303	0.083	0.095	9.488
-	-0.572	0.134	5.117	2.122	0.098	0.077	13.77
0.925	-0.606	0.131	2.552	4.255	0.115	0.061	20.42
0.843	-0.591	0.127	1.187	9.145	0.142	0.043	35.88
0.753	-0.589	0.127	0.742	14.64	0.149	0.039	41.63
0.708	-0.590	0.124	0.582	18.65	0.158	0.031	55.99
0.618	-0.575	0.121	0.398	27.31	0.164	0.026	67.46
0.500	-0.564	0.117	0.230	47.24	0.169	0.022	84.95
0.330	-0.522	0.105	0.199	54.63†	0.201	0.000(2)	-

* see Table 8.4 for alphabetic footnotes

† low value for solution concentration by comparison with results in Table 8.10 at low water activity. Reasons for this are unclear.

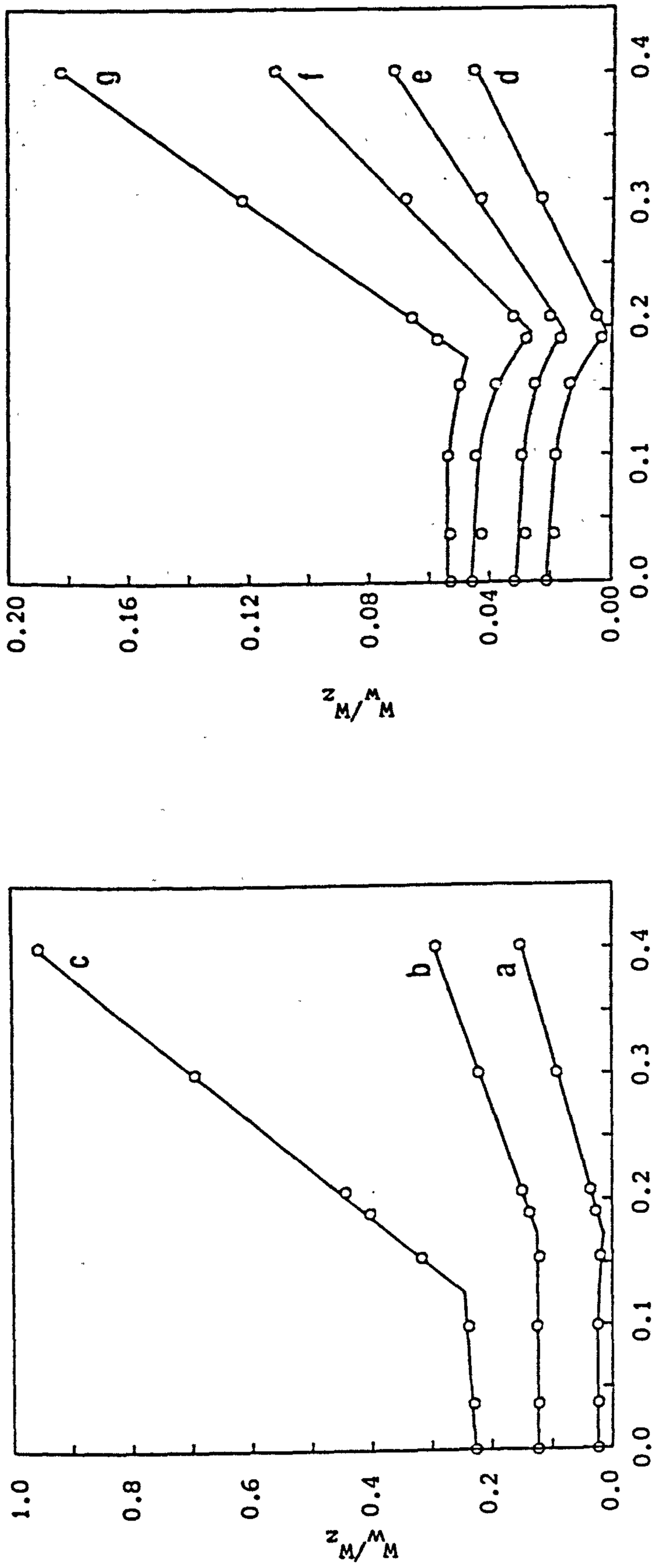

Figure 8.31 Imbibition plots for the glycerol/silicalite(S17) system at different water activities: (a) 0.708; (b) 0.753; (c) 0.925 (d) 0.428; (e) 0.500; (f) 0.618; (g) 0.708

Plots (b) and (c) are displaced by 0.1 and 0.2 units respectively on the ordinate axis.

Plots (e), (f) and (g) are displaced by 0.01, 0.02 and 0.03 units respectively on the ordinate axis.

Table 8.12 Imbibition results for glycerol + silicalite(S17)

a_w [a]	U_w^o	m [b]	U_s	U_w
-	0.030	0.721	0.008	0.030 [c]
-	0.033	1.681	0.014	0.033 [c]
-	0.031	1.860	0.016	0.031 [c]
-	0.030	2.900	0.028	0.030 [c]
-	0.030	3.923	0.072	0.034 [d]
0.925	0.027	4.170	0.128	0.042 [d]
0.843	0.026	8.914	0.162	0.028 [d]
0.753	0.023	14.73	0.169	0.023
0.708	0.023	18.26	0.175	0.017
0.618	0.026	26.77	0.193	0.007
-	0.022	34.81	0.193	0.010
0.500	0.022	40.92	0.193	0.005
0.428	0.021	51.98	0.195	0.002

[a] water activity of saturated salt solutions used for vapour pressure control (refer to Table 8.3)

[b] solution molality, mol Kg^{-1}

[c] assumed to be the same as U_w^o (solid phase lines assumed to be of zero gradient)

[d] $U_w > U_w^o$ because solid phase portions of the imbibition plots were of positive gradient

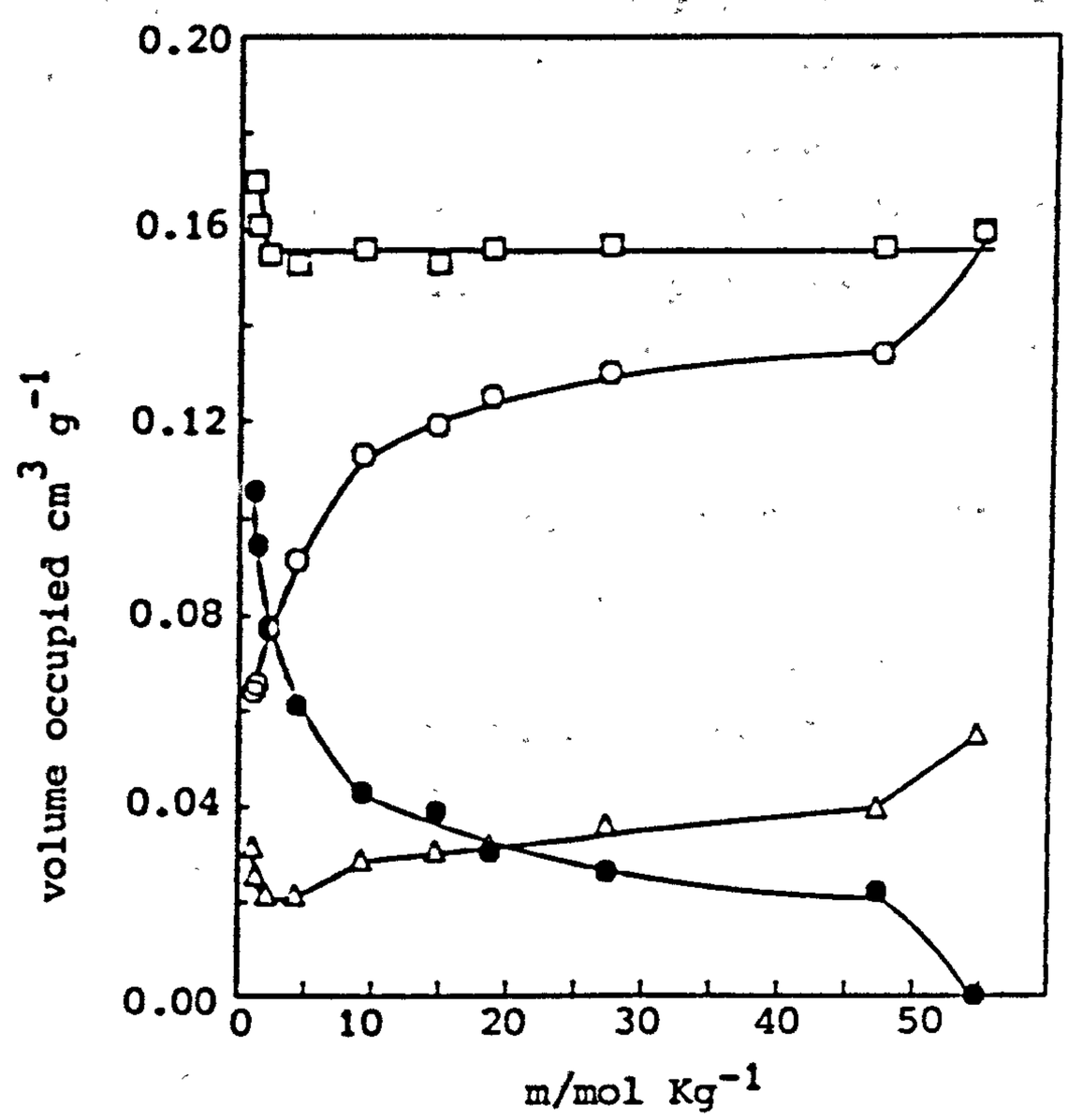

Figure 8.32 Glycerol and water contents ($cm^3\ g^{-1}$ anhydrous solid) of ZSM-5(15.5) as a function of the equilibrium solution concentration (m). Key:

○ glycerol (density taken to be 1.259 g cm^{-3})

● water (density taken to be 1 g cm^{-3})

□ glycerol + water

△ glycerol - volume of water displaced ($U_w^o - U_w$)

a greater volume of glycerol is adsorbed than water is displaced. A similar trend was found for glycerol adsorption by FAU(1.6).

The imbibition plots for silicalite(S17) (Figure 8.31) had a form somewhat different to those of FAU(1.6) and ZSM-5(15.5). At low and intermediate glycerol loadings, none of the adsorbed water is displaced and it is only when the loading begins to approach pore filling that the water content is lowered. Hence the progressive 'dipped' natures of the solid phase portions of the plots in Figure 8.31. Intersections from these plots were interpolated from large scale graphs.

Full isotherms for glycerol adsorption by the three materials are shown and compared in Figure 8.33. At low concentrations, glycerol, a polar non-electrolyte, is sorbed to a greater extent by the ZSM-5 than silicalite. At intermediate molalities, the two pentasil materials adsorb more glycerol than FAU(1.6) even though their pore volumes are smaller; the faugasite has a strong affinity for water. The results for the pentasils highlight that to remove organic molecules from aqueous solutions, materials that are devoid of aluminium and associated cations are not necessarily the best suited. Studies by Bibby et al [16] also showed this.

Interestingly the S-shaped form of the silicalite isotherm in Figure 8.33 bears some resemblance to those obtained for the uptake of alkanediols (Figure 6.2, Chapter 6). The maximum uptake of glycerol (0.195 g/g) corresponds to 12.2 molecules per unit cell.

Upon completion of these isopiestic experiments, some properties of the glycerol-loaded materials were investigated. The presence of a substantial amount of glycerol in the pores of FAU(1.6) did not alter its X-ray diffraction pattern (Figure 8.34). This was not the case for the ZSM-5 and silicalite (Figures 8.35 and 8.36). For these pentasil materials, peaks at low 2θ ($\sim$8-9°) decrease in intensity and those at high 2θ ($\sim$23-24°) increase in intensity with glycerol loading. There is also a considerable number of minor intensity changes, splitting differences and small peak shifts that are dependent on the organic loading.

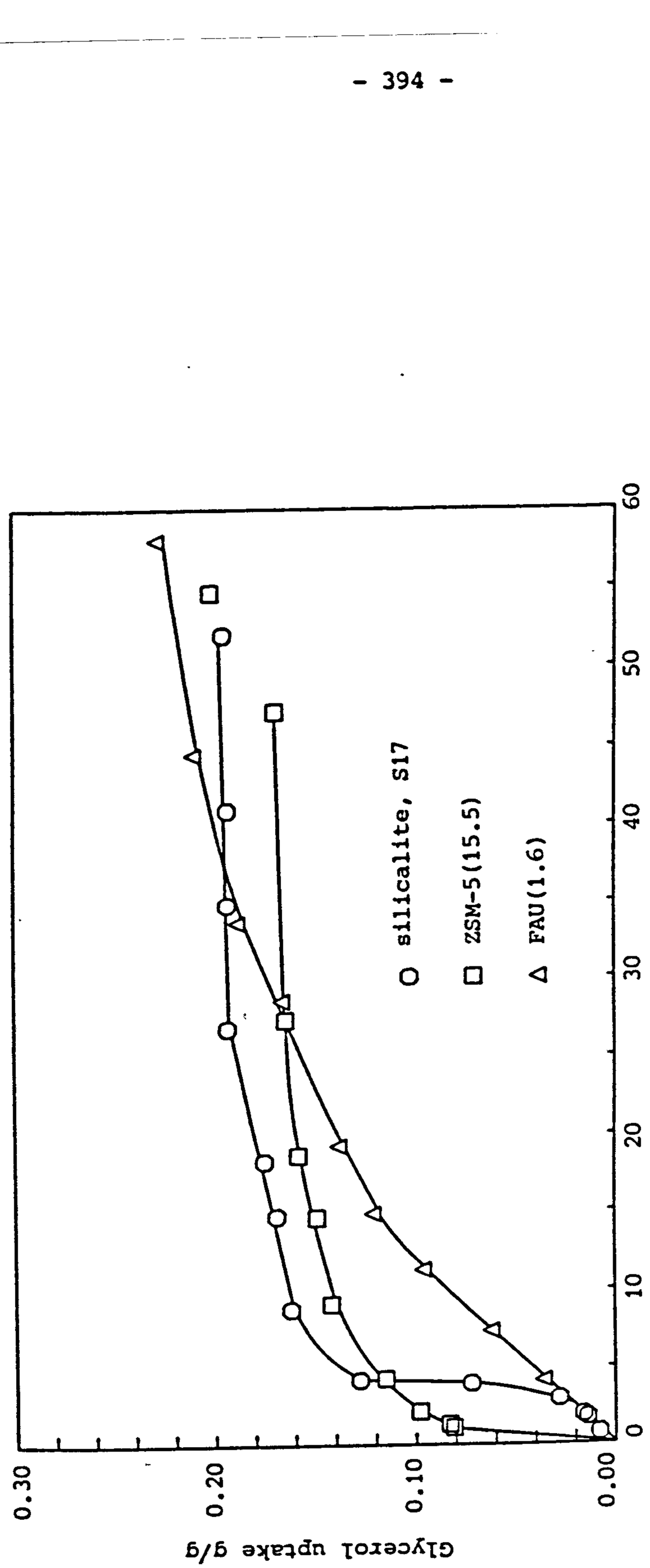

Figure 8.33 Adsorption isotherms showing the uptake of glycerol from aqueous (molality, m) into different zeolitic materials

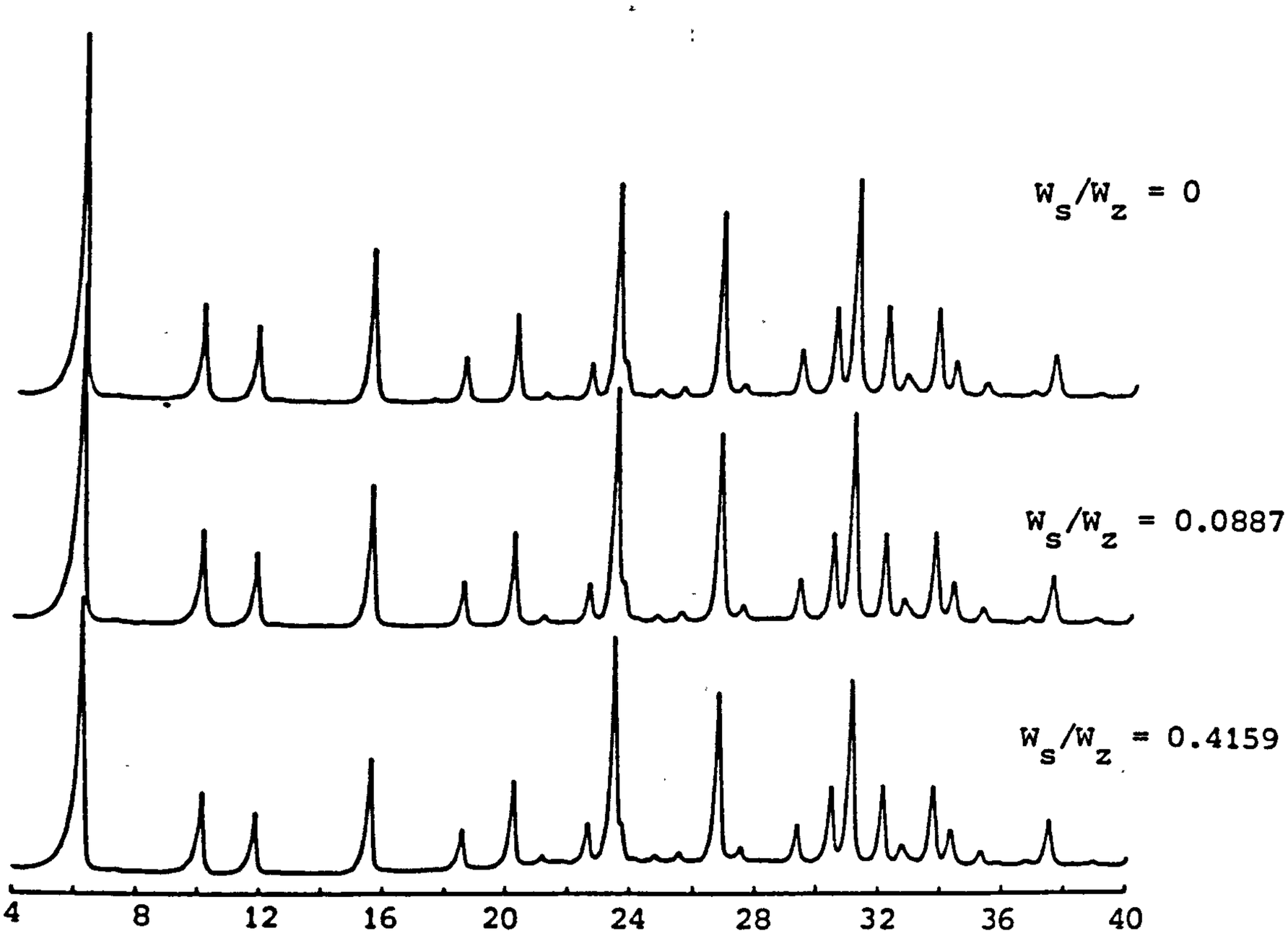

Figure 8.34 X-ray powder diffraction patterns of glycerol/FAU(1.6) mixtures after equilibration at a_w = 0.753. The imbibition results at this water activity are shown in Figure 8.29 and Table 8.10; U_s = 0.121. The presence of a glycerol solution in contact with zeolite crystals in the mixture with W_s/W_z = 0.416 caused a reduction in the diffraction line intensities.

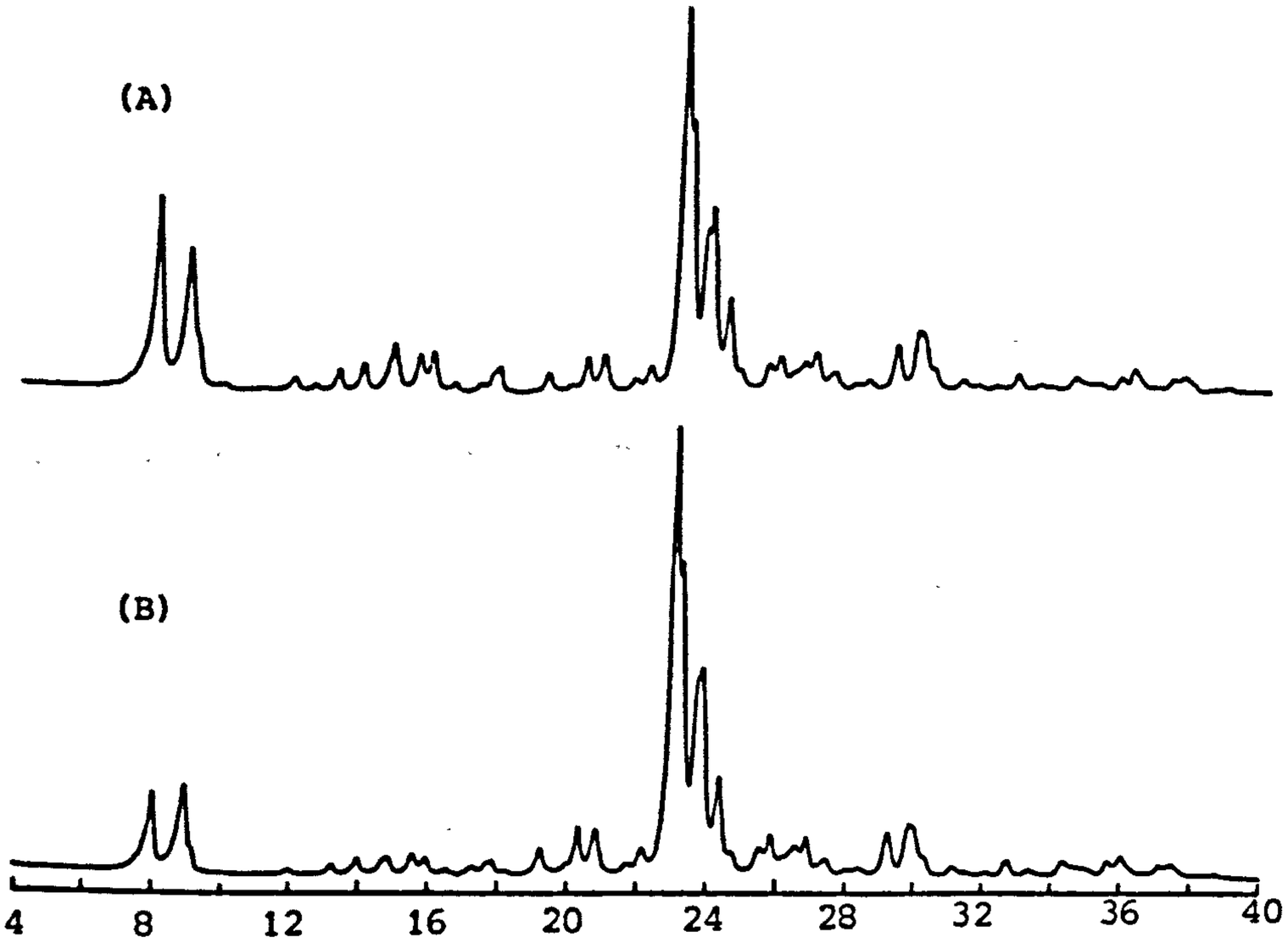

Figure 8.35

X-ray diffraction patterns of (A) ZSM-5(15.5) and (B) glycerol/ZSM-5(15.5) mixture (W_s/W_z = 0.171), both after equilibration at a_w = 0.330. In the latter case, all the glycerol was imbibed (see Figure 8.30).

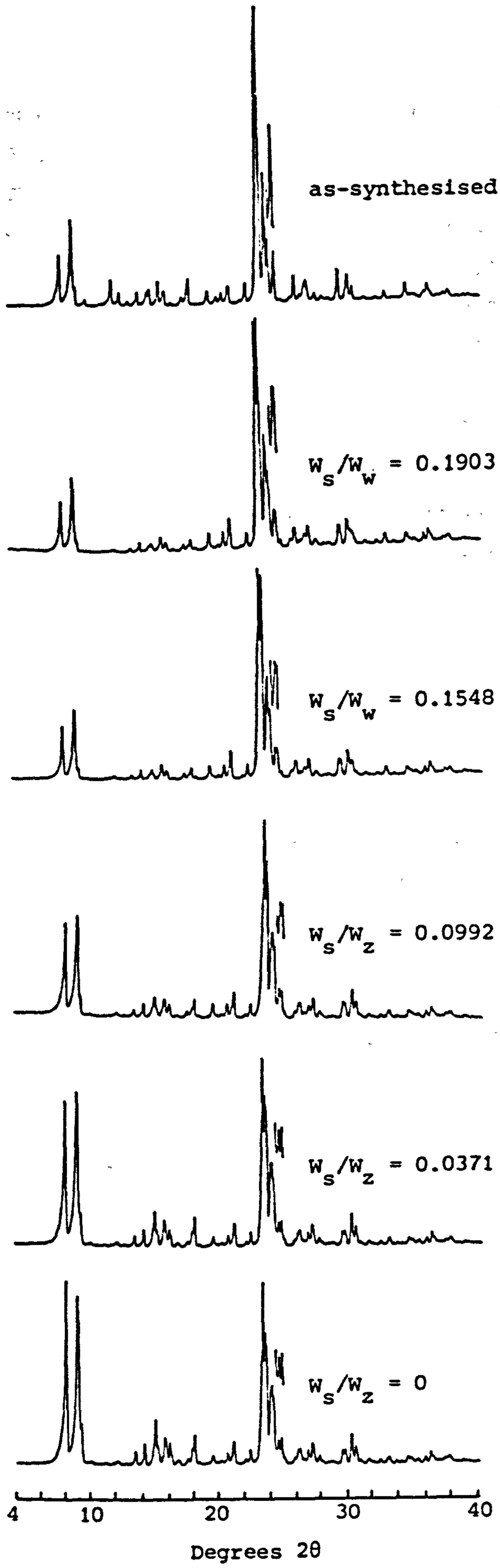

Figure 8.36 X-ray powder diffraction patterns of as-synthesised silicalite(S17) and glycerol/silicalite(S17) mixtures after equilibration at a_w = 0.500 (U_s = 0.193 g/g). As the glycerol loading increases, the peaks at ∿8.0 and 8.9° 2θ decrease in intensity and the doublet at ∿24.5° 2θ becomes a singlet. The peak(s) at ∿24.5° 2θ are shown enlarged above each pattern.

The glycerol-loaded silicalite samples show the major intensity changes particularly well (Figure 8.36). Also very clear is the doublet→singlet transition at ∿24.5° 2θ as the organic content increases. This transition indicates a change from monoclinic to orthorhombic symmetry [17]. Two points are mentioned in connection with this:

(i) The XRD pattern of as-synthesised silicalite (S17) (see Figure 8.36) bears resemblance to those of samples loaded with considerable amounts of glycerol; both entrapped TPA ions and adsorbed glycerol affect peak intensities in the same manner and both organics confer orthorhombic symmetry on the crystals.

(ii) The XRD pattern of ZSM-5(15.5) loaded with glycerol shows, in relation to the organic free material, slightly reduced peaks at low 2θ, and slightly increased peaks at high 2θ. The effects are much less marked than for the silicalite and its glycerol loaded counterparts (c.f. Figures 8.35 and 8.36). Also, ZSM-5(15.5), both organic free and loaded with glycerol, is orthorhombic (no splitting of the peak at ∿24.5° 2θ).

Thermal analysis of the FAU(1.6) samples loaded with glycerol (Figure 8.37) showed the organic was lost in two stages - a low temperature physical desorption and a higher temperature exothermic event. Thermal analysis of samples from the ZSM-5(15.5) and silicalite(S17) experiments showed that glycerol was not completely involatile (see Figure 8.38); the supposedly organic free materials (W_s/W_z = 0) were found to contain small amounts of sorbed glycerol. Whilst this was unexpected, the experiments are not believed to have been seriously affected by this.

At low water activities, glycerol solutions are viscous and water is effectively the solute (the minor component). This fact may be partly the reason why some of the calculated equilibrium solution concentrations at low water activities varied more than expected from system to system.

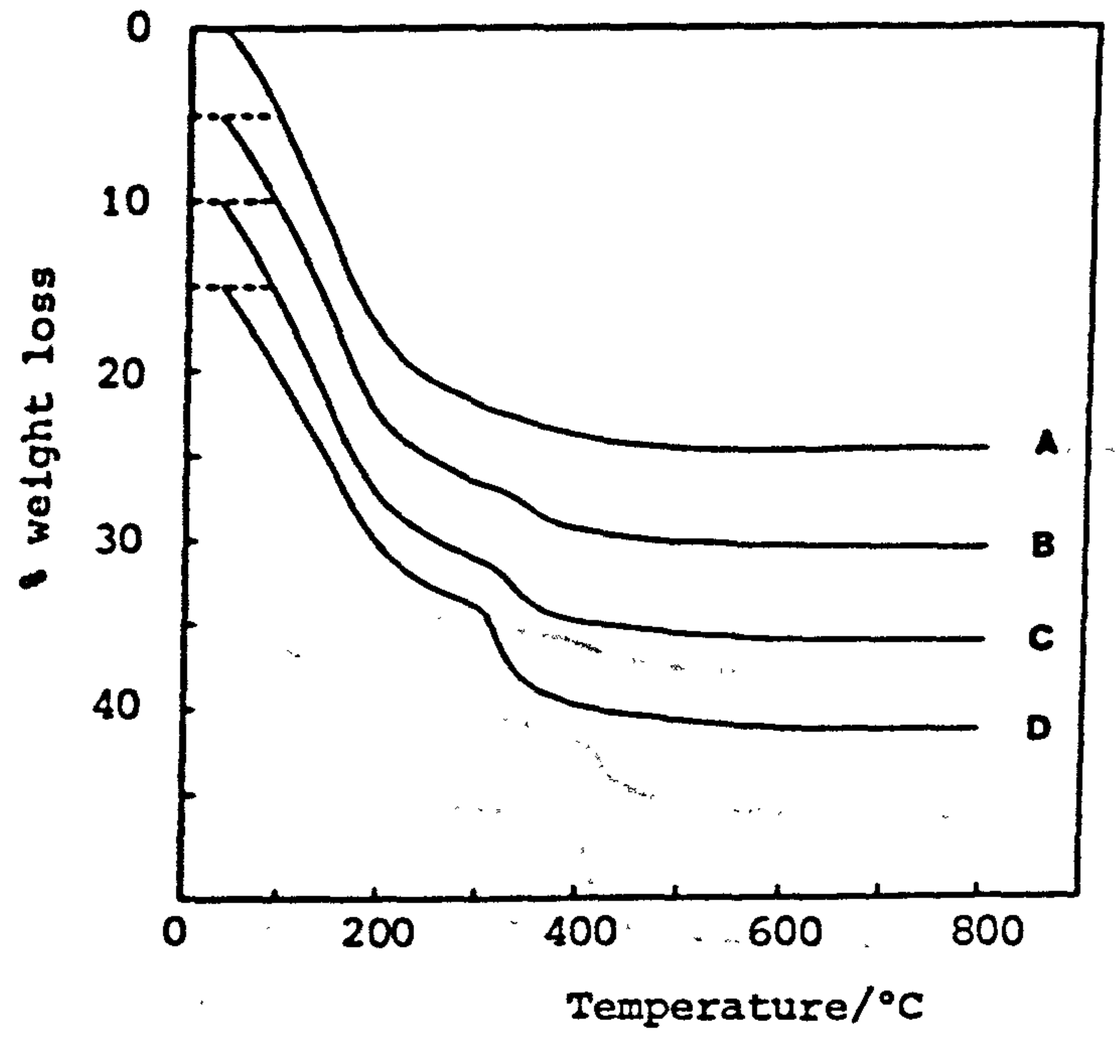

Figure 8.37 TGA and DTA curves of glycerol/FAU(1.6) mixtures after equilibration at a_w = 0.753. The W_s/W_z values of the mixtures were (A) 0, (B) 0.022, (C) 0.045 and (D) 0.089. In each case, all the glycerol was sorbed; the imbibition plot at a_w = 0.753 in Figure 8.29 shows this clearly.

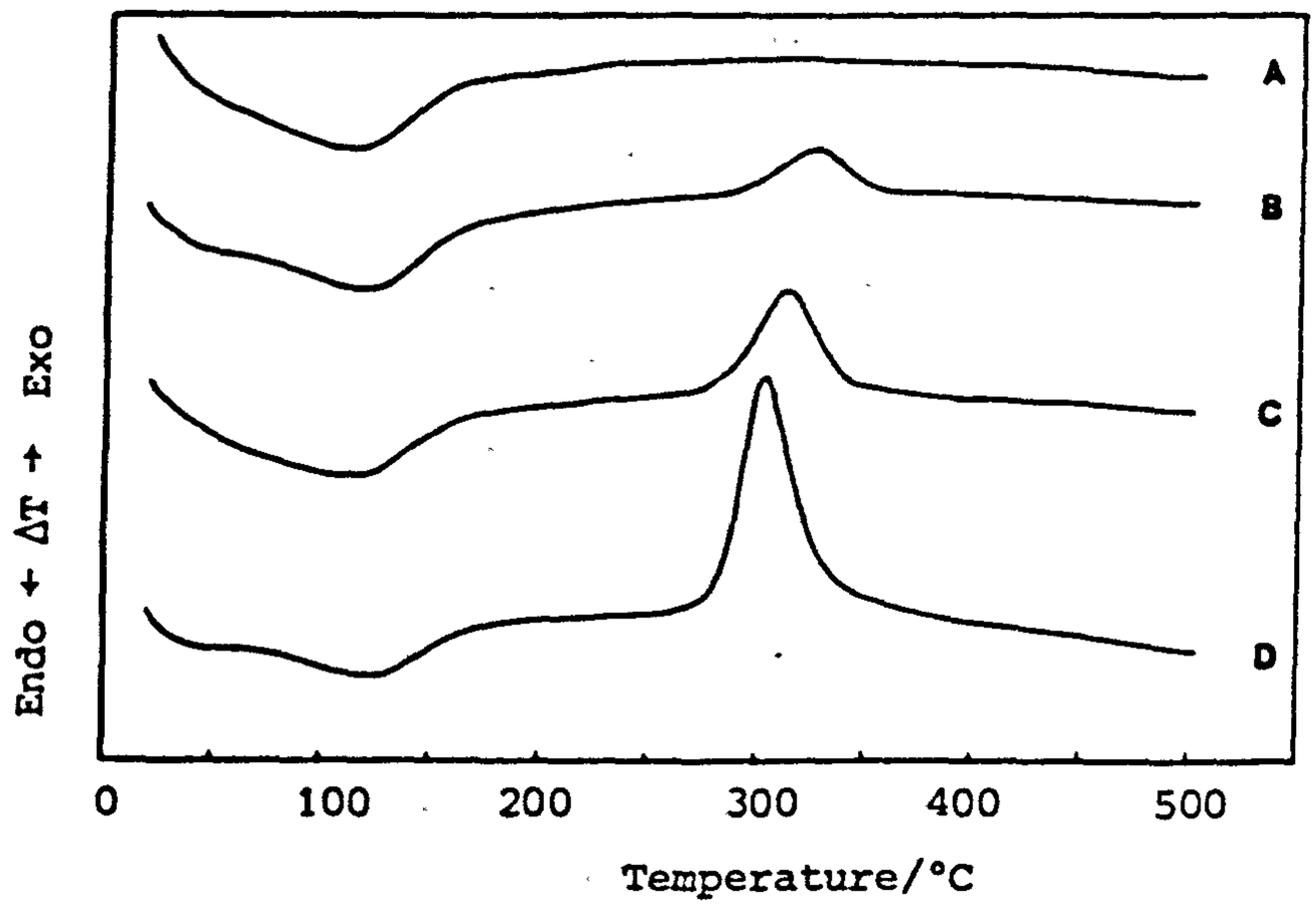

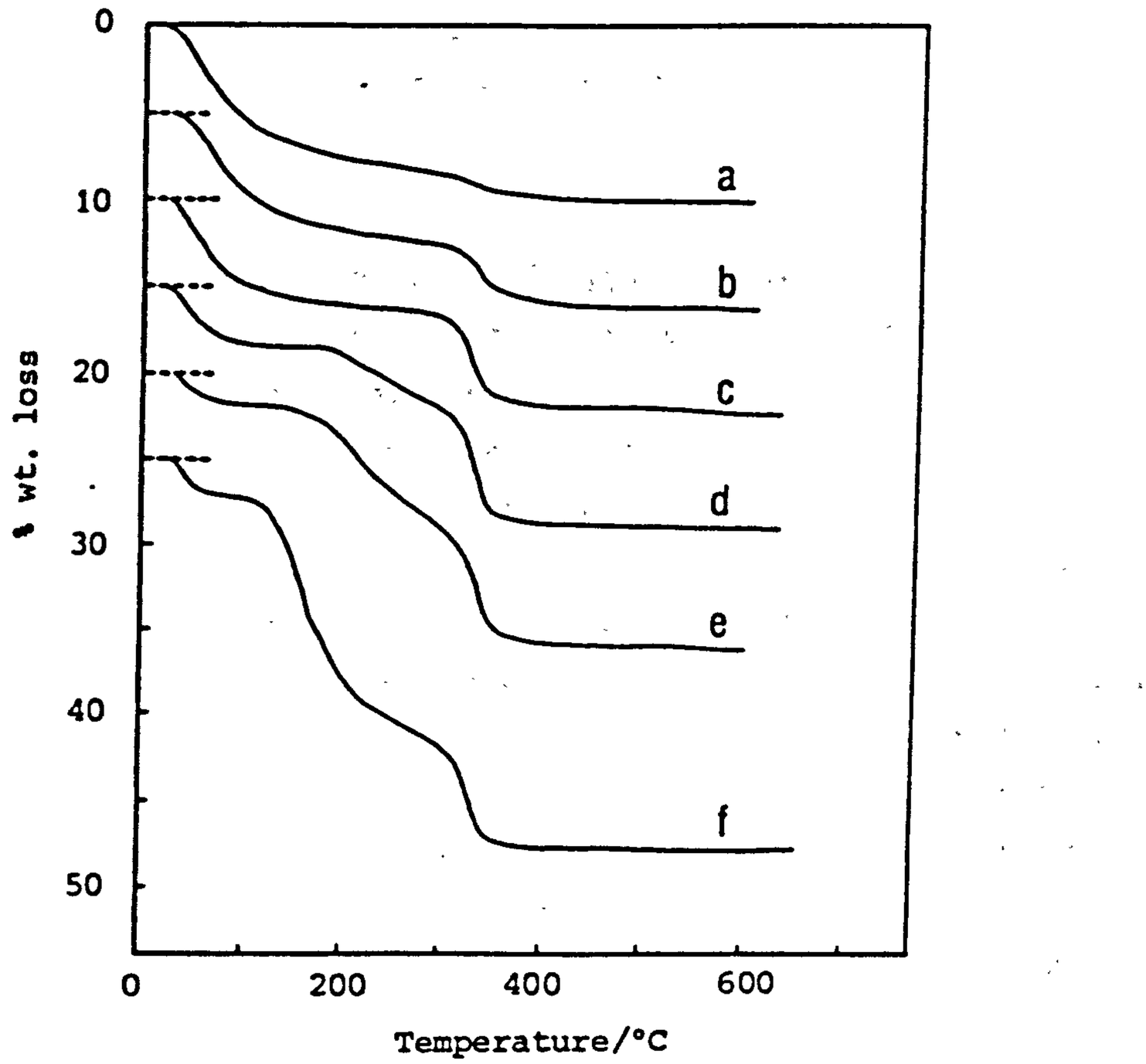

Figure 8.38 TGA curves for glycerol/ZSM-5(15.5) mixtures after equilibration at a_w = 0.330 (at this water activity U_s = 0.201). The curves correspond to the following W_s/W_z values: (a) 0, (b) 0.0289, (c) 0.0602, (d) 0.1197, (e) 0.1705, (f) 0.2713. The plots have been successively displaced by 5 units on the ordinate axis. Curve (a) shows a small weight loss at ∿320°C (c.f. other curves) due to glycerol adsorbed through the vapour phase.

The results for glycerol adsorption have brought interesting information to light and have shown that the isopiestic method can be well applied to solutions of non-electrolytes. Obvious solutes for future study include sugars and water soluble polymers. A further variant when involved with non-electrolytes is the possibility of investigating the adsorption of one particular solute on different cationic forms of the same zeolite. The isopiestic technique could reveal much about as yet unknown cation sieving and selectivity effects.

8.5 Concluding Remarks

This chapter has described a novel approach, based on isopiestic vapour pressure measurements, to solution phase adsorption by zeolitic materials. Ways in which the results interrelate with other work in this thesis have already been mentioned. The results presented have demonstrated the powerful nature of the isopiestic technique and some of its many applications. Theoretical considerations of the imbibition/adsorption processes have not been discussed; the large number of sorbate/sorbent systems researched makes this a task of some magnitude. An insight into the theory involved will be given when these results, along with others not described here, are reported in the literature. A full list of all the sorbate/sorbent systems investigated is given in Appendix IV. To date, only one paper, introducing the application of the isopiestic technique to zeolite adsorption studies, has been published (Appendix V).

The chief advantages and applications of the isopiestic method are summarised below:

(1) All information is obtained from weighings - the method does not rely on a specific property of the solute. The equilibrium contents of the zeolite and the solution phase concentration can all be determined gravimetrically.

(2) The technique is equally applicable to the adsorption of electrolytes and non-electrolytes. The solute under study must, however, be involatile.

(3) The technique can be applied to adsorption/imbibition from non-aqueous solutions. Preliminary experiments with methanolic solutions have been carried out - the results will be described elsewhere.

(4) Adsorption/imbibition by other porous solids besides zeolites can be studied by the method.

(5) The technique can be applied to adsorption on non-porous solids providing they have sufficiently large specific surface areas. It should be mentioned that, when working with porous solids, internal and external adsorption can not be distinguished. The external surface areas of zeolite crystals are seldom significant by comparison with the internal surface area of their channels and hence in zeolite work external adsorption can be deemed negligible. However this is unlikely to be the case with other porous solids.

Clearly there are many applications of the isopiestic technique that have yet to be investigated. The generality of the method makes it one which could find application in many laboratories in the future. The experimental equipment required is specialised but at the same time relatively inexpensive. In fact, trial experiments carried out latterly with a much simpler experimental arrangement (with the zeolite samples contained in glass bottles in a standard dessicator) yielded promising results. This indicated that, with care, far 'cruder' apparatus than originally thought could in some instances suffice to give satisfactory results.

Chapter 8 - References

[1] W.R. Bousfield
Trans. Faraday Soc., 1917, 13, 401.

[2] D.A. Sinclair
J.Phys.Chem., 1933, 37, 495.

[3] R.A. Robinson and D.A. Sinclair
J.Amer.Chem.Soc., 1934, 56, 1830.

[4] R.A. Robinson and R.H. Stokes
"Electrolyte Solutions", Butterworths, London, 1955.

[5] G. Scatchard, W.J. Hamer and S.E. Wood
J.Amer.Chem.Soc., 1938, 60, 3061.

[6] O.D. Bonner and W.H. Breazeale
J.Chem.Eng. Data, 1965, 10, 325.

[7] R. Mallinson
Ph.D. Thesis, University of Edinburgh, 1975.

[8] A.V. Luk'yanov
Siberian Chemical Journal, 1967, 67, 707.

[9] G. Scatchard, W.J. Hamer and S.E. Wood
J.Amer.Chem.Soc., 1938, 60, 3061.

[10] R.E. Wilson
J.Amer.Chem.Soc., 1921, 43, 704.

[11] N. McGhilp
Ph.D. Thesis, University of Edinburgh, 1976.

[11a] R.H. Stokes and R.A. Robinson
Ind.Eng.Chem., 1948, 2013.

[12] W.M. Meier and D.H. Olson
"Atlas of Zeolite Structure Types", published by the Structure Commission of the International Zeolite Association (1978).

[13] R.M. Barrer and A.J. Walker
Trans. Faraday Soc., 1964, 60, 171.

[14] R.M. Barrer and W.M. Meier
J.Chem.Soc., 1958, 299.

[16] N.B. Milestone and D.M. Bibby
J.Chem.Techn. Biotechnol., 1983, 34A, 73.

[17] E.L. Wu, S.L. Lawton, D.H. Olson, A.C. Rohrman Jr., and G.T. Kokotailo
J.Phys.Chem., 1979, 83, 2777.

PAGE
MISSING
IN
ORIGINAL

Chapter 9

Final Comments

The hydrophilic and organophilic properties of zeolites and silica molecular sieves are topics that encompass a spectrum of different aspects of zeolite science, indeed so many that a thesis entitled as such could include in its pages results from a host of subject areas. Several different although closely interrelated topics have been covered in this work. The most obvious common factor has been the involvement with the aqueous solution chemistry of zeolitic materials but many less apparent inter-connecting features have been discussed in the text. Conclusions drawn from results have been described chapter by chapter and it is not possible to succinctly summarise them again here. All the work accomplished during the three year research program could not be incorporated in this thesis but it is hoped that some of the results that remain outstanding will be published in the literature in the near future.

Several ideas for future research have emanated from the presented work and pointers to these have been given at appropriate places in previous chapters. Zeolite science is an unusually rich field for research and work will no doubt continue to flourish in both academic and industrial circles. It is somewhat ironic though that by far the majority of zeolites remain laboratory curiosities; of the hundred or so zeolites now known, with the wealth of knowledge now available and with the level of research being undertaken, it is surprising that only a handful of zeolites are used on a commercial scale. The inception of novel uses and increased understanding of their science are clearly two of the important factors that will determine what the commercial future holds for these fascinating solids.

Appendices

Appendix I

Spectrophotometric Determination of Soluble Silica by the Molybdate Method

The molybdate method [1,2,3] was used to quantify the amount of silica in solution at the end of crystallisations. Under certain conditions, orthosilicic acid reacts with a solution of molybdate in an acid medium to give an intense yellow coloration due to α-molybdosilicic acid. Conditions were chosen such that only the α-acid, and not the β-acid, formed.

A calibration procedure was carried out as follows. A standard silicate solution was prepared by the fusion of ca. 0.1 g anhydrous SiO_2 (BDH colloidal silica powder, low in iron, accurately weighed after heating at 1000°C for 15 minutes and cooling to room temperature over P_2O_5) with about five times that weight (accurate weighing not necessary) of sodium carbonate (AnalaR grade). The fusion process was carried out over a meker burner. The resultant glass was then cooled and dissolved in distilled water to give a concentrated silicate solution of known concentration. Small aliquots of this solution were diluted (glass distilled water was used throughout) to give a series of standard solutions that contained 0-25 ppm SiO_2. Although all solutions were made up in glass, they were immediately transferred to air-tight screw-top plastic bottles after preparation.

A buffered molybdate solution, 0.2M in both acetic acid and sodium acetate, 0.1M in molybdenum (derived from ammonium molybdate (AnalaR)) and adjusted to pH = 4.0 with concentrated sulphuric acid (AnalaR) was prepared and likewise stored in a plastic bottle. This solution was made up just before analyses were carried out, as after storage for a few hours a white solid began to precipitate out. 25 cm^3 of the molybdate buffer were added to (a) 25 cm^3 of each of the standard solutions and also to (b) 25 cm^3 of distilled water (this solution was used as the spectrophotometric blank). After leaving to stand for 15 minutes whilst the acid reacted with the molybdate to form the yellow complex, absorbance measurements were made at 390 nm using a Pye Unicam SP500 spectrophotometer. The solutions had a pH of 4.0 ± 0.1.

Mother liquors to be analysed for soluble silica were filtered through 0.2 μm membrane filters (Gallenkamp) (to remove all solid matter) immediately after reactions were complete and stored in sealed plastic bottles. For analysis, portions of the mother liquors were diluted (to known extents) and reacted with the molybdate buffer in the same way as the standards. The dilutions were carried out by trial and error until absorbance readings were within the calibration range.

Formation of the α-acid was seen to be rapid (development of a yellow coloration) and stable absorbance readings were obtained. Only orthosilicic acid reacts with molybdate and as no time-dependent changes in the absorbance readings were noted this indicated that virtually all the soluble silica was near-monomeric (the dilution state of the analytical procedure no doubt contributed in part to this). Had larger polymeric species been present absorbance readings would have increased with time as depolymerisation to monomeric species occurred. (Solutions that contain polymeric species can be treated with strong alkali prior to analysis. This treatment renders all soluble silica monomeric).

The presence of large concentrations of tetrapropylammonium bromide in solutions interferred with the analysis; a white precipitate formed on addition of the molybdate buffer. This problem was overcome by using a cation-exchange resin (in the sodium form) to reduce the amount of quaternary ion in some of the mother liquors. The presence of sodium salts in the mother liquors did not appear to upset the analysis.

[1] V.W. Truesdale and C.J. Smith
Analyst, 1975, 100, 203.

[2] V.W. Truesdale and C.J. Smith
Analyst, 1975, 100, 797.

[3] V.W. Truesdale and C.J. Smith
Analyst, 1976, 101, 19.

Appendix II

Exploratory Crystallisations in Capillary Tubes

The table below gives details of reaction mixtures that were successfully crystallised (as observed by optical microscopy) in sealed capillary tubes. Although no product analysis was carried out, ZSM-48 was believed to be the product in many cases (see European patent applications 15,132 (1980, L.D. Rollmann and E.W. Valyocsik) and 46,504 (1982, L. Marosi, M. Schwarzmann and J. Stabenow)).

Amine	Moles Amine	SiO_2	H_2O	Temp./°C	Time/Days
piperazine	10	20	1500	180	4
1-methylbenzylamine	10	10	1000	180	15
d-methylbenzylamine	10	10	1000	175	7
DABCO[a]	10	10	1000	150	17
DABCO[a]	10	10	1000	175	7
hexylamine	5	5	1000	150	20
hexylamine	5	5	1000	175	8
diethanolamine	50	10	1000	125	25
diethanolamine	50	10	1000	150	11
diethanolamine	50	10	1000	175	4
cyclohexylamine	50	10	1000	150	17
cyclohexylamine	50	10	1000	175	4
diethylamine	50	10	1000	125	25
diethylamine	50	10	1000	150	17
diethylamine	50	10	1000	175	8
1,2-diaminoethane	50	10	1000	125	25
1,2-diaminoethane	50	10	1000	150	11
1,2-diaminoethane	50	10	1000	175	4
triethylenetetramine	50	10	1000	150	11
triethylenetetramine	50	10	1000	175	4
N,N'-dimethylpiperazine	50	10	1000	150	17
N,N'-dimethylpiperazine	50	10	1000	175	8

[a] 1,4-diazabicyclo[2,2,2]octane

APPENDIX III

Computer Programs Referred to in Chapter 5

```
10   REM  THIS IS FILE 'PHUP1'
20   REM  THIS PROGRAM MODELS CRYSTALLISATION OF DENSE SILICAS FROM
          MIXTURES OF COMPOSITION : XM2O 2OSIO2 1OOOH2O
30   REM  THIS PROGRAM ASSUMES 1000 GRAMS OF WATER ARE USED TO PREPARE
          REACTION MIXTURES.
40   REM  INPUT VALUES FOR CONSTANTS
50   K1 = 2E - 10:K2 = 2E - 12
60   KS = 2.5E - 03: PR£ 1
70   PRINT "K1=";K1: PRINT "K2=";K2
90   PRINT "RESULTS OUTPUT : KS,X,(M+),PH,(ST),% SOLID"
100  PRINT
110  REM  INPUT ALKALINITY FROM REACTION COMPOSITION (X)
120  PR£0: KS = 2.5E - 03: INPUT "X=";X1
130  REM  CALCULATE THE CONCENTRATION OF BASE CATIONS (A)
140  A = 2 * X1 / 18.015
150  REM  STATEMENTS 160 - 200 ALLOW THE PH TO BE CALCULATED
160  B =  - (K1 * KS + 1E - 14):C =  - 2 * K1 * K2 * KS
170  D = B * B - 4 * A * C
180  E =  SQR (D)
190  F = ( - B + E) / (2 * A)
200  PH =  - LOG (F) / LOG (10)
210  REM  CALCULATE THE CONCENTRATIONS OF SILICATE IONS IN
          SOLUTION (S1 AND S2)
220  S1 = K1 * KS / F
230  S2 = K1 * K2 * KS / (F * F)
240  REM  CALCULATE THE TOTAL CONCENTRATION OF SOLUBLE SILICA (ST)
          (INCLUDES ORTHOSILICIC ACID)
250  ST = S1 + S2 + KS
260  REM  CALCULATE THE AMOUNT OF SILICA THAT IS SOLID (NS)
270  NS = 20 / 18.015 - ST
280  REM  CALCULATE THE % OF THE TOTAL SILICA THAT IS SOLID (PN)
290  PN = NS * 100 * 18.015 / 20
300  REM  PRINT STATEMENTS FOR OUPUT
310  PR£ 1
320  PRINT KS;"  ";X1;"  ";A;"  ";PH;"  ";ST;"  ";PN
330  REM  LOOP REPEATING CALCULATIONS WITH KS=1.8E-04
340  IF KS = 1.8E - 04 THEN  GOTO 120
350  KS = 1.8E - 04
360  PR£ 0
370  GOTO 160
```

```
10  REM  THIS IS FILE 'PHUP2'
20  REM  THIS PROGRAM MODELS SILICALITE CRYSTALLISATION
         CHEMICAL COMPOSITION OF CRYSTALS : 4TPAOH 96SIO2
30  PRE 1
40  REM  PRINT REACTION SYSTEM BEING INVESTIGATED
50  PRINT "XNA2O-2OSIO2-2TPABR-1OOOH2O"
60  PRINT "-----------------------------" : PRINT
70  PRINT "THIS PROGRAM ASSUMES 1000 GRAMS OF WATER ARE USED IN MIXTURES"
80  PRINT
90  PRE 0
100 REM  INPUT REACTION ALKALINITY (X1)
110 INPUT "X=";X1
120 REM  CALCULATE INITIAL BASE CATION CONCENTRATION (A)
130 A = 2 * X1 / 18.015
140 REM  INPUT VALUES FOR CONSTANTS
150 K1 = 2E - 10:K2 = 2E - 12
160 KS = 2.5E - 03
170 PRE 1
180 PRINT "X=";X1
190 PRINT "K1=";K1: PRINT "K2=";K2
200 PRINT "KS=";KS: PRINT : PRE 0
210 REM  CALCULATE NOS MOLES SIO2 CRYSTALLISED (FS). NOTE FS IS INITIALLY ZERO
220 FS = RS / 2 + FS
230 REM  CALCULATE NOS MOLES BASE LOST (BL). NOTE BL IS INITIALLY ZERO
240 BL = FS * 4 / 96
250 REM  CALCULATE THE EFFECTIVE BASE CATION CONCENTRATION (A), ALLOWANCE BEING
         MADE FOR BASE TIED UP IN THE CRYSTALS
260 A = 2 * X1 / 18.015 - BL
270 REM  STATEMENTS 280 - 320 ALLOW THE PH TO BE CALCULATED
280 B =  - (K1 * KS + 1E - 14):C =  - 2 * K1 * K2 * KS
290 D = B * B - 4 * A * C
300 E =  SQR (D)
310 F = ( - B + E) / (2 * A)
320 PH =  -  LOG (F) /  LOG (10)
330 REM  CALCULATE THE CONCENTRATION OF SINGLY CHARGED SILICATE ANION (S1)
340 S1 = K1 * KS / F
350 REM  CALCULATE THE CONCENTRATION OF DOUBLY CHARGED SILICATE ANION (S2)
360 S2 = K1 * K2 * KS / (F * F)
         MADE FOR BASE TIED UP IN THE CRYSTALS
370 REM  CALCULATE THE TOTAL CONCENTRATION OF SOLUBLE SILICA (ST) (INCLUDES
         ORTHOSILICIC ACID)
380 ST = S1 + S2 + KS
390 REM  CALCULATE NOS MOLES SOLID SIO2 (GEL + XALS) (NS)
400 NS = 20 / 18.015 - ST
410 REM  CALCULATE NOS MOLES GEL (RS)
420 RS = 20 / 18.015 - ST - FS
430 REM  CALCULATE % CRYSTALLNITY OF THE SOLID PHASE (XL) ON A MASS BASIS
440 XL = FS * 100 / NS
450 REM  CALCULATE PRODUCT YIELD (YD)
460 YD = FS * 100 * 18.015 / 20
470 REM  CALCULATE % OF THE TOTAL SIO2 THAT IS SOLID (GEL + XALS) (PN)
480 PN = NS * 100 * 18.015 / 20
490 REM  CALCULATE MOLAR NA/TPA RATIO IN SOLUTION (CR)
500 CR = (2 * X1 / 18.015) / (2 / 18.015 - BL)
510 REM  CALCULATE MOLE FRACTION SODIUM IONS IN SOLUTION (MC)
520 MC = (2 * X1 / 18.015) / (2 * X1 / 18.015 + 2 / 18.015 - BL)
530 PRE 1
540 IF XL > 95 THEN  PRE 0
550 IF XL > 99.9 THEN  PRE 1
560 REM  PRINT STATEMENTS FOR OUTPUT
570 PRINT "(C+)=";A: PRINT "PH="PH
580 PRINT "(S1)=";S1: PRINT "(S2)=";S2
590 PRINT "NOS MOLES SIO2 IN SYSTEM=";20 / 18.015
600 PRINT "NOS MOLES SIO2 IN SOLUTION=";ST
610 PRINT "NOS MOLES SOLID SIO2 PRESENT(GEL+XALS)=";NS
620 PRINT "% TOTAL SIO2 PRESENT AS SOLID(GEL+XALS)=";PN
630 PRINT "NOS MOLES GEL PRESENT=";RS
640 PRINT "NOS MOLES SIO2 XALLISED=";NS - RS
650 PRINT "NOS MOLES BASE IN XALS=";BL
660 PRINT "% TOTAL BASE TIED UP IN XALS=";BL * 100 / (2 * X1 / 18.015)
670 PRINT "% CRYSTALLINITY=";XL: PRINT "% YIELD=";YD
680 PRINT "NA/TPA RATIO IN SOLUTION=";CR
690 PRINT "NA/(NA+TPA)=";MC
700 PRINT : PRINT
710 REM  CONDITIONAL STATEMENT : IF % CRYSTALLINITY > 99.9 PROGRAM STOPS
720 IF XL > 99.9 THEN  END
730 REM  LOOP TO CONTINUE CRYSTALLISATION
740 GOTO 220
```

```
10    REM  THIS IS FILE 'PHAMINE'
20    REM  THIS PROGRAM MODELS SILICALITE CRYSTALLISATION. IT IS
           ASSUMED THAT 1000 GRAMS OF WATER ARE USED TO PREPARE
           REACTION MIXTURES.
           CHEMICAL COMPOSITION OF CRYSTALS : 4TPAOH 96SIO2
30    REM  INPUT VALUES FOR CONSTANTS
40    K1 = 2E - 10:K2 = 2E - 12:KW = 1E - 14
50    KS = 1.8E - 04
60    KA = 1E - 10
70    PR£ 1
80    REM  PRINT REACTION SYSTEM BEING INVESTIGATED
90    PRINT "N-AMINE 20SIO2 2TPABR 1000H2O"
100   PRINT "----------------------------"
110   PRINT "K1=";K1: PRINT "K2=";K2
120   PRINT "KA=";KA: PRINT "KS=";KS
130   PR£ 0
140   REM  INPUT REACTION ALKALINITY (N) - NOS MOLES AMINE IN MIXTURE
      COMPOSITION
150   INPUT "N=";N
160   REM  CALCULATE CONCENTRATION OF AMINE (AM)
170   AM = N / 18.015
180   REM  STATEMENTS 190 - 340 ALLOW THE REACTION PH TO BE CALCULATED.
           PH VALUES ARE SELECTED UNTIL THE RHS AND LHS OF THE CHARGE
           EQUIVALENCE EQUATION (SEE TEXT IN CHAPTER 5) MATCH
190   INPUT "PH=";PH
200   LG =  - PH *  LOG (10)
210   H =  EXP (LG)
220   REM :CALC LHS EQUATION
230   LH = AM * H / (H + KA) + H
240   REM :CALC RHS EQUATION
250   S1 = K1 * KS / H
260   S2 = K1 * K2 * KS / (H * H)
270   ST = S1 + S2 + KS
280   REM  CALC RHS EQUATION
290   RH = S1 + 2 * S2 + KW / H + BL
300   PRINT "LH=";LH: PRINT "RH=";RH
310   PRINT "LH-RH=";LH - RH: PRINT
320   REM  CONDITIONS FOR DETERMINING WHEN LHS = RHS.
           CAN BE VARIED TO SUIT SYSTEM SENSITIVITY.
330   IF LH - RH > 1E - 04 THEN  GOTO 190
340   IF LH - RH <  - 1E - 04 THEN  GOTO 190
350   REM  CALCULATE NOS MOLES SOLID SIO2 (GEL + XALS) (NS)
360   NS = 20 / 18.015 - ST
370   REM  CALCULATE NOS MOLES AMORPHOUS SOLID (GEL) (RS)
380   RS = NS - FS
390   REM  CALCULATE PRODUCT YIELD (YD)
400   YD = FS * 100 * 18.015 / 20
410   REM  CALCULATE % CRYSTALLINITY OF SOLID PHASE ON A MASS
           BASIS (XL)
420   XL = FS * 100 / NS
430   REM  CALCULATE CONCENTRATION OF PROTONATED AMINE (RP)
440   RP = LH - H
450   REM  CALCULATE CONCENTRATION OF UNPROTONATED AMINE (RN)
460   RN = AM - RP
470   REM  PRINT STATEMENTS FOR OUTPUT
480   PR£ 1
490   PRINT : PRINT "N(IN MIXTURE COMPOSITION)="N
500   PRINT "PH=";PH
510   PRINT "(RNH2 + RNH3+)=";AM
520   PRINT "(RNH3+)=";RP
530   PRINT "(RNH2)=";RN
540   PRINT "(RNH3+)/(RNH2)=";RP / RN
550   PRINT "(RNH3+)/(RNH2 + RNH3+)=";RP / (AM)
560   PRINT "(S1)=";S1
570   PRINT "(S2)=";S2
580   PRINT "(ST)=";ST
590   PRINT "NOS MOLES SIO2 IN SYSTEM=";20 / 18.015
600   PRINT "% TOTAL SIO2 PRESENT AS SOLID(GEL + XALS)=";NS * 100 *
           18.015 / 20
610   PRINT "NOS MOLES SIO2 PRESENT AS SOLID(GEL+XALS)=";NS
620   PRINT "NOS MOLES GEL PRESENT=";RS
630   PRINT "NOS MOLES SIO2 XALLISED=";FS
640   PRINT "% YIELD=";YD
650   PRINT "% CRYSTALLINITY=";XL
```

(contd...)

```
660  PRINT "NOS MOLES BASE IN XALS=";BL
670  PRINT "(RNH3+)/(TPA+)=";RP / (2 / 18.015 - BL)
680  PRINT "(RNH3+)/(RNH3+ + TPA+)=";RP / (RP + 2 / 18.015 - BL)
690  PRINT : PRINT 0
700  PRINT "MOLES XALS=";FS
710  PRINT "MOLES TOTAL SOLID SIO2=";NS
720  PRINT "% CRYSTALLINITY=";XL
730  REM  CHOOSE THE NOS OF MOLES SIO2 THAT ARE TO BE
          CRYSTALLISED (FS)
740  INPUT "MOLES SIO2 CRYSTALLISED=";FS
750  REM  CALCULATE BASE (TPAOH) LOST AS A RESULT
          OF CRYSTALLISATION (BL)
760  BL = FS * 4 / 96
770  REM  LOOP TO CONTINUE CRYSTALLISATION
780  GOTO 190
```

Appendix IV

List of Systems Investigated by the Isopiestic Technique

A list of all the systems investigated by the isopiestic technique is given below. Some were studied in greater detail than others. It was only possible to include a portion of the results in Chapter 8.

Solute	Zeolite Type	
Sodium chloride	Na-A	
Sodium chloride	Na-Faujasite (x 3)	
Sodium bromide	Na-Faujasite	
Sodium iodide	Na-Faujasite	
Sodium carbonate	Na-Faujasite	
Sodium acetate	Na-Faujasite	
Sodium benzenesulphonate	Na-Faujasite	
Sodium pentanesulphonate	Na-Faujasite	
Caesium chloride	(Cs, Na)-Faujasite	
Sodium chloride	Na-ZSM-5	
Sodium acetate	Na-ZSM-5	
Sodium benzenesulphonate	Silicalite	
Sodium pentanesulphonate	Silicalite	
Nickel nitrate	Silicalite	
Sodium chloride	Na-Faujasite	(experiments carried out in glass bottles)
Sodium chloride	Na-S	
Glycerol	Na-Faujasite	
Glycerol	Na-ZSM-5	
Glycerol	Silicalite	
Glycerol	(Cs, Na)-Faujasite	
Glycerol	H-Mordenite	
Polyethyleneglycol 6000	Na-ZSM-5	
Tetrapropylammonium bromide	Silicalite	(experiment with methanol as solvent)

Appendix V

Published Papers

(1) S.G. Fegan and B.M. Lowe
"Crystallisation of Silicalite-1 Precursors",
J.Chem.Soc., Chem.Commun., 1984, 437.

(2) S.G. Fegan and B.M. Lowe
"The Use of Isopiestic Vapour Pressure Measurements to Study Salt Imbibition by Zeolites"
Proceedings of the 6th Int.Conf. on Zeolites (Reno, 1983), p. 288.

(3) S.G. Fegan and B.M. Lowe
"Effect of Alkalinity on the Crystallisation of Silicalite-1 Precursors"
(submitted for publication).

(4) S.G. Fegan and B.M. Lowe
"Crystallisation of Silicalite-1 Precursors in the Amine-TPABr-SiO_2-H_2O System"
(submitted for publication).

Crystallisation of Silicalite-1 Precursors

Stuart G. Fegan and Barrie M. Lowe*
Department of Chemistry, University of Edinburgh, West Mains Road, Edinburgh EH9 3JJ, U.K.

The composition of the (Na, TPA) (TPA = tetrapropylammonium) precursor to silicalite-1 is determined by the base content of the reaction mixture, and for both low and high base contents the crystallisation is accompanied by apparently anomalous pH changes.

High silica zeolites are less soluble in water than the amorphous alumino-silicate gel solids from which they are crystallised and hence their formation is normally associated with an increase in pH.[1,2] A simple theoretical treatment shows that the pH rise and the yield of zeolite both decrease when the base content of the reaction mixture is increased.[2] The present investigation into the crystallisation of the precursor to silicalite-1[3-5] provides the first systematic set of experimental observations against which this theory may be tested.

Silicalite-1 precursors were crystallised at 95 °C in stirred polypropylene reactors from the mixtures xNa$_2$O 2TPABr 20SiO$_2$ 1000H$_2$O (TPA = tetrapropylammonium, $0.25 < x < 6.5$, SiO$_2$ = Cab-o-sil M5). The pH values of samples taken throughout the crystallisation were determined[1] and the final solid products were washed, dried, equilibrated with water vapour, and examined by *X*-ray powder diffraction, *X*-ray fluorescence, and thermal gravimetric analysis. All the reaction mixtures, except that with $x = 0.25$, gave pure well crystallised products with organic contents close to the ideal unit cell composition 4TPAOH 96SiO$_2$. The mixture with $x = 0.25$ contained insufficient base for complete crystallisation and its percentage crystallinity (63%) estimated from *X*-ray powder diffraction measurements was close to the maximum (60%) that could be produced if all the crystalline material had the ideal unit cell composition.

The highest yields (Figure 1) were obtained as predicted[2] from the reaction mixtures that had the lowest base contents. These high yields were not however accompanied by the large increases in pH required by the theory. For $x = 0.5$ and 0.7 the calculated[2] increases in pH are in the ranges 0.78—0.99 and 0.75—0.94 whereas the experimental values are −2.77 and −0.04 respectively. Only for the higher base contents $x = 2$ and $x = 3.5$ are the experimental values (0.78, 0.72) in good agreement with the calculated ones (0.69—0.84, 0.66—0.80).[2] The apparently anomalous decrease in pH obtained for $x = 0.5$ and 0.7 and the abnormally small increases (0.42, 0.42) obtained for $x = 0.85$ and 1.00 are readily interpreted as a consequence of base occlusion. The cations in the silicalite channels must be associated with hydroxide ions or broken siloxane bonds {≡Si–O$^-$ HO–Si≡}; in either case hydroxide ions are removed from the solution phase, and for reaction mixtures with low base contents their removal has a dominant effect on the pH. This is much less significant for reaction mixtures with high base contents and so in these cases there is a reasonable agreement with the theory. For the highest base content the pH increase (0.22) is again less than the calculated value (*ca.* 0.70) but in this case the discrepancy probably arises from an increase in the solubility of the crystalline solid consequent on the incorporation of sodium ions. In particular the outer surface is likely to be rich in sodium and it may have some amorphous character[6] that gives it increased solubility.

All the fully crystalline products contained substantial quantities of sodium ions. The number of sodium atoms per unit cell was found to be linearly dependent on the cation fraction, $2x/(2 + 2x)$, in the reaction mixture (Figure 2). The

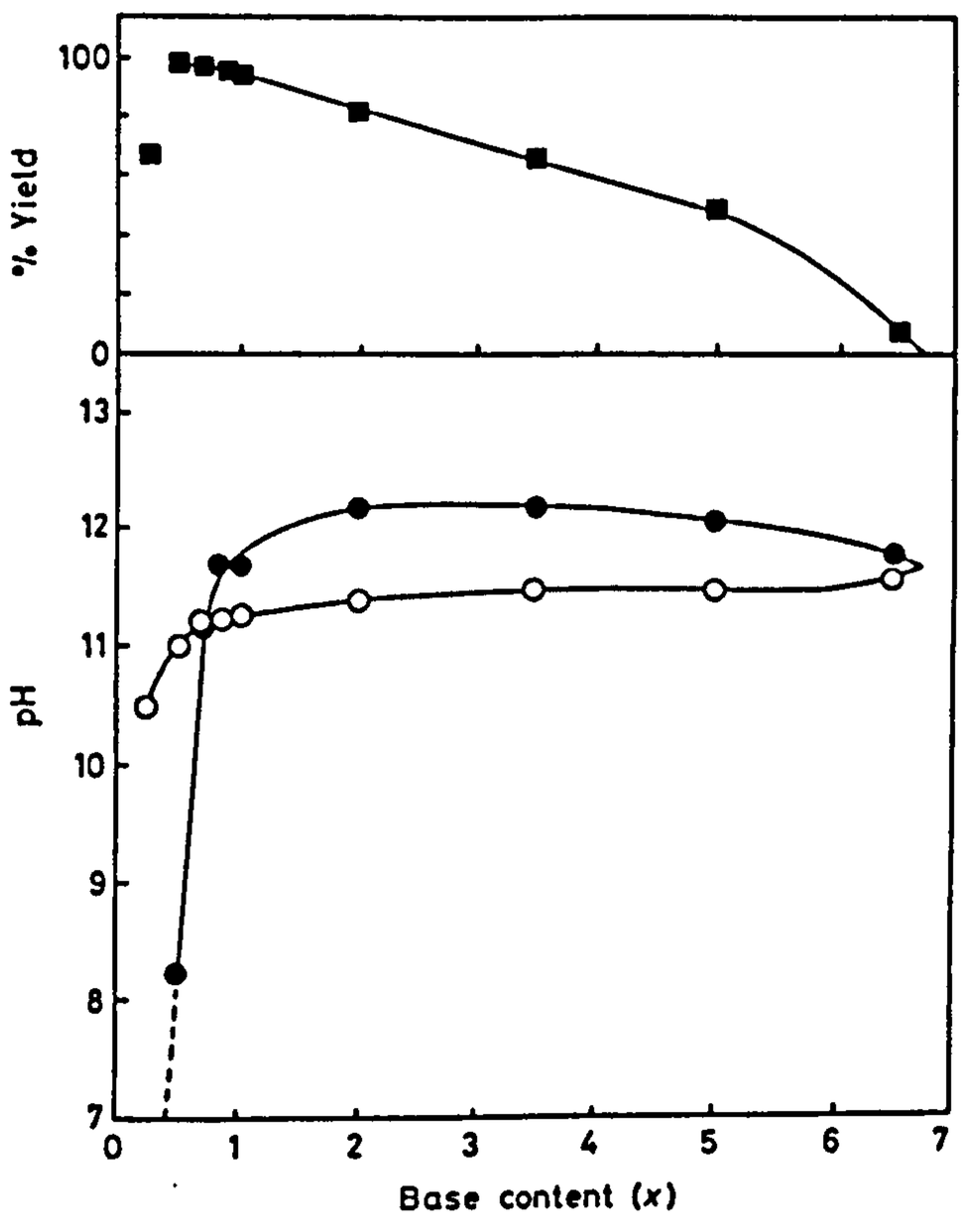

Figure 1. % Yield based on SiO$_2$ (■) and pH of initial gel (○) and final mother liquor (●) as a function of base content, x.

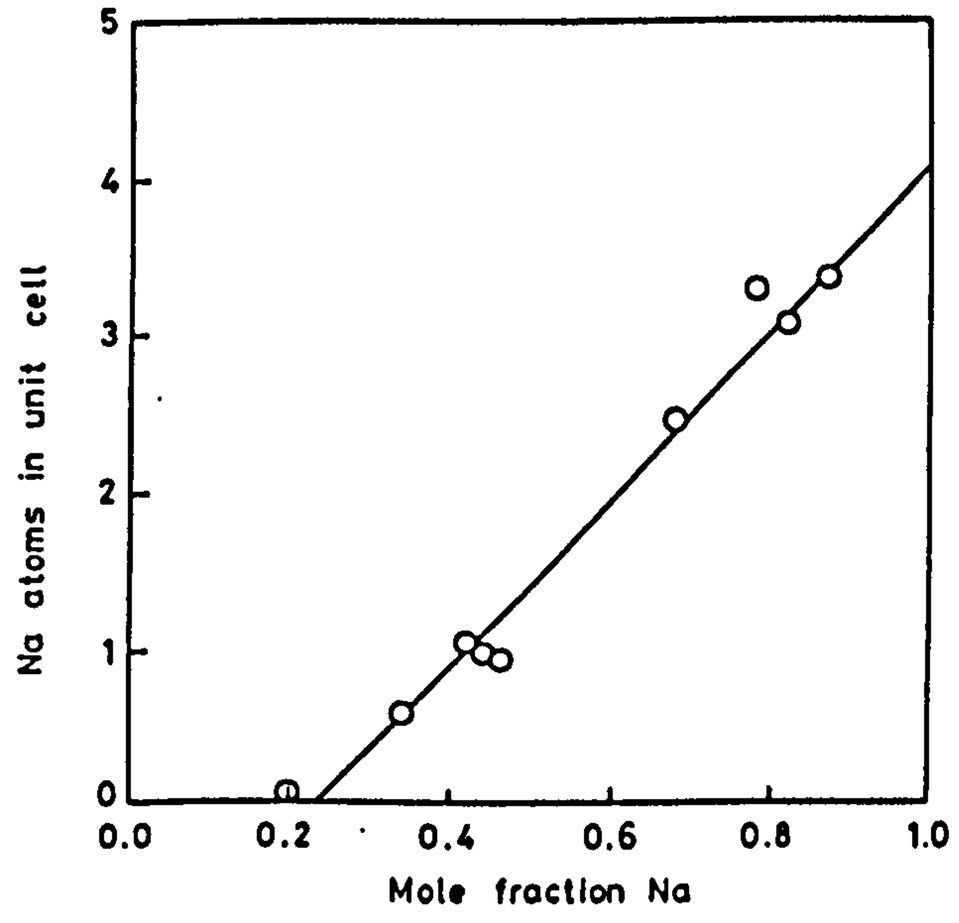

Figure 2. Number of sodium atoms in unit cell as a function of mole fraction $2x/(2x + 2)$ of sodium ions in reaction mixture.

minimum cation fraction for incorporation of sodium into the molecular sieve (0.24 ± 0.08) is within experimental error of the value (0.294) required to provide sufficient base for complete crystallisation of all the silica as 4TPAOH 96SiO_2. Extrapolation of the straight line to a sodium cation fraction of unity gives the maximum number of sodium ions per unit cell that could be incorporated from these reaction mixtures. The value (4.1 ± 0.5) suggests that the limiting unit cell composition of (Na, TPA) silicalite-1 in this system is 4NaOH 4TPAOH 96SiO_2.

The dominant feature of this crystallisation and no doubt that of related zeolitic materials with very low aluminium contents is base occlusion. It is not possible to tell from the present measurements whether the charge on the occluded cations is balanced by hydroxide ions or broken siloxane bonds, though it seems likely that both are present and probably in equilibrium with each other. If the negative charge is present as a broken siloxane bond the sodium ions should be exchangeable and thus these materials may be ion exchangers despite the absence of aluminium in the frameworks.

S. G. F. thanks the S.E.R.C. for a studentship.

Received, 15th December 1983; Com. 1628

References

1 J. L. Casci and B. M. Lowe, *Zeolites*, 1983, 3, 186.
2 B. M. Lowe, *Zeolites*, 1983, 3, 300.
3 E. M. Flanigen, J. M. Bennett, R. W. Grose, J. P. Cohen, R. L. Patton, R. M. Kirchner, and J. V. Smith, *Nature*, 1978, 271, 512.
4 R. W. Grose and E. M. Flanigen, U.S.P. 4061724.
5 F. G. Dwyer and E. E. Jenkins, U.S.P. 3941871.
6 R. K. Iler, 'The Chemistry of Silica,' Wiley, New York, 1979, p. 30.

THE USE OF ISOPIESTIC VAPOUR PRESSURE MEASUREMENTS TO STUDY SALT IMBIBITION BY ZEOLITES

S. G. Fegan and B. M. Lowe

Department of Chemistry, University of Edinburgh, West Mains Road, Edinburgh EH9 3JJ. Scotland, UK

An isopiestic method for measuring salt imbibition by zeolites is described. The method can be used to measure the amount of salt and water imbibed at preset water activities. Isotherms for the imbibition of NaCl, Na_2CO_3 and sodium benzenesulphonate in zeolite Na-X at 25°C are presented.

INTRODUCTION

Amongst the many ways in which the sorbent properties of zeolites can be modified the inclusion of salts by imbibition from aqueous solution is particularly effective (1). It is possible to control both the shape and size selectivity of the parent zeolite, and it appears that small amounts of intracrystalline salt can have very marked effects. Imbibition from aqueous solution is preferable to inclusion from melts in that it allows the controlled introduction of variable amounts of salt into the zeolite channel system. The quantity of salt imbibed depends on the concentration in the solution phase and for some systems it can be represented by a Donnan membrane process (2,3).

Salt imbibition from aqueous solution also has important implications for the study of zeolite crystallization. The addition of salts to reaction mixtures can have marked effects on the induction period, the growth rate, and the shape of the zeolite crystals produced (4), and in some systems different salts can cause the formation of different framework structures (5). Often the salt molecule is encapsulated in the aluminosilicate framework and cannot be readily extracted by washing with water, however, it seems likely that in some cases the framework could form around a salt molecule which is subsequently replaced by water either at a later stage of the crystallization or during the washing of the product.

It is evident that salt imbibition has important implications for at least these two areas of zeolite chemistry and we have therefore begun a systematic study of salt imbibition.

For a complete study of the equilibrium it is necessary to determine the concentration of the solution phase and the amounts of salt and water imbibed by the zeolite. To measure all three quantities is experimentally difficult and previous workers have made various assumptions about the way in which the water content of the zeolite is affected by the imbibed salt. Since the measurements are required for each point on an imbibition isotherm it is necessary that the analytical procedure is straightforward and rapid, and ideally it should not rely on a specific property of the salt under investigation. Perhaps the most intractable experimental problem is the requirement that before analysis the

equilibrated zeolite must be separated from the solution phase and washed free of adhering salt without upsetting its internal salt and water content. In an attempt to avoid this problem and at the same time reduce the analytical procedure to an absolute minimum, and provide accurate values for all the required quantities, we have developed a procedure based on isopiestic vapour equilibration.

Isopiestic vapour pressure measurements have been used by many workers to provide osmotic and activity coefficients for aqueous electrolyte solutions (6), but we are not aware of any previous application to salt imbibition by zeolites. The method which we have developed solves all of the major problems associated with the determination of imbibition isotherms. The apparatus is inexpensive, and with care the method produces accurate results. It has two major advantages over previous methods; it gives both the water and salt content of the zeolite, and it does not rely on a specific property of the salt.

METHOD

Consider a group of small dishes, each of which contains roughly the same accurately known weight of anhydrous zeolite, different known weights of a salt, and a volatile solvent, normally water. If the dishes are in good thermal contact in an evacuated thermostated chamber, solvent will distill from one dish to another until the solution phase in each dish has the same water activity. Hence at equilibrium the solutions in each dish have the same concentration irrespective of the amount of zeolite present, and provided the zeolite samples are in contact with solution they will all contain the same amount of imbibed salt and solvent per unit weight of anhydrous zeolite. It is readily shown that this situation is represented by the equation

$$(W_w/W_z) = U_s(R_{zeo} - R_{sol}) + R_{sol}(W_s/W_z) \qquad (1)$$

in which W_w, W_s and W_z are the total weights of water, salt and anhydrous zeolite present in the dishes at equilibrium; R_{zeo} and R_{sol} are the weight ratios of water to salt in the zeolite and solution phases and U_s is the amount of salt imbibed by unit weight of zeolite. For a given water activity, R_{zeo}, R_{sol} and U_s are constant and hence (W_w/W_z) is linearly dependent on (W_s/W_z). The slope of this line can be used to determine the concentration of the solution. The intercept contains two terms U_s and R_{zeo} which cannot be separated without further experimental information. This is obtained as follows.

If the ratio of salt to zeolite (W_s/W_z) is small all of the salt is imbibed by the zeolite and at equilibrium there is no solution phase present. In this case U_s is simply equal to the ratio of weights of salt and anhydrous zeolite placed in each dish, and the amount of water sorbed by the zeolite is controlled by the water activity of the solution phase present in the dishes for which (W_s/W_z) is large and by the amount of salt in the zeolite. It is observed that for dishes in which there is no solution phase present,

$$(W_w/W_z) = U^o_w + k(W_s/W_z) \qquad (2)$$

in which U^o_w is the amount of water sorbed when there is no salt in the zeolite and k is an empirical constant. The linear form of this equation is an empirical result, not demanded by mass balance or thermodynamic considerations.

At the intersection of the lines represented by equations 1 and 2 the experimental ratios (W_s/W_z), (W_w/W_z) and (W_w/W_s) are the values of U_s, $U_w(= U_sR_{zeo})$ and R_{zeo} for the zeolite in equilibrium with the solution phase. This is true irrespective of the form of equation 2. Obviously the accurate determination

of the intersection point is critical to the success of the experiment; and the amounts of solute and zeolite in each dish must be carefully chosen so that points on both sides are obtained.

Each set of experimental measurements corresponds to a particular water vapour pressure which is determined by the concentration of the solution phase. To make comparison with results obtained for different zeolites and salts it is best to arrange for each equilibration to be carried out under a pre-determined water vapour pressure. This is achieved by introducing a large quantity of a saturated solution plus excess solid into the evacuated chamber. Provided this solution remains saturated the vapour pressure will remain constant and may be determined by a separate experiment or obtained from the literature (6). When the equilibration is carried out in this way the concentration of the solution phase in each dish changes until it has the same vapour pressure as the saturated solution.

EXPERIMENTAL

1. Apparatus

Two types of dish were used for the experiment: gold-plated silver dishes fitted with teflon lids and stainless steel dishes with stainless steel lids. Each dish held about 9 cm^3. The silver dishes sat in a gold-plated copper block and the stainless steel dishes sat in a stainless steel block. Each block held eight dishes. The blocks sat in Jencons type 4 6-inch dry seal dessicators which were modified to allow the lids of the dishes to be raised or lowered from the outside. The blocks were supported from the side of the dessicator and the saturated solution which controlled the vapour pressure was contained in a petri-dish which sat in the bottom of the dessicator below the metal block. During equilibration the dessicators were placed on a rocking board in a water thermostat bath at 25.00 ± 0.04°C. Six dessicators could be accommodated at once.

2. Procedure

The dishes were first carefully dried and weighed. Approximately 0.35g of zeolite was placed in each dish and a saturated solution of AnalaR-grade sodium chloride ($a_w \sim 0.75$) was placed in the petri-dish. The lids were raised from the dishes and the dessicator slowly evacuated with a water pump. Evacuation speeds up equilibration, but must be done carefully so as to avoid spluttering and loss of material. The zeolite was allowed to equilibrate with the sodium chloride solution for about 3 days. The dessicator was then removed from the thermostat bath, the lids were lowered onto the dishes, and air carefully admitted. The dishes were then weighed to obtain the amount of equilibrated zeolite in each dish. Thermal gravimetric analysis of a sample of the same zeolite equilibrated in the same manner was used to obtain the water content of the equilibrated zeolite, and hence the weight of the dry zeolite in each dish.

Different quantities of the salt to be imbibed by the zeolite were added to each dish and the exact amount determined by careful weighing. Distilled water was also added to each dish and a saturated solution of the salt plus excess solid was placed in the petri-dish. The system was then equilibrated as before for several days, and the total amount of water in each dish at equilibrium (sorbed and free) obtained by weighing. At this stage the solution phase in each dish was saturated and the amount of solute imbibed by the zeolite was the maximum that could be achieved from aqueous solution at 25°C.

The solution in the petri-dish was now replaced by a saturated solution (of a different salt) with a vapour pressure higher than that used previously and the system was re-equilibrated. At equilibrium the solution phase in the dishes was no longer saturated and the amount of salt imbibed by the zeolite was reduced.

The experiment was then repeated with saturated solutions of other salts until a sufficient range of vapour pressures had been covered.

Finally, in some cases, an independent measurement of U_w^0 and solute concentration was made for each chosen vapour pressure by separately equilibrating the zeolite and salt over each saturated salt solution.

The method worked best with high solute concentrations and low vapour pressures; at high vapour pressures care must be taken to recognize the occurrence of capillary condensation.

3. Materials

Zeolite Na-X was synthesized at 95°C from the reaction mixture 4.3 Na_2O Al_2O_3 8.6 SiO_2 172 H_2O and had Si/Al ~ 1.35 as determined by XRD. Zeolite Na-A was obtained from BDH. Both zeolites were exchanged several times with NaCl solution and washed thoroughly before use.

Merck suprapure NaCl and BDH analar Na_2CO_3 were dried in vacuo at 180°C and stored over P_2O_5. Fluka purum-grade sodium benzenesulphonate was used as supplied.

Glass-distilled water was used throughout.

RESULTS and DISCUSSION

The systems described here are chosen to illustrate the scope of the isopiestic method.

1. NaCl + Zeolite Na-X

Figure 1 shows a selection of the experimental results as plots of W_w/W_z against W_s/W_z. Sodium chloride is readily imbibed by zeolite X and straight lines corresponding to equations 1 and 2 are observed. These lines have substantially different slopes and the intersection points are readily obtained. Each plot refers to a different water activity, $a_w(=P/P^0)$, and a different sodium chloride concentration. The lines with zero or negative gradients correspond to the situation in which there is no solution phase present in the dishes. This is represented by equation 2. The slope of these lines becomes more negative as the water activity is decreased; corresponding to an increase in the amount of water displaced from the zeolite by unit amount of imbibed salt. The lines with positive slopes are for zeolite in contact with sodium chloride solution (equation 1). The slopes of these are proportional to the reciprocal of the solution phase concentration. Parameters derived from the results shown in Figure 1 and similar results for other water activities are shown in Table 1.

Figure 2 shows how the salt and water content of the zeolite change with the molality of the sodium chloride solution. The water content of the zeolite depends both on the water activity in the solution phase and on the amount of salt imbibed by the zeolite. The effect of salt imbibition on the water content can be seen at high molalites as the difference between U_w and U_w^0 and it is clear that the salt displaces some of the water.

As the water and salt content of the zeolite are both known it is possible to calculate an "effective molality" m_i (defined as mol salt per kg water) for the salt "solution" in the zeolite. Figure 3 shows how m_i varies with the molality m of the solution phase.

Table I - Imbibition Results for NaCl + Zeolite Na-X.

Salt[a]	a_w	U_w^0	R_{sol}	m^c	$10^3 U_s$	U_w	m_f^e
[b]	-	0.384	27.55	0.621	0.0	0.384	0.000
[b]	-	0.376	15.72	1.089	0.534	0.376	0.024
[b]	-	0.372	9.225	1.855	1.917	0.377	0.087
KNO_3	0.925	0.369	7.625	2.244	3.08	0.371	0.142
$BaCl_2$	0.902	0.363	6.025	2.840	10.5	0.368	0.487
$ZnSO_4$	0.871	0.362	4.619	3.705	16.2	0.358	0.776
KCl	0.843	0.358	4.023	4.254	25.2	0.362	1.194
KBr	0.807	0.360	3.388	5.051	31.9	0.349	1.565
NH_4Cl	0.771	0.357	2.871	5.961	37.0	0.337	1.879
NaCl	0.753	0.357	2.834	6.039	42.9	0.332	2.211
NaBr	0.577	0.352	[d]	[d]	49.1	0.327	2.572
K_2CO_3	0.428	0.346	[d]	[d]	51.8	0.317	2.779
$MgCl_2$	0.330	0.337	[d]	[d]	59.9	0.306	3.378
LiCl	0.111	0.313	[d]	[d]	78.2	0.274	4.878

[a] Salt used for saturated solution.
[b] Not used.
[c] Molality of solution phase, mol/kg.
[d] No solution phase present.
[e] Molality of "solution" in zeolite, mol/kg.

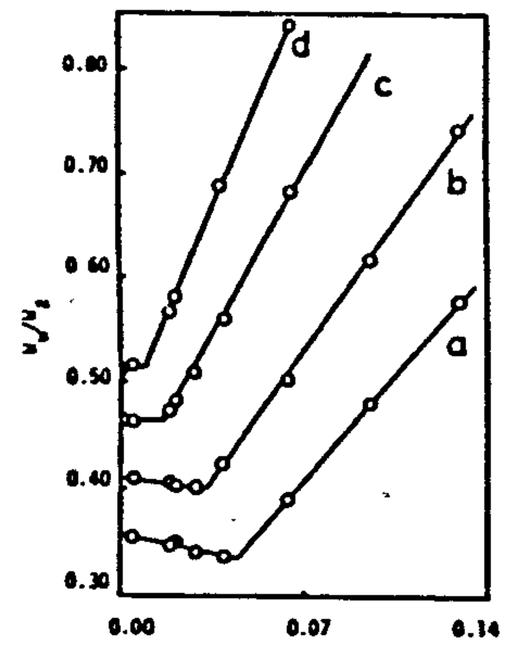

FIGURE 1.
Imbibition results for NaCl+zeolite Na-X. For clarity the plots have been displaced by 0.05 units on the U_w/U_z axis relative to plot (a). The saturated solutions were (a) NaCl, a_w = 0.753; (b) KBr, a_w = 0.807; (c) $ZnSO_4$, a_w = 0.871; (d) $BaCl_2$, a_w = 0.902.

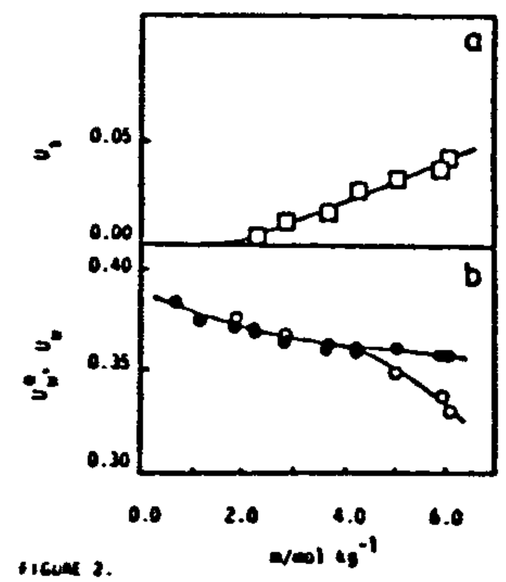

FIGURE 2.
Uptake of NaCl and water by zeolite Na-X against solution molality m. (a) NaCl, □; (b) H_2O, U_w, ●; U_w, ○.

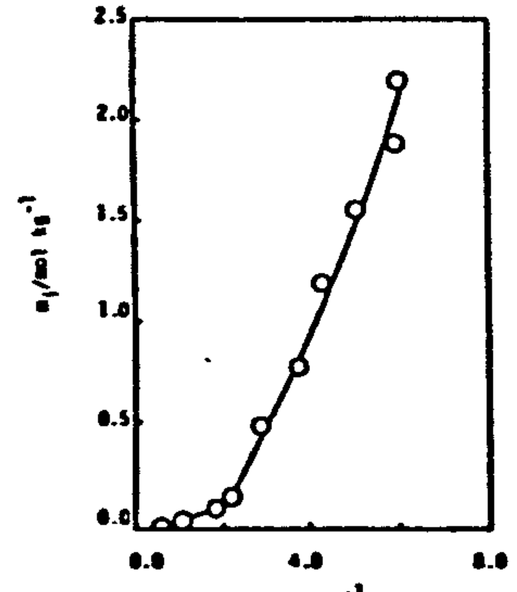

FIGURE 3.
Internal molality, m_f, of NaCl in zeolite Na-X as a function of solution phase molality.

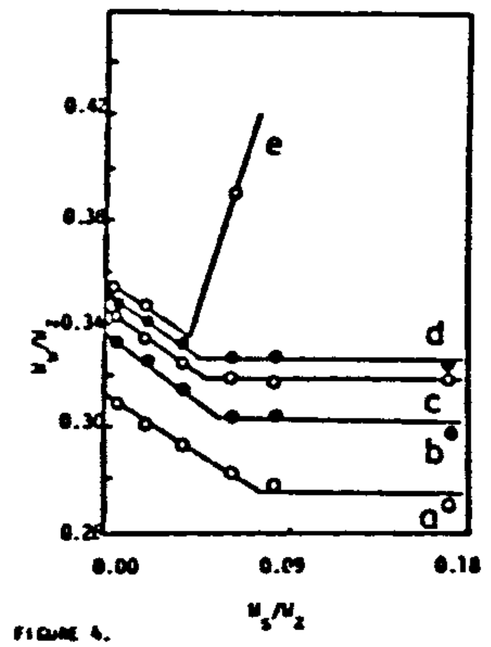

FIGURE 4.
Imbibition results for NaCl in zeolite Na-X for water activities below that of saturated sodium chloride solution. The saturated solutions were (a) LiCl, a_w=0.111; (b) $MgCl_2$, a_w = 0.330; (c) K_2CO_3, a_w = 0.428; (d) NaBr, a_w=0.577, (e) NaCl, a_w = 0.753.

The maximum value of m is determined by the solubility of NaCl (6.15 mol/kg) and this corresponds to an internal molality m_i of 2.21 mol/kg. To achieve internal molalities larger than this it is necessary to equilibrate NaCl with the zeolite under water vapour pressures below that of saturated sodium chloride solution (a_w = 0.753). Figure 4 shows experimental results obtained under these conditions. In these plots the lines with negative slopes correspond as before, to the situation in which all the NaCl is imbibed by the zeolite, whereas the horizontal lines are for mixtures of NaCl + zeolite containing the maximum amount of imbibed salt attainable at the specified water vapour pressure. In these experiments there is no solution phase present in the dishes; the excess salt is simply in contact with the external surface of the zeolite. The intersection points in Figure 4 correspond to the values of U_w and U_s for the maximum amount of imbibed salt and these are given in Table 1. The salt uptake increases as the water activity is lowered. Figure 5 shows the internal molality of NaCl in the zeolite as a function of water activity.

2. Na_2CO_3 + Zeolite Na-X.

This system behaves in a similar way to the previous one, except that because sodium carbonate solutions are readily supersaturated by isothermal distillation (8) it was possible to observe imbibition from solutions many times more concentrated than the saturated solution (2.77 mol/kg) (8). However, it is perhaps possible that at the high concentrations the 'solution phase' was a mixture of slowly equilibrating hydrates.

Figure 6 shows that the uptake of sodium carbonate, as with sodium chloride, produces a corresponding decrease in water content of the zeolite. However, despite the high solution phase molalities (up to 14 mol/kg) the highest internal molality was only 3.205 mol/kg (see Figure 7). The internal molality is shown as a function of water activity in Figure 8. In this case, unlike the NaCl one (Figure 5) no discontinuity is observed.

3. Sodium Benzenesulphonate + Zeolite Na-X

Figure 9 shows experimental results for sodium benzenesulphonate at a concentration close to saturation. It can be seen that no salt imhibition occurs under these conditions. However, at lower water activities (Figure 10) salt imbibition does occur. In this figure the lines for zeolite in contact with excess salt are not horizontal (compare with NaCl in Figure 4). This is because sodium benzenesulphonate crystallizes as a monohydrate as can be deduced from the slope of the line. From the intersection points in Figure 10 it is possible to deduce the internal salt molality and this is shown as a function of water activity in Figure 11.

4. NaCl + Zeolite 4A.

In this case no imbibition occurs even from saturated aqueous solutions as may be deduced from Figure 12. However, it is possible that imbibition may occur at lower water activities.

5. Other Systems

Preliminary investigations have indicated that high silica zeolites, e.g. ZSM-5, imbibe much less inorganic salt than low silica ones. However, the low levels of imbibition (U_s<0.01) are readily detected by this method and work on high silica zeolites is in progress.

The method has many other possibilities which are not illustrated in this paper. Amongst these its application to sorption of involatile non-electrolytes is particularly promising. It should also be noted that imbibition by many other porous materials besides zeolites may be studied by the isopiestic method.

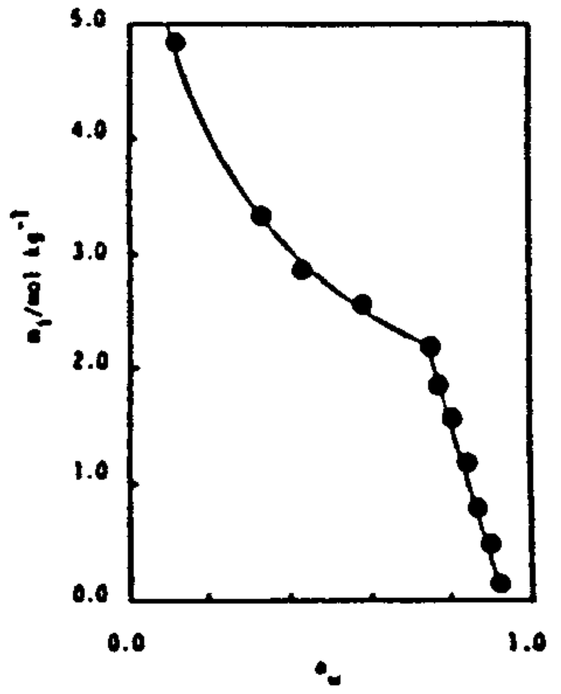

FIGURE 5.
Internal molality, m_i, of NaCl in zeolite Na-X as a function of water activity.

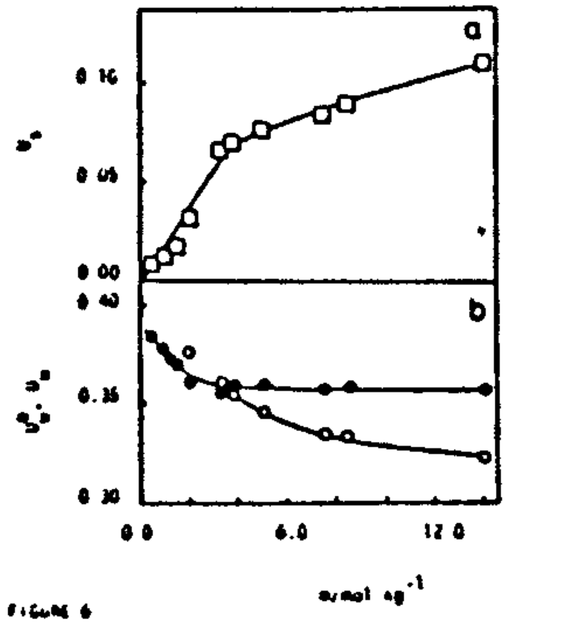

FIGURE 6
Uptake of Na_2CO_3 and water by zeolite Na-X against solution molality m. ○ Na_2CO_3, □ H_2O, U_w.●, U_s.○.

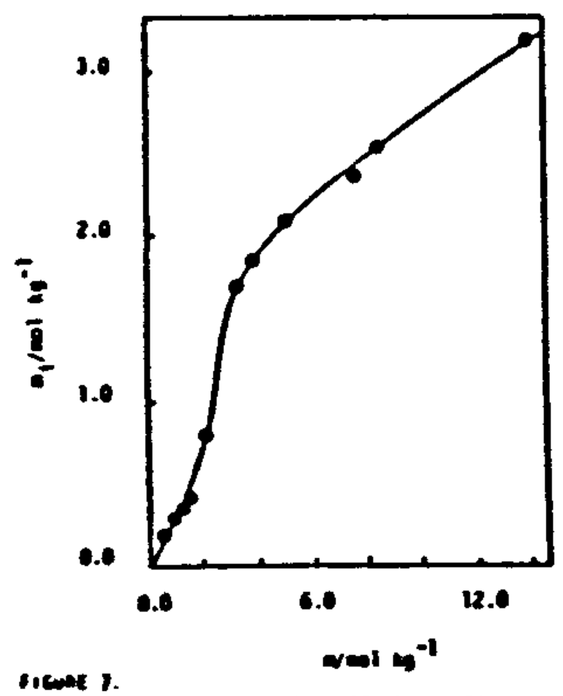

FIGURE 7.
Internal molality, m_i, of Na_2CO_3 in zeolite Na-X as a function of solution phase molality.

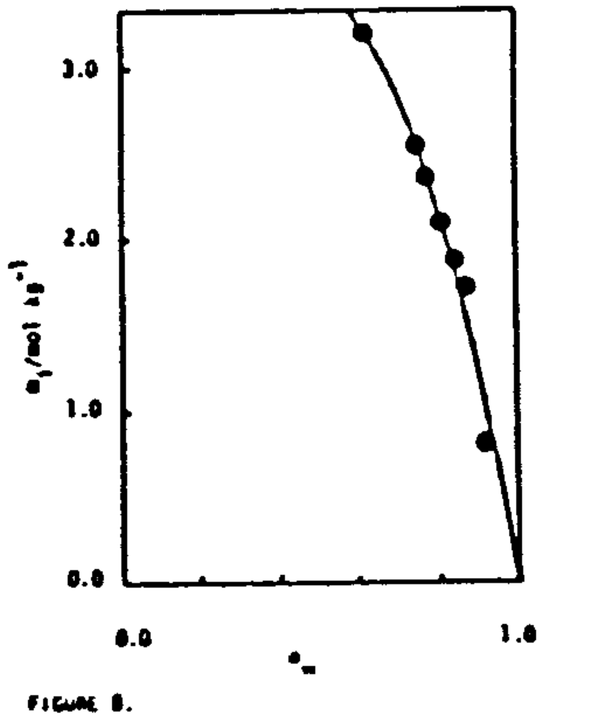

FIGURE 8.
Internal molality, m_i, of Na_2CO_3 in zeolite Na-X as a function of water activity.

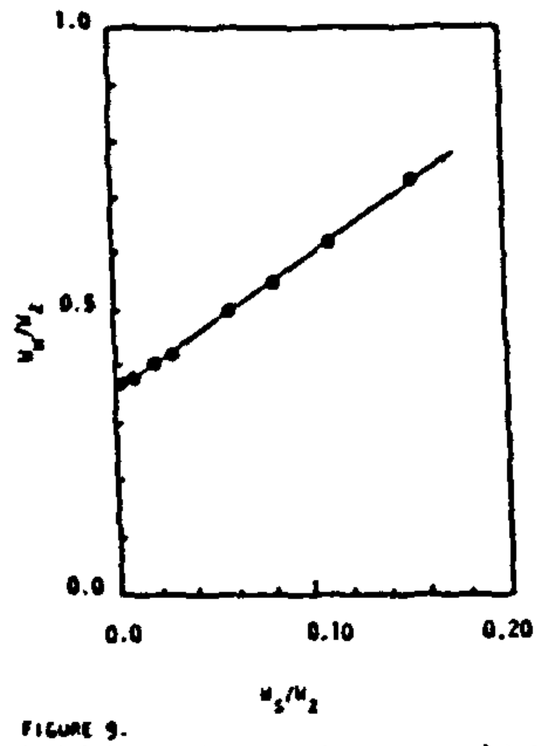

FIGURE 9.
Imbibition results for sodium benzenesulphonate + zeolite Na-X. ρ = 2.34 mol kg^{-1}, a_w = 0.925.

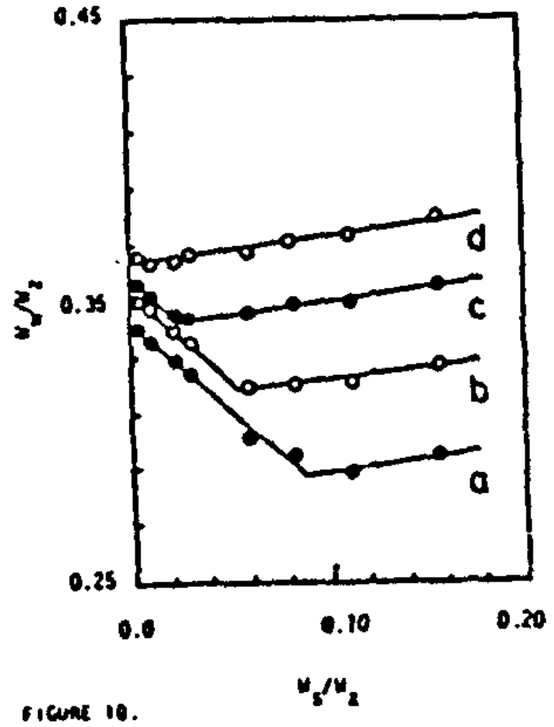

FIGURE 10.
Imbibition results for sodium benzenesulphonate + zeolite Na-X at different water activities. The saturated solutions were (a) $MgCl_2$, a_w = 0.330; (b) $Ca(NO_3)_2$, a_w = 0.500, (c) NH_4NO_3, a_w = 0.618, (d) NaBr, a_w = 0.807.

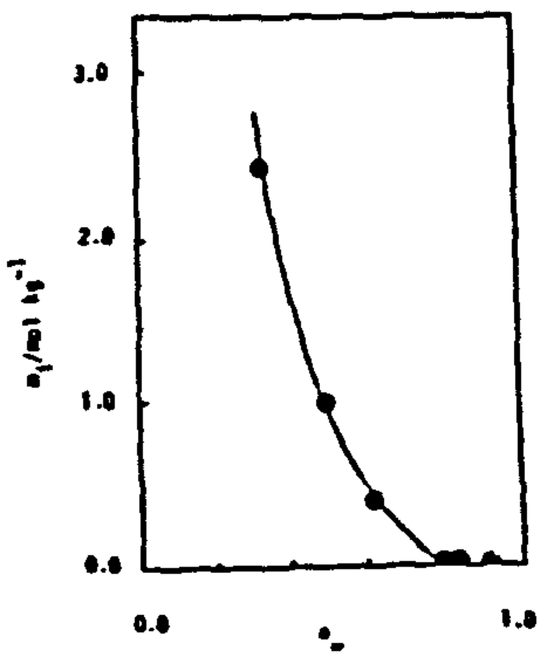

FIGURE 11.
Internal molality, ρ_i, of sodium benzenesulphonate in zeolite Na-X as a function of water activity.

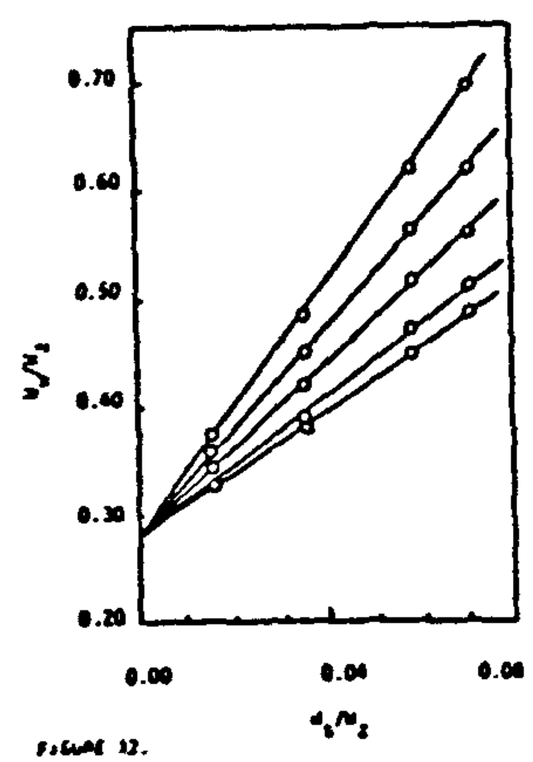

FIGURE 12.
Imbibition results for NaX + zeolite 4A. Lines correspond to the following solution concentrations, 6.01, 5.39, 4.39, 3.63, 2.56 mol kg^{-1}.

ACKNOWLEDGMENT

SJF thanks SERC for a studentship.

REFERENCES

1. R. M. Barrer, D. A. Harding and A. Sikand, J. C. S. Faraday I, 1980, 76, 180.

2. R. M. Barrer and W. M. Meier, J. Chem. Soc., 1958, 299.

3. R. M. Barrer and A. J. Walker, Trans. Faraday Soc., 1964, 60, 171.

4. A. Erdem and L. B. Sand, J. Cat., 1979, 60, 241.

5. R. M. Barrer, J. F. Cole and H. Villiger, J. Chem. Soc. (A), 1970, 1523.

6. R. A. Robinson and R. H. Stokes, "Electrolyte Solutions" (Butterworth, London, 1959).

7. T. V. Whittam, Brit. Patent 1,145,995, (1965).

8. R. A. Robinson and J. M. Macaskill, J. Solution Chem., 1979 8, 35.

Appendix VI

Lecture Series and Courses

The following lecture series and courses were attended during the three year research period:

Courses

Fortran77 computing course
Edinburgh Regional Computing Centre

SERC/CRAC Graduate School
University of Surrey, Guildford

NATO Advanced Study Institute (Zeolites: Science and Technology)
Alcabibeche, Portugal

Lecture Series

Crystallography
Drs. R.O. Gould, B.M. Lowe and M.D. Walkinshaw (University of Edinburgh)

Modern Liquid Phase Separation Processes
Professor J.H. Knox (University of Edinburgh)

The Chemistry of Photographic Processes
Dr. L.A. Williams (Kodak Ltd.)

Fourier-Transform Infrared Spectroscopy
Drs. A. Morrison and J.L. Duncan (University of Aberdeen),
Dr. S. Cradock (University of Edinburgh)

Radiochemical Methods of Analysis
Drs. A.B. McKenzie and J.E. Whitley (Scottish Universities Research and Reactor Centre)

Seminars

Research Group seminars and Departmental seminars were also attended.